



UNIVERSIDAD NACIONAL AUTÓNOMA DE MÉXICO
DOCTORADO EN CIENCIAS BIOMÉDICAS
FACULTAD DE MEDICINA

ESTUDIO DE LA MODIFICACIÓN POST-TRADUCCIONAL DE LA CINASA
WNK4 POR CORTE PROTEOLÍTICO Y REGULACIÓN POR
FOSFORILACIÓN

TESIS

QUE PARA OPTAR POR EL GRADO DE:
DOCTOR EN CIENCIAS

PRESENTA:

ADRIAN RAFAEL MURILLO DE OZORES

DIRECTOR DE TESIS

DRA. MARIA CASTAÑEDA BUENO
FACULTAD DE MEDICINA

COMITÉ TUTOR

DR. GERARDO GAMBA AYALA
INSTITUTO DE INVESTIGACIONES BIOMÉDICAS

DR. ALEJANDRO ZENTELLA DEHESA
INSTITUTO DE INVESTIGACIONES BIOMÉDICAS

CIUDAD DE MÉXICO, AGOSTO DE 2021



Universidad Nacional
Autónoma de México



UNAM – Dirección General de Bibliotecas
Tesis Digitales
Restricciones de uso

DERECHOS RESERVADOS ©
PROHIBIDA SU REPRODUCCIÓN TOTAL O PARCIAL

Todo el material contenido en esta tesis esta protegido por la Ley Federal del Derecho de Autor (LFDA) de los Estados Unidos Mexicanos (México).

El uso de imágenes, fragmentos de videos, y demás material que sea objeto de protección de los derechos de autor, será exclusivamente para fines educativos e informativos y deberá citar la fuente donde la obtuvo mencionando el autor o autores. Cualquier uso distinto como el lucro, reproducción, edición o modificación, será perseguido y sancionado por el respectivo titular de los Derechos de Autor.

RECONOCIMIENTOS

El presente trabajo se realizó bajo la tutoría de la Dra. María Castañeda Bueno en el Departamento de Nefrología y Metabolismo Mineral del Instituto Nacional de Ciencias y Nutrición Salvador Zubirán, y en colaboración con el grupo del Dr. Gerardo Gamba del Instituto de Investigaciones Biomédicas y del Instituto Nacional de Ciencias y Nutrición Salvador Zubirán.

Al Programa de Doctorado en Ciencias Biomédicas de la Universidad Nacional Autónoma de México, por todas las facilidades otorgadas, especialmente a la Dra. Aurea Orozco y a Evangelina Vargas.

El comité tutor que asesoró el desarrollo de esta tesis estuvo formado por:

Dra. María Castañeda Bueno	Facultad de Medicina
Dr. Gerardo Gamba Ayala	Instituto de Investigaciones Biomédicas
Dr. Alejandro Zentella Dehesa	Instituto de Investigaciones Biomédicas

A los miembros del jurado por sus valiosas aportaciones:

Dr. Luis Alfonso Vaca Dominguez	Instituto de Fisiología Celular
Dra. María Castañeda Bueno	Facultad de Medicina
Dra. Norma Araceli Bobadilla Sandoval	Instituto de Investigaciones Biomédicas
Dr. Leon David Islas Suarez	Facultad de Medicina
Dr. Jose Pedraza Chaverri	Facultad de Medicina

Este trabajo fue realizado gracias a apoyos otorgados a la Dra. María Castañeda por el Consejo Nacional de Ciencia y Tecnología (CONACYT) No. 257726 y 101720.

Durante la realización de mis estudios de doctorado recibí una beca otorgada por CONACYT con el número de registro 606808.

A la QFB Norma Vázquez por su apoyo técnico durante la realización de este trabajo.

A la Red de Apoyo a la Investigación (RAI) por el uso de sus servicios de cultivo celular y microscopía.

Al personal del bioterio del Instituto Nacional de Ciencias y Nutrición Salvador Zubirán.

A la Unidad de Secuenciación del Instituto de Biotecnología.

A la American Society of Nephrology, por permitirme presentar parte de este trabajo en el congreso Kidney Week, y al Programa de Apoyo a los Estudios de Posgrado de la UNAM por su apoyo para asistir a dicho congreso.

AGRADECIMIENTOS

A mis papás, **María Elena y Adrián Fabio**. Por todos los sacrificios que han hecho a lo largo de su vida con tal de apoyarme y permitirme llegar hasta donde he llegado. Nada de esto sería posible sin ustedes. Son lo más importante en mi vida.

A mis tías **Leda y Ligia**, por brindarme todo su amor, así como a mis tíos **Luis y María Elena**, por todos sus consejos y apoyo durante toda mi vida.

A mis primos, **Leonel, Claudia y Coqui**, que a pesar de la distancia me han apoyado incondicionalmente.

A mis mascotas, **Kira y Coffee**, por acompañarme en casa todos estos años.

A **María Castañeda**, por su amistad y por el tiempo que se ha dado para enseñarme tanto, como científico y como persona.

A **Gerardo Gamba**, por haberme apoyado desde los inicios de mi carrera hasta el día de hoy.

A **Alejandro Zentella**, cuya amistad ha sido invaluable durante estos años.

A **Félix Recillas y Victoria Chagoya**, mis tutores de la licenciatura, cuyas enseñanzas fueron esenciales para mi formación como científico.

A **Norma Vázquez**, por todo el apoyo día a día en el laboratorio, tanto personal como académico.

A mis tutorcitos de mis diferentes laboratorios, **Zesergio Melo, Rodrigo Arzate, Francisco Carmona y Jesús Rodríguez**, quienes son un pilar esencial de mi carrera académica. Les agradezco el tiempo que se tomaron para enseñarme tantas cosas.

A mis compañeros de la LIBB, especialmente a **Dominique, Roberto Carlos y Abiram**, por todas las risas durante la carrera y las salidas a comer pizza.

A los amigos que he hecho durante mi estancia en el laboratorio: **Alex, Anahí, Braulio, Daniel, Diego, Eli, Gerardito, Germán, Jessica, Jonatan, Lalito, Lalo, Leni, Lore, Luz, Michelle, Migue, Raquel, Rosy, Rox, Sebastián, Silvana y Yolik**, quienes han hecho esta etapa de mi vida una de las más felices.

A **Héctor**, por brindarme su amistad y su apoyo en todos los momentos difíciles del doctorado. Nunca olvidaré nuestras partidas de *Super Smash Bros. Ultimate* o cuando ponías los capítulos de *Dragon Ball Super*.

A **Andrea**, quien me ha apoyado incondicionalmente durante todos estos años. Por permitirme ser parte de su vida, y haberse acercado a la mía. Eres increíblemente importante para mí.

A mis amigos de toda la vida, **Jorge y Víctor**, que siguen siendo tan cercanos, aunque hayan pasado años. Gracias por todos los buenos momentos.

A todos los integrantes de la **Unidad de Fisiología Molecular**, por todas sus enseñanzas.

A la **Universidad Nacional Autónoma de México**.

Tabla de contenido

1.	<i>LISTA DE ABREVIATURAS</i>	5
2.	<i>RESUMEN</i>	6
3.	<i>INTRODUCCIÓN</i>	7
3.1.	Compartimentalización de fluidos	7
3.2.	Homeostasis del K^+	8
3.3.	Balance interno y externo de K^+	8
3.4.	Estructura funcional del riñón	9
3.5.	La nefrona como unidad funcional del riñón.....	9
3.6.	Manejo renal de K^+	10
3.7.	Regulación de la excreción renal de K^+	12
3.8.	El túbulo contorneado distal (DCT) y el cotransportador de Na^+/Cl^- , NCC.....	13
3.9.	Enfermedades genéticas que afectan la función de NCC.....	14
3.10.	Las cinasas WNK.....	15
3.11.	WNK4 y su papel en la regulación de NCC	16
3.12.	Características estructurales de la cinasa WNK4	16
3.13.	WNK4 como cinasa sensible a Cl^-	19
3.14.	Sitios de fosforilación que regulan la actividad de WNK4	19
3.15.	Regulación de la degradación de WNK4.....	20
3.16.	Relación recíproca entre NCC y el K^+	21
3.17.	Papel natriurético y diurético del K^+ y su relación con la presión arterial.....	21
3.18.	Mecanismos propuestos para la regulación de NCC por K^+	21
4.	<i>JUSTIFICACIÓN</i>	23
5.	<i>OBJETIVOS</i>	23
6.	<i>MATERIALES Y MÉTODOS</i>	25
7.	<i>RESULTADOS</i>	29
8.	<i>DISCUSIÓN Y CONCLUSIONES</i>	32
9.	<i>BIBLIOGRAFÍA</i>	35
10.	<i>APÉNDICE</i>	45

1. LISTA DE ABREVIATURAS

11 β -HSD2: 11 β hidroxiesteroide deshidrogenasa tipo 2
AngII: angiotensina II
ATL: asa ascendente delgada de Henle
ASDN: nefrona distal sensible a aldosterona
BCA: ácido bicinconínico
BIM: Bisindolilmaleimida 1
BK: canales iónicos “Big K⁺”
BSA: albúmina de Suero bovino
C-terminal: carboxilo-terminal
CaM: calmodulina
cAMP: adenosín monofosfato cíclico
CBD: sitio de unión a calmodulina
CCD: ducto colector cortical
[Cl]_i: concentración intracelular de Cl⁻
ClC-Kb: canal iónico de Cl⁻ “Chloride Channel-Kb”
CNT: túbulo conector
COPAS: del inglés “Complex Object Parametric Analyzer and Sorter”
CRISPR/Cas9: del inglés “clustered regularly interspaced short palindromic repeats” y “CRISPR-associated protein 9”
CT-CCD: dominio “coiled-coil” del C-terminal
CUL3: del inglés “cullin-3”
DCT: túbulo contorneado distal
DNA: ácido desoxirribonucleico
DTL: asa descendente delgada de Henle
EAST: del inglés “epilepsy, ataxia, sensorineural deafness and salt-wasting renal tubulopathy”
ENaC: canal epitelial de Na⁺
FHHt: hipertensión hiperkalémica familiar
FLAG: epítipo artificial usado para etiquetar proteínas recombinantes
GFP: proteína verde fluorescente
HA: epítipo de la hemaglutinina usado para etiquetar proteínas recombinantes
HCTZ: hidroclorotiazida
HEK293: del inglés “human embryonic kidney 293”
HKM: medio de incubación para células HEK293 con concentración de K⁺ 10mM
HLC: medio de incubación para células HEK293 hipotónico bajo en Cl⁻
HRP: peroxidasa de rábano
IMCD: ducto colector de la médula interna
[K⁺]_e: concentración de K⁺ extracelular
KCC3: cotransportador de K⁺:Cl⁻ 3
KCC4: cotransportador de K⁺:Cl⁻ 4
KCNJ10: del inglés “potassium inwardly rectifying channel subfamily J member 10”
kDa: kilodalton
Kir4.1: del inglés “inwardly-rectifying K⁺ channel 4.1”
Kir5.1: del inglés “inwardly-rectifying K⁺ channel 5.1”
KLHL3: del inglés “Kelch-like-3”
KLHL3/CUL3: componentes de un complejo de ligasa de ubiquitina
KO: del inglés “knockout”
KS-WNK1: del inglés “kidney-specific WNK1”
LC-MS/MS: del inglés “liquid chromatography–mass spectrometry”
LKM: medio de incubación para células HEK293 con concentración de K⁺ 1mM
mRNA: RNA mensajero
mTORC2: del inglés “mammalian target of rapamycin complex 1”

N-terminal: amino-terminal
NCC: cotransportador de $\text{Na}^+:\text{Cl}^-$
NEM: N-etilmaleimida
NHEJ: del inglés “non-homologous end joining”
NKCC1: cotransportador de $\text{Na}^+:\text{K}^+:2\text{Cl}^-$ 1
NKCC2: cotransportador de $\text{Na}^+:\text{K}^+:2\text{Cl}^-$ 2
NKM: medio de incubación para células HEK293 con concentración de K^+ 5mM
OMCD: ducto colector de la médula externa
OMIM: del inglés “Online Mendelian Inheritance in Man”
OSR1: del inglés “Oxidative Stress Responsive Kinase 1”
PCT: túbulo contorneado proximal
PF2-like: dominio similar a Pask-Fray 2
PHAI: Pseudohipoaldosteronismo tipo I
PKA: proteína cinasa A
PKC: proteína cinasa C
PP1: proteína fosfatasa 1
PV: parvalbúmina
RACE 3’: del inglés “Rapid Amplification of cDNA Ends”
RIA: radioinmunoanálisis
RING: del inglés “Really Interesting New Gene”
RM: receptor de mineralocorticoides
RNA: ácido ribonucleico
ROMK: del inglés “renal outer medullary K^+ channel”
SDS: duodecil sulfato de sodio
SGK1: del inglés “Serum/glucocorticoid-regulated kinase 1”
SLC12A3: del inglés “Solute Carrier 12A3”
SPAK: del inglés “Ste-20 Related Proline-Alanine Rich Kinase”
TAL: asa ascendente gruesa de Henle
WNK1: cinasa “*With No Lysine “K” 1*”
WNK4: cinasa “*With No Lysine “K” 4*”
WNK4-L319F: WNK4 con sustitución de Leu319 por Phe, incapaz de unir Cl^-

2. RESUMEN

La cinasa *With No Lysine “K” 4* (WNK4) es una proteína importante en la regulación del manejo de electrolitos en el riñón. Mutaciones en el gen que la codifica, son causa de Hipertensión Hiperkalémica Familiar (FHht), debido a un aumento en la fosforilación y actividad del cotransportador renal de Na^+/Cl^- , NCC, en el túbulo contorneado distal (DCT) de la nefrona. En contraste, la ausencia de WNK4 en modelos murinos se asocia a una pérdida de la función de NCC y menores niveles de K^+ en plasma. La concentración extracelular de K^+ y la actividad de NCC forman un asa de retroalimentación negativa que es esencial para los mecanismos renales encargados de mantener la homeostasis del K^+ en el organismo.

La actividad de la cinasa WNK4 puede ser regulada de distintas maneras: 1) la unión directa de un ion Cl^- en su sitio activo, inhibiendo su autofosforilación, 2) fosforilación en distintos sitios en sus dominios amino (N)- y carboxilo (C)-terminal que promueven un aumento en su actividad, 3) degradación mediada por un complejo de ligasa de ubiquitina de la cual forma parte la proteína Kelch-like-3 (KLHL3), la cual es inhibida por fosforilación. La presencia de WNK4 es indispensable para la activación de NCC ante hipokalemia, y se ha propuesto que la disminución en la concentración extracelular de K^+ promueve una disminución en la concentración intracelular de Cl^- ($[\text{Cl}^-]_i$) lo cual activa

a la cinasa WNK4. Sin embargo, se desconoce la contribución de los otros dos mecanismos en este fenómeno.

Además de la WNK4 completa, variantes de menor tamaño se han observado en inmunoensayos de lisados de riñón de ratón, lo cual sugiere que podrían tratarse de variantes previamente desconocidas de WNK4. En la primera mitad de este trabajo se confirmó la identidad de estas variantes por distintas metodologías. Las variantes cortas de WNK4 sólo fueron detectadas en riñón, son generadas por corte proteolítico y carecen del sitio de unión a la proteína Ste-20 Related Proline-Alanine Rich Kinase (SPAK), el sustrato de la cinasa WNK4, por lo que podrían tratarse de un mecanismo inhibitorio. Además, en estudios in vitro encontramos un sitio fidedigno de unión a la proteína fosfatasa 1 (PP1) en el dominio C-terminal de WNK4, el cual es responsable de la unión a PP1, y la defosforilación e inhibición de WNK4.

La segunda mitad de este proyecto consistió en estudiar la regulación de WNK4 en un modelo de hipokalemia. Primero demostramos que la fosforilación de la Ser64 y Ser1196 de WNK4 incrementan en respuesta a una disminución en la ingesta de K^+ en ratones. Estudios in vitro y ex vivo sugieren que este efecto es independiente de factores adicionales en el organismo, y se debe directamente a la disminución de la concentración extracelular de K^+ . Dado que este parámetro es directamente proporcional a la $[Cl^-]_i$, decidimos estudiar si la $[Cl^-]_i$ pudiese regular la fosforilación de WNK4 en la Ser64 y Ser1196. Usando diferentes maniobras para disminuir $[Cl^-]_i$ encontramos que esto se asocia a un aumento en la fosforilación de WNK4 en estos sitios. Este fenómeno es independiente de la actividad de las cinasas WNK, por lo que un mecanismo sensible a $[Cl^-]_i$ aún no descrito puede converger en la activación de la señalización por WNK4. De manera similar, demostramos que la actividad de KLHL3 disminuye al reducir la $[Cl^-]_i$, lo cual promueve un incremento en la abundancia de WNK4.

La generación de ratones transgénicos WNK4-L319F, los cuales tienen una WNK4 que es incapaz de unir directamente al ion Cl^- , nos permitió estudiar si existen mecanismos adicionales involucrados en la activación de NCC ante hipokalemia. Después de 7 días de ingesta deficiente en K^+ , los ratones WNK4-L319F muestran un aumento en la fosforilación y abundancia de NCC, al igual que los ratones silvestres. Esto sugiere que existen vías redundantes que permiten la activación de WNK4-NCC en hipokalemia, las cuales constituyen mecanismos de adaptación renal ante esta condición.

3. INTRODUCCIÓN

3.1. Compartimentalización de fluidos

El agua corporal total compone aproximadamente un 60% del peso corporal de un adulto humano promedio, lo cual corresponde aproximadamente a 42L. De este volumen, un 60% (~25L) se encuentra dentro de las células, con el restante 40% (~17L) en el fluido extracelular. Del fluido extracelular, sólo el 20% (~3L) se localiza en el corazón y los vasos sanguíneos, es decir, el compartimento intravascular(1).

La composición de los fluidos intra- y extracelular son distintas, tanto en la concentración de electrolitos como en la de moléculas orgánicas. Una característica del fluido intracelular es su alta concentración del ion K^+ y su baja concentración del ion Na^+ , mientras que el fluido extracelular es rico en Na^+ y contiene bajos niveles de K^+ . Esta distribución se mantiene gracias a la actividad de la ATPasa de Na^+/K^+ , la cual promueve la salida de Na^+ y la entrada de K^+ a la célula(1).

3.2. Homeostasis del K⁺

El K⁺ es el catión intracelular más abundante, con un 98% del K⁺ del organismo contenido dentro de las células. Por lo tanto, la concentración intracelular de K⁺ es de aproximadamente 120mM, mientras que en el fluido extracelular puede oscilar entre 3.5 y 5mM. Esta distribución asimétrica juega un papel en el establecimiento del potencial de membrana celular y también es un componente esencial de la fisiología de las células excitables. El mantenimiento de la concentración extracelular de K⁺ ($[K^+]_e$) es de vital importancia, pues alteraciones en este parámetro tienen serias repercusiones en la salud, como debilidad muscular o arritmias, por ejemplo(1, 2).

Dado que la ingesta diaria de K⁺ de un adulto promedio es de aproximadamente 70 mmoles, lo cual es comparable a la cantidad total de K⁺ en el fluido extracelular (4mmol/L x 17L = 68 mmoles), los mecanismos de balance de K⁺ son esenciales para evitar desviaciones en la concentración plasmática de K⁺(2, 3) (**Figura 1**).

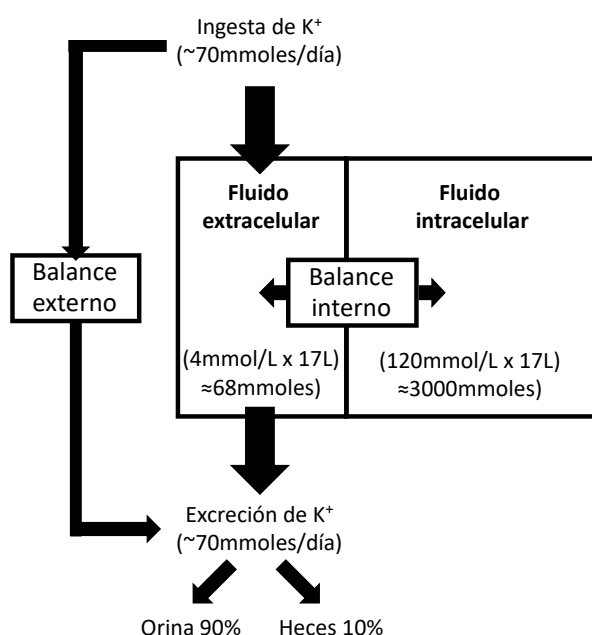


Figura 1. Representación esquemática de la homeostasis del K⁺. Modificado de Zacchia *et al.* 2016(2).

3.3. Balance interno y externo de K⁺

El balance de K⁺ se puede dividir en interno y externo. El balance interno de K⁺ se refiere a los mecanismos de intercambio de este ion entre el fluido intracelular y extracelular. Después de una ingesta de K⁺, existe un flujo neto de K⁺ del fluido extracelular al intracelular, lo cual impide un incremento súbito en la concentración plasmática de K⁺. Este fenómeno está mediado por diferentes hormonas, como la insulina, la epinefrina y la aldosterona, las cuales promueven la entrada de K⁺ a las células por la ATPasa de Na⁺/K⁺(1).

En contraste, el balance externo de K⁺ se refiere a los mecanismos de excreción de K⁺ del organismo, los cuales están balanceados con la ingesta del mismo ion, de modo que no haya ganancias o pérdidas netas de K⁺, manteniendo así la homeostasis de $[K^+]_e$. El riñón es el principal órgano encargado del balance externo de K⁺, pues el 90% de la excreción de K⁺ se da a través de la orina. Un ejemplo de su importancia es la enfermedad renal crónica, donde la disfunción de los riñones aumenta considerablemente la probabilidad de desarrollar hiperkalemia, siendo ésta una

complicación grave para los pacientes que la sufren(2). El 10% restante de la excreción de K^+ se da en las heces. Si bien el colon puede aumentar la excreción de K^+ en ciertas condiciones, no es capaz de mantener el balance externo de K^+ por sí mismo(1).

3.4. Estructura funcional del riñón

El riñón es el órgano encargado de la excreción de sustancias del organismo, del mantenimiento del balance hídrico y electrolítico, así como de la regulación ácido-base de la sangre, entre otros procesos(1). La nefrona es la unidad funcional del riñón, y cada una está compuesta por un glomérulo y una serie de túbulos epiteliales especializados. El glomérulo está formado por el endotelio vascular, la membrana basal y células epiteliales que forman la cápsula de Bowman. Esta estructura permite la filtración de ciertos componentes de la sangre, como el agua, los iones y biomoléculas pequeñas, mientras que impide el paso de las células y las proteínas de alto peso molecular de la sangre.

El filtrado glomerular pasa al espacio de Bowman y posteriormente a la luz del epitelio tubular. El túbulo renal está encargado de la reabsorción de ciertos componentes del filtrado y de la secreción de algunos otros. Estos dos procesos modifican la composición del filtrado convirtiéndolo en orina, la cual finalmente se excreta, después de pasar por el uréter, la vejiga y la uretra(1). El proceso de formación de orina es un producto secundario que le permite al riñón mantener la homeostasis del organismo.

3.5. La nefrona como unidad funcional del riñón

El túbulo epitelial de la nefrona se divide en diferentes segmentos, según su morfología y su función fisiológica: el túbulo proximal (PCT), el asa descendente delgada de Henle (DTL), el asa ascendente delgada de Henle (ATL), el asa ascendente gruesa de Henle (TAL), el túbulo contorneado distal (DCT), el túbulo conector (CNT), el ducto colector cortical (CCD), el ducto colector de la médula externa (OMCD) y el ducto colector de la médula interna (IMCD). (**Figura 2**).

El túbulo proximal reabsorbe un gran porcentaje de los componentes filtrados por el glomérulo. Está encargado de la reabsorción de biomoléculas orgánicas como aminoácidos y glucosa, así como de ~65% de agua y electrolitos.

El asa descendente delgada de Henle es impermeable a iones, por lo que su papel principal es la reabsorción de agua. Por otro lado, el asa ascendente de Henle es impermeable a agua y solamente permite el paso de iones. Este segmento juega un papel importante en la concentración de la orina y en la reabsorción de iones como Na^+ , Cl^- , K^+ , Ca^{2+} y Mg^{2+} .

La mácula densa es un parche de células epiteliales especializadas que forman parte del aparato yuxtglomerular, junto con las células mesangiales y las células granulares secretoras de renina. Este conjunto celular está encargado de un asa de retroalimentación encargada de la regulación del flujo sanguíneo renal, el balance de Na^+ y la presión arterial(1).

El DCT se encarga de la regulación de la reabsorción renal de sal, lo que tiene repercusiones en la cantidad del fluido extracelular y, por lo tanto, en la presión arterial. Asimismo, este segmento es determinante en la homeostasis del K^+ (4).

Finalmente, el túbulo conector y el conducto colector conforman la nefrona distal sensible a aldosterona (ASDN), la cual está encargada de la secreción de K^+ en respuesta a aldosterona. Esto se logra gracias a la reabsorción electrogénica de Na^+ , lo que altera el gradiente eléctrico transepitelial y promueve la salida de K^+ de la célula. El

ducto colector también es importante en el proceso de concentración de orina, pues es el blanco de la hormona antidiurética, la cual estimula la reabsorción de agua por medio de la modulación de la acuaporina 2(5).

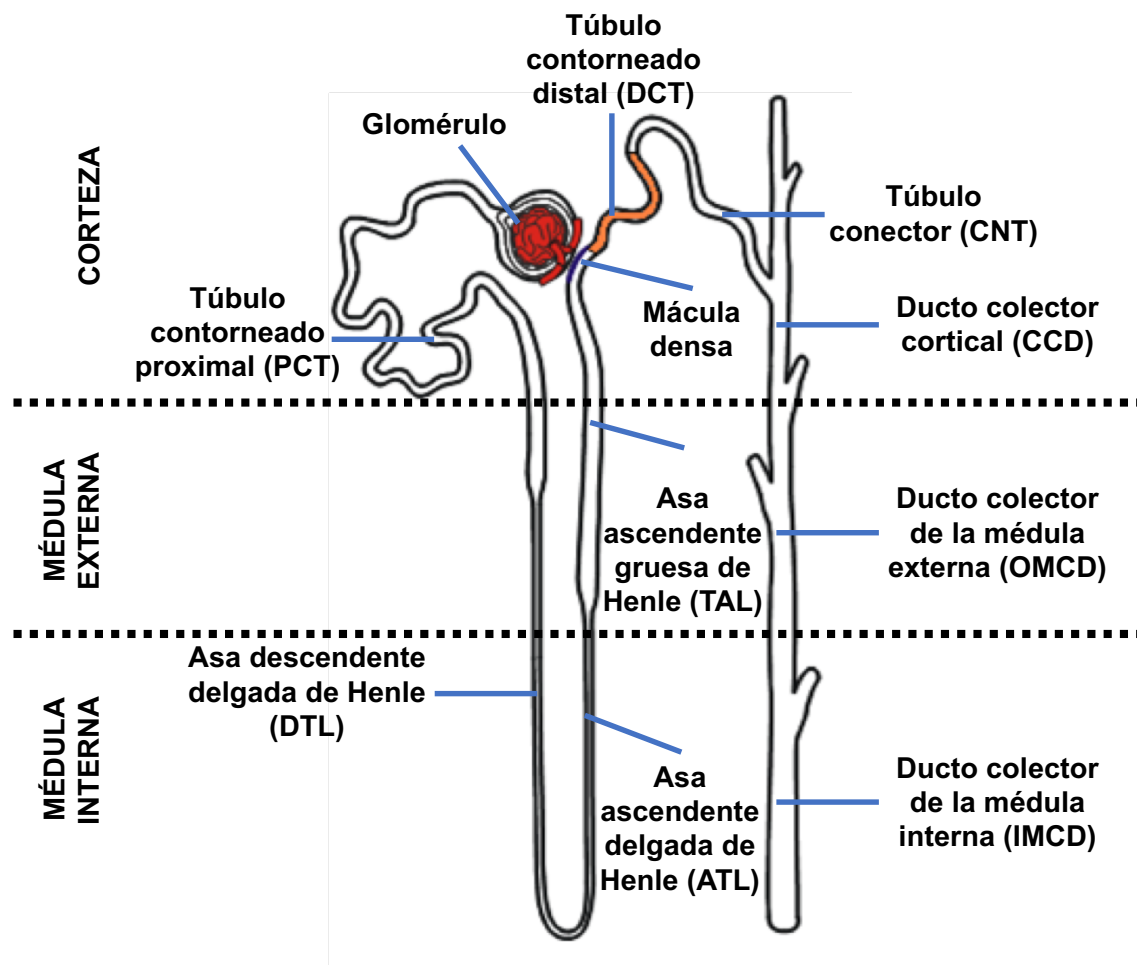


Figura 2. Representación esquemática de la división estructural y funcional de los distintos segmentos tubulares de la nefrona: túbulo contorneado proximal (PCT), asa descendente delgada de Henle (DTL), asa ascendente delgada de Henle (ATL), asa ascendente gruesa de Henle (TAL), túbulo contorneado distal (DCT), túbulo conector (CNT), ducto colector cortical (CCD), ducto colector de la médula externa (OMCD) y ducto colector de la médula interna (IMCD).

3.6. Manejo renal de K^+

El manejo renal tubular de K^+ es un proceso complejo, dado que algunos segmentos de la nefrona se encargan de reabsorber K^+ , mientras que otras células situadas principalmente en la ASDN, juegan un papel importante en la secreción de K^+ (**Figura 3**), fenómeno que es modulable por la acción de una gran variedad de parámetros fisiológicos, como pueden ser hormonas, el balance ácido-base o la misma concentración plasmática de K^+ , como se mencionará a detalle más adelante.

Los iones K^+ son filtrados libremente en el glomérulo, para posteriormente pasar al espacio de Bowman y después al túbulo proximal. En este primer segmento tubular de la nefrona, se lleva a cabo la reabsorción de aproximadamente el 80% del K^+ filtrado.

Mientras que en el túbulo proximal la reabsorción de K^+ es paracelular y altamente dependiente del transporte de agua (**Figura 3A**), en los segmentos posteriores de la nefrona, el manejo de K^+ se da principalmente de manera transcelular y está mediada

por diferentes transportadores, canales y bombas sujetos a diferentes mecanismos de regulación.

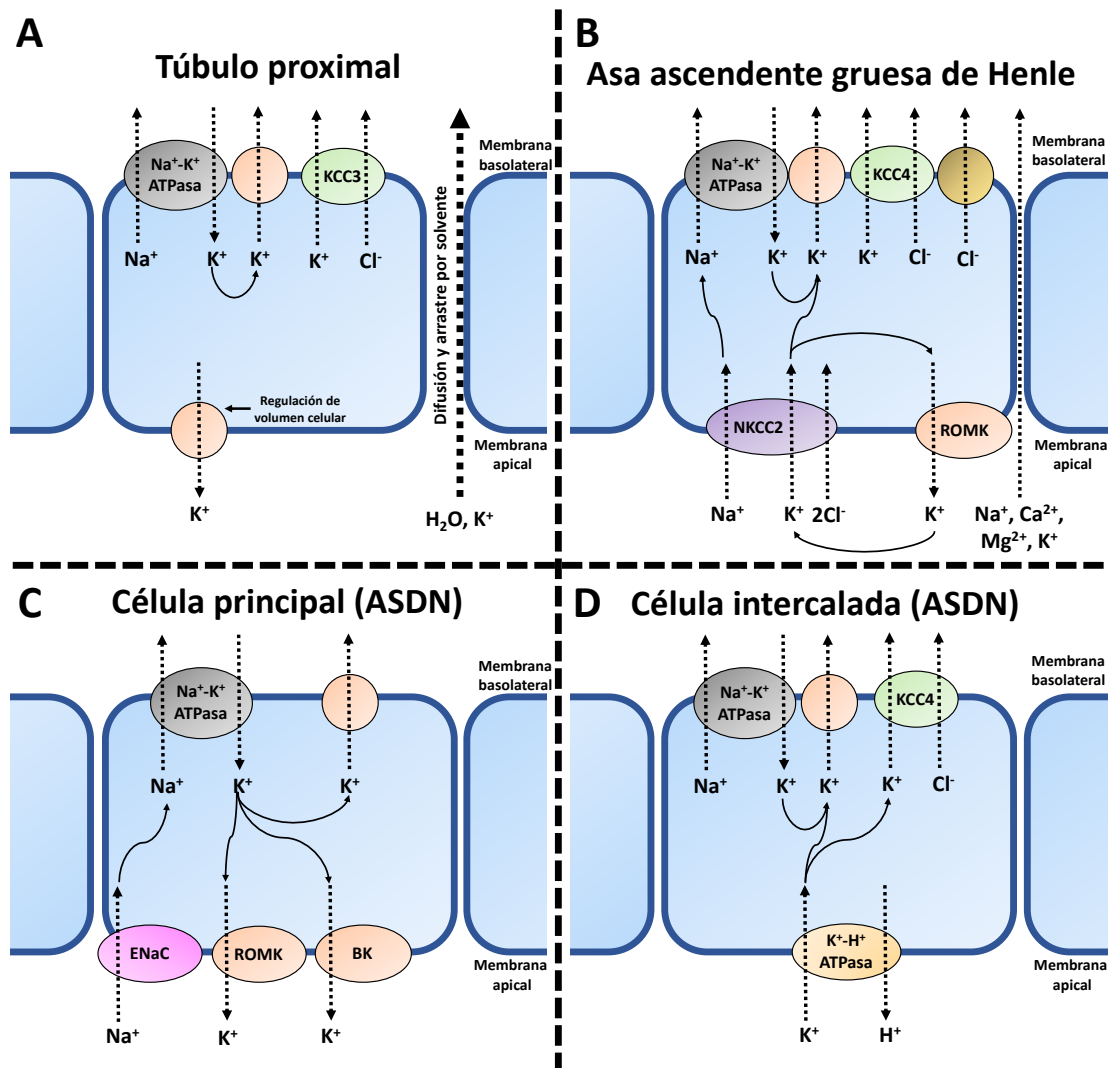


Figura 3. Modelo de los mecanismos de transporte de K^+ a lo largo de la nefrona, específicamente el túbulo proximal (A), asa ascendente gruesa de Henle (B), células principales de la nefrona distal sensible a aldosterona (ASDN) (C) y células intercaladas de la ASDN (D). Cotransportador de $K^+:Cl^-$ 3 (KCC3), cotransportador de $K^+:Cl^-$ 4 (KCC4), cotransportador de $Na^+:K^+:2Cl^-$ 2 (NKCC2), Renal Outer Medullary K^+ channel (ROMK), Epithelial Na^+ Channel (ENaC), Big K^+ channels (BK).

En el asa ascendente gruesa de Henle se da la reabsorción del 10% del K^+ filtrado. En este segmento de la nefrona, la entrada de K^+ depende del cotransportador electroneutro de $Na^+/K^+/2Cl^-$, NKCC2 (**Figura 3B**). Posteriormente, parte del K^+ regresa a la circulación al salir a través de canales y cotransportadores basolaterales de K^+ . Sin embargo, la membrana apical de estas células también presenta permeabilidad a K^+ en la forma del canal iónico ROMK. Esta proteína es importante para el reciclaje de K^+ que permite a NKCC2 mantener su actividad. La disfunción de NKCC2(6) o de ROMK(7) son causa del Síndrome de Bartter (tipo I y tipo II, respectivamente), caracterizado por pérdidas de K^+ , entre otras manifestaciones(8).

En los segmentos posteriores de la nefrona, específicamente la ASDN, se lleva a cabo la secreción de K^+ . En el caso de las células principales, la reabsorción electrogénica

de Na^+ a través del canal ENaC, promueve la salida de K^+ hacia la luz tubular a través de los canales iónicos ROMK y BK (**Figura 3C**). Mutaciones de tipo pérdida de función en los genes que codifican a las subunidades del canal ENaC son causa de Pseudohipoaldosteronismo tipo I (PHA1), caracterizado por hiperkalemia, debido a la incapacidad de estas células de secretar K^+ (9, 10). Por otro lado, mutaciones de tipo ganancia de función en estos genes causan Síndrome de Liddle, en donde la incrementada secreción de K^+ promueve hipokalemia(11–13).

Finalmente, las células α - y β -intercaladas se encargan de reabsorber K^+ a través de una H^+/K^+ ATPasa en la membrana apical (**Figura 3D**), principalmente en condiciones de privación de K^+ (14).

3.7. Regulación de la excreción renal de K^+

La secreción de K^+ mediada por las células principales es modulada por una variedad de factores. Uno de ellos es el flujo luminal que llega a este segmento. Los canales BK son activados por el alto flujo luminal, lo cual aumenta la permeabilidad apical a K^+ y, por lo tanto, su secreción(15). El efecto del flujo luminal sobre la secreción de K^+ explica el hecho de que los diuréticos que actúan río arriba del túbulo conector (como la furosemida en el asa de Henle, o las tiazidas en el túbulo contorneado distal) promueven pérdida de K^+ . Sin embargo, existe evidencia que muestra que la actividad del túbulo contorneado distal puede promover una remodelación de la nefrona, comprometiendo la longitud del túbulo conector y, por lo tanto, la capacidad secretora de K^+ (4).

La aldosterona es una hormona esteroidea producida en la zona glomerulosa de la glándula suprarrenal. Su síntesis y secreción aumentan en respuesta a un incremento de la $[\text{K}^+]_e$. El receptor de mineralocorticoides (RM) es un receptor nuclear y el blanco de la aldosterona. Sin embargo, éste también es capaz de unir cortisol, cuya concentración plasmática es mucho mayor a la de la aldosterona. Por lo tanto, la capacidad de respuesta de una célula ante las oscilaciones en la concentración plasmática de aldosterona depende de una enzima llamada 11- β -hidroxiesteroide-deshidrogenasa tipo II (11 β -HSD2), la cual cataliza la conversión de cortisol a cortisona, que es incapaz de unirse al RM. Por lo tanto, en estas células, como las de la ASDN, la aldosterona se encarga de la modulación del transporte de iones(1).

En las células principales de la ASDN, la ocupación del RM por la aldosterona permite su translocación al núcleo promoviendo la transcripción de distintos genes, como los que codifican para la Na^+/K^+ ATPasa y la cinasa SGK1(16). Esta cinasa fosforila e inactiva a la ligasa de ubiquitina Nedd4-2, cuya función es la degradación del canal ENaC. Por lo tanto, SGK1 promueve un aumento en la cantidad de ENaC y un incremento en el intercambio electrogénico de Na^+ por K^+ que permite la secreción de este último(17).

Experimentos realizados en diferentes modelos animales con ausencia de aldosterona(18), o bien, niveles fijos de ésta por medio de adrenalectomía e infusión constante(19), sugieren que existen mecanismos independientes a esta hormona que permiten aumentar la secreción de K^+ en respuesta a un aumento de $[\text{K}^+]_e$.

Uno de los mecanismos propuestos es la activación de SGK1 por efectos directos de la $[\text{K}^+]_e$, a través del complejo mTORC2(20), lo cual se asocia con un aumento en la actividad del canal ENaC.

Quizá el mecanismo más estudiado hasta el momento por el cual la concentración de K^+ regula su propia secreción, es la modulación del cotransportador renal de Na^+/Cl^- ,

NCC, en el túbulo contorneado distal de la nefrona(21), lo cual tiene repercusiones importantes en la homeostasis del K^+ , como se describe en la siguiente sección.

3.8. El túbulo contorneado distal (DCT) y el cotransportador de Na^+/Cl^- , NCC

El segmento siguiente de la mácula densa se denomina túbulo contorneado distal. Este segmento tubular se encarga de la reabsorción transcelular de cerca del 5% del NaCl filtrado, lo cual tiene repercusiones importantes en la presión arterial. Las células del DCT se caracterizan por la expresión del gen *SLC12A3*, que codifica para el cotransportador de Na^+/Cl^- , NCC, el cual es el blanco farmacológico de los diuréticos de tipo tiazida(22). Esta proteína se localiza en la membrana apical, promoviendo la entrada de Na^+ y Cl^- con una estequiometría 1:1. Posteriormente, el Na^+ sale de la célula por la membrana basolateral a través de la Na^+-K^+ -ATPasa, mientras que el Cl^- sale por la membrana basolateral a través de un canal iónico llamado ClC-Kb (**Figura 4**). Además, la actividad de NCC determina de manera indirecta la secreción de K^+ y, por lo tanto, los niveles plasmáticos de K^+ .

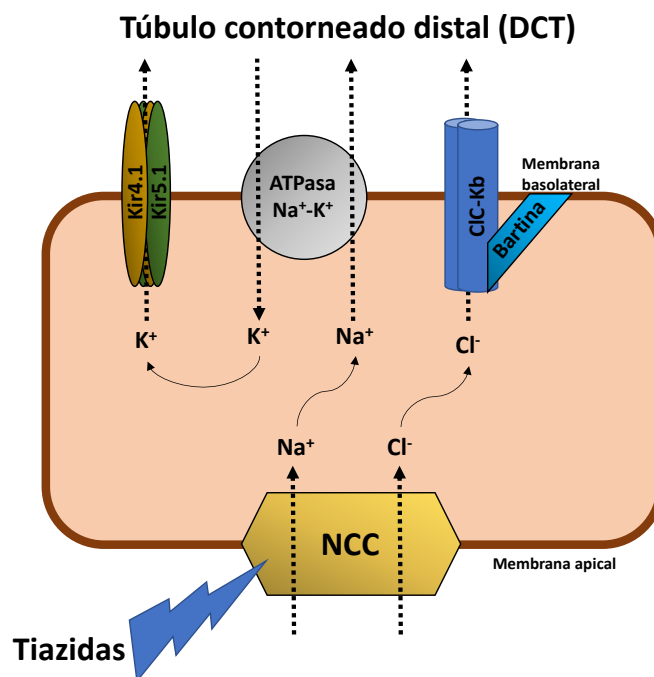


Figura 4. Modelo de transporte de NaCl en las células del DCT. Cotransportador de $Na^+:Cl^-$ (NCC), inwardly-rectifying K^+ channels 4.1 y 5.1 (Kir4.1 y Kir 5.1), Chloride channel Kb (ClC-Kb).

La importancia de NCC en la regulación del balance hidroelectrolítico queda de manifiesto con la descripción y el estudio de dos patologías en las que se afecta la actividad de este cotransportador: el Síndrome de Gitelman y la Hipertensión Hiperkalémica Familiar (**Figura 5**).

Síndrome de Gitelman	Hipertensión Hiperkalémica Familiar (FHt)
<u>Hipokalemia</u>	<u>Hiperkalemia</u>
Menor presión arterial	Hipertensión arterial
Alcalosis metabólica	Acidosis metabólica
Hipocalciuria	Hiper calciuria
Mutaciones pérdida de función en el gen codificante para NCC (<i>SLC12A3</i>)	Mutaciones ganancia de función en <i>WNK1</i> o <i>WNK4</i> Mutaciones pérdida de función en <i>KLHL3</i> o <i>CUL3</i>

Figura 5. Características del síndrome de Gitelman y la Hipertensión Hiperkalémica Familiar. Cotransportador de Na⁺:Cl⁻ (NCC), Solute Carrier 12A3 (*SLC12A3*), *With No Lysine "K" 1 y 4* (*WNK1* y *WNK4*), Kelch-like-3 (*KLHL3*), Cullin-3 (*CUL3*).

3.9. Enfermedades genéticas que afectan la función de NCC

El síndrome de Gitelman (Online Mendelian Inheritance in Man, OMIM #263800) es una enfermedad genética autosómica recesiva, caracterizada por hipotensión arterial, hipokalemia, alcalosis metabólica, hipocalciuria e hipomagnesemia. Esta patología está ocasionada por mutaciones de tipo pérdida de función en el gen *SLC12A3*, el cual codifica al cotransportador NCC(23). La generación y descripción de distintos modelos murinos con delección o mutaciones específicas sobre este gen han corroborado la relación causal entre NCC y el fenotipo del síndrome de Gitelman(24–26).

En contraposición al síndrome de Gitelman, la Hipertensión Hiperkalémica Familiar, FHt (OMIM #614491-2 y #614495-6) es una enfermedad genética que cursa con hipertensión arterial, hiperkalemia, acidosis metabólica hiperclorémica y, en algunos casos, hiper calciuria. Los pacientes con FHt responden a bajas dosis de diuréticos de tipo tiazida(27), lo cual sugirió inicialmente que el FHt se debe principalmente a la sobreactivación de NCC, sin embargo, no se han descrito mutaciones con ganancia de función para el gen que codifica a NCC. En 2001, Wilson y colaboradores describieron que mutaciones en los genes *WNK1* y *WNK4* (que codifican serina/treonina cinasas, como se detallará posteriormente) pueden causar FHt(28). En el caso de *WNK1* se encontraron delecciones en el primer intrón, las cuales se han asociado a mayor expresión del RNA mensajero correspondiente. En cuanto al gen *WNK4*, se hallaron mutaciones cambio de sentido en una región conservada que codifica un segmento de la proteína llamado dominio ácido, involucrado en la degradación de *WNK4* por el complejo *KLHL3-CUL3*, que funciona como un ligasa de ubiquitina. En 2020, mutaciones similares a las originalmente encontradas en *WNK4* también fueron descritas para el caso de *WNK1*(29). Mutaciones en los genes *KLHL3* y *CUL3* también son causa de FHt(30, 31) (descrito más adelante).

De esta manera, podemos observar que NCC juega un papel importante, entre otras cosas, en la homeostasis del K⁺. La pérdida de función de NCC se ve asociada a hipokalemia, mientras que un aumento en la actividad de éste provoca hiperkalemia. Se

ha propuesto que esto se debe a que la reabsorción mediada por NCC determina el flujo que llega a segmentos más distales de la nefrona, lo cual es esencial para reabsorción electrogénica de Na^+ mediada por el canal ENaC y, por lo tanto, la secreción de K^+ a través de los canales ROMK y BK. También se ha observado en un modelo murino transgénico que la sobreactividad de NCC tiene como repercusión la hipotrofia del túbulo conector, lo cual afecta negativamente la secreción de K^+ en este segmento y, por ende, provoca hiperkalemia(4) (**Figura 6**).

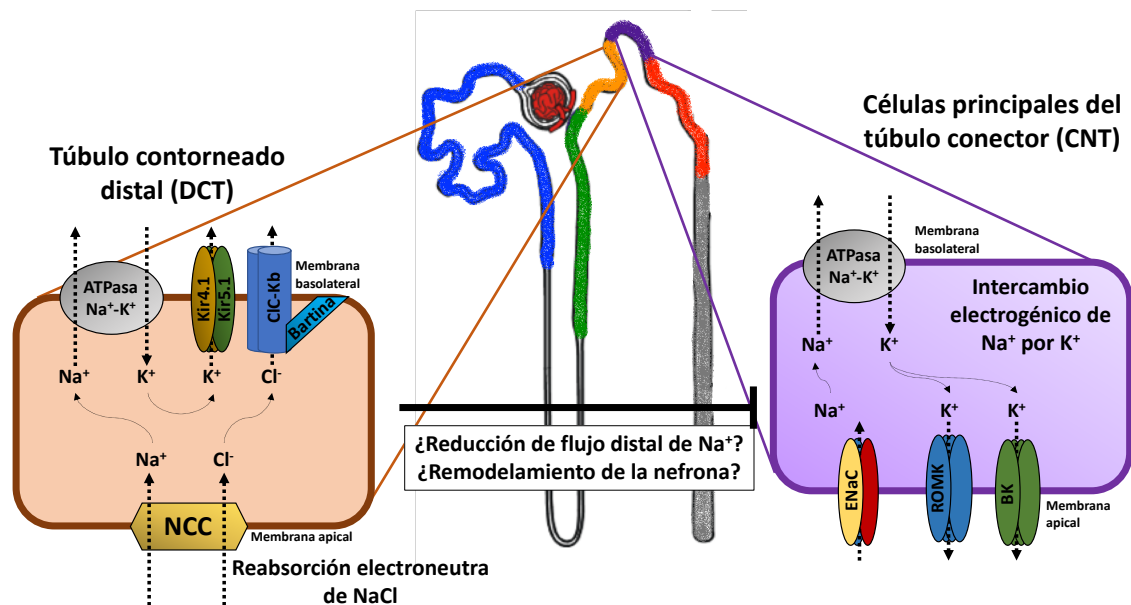


Figura 6. Modelo fisiológico de la relación entre NCC en el DCT y las células secretoras de K^+ en el túbulo conector. Modificado de Murillo-de-Ozores, *et al.* 2019(21). Cotransportador de $\text{Na}^+:\text{Cl}^-$ (NCC), inwardly-rectifying K^+ channels 4.1 y 5.1 (Kir4.1 y Kir 5.1), Chloride channel Kb (CIC-Kb), Epithelial Na^+ Channel (ENaC), Renal Outer Medullary K^+ channel (ROMK), Big K^+ channels (BK).

3.10. Las cinasas WNK

La familia de cinasas de serina-treonina 'WNK' (*With No Lysine "K"*) se caracteriza por la posición atípica de su lisina catalítica en el subdominio I, mientras que en la mayoría de las cinasas se encuentra en el subdominio II. Existen cuatro miembros de esta familia en mamíferos. El papel principal que se ha atribuido a esta familia de cinasas es la regulación del transporte de electrolitos(32).

Actualmente se conoce que el papel principal de las cinasas WNK es la fosforilación de las cinasas Ste-20 Related Proline-Alanine Rich Kinase (SPAK) y Oxidative Stress Responsive Kinase 1 (OSR1), quienes a su vez son responsables de la fosforilación y activación de los cotransportadores electroneutros de Na^+ acoplados a Cl^- (33–35).

Si bien, existen diferentes ejemplos del papel fisiológico del cual son responsables las cinasas WNK en distintos tejidos(36), específicamente en el caso de NCC, diversos estudios sugieren que WNK4 es la cinasa que juega un papel preponderante en las células del DCT. Por ejemplo, estudios de transcriptómica de túbulos microdisecados de rata(37) y ratón(38) muestran que no hay expresión detectable de los genes *WNK2* o *WNK3* en la nefrona, mientras que sí hay RNA mensajero de los genes *WNK1* y

WNK4. Sin embargo, para el caso de *WNK1* en el DCT específicamente, el RNA presente se trata de una isoforma más corta(38) generada por un promotor alternativo, cuya proteína codificada carece de dominio cinasa y, por ende, de actividad catalítica. Esta isoforma es llamada KS-*WNK1* (*k*idney-*s*pecific, pues sólo se ha hallado en el riñón)(39). A pesar de no ser una enzima, se ha sugerido que KS-*WNK1* juega un papel regulador en la actividad de NCC, funcionando como una proteína de andamiaje que puede promover un aumento en la actividad de *WNK4*(29, 40).

3.11. *WNK4* y su papel en la regulación de NCC

La descripción de tres distintos modelos “knockout” (KO) para *WNK4* (el primero de ellos descrito por Maria Castañeda en el laboratorio del Dr. Gerardo Gamba en México) muestran una reducción en la cantidad total y fosforilación de NCC, acompañada de alteraciones electrolíticas similares a los pacientes con síndrome de Gitelman(41–43). Por otro lado, ratones “knockin” con una mutación puntual en uno de los alelos de *WNK4* (*WNK4*^{+/*D561A*}), correspondiente a una de las mutaciones halladas en los pacientes con FHHT, muestran mayores niveles de presión arterial, hiperkalemia, así como niveles de NCC total y fosforilado(44).

Estos experimentos muestran una correlación fisiológica entre la presencia de *WNK4* y la actividad de NCC, lo cual repercute en el balance hidroelectrolítico del organismo. A continuación, se describen características estructurales de la proteína *WNK4*, así como los mecanismos de señalización celular que se han vinculado a la modulación de la actividad cinasa de *WNK4*.

3.12. Características estructurales de la cinasa *WNK4*

La cinasa *WNK4* es el miembro más pequeño de la familia en mamíferos, con un peso teórico aproximado de 135kDa, aunque en los ensayos de Western Blot se observa con un peso aparente cercano a 180kDa(45). Esto para el caso de *WNK4* recombinante. En el caso del ratón, se han detectado bandas adicionales de menor peso que presumiblemente corresponden a *WNK4* dado que no son detectables en el ratón *WNK4*-KO. Esto únicamente usando un anticuerpo que reconoce al dominio amino (N)-terminal de la cinasa, mientras que anticuerpos contra el dominio carboxilo (C)-terminal únicamente reconocen a la forma completa de *WNK4* (**Figura 7**). La primera mitad de este proyecto de doctorado consistió en la descripción de dichas variantes cortas de *WNK4*.

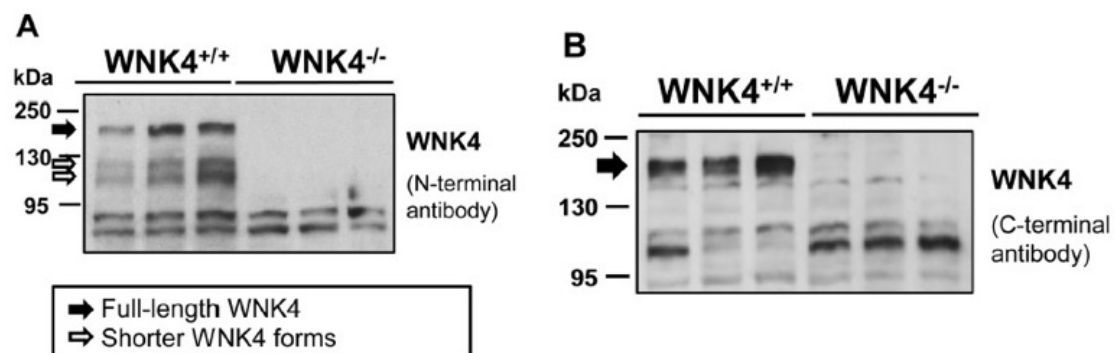


Figura 7. Ensayos de Western Blot con lisados de riñón de ratones silvestres y ratones *WNK4*-KO (knockout de *With No Lysine “K” 4*), usando anticuerpos que reconocen el

dominio N-terminal (panel A) o al dominio C-terminal (panel B) de WNK4. Al analizar las bandas ausentes en el ratón WNK4-KO, se observan variantes cortas con el anticuerpo contra el dominio N-terminal, pero no con el anticuerpo contra el dominio C-terminal.

La cinasa WNK4 está compuesta por un segmento N-terminal pequeño con función reguladora, el dominio cinasa dividido en 12 subdominios, característico de una serina-treonina cinasa, y un segmento C-terminal de mayor tamaño (**Figura 8**), que contiene distintos dominios, sitios de unión y residuos fosforilables, los cuales se ha propuesto pueden modular la actividad de WNK4(46).

Además del dominio cinasa, las WNKs contienen dos dominios globulares que se han denominado “similares a PF2” (PF2-like y PF2-like’, respectivamente). Este nombre proviene de su similitud con un dominio llamado PF2 encontrado en el dominio C-terminal de las cinasas SPAK y OSR1. Este dominio tiene la función de unir motivos con la secuencia RFXV/I. Estos motivos se han hallado en las cinasas WNK y en los cotransportadores electroneutros. Por lo tanto, se ha propuesto que el dominio PF2 de SPAK y OSR1 permite unir a los demás elementos de esta vía de señalización, tanto río arriba (WNKs), como río abajo (cotransportadores electroneutros, como NCC)(47). No se conoce el papel que juegan los dominios PF2-like y PF2-like’ en las WNKs, aunque en el caso del PF2-like de WNK1 se ha observado que también es capaz de unir motivos RFXV/I. Si esto es relevante para la interacción de una WNK con otra WNK o con alguna otra proteína aún se desconoce.

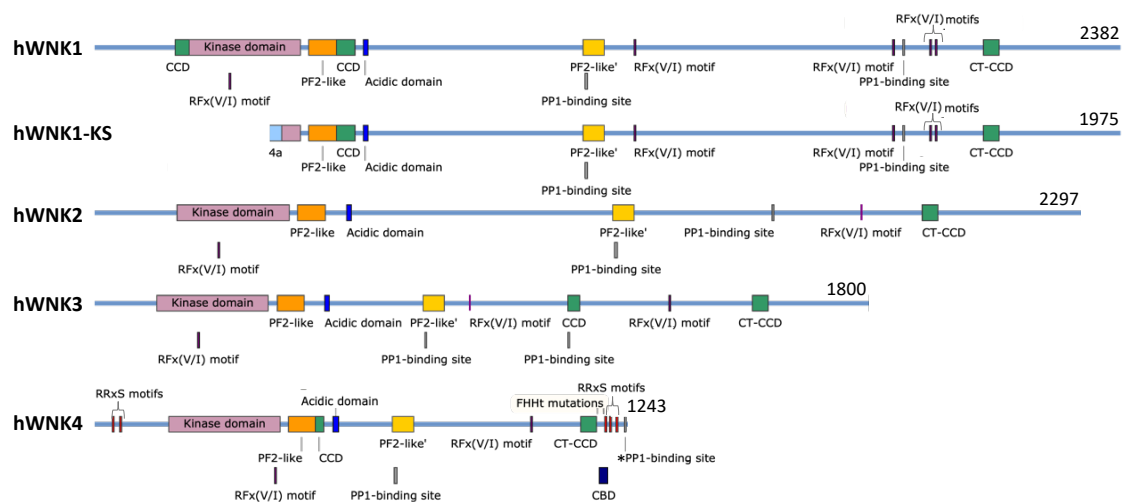


Figura 8. Representación esquemática de los dominios y sitios descritos en las cinasas WNK (de humano). Si bien existen cuatro genes de la familia en mamíferos, la isoforma KS-WNK1 se genera a partir de un promotor alternativo y carece de dominio cinasa(48). Modificado de Murillo-de-Ozores, *et al.* 2020(36). Similar a Pask-Fray-2 (PF2-like), Proteína Fosfatasa 1 (PP1), coiled-coil domain del dominio carboxilo-terminal (CT-CCD), sitio de unión a calmodulina (CBD).

WNK4 contiene dos motivos que cumplen la secuencia consenso RFXV/I, por lo que teóricamente podrían funcionar como sitios de unión a SPAK/OSR1. Evidencia inicial (mutando la F de uno u otro sitio por A) sugería que ambos eran esenciales para la fosforilación de SPAK. Sin embargo, evidencia experimental generada en nuestro laboratorio muestra que el primer sitio, localizado en el dominio cinasa, no es un sitio de

interacción con SPAK. La mutación de la F421 (correspondiente al primer motivo RFxV/I en la WNK4 de humano, hWNK4) por Y no tiene ningún efecto sobre la actividad de la cinasa sobre SPAK, aunque se ha descrito que SPAK es incapaz de unir motivos RYxV/I. Esto concuerda con la conservación de dicho sitio de WNK4 en distintos organismos, dado que las aves, reptiles, anfibios y peces tienen una Y en dicha posición, lo que sugiere que simplemente se requiere un aminoácido aromático en esta posición para el correcto funcionamiento de la cinasa WNK4(46).

El motivo ácido de WNK4 es una secuencia altamente conservada de 10 aminoácidos enriquecida en residuos de carga negativa. La importancia de esta región radica en su papel como sitio de unión para la proteína adaptadora KLHL3, la cual forma parte de un complejo de ligasa de ubiquitina junto con CUL3. Mutaciones en esta región de WNK4, así como mutaciones en los genes codificantes para KLHL3 o CUL3, previenen la degradación de la cinasa WNK4, lo cual promueve la sobreactivación de la vía WNK4-SPAK/OSR1-NCC y, por lo tanto, causan FHHT(49–51).

WNK4 contiene dos dominios de hélice helicoidal (coiled-coil domains). El primero se localiza justo después del dominio PF2-like, mientras que el segundo (CT-CCD) se encuentra hacia el dominio C-terminal de la proteína. Hasta el momento, no existen estudios de la relevancia funcional del primero de estos dominios. En cuanto al segundo, Thastrup y colaboradores demostraron que esta región se encarga de mediar interacción entre WNKs. Específicamente, se encontraron tres residuos altamente conservados (H1145, E1148, Q1156 en hWNK4) cuya presencia es esencial para mediar interacción entre WNKs, lo cual tiene una repercusión funcional en la vía de señalización(52).

Después del CT-CCD, existe una región en WNK4 de aproximadamente 70 residuos altamente conservada entre vertebrados, con diversos sitios de relevancia funcional: tres sitios de fosforilación por PKC/PKA/SGK1(53), un sitio de unión a calmodulina(54), dos residuos que se han hallado mutados en pacientes con FHHT: K1169E(55) y R1185C(28) y un sitio de unión a la proteína fosfatasa 1 (PP1)(45, 56) (**Figura 9**).

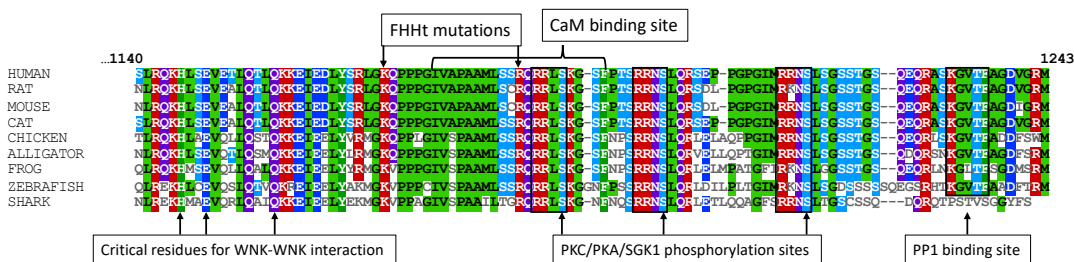


Figura 9. Alineamiento de la estructura primaria de los últimos ~100 aminoácidos de la cinasa WNK4 de organismos de diferentes clases. Los números en la parte superior indican la posición correspondiente a la WNK4 de humano. Se destacan distintos aminoácidos conservados que se han relacionado a la regulación de la actividad de WNK4. Modificado de Murillo-de-Ozores et al. 2021(46). Hipertensión Hiperkalémica Familiar (FHHT), calmodulina (CaM), proteína cinasa C (PKC), proteína cinasa A (PKA), Serum/glucocorticoid-regulated kinase 1 (SGK1), proteína fosfatasa 1 (PP1).

3.13. WNK4 como cinasa sensible a Cl⁻

La actividad de NCC es modulada por la concentración intracelular de Cl⁻ ([Cl⁻]_i)(34), mecanismo que depende de las cinasas WNK. Al determinar la estructura del dominio cinasa de WNK1 por cristalografía de rayos X, se encontró que éste contiene un sitio de unión a Cl⁻ en el sitio activo, entablando interacciones con los residuos F283, L299, L369, G370 y L371 (posiciones correspondientes a WNK1 de rata). La presencia de este anión previene la autofosforilación y activación de la cinasa. Disminuir la concentración de Cl⁻ o mutar el residuo L369 por F promueven un incremento en la actividad de la cinasa y su autofosforilación en la S382(57).

En el laboratorio del Dr. Gerardo Gamba se demostró que la regulación de NCC por WNK4 se ve modulada por la [Cl⁻]_i (**Figura 10**). En un modelo de sobreexpresión heteróloga en ovocitos de *Xenopus laevis*, WNK4 no tiene un efecto activador sobre NCC en condiciones basales. Sin embargo, cuando la célula se depleta de Cl⁻ la cinasa WNK4 se activa y promueve un aumento en la actividad de NCC dependiente de fosforilación(58). Este efecto activador también se puede emular al coexpresar a NCC con la mutante de WNK4 L319F (correspondiente a la L369F de WNK1), la cual es incapaz de unir al Cl⁻ y se comporta como constitutivamente activa, al tener incrementada su fosforilación en la S332 (posición correspondiente a WNK4 de ratón, mWNK4). En un estudio realizado por el grupo del Dr. David Ellison, se realizaron ensayos de actividad cinasa *in vitro* con el dominio cinasa recombinante de WNK4 y SPAK como sustrato(59). En estos experimentos se encontró que WNK4 es inhibida en un rango de concentración relativamente bajo de Cl⁻ (entre 0 y 40mmol/L), lo cual es compatible con mediciones realizadas en el túbulo contorneado distal nativo(60).

La generación de un ratón transgénico con una mutación en WNK4 (L319F/L321F) muestra que WNK4 es un sensor de Cl⁻ fisiológico *in vivo*. Estos ratones muestran un aumento en la cantidad de NCC total y fosforilado, así como un fenotipo similar al FHht(61).

3.14. Sitios de fosforilación que regulan la actividad de WNK4

Dentro de la estructura primaria de WNK4, se encuentran cinco motivos RRxS, los cuales cumplen con la secuencia consenso de fosforilación por PKC(62). Castañeda-Bueno y colaboradores, demostraron en un modelo *in vitro* en células HEK293 transfectadas de manera transitoria con WNK4, que la estimulación del receptor de angiotensina II (AngII) y la activación farmacológica de PKC promueven la fosforilación de estos cinco sitios de WNK4 (Ser47, Ser64, Ser1169, Ser1180 y Ser1196, posiciones correspondientes a mWNK4)(53) (**Figura 10**). Asimismo, mediante ensayos cinasa se observó que WNK4 es un sustrato directo de PKC. Experimentos similares también muestran que estos sitios de WNK4 también pueden ser fosforilados por la cinasa PKA. Específicamente los residuos Ser64 y Ser1196 parecen ser los más importantes, pues mutar estos dos sitios previene la activación río abajo de SPAK (usada como un indicador de la actividad de WNK4 en este sistema) en respuesta a AngII. Además, la fosforilación de estos residuos se ve aumentada específicamente en el DCT en un modelo murino de hipovolemia, lo que sugiere que pudiera ser importante para la posterior activación de NCC en estas condiciones *in vivo*.

Cabe notar que la fosforilación de estos sitios en WNK4 constituye un mecanismo de activación independiente a la disociación del Cl⁻ descrita anteriormente. La WNK4 L319F (incapaz de inhibirse por Cl⁻ al no poder unirlo directamente) muestra un aumento en su actividad en respuesta a AngII, lo cual se ve abolido al mutar los motivos RRxS(53). Esto sugiere que ambos mecanismos de regulación pueden funcionar de manera sinérgica en la activación de WNK4.

3.15. Regulación de la degradación de WNK4

Como se mencionó con anterioridad, otro mecanismo por el cual se regula la cinasa WNK4 es su degradación. La cantidad total de WNK4 es regulada por un complejo de ligasa de ubiquitina compuesto por las proteínas KLHL3 y CUL3 (**Figura 10**).

En un estudio donde se analizó el estado de fosforilación de KLHL3 mediante espectrometría de masas, se encontró que la Ser433 de esta proteína era sometida a esta modificación post-traduccional(63). Previamente se había descrito que este residuo es esencial para la interacción con las cinasas WNK, e incluso la mutación de este aminoácido es una causa de FHHt(64). Shibata *et al.* observaron que la Ser433 de KLHL3 puede ser fosforilada por la cinasa PKC en respuesta a AngII(63). Por lo tanto, se propuso que un mecanismo por el que la AngII activa a NCC es la prevención de la degradación de la cinasa WNK4 por KLHL3.

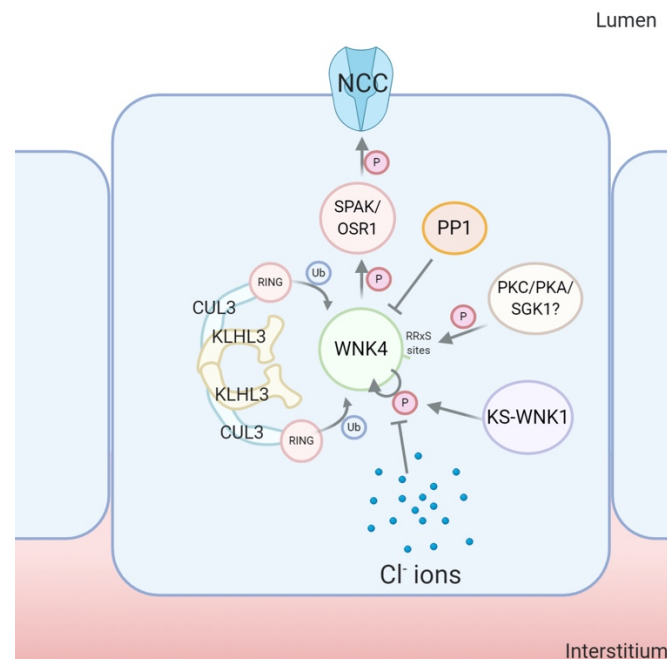


Figura 10. Mecanismos de regulación de la cinasa WNK4 en el DCT. Modificada de Murillo-de-Ozores, et al. 2021(46). Cotransportador de Na⁺:Cl⁻ (NCC), Ste-20 Related Proline-Alanine Rich Kinase (SPAK), Oxidative Stress Responsive Kinase 1 (OSR1), *With No Lysine "K" 4* (WNK4), proteína fosfatasa 1 (PP1), proteína cinasa C (PKC), proteína cinasa A (PKA), Serum/glucocorticoid-regulated kinase 1 (SGK1), kidney-specific *With No Lysine "K" 1* (KS-WNK1), Cullin-3 (CUL3), Kelch-like-3 (KLHL3), Really Interesting New Gene (RING), ubiquitina (Ub), fosforilación (P).

Otra evidencia del papel preponderante de WNK4 en la fisiología y fisiopatología del DCT se observó al realizar una cruce entre ratones con una mutación FHHT en KLHL3 (KLHL3^{R528H/R528H}) y ratones WNK4-KO. De manera interesante, se observó que los ratones KLHL3^{R528H/R528H}/WNK4-KO conservan el fenotipo tipo Gitelman, pues tienen niveles casi indetectables de NCC fosforilado, a pesar de observar un aumento en WNK1 (probablemente KS-WNK1 en el DCT y/o L-WNK1 en otras células) como era de esperarse por la mutación en KLHL3(65). Estos resultados sugieren que el principal modulador positivo de NCC in vivo es WNK4, y la sobreactivación patológica de NCC en el FHHT depende de esta cinasa.

3.16. Relación recíproca entre NCC y el K⁺

El estudio del fenotipo de los pacientes con síndrome de Gitelman o con FHHT, así como los modelos murinos correspondientes, evidencian la importancia de NCC sobre la concentración plasmática de K⁺. Asimismo, en estudios posteriores se demostró que la ingesta de K⁺ es capaz de modular la actividad de NCC, formando una regulación recíproca en un asa de retroalimentación negativa.

Estas observaciones tienen implicaciones importantes, ya que apoyan un mecanismo por el cual el K⁺ por sí mismo puede regular su propia excreción. Se ha propuesto que al ingerir K⁺, la defosforilación e inhibición de NCC son importantes para permitir que el túbulo conector se encargue de la secreción de K⁺ y así evitar un incremento en la concentración plasmática de K⁺. Este mecanismo en particular no depende de la aldosterona, pues se ha descrito que la delección del RM en células del DCT no tiene una repercusión sobre la actividad de NCC(66), mientras que la aldosterona actuaría principalmente en las células principales del túbulo conector en donde promueve la secreción de K⁺ mediada por ENaC y ROMK.

De manera adicional a su papel en la homeostasis del K⁺ per se, la sensibilidad de NCC ante el K⁺ podría ser un mecanismo para explicar la observación poblacional sobre una relación inversamente proporcional entre la ingesta de K⁺ y la salud cardiovascular(21).

3.17. Papel natriurético y diurético del K⁺ y su relación con la presión arterial

Desde hace siglos es conocido el efecto diurético y natriurético de las sales de K⁺, las cuales se han usado en el tratamiento de edema(67). Estas observaciones pueden explicar una parte del efecto benéfico que tienen las dietas altas en K⁺. Estudios publicados en el *New England Journal of Medicine* donde se estudiaron a más de 100,000 sujetos muestran una correlación negativa entre la ingesta de K⁺ y el riesgo a sufrir un evento cardiovascular(68), así como con los niveles de presión arterial(69). Incluso existen estudios que promueven una estrategia de sustitución de Na⁺ por K⁺ en la sal para la prevención de la hipertensión(70). En cuanto a los mecanismos moleculares responsables del efecto natriurético del K⁺, estudios recientes han sugerido que la nefrona distal (y específicamente NCC) juega un papel preponderante en la relación inversamente proporcional entre el K⁺ y la presión arterial(21). Por ejemplo, al administrar a ratones una dieta alta en Na⁺ y baja en K⁺ se observa una activación de NCC que va acompañada con un aumento en la presión arterial. Este fenómeno no se observa en ratones KO para NCC(71).

3.18. Mecanismos propuestos para la regulación de NCC por K⁺

Mediante la modificación del contenido de K⁺ en la dieta de ratones, se ha observado que los niveles de fosforilación del cotransportador NCC están modulados de manera

inversamente proporcional a la ingesta y, por ende, a la concentración plasmática de K^+ (59, 72, 73).

Recientemente se ha descrito que esta regulación se da directamente en las células del túbulo contorneado distal(74), en donde la disminución de $[K^+]_e$ provoca la hiperpolarización de la membrana, lo que promueve la salida de Cl^- de la célula. La disminución de la $[Cl^-]_i$ activa a la cinasa WNK4 lo cual se ve reflejado en un aumento en la fosforilación y actividad de SPAK/OSR1 y, por lo tanto, NCC(71).

Este proceso depende de canales basolaterales de K^+ localizados en el DCT compuestos por el heterotetrámero Kir4.1/Kir5.1. Este canal iónico es responsable del mantenimiento del potencial de membrana de reposo de las células del DCT(75). La relevancia de Kir4.1 en el riñón se conoció gracias a la descripción de una enfermedad genética denominada EAST/SESAME, la cual está causada por mutaciones de tipo pérdida de función en el gen *KCNJ10*(76, 77), que codifica a Kir4.1. Este complejo síndrome causa afectaciones en el sistema nervioso, auditivo y renal. Estas últimas son similares a las alteraciones observadas en el síndrome de Gitelman, como pérdida de sal y de K^+ .

De manera congruente, ratones KO para Kir4.1 tienen niveles reducidos de expresión y actividad de NCC(78, 79). Observaciones similares se han descrito en ratones con expresión disminuida de Kir4.1(80). En estos ratones, Kir5.1 no confiere una conductancia a K^+ , pues se ha descrito que los homotetrámeros Kir5.1 no son funcionales(81, 82). En contraste, el fenotipo de los ratones Kir5.1 KO se caracteriza por un aumento en la expresión, fosforilación y actividad de NCC(83, 84). Estas observaciones podrían explicarse por diferencias funcionales entre el homotetrámero Kir4.1 y el heterotetrámero Kir4.1/Kir5.1 porque en estudios *in vitro*(85, 86), y *ex vivo*(83), la presencia de Kir5.1 confiere sensibilidad al pH intracelular.

Otro elemento importante para la fisiología de las células del DCT y su capacidad para responder ante cambios en la $[K^+]_e$ es el canal basolateral de Cl^- , CIC-Kb. Esta proteína, cuyo tráfico a membrana depende la subunidad accesoria barttina(87, 88), está encargada del transporte transepitelial de Cl^- (89). Mutaciones pérdida de función en los genes codificantes para CIC-Kb y barttina son causa de síndrome de Bartter tipo III(90) y IV(91), respectivamente. Estos tipos de Bartter suelen compartir características con el síndrome de Gitelman, como normo- o hipocalciuria, así como sensibilidad disminuida a tiazidas(92, 93). Observaciones en modelos murinos donde se han afectado la expresión de estos genes corroboran estas observaciones al producir un efecto negativo no sólo sobre NKCC2 en el asa de Henle, sino también sobre la función y fosforilación de NCC en el DCT(94–96).

Las últimas décadas de investigación han establecido a estos genes, y las proteínas correspondientes, como esenciales para mantener la homeostasis electrolítica, formando una vía de señalización que converge en la activación de NCC ante una disminución de la concentración plasmática de K^+ . De manera congruente, este fenómeno está abatido en los ratones Kir4.1 KO(97), Kir5.1 KO(84), barttina hipomórficos(98) y WNK4 KO(73).

Un modelo interesante que se ha estudiado con relación a la respuesta ante cambios en el contenido de K^+ en la dieta es el ratón WNK4-L319F/L321F, el cual tiene una WNK4 incapaz de unir directamente al ion Cl^- . Estos ratones no muestran un aumento en la fosforilación de NCC cuando son alimentados con una dieta deficiente en K^+ por 4 días, lo cual sugiere que la unión/disociación del Cl^- en el dominio cinasa de WNK4 es el mecanismo por el cual NCC se activa en condiciones de bajo K^+ . Sin embargo, en dicho estudio, los niveles de K^+ plasmático siguen estando elevados en estos ratones, en comparación con ratones WT(61). Por lo tanto, es de interés averiguar si menores concentraciones de K^+ en plasma pueden provocar un aumento en la fosforilación de NCC incluso en los ratones WNK4-L319F/L321F. Esto sugeriría que existen mecanismos adicionales responsables del aumento en NCC ante este estímulo.

Uno de estos mecanismos es el aumento en la fosforilación de la S433 de KLHL3, la cual está aumentada al alimentar a ratones con una dieta deficiente en K^+ por 7 días(99), comparado con ratones mantenidos con una dieta control. Esto va acompañado en un aumento en la cantidad de WNK4 total en lisados de riñón. De manera equivalente, los niveles totales de KS-WNK1 también aumentan al mantener a ratones en una dieta sin K^+ (100). La presencia de KS-WNK1 parece ser esencial para la formación de 'puntos citoplasmáticos' que son agregados protéicos que contienen a diversos componentes de esta vía de señalización, como WNK1, WNK4 o SPAK(101). Estos 'cuerpos de WNK' o 'WNK bodies' se forman en respuesta a una disminución de $[K^+]_e$, y se ha propuesto que juegan un papel en la fosforilación de SPAK y su translocación a la membrana apical(102).

4. JUSTIFICACIÓN

De acuerdo con lo expuesto en la introducción, la existencia de variantes cortas de la cinasa WNK4 no ha sido estudiada a profundidad hasta antes de la realización de este trabajo. Por lo tanto, en este proyecto se planteó describir detalladamente la localización de estas variantes en el ratón, así como su generación y características bioquímicas, con relación a la vía de señalización WNK4-SPAK/OSR1.

Asimismo, se ha propuesto que la capacidad de WNK4 de unir Cl^- es el mecanismo principal a través del cual la fosforilación de NCC aumenta en respuesta a niveles bajos de K^+ en plasma. Sin embargo, no existe evidencia clara en la literatura que apoye este fenómeno como único e indispensable en este proceso, mientras que otros mecanismos, como la fosforilación de KLHL3 y de WNK4 en los motivos RRxS, también podrían constituir elementos importantes en la respuesta de NCC. Es por esto, que en este proyecto se estudió la contribución de estos mecanismos alternativos en modelos *in vivo*, *ex vivo* e *in vitro*.

5. OBJETIVOS

El objetivo general del trabajo consiste en la descripción de las variantes cortas de WNK4, su localización en riñón, el mecanismo de su generación y el estudio del papel del dominio C-terminal de WNK4 sobre su fosforilación y la actividad sobre su sustrato, SPAK.

- Confirmar la identidad de las bandas detectadas en lisados de riñón de ratones WT con un anticuerpo dirigido hacia el dominio N-terminal de WNK4.
 - Usar anticuerpos dirigidos contra diferentes regiones de WNK4 para encontrar más información sobre las variantes cortas de WNK4, lo cual será complementado con información derivada de espectrometría de masas.
 - Estudiar si las variantes cortas de WNK4 están presentes en otros tejidos que también contienen WNK4 completa, como testículo, cerebro o pulmón o, si bien, muestran un patrón tejido específico en riñón.
 - Generar distintas construcciones con deleciones de distinto tamaño para describir el papel regulador del dominio C-terminal de WNK4, al analizar la fosforilación de WNK4 y de SPAK.
 - Encontrar si estas variantes cortas se generan de manera post-transcripcional o post-traducciona, mediante ensayos de RACE 3' y ensayos *in vitro* de corte proteolítico de WNK4 recombinante.

El segundo objetivo general, es encontrar si existen mecanismos adicionales a la unión del Cl⁻ de WNK4 para la activación de NCC en condiciones de hipokalemia.

- Analizar si los niveles de fosforilación de WNK4 en los motivos RRxS son regulados por [K⁺]_e
 - Analizar de los niveles totales de WNK4 y su fosforilación en la Ser64 y S1196 en un modelo murino de hipokalemia.
 - Estudiar si la concentración de K⁺ ejerce un efecto directo sobre la regulación de WNK4 en estos sitios usando una línea celular transfectada con WNK4 y rebanadas de riñones de ratón.
- Analizar si la actividad de KLHL3 y, por lo tanto, la abundancia de WNK4 y/o KS-WNK1, puede ser modulada por [Cl⁻]_i
 - Co-transfectar KLHL3 con WNK4 y analizar los niveles de WNK4 en un medio control, medio con baja [K⁺]_e, o un medio hipotónico bajo en Cl⁻
 - Medir niveles de abundancia de KS-WNK1 en modelos *in vivo* con una menor función de NCC, lo cual se ha asociado a una disminución en [Cl⁻]_i, como son los ratones WNK4-KO o ratones silvestres con una administración aguda de hidroclorotiazida.
- Estudiar si existen mecanismos alternativos a la disociación del Cl⁻ de WNK4 en la activación de NCC ante hipokalemia *in vivo*
 - Encontrar si la fosforilación de NCC aún es modulable por la ingesta de K⁺ en un modelo *in vivo* en donde WNK4 no puede unir directamente al Cl⁻, mediante la generación de ratones WNK4-L319F

6. MATERIALES Y MÉTODOS

Ratones

Los estudios en animales fueron aprobados por el Comité de Ética del Instituto Nacional de Ciencias Médicas y Nutrición Salvador Zubirán. Se usaron ratones machos C57BL/6 de 12 a 16 semanas de edad. La dieta baja en K⁺ fue obtenida de TestDiet (St. Louis, MO), y la dieta control se preparó añadiendo KCl para una concentración final de 1.2% de K⁺. Los ratones fueron alimentados con estas dietas y agua *ad libitum* por 7 días. Para el modelo de hidroclorotiazida (HCTZ), se añadió este fármaco en la dieta de ratones silvestres para una dosis de 60mg/kg peso corporal. Los ratones WNK4-KO(41) han sido descritos previamente, así como los ratones Kir5.1-KO(84). Al final del experimento, los ratones se anestesiaron con isofluorano, se extrajo sangre a través de punción cardiaca para análisis de electrolitos con el equipo iStat (Abbott) y se extrajeron los riñones y se congelaron en N₂ líquido.

Generación de ratones WNK4-L319F

El ratón con una mutación en L319F en el gen *Wnk4* fue generado usando CRISPR/Cas9. Se usaron dos RNAs guías sobrelapados hacia el exón 3 del gen *Wnk4*. Cada RNA guía consistió en 20 bases (GCTTGAGCGTGGCCAGTCCG y AAAGGAGGCGCGCTTGAGCG) precediendo directamente una secuencia NGG como PAM (proto-spacer adjacent motifs). Cada RNA guía fue seleccionado basado en una predicción de alta probabilidad de corte y baja probabilidad de eventos inespecíficos. Cas9 fue dirigida hacia los codones G320 y L324, y un oligonucleótido de DNA de cadena sencilla de 12 bases para la reparación, y brazos de homología 5' de 71 bases y 3' de 109 bases se usó para la reparación del DNA. La mutación introducida sustituye el codón L319 por F. Mutaciones silenciosas adicionales se insertaron para proteger al DNA reparado de Cas9, así como para introducir un sitio de restricción de NheI con el propósito de facilitar la genotipificación. Los dos RNAs guías, el DNA de reparación y Cas9 recombinante fueron mezclados e inyectados en 289 embriones de ratón aislados de hembras B6:D2. Después de la inyección, los embriones se transfirieron a hembras pseudo-embarazadas, resultando en el nacimiento de 29 crías. De estas, 9 fueron silvestres, 14 tuvieron mutaciones por “non-homologous end joining” (NHEJ) y 6 ratones tenían la mutación esperada en un alelo y NHEJ en el otro. Después de separar el alelo correcto mediante cruza y genotipificación, dos líneas separadas se establecieron y se montaron retrocruzas con ratones C57BL6/J por 4 generaciones, para eliminar posibles efectos inespecíficos. Después se generaron ratones homocigotos al cruzar ratones heterocigotos entre sí y se estudiaron.

Western Blot

Los tejidos se homogenizaron con el siguiente buffer de lisis: 250mM sacarosa, 10mM trietanolamina, 50mM fluoruro de sodio, 5mM pirofosfato de sodio, 1mM ortovanadato de sodio, 1x inhibidores de proteasas (Roche). Los homogenados fueron centrifugados a 10,000 rpm por 10 minutos a 4°C. La concentración de proteína fue determinada por el ensayo de BCA (Pierce). A las muestras se les añadió buffer Laemmli (concentración final: Tris-HCl 50mM pH6.8, 2% SDS, 10% glicerol, 5% β-mercaptoetanol, 0.05% azul de bromofenol) y se calentaron a 95°C por 10 minutos.

Las muestras de proteína (~30µg de proteína por pozo) se cargaron en un gel de SDS-poliacrilamida (7.5%) de 1mm de espesor y se llevó a cabo una electroforesis seguida de transferencia con un Trans-Blot Turbo (BioRad) a una membrana de fluoruro de polivinilideno (PVDF). El bloqueo de las membranas se hizo con leche 10% en TBST (50mM Tris, 150mM NaCl, 0.1% Tween20, pH 7.5) durante 1 hora a temperatura ambiente. Los anticuerpos se diluyeron en TBST con 5% de leche. Las membranas se incubaron durante la noche a 4°C con los anticuerpos primarios y durante 90 minutos a

temperatura ambiente con los anticuerpos secundarios. La señal fue detectada con un sustrato quimioluminiscente y con placas radiográficas.

Se hizo uso de los siguientes anticuerpos:

- WNK4 (epítotope N-terminal; Oregon Health & Science University (OHSU), laboratorio del Dr. David H. Ellison)(103)
- WNK4 (epítotope N-terminal; MRC, Universidad de Dundee, S121B)(53)
- WNK4 (epítotope C-terminal; MRC, Universidad de Dundee, S064B)(41)
- pWNK4 S64 (Universidad de Yale, laboratorio del Dr. Richard Lifton)(53)
- pWNK4 S1196 (Universidad de Yale, laboratorio del Dr. Richard Lifton)(53)
- pWNK4 S1196 (OHSU, laboratorio del Dr. David H. Ellison)(104)
- pWNK4 S332 (MRC, Universidad de Dundee, S099B)(52)
- pSPAK S373 (MRC, Universidad de Dundee, S670B)(105)
- pNCC 3P (MRC, Universidad de Dundee, S108B)(73)
- NCC (OHSU, laboratorio del Dr. David H. Ellison)(104)
- WNK1 (epítotope C-terminal; Bethyl Laboratories, A301-515A)(100)
- PKC δ (BD Transduction Laboratories, 610398)(106)
- PKC ϵ (BD Transduction Laboratories, 610085)(107)
- HA-HRP (Sigma, H6533)
- FLAG-HRP (Sigma, A8592)
- Actina-HRP (Santa Cruz, sc-1616 HRP)
- RRXp(S/T) (Cell Signaling Technology (CST), #9624)
- Secundario anti-oveja-HRP (Jackson Immunoresearch)
- Secundario anti-conejo-HRP (Jackson Immunoresearch)
- Secundario anti-ratón-HRP (Jackson Immunoresearch)

Inmunofluorescencia

Al momento del sacrificio, los ratones fueron perfundidos con 20mL de solución salina 0.9% y después con 20mL de paraformaldehído 4%. Posteriormente los riñones se colocaron en la misma solución por 3 horas y después se incubaron durante la noche con sacarosa 30% para deshidratarlos. Al día siguiente, los riñones se cortaron en un criostato en rebanadas de 5 μ m que fueron colocados en laminillas y congelados hasta el momento de la tinción. Para esto, se realizó una activación antigénica sumergiendo las laminillas en un buffer de citrato de sodio 10mM y calentando las muestras en un microondas comercial por 10 minutos. Después de lavar las laminillas con TBST, los riñones se bloquearon con BSA 5% por 1 hora, e incubados con el anticuerpo primario (WNK4, pWNK4-S64 o pWNK4-S1196 (Ellison)) durante una noche a 4°C. Después de tres lavados con TBST, se incubó con anticuerpo secundario (Goat Anti-Rabbit IgG H&L (Alexa Fluor® 594) (ab150080)), durante 1 hora. Posteriormente se incubó con el segundo anticuerpo primario (NCC (MRC, Universidad de Dundee, S965B)(41); 1:100); y con el anticuerpo secundario (Donkey Anti-Sheep IgG H&L (Alexa Fluor® 488) (ab150177)) por 1 hora cada uno. Finalmente se usó Vectashield con DAPI (Vector Laboratories; H-1200) para montar las preparaciones. Las imágenes se tomaron en un microscopio confocal (LSM710 Duo; Zeiss) y analizadas con el software ImageJ.

COPAS (Complex Object Parametric Analyzer and Sorter)

El aislamiento del DCT se ha descrito previamente(108). Brevemente, ratones con expresión de GFP bajo el promotor de PV fueron anestesiados y perfundidos con solución Krebs fría. La corteza renal fue molida antes de incubarla en solución de digestión (1 mg/ml colagenasa tipo 1 y 2,000 unidades/ml hialuronidasa en solución Krebs, pH 7.3) por 15 minutos a 37 °C. Los túbulos de colectaron y se colocaron en hielo y sorteados por COPAS. Cada suspensión de túbulos fluorescentes fue colocada en un

tubo de 1.5mL, previamente con 0.5% (w/v) BSA en PBS/NaOH, pH 7.4. Los túbulos fueron lisados con buffer Laemmli.

Espectrometría de masas (MS)

Los lisados de riñón se prepararon como se describió anteriormente. Para inmunoprecipitar WNK4, 1mg de lisado fue incubado con 10 μ g de anticuerpo contra WNK4 (MRC, Dundee, S121B) y perlas magnéticas con Proteína A/G (Pierce) por 2 horas a 4°C. Las perlas se lavaron 5 veces con un buffer con 25mM Tris pH 7.4, 150mM NaCl, 1mM EDTA, 1% NonidetP40 y 5% glicerol. Las proteínas unidas se eluyeron con buffer de glicina pH 2.0 por 10 minutos y preparadas para electroforesis. Las bandas se cortaron del gel y se procesaron en la Unidad de MS y Proteómica de la Universidad de Yale. Brevemente, las bandas del gel se lavaron con 250 μ l de acetonitrilo 50% por 5 minutos, seguidos de 250 μ l de acetonitrilo 50% con 50mM NH₄CO₃ por 10-30 minutos, y finalmente con 250 μ l de acetonitrilo 50% con 10mM NH₄CO₃ por 10-30 minutos. El lavado final fue removido y el gel fue secado al vacío. 60 μ l de una dilución 1:15 de 0.1mg/ml de tripsina fueron añadidos por 10 minutos, para después añadir un volumen de 10mM NH₄CO₃ para cubrir las piezas de gel y se incubaron a 37°C por 18 horas.

Los péptidos se extrajeron añadiendo 250 μ l de 0.1% TFA, 80% acetonitrilo y agitando por 30 minutos. El extracto se pasó a un tubo nuevo para secarse. El pellet de péptidos se diluyó con 0.1% TFA y finalmente sometido a LC-MS/MS. La identificación de proteínas se hizo con un algoritmo de búsqueda Mascot (Matrix Science)(109), con una base de datos del proteoma de ratón SWISSPROT, así como una base de datos de la proteína WNK4 generada por el usuario.

Cultivo celular

Las células HEK293 (ATCC® CRL-1573) fueron usadas para transfección transitoria de FLAG-mWNK4-HA(53), GFP-HA-SPAK (Dundee; DU6188), SPAK-FLAG (generada por FastCloning), PP1 α , PP1 β , y PP1 γ -FLAG (donación del Dr. Jeremy Nichols)(110), hKLHL3-FLAG(50) o PKC δ (donación del Dr. Bernard Weinstein (Addgene #16386; <http://n2t.net/addgene:16386>; RRID:Addgene_16386))(111). Las células se sembraron en un 70-80% de confluencia y se transfectaron con Lipofectamina 2000 (Life Technologies). Las mutaciones en la clona de WNK4 se introdujeron por mutagénesis sitio dirigida con la enzima Phusion® High-Fidelity DNA Polymerase (New England Biolabs) y se confirmaron por secuenciación Sanger. Las deleciones fueron hechas por medio de FastCloning(112). 48 horas después de la transfección, las células se lisaron con un buffer de lisis (50mM Tris·HCl (pH 7.5), 1mM EGTA, 1mM EDTA, 50mM fluoruro de sodio, 5mM pirofosfato de sodio, 1mM ortovanadato de sodio, 1% Nonidet P-40, 270mM sacarosa, 0.1% β -mercaptoetanol, 1x inhibidores de proteasas (Roche)), y la concentración de proteína se determinó por BCA.

Para la estimulación con medios con diferentes concentraciones de K⁺, se incubaron a las células 16 horas antes de la lisis en los respectivos medios: LKM (135mM NaCl, 1mM KCl, 0.5mM CaCl₂, 0.5mM MgCl₂, 0.5mM Na₂HPO₄, 0.5mM Na₂SO₄, 15mM HEPES, 27.75mM glucosa, 18mM sacarosa; pH 7.4); NKM (135mM NaCl, 5mM KCl, 0.5mM CaCl₂, 0.5mM MgCl₂, 0.5mM Na₂HPO₄, 0.5mM Na₂SO₄, 15mM HEPES, 27.75mM glucosa, 10mM sacarosa; pH 7.4); HKM (135mM NaCl, 10mM KCl, 0.5mM CaCl₂, 0.5mM MgCl₂, 0.5mM Na₂HPO₄, 0.5mM Na₂SO₄, 15mM HEPES, 27.75mM glucosa; pH 7.4). Por otra parte, el medio hipotónico bajo Cl⁻ (67.5mM Na-Gluconato, 5mM K-Gluconato, 0.5mM CaCl₂, 0.5mM MgCl₂, 0.5mM Na₂HPO₄, 0.5mM Na₂SO₄, 7.5mM HEPES, 27.75mM glucosa; pH 7.4) se usó durante 2 horas, excepto en el experimento correspondiente para analizar el efecto sobre la degradación de WNK4 por KLHL3, donde también se usó por 16 horas.

Los inhibidores farmacológicos WNK463 (10 μ M; donación del Dr. Dario Alessi, Dundee University), BIM (4 μ M; CST #9841) se colocaron 15 minutos antes del respectivo estímulo con el que se estudiaron. La N-etilmaleimida (NEM) (Sigma) se colocó a una concentración final de 100 μ M por un periodo de 30 minutos.

Inmunoprecipitación

Se usaron perlas de agarosa acopladas a anticuerpo anti-FLAG (Sigma-Aldrich A2220). Las perlas se lavaron 3 veces con PBS (137mM NaCl; 2.7mM KCl; 8.1mM Na₂HPO₄; 1.5mM KH₂PO₄; pH 7.4) antes de la incubación con el lisado. 350 μ g de proteína se usaron por cada reacción, junto con 15 μ l de perlas. La mezcla se llevó a 500 μ l con buffer de lisis y se incubó por 2 horas a 4°C, con agitación por inversión. Posteriormente las perlas se lavaron 2 veces con buffer de lavado (25mM Tris-HCl pH 7.5; 150mM NaCl; 1mM EDTA; 1% v/v NP-40; 5% v/v glicerol) y 2 veces con PBS. La elusión se hizo con buffer Laemmli e incubando a 95°C por 10 minutos. Finalmente las muestras se analizaron por Western Blot.

Ensayo de proteólisis

FLAG-mWNK4-HA recombinante fue inmunoprecipitada con perlas anti-FLAG (Sigma-Aldrich A2220), como indicado anteriormente. Después de los lavados, se añadieron 70 μ g de proteína de riñón (lisado en buffer con 125mM NaCl, 10% v/v glicerol, 1mM EGTA, 1mM EDTA, 1mM PMSF, 10 μ M leupeptina, 4 μ M aprotinina, 10 μ M pepstatina, 1% Triton X-100, 0.5% SDS, 20mM HEPES, pH 7.4) y se incubó la reacción por 90 minutos a 37°C (volumen final de la reacción de 30 μ l en 50mM HEPES, 140mM NaCl, pH 7.4; en ausencia o presencia de inhibidores de proteasas como sea el caso). Las reacciones se detuvieron añadiendo buffer Laemmli y calentándolas a 95 °C por 10 min. La elusión se usó para ensayos de Western Blot.

Experimentos de captación de ²²Na⁺ en ovocitos

El uso de ranas *Xenopus laevis* fue aprobado por el Comité de Ética del Instituto Nacional de Ciencias Médicas y Nutrición Salvador Zubirán. La actividad de NCC fue analizada en ovocitos de rana inyectados con RNA sintetizado *in vitro*, en ausencia o presencia de WNK4 WT o WNK4 T1029X. Dos días después de la inyección, se midió la captación de ²²Na⁺ sensible a tiazida, como descrito previamente(34). De manera breve, la captación de ²²Na⁺ se llevó a cabo en grupos de 10-15 ovocitos. Después de una incubación de 30 minutos a 32°C en un medio ND96 libre de Cl⁻ con 1mM ouabaína, 0.1mM amilorida y 0.1mM bumetanida, los ovocitos se cambiaron a un medio de captación sin K⁺ (40mM NaCl, 56mM gluconato de sodio, 4mM CaCl₂, 1mM MgCl₂ y 5mM HEPES, pH 7.4) con ouabaina, amilorida, bumetanida y 2 μ Ci de ²²Na⁺. Los ovocitos se lavaron cinco veces con solución fría para remover el ²²Na⁺ extracelular. Ovocitos individuales se lisaron con 10%SDS y la medición de ²²Na⁺ se llevó a cabo por conteo por β -centelleo.

Ensayo de actividad de PKC

El ensayo se realizó con el kit PKC Kinase Activity Assay Kit (ab139437) de acuerdo a las recomendaciones del fabricante, usando lisados de células HEK293 transfectadas con WNK4 48 después de la transfección.

Medición de cAMP

Células HEK-293 fueron transfectadas con WNK4, 48 horas después de la transfección, las células fueron estimuladas en presencia de 0.125 mM de 3-isobutyl-methyl-xanthine (IBMX) (Sigma). Después de 2 horas de estímulo las células fueron congeladas a -70°C por 24 horas. El contenido de cada pozo se recuperó en un tubo de ensayo de 12x75 y estos fueron calentados por 3 minutos a 95°C. La cuantificación de cAMP total se analizó por Radioinmunoanálisis (RIA) utilizando como trazador 2-O-monosuccinil tirosil-metiléster cAMP (Sigma) radiomarcado con NaI¹²⁵ por el método de cloramina-T. Tanto la curva estándar como las muestras problema fueron previamente acetiladas con 25µl de trietilamina-anhidrido acético (2:1 v/v) y diluidas en acetato de sodio 5mM, pH=4.75, el anticuerpo empleado fue cAMP (Merck-Millipore Cat. 116820) a una dilución final 1:3,000. Todas las muestras fueron analizadas por duplicado y la sensibilidad del ensayo fue de 4 fmol/tubo(113).

Modelo ex vivo de rebanadas de riñón.

Brevemente, ratones macho C57BL/6 de 12 a 16 semanas de edad fueron anestesiados con isoflurano y perfundidos con 20mL de solución Ringer con alto K⁺ (98.5mM NaCl; 35mM NaHCO₃; 5mM KCl; 1mM NaH₂PO₄; 2.5mM CaCl₂; 1.8mM MgCl₂; 25mM glucosa). Al extraer los riñones se les hizo un corte coronal y fueron incubados en solución Ringer con alta [K⁺] (93.5mM NaCl; 25mM NaHCO₃; 10mM KCl; 1mM NaH₂PO₄; 2.5mM CaCl₂; 1.8mM MgCl₂; 25mM glucosa) con burbujeo constante de carbógeno para mantener pH fisiológico. Posteriormente, una mitad de riñón se pegó en una plataforma para realizar cortes de 300µm en el vibratomo PELCO easiSlicer™. Se obtuvieron entre 1 y 3 rebandas de cada mitad de riñón, las cuales se incubaron por 30 minutos en la misma solución Ringer a 30.5°C. Después de este paso, las rebandas control se pasaron a una solución con [K⁺] normal (93.5mM NaCl; 25mM NaHCO₃; 10mM KCl; 1mM NaH₂PO₄; 2.5mM CaCl₂; 1.8mM MgCl₂; 25mM glucosa) por 60 minutos más, mientras que las demás se pasaron a una solución similar baja en K⁺ (102.5mM NaCl; 25mM NaHCO₃; 1mM KCl; 1mM NaH₂PO₄; 2.5mM CaCl₂; 1.8mM MgCl₂; 25mM glucosa). Finalmente, las rebandas se congelaron en N₂ líquido para posteriormente ser homogenizadas de manera similar a los riñones completos para realizar ensayos de Western Blot.

Análisis estadístico

Para comparaciones entre dos grupos, se usó una t de Student no pareada. Para comparación entre múltiples grupos, se usó una ANOVA, seguida de un test Bonferroni post hoc. Una diferencia se señaló como significativa cuando p<0.05.

7. RESULTADOS

La primera mitad de los resultados de esta tesis ya fueron publicados en un artículo que se presenta más adelante, cuya referencia es la siguiente:

Murillo-de-Ozores AR, Rodríguez-Gama A, Bazúa-Valenti S, Leyva-Ríos K, Vázquez N, Pacheco-Álvarez D, De La Rosa-Velázquez IA, Wengi A, Stone KL, Zhang J, Loffing J, Lifton RP, Yang CL, Ellison DH, Gamba G, Castañeda-Bueno M. C-terminally truncated, kidney-specific variants of the WNK4 kinase lack several sites that regulate its activity. J Biol Chem. 2018 Aug 3;293(31):12209-12221. doi:

10.1074/jbc.RA118.003037. Epub 2018 Jun 19. PMID: 29921588; PMCID: PMC6078442.

A continuación, un resumen de esta parte de los resultados:

En ensayos de Western Blot con lisados de riñón de ratón, además de la banda correspondiente a la WNK4 completa, se han observado bandas correspondientes a un menor tamaño (entre 95 y 130kDa). Por lo tanto, hipotetizamos que se podrían tratar de variantes de WNK4 no descritas. En este trabajo, usando diferentes anticuerpos contra WNK4 y contando con ratones WNK4-KO como control negativo, mostramos que estas bandas sí corresponden a variantes más cortas de la cinasa WNK4, las cuales son detectadas en riñón, pero no en otros tejidos que sí tienen WNK4 completa, como testículo, cerebro o pulmón. Ensayos de espectrometría de masas confirman estas bandas como WNK4 carente del segmento C-terminal. En células HEK293, constructos con WNK4 trunca muestran mayor actividad cinasa al fosforilar a SPAK en comparación con la WNK4 completa, a menos de que también se elimine el sitio de unión a SPAK. Esta ganancia de función de las WNK4 truncas se debe a la eliminación de un sitio consenso de unión a PP1. Cotransfección de PP1 promovió la defosforilación de WNK4, efecto que se vio abatido en una mutante del sitio de unión a PP1 de WNK4. Sin embargo, la movilidad electroforética de las variantes cortas de WNK4 encontradas *in vivo* sugiere que carecen del sitio de unión a SPAK, por lo que podrían tratarse de un mecanismo inhibitorio de esta vía de señalización. Finalmente, mostramos que al menos una de estas variantes puede ser producida por proteólisis por una metaloproteasa dependiente de Zn^{2+} , dado que la WNK4 completa recombinante es cortada cuando es incubada con un lisado de riñón.



C-terminally truncated, kidney-specific variants of the WNK4 kinase lack several sites that regulate its activity

Received for publication, March 20, 2018, and in revised form, June 14, 2018. Published, Papers in Press, June 19, 2018, DOI 10.1074/jbc.RA118.003037

Adrián Rafael Murillo-de-Ozores,^{a1} Alejandro Rodríguez-Gama,^b Silvana Bazúa-Valenti,^b Karla Leyva-Ríos,^c Norma Vázquez,^b Diana Pacheco-Álvarez,^c Inti A. De La Rosa-Velázquez,^d Agnieszka Wengi,^e Kathryn L. Stone,^f Junhui Zhang,^g Johannes Loffing,^e Richard P. Lifton,^{g,h} Chao-Ling Yang,^{i,j} David H. Ellison,^{i,j} Gerardo Gamba,^{b,k,l} and María Castañeda-Bueno^{k2}

From the ^aFacultad de Medicina, and ^bInstituto de Investigaciones Biomédicas, Universidad Nacional Autónoma de México, Mexico City 14080, Mexico, the ^cEscuela de Medicina, Universidad Panamericana, Mexico City 03920, Mexico, the ^dGenomics Laboratory, RAI, Universidad Nacional Autónoma de México-Instituto Nacional de Ciencias Médicas y Nutrición Salvador Zubirán, Mexico City 14080, Mexico, the ^eInstitute of Anatomy and Swiss National Centre of Competence in Research "Kidney Control of Homeostasis," University of Zurich, Zurich 8057, Switzerland, the ^fMS and Proteomics Resource, W. M. Keck Biotechnology Resource Laboratory and ^gDepartment of Genetics, Yale University School of Medicine, New Haven 06510, Connecticut, the ^hLaboratory of Human Genetics and Genomics, Rockefeller University, New York, New York 10065, the ⁱDivision of Nephrology and Hypertension, Department of Medicine, Oregon Health and Science University, Portland, Oregon 97239, the ^jVeterans Affairs Portland Health Care System, Portland, Oregon 97239, the ^kDepartment of Nephrology and Mineral Metabolism, Instituto Nacional de Ciencias Médicas y Nutrición Salvador Zubirán, Mexico City 14080, Mexico, and the ^lTecnológico de Monterrey, Escuela de Medicina y Ciencias de la Salud, Monterrey 64710, Nuevo León, Mexico

Edited by Roger J. Colbran

WNK lysine-deficient protein kinase 4 (WNK4) is an important regulator of renal salt handling. Mutations in its gene cause pseudohypoaldosteronism type II, mainly arising from overactivation of the renal Na⁺/Cl⁻ cotransporter (NCC). In addition to full-length WNK4, we have observed faster migrating bands (between 95 and 130 kDa) in Western blots of kidney lysates. Therefore, we hypothesized that these could correspond to uncharacterized WNK4 variants. Here, using several WNK4 antibodies and WNK4^{-/-} mice as controls, we showed that these bands indeed correspond to short WNK4 variants that are not observed in other tissue lysates. LC-MS/MS confirmed these bands as WNK4 variants that lack C-terminal segments. In HEK293 cells, truncation of WNK4's C terminus at several positions increased its kinase activity toward Ste20-related proline/alanine-rich kinase (SPAK), unless the truncated segment included the SPAK-binding site. Of note, this gain-of-function effect was due to the loss of a protein phosphatase 1 (PP1)-binding site in WNK4. Cotransfection with PP1 resulted in WNK4 dephosphorylation, an activity that was abrogated in the PP1-binding site WNK4 mutant. The electrophoretic mobility of the *in vivo* short variants of renal WNK4 suggested that they lack the SPAK-binding site and thus may not behave as constitutively active kinases toward SPAK. Finally, we show that at least one of the WNK4 short variants may be produced by proteolysis

involving a Zn²⁺-dependent metalloprotease, as recombinant full-length WNK4 was cleaved when incubated with kidney lysate.

WNK lysine-deficient protein kinase 4 (WNK4)³ is a serine-threonine kinase that is present in several tissues, including brain, lungs, liver, and heart, with the highest expression levels observed in kidney, colon, and testes (1). Mutations occurring within a specific motif in WNK4, the acidic motif, produce the human genetic disease pseudohypoaldosteronism type II (PHAII) (2). This disease features hypertension, hyperkalemia, metabolic acidosis, and marked sensitivity to thiazide diuretics, alterations that are thought to be mainly due to higher basal activity of the renal thiazide-sensitive Na⁺/Cl⁻ cotransporter (NCC), which is specifically expressed in the distal convoluted tubule (DCT) of the nephron (3, 4). Decreased activity levels of the K⁺ channel ROMK and Na⁺ channel ENaC may also contribute (5). The acidic motif of WNK4 constitutes the binding site for the cullin-RING E3 ubiquitin ligase complex formed by cullin 3, Kelch-like 3, and an E3 ring ubiquitin ligase, which regulates the degradation of the kinase (6, 7). Thus, PHAII mutations occurring in this motif decrease the degradation rate of the kinase, leading to its overexpression.

WNK4-knockout mice present markedly decreased levels of NCC expression and virtually no NCC phosphorylation. Accordingly, the phenotype of WNK4-knockout mice resembles that of patients with Gitelman disease, featuring hypoten-

This work was supported by National Institutes of Health Grant DK51496 (to G. G., C.-L. Y., and D. H. E.) and Conacyt Grants 23 (to G. G.) and 257726 (to M. C.-B.). The authors declare that they have no conflicts of interest with the contents of this article. The content is solely the responsibility of the authors and does not necessarily represent the official views of the National Institutes of Health.

This article contains Tables S1–S3 and Figs. S1–S4.

¹ Graduate student from the "Programa de Doctorado en Ciencias Biomédicas, Universidad Nacional Autónoma de México (UNAM)" and recipient of CONACYT Fellowship 606808.

² To whom correspondence should be addressed. Tel.: 5255-5487-0900 (ext. 2511); E-mail: mcasta85@yahoo.com.mx.

³ The abbreviations used are: WNK4, WNK lysine-deficient protein kinase 4; ROMK, renal outer medullary potassium channel; ENaC, epithelial Na channel; PHAII, pseudohypoaldosteronism type II; NCC, Na⁺/Cl⁻ cotransporter; DCT, distal convoluted tubule; SPAK, Ste20-related proline/alanine-rich kinase; pSPAK, SPAK phosphorylation; RACE, rapid amplification of cDNA ends; HRP, horseradish peroxidase; COPAS, Complex Object Parametric Analyzer and Sorter.

Kidney-specific WNK4 short variants and regulation by PP1

sion, hypokalemia, and metabolic alkalosis, which is caused by inactivating mutations in NCC (8). Thus, WNK4 is a key regulator of NCC, and its activity is essential to maintain basal NCC activity levels.

WNK4 promotes NCC activation through the phosphorylation of the T-loop of the Ste20-related proline/alanine-rich kinase (SPAK), which in turn phosphorylates key residues for NCC activation located in the N-terminal, cytoplasmic domain of the cotransporter (9, 10). In contrast, the regulatory effect of WNK4 on ROMK and ENaC appears to be independent of kinase activity (11, 12). Recently, it was shown that knock-in mice carrying a constitutively active form of SPAK in the DCT develop PHAII (3). Thus, WNK4's direct effects on ROMK and ENaC do not seem to be essential to develop the disease.

WNK4 kinase activity is regulated by at least two different mechanisms. Binding of a chloride ion within a site located near the active site of the kinase stabilizes an inactive conformation and prevents kinase activity (13, 14). Thus, at high intracellular chloride concentrations ($[Cl^-]_i$), chloride ions remain bound to these sites, inhibiting WNK4 activity. Conversely, when $[Cl^-]_i$ decreases, dissociation of Cl^- ions allows kinase activation. This mechanism has been shown to be important for NCC modulation in response to changes in extracellular K^+ concentration ($[K^+]_e$), because changes in $[K^+]_e$ affect the intracellular Cl^- concentration of DCT cells (15).

The second known regulatory mechanism of WNK4 kinase activity involves phosphorylation of at least two sites, Ser-64 and Ser-1196, located within the regulatory N- and C-terminal domains of WNK4, respectively (16). Phosphorylation of these sites promotes kinase activation; it can be conducted by protein kinase C or protein kinase A, and it is stimulated, for example, in response to AT1 receptor activation by angiotensin II. So far, the mechanism linking phosphorylation to kinase activation is unknown; however, both the N-terminal and C-terminal domains of WNK4 have long been thought to play a regulatory role (17–19), and several functional motifs have been described in the C-terminal domain (16). For instance, the acidic domain (2), two PF2-like domains (20), two putative PP1-binding motifs (21), one RFXV motif (22), and the HQ motif important for WNK dimerization (23, 24) have been described within the C-terminal domain of WNK4.

During our recent characterization of the WNK4-knockout mouse strain (8), we noticed that several bands smaller than that corresponding to the full-length WNK4 were observed in blots of renal tissues performed with an antibody directed against an N-terminal epitope; these were absent in samples from the knockout animals, ruling them out as nonspecific signals. Thus, we hypothesized that these bands could correspond to previously unrecognized variants of WNK4. Here, we present evidence that confirms the identity of these short bands as WNK4 short variants that lack a portion of the C-terminal domain. In addition, the characterization of these short variants of WNK4 has led us to the identification of a *bona fide* PP1-binding site located at the final portion of WNK4's C terminus, which regulates WNK4 phosphorylation levels and, thus, kinase activity.

Results

WNK4 short variants lacking a segment of the C-terminal domain are observed in mouse kidney lysates

Mouse kidney lysates from WNK4^{+/+} and WNK4^{-/-} mice were analyzed by Western blotting using antibodies directed against three distinct WNK4 epitopes. Using two different antibodies directed against N-terminal epitopes, we observed, in addition to the band corresponding to the full-length protein, at least two smaller bands that were absent in the WNK4^{-/-} mouse samples (Fig. 1A and Fig. S1A). These smaller bands were more abundant in samples from TgWNK4^{PHAII} mice (4) (Fig. S1B) and were not detected when an antibody directed against a C-terminal WNK4 epitope was used (Fig. 1B). These results suggest that the small bands observed correspond to shorter variants of WNK4, with an intact N-terminal domain and probably lacking a segment of the C terminus. These shorter WNK4 variants appear to be kidney-specific, as they were not observed in lysates from testis, brain, and lung when analyzed with a WNK4 N-terminal antibody (Fig. 1C).

Full-length WNK4 and the shorter variants were immunoprecipitated from mouse kidney lysates and separated by SDS-PAGE (Fig. 1D). Bands were excised from gel and individually analyzed by MS (LC-MS/MS). For the excised gel sample containing the full-length protein, tryptic peptides generated from the whole length of the protein were detected, including peptides from the C-terminal region (Fig. 1E and Table S1). In contrast, for the gel sample containing the smaller WNK4 variants, only peptides generated from the N-terminal and middle region of the protein were observed, whereas no peptides from the last portion of the C-terminal domain were detected (Fig. 1E and Table S2). This confirms the identity of the small-sized bands observed in Western blots as smaller variants of WNK4 lacking a portion of the C terminus. In addition, given that the 781–787 peptide was observed in the sample corresponding to the short WNK4 variants (Table S2), at least the segment comprising amino acid residues 1–787 must be present in the longest of the short variants. It should be noted that the large tryptic peptide comprising residues 788–970 was not expected to be detected in these assays due to its large size, and thus, the absence of detection of this peptide may not have been due to absence of this segment in the short WNK4 variants.

C-terminally truncated WNK4 constructs are more active than full-length WNK4, as long as they contain the C-terminal SPAK-binding site

To understand the impact that C-terminal truncations may have on WNK4 activity, we generated several WNK4 mutant constructs in which STOP codons were inserted at strategic positions between functional motifs (Fig. 2A). This allowed us to test the impact of the additive elimination of these motifs. The activity of these constructs was tested in HEK293 cells that were cotransfected with SPAK. SPAK phosphorylation (pSPAK; Ser-373) was measured as an indicator of WNK4 activity. Almost all mutant constructs presented a higher level of activity than WNK4-WT (Fig. 2, B and C), which was comparable with the activity of the WNK4-L319F mutant that is considered to be a constitutively active mutant due to

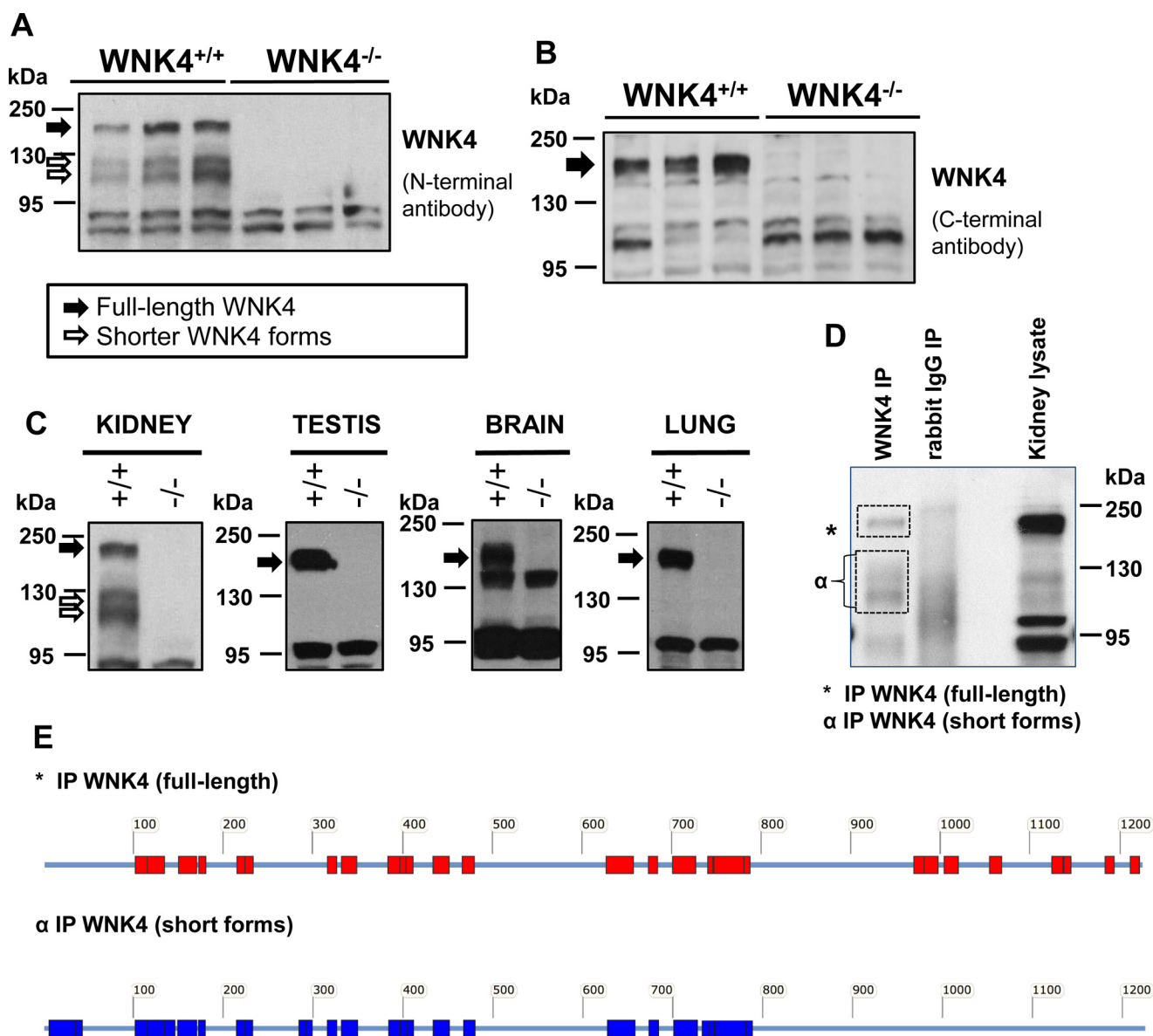


Figure 1. Identification of WNK4 short variants present in kidney lysates. A, Western blotting of kidney lysates of WNK4^{+/+} and WNK4^{-/-} mice using an antibody that recognizes an N-terminal epitope of WNK4 (residues 2–167 of mouse WNK4) (WNK4 antibody A described under “Experimental procedures”) (41). In addition to the band corresponding to the full-length WNK4 (indicated by a *black arrow*), this antibody detects at least two additional bands that are absent in the WNK4^{-/-} samples (*white arrows*). This image has been previously used by Yang *et al.* (41), as part of the WNK4 antibody characterization; however, no emphasis was made at this time in the WNK4 short variants. B, same as in A, but an antibody that recognizes a C-terminal epitope of WNK4 was used (residues 1221–1243 of human WNK4) (antibody B) (8). Only the full-length WNK4 is observed. Thus, the smaller bands observed in A might correspond to shorter WNK4 variants lacking a segment of the C-terminal region. C, Western blots performed with samples of different tissues from WNK4^{+/+} and WNK4^{-/-} mice using the same antibody as in A. The additional bands corresponding to putative WNK4 short variants are only observed in kidney lysates. Different exposure times are presented for clarity: 30 s for kidney and testis, 10 min for brain and lung. D, WNK4 was immunoprecipitated from kidney lysates and subjected to SDS-PAGE. A gel fragment containing the full-length band and another one containing the smaller bands were excised as indicated, and the extracted tryptic peptides were analyzed by LC-MS/MS. E, schematic representation of the peptides observed in LC-MS/MS assays. For the full-length band, peptides from every domain of WNK4 were observed. For the short bands, WNK4 peptides were observed, but none of them corresponded to the C-terminal region (see also Tables S1 and S2). This confirms that the smaller bands correspond to short WNK4 fragments that lack a portion of the C-terminal region. IP, immunoprecipitation.

impaired chloride binding in the kinase domain (14). This effect depended on WNK4 catalytic activity, because it was prevented by introduction of the D318A mutation, which renders the kinase catalytically inactive (Fig. 2F and Fig. S2A) (25). The only mutant construct that did not present higher activity levels than WNK4-WT was WNK4-R996X. Because this mutant is only 35 amino acid residues shorter than the WNK4-T1029X mutant, and the only functional motif known in this segment is the SPAK-binding site comprising residues 996–999 (RFXV motif)

(26), we deduced that the lower pSPAK levels observed with this mutant were due to the loss of this motif. We also assessed T-loop phosphorylation of the truncated mutants WNK4-K1211X and -T1029X as an alternative indicator of activation level. For both mutants, we observed higher T-loop phosphorylation levels than for WNK4-WT (Fig. 2, D and E). Finally, a representative WNK4-truncated mutant was tested for its ability to promote NCC activation in *Xenopus laevis* oocytes. In accordance with the results obtained in HEK293 cells, the

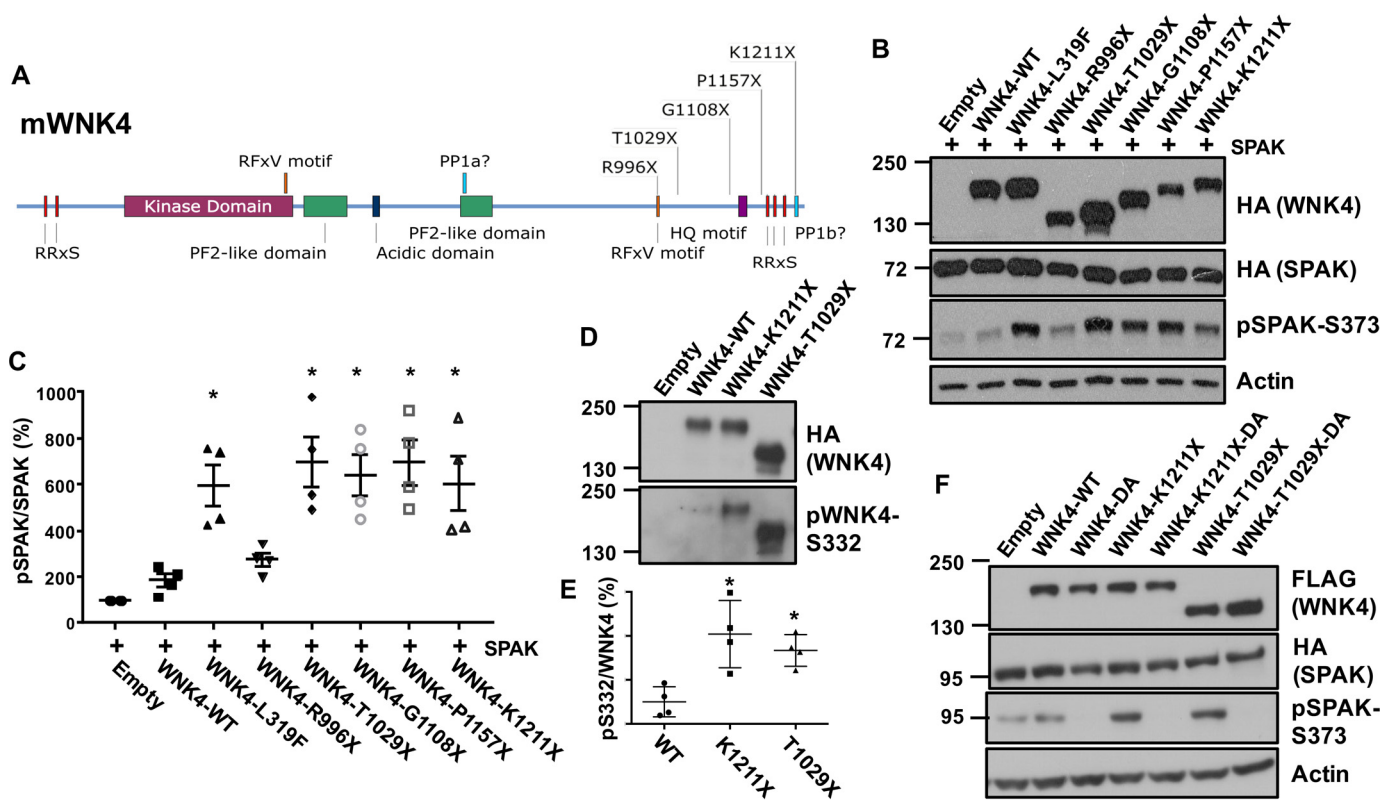


Figure 2. Effect of C-terminal deletions on WNK4 kinase activity. *A*, schematic representation of WNK4 protein depicting its important domains and motifs. The position of insertion of STOP codons for the generation of the truncated mutants is indicated. *RRxS*, sites of phosphorylation by protein kinase C/protein kinase A (16); *RFXV*, motifs presenting consensus sequence for SPAK interaction (22); *PF2-like*, domain similar to the PF2 domain present in SPAK/OSR1 that in SPAK/OSR1 forms the binding pocket for the RFXV motif present in WNKs and Slc12 cotransporters (20, 47); *Acidic domain*, motif that mediates interaction with the KLHL3–CUL3–RING complex (6) (PHAI1-causing mutations found in WNK4 lie within this motif); *PP1a/PP1b*, putative protein phosphatase 1-binding sites (21); *HQ motif*, motif implicated in WNK homo- and heterodimerization (23). *B*, representative Western blots of lysates from HEK293 cells transfected with SPAK-HA and different WNK4 mutants to assess their effect on SPAK phosphorylation. *C*, densitometric analysis of blots presented in *A* shows that C-terminally truncated WNK4 constructs have increased activity compared with full-length WNK4, and similar to that of the chloride-insensitive, constitutively active mutant (L319F), unless the SPAK-binding site is absent. Data are mean \pm S.E. (error bars); *, $p < 0.05$ versus WNK4-WT, $n \geq 4$ in at least three independent experiments. *D*, HEK293 cells were transfected with WNK4-WT or the indicated truncated mutants. WNK4 was immunoprecipitated, and T-loop phosphorylation (Ser-332) was assessed by Western blotting. *E*, densitometric analysis shows that the baseline T-loop phosphorylation of the truncated mutants WNK4-K1211X and T1029X is higher than that of WNK4-WT. *, $p < 0.05$ versus WNK4-WT, $n = 4$ in at least three independent experiments. *F*, HEK293 cells were transfected with WNK4 truncated mutants that were made catalytically inactive by introduction of the D318A mutation. These mutants were unable to phosphorylate SPAK, showing that the higher pSPAK levels observed in the presence of catalytically active truncated mutants are due to higher WNK4 kinase activity.

WNK4-T1029X mutant promoted NCC activation, whereas no NCC activation was observed with the WNK4-WT under the experimental conditions tested (Fig. S2B).

Elimination of a PP1-binding site located at the final portion of the C-terminal domain increased activity of the truncated WNK4 mutants

We noted that the only common feature between the four truncated mutants that presented higher activity levels than WNK4-WT was the absence of the last 12 amino acid residues of the protein. Within this region, a motif presenting the consensus sequence for interaction with PP1 is present (KXVXF) (27). Lin *et al.* (21) have shown that when this site and a second putative PP1-binding site (located at positions 695–699) are mutated, the WNK4–PP1 interaction is lost. In our hands, however, the WNK4–PP1 interaction was preserved in a WNK4 mutant lacking both putative PP1-binding sites (here termed PP1a and PP1b) (Fig. 3A). However, when only a fragment of WNK4's C terminus was expressed (residues 770–1222), which contains only the PP1b site, the absence of this site

disrupted the interaction with PP1. This result suggests that the PP1b site is indeed a PP1-binding site but that, in addition to the PP1a and PP1b sites, additional motifs present in WNK4 may be involved in the interaction.

We hypothesized that the gain of function observed in the truncated WNK4 mutants was due to the loss of the PP1b site. We thus tested whether elimination of the PP1a, PP1b, or both sites could replicate the gain of function observed with the truncated mutants. Interestingly, we observed that only the individual elimination of the PP1b site replicated the gain-of-function effect (Fig. 3, B and C) and that when the PP1a site was mutated in addition to the PP1b site, the gain-of-function effect was lost.

We next tested the effect of the cotransfection of the different PP1 isoforms (PP1 α , PP1 β , and PP1 γ) on the phosphorylation levels of WNK4-WT at previously described phosphorylation sites (RRXS sites) (16). We observed that coexpression of PP1 α and PP1 γ promoted WNK4 dephosphorylation, whereas coexpression of PP1 β had no effect (Fig. 3D). The inability of PP1 β to dephosphorylate WNK4 may be because it binds to

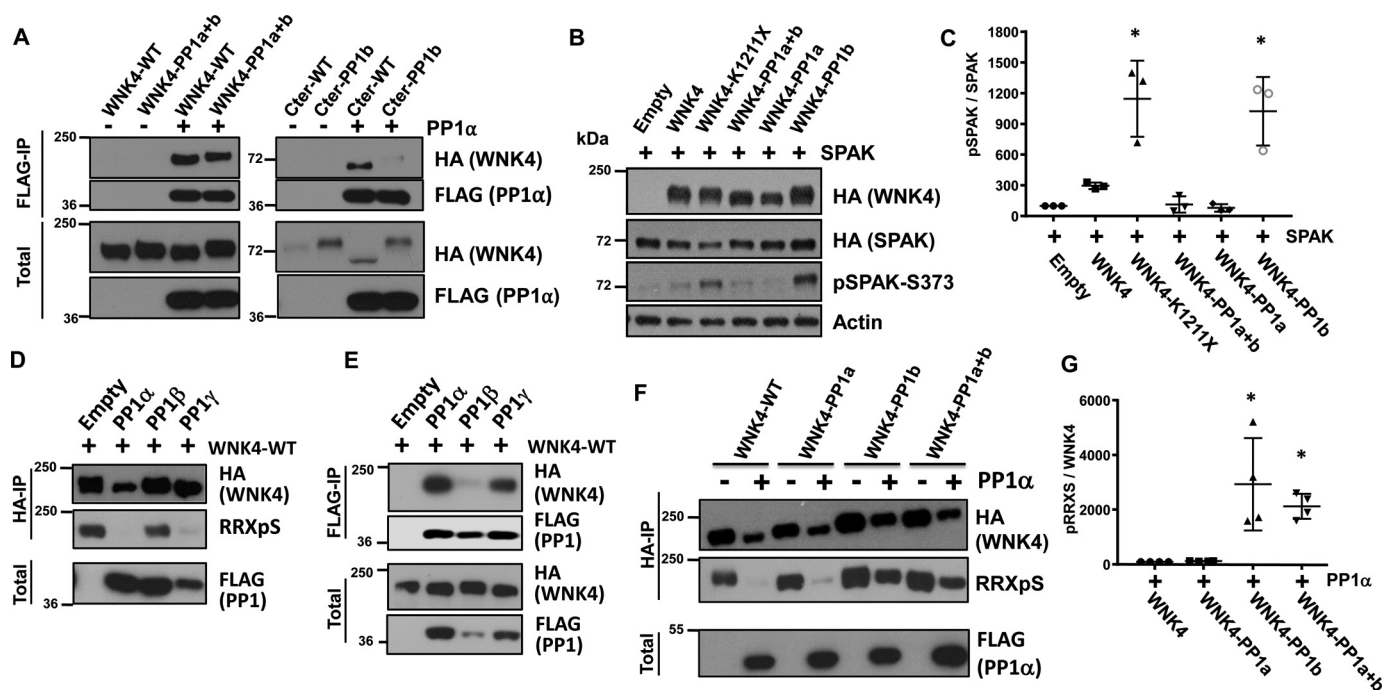


Figure 3. A PP1-binding site located in the C terminus of WNK4 regulates its phosphorylation and activity. *A*, co-immunoprecipitation assay of WNK4 and PP1 α . HEK293 cells were transfected with PP1 α and either full-length WNK4 (*left*) or a C-terminal fragment of WNK4 (residues 770–1222) (*right*). The effect of elimination of the predicted PP1-binding sites was assessed. A shift in the electrophoretic mobility of the WNK4–PP1a+b mutant is observed (migrates slower). This is even more evident with the C-terminal fragment harboring the PP1b mutation. Such a shift may be related to the phosphorylation levels of the protein, given that, as shown in the following panels, elimination of the PP1b site prevents WNK4 dephosphorylation. *B*, Western blots of lysates from HEK293 cells transfected with WNK4 constructs in which the putative PP1-binding sites were mutated (21). Their effect on pSPAK was assessed. PP1a mutant contains mutations V697A/T698A/F699A, and PP1b contains V1213A/T1214A/F1215A. PP1b mutant is more active than WT. *C*, results of quantitation of blots represented in *B*. Data are mean \pm S.E. (error bars). *, $p < 0.05$ versus WNK4-WT, $n = 3$. *D*, HEK293 cells were cotransfected with WNK4-WT and different PP1 isoforms. Before Western blots were performed, WNK4 was immunoprecipitated from cell lysates to eliminate signal detected from other proteins with the RRXpS antibody. Only PP1 α and PP1 γ promoted WNK4 dephosphorylation at RRXS sites. *E*, WNK4 interaction with the different PP1 isoforms was assessed by co-immunoprecipitation. Similar results were observed in three independent experiments. *F*, cells were cotransfected with PP1 α and the indicated WNK4 mutants. WNK4 was immunoprecipitated, and blots were performed with the indicated antibodies. PP1 α promotes dephosphorylation of WNK4 at RRXS sites (41) unless the PP1b site is mutated. *G*, results of quantitation of blots presented in *F*: phosphorylation levels of WNK4 in the presence of PP1 α . Data are mean \pm S.E.; *, $p < 0.05$ versus WNK4-WT, $n = 4$. IP, immunoprecipitation.

WNK4 with lower affinity than the other isoforms (Fig. 3E). The effect of PP1 α co-expression on WNK4 phosphorylation levels depended on PP1 catalytic activity (Fig. S3).

Finally, we tested the effect of PP1 α cotransfection on the phosphorylation levels of the PP1 binding mutants. We observed that the presence of the PP1b mutation (either alone or together with the PP1a mutation) prevented the PP1 α -mediated dephosphorylation of WNK4 (Fig. 3, F and G), whereas the WNK4–PP1a mutant behaved similarly to the WT.

Altogether, these results suggest that PP1 α and PP1 γ are important regulators of WNK4 phosphorylation levels and that they require the presence of the C-terminal binding site, here described as PP1b, to achieve dephosphorylation. Impaired dephosphorylation of WNK4 in the presence of the PP1b mutation leads to kinase activation. This activation is lost in the presence of the PP1a mutation despite high WNK4 phosphorylation levels observed in this double mutant, suggesting that the PP1a mutation impairs the kinase activity of WNK4. Of note, the PP1a site lies within a region of WNK4 that has been described to have a PF2-like fold similar to the one present in SPAK and OSR1. This PF2-like domain present in SPAK and OSR1 has been implicated in the binding of RFXV motifs present in WNK kinases and SLC12 cotransporters (26), and thus, it may play a role in a key functional WNK4 interaction.

At least one of the short WNK4 variants observed in kidney lysates may be the product of a proteolytic event

The presence of two different kidney-specific short variants of the SPAK kinase has been described. McCormick *et al.* (28) reported the existence of an alternative transcript of SPAK that was identified through a 5'-RACE assay. Markadieu *et al.* (29) showed that a proteolytic activity present in kidney lysates produces a cleavage in SPAK that generates SPAK fragments truncated at the N terminus similar to those observed in kidney lysates. Interestingly, it was recently shown that kidney lysates of mice that express SPAK only in the DCT, from a transgene carrying SPAK's ORF, display the same pattern of bands in SPAK blots compared with those observed with lysates of WT mice. This suggests that the shorter variants of SPAK are primarily produced by proteolytic cleavage and are present in the DCT (3).

To investigate the origin of the short variants of WNK4 observed in kidney samples, we performed 3'-RACE assays designed to detect alternative transcripts that would produce WNK4 proteins lacking a portion of the C terminus (Table S3) (30). Only the previously described full-length transcript of WNK4 was successfully amplified by this method. In addition, we searched for alternative WNK4 transcripts in published

Kidney-specific WNK4 short variants and regulation by PP1

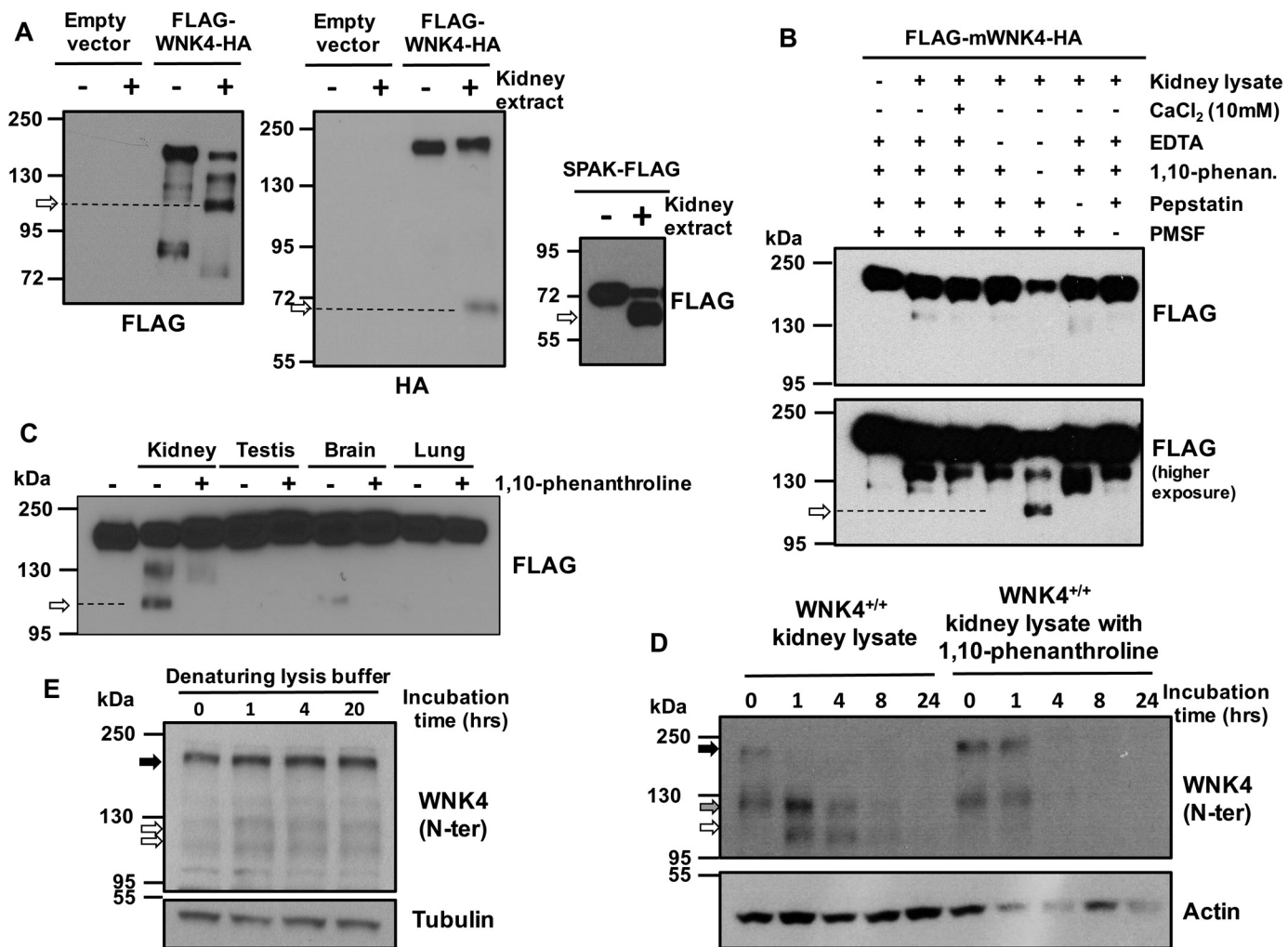


Figure 4. At least one of the short WNK4 variants observed in kidney lysates may be produced by a proteolytic event. **A**, FLAG-WNK4-HA (N- and C-terminal tags) and SPAK-FLAG (C-terminal tag) were immunopurified from HEK293 lysates and incubated with kidney lysates (70 mg) at 37 °C for 1.5 h. Western blots were performed with FLAG and HA antibodies as indicated. In the samples treated with kidney lysate, a decrease in the amount of full-length WNK4 and SPAK was observed, and a lower-sized band became apparent (white arrow), presumably due to a proteolytic cleavage event. For WNK4, lower-sized bands were observed with both FLAG and HA antibodies, suggesting that these bands may correspond to the N-terminal and C-terminal proteolytic fragments, respectively. This observation was reproducible in more than 10 independent experiments, some of which are presented in the following panels and in Fig. 5. **B**, proteolytic assays were performed as described in **A** in the presence of different protease inhibitors: phenylmethylsulfonyl fluoride (1 mM), pepstatin A (10 μM), EDTA (1 mM), and 1,10-phenanthroline (5 mM). The proteolytic event was only observed in the absence of 1,10-phenanthroline (indicated by a white arrow), suggesting that the protease responsible of this cleavage is Zn²⁺-dependent. The same observation was made in two independent experiments. **C**, proteolytic assays performed as described in **A** with lysates of different tissues. WNK4 cleavage is more prominent using kidney lysate (indicated by a white arrow). Four independent assays were performed with similar results. **D**, incubation of kidney lysates at room temperature promotes an increase in the abundance of the shortest WNK4 fragment (white arrow). This is prevented by the addition of 1,10-phenanthroline (5 mM). Other forms of WNK4 are indicated by black and gray arrows. Three independent assays were performed with similar results. WNK4 antibody A was used. **E**, a kidney lysate was prepared by immediate homogenization of frozen tissue in lysis buffer containing 1% SDS, which prevents all enzymatic activity. The short WNK4 variants were detected (white arrows), suggesting that they are not artificially produced during tissue lysis. WNK4 antibody A was used.

databases from mouse kidney RNA-Seq studies (GEO accession numbers GSE79443 (31) and GSE81055). Only one alternative transcript was found that lacks exons 14 and 15 (Fig. S4). This transcript, however, could not explain the short WNK4 variants that we observe in kidney lysates, because it would produce a protein containing a portion of the C-terminal domain that is absent in the short variants that we detect (Fig. 1).

We hypothesized that the short WNK4 variants could be produced by proteolytic events. Full-length WNK4 carrying a FLAG and HA epitopes at the N and C termini, respectively, was produced in HEK293 cells. Following immunopurification, FLAG-WNK4-HA was incubated with 70 μg of kidney lysate at 37 °C for 1.5 h. Incubation with kidney lysate reduced the

amount of full-length WNK4 detected with the FLAG antibody and produced a smaller band that ran between the 95 and 130 kDa markers (Fig. 4A). When probed with the HA antibody, a smaller band of approximately 70 kDa was also observed in the presence of kidney lysate (Fig. 4A). These small bands may correspond to the N-terminal and C-terminal proteolytic fragments, respectively. They were not detected in the lysate samples in the absence of FLAG-WNK4-HA (Fig. 4A), ruling them out as nonspecific bands recognized in the kidney lysate by these antibodies. As control, a SPAK proteolytic assay was performed in parallel using immunopurified SPAK-FLAG (C-terminal tag), and the previously reported proteolytic event was clearly observed (29).

To assess which type of protease is responsible for the cleavage, FLAG-WNK4-HA proteolytic assays were carried out in the presence of multiple combinations of protease inhibitors. The proteolytic event was only observed in the reaction lacking EDTA and 1,10-phenanthroline (Fig. 4B) and was not observed in the reaction containing EDTA and 1,10-phenanthroline in which Ca^{2+} was added in a concentration that exceeds the chelating capacity of EDTA (32). Moreover, previous reactions in which WNK4 cleavage was observed were carried out in the presence of the protease inhibitor mixture Complete (Roche Applied Science), which contains EDTA at low concentrations that are sufficient to chelate Ca^{2+} but not Zn^{2+} ions due to the lower affinity against the latter. These observations suggest that, similar to what was reported for SPAK (29), the protease responsible for the cleavage of WNK4 is probably a Zn^{2+} -dependent metalloprotease.

When lysates from different tissues were tested, the 1,10-phenanthroline-sensitive cleavage of WNK4 was noticeably more prominent upon incubation with kidney lysate than with other lysates (Fig. 4C). This is consistent with the expression pattern of the WNK4 short variants reported in Fig. 1C.

We then tested whether the proteolytic activity could be observed in endogenous WNK4 of mouse kidney lysates. Lysates were freshly prepared, and, immediately after homogenization, the lysate was split in two, and 1,10-phenanthroline was added to one of the tubes. Aliquots were then prepared from each tube that were incubated at 25 °C for the indicated amounts of time (Fig. 4D). In the absence of 1,10-phenanthroline, a decrease in the full-length band was observed after only 1 h of incubation, and, at this time point, the abundance of the band of lowest size already increased with respect to time 0 (Fig. 4D). This increase was not observed in the lysates treated with 1,10-phenanthroline, suggesting that the band of lowest size was generated by a proteolytic cleavage mediated by a Zn^{2+} -dependent protease. Generalized protein degradation was also observed, which explains the absence of band detection in the final time points.

Finally, given the observations just mentioned, we wanted to rule out the possibility that the short WNK4 bands observed in blots were produced as an artifact during lysate preparation, because this would mean that the short variants of WNK4 do not really exist within intact renal cells. To do this, a kidney lysate was prepared by immediate homogenization of frozen tissue in lysis buffer containing 1% SDS (33). This lysis method prevents all enzymatic activity. The short WNK4 variants were detected in this lysate (Fig. 4E), suggesting that they are not artificially produced during tissue lysis when WNK4 proteins come in contact with extracellular proteases or other proteases present in cell types that lack WNK4 expression.

Renal WNK4 short variants probably lack a SPAK-binding site and may be unable to phosphorylate SPAK

WNK4 *in vitro* proteolytic reactions were run in parallel to kidney lysates from WNK4^{+/+} and WNK4^{-/-} mice to compare the electrophoretic mobility of the WNK4 N-terminal fragment produced in proteolytic assays with that of the short WNK4 variants observed in lysates. Proteolytic reactions were performed using kidney lysates from WNK4^{-/-} mice. This

allowed us to use an antibody directed against a WNK4 N-terminal epitope to detect the proteolytic fragments without detecting any WNK4 signal from the lysates used for the proteolytic reaction. We observed that the WNK4 N-terminal proteolytic fragment runs at a height similar to that of the shortest WNK4 variant observed in WNK4^{+/+} kidney lysates (Fig. 5A). We then compared the electrophoretic mobility of the different variants of WNK4 observed in kidney lysates with that of several WNK4 mutant constructs truncated at the C terminus. The full-length WNK4 expressed in HEK293 cells presented an electrophoretic mobility similar to that of the full-length WNK4 observed in kidney lysates (Fig. 5B). The next WNK4 band observed in kidney lysates (the middle band) ran at a similar height as the WNK4-L866X mutant, and the shortest WNK4 kidney band ran faster than the WNK4-L866X mutant and slower than the WNK4-V740X mutant. Thus, assuming that the mobility of the renal WNK4 variants is not affected by an unknown modification or factor that is absent in HEK293 cells, or vice versa, we can conclude that the short renal WNK4 variants probably lack the C-terminal SPAK-binding motif (residues 996–999). According to the results presented in Fig. 2B, this would render them unable to phosphorylate SPAK.

Finally, with the purpose of narrowing down the segment of the protein containing the site in which WNK4 is cleaved *in vitro*, and probably *in vivo*, we generated new WNK4 mutants harboring deletions of different portions of the C terminus (Fig. 5C). We hypothesized that the *in vitro* cleavage would not be observed with the mutant lacking the cleavage site. As expected, all but one of the five deletion mutants were cleaved in *in vitro* proteolytic reactions, and cleavage was prevented by the addition of 1,10-phenanthroline (Fig. 5D). We failed to observe cleavage of the WNK4-Δ740–781 mutant, suggesting that the cleavage site may be present within the segment flanked by residues 740–781. Consistent with this conclusion, all three mutants harboring deletions of segments located downstream of the putative cleavage region produced N-terminal proteolytic fragments of a similar size to the one observed with the WNK4-WT. In contrast, the WNK4-Δ601–739 mutant produced an N-terminal proteolytic fragment of smaller size, presumably because in this mutant, the cleavage site is located downstream of the deletion, and thus the 601–739 region is normally located within the N-terminal proteolytic fragment.

Abundance of short WNK4 variants is not altered by changes in dietary Na^+ and K^+ content

Given that modifications in the dietary content of Na^+ and K^+ affect the activity of NCC and other targets of regulation of WNK4 (like ROMK and ENaC), we decided to test whether these dietary modifications could also affect the abundance of WNK4 isoforms, rationalizing that this could have an impact on the activity of the downstream targets. No changes were observed with the low- Na^+ diet, and an increase in the abundance of all isoforms was observed in mice given a low- K^+ diet (Fig. 6, A and B). The latter result is consistent with a previous report (34), and the changes observed are probably due to a decrease in KLHL3–CUL3–RING-mediated WNK4 degradation. However, no changes in the relative abundance

Kidney-specific WNK4 short variants and regulation by PP1

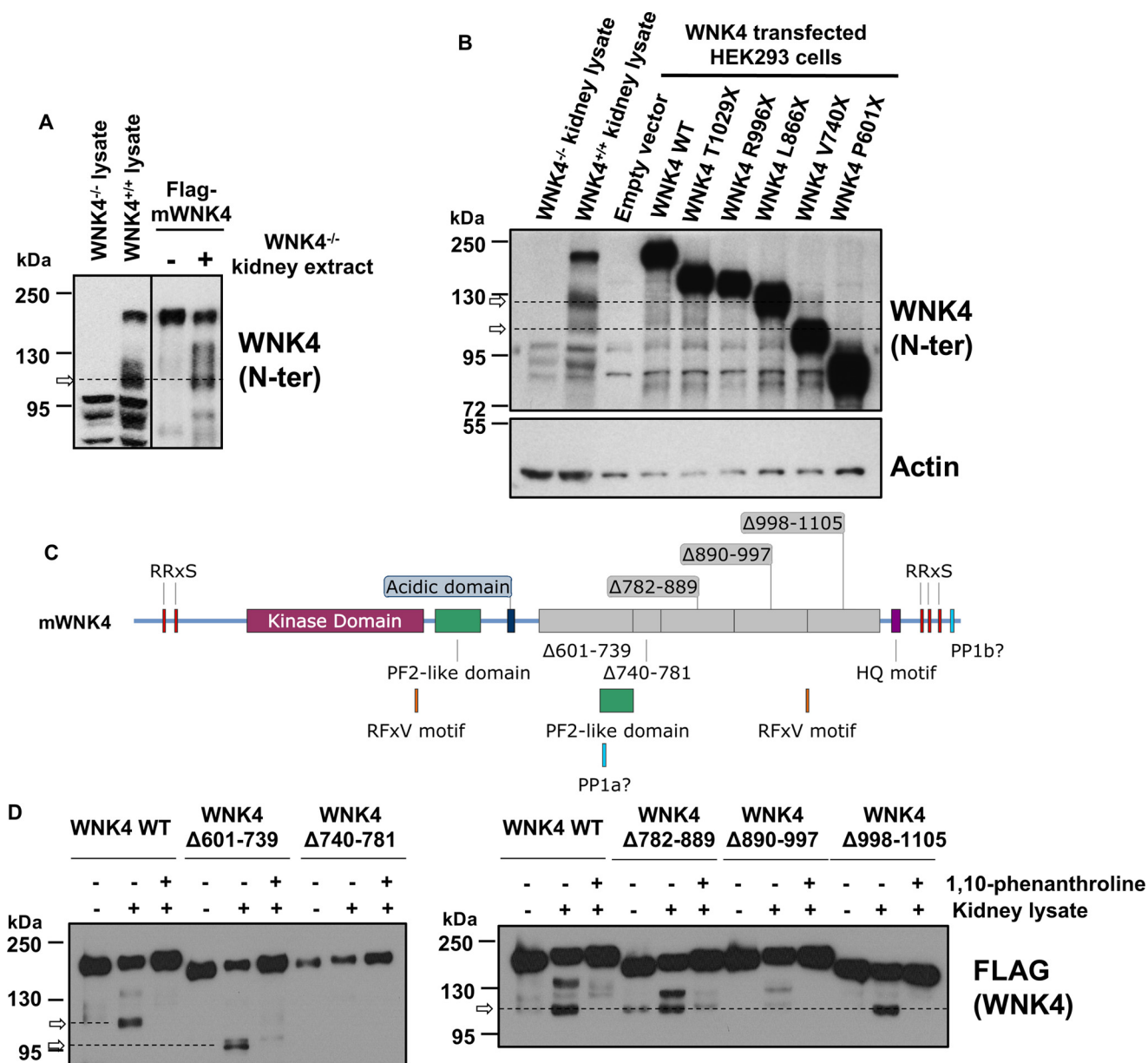


Figure 5. Size analysis of WNK4 short variants. A, Western blotting of WNK4^{+/+} and WNK4^{-/-} kidney lysates run in parallel with WNK4 proteolytic reactions (performed as in Fig. 4A, but using kidney lysates from WNK4^{-/-} mice) to compare the electrophoretic mobility of the WNK4 fragments with that of the short band that is product of the *in vitro* proteolytic cleavage (white arrow). For clarity, the blot image was split in two to present two different film exposure times. Three independent experiments were performed. WNK4 antibody A was used. B, Western blotting of WNK4^{+/+} and WNK4^{-/-} kidney lysates run in parallel with lysates of HEK293 cells transfected with different truncated WNK4 mutants. WNK4 antibody A was used. The electrophoretic mobility of the renal WNK4 short variants (white arrows) suggests that they may be around 740–866 amino acids long and might lack a SPAK-binding site. C, schematic representation of WNK4 constructs in which different segments were deleted to narrow down the region containing the cleavage site in WNK4. D, proteolytic assays performed with different WNK4 constructs harboring deletions in the C-terminal region. All constructs were cleaved upon incubation with kidney lysate (proteolytic fragment indicated by the white arrow), except for the one that lacks residues 740–782. This suggests that the cleavage site might be located within this segment of the protein. Four independent experiments were performed.

of WNK4 forms were observed, suggesting that the cleavage of WNK4 is not regulated in response to these dietary manipulations.

Finally, given that it is clear that WNK4 plays an important role in DCT physiology, we decided to analyze the expression of the WNK4 short variants in samples from DCT tubules isolated by COPASTM. Indeed, we were able to observe at least one of the short variants in these samples. Due to the low signal detected, it was unclear whether the second short variant is expressed in DCT cells.

Discussion

Kidney-specific isoforms of the kinases WNK1 and SPAK have been described. These isoforms present functional properties that differ from those of the full-length proteins (28, 35). Hence, their characterization has been important to understand the molecular pathways implicated in the regulation of renal salt transport. Similarly, the characterization of the WNK4 short variants described in this work may be important to gain a more accurate understanding of WNK4's role in kidney physiology.

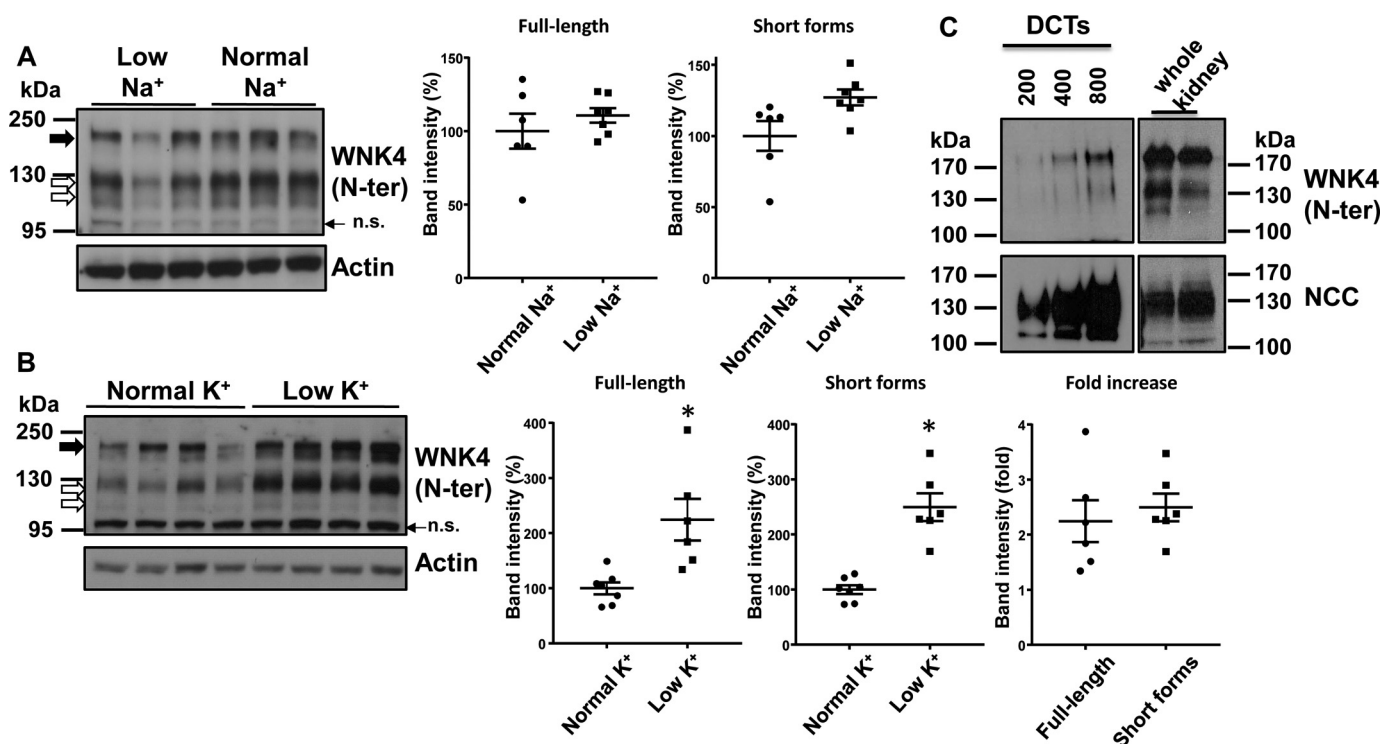


Figure 6. Effect of changes in dietary electrolyte intake on the abundance of renal WNK4 forms. A, WT C57Bl/6 mice were given normal Na⁺ diet ($n = 6$) or low Na⁺ diet ($n = 7$) for a period of 4 days. Kidney lysates were prepared and WNK4 Western blots were performed with an antibody directed against an N-terminal epitope (antibody A) (41). The full-length form is indicated with a *black arrow*. Short WNK4 variants are indicated with *white arrows*. *n.s.*, nonspecific bands. Results of quantitation of band intensities for the full-length and short forms of WNK4 are presented. Data are mean \pm S.E. (*error bars*). B, same as in A, but mice were fed with normal or low-K⁺ diets for 7 days ($n = 6$ for each group). Results of quantitation of band intensities for the full-length and short forms of WNK4 are presented. Data are mean \pm S.E. *, $p < 0.01$ versus normal K⁺. No apparent shift in the relative abundance of WNK4 forms was observed with any of these dietary manipulations. C, DCTs were enriched by COPAS (43) and then subjected to Western blot analysis. At least one of the short WNK4 fragments was observed. NCC blot was performed to confirm DCT enrichment.

Here, we used multiple antibodies for Western blotting assays and LC-MS/MS studies, which helped us to confirm that indeed short fragments of WNK4 are present in kidney lysates that lack a portion of the C-terminal domain (Fig. 1 and Fig. S1).

Given that alternative WNK4 transcripts that could explain the short WNK4 variants were not observed, we tested the possibility that they could be the product of a proteolytic event. Indeed, we observed that kidney lysates appear to possess proteolytic activity toward WNK4 and that this activity produces a band of a size similar to that of the shortest WNK4 variant observed *in vivo* (Figs. 4 and 5). This phenomenon was similar to the one characterized by Markadieu *et al.* (29) for the kinase SPAK: a proteolytic event giving rise to SPAK short variants that is observed upon incubation with kidney lysates, which was prevented by the addition of 1,10-phenanthroline, an inhibitor of Zn²⁺ metalloproteases (36). It remains unclear which is the protease responsible for the SPAK cleavage (37).

It should be noted that only one short WNK4 fragment was produced upon incubation of recombinant WNK4 with kidney lysates. Thus, the origin of only one of the two short WNK4 bands observed in kidney lysates may be explained by a proteolytic event. The second band may be the product of an alternative transcript that we failed to identify or the product of a proteolytic event that was not observed in the conditions tested.

Our experiments narrowed down the location of the cleavage site to a 41-residue-long segment of the protein (within resi-

dues 740–781) (Fig. 5). Cleavage in this region would produce a WNK4 fragment that would lack the C-terminal SPAK-binding site (26) and the HQ motif that is important for WNK homo- or heterodimerization (23, 24). The same would be true for the second short variant of larger size observed in kidney, based on its electrophoretic mobility. Thus, these short variants may be unable to autophosphorylate and to phosphorylate SPAK, so one possibility is that their generation may be a mechanism to inactivate the pathway. Another possibility is that they may play a role in the kinase activity-independent regulation of targets like ENaC and ROMK (11, 12), or in the SPAK-independent regulation of Slc12 cotransporters (26). Because no shift in the abundance of WNK4 forms was observed in mice exposed to low-Na⁺ or low-K⁺ diets, it is not yet clear whether this process is regulated. Further research will be necessary to understand the physiological significance of the WNK4 short variants. Interestingly, it has been recently reported that Zn²⁺ deficiency in DCT cells and in mice is associated with an increase in NCC expression and activity (38). Although the mechanism is currently unknown, one possibility is that Zn²⁺ depletion in DCT cells may lead to decreased WNK4 and SPAK cleavage and, thus, NCC activation.

Finally, it has been recognized that the PP1 phosphatase is an important regulator of the WNK-SPAK/OSR1-Slc12 pathway. For instance, it was shown that inhibition of PP1 activity by calyculin A prevents the activation of KCCs that is observed in the presence of kinase-inactive WNK3 (39) and inhibits the

Kidney-specific WNK4 short variants and regulation by PP1

activity of KCC4 observed in hypotonic conditions (40). Later, Lin *et al.* described two motifs within WNK4 that harbor the consensus sequence required for interaction with PP1, and they showed that elimination of these motifs prevents WNK4–PP1 co-immunoprecipitation (21). More recently, Frenette-Cotton *et al.* (40) showed that mutation of both of these motifs prevents WNK4's ability to inhibit KCC4, and, thus, they proposed that WNK4 inhibits PP1 activity, which translates into KCC4 down-regulation.

In the present work, the study of the short variants of WNK4 has led us to a more comprehensive characterization of the putative PP1-binding sites in WNK4. By directly analyzing the ability of the WNK4–PP1 binding mutants to phosphorylate SPAK and their phosphorylation levels in the presence of PP1, we have obtained robust results showing that PP1 α and PP1 γ are strong regulators of WNK4 activity by promoting WNK4 dephosphorylation (Fig. 3). We also observed that only the second KXVXF motif present in WNK4 (here termed PP1b) is necessary for PP1-mediated regulation of WNK4. Elimination of this site turned WNK4 into a constitutively active kinase, suggesting that WNK4 activity depends on the balance between phosphorylating stimuli (*e.g.* low intracellular chloride (14) or increased angiotensin II (16)) and dephosphorylating stimuli through PP1 α and PP1 γ . Of note, these results fit well with our previous description of a “negative signal regulatory domain” in WNK4 that comprises the terminal 50 residues of the protein (18).

Regarding the first KXVXF motif (PP1a), we show that it may not function as a PP1-binding site, because elimination of this site does not alter PP1-mediated WNK4 dephosphorylation. Instead, mutation of this site ablates WNK4 activity, even in the context of the high levels of WNK4 phosphorylation observed when both sites are mutated together (Fig. 3). Thus, we hypothesize that this loss of activity is due to disruption of a domain that is functionally important. Indeed, the PP1a site lies within a region of WNK4 that has been predicted to have a PF2-like fold similar to the one present in SPAK and OSR1. In these kinases, the PF2 domain constitutes the binding site for RFXV motifs present in WNK kinases and Slc12 transporters. Thus, although we cannot yet ascribe a particular role for this domain in WNK4, we can argue that the PP1a motif probably does not constitute a PP1-binding site. From this perspective, the results of Frenette-Cotton *et al.* (40) acquire a different interpretation; WNK4 is not a regulator of PP1, but instead, PP1 regulates WNK4 activity, and the observation that the WNK4 mutant with both putative PP1-binding sites eliminated is unable to inhibit KCC4 may be explained by the fact that this is a mutant that is unable to phosphorylate SPAK.

In conclusion, we have identified C-terminally truncated, kidney-specific, short variants of the kinase WNK4. At least one of these short variants appears to be a product of a proteolytic event, and our experiments suggest that they both probably lack a SPAK-binding site and an HQ motif. Thus, they are probably inactive, and their physiological relevance remains to be determined. Finally, this work has led us to the identification of a *bona fide* PP1-binding site in WNK4, which is located within the last 12 amino acid residues of the kinase. We have shown

that PP1 regulates WNK4 phosphorylation levels and, thus, WNK4 activity.

Experimental procedures

Mouse studies

Animal studies were approved by the animal care and use committees of our institutions. Most studies were performed in male WT C57BL/6 mice (age 12–16 weeks). WNK4-knockout mice and WNK4-PHAI transgenic mice were also used (C57BL/6 background) (4, 8). Teklad custom normal diet (containing 0.49% NaCl; TD.96208) and NaCl-deficient diet (TD.90228) were given for 4 days (8). Low-K⁺ (0% K⁺) diet was obtained from TestDiet (St. Louis, MO), whereas normal K⁺ was prepared by adding KCl to make a 1.2% K⁺ diet. Mice were given these modified diets for 7 days before being sacrificed.

Western blots

Tissues were snap-frozen in liquid nitrogen and later homogenized (250 mM sucrose, 10 mM triethanolamine, 1 \times protease inhibitors (Roche Applied Science), 1 \times phosphatase inhibitors (Sigma)). Protein concentration was determined by the BCA protein assay (Pierce). Protein extracts were subjected to SDS-PAGE and transferred to polyvinylidene difluoride membranes. Membranes were blocked for 1 h in 10% (w/v) nonfat milk dissolved in TBS-Tween 20 (TBSt). Antibodies were diluted in TBSt containing 5% (w/v) nonfat milk. Membranes were incubated with primary antibodies overnight at 4 °C and with HRP-coupled secondary antibodies at 25 °C for 1 h. Signals were detected with enhanced chemiluminescence reagent. Immunoblots were developed using film.

The following antibodies were used: WNK4 (N-terminal epitope, raised in rabbit, generated by Dr. David H. Ellison's group (41), antibody A); tubulin (Sigma, T5168, raised in mouse); actin (Santa Cruz Biotechnology, Inc., sc-1616 HRP, raised in goat); HA (Sigma, H6533, raised in mouse); FLAG (Sigma, A8592, raised in mouse); pRRXS (Cell Signaling, 9624 (16), raised in rabbit); sheep-HRP (Jackson ImmunoResearch); and rabbit-HRP (Jackson ImmunoResearch). Several antibodies were obtained from the Medical Research Council phosphorylation unit at Dundee University (all are polyclonal antibodies raised in sheep): WNK4 (C-terminal epitope, S064B (8), antibody B); WNK4 (N-terminal epitope, S121B (41), antibody C); pSPAK-Ser-373 (S670B) (42); and NCC (S965B) (8). The specificity of all antibodies used has been previously tested.

COPAS

Isolation of DCT has been described previously (43). Briefly, mice expressing enhanced GFP under the PV promoter were anesthetized and perfused with ice-cold Krebs buffer. Kidney cortex was finely minced before incubation in digestion solution (1 mg/ml collagenase type 1 and 2,000 units/ml hyaluronidase in Krebs buffer, pH 7.3) for 15 min at 37 °C. Tubules collected from digestion reactions were placed on ice and sorted by the COPAS. Each suspension of fluorescent tubules was collected in a 1.5-ml Eppendorf tube, previously coated with 0.5% (w/v) BSA in PBS/NaOH, pH 7.4. Tubules were lysed with Laemmli buffer.

Mass spectrometry

Mouse kidney lysates were prepared as described above. For WNK4 immunoprecipitation, 1 mg of lysate was incubated with 10 μ g of sheep anti-WNK4 antibody (MRC Dundee S121B) (23) and Protein A/G magnetic beads (Pierce) for 2 h at 4 °C. Beads were washed five times with a buffer containing 0.025 M Tris, pH 7.4, 0.15 M NaCl, 0.001 M EDTA, 1% Nonidet P40, 5% glycerol. Bound proteins were eluted by incubation in glycine buffer, pH 2, for 10 min and then prepared for SDS-PAGE. Bands were excised from the gel and processed at the MS and Proteomics Resource at Yale. Briefly, on a tilt table, the gel band was washed with 1) 250 μ l of 50% acetonitrile for 5 min, followed by 2) 250 μ l of 50% acetonitrile containing 50 mM NH_4HCO_3 for 10–30 min, and then finally with 3) 250 μ l of 50% acetonitrile containing 10 mM NH_4HCO_3 for 10–30 min. The final wash was removed, and the gel was SpeedVac-dried. 60 μ l of a 1:15 dilution of a 0.1 mg/ml trypsin stock solution was added to the gel and allowed to absorb for 10 min. An additional volume of 10 mM NH_4HCO_3 was added to cover the gel pieces and then incubated at 37 °C for 18 h. Peptides were then extracted by adding 250 μ l of 0.1% TFA, 80% acetonitrile and shaking for 30 min. Extract was transferred to a new tube and dried. Dried peptide pellet was dissolved in 70% formic acid, diluted with 0.1% TFA, and finally subjected to LC-MS/MS analysis using the LTQ Orbitrap XL that is equipped with a Waters nanoACQUITY UPLC system and uses a Waters Symmetry C18 180 μ m \times 20-mm trap column and a 1.7 μ m, 75 μ m \times 250-mm nanoACQUITY UPLC column for peptide separation. The acquired data were peak-picked and searched using the Mascot Distiller and the Mascot search algorithm, respectively. Protein identification was achieved using the Mascot search algorithm (Matrix Science) as described (44), and MS spectral features were searched against the SWISSPROT Mouse database along with a user-generated WNK4 protein database.

Cell culture

HEK293 cells (ATCC® CRL-1573) were used for transient transfection of mWNK4-HA, FLAG-mWNK4 (16), HA-SPAK, SPAK-FLAG (FLAG inserted in the C-terminal by FastCloning (45)), and FLAG-PP1- α , - β , and - γ (kindly provided by Dr. Jeremy Nichols) (46). Cells were grown to 70–80% confluence and transfected with Lipofectamine 2000 (Life Technologies, Inc.). Mutations were introduced into the WNK4 clone by site-directed mutagenesis using Phusion® high-fidelity DNA polymerase (New England Biolabs) and confirmed by Sanger sequencing. Deletions were performed by FastCloning (45). 48 h after transfection, cells were lysed with a lysis buffer containing 50 mM Tris·HCl (pH 7.5), 1 mM EGTA, 1 mM EDTA, 50 mM sodium fluoride, 5 mM sodium pyrophosphate, 1 mM sodium orthovanadate, 1% (w/v) Nonidet P-40, 270 mM sucrose, 0.1% (v/v) 2-mercaptoethanol, and protease inhibitors (Complete tablets; Roche Applied Science), and protein concentration was quantified.

In vitro proteolytic assays

Recombinant FLAG-mWNK4-HA was immunoprecipitated using a FLAG® Immunoprecipitation Kit (FLAGIPT1, Sigma).

After washing the beads, 70 μ g of kidney lysate (prepared with lysis buffer containing 125 mM NaCl, 10% glycerol, 1 mM EGTA, 1 mM EDTA, 1 mM phenylmethylsulfonyl fluoride, 10 μ M leupeptin, 4 μ M aprotinin, 10 μ M pepstatin, 1% Triton X-100, 0.5% SDS, 20 mM HEPES, pH 7.4) was added to the beads and incubated for 90 min at 37 °C (final reaction volume of 30 μ l in 50 mM HEPES, 140 mM NaCl, pH 7.4, with protease inhibitors as indicated). Reactions were stopped by adding Laemmli buffer and heating at 95 °C for 10 min. Eluates were used for Western blotting assays.

Statistical analysis

For comparison between two groups, unpaired Student's *t* test (two-tailed) was used. For comparison between multiple groups, analysis of variance tests were performed, followed by Tukey post hoc tests. A difference between groups was considered significant when *p* < 0.05.

Na⁺ uptake experiments

The use of *X. laevis* frogs was approved by our institutional committee on animal research. NCC activity was assessed in *X. laevis* oocytes microinjected with NCC cRNA alone or together with WT WNK4 or WNK4-T1029X. Two days post-injection, the thiazide-sensitive Na⁺ uptake was assessed as described previously (9). Briefly, ²²Na⁺ tracer uptake was assessed in groups of 10–15 oocytes. A 30-min incubation at 32 °C in a Cl⁻-free ND96 medium containing 1 mM ouabain, 0.1 mM amiloride, and 0.1 mM bumetanide was followed by a 60-min uptake period in a K⁺-free NaCl medium (40 mM NaCl, 56 mM sodium gluconate, 4.0 mM CaCl₂, 1.0 mM MgCl₂, and 5.0 mM HEPES, pH 7.4) containing ouabain, amiloride, bumetanide, and 2 μ Ci of ²²Na⁺/ml. Oocytes were washed five times in ice-cold uptake solution to remove tracer in the extracellular fluid. Individual oocytes were dissolved in 10% SDS, and the tracer activity was determined for each oocyte by β -scintillation counting.

Author contributions—A. R. M.-d.-O., C.-L. Y., D. E., G. G., and M. C. B. conceptualization; A. R. M.-d.-O., K. L. S., C.-L. Y., and M. C. B. formal analysis; A. R. M.-d.-O., A. R.-G., S. B.-V., K. L.-R., N. V., D. P.-A., I. A. D.-L. R.-V., A. W., K. L. S., J. Z., C.-L. Y., and M. C. B. investigation; A. R. M.-d. O., I. A. D.-L. R.-V., and M. C. B. visualization; A. R. M.-d. O., I. A. D.-L. R.-V., J. L., and M. C. B. methodology; A. R. M.-d. O., G. G., and M. C. B. writing-original draft; A. W. and J. L. resources; R. P. L., C.-L. Y., D. E., G. G., and M. C. B. supervision; R. P. L., C.-L. Y., D. E., G. G., and M. C. B. funding acquisition; M. C. B. project administration; M. C. B. writing-review and editing.

Acknowledgments—We thank Dr. Jeremy Nichols (Parkinson's Institute and Clinical Center, Sunnyvale, CA) for kindly providing the PP1 clones. We also thank Mary LoPresti, Jean Kanyo, and Dr. TuKiet Lam from the MS and Proteomics Resource at Yale University for assistance in the MS sample preparation, data collection, and MS methodology write-up, respectively.

References

1. Kahle, K. T., Gimenez, I., Hassan, H., Wilson, F. H., Wong, R. D., Forbush, B., Aronson, P. S., and Lifton, R. P. (2004) WNK4 regulates apical and

Kidney-specific WNK4 short variants and regulation by PP1

- basolateral Cl⁻ flux in extrarenal epithelia. *Proc. Natl. Acad. Sci. U.S.A.* **101**, 2064–2069 [CrossRef Medline](#)
- Wilson, F. H., Disse-Nicodème, S., Choate, K. A., Ishikawa, K., Nelson-Williams, C., Desitter, I., Gunel, M., Milford, D. V., Lipkin, G. W., Achard, J. M., Feely, M. P., Dussol, B., Berland, Y., Unwin, R. J., Mayan, H., et al. (2001) Human hypertension caused by mutations in WNK kinases. *Science* **293**, 1107–1112 [CrossRef Medline](#)
 - Grimm, P. R., Coleman, R., Delpire, E., and Welling, P. A. (2017) Constitutively active SPAK causes hyperkalemia by activating NCC and remodeling distal tubules. *J. Am. Soc. Nephrol.* **28**, 2597–2606 [CrossRef Medline](#)
 - Lalioti, M. D., Zhang, J., Volkman, H. M., Kahle, K. T., Hoffmann, K. E., Toka, H. R., Nelson-Williams, C., Ellison, D. H., Flavell, R., Booth, C. J., Lu, Y., Geller, D. S., and Lifton, R. P. (2006) Wnk4 controls blood pressure and potassium homeostasis via regulation of mass and activity of the distal convoluted tubule. *Nat. Genet.* **38**, 1124–1132 [CrossRef Medline](#)
 - Zhang, C., Wang, L., Su, X.-T., Zhang, J., Lin, D.-H., and Wang, W.-H. (2016) ENaC and ROMK activity are inhibited in the DCT2/CNT of TgWnk4PHAI mice. *Am. J. Physiol. Renal Physiol.* **312**, F622–F688
 - Shibata, S., Zhang, J., Puthumana, J., Stone, K. L., and Lifton, R. P. (2013) Kelch-like 3 and Cullin 3 regulate electrolyte homeostasis via ubiquitination and degradation of WNK4. *Proc. Natl. Acad. Sci. U.S.A.* **110**, 7838–7843 [CrossRef Medline](#)
 - Wakabayashi, M., Mori, T., Isobe, K., Sahara, E., Susa, K., Araki, Y., Chiga, M., Kikuchi, E., Nomura, N., Mori, Y., Matsuo, H., Murata, T., Nomura, S., Asano, T., Kawaguchi, H., Nonoyama, S., Rai, T., Sasaki, S., and Uchida, S. (2013) Impaired KLHL3-mediated ubiquitination of WNK4 causes human hypertension. *Cell Rep.* **3**, 858–868 [CrossRef Medline](#)
 - Castañeda-Bueno, M., Cervantes-Pérez, L. G., Vázquez, N., Uribe, N., Kantesaria, S., Morla, L., Bobadilla, N. A., Doucet, A., Alessi, D. R., and Gamba, G. (2012) Activation of the renal Na⁺:Cl⁻ cotransporter by angiotensin II is a WNK4-dependent process. *Proc. Natl. Acad. Sci. U.S.A.* **109**, 7929–7934 [CrossRef Medline](#)
 - Pacheco-Alvarez, D., Cristóbal, P. S., Meade, P., Moreno, E., Vazquez, N., Muñoz, E., Díaz, A., Juárez, M. E., Giménez, I., and Gamba, G. (2006) The Na⁺:Cl⁻ cotransporter is activated and phosphorylated at the amino-terminal domain upon intracellular chloride depletion. *J. Biol. Chem.* **281**, 28755–28763 [CrossRef Medline](#)
 - Richardson, C., Rafiqi, F. H., Karlsson, H. K. R., Moleleki, N., Vandewalle, A., Campbell, D. G., Morrice, N. A., and Alessi, D. R. (2008) Activation of the thiazide-sensitive Na⁺-Cl⁻ cotransporter by the WNK-regulated kinases SPAK and OSR1. *J. Cell Sci.* **121**, 675–684 [CrossRef Medline](#)
 - Kahle, K. T., Wilson, F. H., Leng, Q., Lalioti, M. D., O'Connell, A. D., Dong, K., Rapson, A. K., MacGregor, G. G., Giebisch, G., Hebert, S. C., and Lifton, R. P. (2003) WNK4 regulates the balance between renal NaCl reabsorption and K⁺ secretion. *Nat. Genet.* **35**, 372–376 [CrossRef Medline](#)
 - Ring, A. M., Cheng, S. X., Leng, Q., Kahle, K. T., Rinehart, J., Lalioti, M. D., Volkman, H. M., Wilson, F. H., Hebert, S. C., and Lifton, R. P. (2007) WNK4 regulates activity of the epithelial Na⁺ channel *in vitro* and *in vivo*. *Proc. Natl. Acad. Sci. U.S.A.* **104**, 4020–4024 [CrossRef Medline](#)
 - Piala, A. T., Moon, T. M., Akella, R., He, H., Cobb, M. H., and Goldsmith, E. J. (2014) Chloride sensing by WNK1 involves inhibition of autophosphorylation. *Sci. Signal.* **7**, ra41 [CrossRef Medline](#)
 - Bazúa-Valenti, S., Chávez-Canales, M., Rojas-Vega, L., González-Rodríguez, X., Vázquez, N., Rodríguez-Gama, A., Argaiz, E. R., Melo, Z., Plata, C., Ellison, D. H., García-Valdés, J., Hadchouel, J., and Gamba, G. (2015) The effect of WNK4 on the Na⁺-Cl⁻ cotransporter is modulated by intracellular chloride. *J. Am. Soc. Nephrol.* **26**, 1781–1786 [CrossRef Medline](#)
 - Terker, A. S., Zhang, C., McCormick, J. A., Lazelle, R. A., Zhang, C., Meermeier, N. P., Siler, D. A., Park, H. J., Fu, Y., Cohen, D. M., Weinstein, A. M., Wang, W. H., Yang, C. L., and Ellison, D. H. (2015) Potassium modulates electrolyte balance and blood pressure through effects on distal cell voltage and chloride. *Cell Metab.* **21**, 39–50 [CrossRef Medline](#)
 - Castañeda-Bueno, M., Arroyo, J. P., Zhang, J., Puthumana, J., Yarborough, O., 3rd, Shibata, S., Rojas-Vega, L., Gamba, G., Rinehart, J., and Lifton, R. P. (2017) Phosphorylation by PKC and PKA regulate the kinase activity and downstream signaling of WNK4. *Proc. Natl. Acad. Sci. U.S.A.* **114**, E879–E886 [CrossRef Medline](#)
 - San-Cristobal, P., Ponce-Coria, J., Vázquez, N., Bobadilla, N. A., and Gamba, G. (2008) WNK3 and WNK4 amino-terminal domain defines their effect on the renal Na⁺-Cl⁻ cotransporter. *Am. J. Physiol. Renal Physiol.* **295**, F1199–F1206 [CrossRef Medline](#)
 - Yang, C. L., Zhu, X., Wang, Z., Subramanya, A. R., and Ellison, D. H. (2005) Mechanisms of WNK1 and WNK4 interaction in the regulation of thiazide-sensitive NaCl cotransport. *J. Clin. Invest.* **115**, 1379–1387 [CrossRef Medline](#)
 - Ring, A. M., Leng, Q., Rinehart, J., Wilson, F. H., Kahle, K. T., Hebert, S. C., and Lifton, R. P. (2007) An SGK1 site in WNK4 regulates Na⁺ channel and K⁺ channel activity and has implications for aldosterone signaling and K⁺ homeostasis. *Proc. Natl. Acad. Sci. U.S.A.* **104**, 4025–4029 [CrossRef Medline](#)
 - Gagnon, K. B., and Delpire, E. (2012) Molecular physiology of SPAK and OSR1: two Ste20-related protein kinases regulating ion transport. *Physiol. Rev.* **92**, 1577–1617 [CrossRef Medline](#)
 - Lin, D.-H., Yue, P., Rinehart, J., Sun, P., Wang, Z., Lifton, R., and Wang, W.-H. (2012) Protein phosphatase 1 modulates the inhibitory effect of With-no-Lysine kinase 4 on ROMK channels. *Am. J. Physiol. Renal Physiol.* **303**, F110–F119 [CrossRef Medline](#)
 - Piechotta, K., Lu, J., and Delpire, E. (2002) Cation chloride cotransporters interact with the stress-related kinases Ste20-related proline-alanine-rich kinase (SPAK) and oxidative stress response 1 (OSR1). *J. Biol. Chem.* **277**, 50812–50819 [CrossRef Medline](#)
 - Thastrup, J. O., Rafiqi, F. H., Vitari, A. C., Pozo-Guisado, E., Deak, M., Mehellou, Y., and Alessi, D. R. (2012) SPAK/OSR1 regulate NKCC1 and WNK activity: analysis of WNK isoform interactions and activation by T-loop trans-autophosphorylation. *Biochem. J.* **441**, 325–337 [CrossRef Medline](#)
 - Chávez-Canales, M., Zhang, C., Soukaseum, C., Moreno, E., Pacheco-Alvarez, D., Vidal-Petiot, E., Castañeda-Bueno, M., Vázquez, N., Rojas-Vega, L., Meermeier, N. P., Rogers, S., Jeunemaitre, X., Yang, C. L., Ellison, D. H., Gamba, G., and Hadchouel, J. (2014) WNK-SPAK-NCC cascade revisited: WNK1 stimulates the activity of the Na-Cl cotransporter via SPAK, an effect antagonized by WNK4. *Hypertension* **64**, 1047–1053 [CrossRef Medline](#)
 - Wilson, F. H., Kahle, K. T., Sabath, E., Lalioti, M. D., Rapson, A. K., Hoover, R. S., Hebert, S. C., Gamba, G., and Lifton, R. P. (2003) Molecular pathogenesis of inherited hypertension with hyperkalemia: the Na-Cl cotransporter is inhibited by wild-type but not mutant WNK4. *Proc. Natl. Acad. Sci. U.S.A.* **100**, 680–684 [CrossRef Medline](#)
 - Ponce-Coria, J., Markadieu, N., Austin, T. M., Flammang, L., Rios, K., Welling, P. A., and Delpire, E. (2014) A novel Ste20-related proline/alanine-rich kinase (SPAK)-independent pathway involving calcium-binding protein 39 (Cab39) and serine threonine kinase with no lysine member 4 (WNK4) in the activation of Na-K-Cl cotransporters. *J. Biol. Chem.* **289**, 17680–17688 [CrossRef Medline](#)
 - Shi, Y. (2009) Serine/threonine phosphatases: mechanism through structure. *Cell* **139**, 468–484 [CrossRef Medline](#)
 - McCormick, J. A., Mutig, K., Nelson, J. H., Saritas, T., Hoorn, E. J., Yang, C. L., Rogers, S., Curry, J., Delpire, E., Bachmann, S., and Ellison, D. H. (2011) A SPAK isoform switch modulates renal salt transport and blood pressure. *Cell Metab.* **14**, 352–364 [CrossRef Medline](#)
 - Markadieu, N., Rios, K., Spiller, B. W., McDonald, W. H., Welling, P. A., and Delpire, E. (2014) Short forms of Ste20-related proline/alanine-rich kinase (SPAK) in the kidney are created by aspartyl aminopeptidase (Dnpep)-mediated proteolytic cleavage. *J. Biol. Chem.* **289**, 29273–29284 [CrossRef Medline](#)
 - Scotto-Lavino, E., Du, G., and Frohman, M. A. (2006) 3'-End cDNA amplification using classic RACE. *Nat. Protoc.* **1**, 2742–2745 [CrossRef Medline](#)
 - Arvaniti, E., Moulos, P., Vakrakou, A., Chatziantoniou, C., Chadjichristos, C., Kavvadas, P., Charonis, A., and Politis, P. K. (2016) Whole-transcriptome analysis of UO mouse model of renal fibrosis reveals new molecular players in kidney diseases. *Sci. Rep.* **6**, 26235 [CrossRef Medline](#)
 - Beynon, R., and Bond, J. S. (2000) *Proteolytic Enzymes*, 2nd Ed., pp. 105–130, Oxford University Press, Oxford, UK

33. Xiao, Y., Pollack, D., Nieves, E., Winchell, A., Callaway, M., and Vigodner, M. (2015) Can your protein be sumoylated? A quick summary and important tips to study SUMO-modified proteins. *Anal. Biochem.* **477**, 95–97 [CrossRef Medline](#)
34. Ishizawa, K., Xu, N., Loffing, J., Lifton, R. P., Fujita, T., Uchida, S., and Shibata, S. (2016) Potassium depletion stimulates Na-Cl cotransporter via phosphorylation and inactivation of the ubiquitin ligase Kelch-like 3. *Biochem. Biophys. Res. Commun.* **480**, 745–751 [CrossRef Medline](#)
35. Argaiz, E. R., Chavez-Canales, M., Ostrosky-Frid, M., Rodriguez-Gama, A., Vazquez, N., Gonzalez-Rodriguez, X., Garcia-Valdes, J., Hadchouel, J., Ellison, D. H., and Gamba, G. (2018) Kidney-specific WNK1 isoform (KS-WNK1) is a potent activator of WNK4 and NCC. *Am. J. Physiol. Renal Physiol.* [CrossRef Medline](#)
36. Correa, L. M., Cho, C., Myles, D. G., and Primakoff, P. (2000) A role for a TIMP-3-sensitive, Zn²⁺-dependent metalloprotease in mammalian gamete membrane fusion. *Dev. Biol.* **225**, 124–134 [CrossRef Medline](#)
37. Koumangoye, R., and Delpire, E. (2017) DNPEP is not the only peptidase that produces SPAK fragments in kidney. *Physiol. Rep.* **5**, e13479 [CrossRef Medline](#)
38. Williams, C. R., Mistry, M., Mallick, R., Mistry, A., Ko, B., Gooch, J. L., and Hoover, R. S. (2017) Sodium chloride cotransporter upregulation in settings of zinc deficiency offers new insight into blood pressure dysregulation in chronic diseases. *FASEB J.* **31**, 855.1
39. de Los Heros, P., Kahle, K. T., Rinehart, J., Bobadilla, N. A., Vázquez, N., San Cristobal, P., Mount, D. B., Lifton, R. P., Hebert, S. C., and Gamba, G. (2006) WNK3 bypasses the tonicity requirement for K-Cl cotransporter activation via a phosphatase-dependent pathway. *Proc. Natl. Acad. Sci. U.S.A.* **103**, 1976–1981 [CrossRef Medline](#)
40. Frenette-Cotton, R., Marcoux, A.-A., Garneau, A. P., Noel, M., and Isenring, P. (2018) Phosphoregulation of K⁺-Cl⁻ cotransporters during cell swelling: novel insights. *J. Cell Physiol.* [CrossRef Medline](#)
41. Yang, C. L., Liu, X., Paliege, A., Zhu, X., Bachmann, S., Dawson, D. C., and Ellison, D. H. (2007) WNK1 and WNK4 modulate CFTR activity. *Biochem. Biophys. Res. Commun.* **353**, 535–540 [CrossRef Medline](#)
42. Rafiqi, F. H., Zuber, A. M., Glover, M., Richardson, C., Fleming, S., Jouanouić, S., Jouanouić, S., O'Shaughnessy, K. M., and Alessi, D. R. (2010) Role of the WNK-activated SPAK kinase in regulating blood pressure. *EMBO Mol. Med.* **2**, 63–75 [CrossRef Medline](#)
43. Markadieu, N., San-Cristobal, P., Nair, A. V., Verkaart, S., Lenssen, E., Tudpor, K., van Zeeland, F., Loffing, J., Bindels, R. J. M., and Hoenderop, J. G. J. (2012) A primary culture of distal convoluted tubules expressing functional thiazide-sensitive NaCl transport. *Am. J. Physiol. Renal Physiol.* **303**, F886–F892 [CrossRef Medline](#)
44. Krishnan, N., Lam, T. T., Fritz, A., Rempinski, D., O'Loughlin, K., Minderman, H., Berezney, R., Marzluff, W. F., and Thapar, R. (2012) The prolyl isomerase Pin1 targets stem-loop binding protein (SLBP) to dissociate the SLBP-histone mRNA complex linking histone mRNA decay with SLBP ubiquitination. *Mol. Cell Biol.* **32**, 4306–4322 [CrossRef Medline](#)
45. Li, C., Wen, A., Shen, B., Lu, J., Huang, Y., and Chang, Y. (2011) Fast Cloning: a highly simplified, purification-free, sequence- and ligation-independent PCR cloning method. *BMC Biotechnol.* **11**, 92 [CrossRef Medline](#)
46. Lobbstaël, E., Zhao, J., Rudenko, I. N., Beylina, A., Gao, F., Wetter, J., Beullens, M., Bollen, M., Cookson, M. R., Baekelandt, V., Nichols, R. J., and Taymans, J.-M. (2013) Identification of protein phosphatase 1 as a regulator of the LRRK2 phosphorylation cycle. *Biochem. J.* **456**, 119–128 [CrossRef Medline](#)
47. Villa, F., Goebel, J., Rafiqi, F. H., Deak, M., Thastrup, J., Alessi, D. R., and van Aalten, D. M. F. (2007) Structural insights into the recognition of substrates and activators by the OSR1 kinase. *EMBO Rep.* **8**, 839–845 [CrossRef Medline](#)

C-terminally truncated, kidney-specific variants of the WNK4 kinase lack several sites that regulate its activity

Adrián Rafael Murillo-de-Ozores, Alejandro Rodríguez-Gama, Silvana Bazúa-Valenti, Karla Leyva-Ríos, Norma Vázquez, Diana Pacheco-Álvarez, Inti A. De La Rosa-Velázquez, Agnieszka Wengi, Kathryn L. Stone, Junhui Zhang, Johannes Loffing, Richard P. Lifton, Chao-Ling Yang, David H. Ellison, Gerardo Gamba and Maria Castañeda-Bueno

J. Biol. Chem. 2018, 293:12209-12221.

doi: 10.1074/jbc.RA118.003037 originally published online June 19, 2018

Access the most updated version of this article at doi: [10.1074/jbc.RA118.003037](https://doi.org/10.1074/jbc.RA118.003037)

Alerts:

- [When this article is cited](#)
- [When a correction for this article is posted](#)

[Click here](#) to choose from all of JBC's e-mail alerts

This article cites 46 references, 22 of which can be accessed free at <http://www.jbc.org/content/293/31/12209.full.html#ref-list-1>

Supporting information.

C-terminally truncated, kidney-specific variants of the WNK4 kinase lack several sites that regulate its activity

Research article

Adrián Rafael Murillo-de-Ozores^a, Alejandro Rodríguez-Gama^b, Silvana Bazúa-Valenti^b, Karla Leyva-Ríos^c, Norma Vázquez^b, Diana Pacheco-Álvarez^c, Inti A. De La Rosa-Velázquez^d, Agnieszka Wengi^e, Kathryn L. Stone^f, Junhui Zhang^g, Johannes Loffing^e, Richard P. Lifton^{g,h}, Chao-Ling Yang^{l,j}, David H. Ellison^{l,j}, Gerardo Gamba^{b,k,l}, Maria Castañeda-Bueno^k.

Molecular Physiology Unit, ^aFacultad de Medicina and ^bInstituto de Investigaciones Biomédicas, Universidad Nacional Autónoma de México, Mexico City 14080, Mexico. ^cEscuela de Medicina, Universidad Panamericana, Mexico City 03920, Mexico. ^dGenomics Laboratory, RAI, Universidad Nacional Autónoma de México-Instituto Nacional de Ciencias Médicas y Nutrición Salvador Zubirán, Mexico City 14080, Mexico. ^eInstitute of Anatomy and Swiss National Centre of Competence in Research 'Kidney Control of Homeostasis', University of Zurich, Zurich 8057, Switzerland. ^fMS & Proteomics Resource, WM Keck Biotechnology Resource Laboratory and ^gDepartment of Genetics, Yale University School of Medicine, New Haven 06510, CT, USA. ^hLaboratory of Human Genetics and Genomics, The Rockefeller University, New York, NY 10065, USA. ⁱDivision of Nephrology & Hypertension, Department of Medicine, Oregon Health & Science University, Portland 97239, OR, USA. ^jVA Portland Health Care System, Portland, OR, USA. ^kDepartment of Nephrology and Mineral Metabolism, Instituto Nacional de Ciencias Médicas y Nutrición Salvador Zubirán, Mexico City 14080, Mexico. ^lTecnológico de Monterrey, Escuela de Medicina y Ciencias de la Salud, Monterrey 64710, NL, Mexico.

Materials included

1. Figure S1
2. Figure S2
3. Figure S3
4. Figure S4
5. Table S1
6. Table S2
7. Table S3

Figure S1.

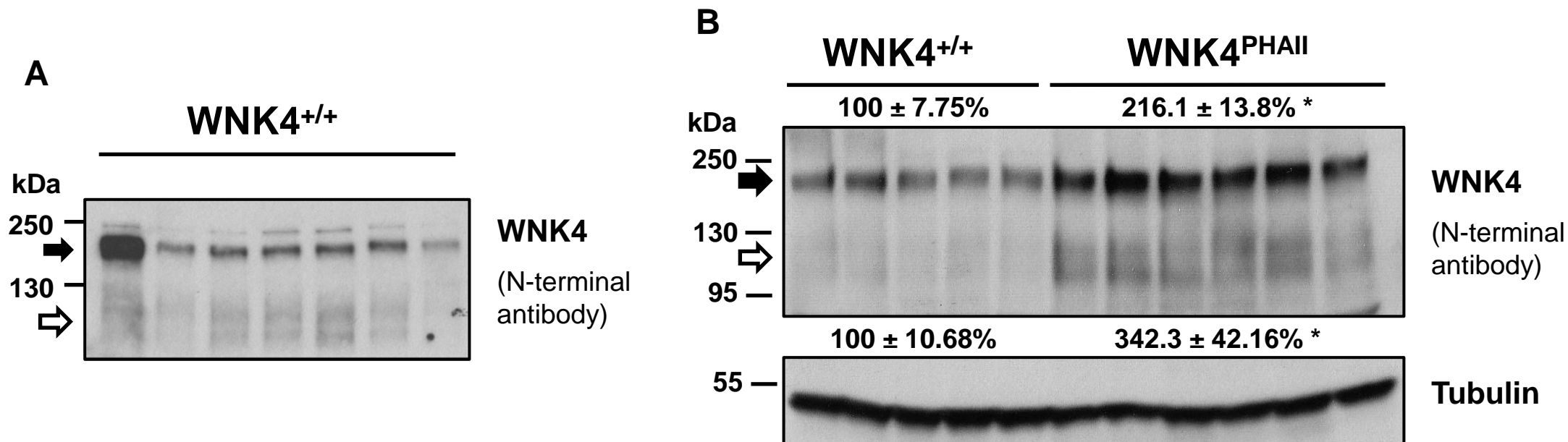


Figure S1. (A) Western blot of mouse kidney lysates using an antibody that recognizes an N-terminal epitope of WNK4 (residues 2-25 of mouse WNK4) (antibody C) (1). In addition to the band corresponding to the full-length WNK4, this antibody detects at least two additional bands that run between the 130 and 95 kDa marker bands. **(B)** Western blot of kidney lysates from TgWNK4^{PHAll} mice (2) performed with the same antibody as in fig.1A. TgWNK4^{PHAll} mice show higher expression of full-length WNK4. The small-sized bands also show higher intensity. Results of quantitation are displayed above and below the blot for the upper and lower bands respectively. *P<0.001.

Figure S2.

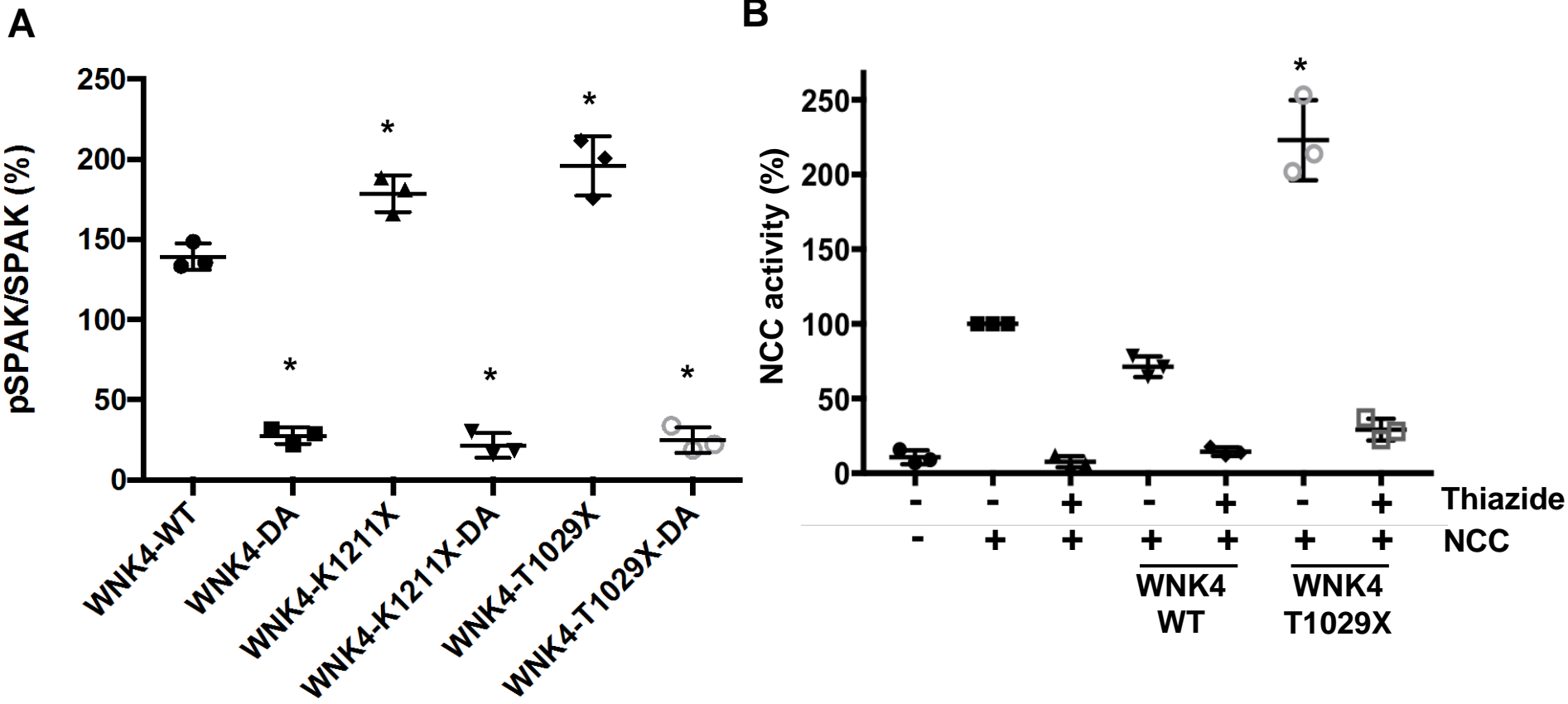


Figure S2. (A) Densitometric analysis of blots represented in figure 2F (*p<0.05 vs. WT, n=3). **(B)** NCC activity (measured as Na⁺ uptake in *Xenopus laevis* oocytes) in the presence of WNK4-WT and WNK4-T1029X (*p<0.05 vs. NCC, n=3).

Figure S3.

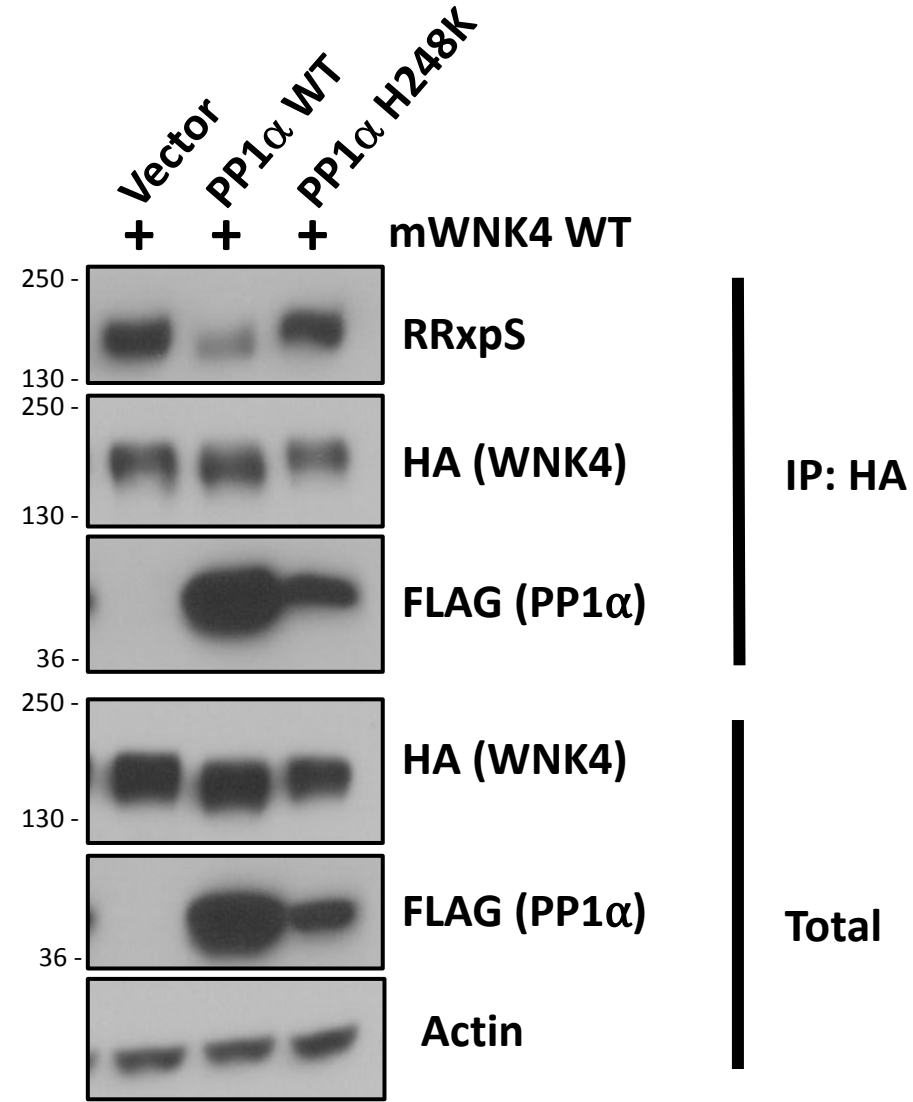


Figure S3. The effect of PP1 co-expression on WNK4 phosphorylation levels is dependent on PP1 catalytic activity. HEK293 cells were cotransfected with WNK4 and wild type PP1 α or the catalytically inactive mutant PP1 α -H248K. Forty eight hours post-transfections cells were lysed and WNK4 was immunoprecipitated in order to analyze WNK4 phosphorylation at RRXS sites. N=6.

Figure S4.

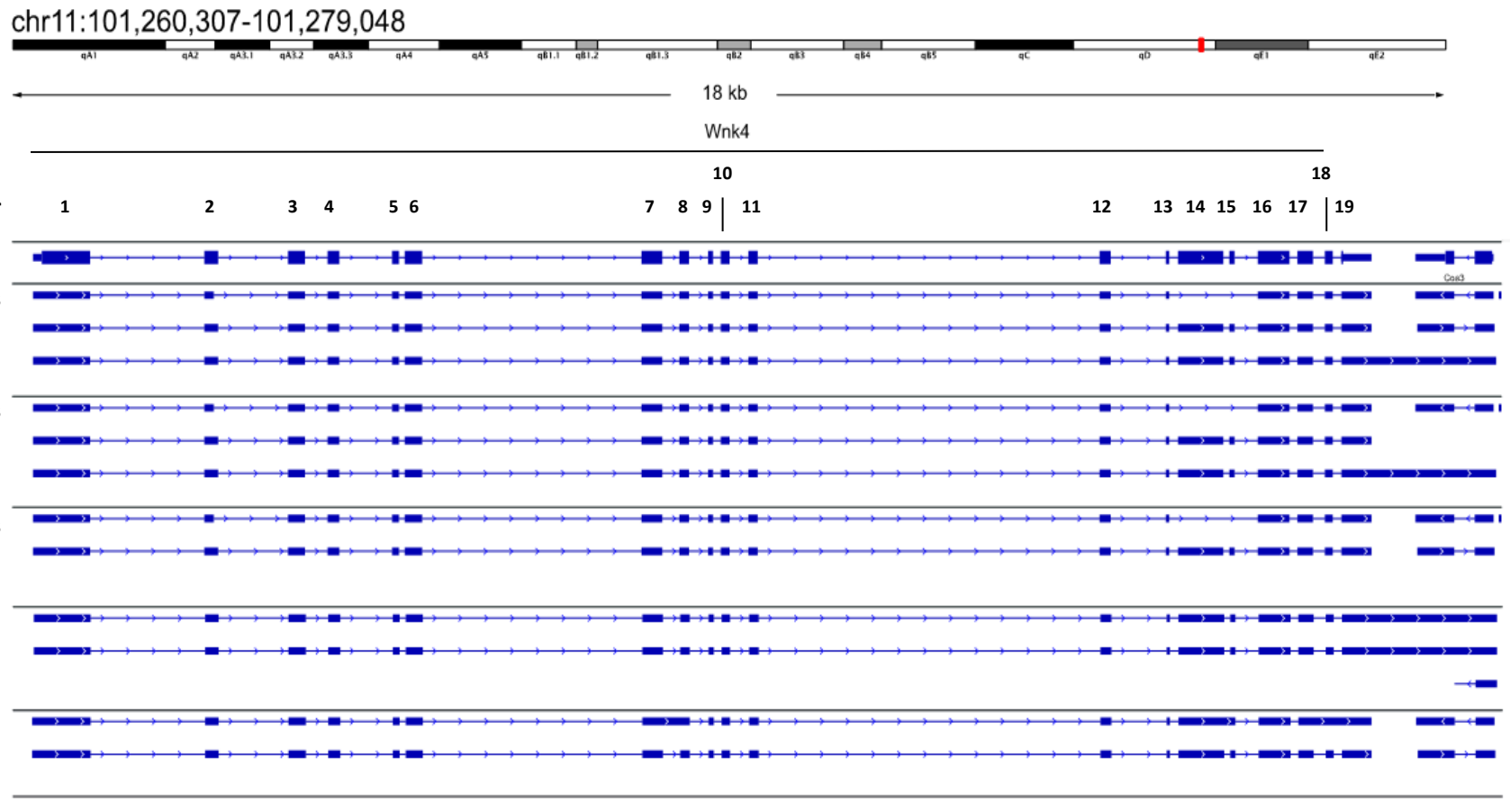


Figure S4. *Wnk4* transcript assembly from published RNA-seq data. C57Bl/6 mouse kidney RNA-seq data was obtained from GSM2095449 to 52 (4 replicates, dataset1)(3) and GSM2141862 to 64 (3 replicates, dataset 2) as raw data. Fastq files were mapped to the mouse genome (mm10) with HISAT2 (Galaxy Version 2.0.5.2) using the default settings. After mapping, the transcripts were assembled using String Tie (Galaxy Version 1.3.3) without GFF/GTF guide to obtain all the potential transcripts (String Tie assembled transcripts) for each replicate of the 2 datasets or for the combined .bam files of each dataset (dataset 1 and 2). After the first assembly, String Tie merge transcripts (Galaxy version 1.3.3) were analysed against the UCSC Known Genes dataset to identify additional transcripts, using each dataset separately or the combination of both (All datasets). All analysis were done using the Galaxy platform at <https://usegalaxy.org/>. Each blue line denotes a predicted transcript and blue boxes indicate exons.

Table S1. LC-MS/MS results for full-length WNK4.

Start	End	Peptide sequence	Score	M/Z	Times observed
102	115	K.EPPEGTWMGAAPVK.A	41.54	735.3625	2
116	134	K.AVDSACPELTGSSGGPGSR.E + Propionamide (C)	75.13	909.9219	2
150	169	R.EQEEKEDTETQAVATSPDGR.Y	23.67	740.6697	2
155	169	K.EDTETQAVATSPDGR.Y	54.05	788.8577	2
173	179	K.FDIEIGR.G	53.97	425.2275	3
215	223	R.FSEEVEMLK.G + Oxidation (M)	59.42	564.2681	4
224	232	K.GLQHPNIVR.F	36.62	517.2992	1
316	325	K.IGDLGLATLK.R	77.8	500.8065	3
332	348	K.SVIGTPEFMAPEMYEEK.Y	51.83	979.456	1
384	396	R.KVTSGTKPNSFYK.V	36.4	728.8941	2
385	396	K.VTSGTKPNSFYK.V	53.4	664.8503	1
397	403	K.VKMPEVK.E + Oxidation (M)	23.48	423.741	1
404	411	K.EIIEGCIR.T	13.59	466.7385	1
434	451	R.GVHVELAEEDDGEKPKLK.L	76.1	641.3215	5
467	479	R.DNQAIEFLFQLGR.D	46.71	775.9019	2
627	657	R.SGPGSDFSPGDSYASDAASGLSDMGEQQMR.K	16.74	998.4139	2
674	683	R.VTSVSDQSDR.V	69.74	547.2603	2
701	726	R.FDLGDGSPEEIAAAMVYNEFILPSER.D	33.13	1464.6863	1
740	745	R.VETLLK.R	28.5	351.7238	1
747	780	R.DAGPPEAAEDALSPQEPAALPGPPNAEPQR.S	28.66	1134.885	1
781	787	R.SISPEQR.S + Phospho (ST)	20.41	448.6959	1
971	981	R.NPAQPLLGDAR.L	44.27	576.3124	3
982	996	R.LAPISEEGKPQLVGR.F	77.23	531.9731	3
1004	1019	K.EPAEPPLQPASPTLSR.S + Phospho (ST)	25.37	590.6238	1
1055	1067	R.AAEGLGVAVDDEK.D	26.37	637.3186	2
1124	1136	K.HLSEVEALQTLQK.K	13.68	499.2763	1
1138	1145	K.EIEDLYSR.L	36.67	512.7514	2
1184	1193	R.SDLPGPGIMR.R	37.92	521.7718	2
1212	1221	K.GVTFAGDIGR.M	68.91	496.7627	3

WNK4 was immunoprecipitated from kidney lysates and separated by SDS-PAGE. Observed peptides for the excised gel fragment containing the full-length WNK4 are presented. Only identified peptides with score higher than homology score are presented. Score, MASCOT score. Peptide sequences are numbered according to position in mouse WNK4.

Table S2. LC-MS/MS results for the short forms of WNK4.

Start	End	Peptide sequence	Score	M/Z	Times observed
6	35	R.NTETGVPMMSQTEADLALRPSPALTSTGPTR.L	54.68	1033.5199	2
36	42	R.LGPPRR.V	28.76	396.7452	1
102	115	K.EPPEGTWMGAAPVK.A	59.13	735.3626	2
116	134	K.AVDSACPELTGSSGGPGSR.E + Propionamide (C)	98.58	909.9187	4
135	145	R.EPPRVPDAAAR.E	22.43	589.817	1
149	169	R.REQEEKEDTETQAVATSPDGR.Y	45.2	792.7024	2
150	169	R.EQEEKEDTETQAVATSPDGR.Y	52	740.6684	4
155	169	K.EDTETQAVATSPDGR.Y	66.11	788.8591	4
173	179	K.FDIEIGR.G	55.12	425.2273	5
215	223	R.FSEEVEMLK.G	71.5	556.2718	5
224	232	K.GLQHPNIVR.F	32.92	345.2017	2
284	291	R.GLHFLHSR.V	24.51	483.7671	1
292	298	R.VPPILHR.D	29.96	416.2665	1
316	325	K.IGDLGLATLK.R	94.68	500.8064	5
332	348	K.SVIGTPEFMAPEMYEEK.Y	75.08	979.4506	4
384	396	R.KVTSGTKPNSFYK.V	52.91	728.8919	3
397	403	K.VKMPEVK.E + Oxidation (M)	39.54	423.741	1
404	411	K.EIIEGCIR.T	28.05	466.7506	3
434	451	R.GVHVELAEEDDGEKPKLK.L	70.43	961.4802	4
467	479	R.DNQAIEFLFQLGR.D	95.12	775.9018	2
474	479	F.LFQLGR.D	26.87	367.2215	1
627	657	R.SGPGSDFSPGDSYASDAASGLSDMGEGGQMR.K	59.19	998.4111	2
674	683	R.VTSVSDQSDR.V	67.49	547.2598	1
701	726	R.FDLDGDSPEEIAAAMVYNEFILPSER.D	38.07	1464.6791	1
733	739	R.IREIIQR.V	36.6	464.2902	1
735	745	R.EIIQRVETLLK.R + Phospho (ST)	9.41	711.3853	1
740	745	R.VETLLK.R	42.26	351.7232	2
747	780	R.DAGPPEAAEDALSPQEPAALPALPGPPNAEPQR.S	23.87	1134.8888	1
781	787	R.SISPEQR.S + Phospho (ST)	23.7	448.6967	1

WNK4 was immunoprecipitated from kidney lysates and separated by SDS-PAGE. Observed peptides for the excised gel fragment containing the short forms of WNK4 are presented. Only identified peptides with score higher than homology score are presented. Score, MASCOT score. Peptide sequences are numbered according to position in mouse WNK4.

Table S3. Primers used for RACE 3' assay.

	Forward primer	Reverse primer (name: sequence)
RT-PCR		QT: CCAGTGAGCAGAGTGACGAGGACTCGAGATGCATCTTTTTTTTTTTTTTTTTT
PCR1	GSP1: TCAgACCCTgCCCTTCag	Q0: CCAGTGAGCAGAGTGACG
PCR2 (nested)	GSP2 TGGGGGGTTACCATCCAG	QI: GAGGACTCGAGATGCATC

Procedure followed was based on the protocol described by Scotto-Lavino, E., *et al.* (4). GSP primers are gene specific primers that align in WNK4 sequence. Q primers were designed to bind at the 3' end of the mRNA (Qt) and cDNA molecules (Q0 and QI).

References

1. Castañeda-Bueno, M., Arroyo, J. P., Zhang, J., Puthumana, J., Yarborough, O., Shibata, S., Rojas-Vega, L., Gamba, G., Rinehart, J., and Lifton, R. P. (2017) Phosphorylation by PKC and PKA regulate the kinase activity and downstream signaling of WNK4. *Proc. Natl. Acad. Sci.* **114**, E879–E886
2. Lalioti, M. D., Zhang, J., Volkman, H. M., Kahle, K. T., Hoffmann, K. E., Toka, H. R., Nelson-Williams, C., Ellison, D. H., Flavell, R., Booth, C. J., Lu, Y., Geller, D. S., and Lifton, R. P. (2006) Wnk4 controls blood pressure and potassium homeostasis via regulation of mass and activity of the distal convoluted tubule. *Nat. Genet.* **38**, 1124–1132
3. Arvaniti, E., Moulos, P., Vakrakou, A., Chatziantoniou, C., Chadjichristos, C., Kavvadas, P., Charonis, A., and Politis, P. K. (2016) Whole-transcriptome analysis of UUO mouse model of renal fibrosis reveals new molecular players in kidney diseases. *Sci. Rep.* **6**, 26235
4. Scotto-Lavino, E., Du, G., and Frohman, M. A. (2007) 3' End cDNA amplification using classic RACE. *Nat. Protoc.* **1**, 2742–2745

La segunda mitad de los resultados se anexa a continuación, en la forma de un manuscrito que está próximo a enviarse al proceso de revisión en una revista de nefrología. A continuación presento un resumen sobre esta parte del trabajo.

Una disminución en la ingesta de K^+ promueve la activación del cotransportador NCC, cuya fosforilación y actividad dependen de la cinasa WNK4. La actividad de WNK4 puede ser inhibida por unión directa de Cl^- a su dominio cinasa. La baja $[K^+]_e$ activa a NCC al disminuir $[Cl^-]$ intracelular, promoviendo la disociación del Cl^- de WNK4. Sin embargo, la señalización mediada por WNK4 también puede ser modulada por su fosforilación de motivos RRxS o por su degradación por el complejo de ligasa de ubiquitina KLHL3/CUL3. Se desconoce la participación de estos mecanismos en la regulación de NCC por $[K^+]_e$. En este trabajo usamos modelos murinos, células HEK293 y rebanadas de riñón de ratón para evaluar el efecto de $[K^+]_e$ y $[Cl^-]$ intracelular en la fosforilación de WNK4, abundancia de WNK4 en el riñón y su localización subcelular. La disminución de $[K^+]_e$ promovió la fosforilación de WNK4 en la Ser64 y Ser1196 en un modelo murino de hipokalemia, en células HEK293 transfectadas con WNK4 y en rebanadas de riñón de ratón. Estos efectos pueden ser secundarios a la disminución de $[Cl^-]$ intracelular, pues reducir este parámetro modificando el medio o con compuestos farmacológicos en células HEK293 incrementó la fosforilación de WNK4 en estos sitios. Asimismo, la actividad de KLHL3, medida como abundancia de WNK4 en células HEK293, se vio disminuida al reducir $[Cl^-]$ intracelular. Esto podría explicar observaciones que hicimos en ratones con una función afectada de NCC, como los ratones WNK4-KO o ratones silvestres administrados de manera aguda con tiazida, donde observamos un aumento en la abundancia de KS-WNK1, otro miembro de la familia también presente en el DCT y sensible a degradación mediada por KLHL3. Finalmente, la generación y estudio del ratón transgénico WNK4-L319F, el cual tiene una WNK4 incapaz de unir Cl^- , nos permitió observar que existen mecanismos adicionales para la activación de NCC ante hipokalemia, pues estos ratones sí son capaces de estimular la fosforilación de NCC después de consumir una dieta deficiente en K^+ por 7 días. En conclusión, nuestros datos sugieren que múltiples y redundantes mecanismos son responsables de la activación de NCC ante una disminución en $[K^+]_e$.

Upregulation of NCC by hypokalemia involves additional mechanisms to direct Cl⁻ sensing by WNK4

Adrián R. Murillo-de-Ozores^{1,2},

Héctor Carbajal-Contreras^{1,3}, Germán R. Magaña-Ávila^{1,2}, Raquel Valdés^{1,4}, Leoneli I. Grajeda-Medina¹, Norma Vázquez⁴, , Alejandro López-Saavedra⁵, Dao-Hong Lin⁶, Wen-Hui Wang⁶, Eric Delpire⁷, David H. Ellison^{8,9,10}, Gerardo Gamba^{1,3,4}, María Castañeda-Bueno*¹

¹Department of Nephrology and Mineral Metabolism, Instituto Nacional de Ciencias Médicas y Nutrición Salvador Zubirán, Tlalpan, Mexico City;

²Facultad de Medicina, Universidad Nacional Autónoma de México, Coyoacan, Mexico City;

³PECEM (MD/PhD), Facultad de Medicina, Universidad Nacional Autónoma de México, Coyoacan, Mexico City, Mexico;

⁴ Molecular Physiology Unit, Instituto de Investigaciones Biomédicas, Universidad Nacional Autónoma de México, Tlalpan, Mexico City.

⁵Unidad de Aplicaciones Avanzadas en Microscopía del Instituto Nacional de Cancerología y la Red de Apoyo a la Investigación, Universidad Nacional Autónoma de México, Mexico City, Mexico;

⁶Department of Pharmacology, New York Medical College, Valhalla, NY, USA;

⁷Department of Anesthesiology, Vanderbilt University School of Medicine, Nashville, TN, USA;

⁸Division of Nephrology and Hypertension, Department of Medicine, Oregon Health and Science University, Portland, OR, USA;

⁹Oregon Clinical & Translational Research Institute, Oregon Health & Science University, Portland, OR, USA;

¹⁰VA Portland Health Care System, Portland, OR, USA.

Type of article: Original article

Running title:

Keywords: distal convoluted tubule, potassium, blood pressure, epithelial transport,
Familial Hyperkalemic Hypertension, Gitelman syndrome.

***Correspondence:** María Castañeda-Bueno, PhD,

maria.castanedab@incmnsz.mx, mcasta85@yahoo.com.mx

Av. Vasco de Quiroga 15. Col. Secc. XVI-Belisario Dominguez. Tlalpan, 14080, CDMX, Mexico.

ABSTRACT

Background

Low K^+ intake activates the renal NaCl cotransporter, NCC, whose phosphorylation and activity depend on the With-No-Lysine kinase WNK4. WNK4 is inhibited by Cl^- binding to its kinase domain. Low extracellular $[K^+]$ ($[K^+]_e$) activates NCC by decreasing intracellular $[Cl^-]$ ($[Cl^-]_i$) and promoting Cl^- dissociation from WNK4. However, WNK4 signaling is also modulated by phosphorylation in RRxS motifs or by its degradation regulated by the KLHL3/CUL3 ubiquitin ligase complex. It is unknown if these mechanisms participate in NCC regulation by $[K^+]_e$.

Methods

We used HEK293 cells, kidney slices, and mouse models to evaluate the effect of low $[K^+]_e$ and $[Cl^-]_i$ on WNK4 phosphorylation, renal WNK abundance, and subcellular localization.

Results

Decreased $[K^+]_e$ promoted WNK4 phosphorylation at S64 and S1196 in *in vivo*, *in vitro*, and *ex vivo* models. These effects might be secondary to $[Cl^-]_i$ depletion, as reduction of $[Cl^-]_i$ in HEK293 cells increased WNK4-RRxS phosphorylation. Moreover, pWNK4-S1196 levels were increased in *Kir5.1^{-/-}* mice, which presumably have decreased distal convoluted tubule (DCT) $[Cl^-]_i$. Similarly, KLHL3 activity was modulated by changes in $[K^+]_e$ and $[Cl^-]_i$ in HEK293. *WNK4^{-/-}* mice and mice acutely treated with hydrochlorothiazide showed higher levels of KS-WNK1 protein, probably due to reduced KLHL3-targeted degradation as a response to reduced $[Cl^-]_i$. Finally, upregulation of NCC in response to low K^+ diet was observed in mice harboring a Cl^- -insensitive WNK4 (L319F), suggesting that in addition to Cl^- sensing by WNK4, other mechanisms participate in NCC upregulation.

Conclusion

Our data suggests that multiple $[Cl^-]_i$ -regulated mechanisms are responsible for NCC upregulation of by low $[K^+]_e$.

SIGNIFICANCE STATEMENT

Modulation of the NaCl cotransporter (NCC) activity by dietary K^+ explain, at least in part, the inverse relationship between K^+ ingestion and blood pressure levels. Here we describe that, in addition to the accepted mechanism mediating NCC activation by low extracellular $[K^+]_e$ ($[K^+]_e$), which involves relief of WNK4 kinase inhibition by Cl^- , alternative mechanisms are at play. These may include modulation of WNK4 activity by phosphorylation of sites within its regulatory domains, and modulation of WNK4/KS-WNK1 degradation by the KLHL3-CUL3 E3 ubiquitin ligase, through phosphorylation of KLHL3's substrate binding domain. Our data suggest that $[K^+]_e$ -induced changes in $[Cl^-]_i$ mediate activation of these alternative pathways, hinting that unidentified Cl^- sensitive molecules may exist that are relevant for distal convoluted tubule physiology.

INTRODUCTION

Recent studies have shown an inverse correlation between K^+ consumption and blood pressure levels in humans^{1,2}. Lower K^+ consumption has been linked to higher blood pressure¹ and higher risk of cardiovascular events³. These effects are probably secondary to renal Na^+ retention under low K^+ intake, according with the central role of the kidneys for the long term regulation of blood pressure⁴. In mice, dietary K^+ restriction causes a salt-sensitive increase in blood pressure^{5,6}, that is not observed in mice deficient in the thiazide-sensitive Na^+Cl^- cotransporter, NCC, suggesting that NCC play a role in this phenomenon⁶.

NCC constitutes the major Na^+ pathway in the apical membrane of the distal convoluted tubule (DCT). The DCT reabsorbs 5-10% of the filtered Na^+ , whereas no net K^+ reabsorption or secretion occur within this segment⁷. Nevertheless, NCC activity influences renal K^+ excretion by affecting the activity of the K^+ secretory mechanisms that operate in the aldosterone-sensitive distal nephron (ASDN)⁸. The role of NCC in maintaining K^+ homeostasis is evidenced by the hypokalemia presented in Gitelman syndrome, caused by loss of function mutations in the gene encoding NCC (*SLC12A3*)⁹. On the other hand, Familial Hyperkalemic Hypertension (FHHT) is caused by mutations in genes that regulate NCC function, such as *WNK1*, *WNK4*¹⁰, *KLHL3*, and *CUL3*^{11,12}. The FHHT phenotype is driven primarily by overactivation of NCC, which causes increased salt retention by the DCT and decreased K^+ secretion by the ASDN^{13,14}.

The activity of NCC is positively regulated by phosphorylation in several sites within its amino-terminal domain¹⁵, by the STE20/SPS1-related Proline-Alanine-rich Kinase (SPAK) and the Oxidative Stress-Responsive 1 kinase (OSR1)¹⁶. Both kinases are substrates of the With-No-Lysine (K) (WNK) family of kinases¹⁷. While this family comprises four members, WNK4 is the major regulator of NCC^{18,19}, and it is responsible for its activation by different stimuli²⁰.

NCC activity is highly sensitive to subtle changes in plasma K^+ concentration²¹⁻²³. Basolateral Kir4.1/Kir5.1 heterotetrameric K^+ channels in the DCT, have been described as the “potassium sensor”, since small decreases in extracellular K^+ concentration ($[K^+]_e$) promote K^+ exit through these channels, and thus, hyperpolarization of the basolateral membrane, while increases in $[K^+]_e$ cause depolarization^{24,25}. These changes in cell membrane potential affect the driving force for basolateral Cl^- efflux, mainly through the Cl^- -Kb channels²⁶. Thus, lower $[K^+]_e$ promotes hyperpolarization, increasing Cl^- efflux, and reducing intracellular Cl^- concentration ($[Cl^-]_i$). Interestingly, the activity of WNK4 has been shown to be highly sensitive to $[Cl^-]$ ^{27,28}, given that a Cl^- ion can bind to the active site of the enzyme that stabilizes an inactive conformation, preventing autophosphorylation and activation^{27,29}. Thus, in the setting of low $[K^+]_e$, the reduction in $[Cl^-]_i$ promotes Cl^- dissociation and activation of the WNK4-SPAK/OSR1-NCC pathway.

An additional mechanism for low $[K^+]_e$ -mediated activation of the WNK4-SPAK/OSR1-NCC pathway has been proposed by Ishizawa et al.³⁰ that involves modulation of the activity of the CUL3-KLHL3 E3 complex that regulates WNK4 ubiquitylation and degradation^{31,32}. Administration of a low K^+ diet to mice promoted an increase in KLHL3 phosphorylation at a PKC-PKA consensus site (RRXS) located within the substrate binding domain of the protein. Previously, Shibata et al. had shown that phosphorylation of this site prevents KLHL3-targeted degradation of WNK4 in cultured cells³³. Accordingly, Ishizawa et al. also observed higher renal WNK4 levels in mice maintained on low K^+ diet.

Finally, Cl⁻ binding is not the only described mechanism for the regulation of WNK4 catalytic activity. Its activity can also be regulated by phosphorylation of sites located within the regulatory amino- and carboxy-terminal domains (Ser64 and Ser1196, here referred to as RRxS sites in allusion to the primary sequence that encompasses the phosphorylated residue)³⁴. Phosphorylation of these sites in vitro and in cultured cells can be mediated by protein kinases A (PKA) and C (PKC). Phosphoablative mutations of these sites drastically reduce kinase activity even in the context of impaired Cl⁻ binding, and phosphorylation of these sites is necessary to achieve maximal activation of the Cl⁻-insensitive mutant (L319F)³⁴.

Given that WNK4 is necessary for NCC activation by low K⁺ intake^{23,35}, and that phosphorylation of its RRxS motifs is essential for full kinase activation, the main goal of this study was to assess the importance of these sites for the modulation of NCC by K⁺. In addition, given the similarities that exist between the regulation of KLHL3 activity and WNK4 activity by phosphorylation at RRxS sites, we began to investigate whether the molecular mechanisms involved in the regulation of WNK4 by RRxS phosphorylation in response to low [K⁺]_e play also a role in the regulation of KLHL3 by low [K⁺]_e.

RESULTS

WNK4 phosphorylation at S64 and S1196 increases in kidneys of mice maintained on a low K+ diet.

In kidneys of mice placed on a low K⁺ diet for 7 days, in addition to the expected increases in WNK4, NCC, and pNCC levels (Figure 1A-B), the ratio of pS64 and pS1196/total WNK4 increased, suggesting that the increase in phosphorylation was not solely the consequence of increased protein expression.

In the DCTs of mice on NKD very low or undetectable signal was observed with the WNK4, pWNK4-S64, and pWNK4-S1196 antibodies by immunofluorescent staining (Figure 1C-H). In contrast, WNK bodies³⁶ were observed in DCT cells of mice on LKD with all three antibodies. Thus, WNK bodies that are formed in DCT cells in response to LKD^{36,37} contain phosphorylated WNK4 at RRxS sites.

Low [K⁺]_e and intracellular Cl⁻ depletion promote WNK4 phosphorylation at S64 and S1196 in HEK293 cells.

To test whether changes in [K⁺]_e can directly modulate WNK4-RRxS phosphorylation we used WNK4-transfected HEK293 cells. Phosphorylation at S64 and S1196 increased after incubation of cells on a low K⁺ medium (LKM), but did not decrease after incubation on a high K⁺ medium (Figure 2A-B). Terker et al. showed that incubation of these cells in LKM decreased [Cl⁻]_i. Thus, we tested whether the increase in WNK4-RRxS phosphorylation could be stimulated by a reduction in [Cl⁻]_i. Incubation in hypotonic low Cl⁻ (HLC) medium^{15,38} for two hours increased pWNK4-S64 and pWNK4-S1196 levels (Figure 2C-D). As an alternative maneuver to reduce [Cl⁻]_i, we used N-ethylmaleimide (NEM). NEM is a known activator of K⁺:Cl⁻ cotransporters (KCCs) and inhibitor of Na⁺-dependent Cl⁻ cotransporters (N(K)CCs),³⁹ that is known to reduce [Cl⁻]_i⁴⁰. Addition of NEM also stimulated an increase in pWNK4-S1196 (Figure 2E-F).

Reasoning that phosphorylation of S64 and S1196 could be stimulated, directly or indirectly, by increased WNK activity under low $[Cl^-]_i$, we tested whether the specific WNK inhibitor WNK463⁴¹ could prevent the stimulation of WNK4-RRXS phosphorylation by LKM. Surprisingly, WNK463 increases S1196 phosphorylation, regardless of the $[K^+]_e$ (Figure 2G-H). Like NEM, WNK463 decreases endogenous SPAK activity, and thus, inhibits NKCC1 and increases KCC activity, leading to decreased $[Cl^-]_i$. Thus, three different maneuvers that reduce $[Cl^-]_i$, increased pWNK4-RRXS levels, suggesting that WNK4-RRXS phosphorylation increases in response to $[Cl^-]_i$ depletion. It is thus likely that the known LKM-induced $[Cl^-]_i$ depletion⁶ was responsible for increased WNK4-RRXS phosphorylation under this condition.

Changes in extracellular $[K^+]_e$ directly modulate levels of WNK4 S64 and S1196 in kidney

WNK4-S64 and S1196 phosphorylation was directly modulated by $[K^+]_e$ in the kidney slices *ex vivo* system^{42,43}. Higher pWNK4-S64 (Figure 3A-B) and pWNK4-S1196 levels (Figure 3C-D) were observed in freshly prepared kidney slices incubated in a low $[K^+]_e$ solution than in those on a normal $[K^+]_e$ solution. Higher pNCC levels were also observed as previously reported⁴². No significant differences in total WNK4 or NCC levels were observed.

Kir5.1^{-/-} mice present higher levels of NCC expression, phosphorylation, and activity⁴⁴. Their DCT cells have higher basolateral K^+ conductance and a more negative membrane potential, which are expected to affect $[Cl^-]_i$. These parameters, as well as the high pNCC levels are not normalized by high K^+ diet, which does normalize plasma $[K^+]_e$. Thus, we investigated pWNK4-RRXS levels in these mice. As shown in Figure 3E-F, renal levels of WNK4 were slightly higher, although not significantly different in Kir5.1^{-/-} mice. However, the pWNK4-S1196/WNK4 ratio was significantly higher. Thus, membrane potential variations in DCT cells that are expected to reduce the $[Cl^-]_i$ can lead to increases in pWNK4-S1196 levels.

Changes in $[Cl^-]_i$ can modulate KLHL3-CUL3 E3 activity and therefore WNK4 and KS-WNK1 levels

Mice maintained on a LKD have higher phosphorylation levels of KLHL3 at the S433 site of the substrate binding domain³⁰ that prevents interaction with WNK4 and decreases KLHL3-targeted degradation³³. Accordingly, these mice display higher renal WNK4 levels than mice maintained on NKD. Given that the KLHL3-S433 site is similar to the WNK-RRXS sites^{30,33,34,45}, we decided to investigate whether KLHL3-targeted degradation of WNK kinases is modulated by $[Cl^-]_i$. In the absence of KLHL3, WNK4 levels did not vary among cells incubated in NKM or LKM. However, in KLHL3 transfected-cells, WNK4 levels were ~2-fold higher in LKM-incubated cells (Figure 4A-B). HLC medium, known to induce $[Cl^-]_i$ depletion, produced a 42 % increase in WNK4 levels, in the absence of exogenous KLHL3, and a 986 % increase in KLHL3-overexpressing cells (Figure 4C-D). Thus, KLHL3-targeted degradation of WNK4 was clearly modulated in response to changes in $[Cl^-]_i$ in this cell model.

Thomson et al. have recently shown that WNK4^{-/-} mice have large WNK bodies in the DCT that are still observed when plasma $[K^+]_e$ levels are corrected by a high K^+ diet. We reasoned that WNK4^{-/-} mice may have higher levels of KS-WNK1 protein that are driving the formation of WNK bodies given that the formation of these structures is dependent on the presence of this protein³⁶. As shown in Figure 4E, this was indeed the case. Because KS-WNK1 is very sensitive to KLHL3-targeted degradation^{46,47} and expression of KS-WNK1 and KLHL3 is restricted to the DCT^{12,48,49}, the level of

KS-WNK1 expression is good indicator of KLHL3-CUL3 E3 activity. We thus hypothesized that low $[Cl^-]_i$ in the DCTs of $WNK4^{-/-}$ mice may be responsible for the high KS-WNK1 levels. To investigate this hypothesis, we administered thiazides to mice, reasoning that this would lower $[Cl^-]_i$ of DCT cells as NCC is the major pathway for Cl^- entry. Supporting this, a mathematical model of the DCT predicts that blockade of 99 % of NCC function would lead to a change in $[Cl^-]_i$ from 18.5 mM at baseline conditions to 12.1 mM (A. Weinstein personal communication: unpublished from the calculations in Weinstein, 2018⁵⁰). After a 12-hour treatment period, plasma $[K^+]$ was similar among thiazide-treated and vehicle treated mice, but higher pNCC levels (likely due to intracellular Cl^- depletion) were observed in the hydrochlorothiazide group. Moreover, slightly increased KS-WNK1 levels were observed by Western blot (Figure 4F) and WNK bodies were detected with the panWNK1 and WNK4 antibodies (Figure 4G-H).

$WNK4^{L319F/L319F}$ mice can still upregulate NCC phosphorylation in response to low K^+ diet, suggesting that alternative pathways participate in this modulation.

The L319F mutation that affects the Cl^- binding site of WNK4 (L322F in human WNK4) has been shown to promote constitutive activation of the kinase due to inability to bind Cl^- ^{34,51}. We generated a mouse model carrying the $WNK4$ -L319F mutation to assess the physiological consequences of such mutation, as well as the ability of these mice to respond to dietary K^+ restriction (Supplemental Figure 1). $WNK4^{L319F/L319F}$ (in C57Bl/6 background) mice presented higher NCC and pNCC levels (Figure 5). Although no significant electrolytic alterations were observed, there was a tendency towards higher plasma $[K^+]$ in the knockin mice (Table 1). Of note, when evaluated in a different genetic background (mixed B6-129/SV) higher pNCC, pSPAK/OSR1, and plasma $[K^+]$ levels were observed (Supplemental Figure 2). Interestingly, upregulation of pNCC, NCC, and pSPAK in response to LKD was observed in both wild type and $WNK4^{L319F/L319F}$ mice, suggesting that the relief of WNK4 inhibition by Cl^- is not the only mechanism behind NCC activation in response to reductions in $[K^+]_e$ (Figure 6B, C, F). We propose that modulation of WNK4 activity by phosphorylation of RRxS sites and modulation of WNKs protein levels by KLHL3 may be part of such mechanisms. Supporting this, in both wild type and $WNK4^{L319F/L319F}$ mice, WNK4 and KS-WNK1 protein levels, as well as WNK4 phosphorylation levels at S64 and S1196 increased with LKD (Figure 6D and E).

Protein kinase C activity may be involved in WNK4-S64 and -S1196 phosphorylation in response to intracellular Cl^- depletion

Given that WNK4-RRxS sites can be phosphorylated by PKC and PKA in *in vitro* kinase assays, we tested whether these kinases are involved in the phosphorylation of S64 and S1196 in response to $[Cl^-]_i$ depletion. Pre-incubation of WNK4-transfected HEK293 cells with the PKC inhibitor Bisindolylmaleimide I (BIM) partially prevented the increase in phosphorylation of S64 and S1196 that occurs upon incubation with HLC medium (Figure 7A, B) and a ~40 % increase in endogenous PKC activity was observed in cells incubated in HLC (Figure 7C). No difference was observed in intracellular cAMP levels (Figure 7C), arguing against the role of the cAMP-regulated PKA in WNK4 phosphorylation under the tested conditions.

Proteomic and transcriptomic studies suggests that PKC delta is the more abundant PKC isoform in the DCTs of mouse and rat^{49,52}. Reported levels for other PKC isoforms are low, suggesting that these isoforms may not be present. However, a report by Sterling et al. showed that renal levels of PKC epsilon are greatly increased in mice on LKD⁵³. Thus, expression of this isoform may be induced in

the DCT under this condition. Here, we observed a higher expression of both PKC δ and PKC ϵ on mice on LKD (Figure 7D-E). However, the increase in PKC ϵ expression was much lower than the previously reported. Unfortunately, we were unable to detect specific signal in immunofluorescent-labeled kidneys. Future experiments will be necessary to confirm protein expression of these isoforms in the DCT. We also tested the ability of PKC δ to promote the phosphorylation of WNK4-S64 and S1196 sites in HEK293 cells. A robust increase in phosphorylation levels was observed in cells with exogenous expression of PKC δ (Figure 7F-G).

DISCUSSION

In the present work we show that decreased $[K^+]_e$ promotes WNK4 phosphorylation at S64 and S1196 and modulates KLHL3 activity, and therefore, WNK4³⁰ and KS-WNK1⁴⁷ abundance. In addition, our data suggest that low $[K^+]_e$ -induced reductions in DCT $[Cl^-]_i$ mediate these effects. We thus propose that modulation of WNK4 activity by direct Cl^- binding is not the sole mechanism for WNK4/NCC regulation in response to low $[K^+]_e$ and that stimulation of WNK4 activity due to increased WNK4 and KS-WNK1 abundance, as well as increased WNK4-RRxS phosphorylation are also relevant. These conclusions are supported by the following observations.

First, an increase was observed in phosphorylation levels of WNK4 at the S64 and S1196 sites in mice maintained on a LKD, and this effect occurred in response to direct sensing of $[K^+]_e$ by DCT cells since it was also observed in kidney slices and WNK4-transfected HEK293 cells incubated in a LKM. Additionally, in HEK293 cells, three different maneuvers that promote $[Cl^-]_i$ depletion stimulated the phosphorylation of WNK4 S64 and S1196. Thus, the $[Cl^-]_i$ depletion that occurs in response to incubation in LKM in these cells⁶ probably mediated the increases observed in WNK4 S64 and S1196 phosphorylation under this condition as well. Supporting that DCT $[Cl^-]_i$ depletion may be behind the increased WNK4-RRxS phosphorylation observed in mice on LKD, increased levels of pWNK4-S1196 were observed in Kir5.1 knockout mice that have been shown to have higher DCT basolateral K^+ conductance and hyperpolarized membranes that are expected to result in reductions in $[Cl^-]_i$ ⁴⁴.

Experiments performed in HEK293 cells suggested that $[Cl^-]_i$ depletion also mediates the regulation of KLHL3-CUL3 E3 activity towards WNKs that promote changes in WNK4 and KS-WNK1 in mice on LKD^{30,47}. According to Ishizawa et al. phosphorylation of the substrate binding domain of KLHL3, that prevents WNK binding, increases in HEK293 cells incubated in LKM and in mice maintained on LKD³⁰. As discussed above, KS-WNK1 protein levels in the kidney are a good indicator of the activity level of the KLHL3-CUL3 E3 complex^{12,48,49,46,47}. We observed that WNK4 knockout mice and mice acutely treated with thiazides had higher levels of KS-WNK1 and this increase may have been due to the inhibition of KLHL3-CUL3 E3 activity that occurs in response to the reduction in DCT $[Cl^-]_i$ expected as a result of the low NCC activity.

The high KS-WNK1 levels observed in WNK4 knockout mice that also present large WNK bodies in their DCT adds up to the existing evidence suggesting that the induction of KS-WNK1 expression promotes the formation of these structures. This evidence includes the observation that in other models, like mice on LKD and KLHL3-R528H knockin mice, high KS-WNK1 protein levels correlate with the observation of WNK bodies^{36,37,47}. Moreover, absence of WNK bodies in KS-WNK1 knockout

mice on LKD suggest that this protein plays a key scaffolding role within these structures³⁶. Thus, observation of WNK bodies may serve as a surrogate for detection of KS-WNK1 induction.

WNK4's inhibition by direct Cl^- binding is the currently accepted mechanism by which NCC phosphorylation is regulated in response to changes in $[\text{K}^+]_e$. Direct evidence supporting this mechanism came with the generation of WNK4-L319F,L321F mice, which present an FHHT-like phenotype, with the inability to upregulate NCC by low K^+ intake⁵⁵. Several differences exist between these mice and the WNK4-L319F presented in this work (Figure 5, Table 1), as our mice did not display for example elevated plasma $[\text{K}^+]$ or $[\text{Cl}^-]$. This might be due to differences in diet composition or genetic background, as suggested by our observation that the WNK4-L319F mutation in a mixed B6-129/Sv background did result in mild hyperkalemia. The contribution of L321F is probably negligible, as it has been shown that mutation of this site's equivalent in WNK1 does not alter kinase's activity²⁹, and WNK4-L319F and WNK4-L319F/L321F have similar effects in *X. laevis* oocytes²⁷.

The fact that we observed pNCC upregulation by LKD in WNK4-L319F mice (Figure 6) could be related to the magnitude of the fall in plasma $[\text{K}^+]$, which can in turn be due to the duration of the dietary regime (4 days vs. 7 days). In the report by Chen et al., WNK4-L319F,L321F mice still displayed higher plasma $[\text{K}^+]$ when compared to WT mice when kept on LKD. Anyhow, our experiments do not discard that direct binding of Cl^- to WNK4 is one of the key mechanisms involved in NCC regulation by K^+ , but support the idea that additional mechanisms, like the ones described above are also physiologically relevant. The relevance of each of these mechanisms may depend on the temporal length of the physiological challenge.

As for the kinase responsible for WNK4 phosphorylation at RRxS sites by low $[\text{Cl}^-]_i$, we present *in vitro* evidence suggesting that a PKC isoform might be involved (Figures 7A and 7C), while PKA activation seems unlikely since cAMP levels are not altered (Figure 7D). We show that PKC δ and PKC ϵ abundance is increased by LKD in total kidney samples, but further research will be necessary to test if these proteins are indeed involved in the modulation of the WNK4-NCC pathway in the DCT.

In summary, this work shows that multiple redundant mechanisms are involved in the activation of WNK4-NCC pathway in the DCT elicited by low $[\text{K}^+]_e$. Moreover, these pathways seem to be modulated by $[\text{Cl}^-]_i$, which plays a central role in the ion-sensitive signaling of DCT cells (Figure 8). It is noteworthy that, our data suggest that yet undescribed Cl^- sensitive molecules exist that participate in this physiological phenomenon.

METHODS

Mice studies

Animal studies were approved by the animal care and use committee of our institution. Male wild type mice or WNK4-L319F mice (C57BL/6 genetic background), 12–16 week-old, were used. Only for the indicated experiment, mice on mixed B6-129/Sv background were used. Low K^+ diet (LKD, 0% K^+) was obtained from Research Diets, Inc. (New Brunswick, NJ), and normal K^+ diet (NKD) was prepared by adding KCl to achieve a final concentration of 1.2 % of K^+ . In all experiments involving

LKD, mice were given these modified diets for 7 days before being sacrificed. Blood samples were obtained through cardiac puncture under isoflurane anesthesia. Kidneys were snap frozen in liquid N₂ and then lysed with a buffer containing: 250 mM sucrose, 10 mM triethanolamine, 50 mM sodium fluoride, 5 mM sodium pyrophosphate, 1 mM sodium orthovanadate, and protease inhibitors (Complete tablets (Roche Applied Science), 10 mM 1,10-phenanthroline and 1 µg/mL pepstatin). Plasma electrolyte concentration was measured by iSTAT by loading whole blood into a EG6+ cartridge (Abbott). WNK4^{-/-18}, Kir5.1^{-/-44} mice have been previously described.

Generation of WNK4-L319F mice

A mouse bearing the Leu319Phe mutation in the *Wnk4* gene was generated using CRISPR/Cas9. To increase the DNA break efficiency, two overlapping guide RNAs located within exon 3 of the *Wnk4* gene were used. Each guide RNA, consisted of a 20-base DNA stretch (GCTTGAGCGTGGCCAGTCCG and AAAGGAGGCGCGCTTGAGCG, boxed in Supplemental Figure 1A) directly preceding NGG as proto-spacer adjacent motifs. Each guide RNA was selected based on high cutting prediction and relatively low possibility of off target event. Cas9 was targeted to within the Gly320 and Leu324 codons. A single strand DNA oligonucleotide consisting of a 12 base repair core fragment and 71-base 5' and 109-base 3' flanking homology arms was used for repair. As shown in Supplemental Figure 1B, mutations were introduced to substitute Leu319 with a Phe residue. Additional silent mutations were introduced to protect the repaired DNA from sgRNA-mediated cas9 retargeting, and to introduce a unique NheI restriction site for genotyping purposes. The two guide RNAs, repair DNA, and recombinant Cas9 were then mixed and injected in 289 mouse embryos isolated from pregnant B6:D2 females. The injection was followed by the transfers of embryos in pseudo-pregnant females, resulting in the birth of 29 pups. Out of 29 pups genotyped, 9 pups were wild-types, 14 pups had non-homologous end joining (NHEJ) mutations, and 6 pups carried the desired mutation in one allele and NHEJs in the other allele. After separating the correct allele from the undesired allele by breeding and genotyping, two separate lines (#5 and #12) were established and backcrossed to C57BL6/J mice for 5 generations to eliminate possible off target events. Homozygote animals were then generated and line #5 was expanded and studied.

Western Blot

Protein concentration of tissue or cell lysates was determined by the BCA protein assay (Pierce). Laemmli buffer was added to protein extracts, and they were heated to 95°C for 5 minutes. Samples were then subjected to SDS-PAGE and transferred to polyvinylidene difluoride (PVDF) membranes. Membranes were blocked for 1 h in 10% (w/v) non-fat milk dissolved in TBS- 0.1%Tween 20 (TBST). Antibodies were diluted in TBST containing 5% (w/v) non-fat milk. Membranes were incubated with primary antibodies overnight at 4°C and with HRP-coupled secondary antibodies at RT for 1 h. Signals were detected with enhanced chemiluminescence reagent. Immunoblots were developed using radiographic film.

Antibodies

Information of the antibodies used in this study is provided in supplementary table 1.

Immunofluorescence

Mice were anesthetized with isoflurane and perfused with 20 mL of PBS and then with 20 mL of 4 % (w/v) paraformaldehyde (PFA) in PBS. Kidneys were harvested and incubated for 3 hours in 4 % PFA, then switched to 30 % (w/v) sucrose in PBS and incubated overnight at 4°C. Tissues were then mounted in OCT (Tissue-Tek) and 5 µm sections were cut and stored at -80°C until use. For

immunostaining, sections were washed three times with TBST. Blocking was performed with 10 % (w/v) BSA diluted in TBST for 30 minutes at room temperature, before sequential incubation with primary and secondary antibodies. Antibodies were diluted in TBST with 5% (w/v) BSA. Imaging was performed using a LSM710-DUO confocal microscope (Carl Zeiss, Jena, Germany). Representative images are shown.

Cells

HEK293 cells (ATCC® CRL-1573) were transiently transfected with mWnk4-HA³⁴, hKlhl3-FLAG³³, or PKC δ -HA (gift from Dr. Bernard Weinstein (Addgene #16386; <http://n2t.net/addgene:16386>; RRID:Addgene_16386))⁵⁶. Cells were grown to 70–80 % confluence and transfected with Lipofectamine 2000 (Life Technologies, Inc.). Forty-eight hours after transfection, cells were lysed with a lysis buffer containing 50 mM Tris-HCl (pH 7.5), 1 mM EGTA, 1 mM EDTA, 50 mM sodium fluoride, 5 mM sodium pyrophosphate, 1 mM sodium orthovanadate, 1% (w/v) IGEPAL CA-630, 270 mM sucrose, 0.1% (v/v) 2-mercaptoethanol, and protease inhibitors (Complete tablets (Roche Applied Science), 10mM 1,10-phenanthroline and 1 μ g/mL pepstatin).

Modified media and small molecules used in HEK293 cells

Cells were incubated with different media for 16 hours before cell lysis to assess the effect of extracellular K⁺ concentration. The media used were the following: Low K⁺ media (LKM): (135 mM NaCl, 1 mM KCl, 0.5 mM CaCl₂, 0.5 mM MgCl₂, 0.5 mM Na₂HPO₄, 0.5 mM Na₂SO₄, 15 mM HEPES, 27.75 mM glucose, 18 mM sucrose, pH 7.4); normal K⁺ media (NKM): (same as LKM except 5 mM KCl and 10mM sucrose to adjust osmolarity), or high K⁺ media (HKM): (same as LKM except 10 mM KCl and no sucrose). Additionally, the effect of intracellular Cl⁻ depletion was assessed by incubating cells for 2 hours with a hypotonic low Cl⁻ media with normal K⁺ (HLC): (67.5 mM Na-gluconate, 5 mM K-gluconate, 0.5 mM CaCl₂, 0.5 mM MgCl₂, 0.5 mM Na₂HPO₄, 0.5 mM Na₂SO₄, 7.5 mM HEPES, 27.75 mM glucose, pH 7.4; modified from Vitari et al.¹⁷). In the indicated experiments, cells were preincubated with Wnk463 (10 μ M, gift from Dario Alessi) or BIM (4 μ M, Cell Signaling Technology) for 15 minutes before and during the maneuver (incubation in media with different K⁺ content or HLC). Stimulation with NEM (100 μ M, Sigma) was performed for 30 minutes before cell lysis.

***Ex vivo* kidney slices**

12–16-week-old male C57BL/6 mice were anesthetized with isoflurane and then perfused with 20 mL of a modified Ringer media with high K⁺ (93.5 mM NaCl; 25 mM NaHCO₃; 10 mM KCl; 1mM NaH₂PO₄; 2.5 mM CaCl₂; 1.8 mM MgCl₂; 25 mM glucose). Kidneys were collected and placed in the same solution. Then, 250 μ m slices were cut using a vibratome (PELCO easiSlicer™). Slices were incubated at 30.5°C for 30 minutes in the same solution and then switched for another 60 minutes to control Ringer media (98.5 mM NaCl; 25 mM NaHCO₃; 5 mM KCl; 1mM NaH₂PO₄; 2.5 mM CaCl₂; 1.8 mM MgCl₂; 25 mM glucose) or to low K⁺ Ringer media (the same as control except for 102.5 mM NaCl and 1 mM KCl). At the end of the experiment, slices were frozen with liquid N₂ and later homogenized as described above for whole mouse kidneys.

PKC activity assay

Wnk4-transfected HEK293 cells lysates were used with the PKC Kinase Activity Assay Kit (ab139437), following manufacturer's instructions.

cAMP measurement

WNK4-transfected HEK293 cells were incubated with NKM or HLC for 2 hours (or DMSO or Forskolin (30 μ M, Cell Signaling) for 30 minutes as controls in the presence of 125 μ M 3-isobutyl-1-methylxanthine (IBMX) (Sigma). After this, cells were frozen at -70 $^{\circ}$ C for 24 hours. The content of each well was recovered and placed in new tubes that were heated at 95 $^{\circ}$ C for 3 minutes. cAMP quantification was analyzed by radioimmunoassay (RIA) using 2-O-monosuccinyl cAMP tyrosylmethyl ester cAMP (Sigma) marked with NaI¹²⁵ by chloramine-T. cAMP standards and samples were previously acetylated and diluted in sodium acetate 5mM pH 4.75. The cAMP antibody used was Merck-Millipore Cat. 116820 at a final dilution of 1:3000. All samples were analyzed by duplicate and the sensibility of the assay was 4fmol/tube ⁵⁷.

Statistical analysis

All values are expressed as mean \pm SEM. For comparison between two groups, unpaired Student's t-test (two-tailed) was used. For comparison between multiple groups, analysis of variance tests was performed, followed by Tukey post hoc tests. A difference between groups was considered significant when $p < 0.05$.

ACKNOWLEDGEMENTS

Adrián Rafael Murillo-de-Ozores is a doctoral student from the “Programa de Doctorado en Ciencias Biomédicas, Universidad Nacional Autónoma de México (UNAM)” and received a fellowship 606808 from CONACYT. We thank Dr. Dario Alessi for kindly gifting us the WNK463 inhibitor. We thank Cristino Cruz for his help with the measurement of electrolytes in mouse plasma samples and Mariela Guadalupe Contreras Escamilla, Berenice Díaz Ramos, Marysol González Yáñez, and Tania Pérez Benhumea, from the animal facility for their help with the wild type and transgenic mice colonies. We thank the “Red de Apoyo a la Investigación” for providing access to the cell culture facility. This work was supported by grant No. DK51496 from NIH to GG, grants No. 101720 and A1-S-8290 from Conacyt Mexico to M-CB, and GG, respectively; and grant No. IN201519 to GG from PAPIIT UNAM.

ARMO, MCB, and GG conceived and designed the study. ARMO, HCC, GRMA, RV, LIGM, NV, ALS, DHL, WHW, ED, DHE, GG, MCB collected, analyzed, and interpreted the data. ARMO, GG, and MCB wrote the manuscript. All authors approved the final version of the manuscript.

DISCLOSURES

None.

SUPPLEMENTAL MATERIAL TABLE OF CONTENTS

Figure S1. Generation of WNK4-L319F and genotyping

Figure S2. Plasma [K⁺] and NCC analysis of WNK4-L319F mice in a mixed B6-129/Sv genetic background

Table S1. Antibodies used for Western blot and immunofluorescent staining

Supplemental references

REFERENCES

1. Mente A, O'Donnell MJ, Rangarajan S, McQueen MJ, Poirier P, Wielgosz A, Morrison H, Li W, Wang X, Di C, Mony P, Devanath A, Rosengren A, Oguz A, Zatonska K, Yusufali AH, Lopez-Jaramillo P, Avezum A, Ismail N, Lanas F, Puoane T, Diaz R, Kelishadi R, Iqbal R, Yusuf R, Chifamba J, Khatib R, Teo K, Yusuf S: Association of Urinary Sodium and Potassium Excretion with Blood Pressure. *N. Engl. J. Med.* [Internet] 371: 601–611, 2014 Available from: <http://www.nejm.org/doi/10.1056/NEJMoa1311989>
2. Sacks FM, Svetkey LP, Vollmer WM, Appel LJ, Bray GA, Harsha D, Obarzanek E, Conlin PR, Miller ER 3rd, Simons-Morton DG, Karanja N, Lin PH, DASH-Sodium Collaborative Research Group: Effects on blood pressure of reduced dietary sodium and the dietary approaches to stop hypertension (DASH) diet. *New Engl. J. Med.* [Internet] 344: 3–10, 2001 Available from: <http://search.proquest.com.ezproxy.endeavour.edu.au/docview/223951601/93462899FFB24AD5PQ/25?accountid=45102>
3. O'Donnell M, Mente A, Rangarajan S, McQueen MJ, Wang X, Liu L, Yan H, Lee SF, Mony P, Devanath A, Rosengren A, Lopez-Jaramillo P, Diaz R, Avezum A, Lanas F, Yusuf K, Iqbal R, Ilow R, Mohammadifard N, Gulec S, Yusufali AH, Kruger L, Yusuf R, Chifamba J, Kabali C, Dagenais G, Lear SA, Teo K, Yusuf S: Urinary Sodium and Potassium Excretion, Mortality, and Cardiovascular Events. *N. Engl. J. Med.* [Internet] 371: 612–623, 2014 Available from: <http://www.nejm.org/doi/10.1056/NEJMoa1311889>
4. Guyton AC: Blood pressure control - Special role of the kidneys and body fluids. *Science (80- .).* 252: 1813–1816, 1991
5. Vitzthum H, Seniuk A, Schulte LH, Müller ML, Hetz H, Ehmke H: Functional coupling of renal K⁺ and Na⁺ handling causes high blood pressure in Na⁺ replete mice. *J. Physiol.* [Internet] 592: 1139–57, 2014 Available from: <http://www.ncbi.nlm.nih.gov/pubmed/24396058>
6. Terker AS, Zhang C, McCormick JA, Lazelle RA, Zhang C, Meermeier NP, Siler DA, Park HJ, Fu Y, Cohen DM, Weinstein AM, Wang WH, Yang CL, Ellison DH: Potassium modulates electrolyte balance and blood pressure through effects on distal cell voltage and chloride. *Cell Metab.* 21: 39–50, 2015
7. Gamba G: Molecular Physiology and Pathophysiology of Electroneutral Cation-Chloride Cotransporters. *Physiol. Rev.* [Internet] 85: 423–493, 2005 Available from: <http://physrev.physiology.org/cgi/doi/10.1152/physrev.00011.2004>
8. Murillo-de-Ozores AR, Gamba G, Castañeda-Bueno M: Molecular mechanisms for the regulation of blood pressure by potassium [Internet]. In: *Current Topics in Membranes*, 1st ed., pp 285–313, 2019 Available from: <http://dx.doi.org/10.1016/bs.ctm.2019.01.004>
9. Simon DB, Nelson-Williams C, Bia MJ, Ellison D, Karet FE, Molina a M, Vaara I, Iwata F, Cushner HM, Koolen M, Gainza FJ, Gitelman HJ, Lifton RP: Gitelman's variant of Bartter's syndrome, inherited hypokalaemic alkalosis, is caused by mutations in the thiazide-sensitive Na-Cl cotransporter. *Nat Genet* 12: 24–30, 1996
10. Wilson FH, Disse-Nicodè S, Choate KA, Ishikawa K, Nelson-Williams C, Desitter I, Gunel M,

Milford DM: Human Hypertension Caused by Mutations in WNK Kinases. *Science* (80-). [Internet] 293: 1107–1112, 2001 Available from: <http://www.ncbi.nlm.nih.gov/pubmed/11498583>

11. Boyden LM, Choi M, Choate KA, Nelson-Williams CJ, Farhi A, Toka HR, Tikhonova IR, Bjornson R, Mane SM, Colussi G, Lebel M, Gordon RD, Semmekrot BA, Poujol A, Välimäki MJ, De Ferrari ME, Sanjad SA, Gutkin M, Karet FE, Tucci JR, Stockigt JR, Keppler-Noreuil KM, Porter CC, Anand SK, Whiteford ML, Davis ID, Dewar SB, Bettinelli A, Fadrowski JJ, Belsha CW, Hunley TE, Nelson RD, Trachtman H, Cole TR, Pinsky M, Bockenhauer D, Shenoy M, Vaidyanathan P, Foreman JW, Rasoulpour M, Thameem F, Al-Shahrouri HZ, Radhakrishnan J, Gharavi AG, Goilav B, Lifton RP: Mutations in kelch-like 3 and cullin 3 cause hypertension and electrolyte abnormalities. *Nature* [Internet] 482: 98–102, 2012 Available from: <http://www.nature.com/doi/10.1038/nature10814>
12. Louis-Dit-Picard H, Barc J, Trujillano D, Miserey-Lenkei S, Bouatia-Naji N, Pylypenko O, Beaurain G, Bonnefond A, Sand O, Simian C, Vidal-Petiot E, Soukaseum C, Mandet C, Broux F, Chabre O, Delahousse M, Esnault V, Fiquet B, Houillier P, Bagnis CI, Koenig J, Konrad M, Landais P, Mourani C, Niaudet P, Probst V, Thauvin C, Unwin RJ, Soroka SD, Ehret G, Ossowski S, Caulfield M, Bruneval P, Estivill X, Froguel P, Hadchouel J, Schott J-J, Jeunemaitre X: KLHL3 mutations cause familial hyperkalemic hypertension by impairing ion transport in the distal nephron. *Nat. Genet.* [Internet] 44: 456–460, 2012 Available from: <http://www.nature.com/doi/10.1038/ng.2218>
13. Lalioti MD, Zhang J, Volkman HM, Kahle KT, Hoffmann KE, Toka HR, Nelson-Williams C, Ellison DH, Flavell R, Booth CJ, Lu Y, Geller DS, Lifton RP: Wnk4 controls blood pressure and potassium homeostasis via regulation of mass and activity of the distal convoluted tubule. *Nat. Genet.* [Internet] 38: 1124–1132, 2006 Available from: <http://www.nature.com/doi/10.1038/ng1877>
14. Grimm PR, Coleman R, Delpire E, Welling PA: Constitutively Active SPAK Causes Hyperkalemia by Activating NCC and Remodeling Distal Tubules. *J. Am. Soc. Nephrol.* 28: 2597–2606, 2017
15. Pacheco-Alvarez D, San Cristóbal P, Meade P, Moreno E, Vazquez N, Muñoz E, Díaz A, Juárez ME, Giménez I, Gamba G: The Na⁺:Cl⁻ cotransporter is activated and phosphorylated at the amino-terminal domain upon intracellular chloride depletion. *J. Biol. Chem.* 281: 28755–28763, 2006
16. Alessi DR, Zhang J, Khanna A, Hochdorfer T, Shang Y, Kahle KT: The WNK-SPAK/OSR1 pathway: Master regulator of cation-chloride cotransporters. *Sci. Signal.* [Internet] 7: re3–re3, 2014 Available from: <http://stke.sciencemag.org/cgi/doi/10.1126/scisignal.2005365>
17. Vitari AC, Deak M, Morrice NA, Alessi DR: The WNK1 and WNK4 protein kinases that are mutated in Gordon's hypertension syndrome phosphorylate and activate SPAK and OSR1 protein kinases. *Biochem. J.* [Internet] 391: 17–24, 2005 Available from: <http://biochemj.org/lookup/doi/10.1042/BJ20051180>
18. Castaneda-Bueno M, Cervantes-Perez LG, Vazquez N, Uribe N, Kantesaria S, Morla L, Bobadilla NA, Doucet A, Alessi DR, Gamba G: Activation of the renal Na⁺:Cl⁻ cotransporter by angiotensin II is a WNK4-dependent process. *Proc. Natl. Acad. Sci.* [Internet] 109: 7929–7934, 2012 Available from: <http://www.pnas.org/cgi/doi/10.1073/pnas.1200947109>

19. Susa K, Sohara E, Takahashi D, Okado T, Rai T, Uchida S: WNK4 is indispensable for the pathogenesis of pseudohypoaldosteronism type II caused by mutant KLHL3. *Biochem. Biophys. Res. Commun.* [Internet] 491: 727–732, 2017 Available from: <http://dx.doi.org/10.1016/j.bbrc.2017.07.121>
20. Murillo-de-Ozores AR, Rodríguez-Gama A, Carbajal-Contreras H, Gamba G, Castañeda-Bueno M: WNK4 kinase: from structure to physiology. *Am. J. Physiol. Physiol.* 320: F378–F403, 2021
21. Vallon V, Schroth J, Lang F, Kuhl D, Uchida S: Expression and phosphorylation of the Na⁺-Cl⁻ cotransporter NCC in vivo is regulated by dietary salt, potassium, and SGK1. *Am. J. Physiol. - Ren. Physiol.* 297: F704–F712, 2009
22. Sorensen M V., Grossmann S, Roesinger M, Gresko N, Todkar AP, Barmettler G, Ziegler U, Odermatt A, Loffing-Cueni D, Loffing J: Rapid dephosphorylation of the renal sodium chloride cotransporter in response to oral potassium intake in mice. *Kidney Int.* [Internet] 83: 811–824, 2013 Available from: <http://linkinghub.elsevier.com/retrieve/pii/S0085253815558353>
23. Castaneda-Bueno M, Cervantes-Perez LG, Rojas-Vega L, Arroyo-Garza I, Vazquez N, Moreno E, Gamba G: Modulation of NCC activity by low and high K⁺ intake: insights into the signaling pathways involved. *Am. J. Physiol. - Ren. Physiol.* [Internet] 306: F1507–F1519, 2014 Available from: <http://ajprenal.physiology.org/cgi/doi/10.1152/ajprenal.00255.2013>
24. Cuevas CA, Su X-T, Wang M-X, Terker AS, Lin D-H, McCormick JA, Yang C-L, Ellison DH, Wang W-H: Potassium Sensing by Renal Distal Tubules Requires Kir4.1. *J. Am. Soc. Nephrol.* [Internet] 28: 1814–1825, 2017 Available from: <http://www.jasn.org/lookup/doi/10.1681/ASN.2016090935>
25. Wang MX, Cuevas CA, Su XT, Wu P, Gao ZX, Lin DH, McCormick JA, Yang CL, Wang WH, Ellison DH: Potassium intake modulates the thiazide-sensitive sodium-chloride cotransporter (NCC) activity via the Kir4.1 potassium channel. *Kidney Int.* [Internet] 93: 893–902, 2018 Available from: <https://doi.org/10.1016/j.kint.2017.10.023>
26. Nomura N, Shoda W, Wang Y, Mandai S, Furusho T, Takahashi D, Zeniya M, Sohara E, Rai T, Uchida S: Role of CIC-K and barttin in low-potassium induced sodium-chloride cotransporter activation and hypertension in mouse kidney. *Biosci. Rep.* [Internet] 38: 2018 Available from: <http://bioscirep.org/lookup/doi/10.1042/BSR20171243>
27. Bazua-Valenti S, Chavez-Canales M, Rojas-Vega L, Gonzalez-Rodriguez X, Vazquez N, Rodriguez-Gama A, Argaiz ER, Melo Z, Plata C, Ellison DH, Garcia-Valdes J, Hadchouel J, Gamba G: The Effect of WNK4 on the Na⁺-Cl⁻ Cotransporter Is Modulated by Intracellular Chloride. *J. Am. Soc. Nephrol.* [Internet] 26: 1781–1786, 2015 Available from: <http://www.jasn.org/cgi/doi/10.1681/ASN.2014050470>
28. Terker AS, Zhang C, Erspamer KJ, Gamba G, Yang C-L, Ellison DH: Unique chloride-sensing properties of WNK4 permit the distal nephron to modulate potassium homeostasis. *Kidney Int.* [Internet] 89: 1–8, 2015 Available from: <http://www.nature.com/doi/10.1038/ki.2015.289>
29. Piali AT, Moon TM, Akella R, He H, Cobb MH, Goldsmith EJ: Chloride Sensing by WNK1 Involves Inhibition of Autophosphorylation. *Sci. Signal.* [Internet] 7: ra41–ra41, 2014

Available from: <http://stke.sciencemag.org/cgi/doi/10.1126/scisignal.2005050>

30. Ishizawa K, Xu N, Loffing J, Lifton RP, Fujita T, Uchida S, Shibata S: Potassium depletion stimulates Na-Cl cotransporter via phosphorylation and inactivation of the ubiquitin ligase Kelch-like 3. *Biochem. Biophys. Res. Commun.* 480: 745–751, 2016
31. Shibata S, Zhang J, Puthumana J, Stone KL, Lifton RP: Kelch-like 3 and Cullin 3 regulate electrolyte homeostasis via ubiquitination and degradation of WNK4. *Proc. Natl. Acad. Sci.* [Internet] 110: 7838–7843, 2013 Available from: <http://www.pubmedcentral.nih.gov/articlerender.fcgi?artid=3651502&tool=pmcentrez&rendertype=abstract%5Cnhttp://www.pnas.org/cgi/doi/10.1073/pnas.1304592110>
32. Wakabayashi M, Mori T, Isobe K, Sohara E, Susa K, Araki Y, Chiga M, Kikuchi E, Nomura N, Mori Y, Matsuo H, Murata T, Nomura S, Asano T, Kawaguchi H, Nonoyama S, Rai T, Sasaki S, Uchida S: Impaired KLHL3-mediated ubiquitination of WNK4 causes human hypertension. *Cell Rep.* [Internet] 3: 858–868, 2013 Available from: <http://dx.doi.org/10.1016/j.celrep.2013.02.024>
33. Shibata S, Arroyo JP, Castaneda-Bueno M, Puthumana J, Zhang J, Uchida S, Stone KL, Lam TT, Lifton RP: Angiotensin II signaling via protein kinase C phosphorylates Kelch-like 3, preventing WNK4 degradation. *Proc. Natl. Acad. Sci.* [Internet] 111: 15556–15561, 2014 Available from: <http://www.pnas.org/cgi/doi/10.1073/pnas.1418342111>
34. Castañeda-Bueno M, Arroyo JP, Zhang J, Puthumana J, Yarborough O, Shibata S, Rojas-Vega L, Gamba G, Rinehart J, Lifton RP: Phosphorylation by PKC and PKA regulate the kinase activity and downstream signaling of WNK4. *Proc. Natl. Acad. Sci.* [Internet] 114: E879–E886, 2017 Available from: <http://www.pnas.org/lookup/doi/10.1073/pnas.1620315114>
35. Yang YS, Xie J, Yang S, Sen, Lin SH, Huang CL: Differential roles of WNK4 in regulation of NCC in vivo. *Am. J. Physiol. - Ren. Physiol.* 314: F999–F1007, 2018
36. Boyd-Shiwarski CR, Shiwerski DJ, Roy A, Namboodiri HN, Nkashama LJ, Xie J, McClain KL, Marciszyn A, Kleyman TR, Tan RJ, Stolz DB, Puthenveedu MA, Huang CL, Subramanya AR: Potassium-regulated distal tubule WNK bodies are kidney-specific WNK1 dependent. *Mol. Biol. Cell* 29: 499–509, 2018
37. Thomson MN, Cuevas CA, Bewarder TM, Dittmayer C, Miller LN, Si J, Cornelius RJ, Su X-T, Yang C-L, McCormick JA, Hadchouel J, Ellison DH, Bachmann S, Mutig K: WNK bodies cluster WNK4 and SPAK/OSR1 to promote NCC activation in hypokalemia. *Am. J. Physiol. Physiol.* [Internet] 318: F216–F228, 2020 Available from: <https://www.physiology.org/doi/10.1152/ajprenal.00232.2019>
38. Richardson C, Rafiqi FH, Karlsson HKR, Moleleki N, Vandewalle A, Campbell DG, Morrice NA, Alessi DR: Activation of the thiazide-sensitive Na⁺-Cl⁻ cotransporter by the WNK-regulated kinases SPAK and OSR1. *J. Cell Sci.* [Internet] 121: 675–684, 2008 Available from: <http://jcs.biologists.org/cgi/doi/10.1242/jcs.025312>
39. Gagnon KBE, England R, Delpire E: Characterization of SPAK and OSR1, Regulatory Kinases of the Na-K-2Cl Cotransporter. *Mol. Cell. Biol.* [Internet] 26: 689–698, 2006 Available from: <http://mcb.asm.org/cgi/doi/10.1128/MCB.26.2.689-698.2006>
40. Conway LC, Cardarelli RA, Moore YE, Jones K, McWilliams LJ, Baker DJ, Burnham MP, Bürli

RW, Wang Q, Brandon NJ, Moss SJ, Deeb TZ: N-Ethylmaleimide increases KCC2 cotransporter activity by modulating transporter phosphorylation. *J. Biol. Chem.* 292: 21253–21263, 2017

41. Yamada K, Park H-M, Rigel DF, DiPetrillo K, Whalen EJ, Anisowicz A, Beil M, Berstler J, Brocklehurst CE, Burdick DA, Caplan SL, Capparelli MP, Chen G, Chen W, Dale B, Deng L, Fu F, Hamamatsu N, Harasaki K, Herr T, Hoffmann P, Hu Q-Y, Huang W-J, Idamakanti N, Imase H, Iwaki Y, Jain M, Jeyaseelan J, Kato M, Kaushik VK, Kohls D, Kunjathoor V, LaSala D, Lee J, Liu J, Luo Y, Ma F, Mo R, Mowbray S, Mogi M, Ossola F, Pandey P, Patel SJ, Raghavan S, Salem B, Shanado YH, Trakshel GM, Turner G, Wakai H, Wang C, Weldon S, Wielicki JB, Xie X, Xu L, Yagi YI, Yasoshima K, Yin J, Yowe D, Zhang J-H, Zheng G, Monovich L: Small-molecule WNK inhibition regulates cardiovascular and renal function. *Nat. Chem. Biol.* [Internet] 12: 896–898, 2016 Available from: <http://www.nature.com/doi/10.1038/nchembio.2168>
42. Penton D, Czogalla J, Wengi A, Himmerkus N, Loffing-Cueni D, Carrel M, Rajaram RD, Staub O, Bleich M, Schweda F, Loffing J: Extracellular K⁺ rapidly controls NaCl cotransporter phosphorylation in the native distal convoluted tubule by Cl⁻-dependent and independent mechanisms. *J. Physiol.* [Internet] 594: 6319–6331, 2016 Available from: <http://doi.wiley.com/10.1113/JP272504>
43. Mukherjee A, Yang C-L, McCormick JA, Martz K, Sharma A, Ellison DH: Roles of WNK4 and SPAK in K⁺ mediated dephosphorylation of the sodium chloride cotransporter. *Am. J. Physiol. Physiol.* 2021
44. Wu P, Gao ZX, Zhang DD, Su XT, Wang WH, Lin DH: Deletion of Kir5.1 impairs renal ability to excrete potassium during increased dietary potassium intake. *J. Am. Soc. Nephrol.* 30: 1425–1438, 2019
45. Yoshizaki Y, Mori Y, Tsuzaki Y, Mori T, Nomura N, Wakabayashi M, Takahashi D, Zeniya M, Kikuchi E, Araki Y, Ando F, Isobe K, Nishida H, Ohta A, Susa K, Inoue Y, Chiga M, Rai T, Sasaki S, Uchida S, Sohara E: Impaired degradation of WNK by Akt and PKA phosphorylation of KLHL3. *Biochem. Biophys. Res. Commun.* 467: 229–234, 2015
46. Louis-Dit-Picard H, Kouranti I, Rafael C, Loisel-Ferreira I, Chavez-Canales M, Abdel-Khalek W, Argaiz ER, Baron S, Vacle S, Migeon T, Coleman R, Do Cruzeiro M, Hureaux M, Thurairajasingam N, Decramer S, Girerd X, O'Shaughnessy K, Mulatero P, Roussey G, Tack I, Unwin R, Vargas-Poussou R, Staub O, Grimm R, Welling PA, Gamba G, Clauser E, Hadchouel J, Jeunemaitre X: Mutation affecting the conserved acidic WNK1 motif causes inherited hyperkalemic hyperchloremic acidosis. *J. Clin. Invest.* [Internet] Oct 26: 94171, 2020 Available from: <https://www.jci.org/articles/view/94171>
47. Ostrosky-Frid M, Chavez-Canales M, Zhang J, Andrukova O, Argaiz ER, Lerdo de Tejada F, Murillo-de-Ozores AR, Sanchez-Navarro A, Rojas-Vega L, Bobadilla NA, Vazquez N, Castaneda-Bueno M, Alessi DR, Gamba G: Role of KLHL3 and dietary K⁺ in regulating KS-WNK1 expression. *Am. J. Physiol. Physiol.* [Internet] ajprenal.00575.2020, 2021 Available from: <https://journals.physiology.org/doi/10.1152/ajprenal.00575.2020>
48. Vidal-Petiot E, Cheval L, Faugueroux J, Malard T, Doucet A, Jeunemaitre X, Hadchouel J: A new methodology for quantification of alternatively spliced exons reveals a highly tissue-specific expression pattern of WNK1 isoforms. *PLoS One* 7: 1–9, 2012

49. Chen L, Chou C, Knepper MA: A Comprehensive Map of mRNAs and Their Isoforms across All 14 Renal Tubule Segments of Mouse. 2021
50. Weinstein AM: A mathematical model of distal nephron acidification: Diuretic effects. *Am. J. Physiol. - Ren. Physiol.* 295: 1353–1364, 2008
51. Bazúa-Valenti S, Gamba G: Revisiting the NaCl cotransporter regulation by with-no-lysine kinases. *Am. J. Physiol. - Cell Physiol.* [Internet] 308: C779–C791, 2015 Available from: <http://ajpcell.physiology.org/lookup/doi/10.1152/ajpcell.00065.2015>
52. Limbutara K, Chou C-L, Knepper MA: Quantitative Proteomics of All 14 Renal Tubule Segments in Rat. *J. Am. Soc. Nephrol.* [Internet] 31: 1255–1266, 2020 Available from: <http://www.ncbi.nlm.nih.gov/pubmed/32358040>
53. Sterling H, Lin DH, Chen YJ, Wei Y, Wang ZJ, Lai J, Wang WH: PKC expression is regulated by dietary K intake and mediates internalization of SK channels in the CCD. *Am. J. Physiol. - Ren. Physiol.* 286: 1072–1078, 2004
54. Su X, Klett NJ, Sharma A, Allen CN, Wang W, Yang C, Ellison DH: Distal convoluted tubule Cl⁻ concentration is modulated via K⁺ channels and transporters. *Am. J. Physiol. Physiol.* [Internet] 319: F534–F540, 2020 Available from: <https://journals.physiology.org/doi/10.1152/ajprenal.00284.2020>
55. Chen J-C, Lo Y-F, Lin Y-W, Lin S-H, Huang C-L, Cheng C-J: WNK4 kinase is a physiological intracellular chloride sensor. *Proc. Natl. Acad. Sci.* [Internet] 116: 4502–4507, 2019 Available from: <http://www.pnas.org/lookup/doi/10.1073/pnas.1817220116>
56. Soh JW, Weinstein IB: Roles of Specific Isoforms of Protein Kinase C in the Transcriptional Control of Cyclin D1 and Related Genes. *J. Biol. Chem.* [Internet] 278: 34709–34716, 2003 Available from: <http://dx.doi.org/10.1074/jbc.M302016200>
57. Zambrano E, Barrios-de-Tomasi J, Cárdenas M, Ulloa-Aguirre A: Studies on the relative in-vitro biological potency of the naturally-occurring isoforms of intrapituitary follicle stimulating hormone. *Mol. Hum. Reprod.* 2: 563–571, 1996

FIGURE LEGENDS

Figure 1. WNK4 phosphorylation at S64 and S1196 is stimulated by low K^+ intake. (A) Representative immunoblots of total kidney proteins of mice maintained on normal K^+ diet (NKD) or low K^+ diet (LKD) for 7 days. Mean plasma $[K^+]_e$ values for each group are shown on top of the blots. (B) Results of the densitometric analysis of the blots represented in A show that WNK4 phosphorylation levels at S64 and S1196 are higher in mice on LKD even after normalization to total WNK4 levels. Ratio values obtained for mice on NKD were normalized to 100%. Bars represent mean and error bars represent SEM. For statistical analysis, student t tests were performed. * $p < 0.01$, ** $p < 0.005$, *** $p < 0.001$, **** $p < 0.0001$, $n = 6$ per group. (C-H) Immunofluorescent labeling of kidney slices from mice maintained on NKD or LKD was performed to detect changes that occur within DCT cells (identified by NCC labeling). WNK bodies were detected in DCT cells of mice maintained in LKD with the pWNK4-S64 (C), pS1196 (E), and WNK4 (G) antibodies, but were not detected in kidney slices from mice in NKD with these same antibodies (D, F, H).

Figure 2. Decreases in extracellular $[K^+]_e$ and intracellular $[Cl^-]_i$ stimulate WNK4-RRXS phosphorylation in HEK293 cells. (A) Representative immunoblots of WNK4-transfected HEK293 cells incubated on media containing 1mM K^+ , 5mM K^+ , or 10mM K^+ (LKM, NKM, or HKM, respectively). (B) Densitometric analysis of pWNK4-S64/WNK4 and pWNK4-S1196/WNK4 from at least 5 independent experiments show a statistically significant increase in S64 and S1196 WNK4 phosphorylation in cells incubated in LKM. Values for NKM group were normalized to 100 % and other groups were normalized accordingly. pSPAK levels were also altered as previously shown⁶. (C) Representative immunoblots of WNK4-transfected HEK293 cells incubated in NKM or hypotonic low Cl^- medium (HLC). (D) Densitometric analysis of the blots represented in C. At least 6 independent experiments were performed. Increased pWNK4-S64/WNK4 and pWNK4-S1196/WNK4 levels were observed in cells incubated in HLC medium. (E) Immunoblots of cells stimulated with N-ethylmaleimide (NEM, 100 μ M) for 30 minutes. (F) Results of quantitation, including data from at least 6 independent experiments. NEM stimulation decreases SPAK phosphorylation, as previously reported⁴⁰, but increases WNK4-S1196 phosphorylation. (G) Immunoblots of cells incubated in LKM, NKM, or HKM in the absence or presence of WNK463 (10 μ M). (H) Results of quantitation, including data from at least 4 experiments. All data are mean \pm SEM. * $p < 0.05$, ** $p < 0.005$, *** $p < 0.001$, **** $p < 0.0005$.

Figure 3. WNK4 S64 and S1196 phosphorylation is directly modulated by $[K^+]_e$ in the kidney. (A) Representative immunoblots showing the levels of pWNK4-S64, WNK4, pNCC, and NCC of kidney slices incubated in normal K^+ (1 mM) and low K^+ (5 mM) containing buffers. (B) Results of quantitation of pWNK4 and pNCC levels normalized to total protein levels. Ratio values for low K^+ samples were normalized to those observed on normal K^+ samples (100 %). (C) Same as in A, but pWNK4-S1196 levels were analyzed. (D) Results of quantitation of blots represented in (C). (E) Representative immunoblots of total kidney protein samples from Kir5.1^{+/+} and Kir5.1^{-/-} mice. (F) Results of quantitation show statistically significant higher pWNK4-S1196/WNK4 levels in Kir5.1^{-/-} mice. Data are mean \pm SEM, * $p < 0.05$, ** $p < 0.005$, *** $p < 0.001$, **** $p < 0.0001$.

Figure 4. KLHL3-targeted degradation of WNK kinases is modulated by $[Cl^-]_i$. (A) HEK293 cells were cotransfected with WNK4 plus empty vector or WNK4 plus KLHL3. After stimulation for 16 hours with the indicated media, cells were lysed and immunoblots were performed. (B) Results of

quantitation of blots represented in (A) show that WNK4 levels are only modulated in response to changes in $[K^+]_e$ when KLHL3 is overexpressed. Bar graphs represent WNK4/Actin values observed in LKM, normalized to those observed in NKM. (C) Same as in A, but cells were stimulated with NKM or HLC medium. (D) Densitometric analysis shows that the upregulation of WNK4 expression observed in response to stimulation with HLC medium, is significantly higher in the presence of KLHL3. (E) Immunoblot analysis of kidney proteins from WNK4^{-/-} mice and wild type littermates. The panWNK1 antibody used was previously shown to recognize a band corresponding to KS-WNK1 at the indicated height (black arrow) in immunoblots⁴⁷. (F) Representative immunoblots of kidney proteins from mice treated with vehicle or hydrochlorothiazide (60mg/kg body weight) for 12 hours. Mean plasma $[K^+]$ values for each group are indicated above. (G-H) Immunofluorescent staining of kidney slices from thiazide-treated mice (same animals analyzed in F). Thiazide treatment induces the formation of WNK bodies (detected with the WNK1 and WNK4 antibodies) in DCT cells (NCC positive) (white arrows). Data are mean \pm SEM. * $p < 0.05$, ** $p < 0.0001$

Figure 5. Analysis of NCC, pNCC and WNK4 abundance in the kidney from WT and WNK4^{L319F/L319F} mice at baseline conditions. Representative immunoblots of NCC, pNCC (A) and WNK4 (B) performed with total kidney lysates of wild type and WNK4^{L319F/L319F} mice. Quantitative analysis of pNCC/Actin (C), NCC/Actin (D) and WNK4/Coomassie (E) levels observed in immunoblots represented in A. Values observed in wild type mice were normalized to 100%. Data are mean \pm SEM. * $p < 0.05$, ** $p < 0.005$.

Figure 6. Low $[K^+]_e$ -induced upregulation of NCC is observed in WNK4^{L319F/L319F}. (A) WNK4^{L319F/L319F} mice were placed on a normal or K^+ deficient diet for 7 days. No significant differences were observed in plasma $[K^+]$ among wild type and knockin mice maintained on normal K^+ diet. In both genotypes, administration of a K^+ deficient diet produced similar reductions in plasma $[K^+]$. (B) Representative immunoblots performed with total kidney lysates of wild type and WNK4^{L319F/L319F} mice on normal and K^+ deficient diets. (C) Quantitative analysis of pNCC/actin and NCC/actin levels observed in immunoblots represented in B. Values observed in wild type mice on normal K^+ diet were normalized to 100% and other groups were normalized accordingly. (D) Quantitative analysis of KS-WNK1/Coomassie and WNK4/actin levels. (E) Quantitative analysis of pWNK4-S64/actin and pWNK4-S1196/actin levels. (F) Quantitative analysis of pSPAK/actin levels. Data are mean \pm SEM, * $p < 0.05$, ** $p < 0.01$, *** $p < 0.001$, **** $p < 0.0001$ vs control.

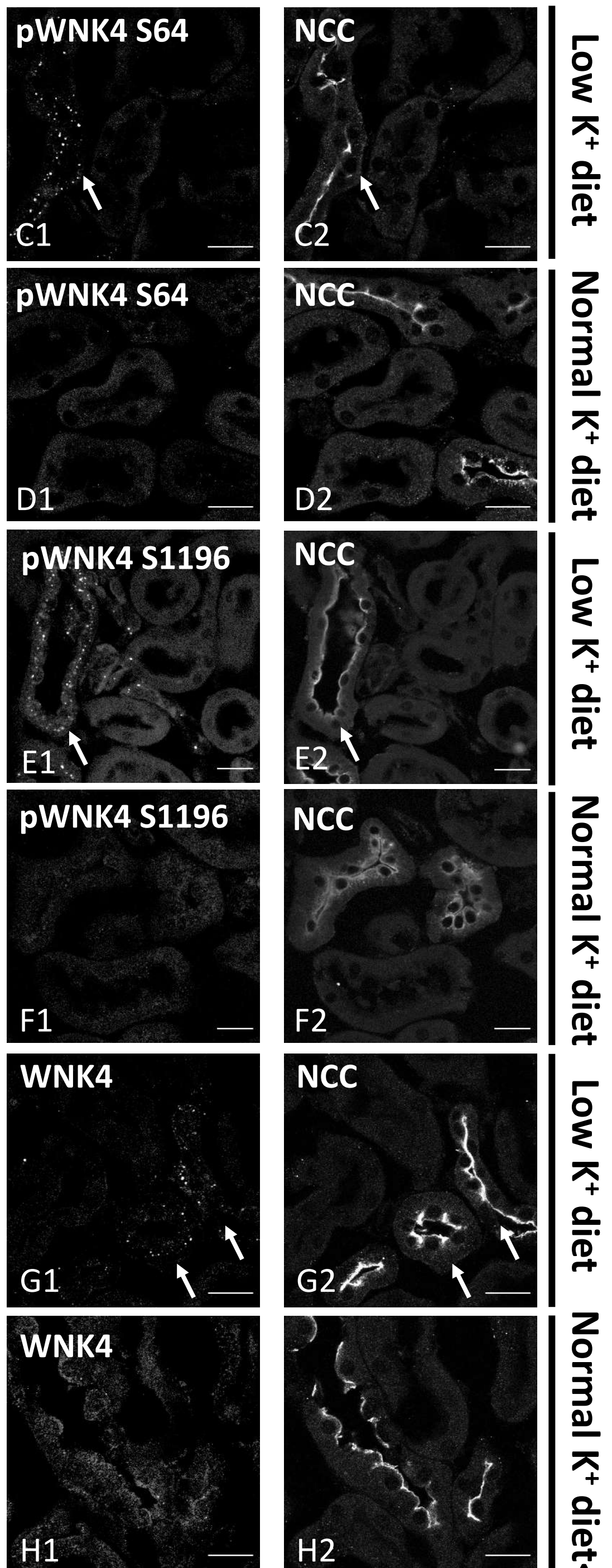
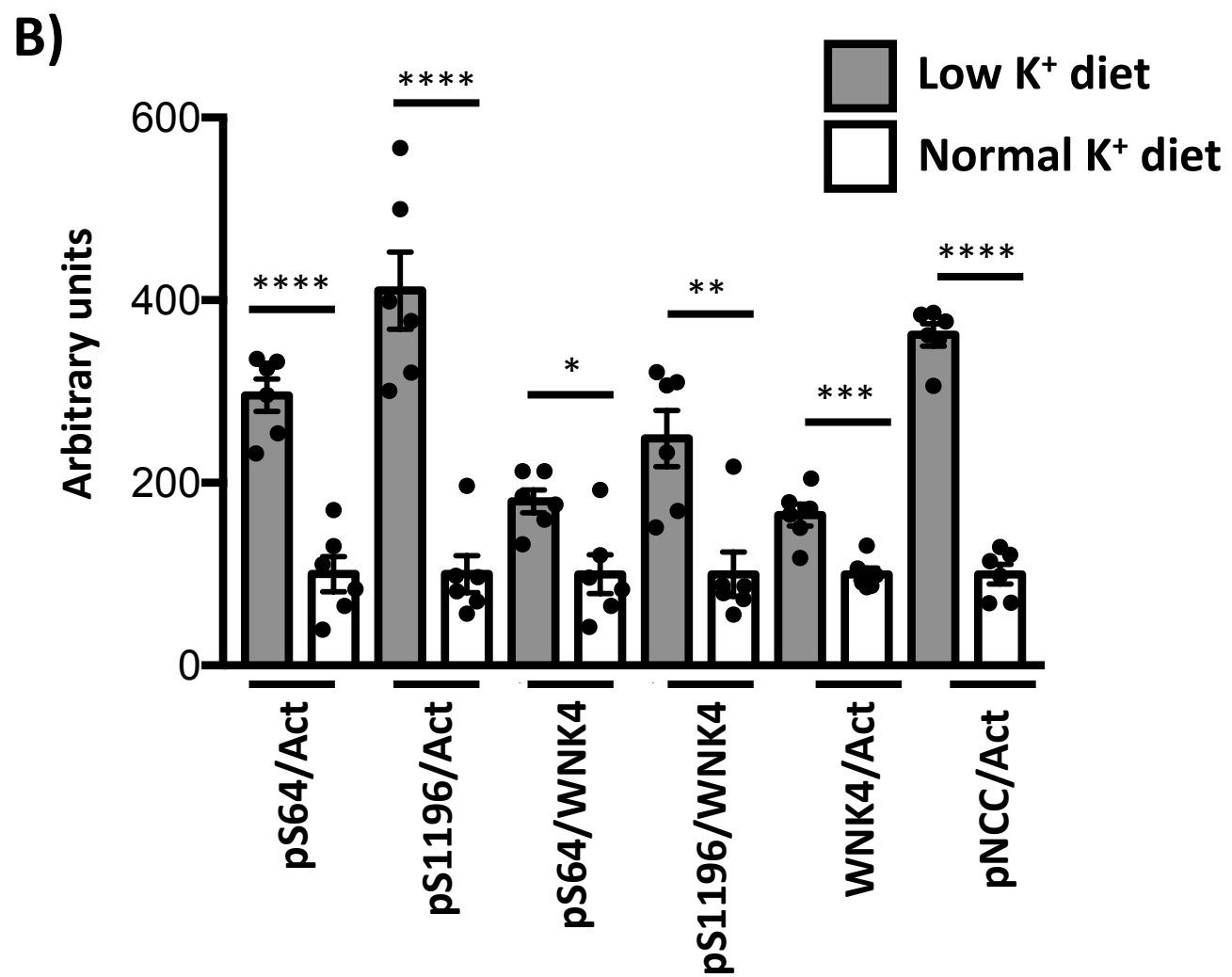
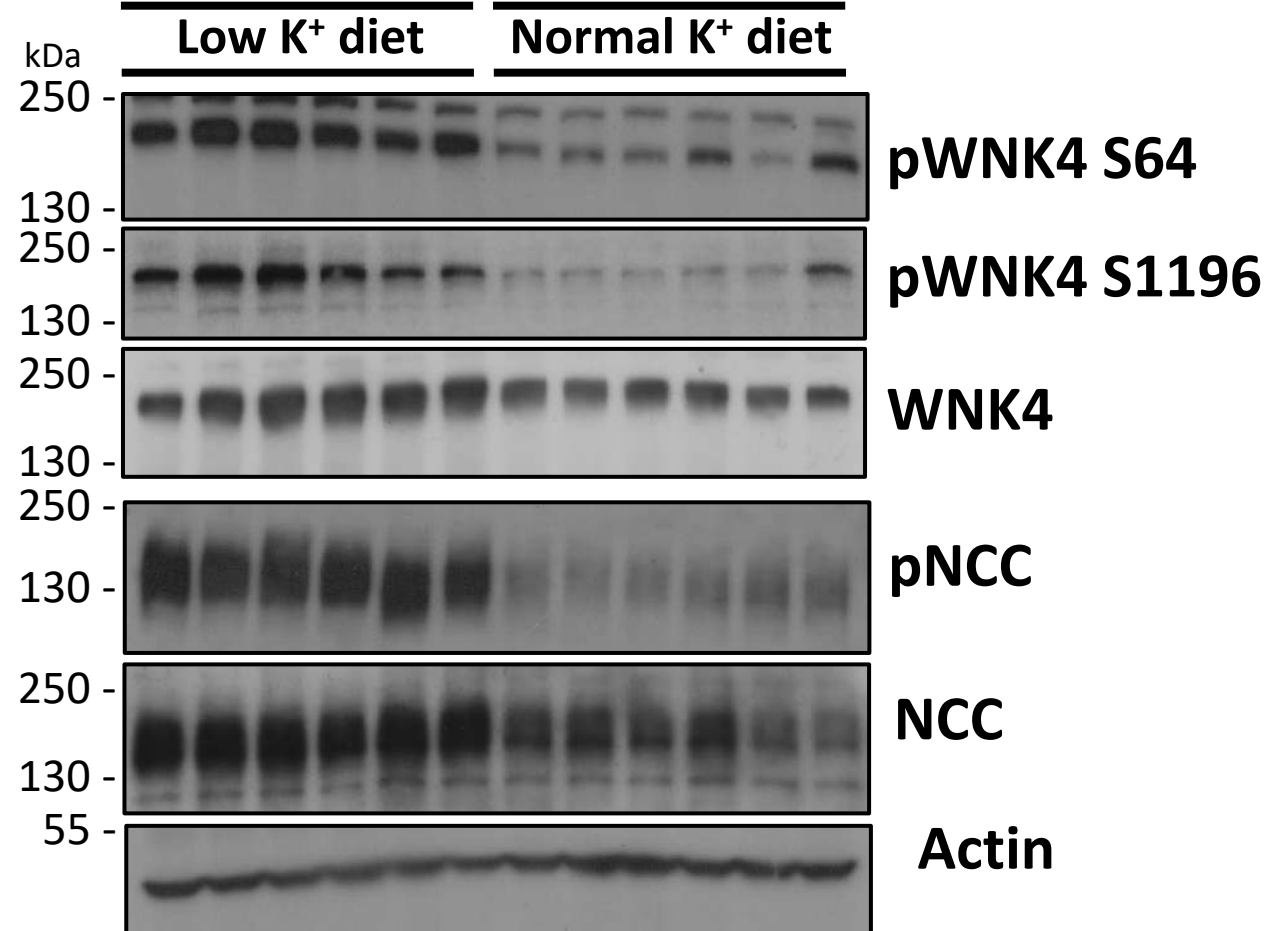
Figure 7. Possible role for PKC in $[Cl^-]_i$ depletion-induced WNK4-S64 and S1196 phosphorylation. (A) Immunoblots showing that PKC inhibition with Bisindoylmaleimide I (BIM) prevents the stimulation of WNK4 phosphorylation at S64 and S1196 by $[Cl^-]_i$ depletion in HEK293 cells. (B) Densitometric analysis of pWNK4-S64/WNK4 and pWNK4-S1196/WNK4 from at least 4 independent experiments. (C) Endogenous PKC activity levels determined by ELISA of HEK293 cells incubated in HLC, normalized to levels observed in NKM. Data from 3 independent experiments is included. (D) Intracellular $[cAMP]$ levels assessed by RIA, of cells incubated on control or HLC medium. Forskolin-stimulated cells were used as a positive control of a maneuver that is known to increase $[cAMP]$ levels. Three independent experiments were performed. (E) PKC δ and PKC ϵ levels, assessed by immunoblot, of kidneys of mice maintained on NKD or LKD for 7 days. (F) Results of quantitation of blots represented in D. $n = 6$ per group. (G) Representative immunoblots showing the effect of PKC δ expression on WNK4-S64 and S1196 phosphorylation in HEK293 cells. (H) Results of quantitation of blots represented in F. $n = 6$ per group. All data are mean \pm SEM, * $p < 0.05$, ** $p < 0.0001$.

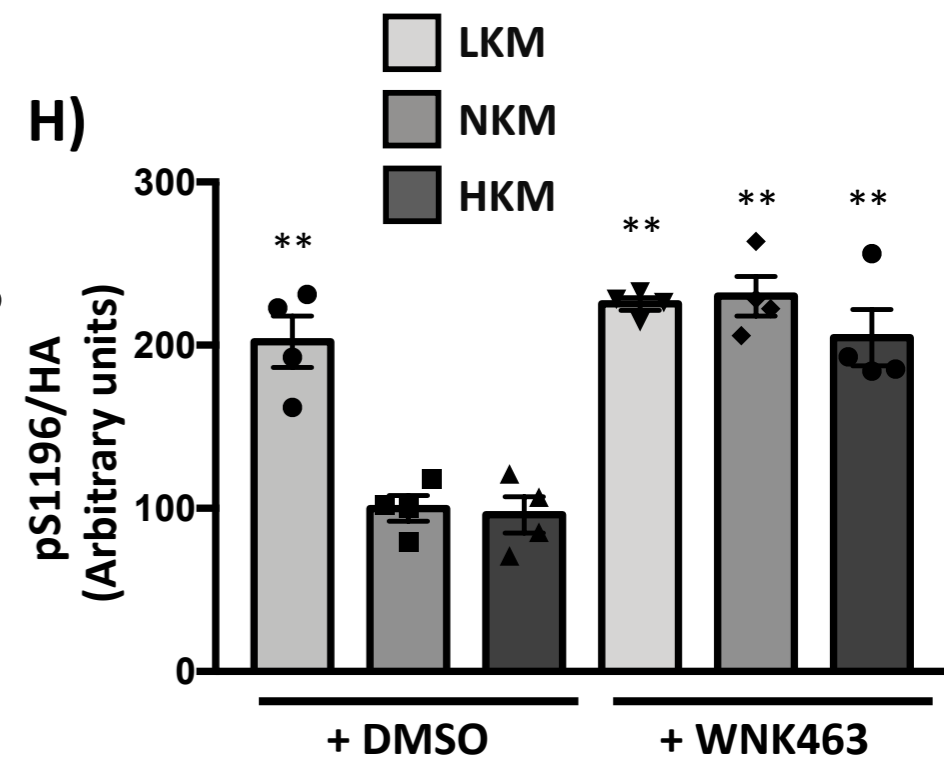
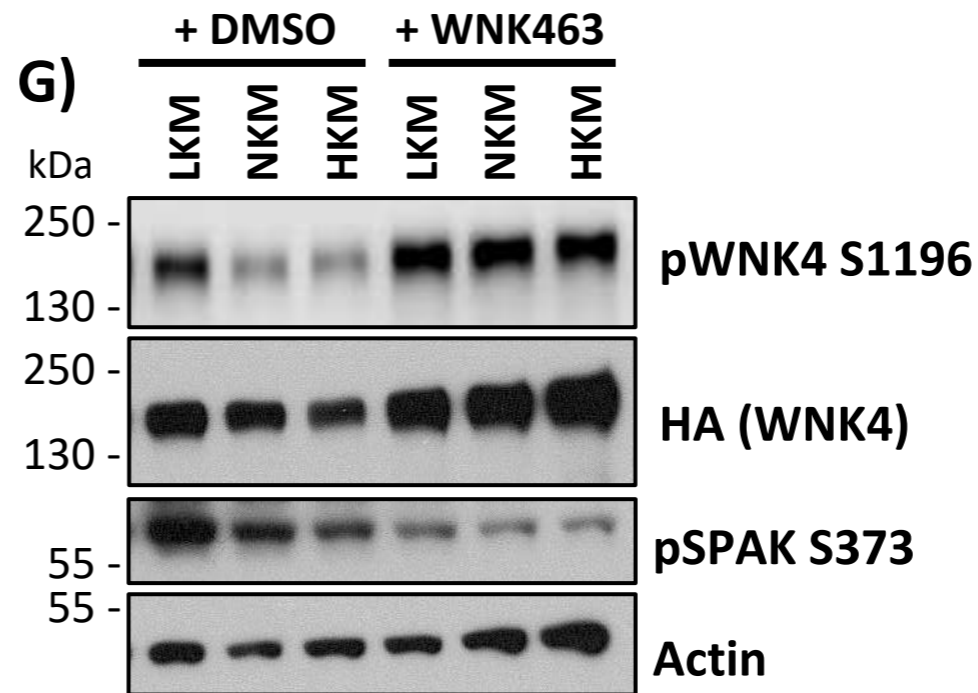
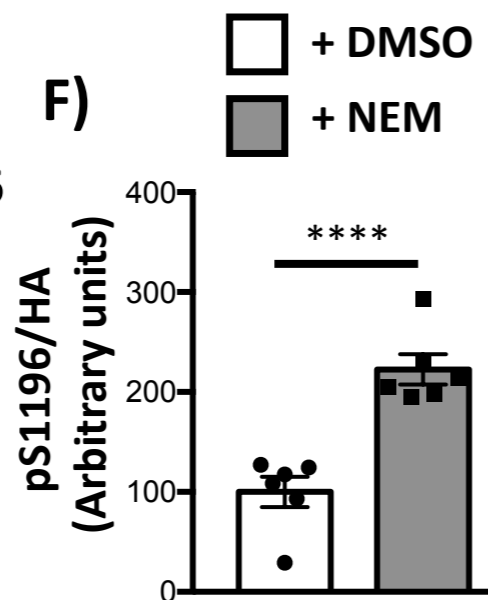
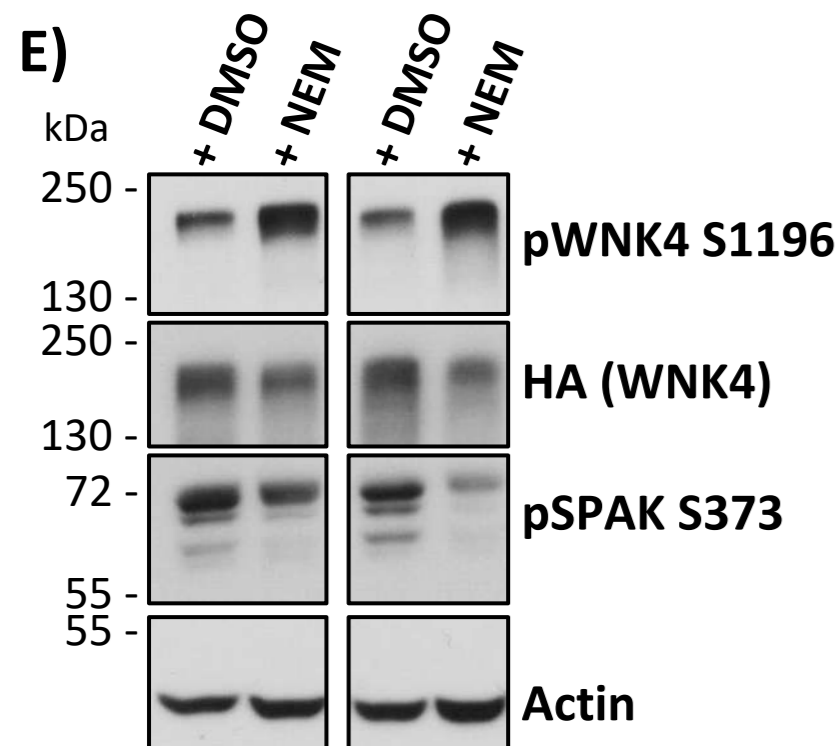
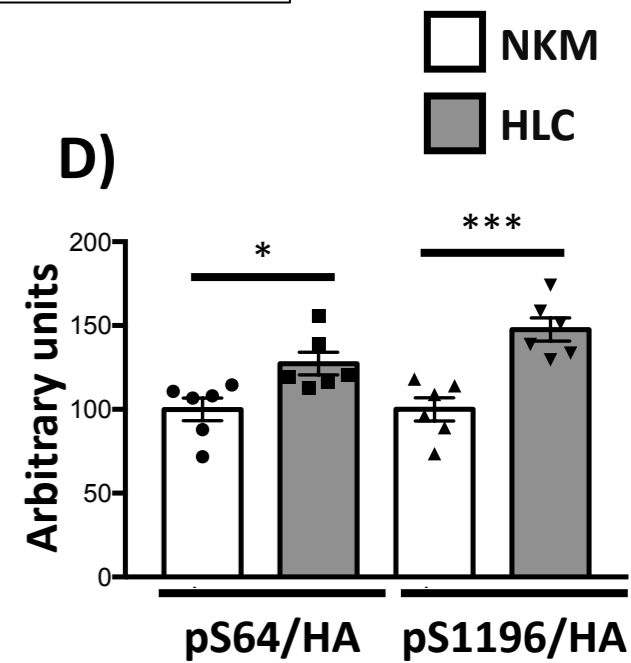
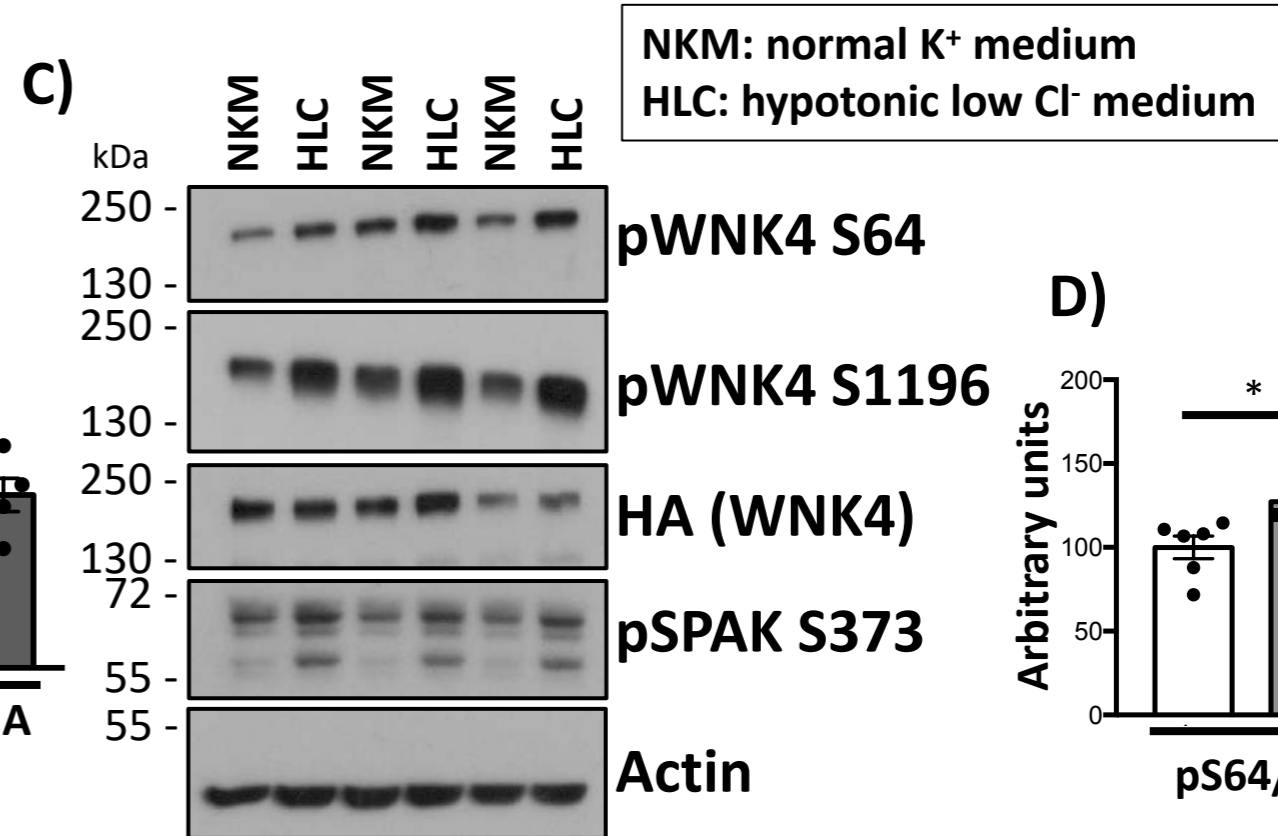
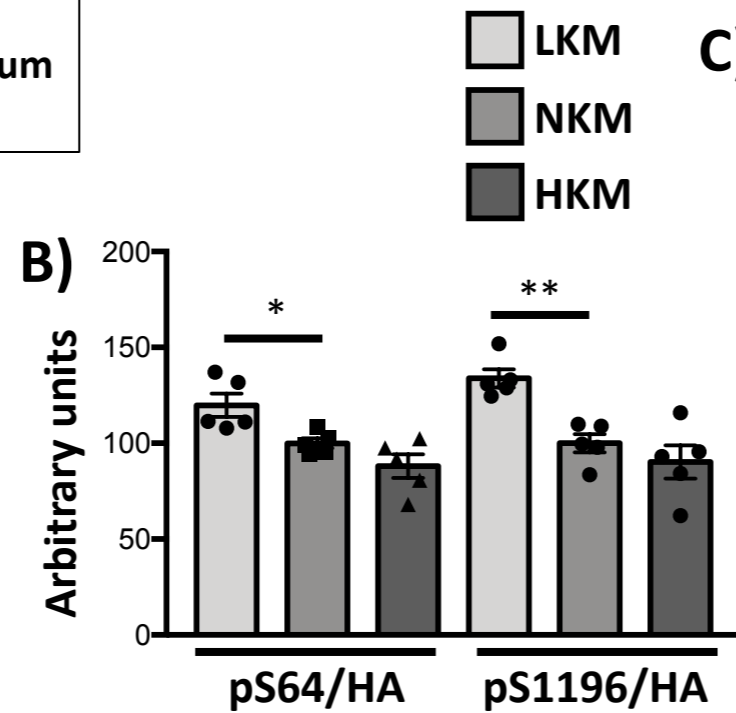
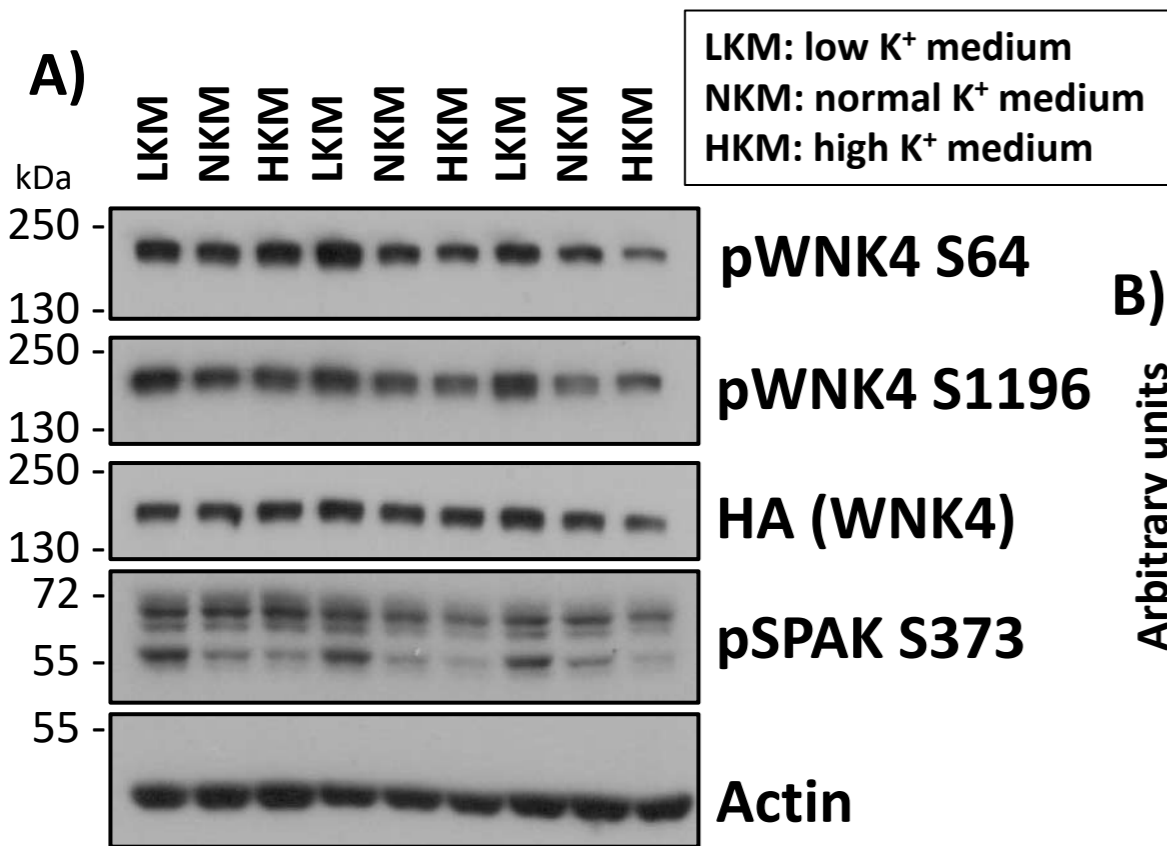
Figure 8. Proposed model of the mechanisms that contribute to NCC's activation during hypokalemia. With a decrease in plasma $[K^+]$, there is an increase in Cl^- efflux in the basolateral membrane of the DCT. This leads to the activation of WNK4 by different mechanisms: a reduction in direct Cl^- binding to WNK4 increases its transautophosphorylation at its T-loop. Moreover, the activation of a kinase that may belong to the PKC family, increases the phosphorylation of WNK4 at its RRxS motifs, also promoting the increase in catalytic activity. Finally, KLHL3 phosphorylation at its RRxS site decreases KLHL3-targeted degradation of WNKs, leading to increased abundance of WNK4 and KS-WNK1 in the DCT.

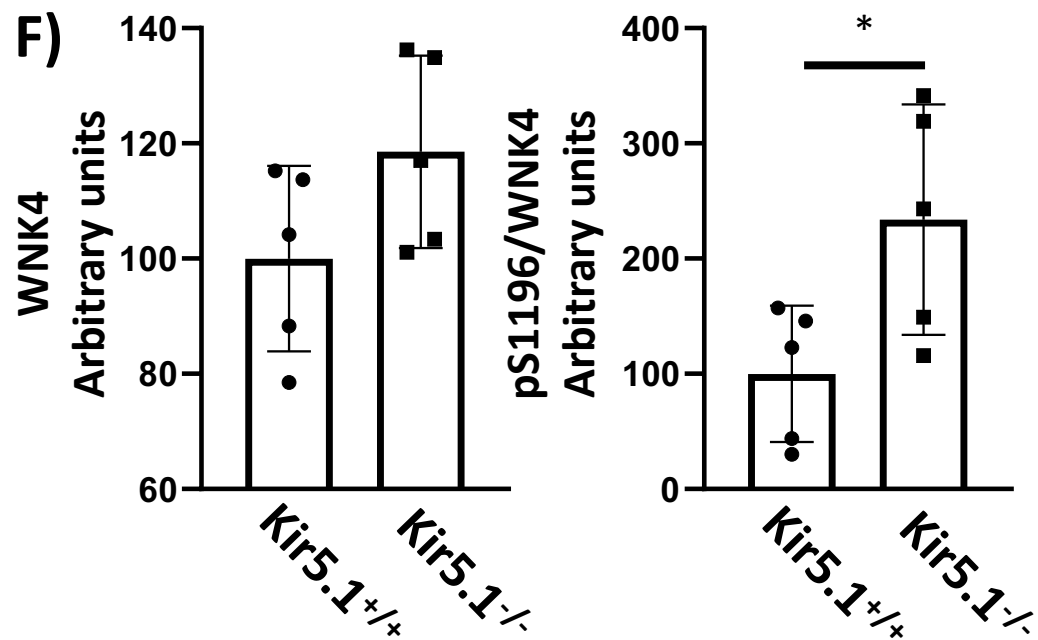
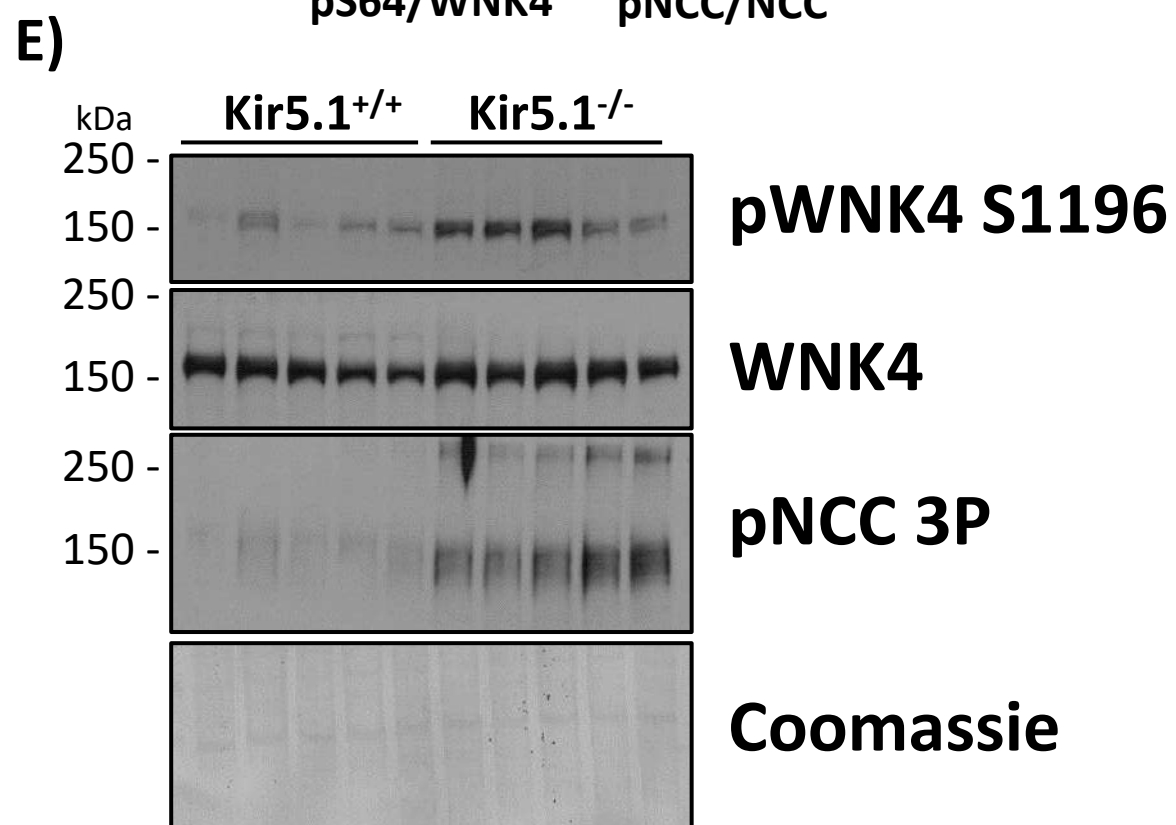
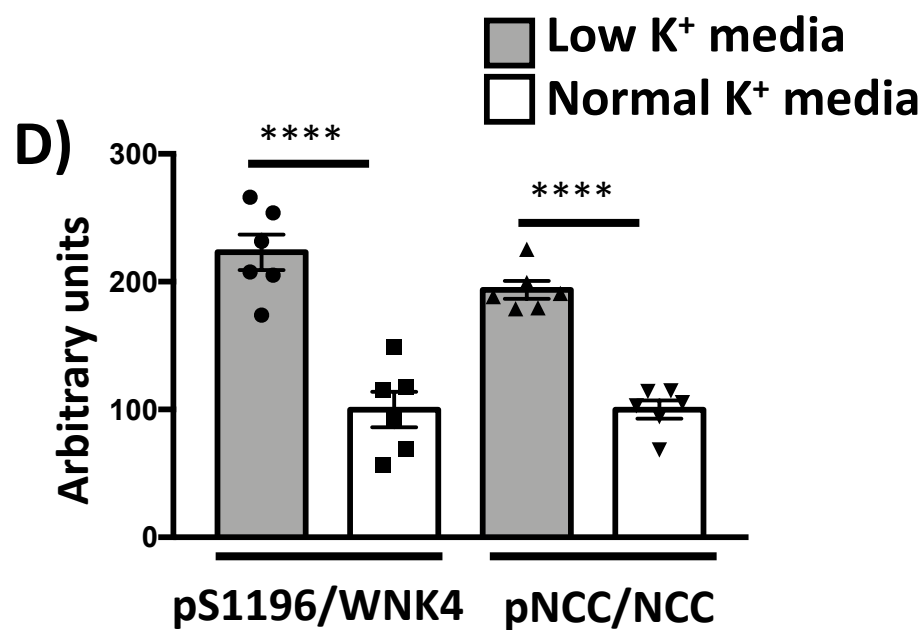
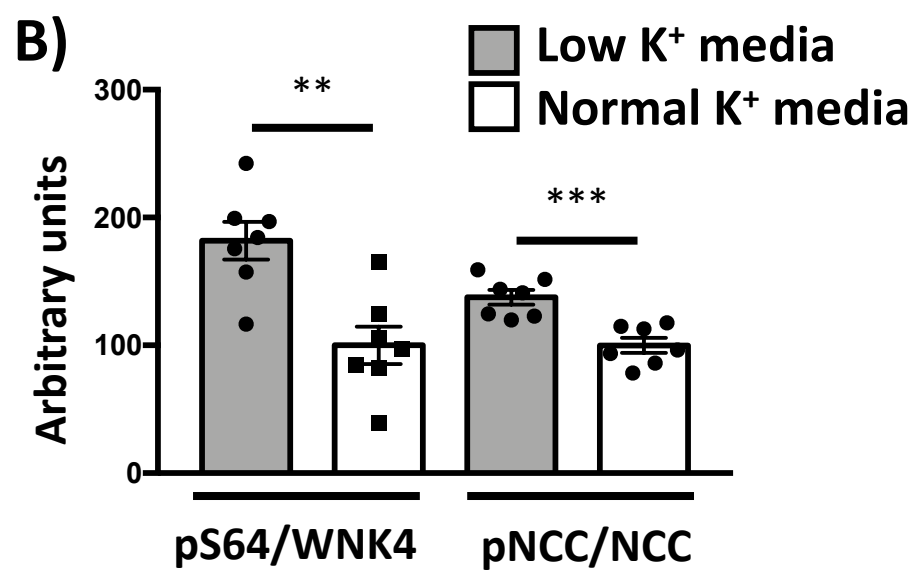
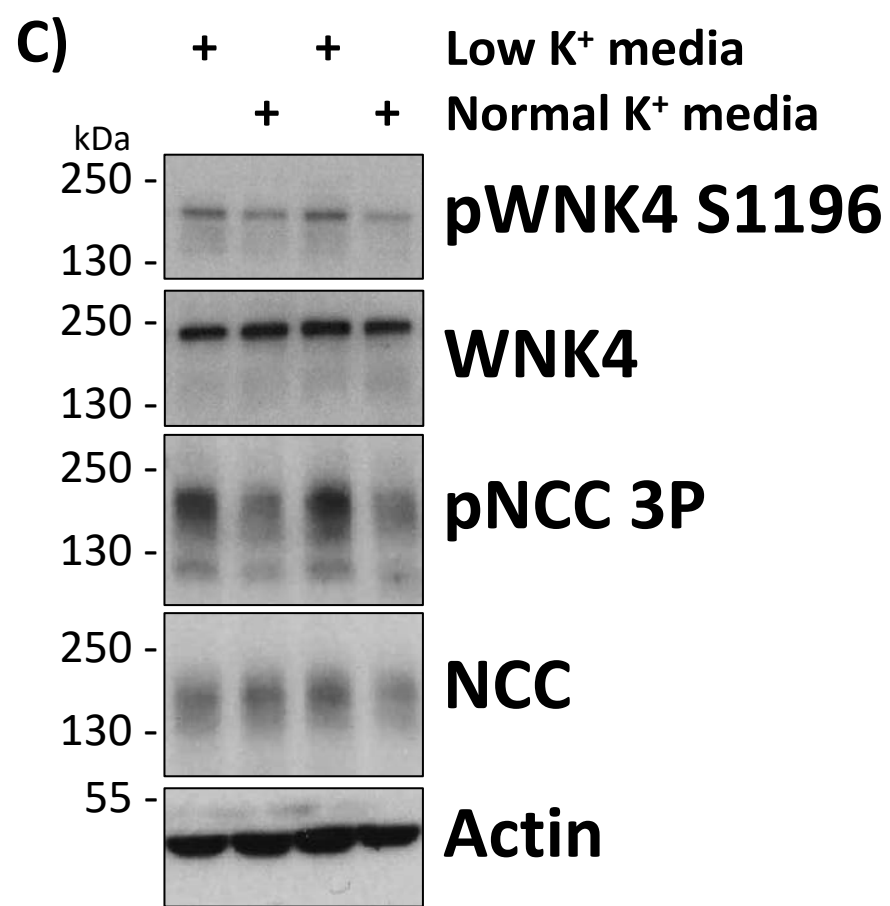
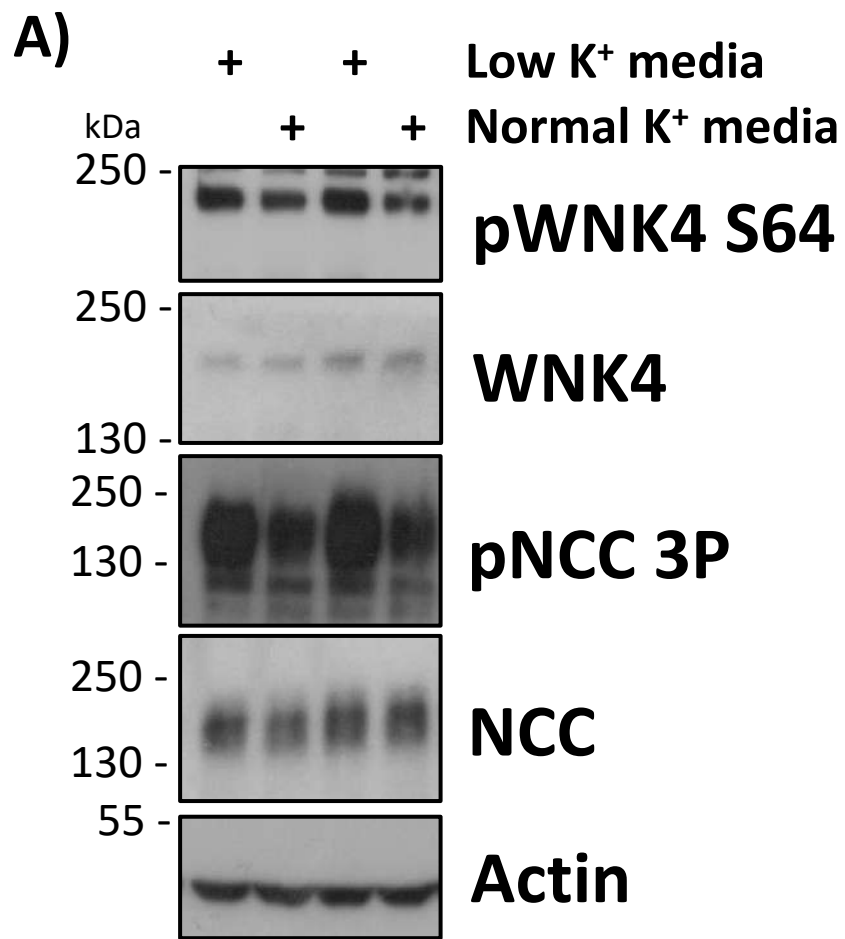
Table 1. Plasma biochemistry of WNK4^{+/+} and WNK4^{L319F/L319F}

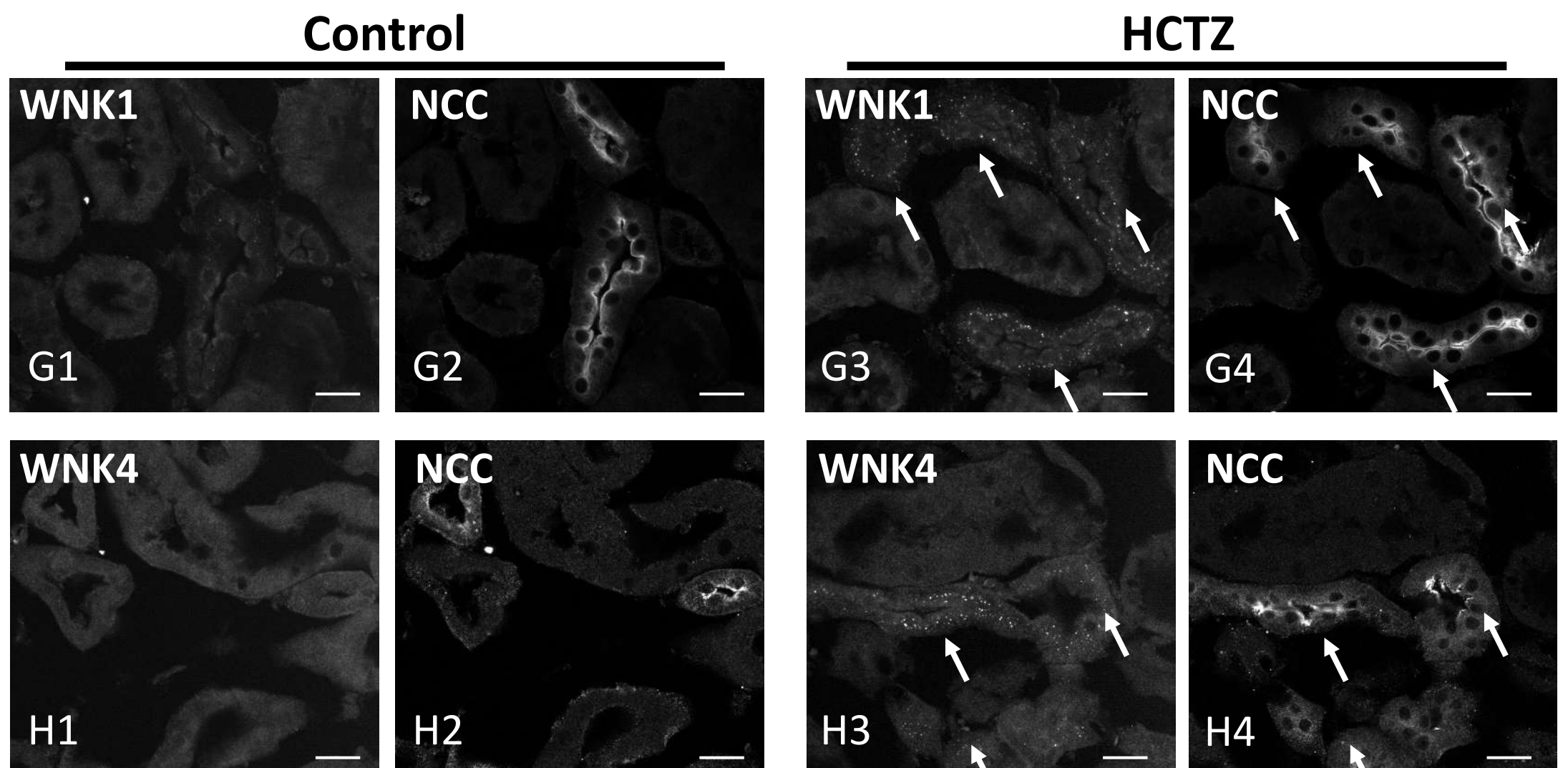
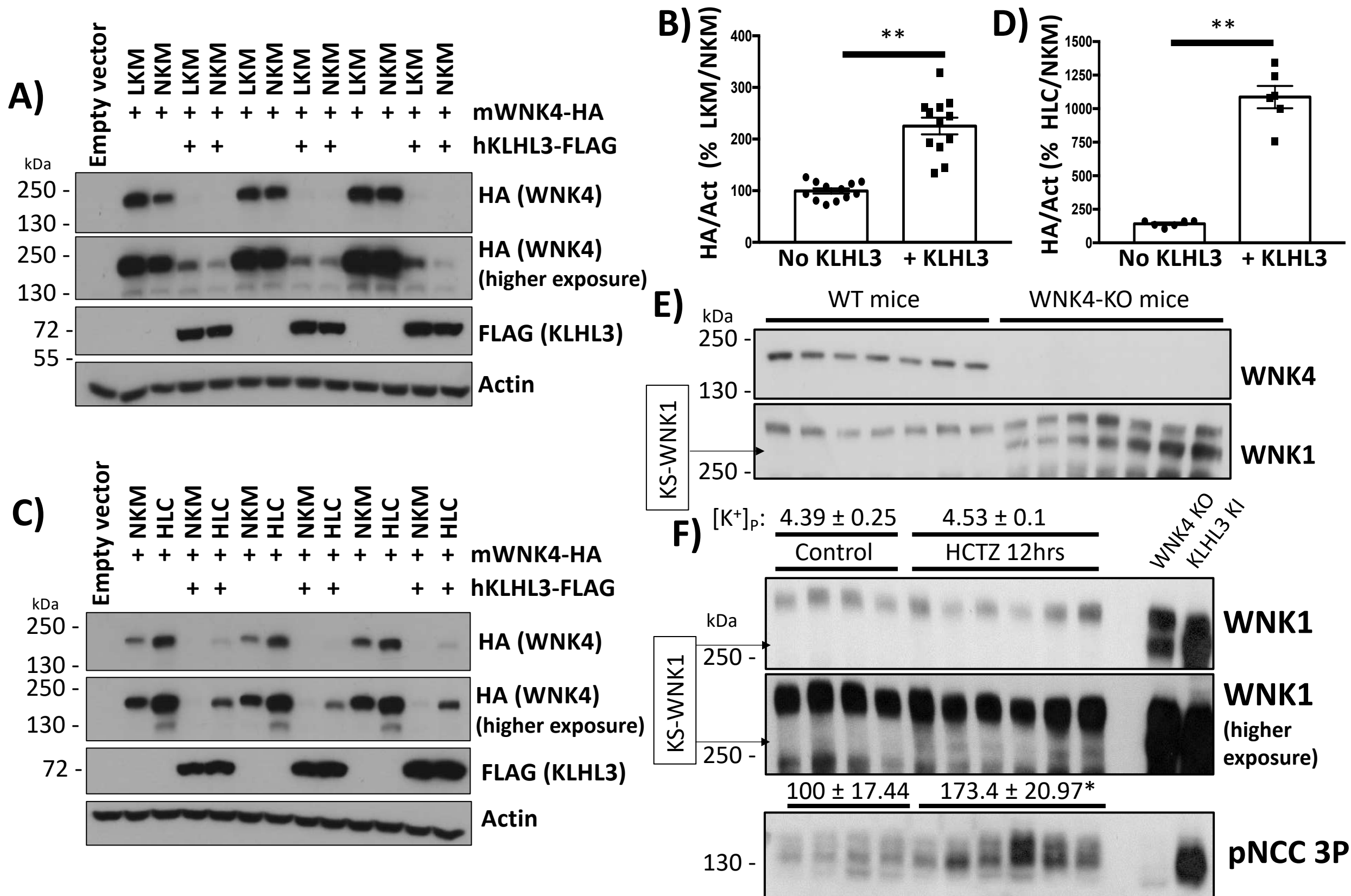
	WNK4 ^{+/+}	WNK4 ^{L319F/L319F}	p value
Body weight (g)	27.84 ± 0.57, n=11	27.3 ± 1.13, n=8	0.6524
Plasma [Na ⁺] (mmol/L)	147.4 ± 0.38, n=13	146.8 ± 0.46, n=9	0.3260
Plasma [K ⁺] (mmol/L)	4.33 ± 0.08, n=13	4.58 ± 0.11, n=9	0.0738
Plasma [Cl ⁻] (mmol/L)	120.8 ± 0.9, n=13	121.1 ± 0.95, n=9	0.8451
Plasma [Mg ²⁺] (mg/dL)	1.743 ± 0.02, n=9	1.759 ± 0.06, n=8	0.7947
Plasma [BUN] (mg/dL)	24.08 ± 0.66, n=12	21 ± 0.85, n=9	0.0088
Plasma [Creatinine] (mg/dL)	0.1082 ± 0.01, n=11	0.0775 ± 0.01, n=8	0.1435
Hematocrit (%)	41.45 ± 0.43, n=11	41.75 ± 0.41, n=8	0.6395

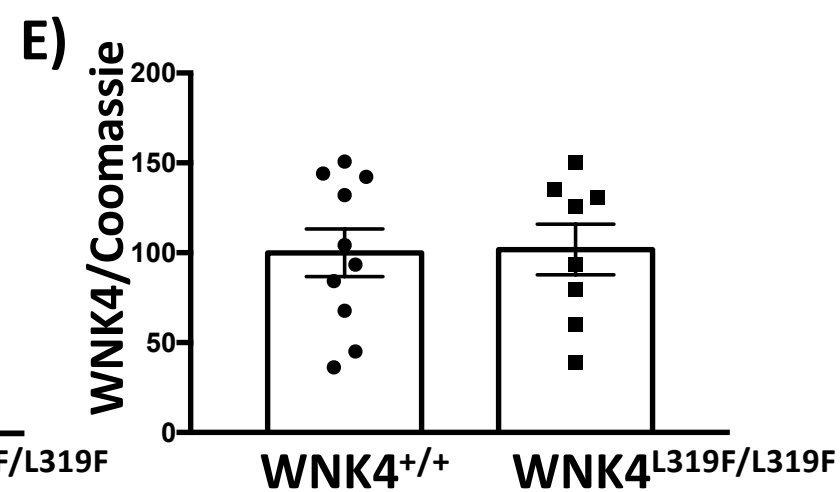
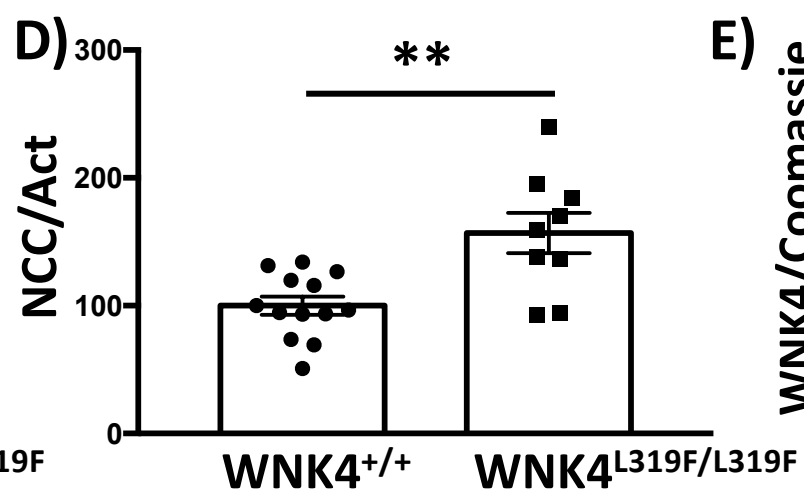
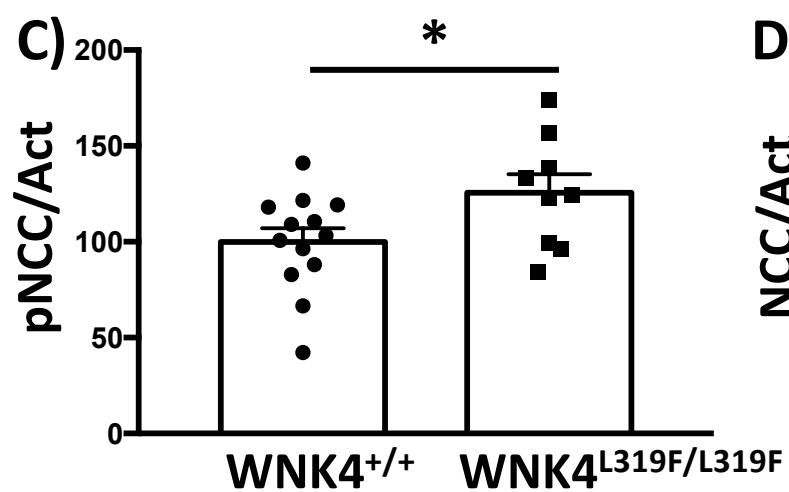
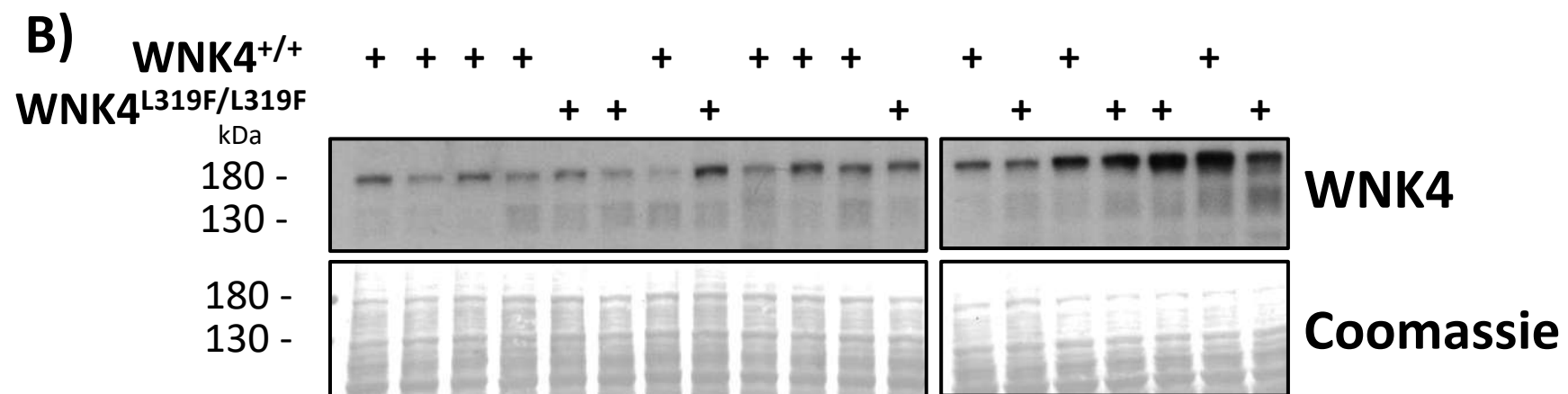
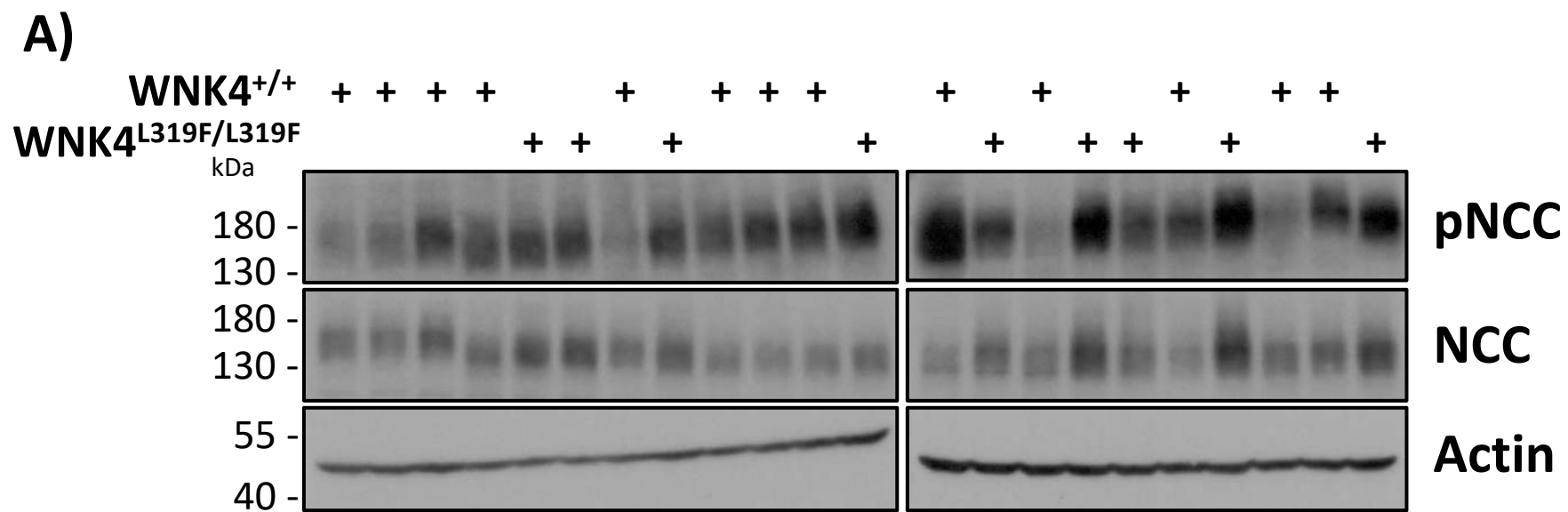
A) $[K^+]_p$: $2.67 \pm 0.08^{****}$ 5.15 ± 0.29



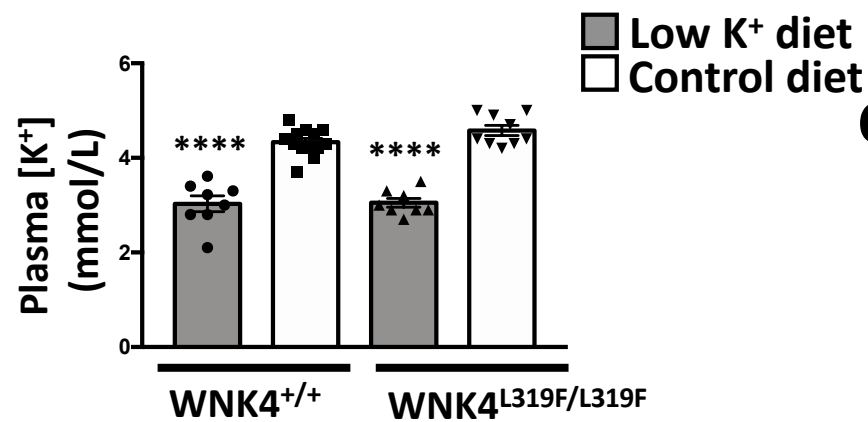




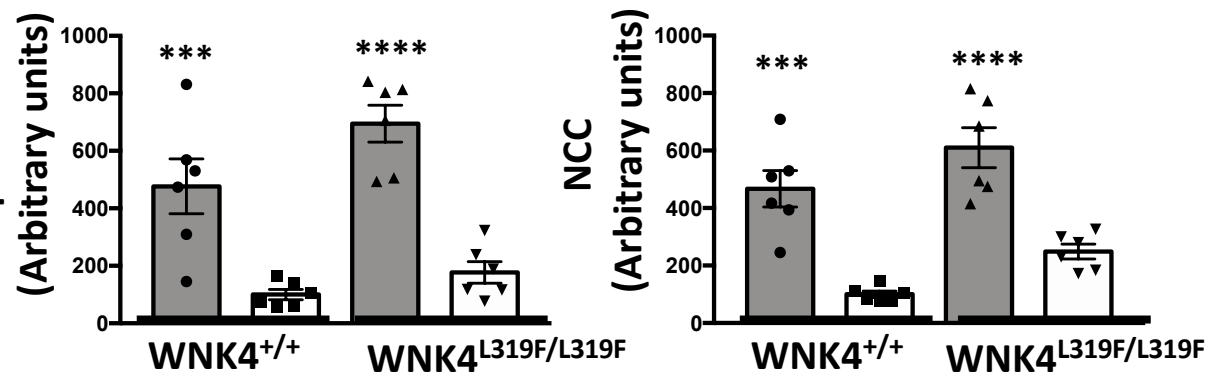




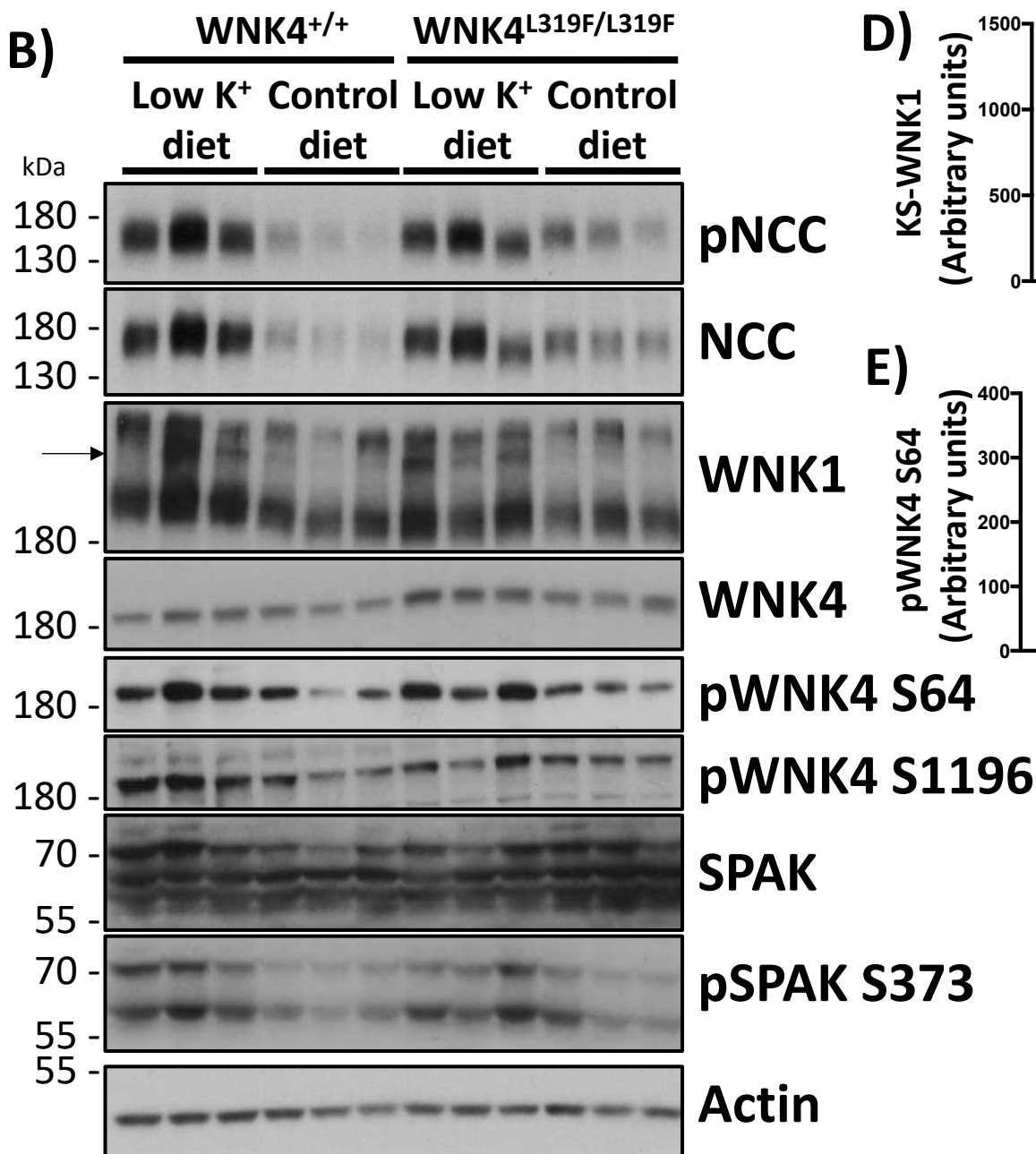
A)



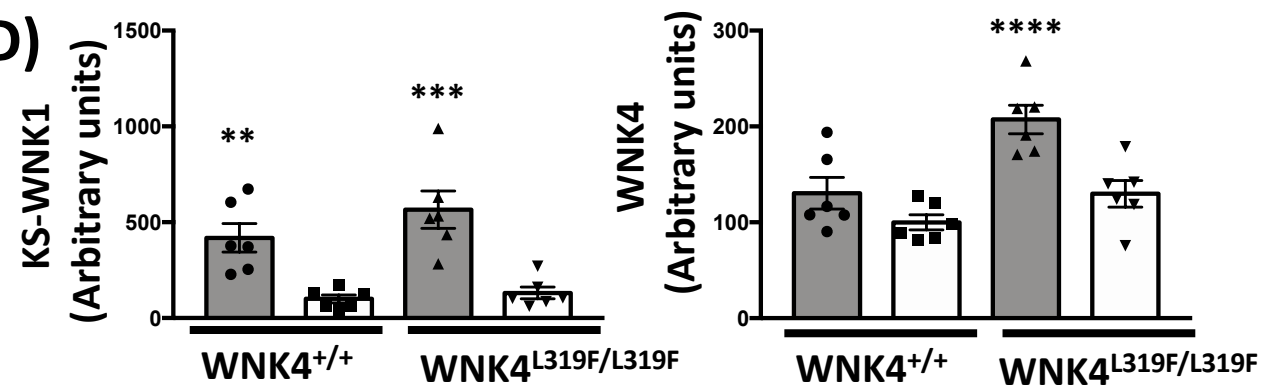
C)



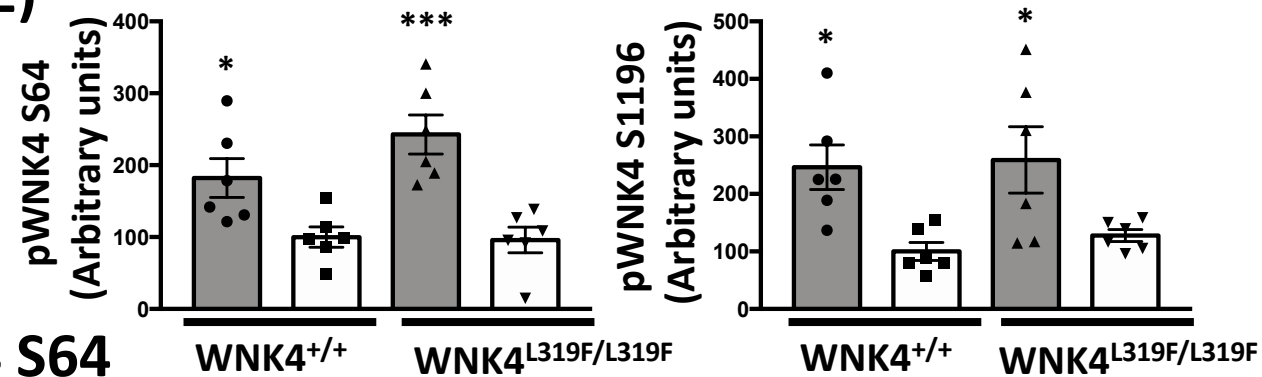
B)



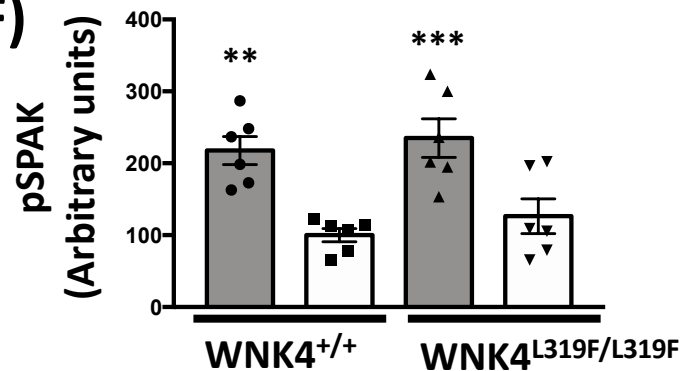
D)

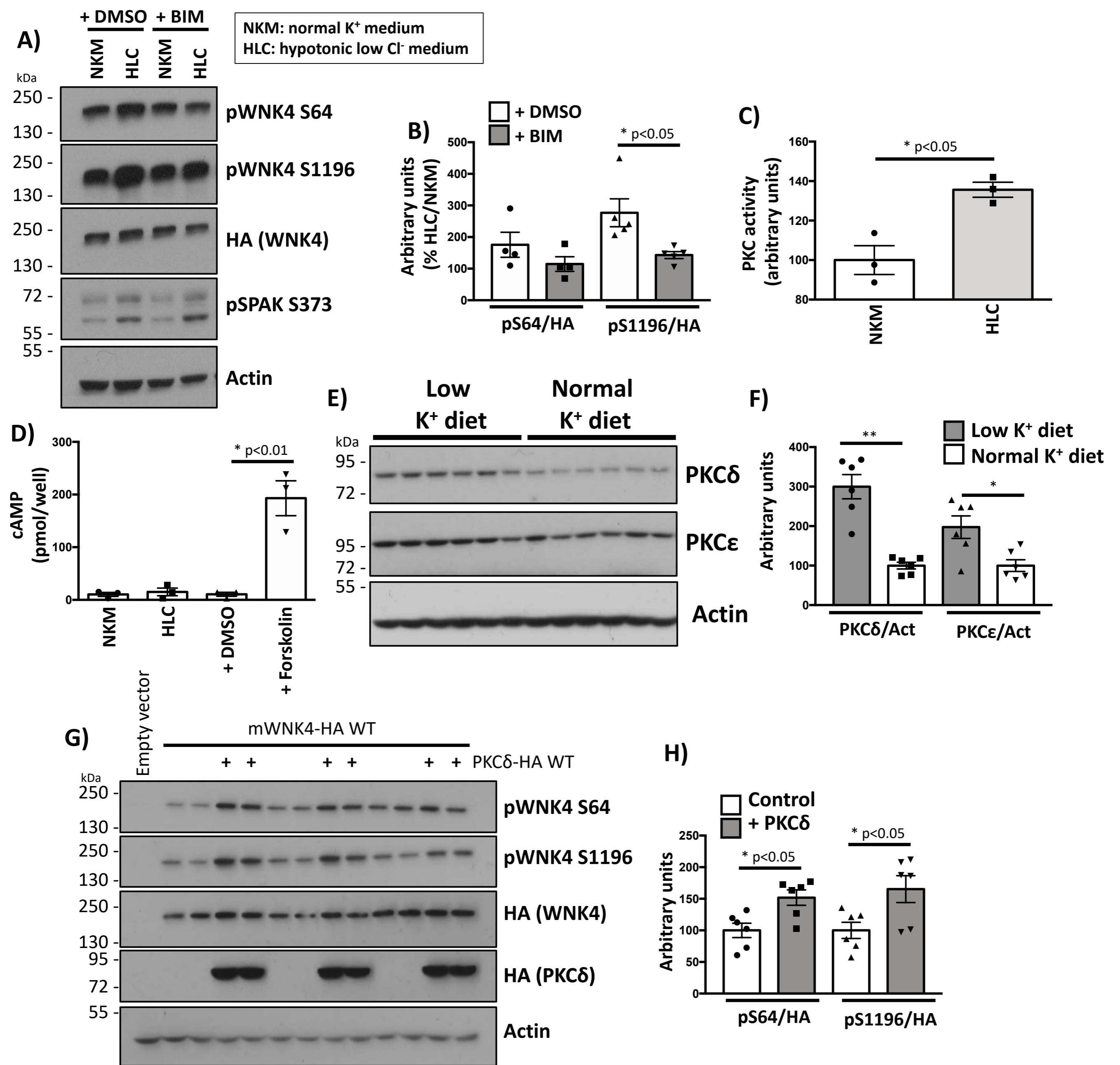


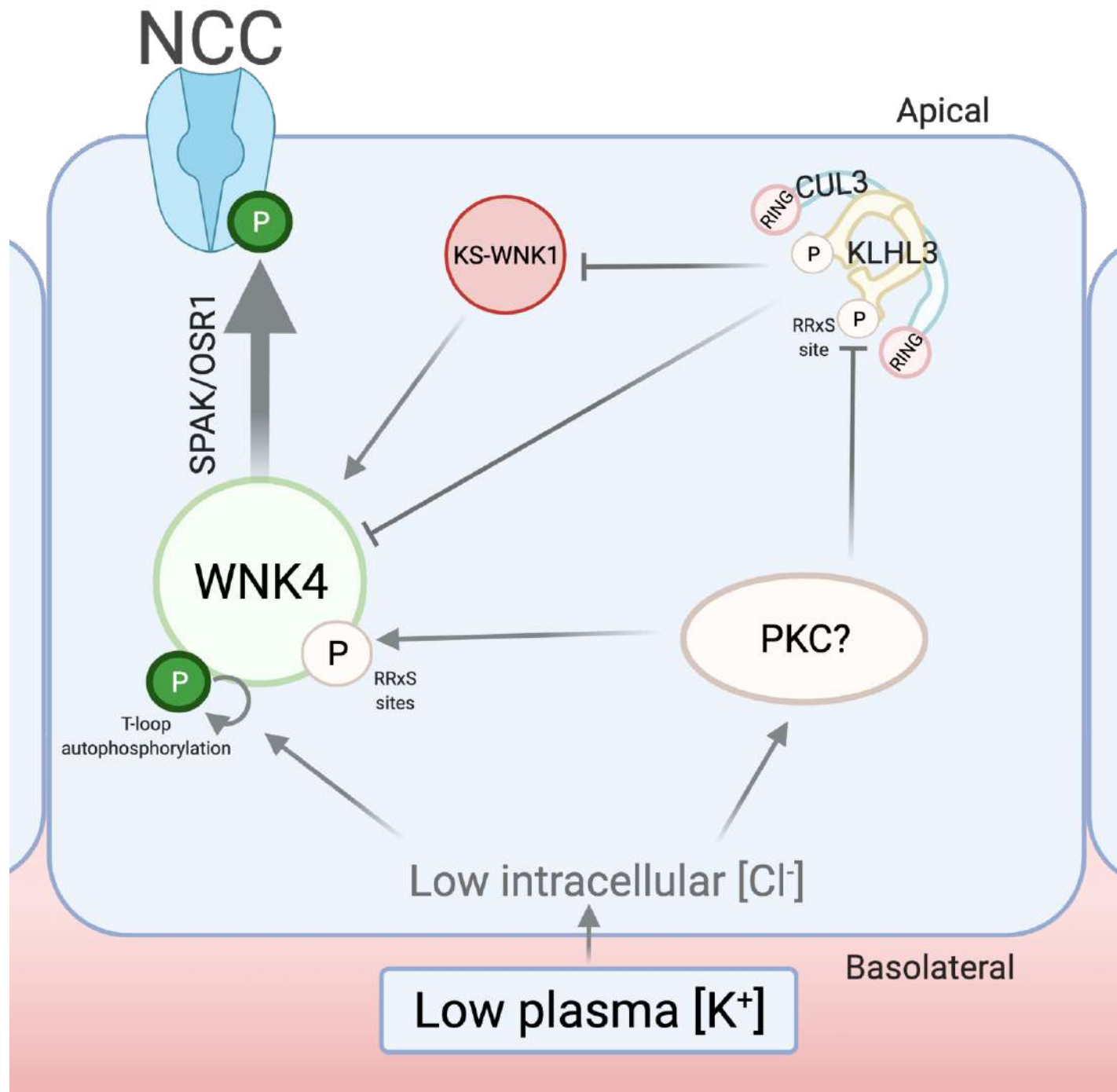
E)



F)







Supplemental Information

Upregulation of NCC by hypokalemia involves additional mechanisms to direct Cl⁻ sensing by WNK4.

Adrián Rafael Murillo-de-Ozores, Héctor Carbajal-Contreras, Germán Ricardo Magaña-Ávila, Raquel Valdés, Leoneli I. Grajeda-Medina, Norma Vázquez, Alejandro López-Saavedra, Dao-Hong Lin, Wen-Hui Wang, Eric Delpire, David H. Ellison, Gerardo Gamba, María Castañeda-Bueno.

Table of contents

Figure S1. Generation of WNK4-L319F and genotyping

Figure S2. Plasma [K⁺] and NCC analysis of WNK4-L319F mice in a mixed B6-129/Sv genetic background

Table S1. Antibodies used for Western blot and immunofluorescent staining

Supplemental references

FIGURE S1. Generation of WNK4-L319F and genotyping

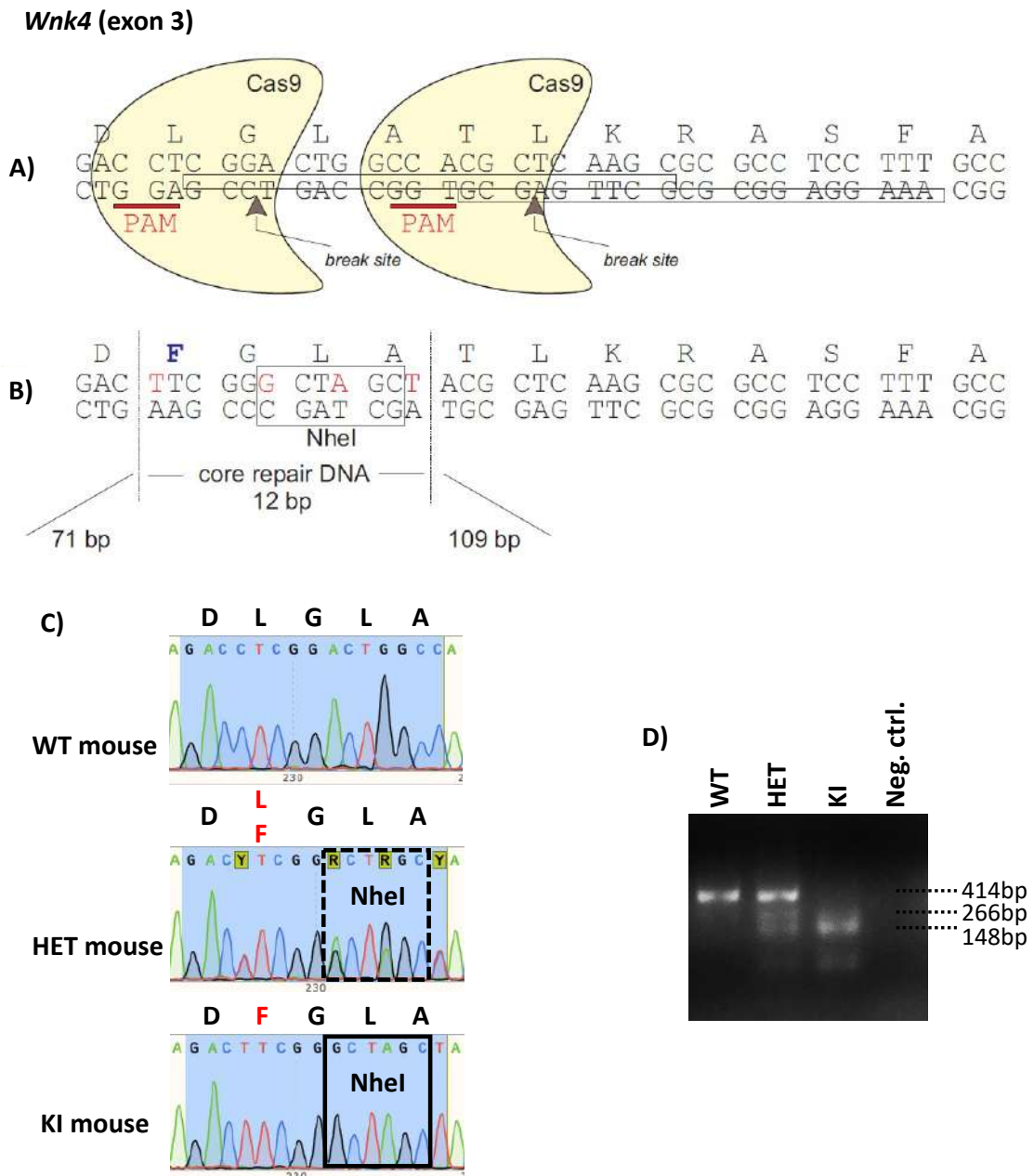


Figure S1. A) Schematic representation of CRISPR/Cas9 and its RNA guides (boxed) targeting exon 3 of *Wnk4* as described in Methods. B) Repaired allele with substitution of Leu319 codon to Phe. Additional silent mutations introduced an *NheI* restriction site (boxed) for genotyping. C) Confirmation by Sanger sequencing of PCR products (Primers: 5'-TCTCCCTAGATCAATAGCTCTG-3' and 5'-AGAGGTGGTGGCAAGGATGG-3') of WT, heterozygous, and homozygous WNK4-L319F mice. D) Genotyping was done by digesting PCR products with *NheI* and analyzing them in agarose gels. Undigested DNA (414 bp) corresponded to products amplified from WT allele, while products amplified from the L319F allele were cut into fragments of 266 bp and 148 bp.

FIGURE S2. Plasma $[K^+]$ and NCC analysis of WNK4-L319F mice in a mixed B6-129/Sv genetic background

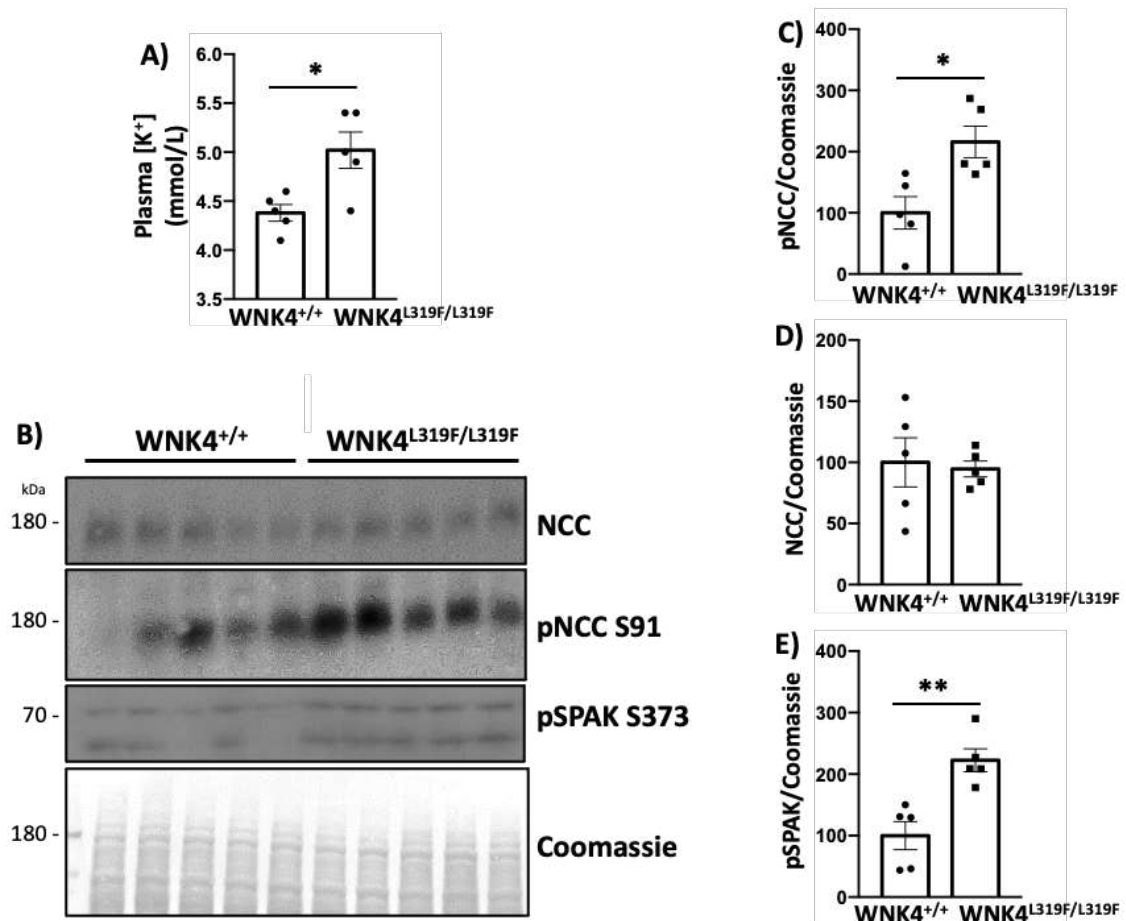


Figure S2. Heterozygous WNK4-L319F mice in a C57BL/6 background were crossed with 129/Sv mice for 2 generations, and then heterozygous WNK4-L319F mice in this mixed B6-129/Sv genetic background were crossed with each other to obtain WT and homozygous WNK4-L319F (KI) mice. KI mice presented higher plasma $[K^+]$ when compared to WT mice (A). Analysis of NCC, pNCC and pSPAK in kidney lysates by Western Blot (B). Quantitative analysis of pNCC/Coomassie (C), NCC/Coomassie (D) and pSPAK/Coomassie (E) levels observed in immunoblots represented in B. Values observed in wild type mice were normalized to 100%. Data are mean \pm SEM. * $p < 0.05$, ** $p < 0.005$. In these mice, we analyzed Ser91 phosphorylation of NCC, given that it has been reported that other NCC phosphoantibodies recognize NKCC2 unspecifically in 129/Sv mice(1). In contrast, NCC Ser91 is not conserved in NKCCs and has been shown to be positively regulated by SPAK (2).

TABLE S1. Antibodies used for Western blot and immunofluorescent staining

Antibody	Concentration (Western Blot)	Source	Reference
pWnk4-S64	1:100 (WB and IF)	Lifton Lab	(3)
pWnk4-S1196	1:2000 (cell samples) (WB)	Lifton Lab	(3)
pWnk4-S1196	1:1000 (kidney samples; WB and IF)	Ellison Lab	(4)
Wnk4	1:5000 (WB) 1:1000 (IF)	Ellison Lab	(5)
pNCC 3P	3 µg/ml (WB)	S108B, MRC, Dundee	(6)
pNCC S91	3 µg/ml (WB)	S996B, MRC, Dundee	(2)
NCC	1:5000 (WB)	Ellison lab	(4)
NCC	1:100 (IF)	S965B, MRC, Dundee	(6)
pSPAK S373	3 µg/ml (WB)	S670B, MRC, Dundee	(7)
Wnk1	1:3000 (WB)	Bethyl A301-515A	(8)
PKCδ	1:2000 (WB)	610398 BD Transduction Lab	(9)
PKCε	1:2000 (WB)	610085 BD Transduction Lab	(10)

HRP coupled antibodies

	Concentration	Source
Actin-HRP	1:10000	Santa Cruz
HA-HRP	1:1000	Sigma
FLAG-HRP	1:5000	Sigma
Rabbit-HRP	1:15000	Jackson Immunoresearch
Sheep-HRP	1:15000	Jackson Immunoresearch
Mouse-HRP	1:2500	Jackson Immunoresearch

Alexa coupled antibodies

	Concentration	Source
Rabbit-Alexa 594	1:400	Thermo Scientific
Sheep-Alexa 488	1:400	Thermo Scientific

Supplemental references

1. Moser, S., Sugano, Y., Wengi, A., Fisi, V., Lindtoft Rosenbaek, L., Mariniello, M., Loffing-Cueni, D., McCormick, J. A., Fenton, R. A., and Loffing, J. (2021) A five amino acids deletion in NKCC2 of C57BL/6 mice affects analysis of NKCC2 phosphorylation but does not impact kidney function. *Acta Physiol.* 10.1111/apha.13705
2. Rafiqi, F. H., Zuber, A. M., Glouer, M., Richardson, C., Fleming, S., Jouanouić, S., Jovanović, A., Kevin, M. O. S., and Alessi, D. R. (2010) Role of the WNK-activated SPAK kinase in regulating blood pressure. *EMBO Mol. Med.* **2**, 63–75
3. Castañeda-Bueno, M., Arroyo, J. P., Zhang, J., Puthumana, J., Yarborough, O., Shibata, S., Rojas-Vega, L., Gamba, G., Rinehart, J., and Lifton, R. P. (2017) Phosphorylation by PKC and PKA regulate the kinase activity and downstream signaling of WNK4. *Proc. Natl. Acad. Sci.* **114**, E879–E886
4. Cornelius, R. J., Si, J., Cuevas, C. A., Nelson, J. W., Gratreak, B. D. K., Pardi, R., Yang, C.-L., and Ellison, D. H. (2018) Renal COP9 Signalosome Deficiency Alters CUL3-KLHL3-WNK Signaling Pathway. *J. Am. Soc. Nephrol.* 10.1681/ASN.2018030333
5. Murillo-de-Ozores, A. R., Rodríguez-Gama, A., Bazúa-Valenti, S., Leyva-Ríos, K., Vázquez, N., Pacheco-Álvarez, D., De La Rosa-Velázquez, I. A., Wengi, A., Stone, K. L., Zhang, J., Loffing, J., Lifton, R. P., Yang, C. L., Ellison, D. H., Gamba, G., and Castañeda-Bueno, M. (2018) C-terminally truncated, kidney-specific variants of the WNK4 kinase lack several sites that regulate its activity. *J. Biol. Chem.* **293**, 12209–12221
6. Castaneda-Bueno, M., Cervantes-Perez, L. G., Rojas-Vega, L., Arroyo-Garza, I., Vazquez, N., Moreno, E., and Gamba, G. (2014) Modulation of NCC activity by low and high K⁺ intake: insights into the signaling pathways involved. *AJP Ren. Physiol.* **306**, F1507–F1519
7. Zagórska, A., Pozo-Guisado, E., Boudeau, J., Vitari, A. C., Rafiqi, F. H., Thastrup, J., Deak, M., Campbell, D. G., Morrice, N. A., Prescott, A. R., and Alessi, D. R. (2007) Regulation of activity and localization of the WNK1 protein kinase by hyperosmotic stress. *J. Cell Biol.* **176**, 89–100
8. Ostrosky-Frid, M., Chávez-Canales, M., Zhang, J., Andrukhova, O., Argaiz, E. R., Lerdo-De-Tejada, F., Murillo-De-Ozores, A., Sanchez-Navarro, A., Rojas-Vega, L., Bobadilla, N. A., Vazquez, N., Castañeda-Bueno, M., Alessi, D. R., and Gamba, G. (2021) Role of KLHL3 and dietary K⁺ in regulating KS-WNK1 expression. *Am. J. Physiol. - Ren. Physiol.* **320**, F734–F747
9. Liu, Y., Deng, X., Wu, D., Jin, M., and Yu, B. (2019) PKC δ promotes fertilization of mouse embryos in early development via the Cdc25B signaling pathway. *Exp. Ther. Med.* 10.3892/etm.2019.7959
10. Kumar, V., Weng, Y. C., Wu, Y. C., Huang, Y. T., Liu, T. H., Kristian, T., Liu, Y. L., Tsou, H. H., and Chou, W. H. (2019) Genetic inhibition of PKC ϵ attenuates neurodegeneration after global cerebral ischemia in male mice. *J. Neurosci. Res.* **97**, 444–455

8. DISCUSIÓN Y CONCLUSIONES

La descripción de variantes cortas de la cinasa WNK4 puede ser de importancia para el entendimiento de los mecanismos finos de regulación de su vía de señalización. Es de llamar la atención que las variantes únicamente se encontraron en riñón, órgano en el cual la cinasa WNK4 juega un papel preponderante. A pesar de que WNK4 se expresa en distintos tejidos(114), es notable que las alteraciones fenotípicas de los ratones con ausencia(41), o ganancia de función de WNK4(44), son únicamente de origen renal.

La estructura del gen de WNK4 ya ha sido descrita con anterioridad. Contiene 19 exones y 18 intrones, tanto en ratón como en humano(28). Ensayos experimentales sólo han sido capaces de detectar el mRNA que contiene los 19 exones. Esto ha sido corroborado en nuestro trabajo en donde se hizo un análisis de posibles isoformas no descritas basándonos en datos ya publicados de RNA-seq de riñón de ratón, en el cual no hallamos información suficiente que respaldara la existencia de transcritos alternativos. En un estudio reciente de RNA-seq de túbulos microdisecados de nefrona de ratón en donde se hizo un análisis profundo sobre splicing alternativo tampoco se encontró evidencia de transcritos alternativos del gen *Wnk4*(38).

Posteriormente, encontramos que un corte proteolítico es capaz de generar estas variantes de WNK4 de menor tamaño. Previamente, se ha descrito que SPAK sufre una modificación similar(115), aunque hasta el momento no existe evidencia contundente sobre la identidad de la proteasa específica responsable de dicho corte(116). Si ambas cinasas WNK4 y SPAK son reguladas por proteasas similares en determinada condición, eso queda por determinarse y será un proyecto interesante en el futuro.

Los experimentos en donde comparamos la movilidad electroforética de distintas proteínas truncas recombinantes de WNK4 contra las isoformas encontradas *in vivo*, sugieren que éstas carecen de sitio de unión a SPAK, por lo que probablemente serían una forma de inhibición de la vía WNK4/SPAK. La determinación de un segmento de 41 residuos (del aminoácido 740 al 781 de WNK4 de ratón) como el probable sitio de corte apunta en la misma dirección.

Otra vertiente interesante estudiada en este trabajo, es la confirmación de un sitio de unión a la proteína fosfatasa 1 (PP1) en los últimos residuos de WNK4. Mientras que la presencia de un sitio consenso ([RK]-X(0,1)-[VI]-{P}-[FW]) puede sugerir que cierta proteína puede entablar una interacción con PP1, se necesita evidencia experimental para validar dicha predicción. Esto porque esta secuencia consenso tiene una baja especificidad (pues ocurre aleatoriamente en un cuarto de todas las proteínas) a pesar de su alta sensibilidad(56). WNK4 tiene dos de estos sitios, el primero se ubica en el dominio PF2-like' y el segundo en los últimos 12 residuos de WNK4. Al mutar uno u otro de estos sitios, observamos efectos diferentes, pues mutar el primero provoca la pérdida de función de la proteína, mientras que mutar el segundo promueve la fosforilación y activación de la cinasa WNK4.

En cuanto al primer sitio consenso, esta evidencia sugiere que no se trata de un sitio de unión a PP1. En cambio, dichos residuos podrían ser importantes para el plegamiento y/o función del dominio PF2-like'(47). Además, este sitio se encuentra conservado en los distintos miembros de la familia, y ensayos de 'pull-down' de este sitio tanto de WNK1 como de WNK4 no muestran interacción con la subunidad catalítica de PP1(56). Al encontrar y validar al segundo de estos sitios como sitio fidedigno de unión a PP1, este trabajo establece al dominio C-terminal como un segmento de regulación negativa de la actividad de la cinasa WNK4. Esto es congruente con observaciones previas en un modelo de ovocitos de *X. laevis*(117).

El análisis a detalle de los sitios o dominios con función reguladora ubicados en el dominio C-terminal de WNK4 ha despertado el interés de estudiar su contribución a la fisiología renal. Se han generado modelos transgénicos de ratones con codones de paro prematuros en posiciones estratégicas de WNK4 (**Figura 11**), con el fin de evaluar las propiedades del extremo C-terminal (como el sitio de unión a PP1) o el sitio de unión a SPAK. De especial interés éste último, pues se han descrito pacientes en la medicina veterinaria con mutaciones de tipo sin sentido que producirían una WNK4 trunca sin sitio de unión a SPAK. Estos gatos birmanos se presentan en la clínica con Parálisis hipokalémica periódica felina(118). Por lo tanto, será interesante observar si existe una relación causal entre estas mutaciones en WNK4 y el fenotipo de estos animales.

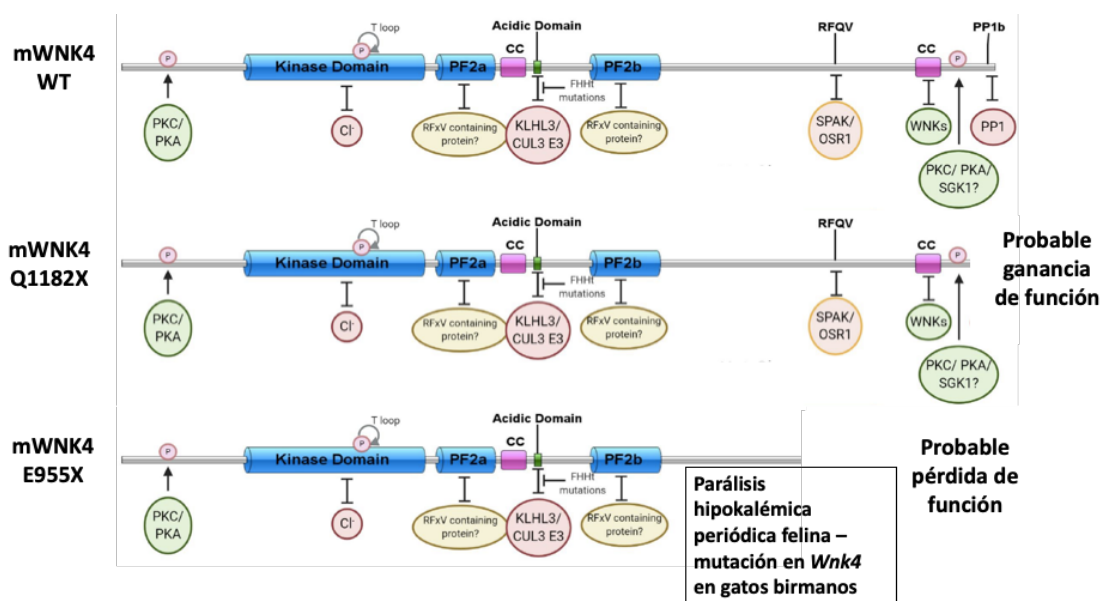


Figura 11. Representación esquemática de la WNK4 modificada en modelos murinos próximos a estudiarse en el laboratorio y en colaboración con otros grupos.

En cuanto a la segunda mitad del proyecto, demostramos que distintos mecanismos están involucrados en la activación de NCC en respuesta a hipokalemia. En primer lugar, encontramos que la fosforilación de WNK4 en la Ser64 y la Ser1196 aumenta en respuesta a menor $[K^+]_e$, en modelos *in vivo*, *in vitro* y *ex vivo*. En el caso del ratón, este proceso parece darse en el DCT, dado que los WNK bodies observados en estas células incluyen WNK4 fosforilada en estos dos residuos. Esto pudiera contribuir a la activación de la vía de señalización WNK4-SPAK/OSR1-NCC en estas condiciones.

Dado que una disminución en la $[K^+]_e$ promueve una reducción en $[Cl^-]_i$, estudiamos si la fosforilación de WNK4 en la Ser64 y Ser1196 también estaban reguladas de esta manera. Distintas maniobras cuyo efecto demostrado es la disminución de $[Cl^-]_i$ promovieron el aumento de la fosforilación de WNK4 en estos sitios. De manera interesante, este efecto es independiente de las cinasas WNK mismas, dado que su inhibición farmacológica más bien aumenta la fosforilación de WNK4. Esto podría explicarse por el efecto del inhibidor WNK463 en la disrupción de la fosforilación de SPAK/OSR1, lo cual promovería la inhibición de la entrada de Cl⁻ a la célula mediante NKCC1 y la activación de su salida a través los cotransportadores de K⁺/Cl⁻, KCCs(8, 36). Esto sería un ejemplo de una interrupción de un asa de retroalimentación negativa que modula la fosforilación y actividad de WNK4.

La regulación de la actividad de KLHL3, y por lo tanto de la degradación de las WNKs, depende al menos en parte de la fosforilación de KLHL3 en la Ser433. Este residuo tiene un sitio consenso similar a la Ser64 y Ser1196 de WNK4 (motivos RRxS) y se ha demostrado que pueden fosforilarse por las mismas cinasas(53, 63, 119). Al igual que la fosforilación de WNK4, encontramos que la actividad de KLHL3 puede modularse por $[Cl^-]_i$, lo cual puede repercutir en la cantidad total de WNK4 y KS-WNK1.

El estudio de los ratones WNK4-L319F nos permitió encontrar que existen mecanismos adicionales a la unión del Cl^- a WNK4 para la regulación de NCC en hipokalemia. Sin embargo, es importante puntualizar algunas diferencias que encontramos con el estudio previo de un ratón con una WNK4 insensible a Cl^- . En primer lugar, no observamos diferencias claras en los electrolitos plasmáticos entre ratones WNK4 WT y WNK4-L319F, mientras que en el estudio por Chen y colaboradores se demostró que los ratones WNK4-L319F/L321F tienen mayores niveles de K^+ y Cl^- en plasma, comparados con ratones WT. Esto puede deberse a diferentes factores, como el fondo genético, la composición de la dieta o la recolección de muestras. Otra diferencia es que Chen et al. realizaron la mutación de dos sitios (L319F y L321F) en comparación con nuestro informe en el cual sólo se mutó la L319F. Sin embargo, estudios *in vitro* sugieren que la mutación L319F es suficiente para disminuir la afinidad por Cl^- y aumentar considerablemente la actividad de las cinasas WNK1(57) y WNK4(58, 59).

No es necesariamente sorprendente que los ratones WNK4-L319F no tengan un fenotipo evidente en comparación con los ratones WT. Estimaciones de la $[Cl^-]_i$ en el DCT son bajas (alrededor de 7mM)(60), por lo que el efecto de ganancia de función de WNK4 puede ser más modesto en comparación a lo observado en modelos de sobreexpresión en cultivo celular. Además, existen mecanismos compensatorios que pudieran evitar un aumento considerable de la vía WNK4-NCC. Uno de ellos pudiera ser la acción de fosfatasas. Inhibidores de la calcineurina, como el tacrolimus, se han asociado a un aumento en la fosforilación de NCC(120), por lo que esta pudiera ser una buena estrategia para abordar esta pregunta. Asimismo, será interesante analizar en el futuro a más detalle el fenotipo de estos ratones, tanto en su respuesta de NCC ante distintos estímulos fisiológicos (como ingesta de K^+ , consumo de NaCl u hormonas) como en otros segmentos de la nefrona o en otros tejidos.

Aunque encontramos que la inhibición farmacológica de PKC tiene un efecto sobre la fosforilación de WNK4 en células HEK293, la identidad de la cinasa responsable de los hallazgos *in vivo* aún es desconocida. Si bien en este trabajo proporcionamos una correlación con el aumento en la abundancia de PKC δ y PKC ϵ en los riñones de ratones hipokalémicos, hacen falta experimentos que estudien una relación causal entre estas cinasas y WNK4.

En conclusión, este trabajo muestra que múltiples y redundantes mecanismos están involucrados en la activación de la vía WNK4-NCC en el DCT por una disminución en $[K^+]_e$. Además, este proceso parece ser modulado por la $[Cl^-]_i$, la cual juega un papel central en la señalización sensible a iones en las células del DCT. Nuestra información sugiere la existencia de moléculas con sensibilidad a Cl^- no descritas que participan en este fenómeno fisiológico.

9. BIBLIOGRAFÍA

1. Boron, W. F., and Boulpaep, E. L. (2017) *Medical Physiology*, 3rd ed., Elsevier, 10.21019/9781582121994.ch1
2. Zacchia, M., Abategiovanni, M. L., Stratigis, S., and Capasso, G. (2016) Potassium: From Physiology to Clinical Implications. *Kidney Dis.* 10.1159/000446268
3. Bazúa-Valenti, S., Rojas-Vega, L., Castañeda-Bueno, M., Barrera-Chimal, J., Bautista, R., Cervantes-Pérez, L. G., Vázquez, N., Plata, C., Murillo-de-Ozores, A. R., González-Mariscal, L., Ellison, D. H., Riccardi, D., Bobadilla, N. A., and Gamba, G. (2018) The Calcium-Sensing Receptor Increases Activity of the Renal NCC through the WNK4-SPAK Pathway. *J. Am. Soc. Nephrol.* **29**, 1838–1848
4. Grimm, P. R., Coleman, R., Delpire, E., and Welling, P. A. (2017) Constitutively active SPAK causes hyperkalemia by activating NCC and remodeling distal tubules. *J. Am. Soc. Nephrol.* **28**, 2597–2606
5. Salhadar, K., Matthews, A., Raghuram, V., Limbutara, K., Yang, C. R., Datta, A., Chou, C. L., and Knepper, M. A. (2021) Phosphoproteomic identification of vasopressin/cAMP/protein kinase A-dependent signaling in kidney. *Mol. Pharmacol.* **99**, 358–369
6. Simon, D. B., Karet, F. E., Hamdan, J. H., DiPietro, A., Sanjad, S. A., and Lifton, R. P. (1996) Bartter's syndrome, hypokalaemic alkalosis with hypercalciuria, is caused by mutations in the Na-K-2Cl cotransporter NKCC2. *Nat. Genet.* **13**, 138–8
7. Simon, D. B., Karet, F. E., Rodriguez-Soriano, J., Hamdan, J. H., DiPietro, A., Trachtman, H., Sanjad, S. A., and Lifton, R. P. (1996) Genetic heterogeneity of Bartter's syndrome revealed by mutations in the K⁺ channel, ROMK. *Nat. Genet.* **14**, 152–156
8. Gamba, G. (2005) Molecular physiology and pathophysiology of electroneutral cation-chloride cotransporters. *Physiol. Rev.* **85**, 423–93
9. Chang, S. S., Grunder, S., Hanukoglu, A., Rösler, A., Mathew, P. M., Hanukoglu, I., Schild, L., Lu, Y., Shimkets, R. A., Nelson-Williams, C., Rossier, B. C., and Lifton, R. P. (1996) Mutations in subunits of the epithelial sodium channel cause salt wasting with hyperkalaemic acidosis, pseudohypoaldosteronism type 1. *Nat. Genet.* **12**, 248–253
10. Strautnieks, S. S., Thompson, R. J., Gardiner, R. M., and Chung, E. (1996) A novel splice-site mutation in the γ subunit of the epithelial sodium channel gene in three pseudohypoaldosteronism type 1 families. *Nat. Genet.* **13**, 248–250
11. Shimkets, R. A., Warnock, D. G., Bositis, C. M., Nelson-Williams, C., Hansson, J. H., Schambelan, M., Gill, J. R., Ulick, S., Milora, R. V., Findling, J. W., Canessa, C. M., Rossier, B. C., and Lifton, R. P. (1994) Liddle's syndrome: Heritable human hypertension caused by mutations in the β subunit of the epithelial sodium channel. *Cell.* **79**, 407–414
12. Hansson, J. H., Nelson-Williams, C., Suzuki, H., Schild, L., Shimkets, R., Lu, Y., Canessa, C., Iwasaki, T., Rossier, B., and Lifton, R. P. (1995) Hypertension caused by a truncated epithelial sodium channel γ subunit: Genetic heterogeneity of Liddle syndrome. *Nat. Genet.* **11**, 76–82
13. Salih, M., Gautschi, I., Van Bemmelen, M. X., Benedetto, M. Di, Brooks, A. S., Lugtenberg, D., Schild, L., and Hoorn, E. J. (2017) A Missense

- Mutation in the Extracellular Domain of aENaC Causes Liddle Syndrome. *J Am Soc Nephrol.* 10.1681/ASN.2016111163
14. Gumz, M. L., Lynch, I. J., Greenlee, M. M., Cain, B. D., and Wingo, C. S. (2010) The renal H⁺-K⁺-ATPases: physiology, regulation, and structure. *Am. J. Physiol. Physiol.* **298**, F12–F21
 15. Liu, W., Xu, S., Woda, C., Kim, P., Weinbaum, S., and Satlin, L. M. (2003) Effect of flow and stretch on the [Ca²⁺]_i response of principal and intercalated cells in cortical collecting duct. *Am. J. Physiol. Physiol.* **285**, F998–F1012
 16. Valinsky, W. C., Touyz, R. M., and Shrier, A. (2018) Aldosterone, SGK1, and ion channels in the kidney. *Clin. Sci.* **132**, 173–183
 17. Palmer, B. F. (2014) Regulation Of Potassium Homeostasis. *Clin. J. Am. Soc. Nephrol.* **10**, 1050–1060
 18. Todkar, A., Picard, N., Loffing-Cueni, D., Sorensen, M. V., Mihailova, M., Nesterov, V., Makhanova, N., Korbmacher, C., Wagner, C. A., and Loffing, J. (2015) Mechanisms of Renal Control of Potassium Homeostasis in Complete Aldosterone Deficiency. *J. Am. Soc. Nephrol.* **26**, 425–438
 19. Young, D. B., and Paulsen, A. W. (1983) Interrelated effects of aldosterone and plasma potassium on potassium excretion. *Am. J. Physiol. Physiol.* **244**, F28–F34
 20. Sørensen, M. V., Saha, B., Jensen, I. S., Wu, P., Ayasse, N., Gleason, C. E., Svendsen, S. L., Wang, W.-H. H., and Pearce, D. (2019) Potassium acts through mTOR to regulate its own secretion. *JCI Insight.* 10.1172/jci.insight.126910
 21. Murillo-de-Ozores, A. R., Gamba, G., and Castañeda-Bueno, M. (2019) Molecular mechanisms for the regulation of blood pressure by potassium. in *Current Topics in Membranes*, 1st Ed., pp. 285–313, Elsevier Inc., **83**, 285–313
 22. Gamba, G., Saltzberg, S. N., Lombardi, M., Miyanoshita, A., Lytton, J., Hediger, M. A., Brenner, B. M., and Hebert, S. C. (1993) Primary structure and functional expression of a cDNA encoding the thiazide-sensitive, electroneutral sodium-chloride cotransporter. *Proc. Natl. Acad. Sci. U. S. A.* **90**, 2749–53
 23. Simon, D. B., Nelson-Williams, C., Bia, M. J., Ellison, D., Karet, F. E., Molina, A. M., Vaara, I., Iwata, F., Cushner, H. M., Koolen, M., Gainza, F. J., Gitelman, H. J., and Lifton, R. P. (1996) Gitelman's variant of Bartter's syndrome, inherited hypokalaemic alkalosis, is caused by mutations in the thiazide-sensitive Na-Cl cotransporter. *Nat. Genet.* **12**, 24–30
 24. Schultheis, P. J., Lorenz, J. N., Meneton, P., Nieman, M. L., Riddle, T. M., Flagella, M., Duffy, J. J., Doetschman, T., Miller, M. L., and Shull, G. E. (1998) Phenotype resembling Gitelman's syndrome in mice lacking the apical Na⁺-Cl⁻ cotransporter of the distal convoluted tubule. *J. Biol. Chem.* **273**, 29150–29155
 25. Yang, S. Sen, Lo, Y. F., Yu, I. S., Lin, S. W., Chang, T. H., Hsu, Y. J., Chao, T. K., Sytwu, H. K., Uchida, S., Sasaki, S., and Lin, S. H. (2010) Generation and analysis of the thiazide-sensitive Na⁺-Cl⁻ cotransporter (Ncc/Slc12a3) Ser707X knockin mouse as a model of Gitelman syndrome. *Hum. Mutat.* **31**, 1304–1315
 26. Yang, S. Sen, Fang, Y. W., Tseng, M. H., Chu, P. Y., Yu, I. S., Wu, H. C.,

- Lin, S. W., Chau, T., Uchida, S., Sasaki, S., Lin, Y. F., Sytwu, H. K., and Lin, S. H. (2013) Phosphorylation regulates NCC stability and transporter activity in vivo. *J. Am. Soc. Nephrol.* **24**, 1587–1597
27. Mayan, H., Vered, I., Mouallem, M., Tzadok-witkon, M., and Pazner, R. (2002) Pseudohypoaldosteronism Type II : Marked Sensitivity to. *J Clin Endocrinol Metab.* **87**, 3248–3254
 28. Wilson, F. H., Disse-Nicodème, S., Choate, K. A., Ishikawa, K., Nelson-Williams, C., Desitter, I., Gunel, M., Milford, D. V., Lipkin, G. W., Achard, J. M., Feely, M. P., Dussol, B., Berland, Y., Unwin, R. J., Mayan, H., Simon, D. B., Farfel, Z., Jeunemaitre, X., and Lifton, R. P. (2001) *Human hypertension caused by mutations in WNK kinases*, 10.1126/science.1062844
 29. Louis-Dit-Picard, H., Kouranti, I., Rafael, C., Loisel-Ferreira, I., Chavez-Canales, M., Abdel-Khalek, W., Argaiz, E. R., Baron, S., Vacle, S., Migeon, T., Coleman, R., Cruzeiro, M. Do, Hureauux, M., Thurairajasingam, N., Decramer, S., Girerd, X., O'Shaugnessy, K., Mulatero, P., Roussey, G., Tack, I., Unwin, R., Vargas-Poussou, R., Staub, O., Grimm, R., Welling, P. A., Gamba, G., Clauser, E., Hadchouel, J., and Jeunemaitre, X. (2020) Mutation affecting the conserved acidic WNK1 motif causes inherited hyperkalemic hyperchloremic acidosis. *J. Clin. Invest.* **130**, 6379–6394
 30. Boyden, L. M., Choi, M., Choate, K. A., Nelson-Williams, C. J., Farhi, A., Toka, H. R., Tikhonova, I. R., Bjornson, R., Mane, S. M., Colussi, G., Lebel, M., Gordon, R. D., Semmekrot, B. A., Pujol, A., Välimäki, M. J., De Ferrari, M. E., Sanjad, S. A., Gutkin, M., Karet, F. E., Tucci, J. R., Stockigt, J. R., Keppler-Noreuil, K. M., Porter, C. C., Anand, S. K., Whiteford, M. L., Davis, I. D., Dewar, S. B., Bettinelli, A., Fadrowski, J. J., Belsha, C. W., Hunley, T. E., Nelson, R. D., Trachtman, H., Cole, T. R. P., Pinsk, M., Bockenhauer, D., Shenoy, M., Vaidyanathan, P., Foreman, J. W., Rasoulpour, M., Thameem, F., Al-Shahroui, H. Z., Radhakrishnan, J., Gharavi, A. G., Goilav, B., and Lifton, R. P. (2012) Mutations in kelch-like 3 and cullin 3 cause hypertension and electrolyte abnormalities. *Nature.* 10.1038/nature10814
 31. Louis-Dit-Picard, H., Barc, J., Trujillano, D., Miserey-Lenkei, S., Bouatia-Naji, N., Pylypenko, O., Beaurain, G., Bonnefond, A., Sand, O., Simian, C., Vidal-Petiot, E., Soukaseum, C., Mandet, C., Broux, F., Chabre, O., Delahousse, M., Esnault, V., Fiquet, B., Houillier, P., Bagnis, C. I. C., Koenig, J., Konrad, M., Landais, P., Mourani, C., Niaudet, P., Probst, V., Thauvin, C., Unwin, R. J. R. R. J., Soroka, S. D. S., Ehret, G., Ossowski, S., Caulfield, M., Bruneval, P., Estivill, X., Froguel, P., Hadchouel, J., Schott, J.-J. J. J., Jeunemaitre, X., Pressure, I. C. for B., Bruneval, P., Estivill, X., Froguel, P., Hadchouel, J., Schott, J.-J. J. J., and Jeunemaitre, X. (2012) KLHL3 mutations cause familial hyperkalemic hypertension by impairing ion transport in the distal nephron. *Nat. Genet.* **44**, 456–60, S1-3
 32. Alessi, D. R., Zhang, J., Khanna, A., Hochdörfer, T., Shang, Y., and Kahle, K. T. (2014) The WNK-SPAK / OSR1 pathway : Master regulator of cation-chloride cotransporters. **7**, 1–10
 33. Vitari, A. C., Deak, M., Morrice, N. A., and Alessi, D. R. (2005) The WNK1 and WNK4 protein kinases that are mutated in Gordon's hypertension

- syndrome phosphorylate and activate SPAK and OSR1 protein kinases. *Biochem. J.* 10.1042/BJ20051180
34. Pacheco-Alvarez, D., San Cristóbal, P., Meade, P., Moreno, E., Vazquez, N., Muñoz, E., Díaz, A., Juárez, M. E., Giménez, I., and Gamba, G. (2006) The Na⁺:Cl⁻ cotransporter is activated and phosphorylated at the amino-terminal domain upon intracellular chloride depletion. *J. Biol. Chem.* **281**, 28755–28763
 35. Richardson, C. J. Z., Rafiqi, F. H., Karlsson, H. K. R., Moleleki, N., Vandewalle, A., Campbell, D. G., Morrice, N. A., and Alessi, D. R. (2008) Activation of the thiazide-sensitive Na⁺-Cl⁻ cotransporter by the WNK-regulated kinases SPAK and OSR1. *J. Cell Sci.* **121**, 675–684
 36. Murillo-de-Ozores, A. R., Chávez-Canales, M., de los Heros, P., Gamba, G., and Castañeda-Bueno, M. (2020) Physiological Processes Modulated by the Chloride-Sensitive WNK-SPAK/OSR1 Kinase Signaling Pathway and the Cation-Coupled Chloride Cotransporters. *Front. Physiol.* **11**, 1–28
 37. Lee, J. W., Chou, C. L., and Knepper, M. A. (2015) Deep sequencing in microdissected renal tubules identifies nephron segment-specific transcriptomes. *J. Am. Soc. Nephrol.* **26**, 2669–2677
 38. Chen, L., Chou, C.-L., and Knepper, M. A. (2021) A Comprehensive Map of mRNAs and Their Isoforms across All 14 Renal Tubule Segments of Mouse. *J. Am. Soc. Nephrol.* **32**, 897–912
 39. Vidal-Petiot, E., Cheval, L., Faugeroux, J., Malard, T., Doucet, A., Jeunemaitre, X., and Hadchouel, J. (2012) A new methodology for quantification of alternatively spliced exons reveals a highly tissue-specific expression pattern of WNK1 isoforms. *PLoS One.* 10.1371/journal.pone.0037751
 40. Argaiz, E. R., Chavez-Canales, M., Ostrosky-Frid, M., Rodríguez-Gama, A., Vázquez, N., Gonzalez-Rodriguez, X., Garcia-Valdes, J., Hadchouel, J., Ellison, D., and Gamba, G. (2018) Kidney-specific WNK1 isoform (KS-WNK1) is a potent activator of WNK4 and NCC. *Am. J. Physiol. - Ren. Physiol.* **315**, F734–F745
 41. Castañeda-Bueno, M., Cervantes-Pérez, L. G., Vázquez, N., Uribe, N., Kantesaria, S., Morla, L., Bobadilla, N. A., Doucet, A., Alessi, D. R., and Gamba, G. (2012) Activation of the renal Na⁺:Cl⁻ cotransporter by angiotensin II is a WNK4-dependent process. *Proc. Natl. Acad. Sci. U. S. A.* **109**, 7929–7934
 42. Takahashi, D., Mori, T., Nomura, N., Khan, M. Z. H., Araki, Y., Zeniya, M., Sohara, E., Rai, T., Sasaki, S., and Uchida, S. (2014) WNK4 is the major WNK positively regulating NCC in the mouse kidney. *Biosci. Rep.* **34**, 195–205
 43. Yang, Y. S., Xie, J., Yang, S. Sen, Lin, S. H., and Huang, C. L. (2018) Differential roles of WNK4 in regulation of NCC in vivo. *Am. J. Physiol. - Ren. Physiol.* **314**, F999–F1007
 44. Yang, S. Sen, Morimoto, T., Rai, T., Chiga, M., Sohara, E., Ohno, M., Uchida, K., Lin, S. H., Moriguchi, T., Shibuya, H., Kondo, Y., Sasaki, S., and Uchida, S. (2007) Molecular Pathogenesis of Pseudohypoaldosteronism Type II: Generation and Analysis of a Wnk4D561A/+Knockin Mouse Model. *Cell Metab.* **5**, 331–344
 45. Murillo-de-Ozores, A. R., Rodríguez-Gama, A., Bazúa-Valenti, S., Leyva-Ríos, K., Vázquez, N., Pacheco-Álvarez, D., De La Rosa-Velázquez, I. A.,

- Wengi, A., Stone, K. L., Zhang, J., Loffing, J., Lifton, R. P., Yang, C. L., Ellison, D. H., Gamba, G., and Castañeda-Bueno, M. (2018) C-terminally truncated, kidney-specific variants of the WNK4 kinase lack several sites that regulate its activity. *J. Biol. Chem.* **293**, 12209–12221
46. Murillo-De-Ozores, A. R., Rodríguez-Gama, A., Carbajal-Contreras, H., Gamba, G., and Castañeda-Bueno, M. (2021) WNK4 kinase: From structure to physiology. *Am. J. Physiol. - Ren. Physiol.* **320**, F378–F403
47. Gagnon, K. B., and Delpire, E. (2012) Molecular physiology of SPAK and OSR1: Two Ste20-related protein kinases regulating ion transport. *Physiol. Rev.* **92**, 1577–1617
48. Delaloy, C., Lu, J., Houot, A.-M., Disse-Nicodeme, S., Gasc, J.-M., Corvol, P., and Jeunemaitre, X. (2003) Multiple Promoters in the WNK1 Gene: One Controls Expression of a Kidney-Specific Kinase-Defective Isoform. *Mol. Cell. Biol.* **23**, 9208–9221
49. Ohta, A., Schumacher, F.-R., Mehellou, Y., Johnson, C., Knebel, A., Macartney, T. J., Wood, N. T., Alessi, D. R., and Kurz, T. (2013) The CUL3–KLHL3 E3 ligase complex mutated in Gordon’s hypertension syndrome interacts with and ubiquitylates WNK isoforms: disease-causing mutations in KLHL3 and WNK4 disrupt interaction. *Biochem. J.* **451**, 111–122
50. Shibata, S., Zhang, J., Puthumana, J., Stone, K. L., and Lifton, R. P. (2013) Kelch-like 3 and Cullin 3 regulate electrolyte homeostasis via ubiquitination and degradation of WNK4. *Proc. Natl. Acad. Sci. U. S. A.* **110**, 7838–7843
51. Wakabayashi, M., Mori, T., Isobe, K., Sohara, E., Susa, K., Araki, Y., Chiga, M., Kikuchi, E., Nomura, N., Mori, Y., Matsuo, H., Murata, T., Nomura, S., Asano, T., Kawaguchi, H., Nonoyama, S., Rai, T., Sasaki, S., and Uchida, S. (2013) Impaired KLHL3-mediated ubiquitination of WNK4 causes human hypertension. *Cell Rep.* **3**, 858–868
52. Thastrup, J. O., Rafiqi, F. H., Vitari, A. C., Pozo-Guisado, E., Deak, M., Mehellou, Y., and Alessi, D. R. (2012) SPAK/OSR1 regulate NKCC1 and WNK activity: Analysis of WNK isoform interactions and activation by T-loop trans-autophosphorylation. *Biochem. J.* **441**, 325–337
53. Castañeda-Bueno, M., Arroyo, J. P., Zhang, J., Puthumana, J., Yarborough, O., Shibata, S., Rojas-Vega, L., Gamba, G., Rinehart, J., and Lifton, R. P. (2017) Phosphorylation by PKC and PKA regulate the kinase activity and downstream signaling of WNK4. *Proc. Natl. Acad. Sci.* **114**, E879–E886
54. Na, T., Wu, G., Zhang, W., Dong, W.-J., and Peng, J.-B. (2013) Disease-causing R1185C mutation of WNK4 disrupts a regulatory mechanism involving calmodulin binding and SGK1 phosphorylation sites. *Am. J. Physiol. Physiol.* **304**, F8–F18
55. Zhang, C., Wang, Z., Xie, J., Yan, F., Wang, W., Feng, X., Zhang, W., and Chen, N. (2011) Identification of a novel WNK4 mutation in Chinese patients with pseudohypoaldosteronism type II. *Nephron - Physiol.* **118**, 53–61
56. Hendrickx, A., Beullens, M., Ceulemans, H., Den Abt, T., Van Eynde, A., Nicolaescu, E., Lesage, B., and Bollen, M. (2009) Docking Motif-Guided Mapping of the Interactome of Protein Phosphatase-1. *Chem. Biol.* **16**, 365–371

57. Piala, A. T., Moon, T. M., Akella, R., He, H., Cobb, M. H., and Goldsmith, E. J. (2014) Chloride sensing by WNK1 involves inhibition of autophosphorylation. *Sci. Signal.* 10.1126/scisignal.2005050
58. Bazua-Valenti, S., Chavez-Canales, M., Rojas-Vega, L., Gonzalez-Rodriguez, X., Vazquez, N., Rodriguez-Gama, A., Argaiz, E. R., Melo, Z., Plata, C., Ellison, D. H., Garcia-Valdes, J., Hadchouel, J., Gamba, G., Bazúa-Valenti, S., Chávez-Canales, M., Rojas-Vega, L., González-Rodríguez, X., Vázquez, N., Rodríguez-Gama, A., Argaiz, E. R., Melo, Z., Plata, C., Ellison, D. H., García-Valdés, J., Hadchouel, J., and Gamba, G. (2014) The Effect of WNK4 on the Na⁺-Cl⁻ Cotransporter Is Modulated by Intracellular Chloride. *J. Am. Soc. Nephrol.* 10.1681/ASN.2014050470
59. Terker, A. S., Zhang, C., Erspamer, K. J., Gamba, G., Yang, C.-L. L., and Ellison, D. H. (2015) Unique chloride-sensing properties of WNK4 permit the distal nephron to modulate potassium homeostasis. *Kidney Int.* **89**, 1–8
60. Su, X. T., Klett, N. J., Sharma, A., Allen, C. N., Wang, W. H., Yang, C. L., and Ellison, D. H. (2020) Distal convoluted tubule Cl⁻ concentration is modulated via K⁺ channels and transporters. *Am. J. Physiol. - Ren. Physiol.* **319**, F534–F540
61. Chen, J. C., Lo, Y. F., Lin, Y. W., Lin, S. H., Huang, C. L., and Cheng, C. J. (2019) WNK4 kinase is a physiological intracellular chloride sensor. *Proc. Natl. Acad. Sci. U. S. A.* **116**, 4502–4507
62. Nishikawa, K., Toker, A., Johannes, F. J., Songyang, Z., and Cantley, L. C. (1997) Determination of the specific substrate sequence motifs of protein kinase C isozymes, 10.1074/jbc.272.2.952
63. Shibata, S., Arroyo, J. P., Castaneda-Bueno, M., Puthumana, J., Zhang, J., Uchida, S., Stone, K. L., Lam, T. T., and Lifton, R. P. (2014) Angiotensin II signaling via protein kinase C phosphorylates Kelch-like 3, preventing WNK4 degradation. *Proc. Natl. Acad. Sci.* **111**, 15556–15561
64. Schumacher, F.-R., Sorrell, F. J. J., Alessi, D. R. R., Bullock, A. N. N., and Kurz, T. (2014) Structural and biochemical characterization of the KLHL3–WNK kinase interaction important in blood pressure regulation. *Biochem. J.* **460**, 237–246
65. Susa, K., Sohara, E., Takahashi, D., Okado, T., Rai, T., and Uchida, S. (2017) WNK4 is indispensable for the pathogenesis of pseudohypoaldosteronism type II caused by mutant KLHL3. *Biochem. Biophys. Res. Commun.* **491**, 727–732
66. Czogalla, J., Vohra, T., Penton, D., Kirschmann, M., Craigie, E., and Loffing, J. (2016) The mineralocorticoid receptor (MR) regulates ENaC but not NCC in mice with random MR deletion. *Pflugers Arch. Eur. J. Physiol.* **468**, 849–858
67. Keith, N. M., and Binger, M. W. (1935) Diuretic Action of Potassium Salts. *JAMA.* **105**, 1584–91
68. O'Donnell, M., Mente, A., Rangarajan, S., McQueen, M. J., Wang, X., Liu, L., Yan, H., Lee, S. F., Mony, P., Devanath, A., Rosengren, A., Lopez-Jaramillo, P., Diaz, R., Avezum, A., Lanas, F., Yusuf, K., Iqbal, R., Ilow, R., Mohammadifard, N., Gulec, S., Yusufali, A. H., Kruger, L., Yusuf, R., Chifamba, J., Kabali, C., Dagenais, G., Lear, S. A., Teo, K., and Yusuf, S. (2014) Urinary Sodium and Potassium Excretion, Mortality, and Cardiovascular Events. *N. Engl. J. Med.* **371**, 612–623

69. Mente, A., O'Donnell, M. J., Rangarajan, S., McQueen, M. J., Poirier, P., Wielgosz, A., Morrison, H., Li, W., Wang, X., Di, C., Mony, P., Devanath, A., Rosengren, A., Oguz, A., Zatonska, K., Yusufali, A. H., Lopez-Jaramillo, P., Avezum, A., Ismail, N., Lanas, F., Puoane, T., Diaz, R., Kelishadi, R., Iqbal, R., Yusuf, R., Chifamba, J., Khatib, R., Teo, K., and Yusuf, S. (2014) Association of Urinary Sodium and Potassium Excretion with Blood Pressure. *N. Engl. J. Med.* **371**, 601–611
70. Bernabe-Ortiz, A., Sal y Rosas, V. G., Ponce-Lucero, V., Cárdenas, M. K., Carrillo-Larco, R. M., Diez-Canseco, F., Pesantes, M. A., Sacksteder, K. A., Gilman, R. H., and Miranda, J. J. (2020) Effect of salt substitution on community-wide blood pressure and hypertension incidence. *Nat. Med.* **26**, 374–378
71. Terker, A. S., Zhang, C., McCormick, J. A., Lazelle, R. A., Zhang, C., Meermeier, N. P., Siler, D. A., Park, H. J., Fu, Y., Cohen, D. M., Weinstein, A. M., Wang, W. H., Yang, C. L., and Ellison, D. H. (2015) Potassium modulates electrolyte balance and blood pressure through effects on distal cell voltage and chloride. *Cell Metab.* **21**, 39–50
72. Vallon, V., Schroth, J., Lang, F., Kuhl, D., and Uchida, S. (2009) Expression and phosphorylation of the Na⁺-Cl⁻ cotransporter NCC in vivo is regulated by dietary salt, potassium, and SGK1. *Am. J. Physiol. Physiol.* **297**, F704–F712
73. Castaneda-Bueno, M., Cervantes-Perez, L. G., Rojas-Vega, L., Arroyo-Garza, I., Vazquez, N., Moreno, E., and Gamba, G. (2014) Modulation of NCC activity by low and high K⁺ intake: insights into the signaling pathways involved. *AJP Ren. Physiol.* **306**, F1507–F1519
74. Penton, D., Czogalla, J., Wengi, A., Himmerkus, N., Loffing-Cueni, D., Carrel, M., Rajaram, R. D., Staub, O., Bleich, M., Schweda, F., and Loffing, J. (2016) Extracellular K⁺ rapidly controls NaCl cotransporter phosphorylation in the native distal convoluted tubule by Cl⁻-dependent and independent mechanisms. *J. Physiol.* **594**, 6319–6331
75. Su, X.-T., and Wang, W.-H. (2016) The expression, regulation, and function of Kir4.1 (*Kcnj10*) in the mammalian kidney. *Am. J. Physiol. - Ren. Physiol.* **311**, F12–F15
76. Bockenhauer, D., Feather, S., Stanescu, H. C., and Bandulik, S. (2009) Epilepsy, Ataxia, Sensorineural Deafness, Tubulopathy, and KCNJ10 Mutations. *N. Engl. J. Med.* **360**, 1960–70
77. Scholl, U. I., Choi, M., Liu, T., Ramaekers, V. T., Häusler, M. G., Grimmer, J., Tobe, S. W., Farhi, A., Nelson-Williams, C., and Lifton, R. P. (2009) Seizures, sensorineural deafness, ataxia, mental retardation, and electrolyte imbalance (SeSAME syndrome) caused by mutations in KCNJ10. *Proc. Natl. Acad. Sci. U. S. A.* **106**, 5842–5847
78. Zhang, C., Wang, L., Zhang, J., Su, X. T., Lin, D. H., Scholl, U. I., Giebisch, G., Lifton, R. P., and Wang, W. H. (2014) KCNJ10 determines the expression of the apical Na-Cl cotransporter (NCC) in the early distal convoluted tubule (DCT1). *Proc. Natl. Acad. Sci. U. S. A.* **111**, 11864–11869
79. Cuevas, C. A., Su, X. T., Wang, M. X., Terker, A. S., Lin, D. H., McCormick, J. A., Yang, C. L., Ellison, D. H., and Wang, W. H. (2017) Potassium sensing by renal distal tubules requires Kir4.1. *J. Am. Soc. Nephrol.* **28**, 1814–1825

80. Malik, S., Lambert, E., Zhang, J., Wang, T., Clark, H. L., Cypress, M., Goldman, B. I., Porter, G. A., Pena, S., Nino, W., and Gray, D. A. (2018) Potassium conservation is impaired in mice with reduced renal expression of Kir4.1. *Am. J. Physiol. - Ren. Physiol.* **315**, F1271–F1282
81. Pessia, M., Tucker, S. J., Lee, K., Bond, C. T., and Adelman, J. P. (1996) Subunit positional effects revealed by novel heteromeric inwardly rectifying K⁺ channels. *EMBO J.* **15**, 2980–2987
82. Tanemoto, M., Abe, T., and Ito, S. (2005) PDZ-binding and dihydrophobic motifs regulate distribution of Kir4.1 channels in renal cells. *J. Am. Soc. Nephrol.* **16**, 2608–2614
83. Paulais, M., Bloch-Faure, M., Picard, N., Jacques, T., Ramakrishnan, S. K., Keck, M., Sohet, F., Eladari, D., Houillier, P., Lourdel, S., Teulon, J., and Tucker, S. J. (2011) Renal phenotype in mice lacking the Kir5.1 (Kcnj16) K⁺ channel subunit contrasts with that observed in SeSAME/EAST syndrome. *Proc. Natl. Acad. Sci. U. S. A.* **108**, 10361–10366
84. Wu, P., Gao, Z. X., Zhang, D. D., Su, X. T., Wang, W. H., and Lin, D. H. (2019) Deletion of Kir5.1 impairs renal ability to excrete potassium during increased dietary potassium intake. *J. Am. Soc. Nephrol.* **30**, 1425–1438
85. Tanemoto, M., Kittaka, N., Inanobe, A., and Kurachi, Y. (2000) In vivo formation of a proton-sensitive K⁺ channel by heteromeric subunit assembly of Kir5.1 with Kir4.1. *J. Physiol.* **525**, 587–592
86. Tucker, S. J., Imbrici, P., Salvatore, L., D'Adamo, M. C., and Pessia, M. (2000) pH Dependence of the inwardly rectifying potassium channel, Kir5.1, and localization in renal tubular epithelia. *J. Biol. Chem.* **275**, 16404–16407
87. Estévez, R., Boettger, T., Stein, V., Birkenhäger, R., Otto, E., Hildebrandt, F., and Jentsch, T. J. (2001) Barttin is a Cl⁻ channel β -subunit crucial for renal Cl⁻ reabsorption and inner ear K⁺ secretion. *Nature.* **414**, 558–561
88. Waldegger, S., Jeck, N., Barth, P., Peters, M., Vitzthum, H., Wolf, K., Kurtz, A., Konrad, M., and Seyberth, H. W. (2002) Barttin increases surface expression and changes current properties of CLC-K channels. *Pflügers Arch. Eur. J. Physiol.* **444**, 411–418
89. Jentsch, T. J., and Pusch, M. (2018) CLC chloride channels and transporters: Structure, function, physiology, and disease. *Physiol. Rev.* **98**, 1493–1590
90. Simon, D. B., Bindra, R. S., Nelson-williams, T. A. M. C., Mendonca, E., Stone, R., Schurman, S., Nayir, A., Alpay, H., Bakkaloglus, A., Rodriguez-soriano, J., Morales, J. M., Sanjad, S. A., Taylor, C. M., Pilz, D., Brem, A., Trachtman, H., Griswold, W., Richard, G. A., John, E., and Lifton, R. P. (1997) Mutations in the chloride channel gene, CLCNKB, cause Bartter's syndrome type III. *Nat. Genet.* **17**, 171–178
91. Birkenhäger, R., Otto, E., Schürmann, M. J., Vollmer, M., Ruf, E. M., Maier-Lutz, I., Beekmann, F., Fekete, A., Omran, H., Feldmann, D., Milford, D. V., Jeck, N., Konrad, M., Landau, D., Knoers, N. V. A. M., Antignac, C., Sudbrak, R., Kispert, A., and Hildebrandt, F. (2001) Mutation of BSND causes Bartter syndrome with sensorineural deafness and kidney failure. *Nat. Genet.* **29**, 310–314
92. Konrad, M., Vollmer, M., Lemmink, H. H., Van Den Heuvel, L. P. W. J., Jeck, N., Vargas-Poussou, R., Lakings, A., Ruf, R., Deschênes, G.,

- Antignac, C., Guay-Woodford, L., Knoers, N. V. A. M., Seyberth, H. W., Feldmann, D., and Hildebrandt, F. (2000) Mutations in the chloride channel gene *CLCNKB* as a cause of classic Bartter syndrome. *J. Am. Soc. Nephrol.* **11**, 1449–1459
93. Cruz, A. J., and Castro, A. (2013) Gitelman or Bartter type 3 syndrome? A case of distal convoluted tubulopathy caused by *CLCNKB* gene mutation. *BMJ Case Rep.* 10.1136/bcr-2012-007929
94. Grill, A., Schießl, I. M., Gess, B., Fremter, K., Hammer, A., and Castrop, H. (2016) Salt-losing nephropathy in mice with a null mutation of the *Clcnk2* gene. *Acta Physiol.* **218**, 198–211
95. Hennings, J. C., Andrini, O., Picard, N., Paulais, M., Huebner, A. K., Cayuqueo, I. K. L., Bignon, Y., Keck, M., Cornière, N., Böhm, D., Jentsch, T. J., Chambrey, R., Teulon, J., Hübner, C. A., and Eladari, D. (2017) The *ClC-K2* chloride channel is critical for salt handling in the distal nephron. *J. Am. Soc. Nephrol.* **28**, 209–217
96. Nomura, N., Tajima, M., Sugawara, N., Morimoto, T., Kondo, Y., Ohno, M., Uchida, K., Mutig, K., Bachmann, S., Soleimani, M., Ohta, E., Ohta, A., Sohara, E., Okado, T., Rai, T., Jentsch, T. J., Sasaki, S., and Uchida, S. (2011) Generation and analyses of R8L barttin knockin mouse. *Am. J. Physiol. - Ren. Physiol.* **301**, 297–307
97. Wang, M. X., Cuevas, C. A., Su, X. T., Wu, P., Gao, Z. X., Lin, D. H., McCormick, J. A., Yang, C. L., Wang, W. H., and Ellison, D. H. (2018) Potassium intake modulates the thiazide-sensitive sodium-chloride cotransporter (NCC) activity via the Kir4.1 potassium channel. *Kidney Int.* **93**, 893–902
98. Nomura, N., Shoda, W., Wang, Y., Mandai, S., Furusho, T., Takahashi, D., Zeniya, M., Sohara, E., Rai, T., and Uchida, S. (2018) Role of *ClC-K* and barttin in low-potassium induced sodium-chloride cotransporter activation and hypertension in mouse kidney. *Biosci. Rep.* 10.1042/BSR20171243
99. Ishizawa, K., Xu, N., Loffing, J., Lifton, R. P., Fujita, T., Uchida, S., and Shibata, S. (2016) Potassium depletion stimulates Na-Cl cotransporter via phosphorylation and inactivation of the ubiquitin ligase Kelch-like 3. *Biochem. Biophys. Res. Commun.* **480**, 745–751
100. Ostrosky-Frid, M., Chávez-Canales, M., Zhang, J., Andrukhova, O., Argaiz, E. R., Lerdo-De-Tejada, F., Murillo-De-Ozores, A., Sanchez-Navarro, A., Rojas-Vega, L., Bobadilla, N. A., Vazquez, N., Castañeda-Bueno, M., Alessi, D. R., and Gamba, G. (2021) Role of *KLHL3* and dietary K⁺ in regulating *KS-WNK1* expression. *Am. J. Physiol. - Ren. Physiol.* **320**, F734–F747
101. Boyd-Shiwarski, C. R., Shiwarski, D. J., Roy, A., Nkashama, L. J., Namboodiri, H. N., Xie, J., McClain, K. L., Marciszyn, A., Kleyman, T. R., Tan, R. J., Stolz, D. B., Puthenveedu, M. A., Huang, C.-L., and Subramanya, A. R. (2017) Potassium-Regulated Distal Tubule WNK Bodies are Kidney-Specific WNK1 Dependent. *Mol. Biol. Cell.* **1**, mbc.E17-08-0529
102. Thomson, M. N., Cuevas, C. A., Bewarder, T. M., Dittmayer, C., Miller, L. N., Si, J., Cornelius, R. J., Su, X. T., Yang, C. L., McCormick, J. A., Hadchouel, J., Ellison, D. H., Bachmann, S., and Mutig, K. (2020) WNK bodies cluster WNK4 and SPAK/OSR1 to promote NCC activation in

- hypokalemia. *Am. J. Physiol. - Ren. Physiol.* **318**, F216–F228
103. McCormick, J. A., Yang, C. L., Zhang, C., Davidge, B., Blankenstein, K. I., Terker, A. S., Yarbrough, B., Meermeier, N. P., Park, H. J., McCully, B., West, M., Borschewski, A., Himmerkus, N., Bleich, M., Bachmann, S., Mutig, K., Argaiz, E. R., Gamba, G., Singer, J. D., and Ellison, D. H. (2014) Hyperkalemic hypertension-associated cullin 3 promotes WNK signaling by degrading KLHL3. *J. Clin. Invest.* **124**, 4723–4736
 104. Cornelius, R. J., Si, J., Cuevas, C. A., Nelson, J. W., Gratreak, B. D. K., Pardi, R., Yang, C.-L., and Ellison, D. H. (2018) Renal COP9 Signalosome Deficiency Alters CUL3-KLHL3-WNK Signaling Pathway. *J. Am. Soc. Nephrol.* 10.1681/ASN.2018030333
 105. Zagórska, A., Pozo-Guisado, E., Boudeau, J., Vitari, A. C., Rafiqi, F. H., Thastrup, J., Deak, M., Campbell, D. G., Morrice, N. A., Prescott, A. R., and Alessi, D. R. (2007) Regulation of activity and localization of the WNK1 protein kinase by hyperosmotic stress. *J. Cell Biol.* **176**, 89–100
 106. Liu, Y., Deng, X., Wu, D., Jin, M., and Yu, B. (2019) PKC δ promotes fertilization of mouse embryos in early development via the Cdc25B signaling pathway. *Exp. Ther. Med.* 10.3892/etm.2019.7959
 107. Kumar, V., Weng, Y. C., Wu, Y. C., Huang, Y. T., Liu, T. H., Kristian, T., Liu, Y. L., Tsou, H. H., and Chou, W. H. (2019) Genetic inhibition of PKC ϵ attenuates neurodegeneration after global cerebral ischemia in male mice. *J. Neurosci. Res.* **97**, 444–455
 108. Markadieu, N., San-Cristobal, P., Nair, A. V., Verkaart, S., Lenssen, E., Tudpor, K., van Zeeland, F., Loffing, J., Bindels, R. J. M., and Hoenderop, J. G. J. (2012) A primary culture of distal convoluted tubules expressing functional thiazide-sensitive NaCl transport. *Am. J. Physiol. Renal Physiol.* **303**, F886–92
 109. Krishnan, N., Lam, T. T., Fritz, A., Rempinski, D., O’Loughlin, K., Minderman, H., Berezney, R., Marzluff, W. F., and Thapar, R. (2012) The Prolyl Isomerase Pin1 Targets Stem-Loop Binding Protein (SLBP) To Dissociate the SLBP-Histone mRNA Complex Linking Histone mRNA Decay with SLBP Ubiquitination. *Mol. Cell. Biol.* **32**, 4306–4322
 110. Lobbstaël, E., Zhao, J., Rudenko, I. N., Beylina, A., Gao, F., Wetter, J., Beullens, M., Bollen, M., Cookson, M. R., Baekelandt, V., Nichols, R. J., and Taymans, J. M. (2013) Identification of protein phosphatase 1 as a regulator of the LRRK2 phosphorylation cycle. *Biochem. J.* **456**, 119–128
 111. Soh, J. W., and Weinstein, I. B. (2003) Roles of Specific Isoforms of Protein Kinase C in the Transcriptional Control of Cyclin D1 and Related Genes. *J. Biol. Chem.* **278**, 34709–34716
 112. Li, C., Wen, A., Shen, B., Lu, J., Huang, Y., and Chang, Y. (2011) FastCloning: a highly simplified, purification-free, sequence- and ligation-independent PCR cloning method. *BMV Biotechnol.* **11**, 1–10
 113. Zambrano, E., Barrios-de-Tomasi, J., Cárdenas, M., and Ulloa-Aguirre, A. (1996) Studies on the relative in-vitro biological potency of the naturally-occurring isoforms of intrapituitary follicle stimulating hormone. *Mol. Hum. Reprod.* **2**, 563–571
 114. Kahle, K. T., Gimenez, I., Hassan, H., Wilson, F. H., Wong, R. D., Forbush, B., Aronson, P. S., and Lifton, R. P. (2004) *WNK4 regulates apical and basolateral Cl⁻ flux in extrarenal epithelia*, 10.1073/pnas.0308434100

115. Markadieu, N., Rios, K., Spiller, B. W., McDonald, W. H., Welling, P. A., and Delpire, E. (2014) Short forms of Ste20-related proline/alanine-rich kinase (SPAK) in the kidney are created by aspartyl aminopeptidase (Dnpep)-mediated proteolytic cleavage. *J. Biol. Chem.* **289**, 29273–29284
116. Koumangoye, R., and Delpire, E. (2017) DNPEP is not the only peptidase that produces SPAK fragments in kidney. *Physiol. Rep.* **5**, 1–9
117. Yang, C. L., Zhu, X., Wang, Z., Subramanya, A. R., and Ellison, D. H. (2005) Mechanisms of WNK1 and WNK4 interaction in the regulation of thiazide-sensitive NaCl cotransport. *J. Clin. Invest.* **115**, 1379–1387
118. Gandolfi, B., Gruffydd-Jones, T. J., Malik, R., Cortes, A., Jones, B. R., Helps, C. R., Prinzenberg, E. M., Erhardt, G., and Lyons, L. A. (2012) First WNK4-Hypokalemia Animal Model Identified by Genome-Wide Association in Burmese Cats. *PLoS One.* **7**, 1–9
119. Yoshizaki, Y., Mori, Y., Tsuzaki, Y., Mori, T., Nomura, N., Wakabayashi, M., Takahashi, D., Zeniya, M., Kikuchi, E., Araki, Y., Ando, F., Isobe, K., Nishida, H., Ohta, A., Susa, K., Inoue, Y., Chiga, M., Rai, T., Sasaki, S., Uchida, S., and Sohara, E. (2015) Impaired degradation of WNK by Akt and PKA phosphorylation of KLHL3. *Biochem. Biophys. Res. Commun.* **467**, 229–234
120. Shoda, W., Nomura, N., Ando, F., Mori, Y., Mori, T., Sohara, E., Rai, T., and Uchida, S. (2017) Calcineurin inhibitors block sodium-chloride cotransporter dephosphorylation in response to high potassium intake. *Kidney Int.* **91**, 402–411

10. APÉNDICE

Además del artículo ya publicado en Journal of Biological Chemistry, y el manuscrito que está próximo a enviarse, durante mi doctorado tuve la oportunidad de publicar otros artículos de revisión sobre el tema y de colaborar como co-autor en distintos trabajos de la Unidad de Fisiología Molecular. Estos se presentan a continuación.

Molecular mechanisms for the regulation of blood pressure by potassium

Adrián Rafael Murillo-de-Ozores^{a,b}, Gerardo Gamba^{a,c,d},
 María Castañeda-Bueno^{a,*}

^aMolecular Physiology Unit, Department of Nephrology and Mineral Metabolism, Instituto Nacional de Ciencias Médicas y Nutrición Salvador Zubirán, Mexico City, Mexico

^bFacultad de Medicina, Universidad Nacional Autónoma de México, Mexico City, Mexico

^cInstituto de Investigaciones Biomédicas, Universidad Nacional Autónoma de México, Mexico City, Mexico

^dTecnológico de Monterrey, Escuela de Medicina y Ciencias de la Salud, Monterrey, NL, Mexico

*Corresponding author: e-mail addresses: maria.castanedab@incmnz.mx; mcasta85@yahoo.com.mx

Contents

1. Evidences of the impact of dietary potassium intake on blood pressure levels	2
2. Natriuretic and diuretic effects of potassium; nephron segments involved in the natriuretic effect of high potassium intake	5
3. Role of the kidney in potassium homeostasis	10
4. Molecular mechanisms implicated in the natriuretic and diuretic effects of potassium	15
4.1 Regulation of the Na-Cl cotransporter NCC by potassium	16
4.2 Additional mechanisms for potassium-mediated regulation of NCC	20
5. Summary and conclusions	21
Acknowledgments	22
References	22

Abstract

It has been well documented that the amount of potassium in the diet is associated with blood pressure levels in the population: the higher the potassium consumption, the lower the blood pressure and the cardiovascular mortality. In the last few years certain mechanisms for potassium regulation of salt reabsorption in the kidney have been elucidated at the molecular level. In this work we discuss the evidence demonstrating the relationship between potassium intake and blood pressure levels in human populations and in animal models, as well as the experimental data that reveal the effects of potassium on transepithelial Na⁺ reabsorption in different nephron segments. We also discuss the physiological relevance of K⁺-induced natriuresis, and finally, we focus on the molecular mechanisms by which extracellular potassium modulates the activity of the renal NaCl cotransporter, which is the mechanism that has been best dissected so far.

Abbreviations

ASDN	aldosterone-sensitive distal nephron
BK	Maxi-K channel
[Cl⁻]_I	intracellular chloride concentration
CCD	cortical collecting duct
CNT	connecting tubule
CUL3	Cullin 3
DCT	distal convoluted tubule
ENaC	epithelial Na ⁺ channel
FHHt	familial hyperkalemic hypertension
[K⁺]_e	extracellular potassium concentration
KIR	inward rectifier K ⁺ channel
KLHL3	kelch like family member 3
NCC	Na ⁺ :Cl ⁻ cotransporter
NKCC	Na ⁺ :K ⁺ :2Cl ⁻ cotransporter
OSR1	oxidative stress-responsive 1 protein
ROMK	renal outer medullary K ⁺ channel
SPAK	Ste20/SPS1-related proline-alanine rich kinase
TAL	thick ascending limb of Henle's loop
WHO	World Health Organization
WNK	<u>with no</u> lysine (K) kinase



1. Evidences of the impact of dietary potassium intake on blood pressure levels

Hypertension affects >1 billion people around the world and it is one of the leading risk factors for cardiovascular disease and death (Mente et al., 2014). Although it has been thoroughly documented that sodium intake plays a determinant role in the pathogenesis of hypertension, potassium content in the diet might be as important as sodium in the regulation of blood pressure.

Compared to ancient diets, the current typical Western diet has a relatively low potassium content (~54 mmol or 2.1 g/day) and a high sodium content (~214 mmol or 4.9 g/day) (Mente et al., 2014). For example, individuals from the Yanomamo tribe in South America have a diet rich in potassium (~150 mmol or 5.9 g/day) (Oliver, Cohen, & Neel, 1975), with a potassium content well above the one recommended by the World Health Organization (WHO) in order to lower the risk of cardiovascular disease (at least 90 mmol or 3.5 g/day) (WHO, 2012b). In contrast, sodium intake of Yanomamo Indians averages (~1 mmol or 0.023 g/day), while WHO recommends ingesting <86 mmol or 2 g/day (WHO, 2012a). It is

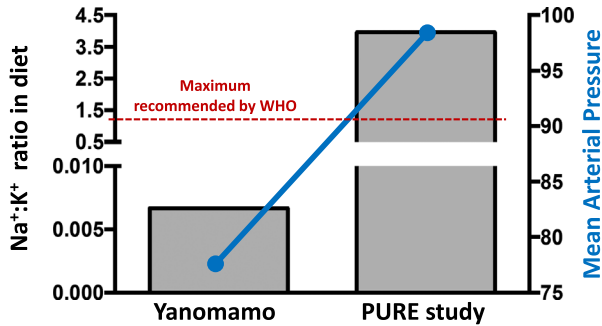


Fig. 1 The ratio of Na⁺:K⁺ contained in diets from different cultures and its relationship to blood pressure. Yanomamo Indians have a diet with an exceptionally low Na⁺:K⁺ ratio and it is likely that the low mean arterial pressure observed in those individuals is related to this variable. On the other hand, individuals from civilized environments, such as the ones included in the PURE cohort (Mente et al., 2014), have diets with very high Na⁺:K⁺ ratios, even higher than the maximum values recommended by the WHO, and it is possible that this is an important factor contributing to the high prevalence of hypertension around the world.

possible that the lower prevalence of hypertension in these isolated communities is the result of the low Na⁺:K⁺ ratio in their diet, as it has been shown that this parameter has a stronger correlation with blood pressure than potassium or sodium intakes alone (Dahl, Leitl, & Heine, 1972; Khaw & Barrett-Connor, 1988; Mente et al., 2014) (Fig. 1).

Several basic, clinical and epidemiological studies have highlighted the inverse relationship between potassium consumption and blood pressure levels. In 1928, Addison reported that potassium salts could alleviate elevated blood pressure in hypertensive patients (Addison, 1928), and this finding was confirmed by subsequent reports by different groups (Kempner, 1974; Mcquarrie, Thompson, & Anderson, 1935; Meneely, Ball, & Youmans, 1957; Priddle, 1931). It has been shown that lowering potassium content in the diet increases blood pressure levels in patients with primary hypertension (Krishna & Kapoor, 1991). Additionally, part of the hypotensive properties of the dietary approaches to stop hypertension (DASH) diet has been attributed to the high content of potassium in such diet (Sacks et al., 2001). Interestingly, potassium depletion may also be involved in the pathogenesis of secondary hypertension caused by mineralocorticoid excess such as primary aldosteronism, as suggested by a rat model where potassium supplementation prevented the increase in blood pressure caused by deoxycorticosterone acetate (DOCA)-salt treatment (Fujita & Sato, 1983). This might also be true in

humans, as it has been shown that potassium supplementation (~ 42 mmol or 3.1 gK^+ /day) reduces sodium retention in healthy volunteers that were administered fludrocortisone for 10 days (Krishna & Kapoor, 1993).

More recent studies published in the *New England Journal of Medicine*, where a large and heterogeneous cohort of $>100,000$ individuals was analyzed as part of the Prospective Urban Rural Epidemiology (PURE) study, showed that potassium excretion (measured as a surrogate for potassium intake) is negatively correlated with risk of major cardiovascular events (O'Donnell et al., 2014) and it is possible that this effect is related to the fact that, in this same cohort, higher potassium excretion is related to lower blood pressure levels, independently to the effect of sodium intake (Mente et al., 2014). A recent meta-analysis also showed a significant effect of potassium supplementation on lowering systolic and diastolic blood pressure, and it has been suggested that potassium could serve as an adjuvant anti-hypertensive agent for patients with essential hypertension (Poorolajal et al., 2017).

The kidney is one of the major organs responsible for both potassium and blood pressure homeostasis. Ninety percent of the ingested K^+ is excreted in the urine, while the remaining 10% is excreted along with the stool. Accordingly, renal failure is often associated with hyperkalemia (Zacchia, Abategiovanni, Stratigis, & Capasso, 2016). The kidney also plays a determinant role in the long-term regulation of blood pressure, and it has been proposed that defective sodium handling by the kidney is a pathogenic hallmark of hypertension (Guyton, 1991). Supporting this concept, all the monogenic forms of hypertension described so far affect, directly or indirectly, sodium reabsorption by the kidney (Lifton, Gharavi, Geller, & Hughes, 2001). Additionally, normotensive kidney transplant recipients whose donor had a familial history of hypertension have a higher probability to develop hypertension later in life (Guidi et al., 1996; Guidi, Cozzi, Minetti, & Bianchi, 1998), and it has been shown that angiotensin II requires the presence of its receptor specifically in the kidney in order to cause hypertension and cardiac hypertrophy (Crowley et al., 2006). The mechanisms linking altered sodium handling by the kidney to hypertension and other mechanisms explaining the “salt-sensitivity” of hypertension have been thoroughly reviewed elsewhere (Lifton et al., 2001; Salt, 2015, complete issue).

Recent evidence has shown that renal handling of sodium, and therefore blood pressure, is directly affected by potassium intake. In this review, we focus on classic micropuncture and microperfusion studies that shed light on the effect of potassium on renal sodium handling by different nephron

segments, and in more recent genetic and molecular studies that have brought attention to the WNK4-SPAK-NCC signaling pathway in the distal convoluted tubule as an important player in the regulation of blood pressure by potassium.



2. Natriuretic and diuretic effects of potassium; nephron segments involved in the natriuretic effect of high potassium intake

The diuretic effect of potassium salts is not new knowledge. In 1935, Keith and Binger wrote: “For two centuries certain potassium salts have been employed as diuretics in clinical medicine” (Keith & Binger, 1935). They go on to cite the works of several physicians who administered potassium salts in large doses that produced diuresis and satisfactory outcomes in patients with edema. In their 1935 work, Keith and Binger analyzed the diuretic effect in normal individuals and edematous patients of potassium chloride, bicarbonate, nitrate, acetate, and citrate, and showed that all potassium salts produced diuresis, with the greater effect produced by potassium nitrate, followed by potassium chloride. A sudden decrease in water excretion was reported after discontinuing administration of the salt (Keith & Binger, 1935). The observed diuresis has been shown to be accompanied by increased rates of sodium and chloride excretion (Kahn & Bohrer, 1967).

In animal models, administration of large amounts of potassium salts has allowed to observe dramatic effects of potassium on diuresis. In these studies, the administered high potassium diets usually contain 5–10 times the amount of K^+ contained in the “control” diets. With a diet containing five times more K^+ , urinary volumes more than doubled ($\sim 2.5 \times$) (Castaneda-Bueno et al., 2014). With diets containing 10 times more K^+ , urinary volumes observed were 4–6 times larger than those observed with the control diets (Cheng, Truong, Baum, & Huang, 2012; O’Reilly et al., 2006). The increase in urinary volume was paralleled by an increase in natriuresis (Castaneda-Bueno et al., 2014; Cheng et al., 2012) and a negative Na^+ balance (Jung et al., 2011).

Despite these clear observations, the diuresis/natriuresis induced by high potassium intake has generally been disregarded as one of the main mechanisms linking high potassium consumption with lower blood pressure (Adrogué & Madias, 2007; He et al., 2010). Other mechanisms including effects on vasculature, sympathetic nervous system, etc. have gained more

attention. This is striking, given that diuretics are among the most common drugs used for the treatment of hypertension.

In 1970, Vander showed that the direct intra-arterial infusion of KCl in the right kidneys of dogs increased Na^+ excretion by the right kidneys, but not by the contralateral kidney (Vander, 1970). This demonstrated that the natriuretic effect of potassium is due to direct renal actions of potassium.

Experiments performed during the micropuncture and microperfusion era began to delineate the nephron segments in which high K^+ intake exerts this inhibitory action on Na^+ reabsorption (Table 1). Free flow micropuncture experiments showed inhibition of absolute rates of fluid reabsorption by the proximal convoluted tubules in rats perfused intravenously with KCl (Brandis et al., 1972). Microperfusion with 10 mM KCl of peritubular capillaries irrigating the micropunctured proximal convoluted tubules also decreased fluid reabsorption, suggesting that the increase in K^+ concentration in peritubular fluid was responsible for such inhibition. Kirchner et al., however, failed to observe an effect on proximal fluid or Cl^- reabsorption in micropunctured tubules of rats acutely infused with KNO_3 (Kirchner, 1983). In rats on normal or high K^+ diets, Wright et al. observed inhibition of proximal tubule Na^+ reabsorption after acute KCl infusion by free flow micropuncture, although the segment they considered as “proximal tubule” comprised proximal tubule and loop of Henle (Wright et al., 1971).

Several works also showed an inhibitory effect of K^+ on Na^+ and Cl^- reabsorption in the loop of Henle. For example, increasing K^+ concentration in the peritubular or luminal fluid of in vitro microperfused medullary thick ascending limbs of mice or rabbits decreased Na^+ and Cl^- reabsorption (Stokes et al., 1982). In vivo, micropuncture of proximal and distal rat nephrons showed that acute K^+ infusion inhibited reabsorption of Cl^- in the loop of Henle (Kirchner, 1983). In rats maintained on a high K^+ diet for 10–14 days, a decrease in the Na^+ reabsorption rate of the loop of Henle was measured by in vivo microperfusion (Unwin et al., 1994). More recently, Cheng et al. performed in vitro microperfusion and detected decreased levels of Na^+ reabsorption in cortical thick ascending limbs of mice that were maintained on high K^+ diet when compared to tubules of mice maintained on normal diet (Cheng et al., 2012). A decrease in furosemide sensitive Na^+ excretion in mice on high K^+ diet has also been reported (Wang et al., 2017).

The increased diuresis on high K^+ diets is not only secondary to the increase in Na^+ and Cl^- excretion, as experiments show that an increase in free water excretion occurs (Cheng et al., 2012; Kahn & Bohrer, 1967).

Table 1 Nephron segments in which a decrease in Na^+ , Cl^- , or fluid reabsorption has been observed in response to a K^+ challenge.

Authors (year)	Nephron segments studied	Employed methodology	K^+ challenge	Effect observed
Brandis, Keyes, and Windhager (1972)	Proximal convoluted tubule	Free flow micropuncture, rats	Intravenous perfusion of KCl	↓ fluid reabsorption
Brandis et al. (1972)	Proximal convoluted tubule	Free flow micropuncture, rats	Microperfusion with 10 mM KCl of peritubular capillaries irrigating the tubules	↓ fluid reabsorption
Kirchner (1983)	Proximal tubule (superficial nephrons)	Micropuncture, rats	Intravenous acute infusion of KNO_3	No change in fluid of Cl^- reabsorption
Kirchner (1983)	Loop of Henle (superficial nephrons)	Micropuncture, rats	Intravenous acute infusion of KNO_3	↓ in Cl^- reabsorption
Wright, Strieder, Fowler, and Giebisch (1971)	Proximal tubule and loop of Henle	Free flow micropuncture, rats	Acute infusion of KCl in rats maintained on normal or high K^+ diets	↓ in Na^+ reabsorption
Stokes, Lee, and Williams (1982)	Medullary thick ascending limb of Henle's loop	In vitro microperfusion, mice or rabbits	Increasing K^+ concentration in peritubular or luminal fluid	↓ in Na^+ and Cl^- reabsorption
Unwin, Capasso, and Giebisch (1994)	Loop of Henle (superficial nephrons)	In vivo microperfusion, rats	High K^+ diet for 10–14 days	↓ in Na^+ reabsorption
Cheng et al. (2012)	Cortical thick ascending limbs of Henle's loop	In vitro microperfusion, mice	High K^+ diet for 2 weeks	↓ in Na^+ reabsorption

Continued

Table 1 Nephron segments in which a decrease in Na⁺, Cl⁻, or fluid reabsorption has been observed in response to a K⁺ challenge.—cont'd

Authors (year)	Nephron segments studied	Employed methodology	K ⁺ challenge	Effect observed
Wang, Wen, Li, Wang-france, and Sansom (2017)	Thick ascending limb of Henle's loop	Measurement of furosemide-sensitive Na ⁺ + excretion, mice	High K ⁺ diet for 4–7 days	↓ in furosemide-sensitive Na ⁺ reabsorption
Vallon, Schroth, Lang, Kuhl, and Uchida (2009)	Distal convoluted tubule	Measurement of NCC phosphorylation (Western blot), mice	Low or high K ⁺ diets for 7 days	↓ in NCC phosphorylation with increased dietary K ⁺
Frindt and Palmer (2010)	Distal convoluted tubule	Measurement of NCC abundance in apical membrane (Western blot), rats	Low or high K ⁺ diets for 6–8 days	↓ in NCC surface expression with increased dietary K ⁺
Castaneda-Bueno et al. (2014)	Distal convoluted tubule	Measurement of NCC phosphorylation (Western blot), mice	High KCl diets for 4 days High K-citrate diet for 4 days	↓ in NCC phosphor. With high KCl diet ↑ in NCC phosphor. With high K-citrate diet
Sorensen et al. (2013)	Distal convoluted tubule	Measurement of NCC phosphorylation (Western blot), mice	Oral gavage with 2% K ⁺ (acute effect)	↓ in NCC phosphorylation (15 min after gavage)

Rengarajan et al. (2014)	Distal convoluted tubule	Measurement of NCC phosphorylation (Western blot), rats	Intravenous KCl infusion	↓ in NCC phosphorylation
Terker, Zhang, Erspamer, et al. (2015); Terker, Zhang, McCormick, et al. (2015)	Distal convoluted tubule	Measurement of NCC phosphorylation (Western blot), mice	Amiloride admin. For 5–7 days (to increase plasma K^+)	↓ in NCC expression and phosphorylation
Terker et al. (2016)	Distal convoluted tubule	Measurement of NCC phosphorylation (Western blot), mice	Inducible, nephron specific MR-knockout mice (that develop hyperkalemia when treated with doxycycline)	↓ in NCC expression and phosphorylation
Jung et al. (2011)	Various segments	Measurement of transporter expression (Western blot)	High K^+ diet for 1 week and 3 weeks	↓ in NHE3, NBC1, and NCC expression
Yang, Xu, et al. (2018)	Various segments	Measurement of transporter expression and phosphoryl. (Western blot)	High K^+ diet for 1 week	↓ in NHE3 and NCC expression ↓ in NKCC2 and NCC phosphoryl.

MR, mineralocorticoid receptor.

In this regard, the decrease in NaCl reabsorption by the thick ascending limb may contribute to a decrease in the urine concentrating ability of the kidney and explain, at least in part, this observation.

Recent evidence shows that high K^+ intakes and increases in plasma K^+ concentration also inhibit Na^+ and Cl^- reabsorption in the distal convoluted tubule (DCT). Phosphorylation of the thiazide sensitive Na-Cl cotransporter NCC, which is the major apical transporter involved in Na^+ and Cl^- reabsorption in this nephron segment, is drastically decreased by high K^+ intake or elevations in plasma K^+ (Sorensen et al., 2013; Vallon et al., 2009). It has been well demonstrated that phosphorylation of NCC is a good indicator of cotransporter activity, and thus, decreased phosphorylation levels of NCC are indicative of low Na^+ and Cl^- reabsorption levels in the DCT.

Finally, in a recent mathematical model of the rat kidney by Weinstein (2017), the effect on Na^+ reabsorption in different nephron segments of increasing peritubular K^+ concentration from 5 to 5.5 mM was analyzed. It was predicted that a 2.3-fold increase in natriuresis would result. The author concluded that, although Na^+ reabsorption in the proximal convoluted tubule, ascending loop of Henle, and DCT were predicted to be inhibited, the main contributor to natriuresis was the inhibition of proximal convoluted tubule reabsorption. The reason for this, according to this model, is that the loop of Henle and the DCT respond to increases in Na^+ delivery with increased Na^+ reabsorption.



3. Role of the kidney in potassium homeostasis

Given the steep K^+ concentration gradient that is maintained between the intracellular and extracellular compartments (120 mM intracellular vs 3.5–5.5 mM extracellular), which is crucial for a variety of cell functions, the majority of K^+ contained in the body is found within the cells, and only a minor part is found in the extracellular fluid, i.e., approximately 63 mmol in a young adult male of 70 kg with an extracellular fluid volume of ~14 L (14 L \times 4.5 mmol/L). More K^+ may be present in a meal than that contained in the extracellular fluid. For instance, the average daily K^+ intake observed in the population of the PURE study was 2.1 g (54 mmol) (Mente et al., 2014). Thus, the dietary intake of K^+ could significantly modify the K^+ concentration of the extracellular fluid if it were not for the existence of mechanisms that buffer these increases by promoting the internalization

of K^+ to the cells. Simultaneously, mechanisms to increase renal K^+ excretion are activated in order to match K^+ excretion to K^+ intake and achieve K^+ balance.

No matter how much K^+ is ingested in the diet, the kidneys filter approximately 720 mmol of K^+ per day ($180\text{ L} \times 4\text{ mmol/L}$), of which 90% are reabsorbed in the proximal tubule and thick ascending limb of Henle's loop (TAL) (Boulpaep & Boron, 2016). Therefore, the distal nephron, in particular the aldosterone-sensitive distal nephron (ASDN), which comprises the late portion of the DCT, the connecting tubule (CNT), and the cortical collecting duct (CCD), is the segment in charge of adjusting urinary excretion to dietary intake in order to maintain K^+ balance. When dietary intake is normal to high, K^+ is secreted in the distal nephron. Secreted K^+ can reach values of 20%–180% of the filtered K^+ and urinary excretion levels can reach to amounts of 10%–150% of the filtered K^+ (because some of the secreted K^+ is reabsorbed in the collecting duct). In contrast, when dietary intake is low, net K^+ reabsorption is observed in the distal nephron, and K^+ excretion is reduced to as much as 2% of the filtered amount.

Within the ASDN, the late portion of the DCT and the CNT are the segments which appear to play a major role in the regulation of K^+ balance (Meneton, Loffing, & Warnock, 2004). Compared to the collecting duct, the late DCT and CNT show a several-fold higher $\text{Na}^+:\text{K}^+$ -ATPase activity per millimeter of tubule length in different mammalian species (Katz, Doucet, & Morel, 1979). In mice, apical accumulation of the K^+ channel ROMK, which participates in K^+ secretion, is only observed in the late DCT and CNT when mice are fed a moderately high K^+ diet, while apical ROMK accumulation is observed in the CCD only when K^+ intake levels are very high (Loffing-Cueni et al., 2003). The activity of the epithelial Na^+ channel ENaC (which contributes to establishing the driving force for K^+ secretion as explained below) is also several times larger in the late DCT/CNT than in the CCD of rats treated with aldosterone or fed a high K^+ diet (Frindt & Palmer, 2004). Moreover, genetic mouse models deficient in ENaC activity in the CCD do not display a salt-losing or K^+ retaining phenotype, even when placed on low Na^+ diet or high K^+ diet, respectively (Rubera et al., 2003), whereas mice lacking ENaC activity in the entire ASDN (Boscardin et al., 2017, 2018; Perrier et al., 2016) or lacking ENaC activity specifically in the CNT (Christensen et al., 2010) do present a Na^+ wasting phenotype when on low Na^+ diet which is accompanied with K^+ retention. Thus, it has been proposed that the collecting duct makes an important contribution to K^+ secretion and for achieving K^+ balance only

when K^+ intake levels are very high. With the low K^+ intake levels observed in modern societies' diets it is thus likely that the majority of aldosterone-regulated K^+ secretion takes place in the late DCT and CNT (Meneton et al., 2004).

The most relevant molecular players involved in the process of K^+ secretion in the distal nephron are the epithelial Na^+ channel (ENaC) and the K^+ channels renal outer medullary K^+ channel (ROMK), and the Maxi-K channel (BK).

ENaC expression in the nephron is found in the apical membrane of the ASDN, specifically in principal cells of the CNT and CCD, and in similar cells that are present in the late portion of the DCT (Loffing et al., 2000). Na^+ entry to the cell via ENaC promotes the depolarization of the apical membrane, thus generating a lumen-negative transepithelial voltage and contributing to the driving force for K^+ secretion. ENaC's role in K^+ secretion is evidenced by the existence of genetic diseases such as pseudohypoaldosteronism type I, which presents with hyperkalemia and is caused by inactivating mutations in any of the three subunits forming the channel (Chang et al., 1996) (Strautnieks, Thompson, Gardiner, & Chung, 1996), or Liddle syndrome, which features hypokalemia and is caused by mutations in β - or γ -ENaC subunits that prevent channel retrieval from the plasma membrane and thus lead to channel overactivation (Hansson et al., 1995; Schild et al., 1996; Shimkets et al., 1994). ENaC is one of the principal targets for regulation by aldosterone that mainly affects the channel's retrieval from the plasma membrane mediated by Nedd4-2 (Debonneville et al., 2002). Another important target for regulation by aldosterone is the Na^+K^+ -ATPase (Férraille et al., 1993). Coordinated upregulation of the Na^+K^+ -ATPase at the basolateral membrane and ENaC at the apical membrane raises the Na^+ reabsorption capacity of the ASDN, which stimulates K^+ secretion.

Potassium secretion across the apical membrane of the ASDN can occur via two mayor pathways: ROMK and BK channels. ROMK expression in the nephron begins in the TAL and continues all the way to the CD (Wade et al., 2011). However, net K^+ secretion mediated by ROMK is only observed in the segments comprising the ASDN, segments in which ROMK is coexpressed with ENaC in principal cells. A high K^+ intake promotes an increase in the apical conductance of K^+ and in the activity of ROMK (Palmer, 1999). Given that ROMK channels have a high basal open probability that virtually makes them constitutively active, regulation of ROMK-mediated K^+ secretion is achieved through the regulation of

translocation of channels from subapical compartments to the plasma membrane (Frindt & Palmer, 2010; Wade et al., 2011). Modulation of the channel's synthesis rate has not been observed (Frindt, Zhou, Sackin, & Palmer, 1998). Although certain controversy exists, several lines of evidence suggest that the regulation of ROMK's translocation to the apical membrane by high K^+ intake is independent of aldosterone (Huang et al., 2004; Wei, Bloom, Lin, Gu, & Wang, 2001).

BK channels are activated by membrane depolarization, elevation of intracellular calcium concentration, hypoosmotic stress, or membrane stretch (Carrisoza-Gaytan, Carattino, Kleyman, & Satlin, 2016). Unlike ROMK, BK channels are normally inactive and only become activated under conditions of high tubular flow rate, such as that observed under high K^+ intake (Woda, Bragin, Kleyman, & Satlin, 2001). Flow-mediated activation is associated with an increase in intracellular calcium (Carrisoza-Gaytan et al., 2016) (Welling, 2013). BK channels in the kidney are expressed in the apical membrane of the ASDN, both in principal cells and intercalated cells (all types); however, expression is low in principal cells and much more robust in intercalated cells (Carrisoza-Gaytan et al., 2016; Welling, 2013). Despite this high expression, it is still under debate whether BK channels expressed in intercalated cells can mediate flow induced K^+ secretion (FIKS). Indeed principal cells present robust expression of the $Na^+ : K^+ - ATPase$ in the basolateral membrane that mediates entry of K^+ ions into the cell that can be extruded to the tubule lumen via BK. However, very low amounts of $Na^+ : K^+ - ATPase$ are present in intercalated cells (Pácha, Frindt, Sackin, & Palmer, 1991). It has been proposed that basolateral K^+ entry to these cells may be mediated by $Na^+ : K^+ : 2Cl^-$ cotransporter type 1 (NKCC1) activity. Evidence favoring this concept is that BK-mediated FIKS is dependent on a basolateral bumetanide sensitive- Cl^- dependent transport pathway (Liu et al., 2011). However, it is unclear how Na^+ entering the cells via NKCC1 can be recycled back to the interstitial fluid, which would be important to maintain NKCC1 activity. The importance of BK channels in K^+ secretion is demonstrated by the fact that its activity can compensate ROMK deficiency in ROMK knockout mice or patients with Bartter syndrome type II (caused by inactivating mutations in ROMK) (Simon, Karet, et al., 1996; Wagner et al., 2008). These mice and patients develop mild hypokalemia which is due to the impaired reabsorption capacity of the TAL which leads to increased distal Na^+ and flow delivery that activates K^+ secretion via BK channels. Finally, high dietary K^+ stimulates BK transcription and channel

translocation to the plasma membrane, a response that is independent of aldosterone (Welling, 2013). However, aldosterone indirectly affects BK-mediated K^+ secretion through the stimulation of ENaC (Cornelius et al., 2015).

The natriuretic and diuretic effects of high K^+ diets described in the previous section, which appear to be due to an inhibition of Na^+ reabsorption pathways in the proximal tubule, TAL, and DCT, are important to maximize renal K^+ excretion (Fig. 2). It is generally argued that this is because: (1) the increase in Na^+ delivery to the ASDN allows the electrogenic Na^+-K^+ exchange through ENaC and ROMK/BK channels; (2) the increased fluid delivery to the ASDN slows down the rise in luminal K^+ concentration which is produced as a consequence of K^+ secretion; (3) increased flow stimulates the flow-activated BK channels. Nevertheless, recent data

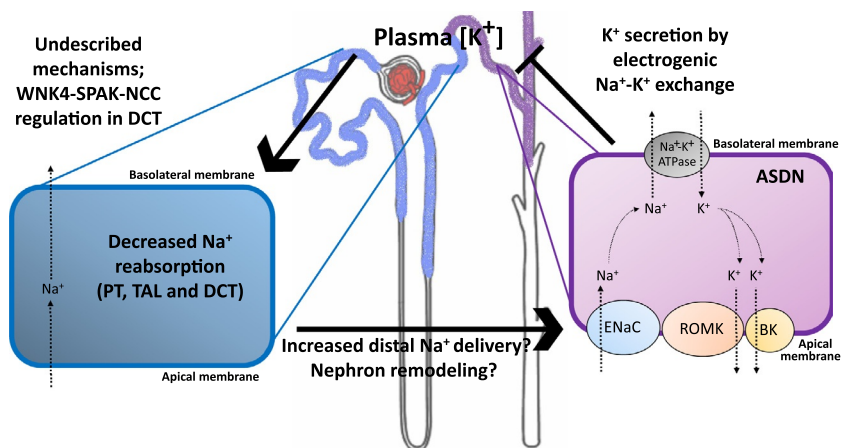


Fig. 2 Physiological relevance of K^+ -induced natriuresis. Experimental evidence suggests that an increase in K^+ intake, and the consequent rise in plasma K^+ concentration, induce natriuresis due to a decrease in Na^+ reabsorption in the proximal tubule (PT), thick ascending limb of Henle's loop (TAL), and distal convoluted tubule (DCT). The resulting increase in Na^+ delivery and flow to the aldosterone-sensitive distal nephron (ASDN) stimulate the K^+ secretory apparatus. However, it is still under debate if high Na^+ delivery and flow directly stimulate K^+ secretion by stimulating ENaC mediated Na^+ reabsorption that generates a lumen negative transepithelial voltage increasing the driving force for K^+ secretion, and by activating flow induced K^+ secretion through BK channels. Recent evidence suggests that acute inhibition of proximal Na^+ reabsorption by itself does not stimulate K^+ secretion (Grimm, Coleman, Delpire, & Welling, 2017; Hunter, Craigie, Homer, Mullins, & Bailey, 2014), but that in a more chronic setting (3 days in mouse), remodeling of the distal nephron occurs with hypertrophy of ASDN, promoting K^+ secretion.

questions the idea that the increase in Na^+ delivery acutely increases the capacity of the ASDN to secrete K^+ . This would mean that not only the higher availability of Na^+ in the tubule lumen favoring ENaC-mediated Na^+ reabsorption may be sufficient to promote Na^+ reabsorption. For example, early in vivo microperfusion studies suggested that luminal Na^+ concentration plays no role in modulating K^+ secretion (Good & Wright, 1979). Moreover, it has been shown recently that acute inhibition of NCC with hydrochlorothiazide elicited immediate natriuresis that was sustained for a 2-h period after diuretic administration, but no kaliuresis was observed (Hunter et al., 2014). Finally, in transgenic mice expressing a constitutively active version of Ste20/SPS1-related proline-alanine rich kinase (SPAK; CA-SPAK mice) in which NCC is thus also constitutively activated, hyperkalemia is observed. However, thiazide administration elicits an immediate natriuretic effect, but a delayed kaliuretic effect, and thiazide normalizes plasma K^+ levels only after 3 days of thiazide administration (Grimm et al., 2017). These mice show remodeling of the distal tubule with hypertrophy of the DCT and hypotrophy of the CNT. Thiazide administration for 3 days normalizes these structural changes, correlating with the correction of plasma K^+ levels. Interestingly, nephron remodeling in response to altered Na^+ and K^+ intake in rabbits was reported decades ago (Kaissling & Le Hir, 1982), and although further investigation is needed to address the molecular mechanisms at play in this process, it is becoming clear that distal Na^+ delivery (or inhibition of proximal Na^+ reabsorption) may affect K^+ secretion in a more complex way than previously thought.



4. Molecular mechanisms implicated in the natriuretic and diuretic effects of potassium

Although, as discussed above, it has been shown that sodium reabsorption by different nephron segments is inhibited by high K^+ intake, most of the molecular mechanisms responsible for these phenomena remain elusive. Some of them, however, are just recently beginning to be understood. For example, decreased protein levels of the sodium-hydrogen exchanger NHE3 and the sodium-bicarbonate cotransporter NBC-1 could explain the effect on proximal tubule and possibly on the loop of Henle (Jung et al., 2011). Negative modulation of the $\text{Na}^+:\text{K}^+:2\text{Cl}^-$ cotransporter NKCC2 phosphorylation could also explain the inhibitory effect of high potassium upon sodium reabsorption in TAL (Yang, Xu, et al., 2018).

4.1 Regulation of the Na-Cl cotransporter NCC by potassium

While it has been suggested by a mathematical model that the proximal nephron is determinant for increased natriuresis by high K^+ intake (Weinstein, 2017), experimental evidence has shown that the distal nephron plays a key role in the relationship between K^+ and blood pressure. For example, it has been shown that the hypertensive effect of a high sodium/low potassium diet, such as the typical western diet, could be explained by increased salt reabsorption by NCC in the DCT in a mouse model. Wild-type mice fed with such diet displayed a significant increase in blood pressure, while NCC knockout mice did not (Terker, Zhang, McCormick, et al., 2015).

So far the best understood molecular mechanism explaining the inverse relationship between K^+ intake and blood pressure levels involves NCC regulation in the DCT. This understanding began with the description of monogenic diseases in which NCC activity is dysregulated, causing alterations in potassium and blood pressure homeostasis.

Gitelman syndrome (OMIM #263800) is caused by loss of function mutations in the gene *SLC12A3*, that codifies NCC, and it is characterized by hypokalemia, low blood pressure, metabolic alkalosis, hypocalciuria, and hypomagnesemia (Simon, Nelson-Williams, et al., 1996). Accordingly, this disease is reminiscent of thiazide overdose, and it manifests that NCC plays a determinant role not only in blood pressure, but also in K^+ regulation.

On the other hand, familial hyperkalemic hypertension (FHHt) (OMIM #614491-2 and #614495-6), also called Gordon syndrome or pseudo-hypoaldosteronism type II (PHAII), is associated with hyperkalemia, hypertension, metabolic acidosis and hypercalciuria (Wilson et al., 2001). Low doses of thiazide diuretics are able to correct all physiological abnormalities of FHHt (Mayan, Vered, Mouallem, Tzadok-witkon, & Pauzner, 2002), which suggests that NCC overactivation is involved in this disease. Nevertheless, no gain of function mutations have been described in *SLC12A3*. In 2001 Richard Lifton's group reported that mutations in the genes *PRKWNK1* and *PRKWNK4* caused FHHt (Wilson et al., 2001). These genes codify two members of the with no lysine (K) (WNK) kinase family that contains four members in total in human. These serine-threonine kinases are characterized by the atypical positioning of their catalytic lysine and they have been described as important regulators of transepithelial ion transport. In particular, WNK4 and WNK1 have been shown to be key regulators of NCC (Alessi et al., 2014) (Hadchouel, Ellison, & Gamba, 2016).

Gain of function mutations in WNK4 cause familial hyperkalemic hypertension (FHHT) due to NCC overactivation (Laloti et al., 2006; Wilson et al., 2001; Yang et al., 2007). FHHT mutations in WNK4 cause an amino acid change in a region of the protein denominated “acidic domain,” responsible for the interaction with kelch like family member 3 (KLHL3), an adaptor protein and receptor for the KLHL3-CUL3-RING ubiquitin ligase complex. Mutated WNK4 cannot interact with this complex and its proteasomal degradation is compromised, leading to increased WNK4 levels in the DCT (Ohta et al., 2013; Shibata, Zhang, Puthumana, Stone, & Lifton, 2013; Wakabayashi et al., 2013). Mutations in the genes coding KLHL3 and Cullin 3 (CUL3) are also a cause for FHHT (Boyden et al., 2012; Louis-Dit-Picard et al., 2012).

NCC activity is positively regulated by phosphorylation at several sites in its cytoplasmic N-terminal domain (Pacheco-Alvarez et al., 2006) by the kinases SPAK and OSR1 (oxidative stress-responsive 1 protein), which in turn are phosphorylated and activated by WNK kinases (Richardson et al., 2008; Vitari, Deak, Morrice, & Alessi, 2005). Although WNK1 and WNK3 are also expressed in the kidney, it has been suggested that WNK4 is the main WNK kinase responsible for NCC regulation in vivo (Castaneda-Bueno et al., 2012; Oi et al., 2012; Susa et al., 2017). Accordingly, WNK4 knockout mice have a phenotype resembling Gitelman syndrome (Castaneda-Bueno et al., 2012; Takahashi et al., 2014; Yang, Xie, et al., 2018).

Kinase activity of WNK kinases has been shown to be negatively modulated by chloride. X-ray crystallography showed that the chloride anion binds close to the active site, within the kinase domain of WNK1. Binding stabilizes an inactive conformation of the kinase. The decrease in Cl^- concentration ($[\text{Cl}^-]$) promotes Cl^- dissociation, and thus WNK1 activation and autophosphorylation in the activation loop (Piala et al., 2014). Later, it was shown that WNK4 has an even higher sensitivity to chloride (Bazua-Valenti et al., 2015) and this modulation could be important for WNK4 activity in vivo, as mathematical modeling of the DCT predicts that intracellular chloride concentration ($[\text{Cl}^-]_i$) fluctuates between ~ 12 and ~ 20 mM, in function of extracellular potassium (Terker, Zhang, McCormick, et al., 2015).

To our knowledge, the first report of the inverse relationship between NCC activity and plasma $[\text{K}^+]$ was published in 2009 by Uchida's group. In this work, mice were fed with high (5%) K^+ diets, which prompted a reciprocal inverse modulation of NCC phosphorylation at Thr53, Thr58

and Ser71 (Vallon et al., 2009). Later, several groups published similar findings performing dietary manipulations in mouse models (Castaneda-Bueno et al., 2014; Frindt & Palmer, 2010; Lubbe et al., 2013; Terker, Zhang, Erspamer, et al., 2015) and even in humans (Terker, Zhang, McCormick, et al., 2015). Sorensen and collaborators used gastric gavage of 2% K^+ (15 $\mu\text{L/g}$) in order to study the rapid response of NCC to acute increases in plasma $[K^+]_e$ (Sorensen et al., 2013). K^+ loading promoted a marked decrease in NCC phosphorylation, accompanied by increased natriuresis, which has significantly blunted in NCC knockout mice. These results suggest that the natriuretic effect of potassium salts depend, at least in part, on decreased salt reabsorption in the DCT.

In 2015, Terker and collaborators proposed that extracellular potassium concentration ($[K^+]_e$) has a direct effect on DCT's $[Cl^-]_i$ due to effects on cell voltage (Fig. 3). They proposed that low $[K^+]_e$ promotes apical membrane hyperpolarization which increases the driving force for chloride efflux from the cell, leading to WNK activation (Terker, Zhang, McCormick, et al., 2015). This hypothesis has been supported by experimental evidence in in vitro and ex vivo models (Penton et al., 2016; Terker, Zhang, Erspamer, et al., 2015). Therefore, the current view is that NCC activity is increased in response to decreases in extracellular $[K^+]_e$ due to higher WNK4 activity.

In the DCT, the basolateral conductance of K^+ is given by KIR4.1/KIR5.1 heterotetramer potassium channels, characterized by $\sim 40\text{ pS}$ K^+ currents. These channels are responsible for the recycling of K^+ that entered through the Na^+-K^+ ATPase (Cuevas et al., 2017; Su & Wang, 2016). KIR4.1 has been called the 'potassium sensor' of the DCT, as *Kcnj10* (which codifies KIR4.1) knockout mice lose NCC modulation by potassium (Cuevas et al., 2017). In fact, loss of function of KIR4.1 causes EAST/SeSAME syndrome, a complex disorder with a renal phenotype similar to Gitelman syndrome (Bockenhauer et al., 2009; Scholl et al., 2009).

In contrast, *Kcnj16* (codifying KIR5.1) knockout mice have increased sensibility to thiazide diuretics, a surrogate for NCC activity in vivo (Paulais et al., 2011). This observation is likely explained because KIR4.1 homomultimers are insensitive to intracellular pH, while KIR4.1/5.1 channels heteromers are sensitive to physiological levels of intracellular pH. Whether modulation of intracellular pH of the DCT is physiologically relevant to NCC modulation remains elusive. However, it has been shown that chronic K^+ depletion causes increased activity of KIR4.1/5.1

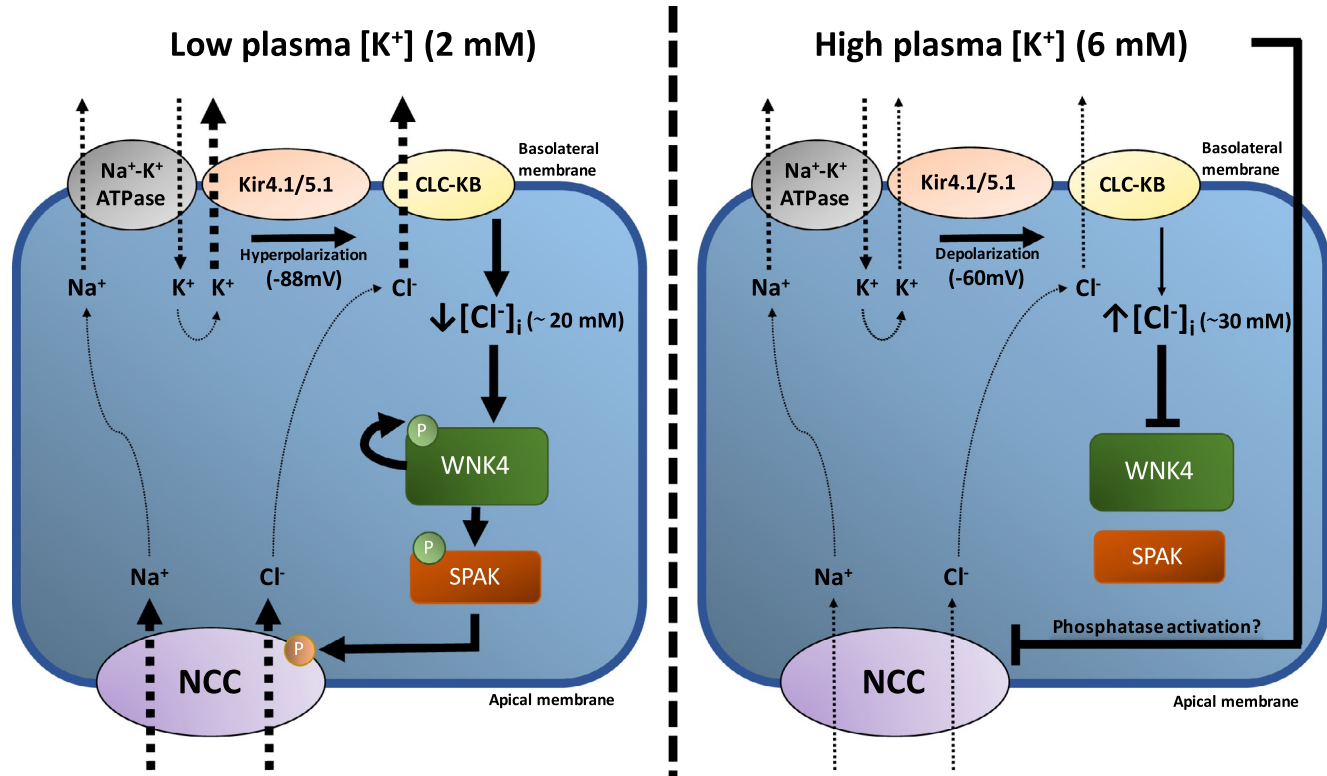


Fig. 3 Molecular mechanisms by which plasma K^+ levels regulate NCC activity in the DCT. During hypokalemic states ($[K^+] = 2\text{mM}$), K^+ extrusion through basolateral Kir4.1/5.1 channels increases, which promotes hyperpolarization (-88mV) of distal convoluted tubule (DCT) cells that leads to increased chloride efflux through CLC-KB. The decrease in intracellular chloride concentration ($[Cl^-]_i \sim 20\text{mM}$) causes phosphorylation and activation of WNK4 kinase, which promotes SPAK and, therefore, NCC activation. On the other hand, high plasma K^+ ($[K^+] = 6\text{mM}$) depolarizes DCT cells (-60mV), which prevents chloride efflux. High $[Cl^-]_i$ ($\sim 30\text{mM}$) renders WNK4 inactive, decreasing SPAK and NCC phosphorylation. Additional mechanisms promote specific NCC dephosphorylation, probably due to activation of protein phosphatases. (Values stated were calculated through mathematical modeling by Terker, Zhang, McCormick, et al. (2015).)

heterotetramers, promoting increased potassium currents, and hyperpolarization of the distal convoluted tubule membrane (Wang et al., 2018).

Basolateral chloride efflux from the DCT cells occurs mainly through the ClC-KB (ClC-K2 in mouse) chloride channel (Hennings et al., 2017), whose translocation to the basolateral membrane and stability depend on the protein Barttin. Nomura and collaborators showed that hypomorphic mice with a mutated Barttin are able to thrive, but display a Gitelman-like phenotype, with the inability to upregulate NCC by further K^+ depletion (Nomura et al., 2018). This was the first evidence that chloride efflux was responsible for the activation of NCC by hypokalemia in vivo.

4.2 Additional mechanisms for potassium-mediated regulation of NCC

Inhibition of NCC by high extracellular potassium seems to involve additional mechanisms independent of $[Cl^-]_i$. For example, in an ex vivo model of mouse kidney slices (Penton et al., 2016) observed that NCC dephosphorylation by high extracellular K^+ occurs even when WNK-SPAK activity is clamped on a low chloride medium. In this work, the mechanism responsible for NCC dephosphorylation remained elusive, as protein phosphatase 1 (PP1)/protein phosphatase 2 (PP2) and calcineurin inhibitors could not prevent dephosphorylation. In contrast, Shoda et al. showed that in mice, rapid NCC dephosphorylation in response to acute K^+ loading was prevented by inhibition of the phosphatase calcineurin with tacrolimus (Shoda et al., 2017). Conflicting data between these works may be due to the use of different models. For example, the results obtained in the in vivo approach may be influenced by systemic factors additional to the direct effects of K^+ on DCT. Further investigation will be helpful to understand the intricacies of the NCC dephosphorylation process and its relationship to potassium homeostasis.

A recent work from our group showed that binding of Cl^- to the kinase domain of WNK4 is not the sole regulatory mechanism of kinase activity. We described that at least two phosphorylation sites, one located within the N-terminal domain (S64) and another one within the C-terminal domain (S1196), modulate WNK4 activity measured as WNK4-mediated SPAK phosphorylation and T-loop autophosphorylation (Castañeda-Bueno et al., 2017). These sites are target for phosphorylation by Protein kinase C (PKC) and Protein kinase A (PKA) and we initially showed that its phosphorylation is induced in response to stimulation of cells with angiotensin II. More recently, we have observed that hypokalemia in

mouse is also an important stimulus that promotes phosphorylation of these sites (Murillo-de-Ozores, Grajeda-Medina, Gamba, & Castañeda-Bueno, 2018). In an *in vitro* cell model, we observed that intracellular chloride depletion, secondary to cell incubation in a low K^+ medium, is responsible for such increase in the phosphorylation levels of these sites. Thus, we have proposed that DCT intracellular Cl^- depletion secondary to decreases in extracellular $[K^+]$, may not only promote WNK4 activation due to Cl^- dissociation, but also through the phosphorylation of these sites.

Finally, it has been observed in several mouse models that hypokalemia promotes an increase in WNK4 expression levels (Ishizawa et al., 2016; Terker, Zhang, McCormick, et al., 2015). It has been recently shown that the molecular mechanism behind this effect involves a decrease in KLHL3-CUL3-RING-mediated degradation of WNK4. Hypokalemia promotes KLHL3 phosphorylation at Ser433, which is a site located within the substrate recognition domain of KLHL3. Thus, phosphorylation prevents substrate binding and subsequent ubiquitination and degradation (Ishizawa et al., 2016).



5. Summary and conclusions

For a long time, it has been known that potassium salts have diuretic and natriuretic effects that ameliorate hypertension and edematous states. Evidence suggests that increased potassium intake decreases sodium reabsorption by the proximal tubule, TAL, and DCT, even though the molecular mechanisms at play are mostly unknown at the moment. However, several groups across the world have shown that the WNK4-SPAK-NCC pathway in the DCT plays a pivotal role in the physiological relationship between potassium and blood pressure regulation. This pathway functions as a molecular switch that determines salt reabsorption in the DCT in response to plasma $[K^+]$. Turning off the switch by increased potassium intake allows appropriate K^+ secretion by the ASDN, while K^+ depletion turns on NCC to prevent electrogenic Na^+-K^+ exchange, and indirectly promotes an increase in blood pressure.

Further work will be required to assess the quantitative contribution of different nephron segments to the phenomenon of K^+ -induced natriuresis. In the meanwhile, it is evident that eating more avocados and bananas is good for your health.

Acknowledgments

A.R.M.-O. is a graduate student from the “Programa de Doctorado en Ciencias Biomédicas, Universidad Nacional Autónoma de México (UNAM)” and received a fellowship 606808 from CONACYT.

This work was supported by National Institutes of Health Grant DK51496 (to G.G.) and Conacyt Grants No. 23 (to G.G.) and 257726 (to M.C.-B.).

References

- Addison, W. L. T. (1928). The use of sodium chloride, potassium chloride, sodium bromide, and potassium bromide in cases of arterial hypertension which are amenable to potassium chloride. *Canadian Medical Association Journal*, 18(3), 281–285.
- Adrogué, H. J., & Madias, N. E. (2007). Sodium and potassium in the pathogenesis of hypertension. *New England Journal of Medicine*, 356(19), 1966–1978.
- Alessi, D. R., Zhang, J., Khanna, A., Hochdorfer, T., Shang, Y., & Kahle, K. T. (2014). The WNK-SPAK/OSR1 pathway: Master regulator of cation-chloride cotransporters. *Science Signaling*, 7(334), re3.
- Bazua-Valenti, S., Chavez-Canales, M., Rojas-Vega, L., Gonzalez-Rodriguez, X., Vazquez, N., & Rodriguez-Gama, A., et al. (2015). The effect of WNK4 on the Na⁺-Cl⁻ cotransporter Is modulated by intracellular chloride. *Journal of the American Society of Nephrology*, 26(8), 1781–1786.
- Bockenbauer, D., Feather, S., Stanescu, H. C., Bandulik, S., Zdebik, A. A., Reichold, M., et al. (2009). Epilepsy, ataxia, sensorineural deafness, tubulopathy, and KCNJ10 mutations. *New England Journal of Medicine*, 360(19), 1960.
- Boscardin, E., Perrier, R., Sergi, C., Maillard, M., Loffing, J., Loffing-Cueni, D., et al. (2017). Severe hyperkalemia is rescued by low-potassium diet in renal β ENaC-deficient mice. *Pflügers Archiv - European Journal of Physiology*, 469(10), 1387–1399.
- Boscardin, E., Perrier, R., Sergi, C., Maillard, M. P., Loffing, J., Loffing-Cueni, D., et al. (2018). Plasma potassium determines NCC abundance in adult kidney-specific γ ENaC knockout. *Journal of the American Society of Nephrology*, 29(3), 977–990.
- Boulpaep, E. L., & Boron, W. F. (2016). *Medical physiology* (3rd Ed.). Elsevier.
- Boyden, L. M., Choi, M., Choate, K. A., Nelson-Williams, C. J., Farhi, A., Toka, H. R., et al. (2012). Mutations in kelch-like 3 and cullin 3 cause hypertension and electrolyte abnormalities. *Nature*, 482(7383), 98–102.
- Brandis, M., Keyes, J., & Windhager, E. (1972). Potassium-induced inhibition of proximal tubular fluid reabsorption in rats. *The American Journal of Physiology*, 222(2), 421–427.
- Carrisoza-Gaytan, R., Carattino, M. D., Kleyman, T. R., & Satlin, L. M. (2016). An unexpected journey: Conceptual evolution of mechanoregulated potassium transport in the distal nephron. *American Journal of Physiology. Cell Physiology*, 310, C243–C259.
- Castañeda-Bueno, M., Arroyo, J. P., Zhang, J., Puthumana, J., Yarbrough, O., Shibata, S., et al. (2017). Phosphorylation by PKC and PKA regulate the kinase activity and downstream signaling of WNK4. *Proceedings of the National Academy of Sciences*, 114(5), E879–E886. <https://doi.org/10.1073/pnas.1620315114>.
- Castaneda-Bueno, M., Cervantes-Perez, L. G., Rojas-Vega, L., Arroyo-Garza, I., Vazquez, N., Moreno, E., et al. (2014). Modulation of NCC activity by low and high K⁺ intake: Insights into the signaling pathways involved. *American Journal of Physiology Renal Physiology*, 306(12), F1507–F1519.
- Castaneda-Bueno, M., Cervantes-Perez, L. G., Vazquez, N., Uribe, N., Kantesaria, S., Morla, L., et al. (2012). Activation of the renal Na⁺: Cl⁻ cotransporter by angiotensin II is a WNK4-dependent process. *Proceedings of the National Academy of Sciences*, 109(20), 7929–7934.

- Chang, S. S., Grunder, S., Hanukoglu, A., Rösler, A., Mathew, P. M., Hanukoglu, I., et al. (1996). Mutations in subunits of the epithelial sodium channel cause salt wasting with hyperkalaemic acidosis, pseudohypoaldosteronism type 1. *Nature Genetics*, *12*(3), 248–253.
- Cheng, C.-J., Truong, T., Baum, M., & Huang, C.-L. (2012). Kidney-specific WNK1 inhibits sodium reabsorption in the cortical thick ascending limb. *American Journal of Physiology. Renal Physiology*, *303*(5), F667–F673.
- Christensen, B. M., Perrier, R., Wang, Q., Zuber, A. M., Maillard, M., Mordasini, D., et al. (2010). Sodium and potassium balance depends on α ENaC expression in connecting tubule. *Journal of the American Society of Nephrology*, *21*(11), 1942–1951.
- Cornelius, R. J., Wen, D., Li, H., Yuan, Y., Wang-France, J., Warner, P. C., et al. (2015). Low Na, high K diet and the role of aldosterone in BK-mediated K excretion. *PLoS One*, *10*(1), 1–16.
- Crowley, S. D., Gurley, S. B., Herrera, M. J., Ruiz, P., Griffiths, R., Kumar, A. P., et al. (2006). Angiotensin II causes hypertension and cardiac hypertrophy through its receptors in the kidney. *Proceedings of the National Academy of Sciences*, *103*(47), 17985–17990.
- Cuevas, C. A., Su, X.-T., Wang, M.-X., Terker, A. S., Lin, D.-H., McCormick, J. A., et al. (2017). Potassium sensing by renal distal tubules requires kir4.1. *Journal of the American Society of Nephrology*, *28*(6), 1814–1825.
- Dahl, L. K., Leitl, G., & Heine, M. (1972). Influence of dietary potassium and sodium/potassium molar ratios on the development of salt hypertension. *The Journal of Experimental Medicine*, *136*, 318–330.
- Debonneville, C., Flores, S. Y., Kamynina, E., Plant, P. J., Tauxe, C., Thomas, M. A., et al. (2002). Phosphorylation of Nedd4-2 by Sgk1 regulates epithelial Na⁺ channel cell surface expression. *EMBO Journal*, *20*(24), 7052–7059.
- Férraille, E., Vogt, B., Rousselot, M., Barlet-Bas, C., Cheval, L., Doucet, A., et al. (1993). Mechanism of enhanced Na-K-ATPase activity in cortical collecting duct from rats with nephrotic syndrome. *Journal of Clinical Investigation*, *91*(4), 1295–1300.
- Frindt, G., & Palmer, L. G. (2004). Na channels in the rat connecting tubule. *American Journal of Physiology. Renal Physiology*, *286*, F669–F674.
- Frindt, G., & Palmer, L. G. (2010). Effects of dietary K on cell-surface expression of renal ion channels and transporters. *American Journal of Physiology. Renal Physiology*, *299*(4), F890–F897. <https://doi.org/10.1152/ajprenal.00323.2010>.
- Frindt, G., Zhou, H., Sackin, H., & Palmer, L. G. (1998). Dissociation of K channel density and ROMK mRNA in rat cortical collecting tubule during K adaptation. *American Journal of Physiology. Renal Physiology*, *274*(3, Pt 2), F525–F531.
- Fujita, T., & Sato, Y. (1983). Natriuretic and antihypertensive effects of potassium in DOCA-salt hypertensive rats. *Kidney International*, *24*(6), 731–739.
- Good, D. W., & Wright, F. S. (1979). Luminal influences on potassium secretion: Sodium concentration and fluid flow rate. *American Journal of Physiology. Renal Physiology*, *236*(2), F192–F205.
- Grimm, P. R., Coleman, R., Delpire, E., & Welling, P. A. (2017). Constitutively active SPAK causes hyperkalemia by activating NCC and remodeling distal tubules. *Journal of the American Society of Nephrology*, *28*(9), 2597–2606.
- Guidi, E., Cozzi, M. G., Minetti, E., & Bianchi, G. (1998). Donor and recipient family histories of hypertension influence renal impairment and blood pressure during acute rejections. *Journal of the American Society of Nephrology*, *9*(11), 2102–2107.
- Guidi, E., Menghetti, D., Milani, S., Montagnino, G., Palazzi, P., & Bianchi, G. (1996). Hypertension may be transplanted with the kidney in humans: A long-term historical prospective follow-up of recipients grafted with kidneys coming from donors with or without hypertension in their families. *Journal of the American Society of Nephrology: JASN*, *7*(8), 1131–1138.

- Guyton, A. C. (1991). Blood pressure control—special role of the kidneys and body fluids. *Science*, 252(5014), 1813–1816.
- Hadchouel, J., Ellison, D. H., & Gamba, G. (2016). Regulation of renal electrolyte transport by WNK and SPAK-OSR1 kinases. *Annual Review of Physiology*, 78(1), 367–389.
- Hansson, J. H., Schild, L., Lu, Y., Wilson, T. A., Gautschi, I., Shimkets, R., et al. (1995). A de novo missense mutation of the beta subunit of the epithelial sodium channel causes hypertension and Liddle syndrome, identifying a proline-rich segment critical for regulation of channel activity. *Proceedings of the National Academy of Sciences*, 92(25), 11495–11499.
- He, F. J., Marciniak, M., Carney, C., Markandu, N. D., Anand, V., Fraser, W. D., et al. (2010). Effects of potassium chloride and potassium bicarbonate on endothelial function, cardiovascular risk factors, and bone turnover in mild hypertensives. *Hypertension*, 55(3), 681–688.
- Hennings, J. C., Andriani, O., Picard, N., Paulais, M., Huebner, A. K., Cayuqueo, I. K. L., et al. (2017). The ClC-K2 chloride channel is critical for salt handling in the distal nephron. *Journal of the American Society of Nephrology*, 28(1), 209–217.
- Huang, D. Y., Wulff, P., Völkl, H., Loffing, J., Richter, K., Kuhl, D., et al. (2004). Impaired regulation of renal K⁺ elimination in the SGK1-Knockout mouse. *Journal of the American Society of Nephrology*, 15(4), 885–891.
- Hunter, R. W., Craigie, E., Homer, N. Z. M., Mullins, J. J., & Bailey, M. A. (2014). Acute inhibition of NCC does not activate distal electrogenic Na⁺ reabsorption or kaliuresis. *American Journal of Physiology. Renal Physiology*, 306(4), F457–F467.
- Ishizawa, K., Xu, N., Loffing, J., Lifton, R. P., Fujita, T., Uchida, S., et al. (2016). Potassium depletion stimulates Na-Cl cotransporter via phosphorylation and inactivation of the ubiquitin ligase Kelch-like 3. *Biochemical and Biophysical Research Communications*, 480(4), 745–751.
- Jung, J. Y., Kim, S., Lee, J. W., Jung, E. S., Heo, N. J., Son, M.-J., et al. (2011). Effects of potassium on expression of renal sodium transporters in salt-sensitive hypertensive rats induced by uninephrectomy. *American Journal of Physiology. Renal Physiology*, 300(6), F1422–F1430.
- Kahn, M., & Bohrer, N. K. (1967). Effect of potassium-induced diuresis on renal concentration and dilution. *American Journal of Physiology*, 212(6), 1365–1375.
- Kaissling, B., & Le Hir, M. (1982). Distal tubular segments of the rabbit kidney after adaptation to altered Na- and K-intake I. Structural changes. *Cell and Tissue Research*, 224(3), 469–492.
- Katz, A. I., Doucet, A., & Morel, F. (1979). Na-K-ATPase activity along the rabbit, rat, and mouse nephron. *American Journal of Physiology*, 237(2), F114–F120.
- Keith, N. M., & Binger, M. W. (1935). Diuretic action of potassium salts. *Journal of the American Medical Association*, 105(20), 1584–1591.
- Kempner, W. (1974). Treatment of hypertensive vascular disease with rice diet. *Archives of Internal Medicine*, 133(5), 758–790.
- Khaw, K. T., & Barrett-Connor, E. (1988). The association between blood pressure, age, and dietary sodium and potassium: A population study. *Circulation*, 77(1), 53–61. <https://doi.org/10.1161/01.CIR.77.1.53>.
- Kirchner, K. A. (1983). Effect of acute potassium infusion on loop segment chloride reabsorption in the rat. *American Journal of Physiology. Renal Physiology*, 244(6), F599–F605.
- Krishna, G. G., & Kapoor, S. C. (1991). Potassium depletion exacerbates essential hypertension. *Annals of Internal Medicine*, 115(2), 77–83.
- Krishna, G. G., & Kapoor, S. C. (1993). Potassium supplementation ameliorates mineralocorticoid-induced sodium retention. *Kidney International*, 43(5), 1097–1103.

- Lalioti, M. D., Zhang, J., Volkman, H. M., Kahle, K. T., Hoffmann, K. E., Toka, H. R., et al. (2006). *Wnk4* controls blood pressure and potassium homeostasis via regulation of mass and activity of the distal convoluted tubule. *Nature Genetics*, *38*(10), 1124–1132.
- Lifton, R. P., Gharavi, A. G., Geller, D. S., & Hughes, H. (2001). Molecular mechanisms of human hypertension. *Cell*, *104*, 545–556.
- Liu, W., Schreck, C., Coleman, R. a., Wade, J. B., Hernandez, Y., Zavilowitz, B., et al. (2011). Role of NKCC in BK channel-mediated net K⁺ secretion in the CCD. *American Journal of Physiology. Renal Physiology*, *301*(5), F1088–F1097.
- Loffing, J., Pietri, L., Aregger, F., Bloch-Faure, M., Ziegler, U., Meneton, P., et al. (2000). Differential subcellular localization of ENaC subunits in mouse kidney in response to high- and low-Na diets. *American Journal of Physiology. Renal Physiology*, *279*(2), F252–F258.
- Loffing-Cueni, D., Schlaepfer, M., Bloch-Faure, M., Hummler, E., Rossier, B., Kaissling, B., et al. (2003). Apical translocation of ROMK and ENaC in mouse distal nephron in response to high K⁺ diet (Abstract). *Nephrology, Dialysis, Transplantation*, *18*, 552.
- Louis-Dit-Picard, H., Barc, J., Trujillano, D., Miserey-Lenkei, S., Bouatia-Naji, N., Pylypenko, O., et al. (2012). KLHL3 mutations cause familial hyperkalemic hypertension by impairing ion transport in the distal nephron. *Nature Genetics*, *44*(4), 456–460.
- Lubbe, N., Moes, A., Rosenbaek, L., Schoep, S., Meima, M., Danser, A., et al. (2013). K⁺-induced natriuresis is preserved during Na⁺ depletion and accompanied by inhibition of the Na⁺-Cl⁻ cotransporter. *American Journal of Physiology. Renal Physiology*, *305*(8), F1177–F1188.
- Mayan, H., Vered, I., Mouallem, M., Tzadok-witkon, M., & Pazner, R. (2002). Pseudo-hypoaldosteronism Type II: Marked sensitivity to Thiazides, hypercalciuria, normomagnesemia, and low bone mineral density. *The Journal of Clinical Endocrinology and Metabolism*, *87*(7), 3248–3254.
- Mcquarrie, I., Thompson, W. H., & Anderson, J. A. (1935). Effects of excessive ingestion of sodium and potassium salts on carbohydrate metabolism and blood pressure in diabetic children. *The Journal of Nutrition*, *11*(1), 77–101.
- Meneely, G. R., Ball, C. O., & Youmans, J. B. (1957). Chronic sodium chloride toxicity: The protective effect of added potassium chloride. *Annals of Internal Medicine*, *47*(2), 263–273.
- Meneton, P., Loffing, J., & Warnock, D. G. (2004). Sodium and potassium handling by the aldosterone-sensitive distal nephron: The pivotal role of the distal and connecting tubule. *American Journal of Physiology. Renal Physiology*, *287*(4), F593–F601.
- Mente, A., O'Donnell, M. J., Rangarajan, S., McQueen, M. J., Poirier, P., Wielgosz, A., et al. (2014). Association of urinary sodium and potassium excretion with blood pressure. *New England Journal of Medicine*, *371*(7), 601–611.
- Murillo-de-Ozores, A. R., Grajeda-Medina, L. I., Gamba, G., & Castañeda-Bueno, M. (2018). Intracellular chloride depletion promotes WNK4-RRXS phosphorylation by a PKC/PKA dependent mechanism. *Journal of the American Society of Nephrology*, *29*, 1005 (meeting abstract).
- Nomura, N., Shoda, W., Wang, Y., Mandai, S., Furusho, T., Takahashi, D., et al. (2018). Role of ClC-K and barttin in low-potassium induced sodium-chloride cotransporter activation and hypertension in mouse kidney. *Bioscience Reports*, *38*(1).
- O'Donnell, M., Mente, A., Rangarajan, S., McQueen, M. J., Wang, X., Liu, L., et al. (2014). Urinary sodium and potassium excretion, mortality, and cardiovascular events. *New England Journal of Medicine*, *371*(7), 612–623.
- Ohta, A., Schumacher, F., Mehellou, Y., Johnson, C., Knebel, A., Macartney, T. J., et al. (2013). The CUL3-KLHL3 E3 ligase complex mutated in Gordon's hypertension

- syndrome interacts with and ubiquitylates WNK isoforms: Disease-causing mutations in KLHL3 and WNK4 disrupt interaction. *Biochemical Journal*, 451, 111–122.
- Oi, K., Sahara, E., Rai, T., Misawa, M., Chiga, M., Alessi, D. R., et al. (2012). A minor role of WNK3 in regulating phosphorylation of renal NKCC2 and NCC co-transporters in vivo. *Biology Open*, 1(2), 120–127.
- Oliver, W. J., Cohen, E. L., & Neel, J. V. (1975). Blood pressure, sodium intake, and sodium related hormones in the Yanomamo Indians, a “no-salt” culture. *Circulation*, 52(1), 146–151.
- O’Reilly, M., Marshall, E., Macgillivray, T., Mittal, M., Xue, W., Kenyon, C. J., et al. (2006). Dietary electrolyte-driven responses in the renal WNK kinase pathway in vivo. *Journal of the American Society of Nephrology*, 17(9), 2402–2413.
- Pácha, J., Frindt, G., Sackin, H., & Palmer, L. G. (1991). Apical maxi K channels in intercalated cells of CCT. *The American Journal of Physiology*, 261(30), F696–F705.
- Pacheco-Alvarez, D., San Cristóbal, P., Meade, P., Moreno, E., Vazquez, N., Muñoz, E., et al. (2006). The Na⁺:Cl⁻ cotransporter is activated and phosphorylated at the amino-terminal domain upon intracellular chloride depletion. *Journal of Biological Chemistry*, 281(39), 28755–28763.
- Palmer, L. G. (1999). Potassium secretion and the regulation of distal nephron K channels. *American Journal of Physiology. Renal Physiology*, 277(46), F821–F833.
- Paulais, M., Bloch-Faure, M., Picard, N., Jacques, T., Ramakrishnan, S. K., Keck, M., et al. (2011). Renal phenotype in mice lacking the Kir5.1 (Kcnj16) K⁺ channel subunit contrasts with that observed in SeSAME/EAST syndrome. *Proceedings of the National Academy of Sciences*, 108(25), 10361–10366.
- Penton, D., Czogalla, J., Wengi, A., Himmerkus, N., Loffing-Cueni, D., Carrel, M., et al. (2016). Extracellular K⁺ rapidly controls NaCl cotransporter phosphorylation in the native distal convoluted tubule by Cl⁻-dependent and independent mechanisms. *Journal of Physiology*, 594(21), 6319–6331.
- Perrier, R., Boscardin, E., Malsure, S., Sergi, C., Maillard, M. P., Loffing, J., et al. (2016). Severe salt-losing syndrome and hyperkalemia induced by adult nephron-specific knock-out of the epithelial sodium channel-subunit. *Journal of the American Society of Nephrology*, 27(8), 2309–2318.
- Piala, A. T., Moon, T. M., Akella, R., He, H., Cobb, M. H., & Goldsmith, E. J. (2014). Chloride sensing by WNK1 involves inhibition of autophosphorylation. *Science Signaling*, 7(324), ra41.
- Poorolajal, J., Zeraati, F., Soltanian, A. R., Sheikh, V., Hooshmand, E., & Maleki, A. (2017). Oral potassium supplementation for management of essential hypertension: A meta-analysis of randomized controlled trials. *PLoS One*, 12(4), 1–16.
- Priddle, W. W. (1931). Observations on the management of hypertension. *Canadian Medical Association Journal*, 25(1), 5–8.
- Rengarajan, S., Lee, D. H., Oh, Y. T., Delpire, E., Youn, J. H., & McDonough, A. A. (2014). Increasing plasma [K⁺] by intravenous potassium infusion reduces NCC phosphorylation and drives kaliuresis and natriuresis. *American Journal of Physiology. Renal Physiology*, 306(9), F1059–F1068.
- Richardson, C., Rafiqi, F. H., Karlsson, H. K. R., Moleleki, N., Vandewalle, A., Campbell, D. G., et al. (2008). Activation of the thiazide-sensitive Na⁺-Cl⁻ cotransporter by the WNK-regulated kinases SPAK and OSR1. *Journal of Cell Science*, 121(5), 675–684.
- Rubera, I., Loffing, J., Palmer, L. G., Frindt, G., Fowler-jaeger, N., Sauter, D., et al. (2003). Collecting duct-specific gene inactivation of aENaC in the mouse kidney does not impair sodium and potassium balance. *Journal of Clinical Investigation*, 112(4), 554–565. <https://doi.org/10.1172/JCI200316956>. Introduction.

- Sacks, F. M., Svetkey, L. P., Vollmer, W. M., Appel, L. J., Bray, G. A., & Harsha, D. DASH-Sodium Collaborative Research Group. (2001). Effects on blood pressure of reduced dietary sodium and the dietary approaches to stop hypertension (DASH) diet. *New England Journal of Medicine*, *344*(1), 3–10.
- Salt. (2015). *Pflügers Archiv - European Journal of Physiology*, *467*(3). complete issue.
- Schild, L., Lu, Y., Gautschi, I., Schneeberger, E., Lifton, R. P., & Rossier, B. C. (1996). Identification of a PY motif in the epithelial Na channel subunits as a target sequence for mutations causing channel activation found in Liddle syndrome. *The EMBO Journal*, *15*(10), 2381–2387.
- Scholl, U. I., Choi, M., Liu, T., Ramaekers, V. T., Hausler, M. G., Grimmer, J., et al. (2009). Seizures, sensorineural deafness, ataxia, mental retardation, and electrolyte imbalance (SeSAME syndrome) caused by mutations in KCNJ10. *Proceedings of the National Academy of Sciences*, *106*(14), 5842–5847.
- Shibata, S., Zhang, J., Puthumana, J., Stone, K. L., & Lifton, R. P. (2013). Kelch-like 3 and Cullin 3 regulate electrolyte homeostasis via ubiquitination and degradation of WNK4. *Proceedings of the National Academy of Sciences*, *110*(19), 7838–7843.
- Shimkets, R. A., Warnock, D. G., Bositis, C. M., Nelson-Williams, C., Hansson, J. H., Schambelan, M., et al. (1994). Liddle's syndrome: Heritable human hypertension caused by mutations in the beta subunit of the epithelial sodium channel. *Cell*, *79*(3), 407–414.
- Shoda, W., Nomura, N., Ando, F., Mori, Y., Mori, T., Sohara, E., et al. (2017). Calcineurin inhibitors block sodium-chloride cotransporter dephosphorylation in response to high potassium intake. *Kidney International*, *91*(2), 402–411.
- Simon, D. B., Karet, F. E., RodriguezSoriano, J., Hamdan, J. H., DiPietro, A., Trachtman, H., et al. (1996). Genetic heterogeneity of Bartter's syndrome revealed by mutations in the K⁺ channel, ROMK. *Nature Genetics*, *14*(2), 152–156. <https://doi.org/10.1038/ng1096-152>.
- Simon, D. B., Nelson-Williams, C., Bia, M. J., Ellison, D., Karet, F. E., Molina, A. M., et al. (1996). Gitelman's variant of Bartter's syndrome, inherited hypokalaemic alkalosis, is caused by mutations in the thiazide-sensitive Na-Cl cotransporter. *Nature Genetics*, *12*(1), 24–30.
- Sorensen, M. V., Grossmann, S., Roesinger, M., Gresko, N., Todkar, A. P., Barmettler, G., et al. (2013). Rapid dephosphorylation of the renal sodium chloride cotransporter in response to oral potassium intake in mice. *Kidney International*, *83*(5), 811–824.
- Stokes, J. B., Lee, I., & Williams, A. (1982). Consequences of potassium recycling in the renal medulla. *Journal of Clinical Investigation*, *70*(2), 219–229.
- Strautnieks, S. S., Thompson, R. J., Gardiner, R. M., & Chung, E. (1996). A novel splice-site mutation in the γ subunit of the epithelial sodium channel gene in three pseudo-hypaldosteronism type 1 families. *Nature Genetics*, *13*(2), 248–250.
- Su, X.-T., & Wang, W.-H. (2016). The expression, regulation, and function of Kir4.1 (*Kcnj10*) in the mammalian kidney. *American Journal of Physiology. Renal Physiology*, *311*(1), F12–F15.
- Susa, K., Sohara, E., Takahashi, D., Okado, T., Rai, T., & Uchida, S. (2017). WNK4 is indispensable for the pathogenesis of pseudohypaldosteronism type II caused by mutant KLHL3. *Biochemical and Biophysical Research Communications*, *491*(3), 727–732.
- Takahashi, D., Mori, T., Nomura, N., Khan, M. Z. H., Araki, Y., Zeniya, M., et al. (2014). WNK4 is the major WNK positively regulating NCC in the mouse kidney. *Bioscience Reports*, *34*(3), 195–206. <https://doi.org/10.1042/BSR20140047>.
- Terker, A. S., Yarbrough, B., Ferdaus, M. Z., Lazelle, R. A., Erspamer, K. J., Meermeier, N. P., et al. (2016). Direct and indirect mineralocorticoid effects determine distal salt transport. *Journal of the American Society of Nephrology*, *27*(8), 2436–2445. <https://doi.org/10.1681/ASN.2015070815>.

- Terker, A. S., Zhang, C., Erspamer, K. J., Gamba, G., Yang, C.-L., & Ellison, D. H. (2015). Unique chloride-sensing properties of WNK4 permit the distal nephron to modulate potassium homeostasis. *Kidney International*, *89*(1), 1–8. <https://doi.org/10.1038/ki.2015.289>.
- Terker, A. S., Zhang, C., McCormick, J. A., Lazelle, R. A., Zhang, C., Meermeier, N. P., et al. (2015). Potassium modulates electrolyte balance and blood pressure through effects on distal cell voltage and chloride. *Cell Metabolism*, *21*(1), 39–50.
- Unwin, R., Capasso, G., & Giebisch, G. (1994). Potassium and sodium transport along the loop of Henle: Effects of altered dietary potassium intake. *Kidney International*, *46*(4), 1092–1099.
- Vallon, V., Schroth, J., Lang, F., Kuhl, D., & Uchida, S. (2009). Expression and phosphorylation of the Na⁺-Cl⁻ cotransporter NCC in vivo is regulated by dietary salt, potassium, and SGK1. *American Journal of Physiology. Renal Physiology*, *297*(3), F704–F712.
- Vander, A. J. (1970). Direct effects of potassium on renin secretion and renal function. *The American Journal of Physiology*, *219*(2), 455–459.
- Vitari, A. C., Deak, M., Morrice, N. A., & Alessi, D. R. (2005). The WNK1 and WNK4 protein kinases that are mutated in Gordon's hypertension syndrome phosphorylate and activate SPAK and OSR1 protein kinases. *Biochemical Journal*, *391*(1), 17–24.
- Wade, J. B., Fang, L., Coleman, R. A., Liu, J., Grimm, P. R., Wang, T., et al. (2011). Differential regulation of ROMK (Kir1.1) in distal nephron segments by dietary potassium. *American Journal of Physiology. Renal Physiology*, *300*(6), F1385–F1393.
- Wagner, C. A., Loffing-Cueni, D., Yan, Q., Schulz, N., Fakitsas, P., Carrel, M., et al. (2008). Mouse model of type II Bartter's syndrome. II. Altered expression of renal sodium- and water-transporting proteins. *American Journal of Physiology. Renal Physiology*, *294*(6), F1373–F1380.
- Wakabayashi, M., Mori, T., Isobe, K., Sahara, E., Susa, K., Araki, Y., et al. (2013). Impaired KLHL3-mediated ubiquitination of WNK4 causes human hypertension. *Cell Reports*, *3*(3), 858–868.
- Wang, M. X., Cuevas, C. A., Su, X. T., Wu, P., Gao, Z. X., Lin, D. H., et al. (2018). Potassium intake modulates the thiazide-sensitive sodium-chloride cotransporter (NCC) activity via the Kir4.1 potassium channel. *Kidney International*, *93*(4), 893–902. <https://doi.org/10.1016/j.kint.2017.10.023>.
- Wang, B., Wen, D., Li, H., Wang-france, J., & Sansom, S. C. (2017). Net K⁺ secretion in the thick ascending limb of mice on a low-Na, high-K diet. *Kidney International*, *92*(4), 864–875.
- Wei, Y., Bloom, P., Lin, D., Gu, R., & Wang, W. H. (2001). Effect of dietary K intake on apical small-conductance K channel in CCD: Role of protein tyrosine kinase. *American Journal of Physiology. Renal Physiology*, *281*(2), F206–F212.
- Weinstein, A. M. (2017). A mathematical model of the rat nephron: K⁺-induced natriuresis. *American Journal of Physiology. Renal Physiology*, *312*, F925–F950.
- Wellng, P. A. (2013). Regulation of renal potassium secretion: Molecular mechanisms. *Seminars in Nephrology*, *33*(3), 215–228.
- WHO. (2012a). *Guideline: Sodium intake for adults and children*. Geneva: World Health Organization (WHO).
- WHO. (2012b). *Guideline: Potassium intake for adults and children*. Geneva: World Health Organization (WHO). <https://doi.org/9789241549028>.
- Wilson, F. H., Disse-Nicodème, S., Choate, K. A., Ishikawa, K., Nelson-Williams, C., Desitter, I., et al. (2001). Human hypertension caused by mutations in WNK kinases. *Science*, *293*(5532), 1107–1112.
- Woda, C. B., Bragin, A., Kleyman, T. R., & Satlin, L. M. (2001). Flow-dependent K⁽⁺⁾ secretion in the cortical collecting duct is mediated by a maxi-K channel. *American Journal of Physiology. Renal Physiology*, *280*(5), F786–F793.

- Wright, F. S., Strieder, N., Fowler, N. B., & Giebisch, G. (1971). Potassium secretion by distal tubule after potassium adaptation. *The American Journal of Physiology*, *221*(2), 437–448.
- Yang, S. S., Morimoto, T., Rai, T., Chiga, M., Sohara, E., Ohno, M., et al. (2007). Molecular pathogenesis of pseudohypoaldosteronism type II: Generation and analysis of a *Wnk4*^{D561A/+} knockin mouse model. *Cell Metabolism*, *5*(5), 331–344.
- Yang, Y., Xie, J., Yang, S., Lin, S., Huang, C., Drive, H., et al. (2018). Differential roles of WNK4 in regulation of NCC in vivo. *American Journal of Physiology. Renal Physiology*, *314*(5), F999–F1007.
- Yang, L., Xu, S., Guo, X., Uchida, S., Weinstein, A. M., Wang, T., et al. (2018). Regulation of renal Na transporters in response to dietary K. *American Journal of Physiology. Renal Physiology*, *315*(4), F1032–F1041.
- Zacchia, M., Abategiovanni, M. L., Stratigis, S., & Capasso, G. (2016). Potassium: From physiology to clinical implications. *Kidney Diseases (Basel, Switzerland)*, *2*(2), 72–79.



Physiological Processes Modulated by the Chloride-Sensitive WNK-SPAK/OSR1 Kinase Signaling Pathway and the Cation-Coupled Chloride Cotransporters

Adrián Rafael Murillo-de-Ozores^{1,2}, María Chávez-Canales³, Paola de los Heros⁴, Gerardo Gamba^{1,5} and María Castañeda-Bueno^{1*}

¹ Department of Nephrology and Mineral Metabolism, Instituto Nacional de Ciencias Médicas y Nutrición Salvador Zubirán, Mexico City, Mexico, ² Facultad de Medicina, Universidad Nacional Autónoma de México, Mexico City, Mexico, ³ Unidad de Investigación UNAM-INC, Instituto Nacional de Cardiología Ignacio Chávez and Instituto de Investigaciones Biomédicas, Universidad Nacional Autónoma de México, Mexico City, Mexico, ⁴ Unidad de Investigación UNAM-INC, Research Division, Facultad de Medicina, Universidad Nacional Autónoma de México, Mexico City, Mexico, ⁵ Molecular Physiology Unit, Instituto de Investigaciones Biomédicas, Universidad Nacional Autónoma de México, Mexico City, Mexico

OPEN ACCESS

Edited by:

Alexander A. Mongin,
Albany Medical College, United States

Reviewed by:

Dandan Sun,
University of Pittsburgh, United States
Hui Cai,
Emory University, United States

*Correspondence:

María Castañeda-Bueno
maria.castanedab@incmnsz.mx;
mcasta85@yahoo.com.mx

Specialty section:

This article was submitted to
Membrane Physiology
and Membrane Biophysics,
a section of the journal
Frontiers in Physiology

Received: 21 July 2020

Accepted: 29 September 2020

Published: 20 October 2020

Citation:

Murillo-de-Ozores AR,
Chávez-Canales M, de los Heros P,
Gamba G and Castañeda-Bueno M
(2020) Physiological Processes
Modulated by the Chloride-Sensitive
WNK-SPAK/OSR1 Kinase Signaling
Pathway and the Cation-Coupled
Chloride Cotransporters.
Front. Physiol. 11:585907.
doi: 10.3389/fphys.2020.585907

The role of Cl⁻ as an intracellular signaling ion has been increasingly recognized in recent years. One of the currently best described roles of Cl⁻ in signaling is the modulation of the With-No-Lysine (K) (WNK) – STE20-Proline Alanine rich Kinase (SPAK)/Oxidative Stress Responsive Kinase 1 (OSR1) – Cation-Coupled Cl⁻ Cotransporters (CCCs) cascade. Binding of a Cl⁻ anion to the active site of WNK kinases directly modulates their activity, promoting their inhibition. WNK activation due to Cl⁻ release from the binding site leads to phosphorylation and activation of SPAK/OSR1, which in turn phosphorylate the CCCs. Phosphorylation by WNKs-SPAK/OSR1 of the Na⁺-driven CCCs (mediating ions influx) promote their activation, whereas that of the K⁺-driven CCCs (mediating ions efflux) promote their inhibition. This results in net Cl⁻ influx and feedback inhibition of WNK kinases. A wide variety of alterations to this pathway have been recognized as the cause of several human diseases, with manifestations in different systems. The understanding of WNK kinases as Cl⁻ sensitive proteins has allowed us to better understand the mechanistic details of regulatory processes involved in diverse physiological phenomena that are reviewed here. These include cell volume regulation, potassium sensing and intracellular signaling in the renal distal convoluted tubule, and regulation of the neuronal response to the neurotransmitter GABA.

Keywords: distal convoluted tubule, GABAergic activity, cell volume regulation, intracellular chloride concentration, arterial blood pressure, potassium

CHLORIDE AS A SIGNALING ION

The chloride (Cl⁻) anion is an important component of all known living beings, where it plays several roles in homeostatic and rheostatic processes in all types of cells. In humans, extracellular Cl⁻ concentration is maintained relatively constant, between 100 and 116 mmol/L, due to tight regulation by the kidneys and intestine (Boulpaep and Boron, 2016). It is notable that there is

interspecies variability of plasma Cl^- concentration. For instance, normal levels in rats and mice are in the range of 90–132 mmol/L and 106–131 mmol/L, respectively (Lea et al., 2018).

Intracellular Cl^- concentration ($[\text{Cl}^-]_i$) varies wildly among different cell types within an organism. For example, it has been reported that most adult neurons have relatively low $[\text{Cl}^-]_i$ (5–15 mmol/L) (Kakazu et al., 1999; Yamada et al., 2004; Glykys et al., 2014), and $[\text{Cl}^-]_i$ of renal epithelial cells such as the ones of the distal convoluted tubule (DCT) has been estimated to be between 10 and 20 mmol/L (Beck et al., 1988; Boettger et al., 2002; Weinstein, 2005; Terker et al., 2015b). Conversely, olfactory sensory neurons (Reuter et al., 1998) and some cells from secretory epithelia, such as pancreatic (O'Doherty and Stark, 1983) and salivary acinar cells (Foskett, 1990), have a $[\text{Cl}^-]_i$ as high as 60–65 mmol/L. Additionally, $[\text{Cl}^-]_i$ can be dynamically modulated by different stimuli, such as cholinergic agonists (Foskett, 1990), cAMP levels (Xie and Schafer, 2004), lectin-stimulation (Lai et al., 2003), and extracellular potassium concentration ($[\text{K}^+]_e$) (Terker et al., 2015b). These reports exemplify the wide variation of $[\text{Cl}^-]_i$, which is important for the role that this anion plays in the physiology of specific cell types.

While some of the most studied roles for Cl^- in physiology are related to cell volume regulation (Hoffmann et al., 2009), establishment of resting membrane potential (Funabashi et al., 2010; Hutter, 2017), and acid-base balance (Seifter and Chang, 2016), it is now becoming clear that this anion is involved in intracellular signaling pathways involved in the regulation of a wider variety of cellular processes, such as gene expression, cell proliferation, apoptosis, among others (reviewed in Valdivieso and Santa-Coloma, 2019; Wilson and Mongin, 2019; Lüscher et al., 2020). For instance, published evidence suggests that $[\text{Cl}^-]_i$ can modulate the activity of different kinases, such as the MAPKs p38, JNK and ERK (Ohsawa et al., 2010; Wu et al., 2016), as well as SGK1 (Zhang et al., 2018), although it is still unclear whether direct effects of Cl^- ions on the kinases themselves are responsible. However, the With-No-lysine (K) (WNK) family of kinases is one example where the direct Cl^- binding to the enzyme's active site (Piala et al., 2014) that modulates kinase activity (Bazua-Valenti et al., 2015) has been thoroughly studied (detailed in sections below). These observations support the novel proposed role of $[\text{Cl}^-]_i$ as a second messenger (Valdivieso and Santa-Coloma, 2019; Wilson and Mongin, 2019; Lüscher et al., 2020), responsible for modulating the activity of several proteins.

Transmembrane transport proteins determine the Cl^- permeability of each cell type. Ion channels that facilitate large Cl^- fluxes across cell membranes include the CLC family (reviewed extensively in Jentsch and Pusch, 2018), the cystic fibrosis transmembrane conductance regulator (CFTR) channel (Csanády et al., 2019), the volume-regulated anion channel (VRAC) channel (Osei-Owusu et al., 2018), and Ca^{2+} -activated Cl^- channels (CaCCs) such as anoctamins (Pedemonte and Galletta, 2014). The direction of Cl^- flux through ion channels is solely determined by the electrochemical gradient of this ion across the membrane. However, secondary active transporters can set the $[\text{Cl}^-]_i$ at levels that diverge from the electrochemical equilibrium by coupling Na^+ influx or K^+ efflux to the movement

of Cl^- . Transporters with this type of activity are all members of the SLC12 family of solute carriers described below.

THE SLC12 FAMILY OF COTRANSPORTERS

The SLC12 family of solute carriers is comprised by the electroneutral cation-coupled Cl^- cotransporters (CCCs). Seven members of this family are arranged in two branches, depending on their ability to use Na^+ as one of the transported cations coupled to Cl^- . The Na^+ -dependent branch includes the Na^+ - K^+ - 2Cl^- cotransporters, known as NKCC1 and NKCC2, and the Na^+ - Cl^- cotransporter, NCC (Gamba, 2005). NKCC1 is expressed in many epithelial and non-epithelial cells (Delpire et al., 1994). Within epithelial cells it is expressed in the basolateral membrane, except in the choroid plexus of the brain, where it is expressed apically (Delpire et al., 1994; Wu et al., 1998). NKCC2 is exclusively expressed in the apical membrane of the thick ascending limb of Henle's loop in the kidney (Gamba et al., 1994) and NCC is present in the apical membrane of the distal convoluted tubule in the kidney and in osteoblasts in bone (Gamba et al., 1994; Dvorak et al., 2007). Identity degree at the amino acid level among these transporters is between 50 and 60%. The Na^+ -independent branch is composed of four K^+ - Cl^- cotransporters, known as KCC1 to KCC4. Of these four, KCC2 is exclusively expressed in neurons, while the other three KCCs are present in many cells throughout the body. Identity degree among KCCs is about 60% and between the Na^+ -dependent and independent branches is around 25% (Gamba, 2005; Arroyo et al., 2013).

The CCCs are secondary active transporters whose activity is driven by the Na^+ and K^+ gradients generated by the Na^+ - K^+ -ATPase. The Na^+ -driven transporters move ions from the extracellular space into the cytoplasm, while the K^+ -driven transporters (of the Na^+ -independent branch) mediate ion extrusion from the cells. In non-epithelial cells, the sustained activity of the Na^+ - K^+ -ATPase maintains a low Na^+ and high K^+ intracellular concentration, respectively. Thus, it is considered that the net effect of the activity of CCCs is the modulation of the $[\text{Cl}^-]_i$. Because of this, the expression of Na^+ -driven and K^+ -driven members of the SLC12 family in the same cell constitutes a system for the dynamic modulation of $[\text{Cl}^-]_i$. This, for example, is particularly relevant in neurons, where, as explained below in detail, the type and magnitude of the response to neurotransmitters that activate Cl^- channels in the postsynaptic membrane depends on the electrochemical Cl^- gradient (Kahle et al., 2008). Regulation of $[\text{Cl}^-]_i$ also plays a relevant role for the regulation of cell volume (de los Heros et al., 2018). In epithelial cells, the CCCs works in conjunction with other apical and/or basolateral channels and transporters to carry out transepithelial ion transport (Gamba, 2005). Thus, the major physiological roles of the CCCs are modulation of $[\text{Cl}^-]_i$, cell volume regulation, and transepithelial ion transport. For this reason, the CCCs are implicated in many organs' and systems' physiological processes (Gamba, 2005).

A variety of human and animal diseases and phenotypes in knockout mice models have been helpful in revealing the many roles of CCCs in physiology (Delpire and Mount, 2002) (Table 1). Inactivating mutations in the renal cotransporters NKCC2 and NCC are the cause of the Bartter syndrome type I (Simon et al., 1996a) and Gitelman disease (Simon et al., 1996b), respectively. NKCC2 constitutes the main apical entryway for Na⁺ and Cl⁻ in the thick ascending limb of Henle's loop and NCC plays a similar role in the downstream adjacent nephron segment known as the distal convoluted tubule. Decreased Na⁺ reabsorption in these segments is not only associated with volume depletion and low blood pressure, but also with hypokalemic metabolic alkalosis due to increased K⁺ secretion in the aldosterone sensitive distal nephron that is stimulated by the increased distal Na⁺ delivery

(Gamba, 2005). The phenotype of both, type I Bartter syndrome and Gitelman syndrome patients, is exclusively the consequence of the lack of activity of these transporters in the nephron, suggesting that indeed their expression is very restricted to the kidney and, if expressed elsewhere, like NCC in bone, its role in other tissues is not essential. Regarding NKCC1, knockout mice were generated and studied before human mutations in this gene were found. These mice have a wide variety of phenotypic alterations, such as small size, inner ear dysfunction, male infertility, altered pain perception, defects in intestinal transit, decreased saliva production, and low blood pressure, among others (Gagnon and Delpire, 2013). Delpire et al. (2016) described a human patient with respiratory weakness, endocrine and pancreatic abnormalities, and multi-organ failure. Genetic

TABLE 1 | SLC12 cotransporters: associated genetic diseases and phenotype of knockout models.

Gene	Protein	Tissue expression	Associated disease (inheritance pattern; effect on protein function)	Knockout mice phenotype
<i>SLC12A1</i>	NKCC2	Kidney (Gamba et al., 1994); gastrointestinal tract (Xue et al., 2009)	Bartter syndrome type I (OMIM 601678) – hypokalemic metabolic alkalosis, low blood pressure, hypercalciuria (autosomal recessive; loss of function) (Simon et al., 1996a) Hydrallantois in <i>Bos taurus</i> (OMIA 002053-9913) – excessive accumulation of fluid within the allantoic cavity in pregnant animals (autosomal recessive; loss of function) (Sasaki et al., 2016)	Bartter-like – severe volume depletion and failure to thrive; partial rescue with indomethacin, with severe polyuria, hydronephrosis, hypokalemia, hypercalciuria, hyperreninemia, and proteinuria (Takahashi et al., 2000)
<i>SLC12A2</i>	NKCC1	Ubiquitous (Delpire et al., 1994)	Multisystem dysfunction – endocrine abnormalities, low blood pressure, intestinal dysfunction (autosomal dominant – mistrafficking of mutant NKCC1 to apical membrane in epithelial cells) (Delpire et al., 2016; Koumangoye et al., 2018) Kilquist syndrome – sensorineural deafness, intestinal and respiratory dysfunction, neuropsychological delay, severe xerostomia (autosomal recessive; loss of function) (Macnamara et al., 2019) Schizophrenia – (autosomal dominant; gain of function) (Merner et al., 2016)	Sensorineural deafness (Delpire et al., 1999; Dixon et al., 1999), growth retardation, low blood pressure, intestinal abnormalities (Flagella et al., 1999), male infertility (Pace et al., 2000), decreased saliva secretion (Evans et al., 2000), altered pain perception (Sung et al., 2000)
<i>SLC12A3</i>	NCC	Kidney (Gamba et al., 1994), bone (Dvorak et al., 2007), placenta, prostate and small intestine (Chang et al., 1996)	Gitelman syndrome (OMIM 263800) – hypokalemic metabolic alkalosis, low blood pressure, hypocalciuria, hypomagnesemia (autosomal recessive; loss of function) (Simon et al., 1996b)	Gitelman-like – low blood pressure in low Na ⁺ diet, hypocalciuria, hypomagnesemia (Schultheis et al., 1998), metabolic alkalosis (Loffing et al., 2004), hypokalemia while in low K ⁺ diet (Morris et al., 2006)
<i>SLC12A4</i>	KCC1	Ubiquitous (Gillen and Forbush, 1999)	None found	No obvious differences compared to littermate WT mice (Rust et al., 2007)
<i>SLC12A5</i>	KCC2	Central nervous system (Payne et al., 1996), pancreas (Kursan et al., 2017)	Idiopathic epilepsy (OMIM 616685) – (autosomal dominant with incomplete penetrance; loss of function) (Kahle et al., 2014; Puskarjov et al., 2014) Epilepsy of infancy with migrating focal seizures (OMIM 616645) – (autosomal recessive; loss of function) (Stödtberg et al., 2015)	Neonatal death due to inability to breathe because of irregular activity of pre-Bötzinger complex (Hubner et al., 2001)
<i>SLC12A6</i>	KCC3	Wide, including muscle, heart, kidney, lung, and brain (Mount et al., 1999).	Andermann syndrome (OMIM 218000) – peripheral neuropathy associated with agenesis of the corpus callosum (autosomal recessive; loss of function) (Howard et al., 2002) Spinocerebellar ataxia in <i>Canis lupus familiaris</i> (OMIA 002279-9615) – (autosomal recessive; loss of function) (Van Poucke et al., 2019)	Locomotor abnormalities, deficit in prepulse inhibition, hypomyelination, axonal swelling fiber degeneration (Howard et al., 2002), progressive hearing loss, arterial hypertension, defective cell volume regulation (Boettger et al., 2003)
<i>SLC12A7</i>	KCC4	Wide, including heart, lung, liver, kidney, pancreas, stomach, thyroid (Mount et al., 1999)	None found	Deafness, renal tubular acidosis (Boettger et al., 2002)

analysis revealed a heterozygous 11-bp deletion in exon 22 of *SLC12A2* (encoding NKCC1) (Delpire et al., 2016) that causes a frameshift resulting in a truncated protein lacking the last 187 amino acid residues of the C-terminus. This mutation causes the mislocalization of the cotransporter to the apical membrane in epithelial cells (Koumangoye et al., 2018). The same mutation has been shown to cause a similar, although milder, phenotype in mice (Koumangoye et al., 2020). Macnamara et al. (2019) reported a novel syndrome, named Kilquist syndrome, in a patient harboring a large homozygous deletion in *SLC12A2*, from intron 1 through exon 7. Such mutation leads to aberrant splicing between exons 1 and 8, introducing a frameshift that would produce a truncated protein. Molecular analysis showed lower mRNA levels and absence of the NKCC1 protein in the patient's fibroblasts. Phenotypic features similar to the ones observed in NKCC1 knockout (−/−) mice were reported, including global developmental delay, bilateral sensorineural hearing loss, gastrointestinal abnormalities, and xerostomia (Macnamara et al., 2019). In addition, a missense variant that increases the activity of NKCC1 was described to be associated with schizophrenia (Merner et al., 2016).

Mutations in *KCC2* have been implicated in a variety of epileptic syndromes (Kahle et al., 2014; Puskarjov et al., 2014) and mutations in *KCC3* are the cause of a very complex inherited neurological disease known as Andermann's syndrome in which patients exhibit absence of the corpus callosum in the brain, together with a variety of neurodegenerative and psychiatric manifestations (Howard et al., 2002). No pathogenic mutations in *KCC4* have been described in humans. However, *KCC4*^{−/−} mice display deafness and renal tubular acidosis, suggesting that this transporter plays an important role in inner ear and kidney physiology (Boettger et al., 2002). Finally, global, constitutive disruption of *KCC1* in mice has no phenotypic consequences, suggesting that the absence of *KCC1* can be compensated by other K^+ - Cl^- cotransporters (Rust et al., 2007).

The Na^+ -driven and K^+ -driven cotransporters are regulated in opposite ways. They are all regulated by a kinase cascade in which the With No lysine (K) kinases (WNKs) phosphorylate and regulate the STE20-Proline Alanine rich Kinase (SPAK), and the Oxidative Stress Responsive Kinase 1 (OSR1). SPAK and OSR1 in turn phosphorylate the CCCs (Richardson and Alessi, 2008; Gagnon and Delpire, 2012; Alessi et al., 2014). Phosphorylation of the Na^+ -driven cotransporters, which occur in a cluster of serine-threonine residues located in the intracellular N-terminal domain, results in upregulation of cotransporter activity. In contrast, phosphorylation of K^+ -driven transporters that occurs in threonine residues of the C-terminal cytoplasmic domain results in downregulation of cotransporter activity. Thus, activation of this kinase cascade is able to simultaneously activate the Na^+ -(K^+)- Cl^- influx and prevent the K^+ - Cl^- efflux, increasing $[Cl^-]_i$ and intracellular osmolarity, while inactivation of the phosphorylating cascade and/or activation of dephosphorylating pathways result in opposite effects.

Stimuli such as the decrease in $[Cl^-]_i$ or the decrease in cell volume (cell shrinkage) result in activation of the WNK-SPAK/OSR1 phosphorylation pathway, increasing the activity of the Na^+ -(K^+)- Cl^- cotransporters and inhibiting the K^+ - Cl^-

cotransporters (Gagnon et al., 2006; Zagórska et al., 2007; Arroyo et al., 2013; Piala et al., 2014; Bazua-Valenti et al., 2015; de los Heros et al., 2018). This results in the increase of $[Cl^-]_i$ or in the net influx of ions that contribute to the regulatory volume increase response. In contrast, an increase in $[Cl^-]_i$ or cell volume (cell swelling) inhibits the phosphorylating pathway and activates protein phosphatases, thus resulting in cotransporters dephosphorylation, and the consequent decrease in $[Cl^-]_i$ or the net efflux of ions that contribute to the regulatory volume decrease response. Thus, a negative feedback loop integrated by the monovalent cation- Cl^- cotransporters of the CCC family, the WNK-SPAK/OSR1 kinase cascade, and protein phosphatases serve to regulate the $[Cl^-]_i$ and/or the cell volume, which in turn modulate the activity of the cotransporters via the kinases and phosphatases. This feedback loop has implications in several physiological processes that are discussed in this work.

THE WNK-SPAK/OSR1 SIGNALING PATHWAY AND ITS MODULATION BY INTRACELLULAR CHLORIDE

The WNK family of Ser/Thr kinases is comprised of four members in mammals: WNK1, WNK2, WNK3, and WNK4. Unlike most kinases, WNKs have their conserved catalytic Lys residue involved in ATP binding located in subdomain I, instead of in subdomain II, a characteristic that earned them their name (Xu et al., 2000) (**Figure 1**). Structurally, WNK kinases are composed by a relatively small regulatory N-terminal domain, followed by a highly conserved kinase domain (divided in the 12 subdomains characteristic of Ser/Thr kinases), and a large C-terminal domain with regulatory functions conferred by a variety of domains and binding sites for different interacting proteins (McCormick and Ellison, 2011; Gagnon and Delpire, 2012) (**Figure 2**). WNK1, WNK3, and WNK4 are expressed in a wide variety of tissues, such as heart, brain, lung, liver, muscle, kidney, testis, and colon, among others (Xu et al., 2000; Holden et al., 2004; Kahle et al., 2004; Vitari et al., 2005; Murillo-de-Ozores et al., 2018), while WNK2 is only expressed in brain, heart, and colon (Verissimo and Jordan, 2001) (**Table 2**).

The first evidence linking WNK kinases to the CCCs was the discovery of mutations in the genes *WNK1* and *WNK4* in Familial Hyperkalemic Hypertension (FHHT), also known as Pseudohypoaldosteronism type 2 (PHAII), or Gordon syndrome (Wilson et al., 2001). FHHT is mainly driven by overactivation of NCC in the distal nephron (Lalot et al., 2006; Grimm et al., 2017). Further studies showed that WNKs activate N(K)CCs and inhibit KCCs by phosphorylating and activating the downstream kinases SPAK and OSR1 (Moriguchi et al., 2005; Vitari et al., 2005; Alessi et al., 2014).

SPAK and OSR1 are two highly similar Ser/Thr kinases of the Ste20 family, that display wide tissue expression (extensively reviewed by Gagnon and Delpire, 2013) (**Table 2**). Initially, these kinases were shown to bind the CCCs by a yeast two-hybrid screen (Piechotta et al., 2002) and it was later shown

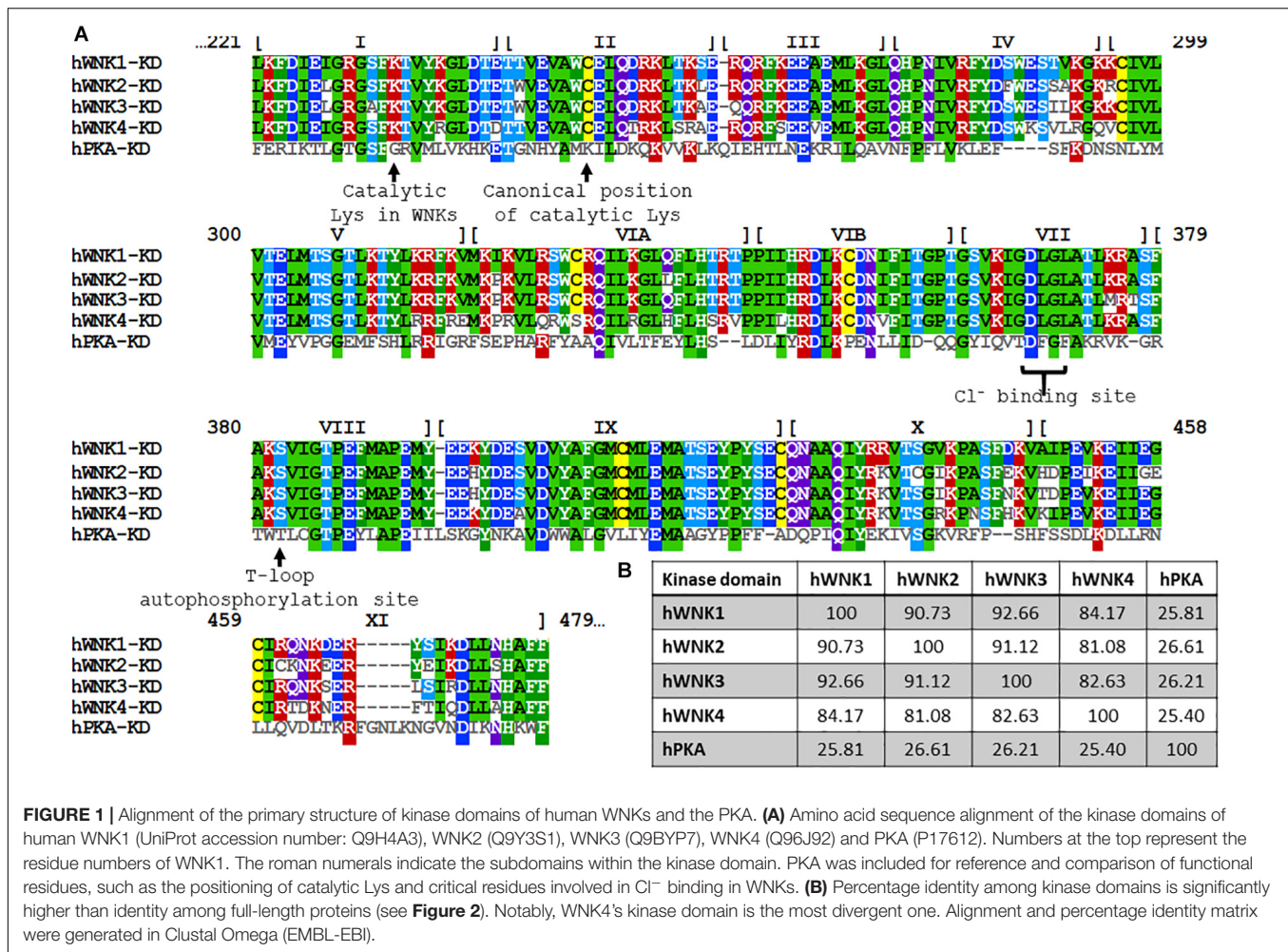


FIGURE 1 | Alignment of the primary structure of kinase domains of human WNKs and the PKA. **(A)** Amino acid sequence alignment of the kinase domains of human WNK1 (UniProt accession number: Q9H4A3), WNK2 (Q9Y3S1), WNK3 (Q9BYP7), WNK4 (Q96J92) and PKA (P17612). Numbers at the top represent the residue numbers of WNK1. The roman numerals indicate the subdomains within the kinase domain. PKA was included for reference and comparison of functional residues, such as the positioning of catalytic Lys and critical residues involved in Cl^- binding in WNKs. **(B)** Percentage identity among kinase domains is significantly higher than identity among full-length proteins (see **Figure 2**). Notably, WNK4's kinase domain is the most divergent one. Alignment and percentage identity matrix were generated in Clustal Omega (EMBL-EBI).

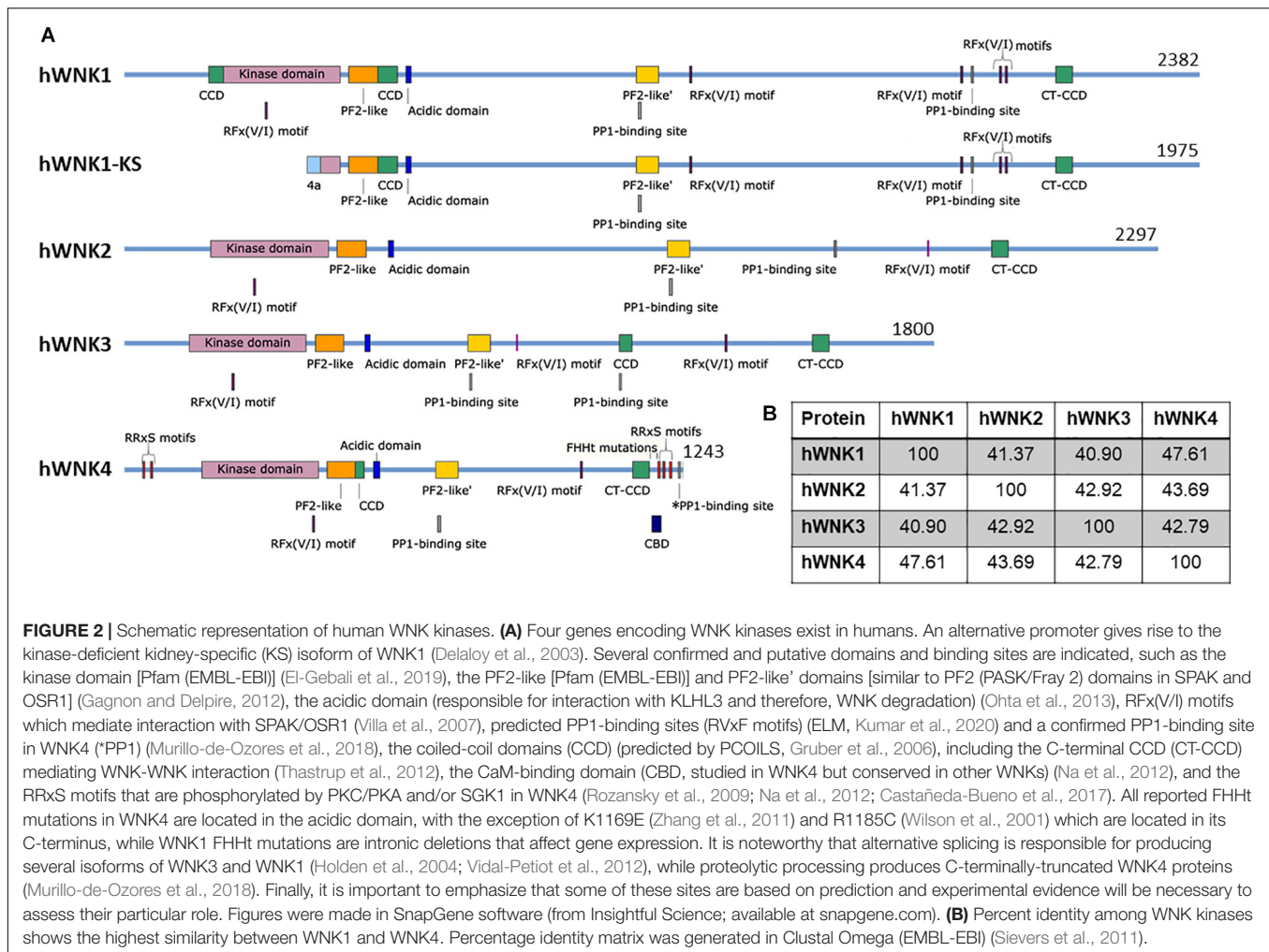
that they are responsible for direct phosphorylation of the CCCs (Dowd and Forbush, 2003; de los Heros et al., 2014). SPAK and OSR1 contain a domain called PF2 in their C-terminal region (also called CCT), that mediates binding with RFX(V/I) motifs in WNK kinases (Villa et al., 2007) and in CCCs (Piechotta et al., 2002). Accordingly, mice with a mutation in SPAK PF2 domain (L502A) display lower SPAK and CCCs phosphorylation levels (Zhang J. et al., 2015). Interestingly, it has been proposed that two regions with a similar tertiary structure exist in WNK kinases themselves (PF2-like and PF2-like') (Gagnon and Delpire, 2013). Mutation of PF2-like' in WNK4 prevents SPAK phosphorylation (Murillo-de-Ozores et al., 2018), and although the role of these regions is currently unknown, they might play a role in WNK binding with each other and/or with the CCCs (Moon et al., 2013).

WNKs as Cl^- -Sensing Kinases

The role of WNK kinases as Cl^- sensing proteins was suggested since their initial characterization. It was shown that the reduction in $[\text{Cl}^-]_i$ induced kinase autophosphorylation and activation (Moriguchi et al., 2005). Increased activation and phosphorylation of NKCC1, NKCC2, and NCC by lowering

$[\text{Cl}^-]_i$ also suggested that WNK kinases were likely modulated by $[\text{Cl}^-]_i$ (Breitwieser et al., 1990; Lytle and Forbush, 1996; Pacheco-Alvarez et al., 2006; Ponce-Coria et al., 2008).

Conclusive evidence that WNK kinases are Cl^- -sensitive proteins came from X-ray crystallography studies performed by Pinal et al. (2014). Crystallographic structure of the kinase domain of rat WNK1 showed the presence of a Cl^- anion bound directly to the kinase, specifically to the backbone amides of Gly370 and Leu371, located in the N-terminus of the activation loop, with additional hydrophobic interactions with Phe283, Leu299, Leu369, and Leu371 (a Cl^- binding pocket structurally similar to the one observed in CIC transporters). Direct Cl^- binding stabilizes a WNK1 inactive conformation, while decreased $[\text{Cl}^-]$ or mutation of the Cl^- binding site, by substituting Leu369 for a Phe (L369F), resulted in increased autophosphorylation and activation of WNK1 kinase. Interestingly, as the Cl^- binding site is located in the catalytic site of the kinase, it might overlap with the canonical positioning of the catalytic Lys in other kinases. Thus, the unique placement of this Lys in WNKs in subdomain I might permit Cl^- binding. Cl^- -sensitivity of WNK kinases seems to be a conserved regulatory mechanism, as it has been shown that Cl^- also inhibits



Drosophila melanogaster WNK (DmWNK) autophosphorylation (Sun et al., 2018).

Reports of WNK4 effect over NCC activity were initially discordant, because evidence showed inhibitory modulation *in vitro* (Wilson et al., 2003; Yang et al., 2003), while *in vivo* evidence pointed to WNK4 as an activator of NCC (Castaneda-Bueno et al., 2012). Later, it was described that this discrepancy could be explained by WNK4 regulation by $[Cl^-]_i$. Bazua-Valenti et al. (2015) showed that while WNK4 coexpression does not upregulate NCC in basal conditions in *Xenopus laevis* oocytes, decreasing $[Cl^-]_i$ promotes WNK4's activating phosphorylation and WNK4-mediated NCC activation. Mutation of the WNK4 Cl^- -binding site (L322F in human WNK4) turned it into a constitutively active kinase that upregulated NCC activity, even without Cl^- depletion. These series of experiments not only helped to understand the different effects of WNK4 over NCC function, but also confirmed WNK kinases as key Cl^- sensing proteins that regulate the activity of the CCCs.

Analysis of WNK1, WNK3, and WNK4 autophosphorylation upon Cl^- depletion in *X. laevis* oocytes (Bazua-Valenti et al., 2015), as well as *in vitro* kinase assays (Terker et al., 2015a) have suggested different Cl^- sensitivities for these three kinases.

While WNK1 and WNK4 autophosphorylation was increased by incubating oocytes in a hypotonic low Cl^- media, WNK3 phosphorylation was not affected by this maneuver as it was already phosphorylated in basal conditions (Bazua-Valenti et al., 2015). *In vitro* kinase assays, incubating the recombinant kinase domains of WNK1, WNK3, or WNK4 with their substrate SPAK in buffers with different $[Cl^-]$, showed that WNK4 was inhibited in a lower range of $[Cl^-]$ s than WNK1 or WNK3 (Terker et al., 2015a). Coexpression of NCC with Cl^- -insensitive mutants of WNK1 (L369F/L371F) and WNK4 (L322F/L324F) dramatically increased NCC phosphorylation when compared to pNCC levels in the presence of their wild type (WT) counterparts. However, WNK3 L295F/L297F did not affect NCC differently from WT WNK3 as this kinase is already active even in cells with high $[Cl^-]_i$ (~70 mM in HEK cells and ~55 mM in oocytes) (Bazua-Valenti et al., 2015; Terker et al., 2015a; Pacheco-Alvarez et al., 2020). These studies suggested that WNK3 activity is independent of $[Cl^-]_i$. Thus, although WNK3 can modify $[Cl^-]_i$ through the regulation of the CCCs, $[Cl^-]_i$ is not the main regulator of WNK3 activity, as we discuss below.

It is worth mentioning that there are some differences in the specific values of $[Cl^-]$ that inhibit WNK activity

TABLE 2 | Components of the WNK-SPAK/OSR1 pathway: associated genetic diseases, and phenotype of knockout models.

Gene	Protein	Tissue expression	Associated disease (inheritance pattern; effect on protein function)	Knockout mice phenotype
<i>STK39</i>	SPAK	Wide, including brain, adrenal gland, thymus, spleen, intestine, heart, kidney, testis, ovary, lung (Ushiro et al., 1998)	None found	Gitelman-like – low blood pressure, hypokalemia, hypocalciuria, hypomagnesemia, decreased NCC activity (Yang et al., 2010)
<i>OXS1</i>	OSR1	Ubiquitous (Tamari et al., 1999)	None found	Early embryonic lethality, similar to <i>WNK1</i> ^{-/-} mice (Xie et al., 2013)
<i>WNK1</i>	WNK1	Wide, including kidney, testis, heart, brain, spleen, muscle, lung, liver, pancreas, adipose tissue (Xu et al., 2000; Vitari et al., 2005)	Familial Hyperkalemic Hypertension (FHHT) (OMIM 614492) – hyperkalemia, hypertension, metabolic acidosis (autosomal dominant; gain of function) (Wilson et al., 2001) Hereditary Sensory and Autonomic Neuropathy type IIA (HSAN2A) (OMIM 201300) – reduced sensation to pain, temperature, and touch (autosomal recessive; loss of function) (Shekarabi et al., 2008)	Early embryonic lethality (Zambrowicz et al., 2003) due to cardiovascular developmental and placental defects (Xie et al., 2009)
<i>WNK2</i>	WNK2	Brain, heart and colon (Verissimo and Jordan, 2001)	None found	Not reported yet
<i>WNK3</i>	WNK3	Wide, including kidney, colon, heart, brain, muscle, lung, liver, pancreas, placenta (Holden et al., 2004)	None found	No obvious differences to littermate WT mice in basal conditions, low blood pressure in low Na ⁺ diet (Oi et al., 2012)
<i>WNK4</i>	WNK4	Wide, including kidney, testis, colon, heart, brain, spleen, lung, liver (Kahle et al., 2004; Murillo-de-Ozores et al., 2018)	Familial Hyperkalemic Hypertension (FHHT) (OMIM 614491) – hyperkalemia, hypertension, metabolic acidosis (autosomal dominant; gain of function) (Wilson et al., 2001) Hypokalemic periodic paralysis in <i>Felis catus</i> (OMIA 001759-9685) – skeletal muscle weakness with intermittent hypokalemia (autosomal recessive; loss of function) (Gandolfi et al., 2012)	Gitelman-like – normal blood pressure with increased renin activity, hypokalemic metabolic alkalosis, hypomagnesemia (Castaneda-Bueno et al., 2012)

(Piala et al., 2014; Terker et al., 2015a; Sun et al., 2018). Discrepancies could be due to the use of different substrates' phosphorylation as a surrogate for WNK activity (such as myelin basic protein, OSR1, SPAK, or WNK itself). Additionally, *in vitro* assays have been performed using only the kinase domain of WNK kinases, while it is possible that the N- and C-terminal regions could affect Cl⁻ sensitivity. However, *in vitro* experiments have served as proof of concept to demonstrate that the kinase activity of WNKs can be directly modulated by Cl⁻ binding. This phenomenon has more recently been corroborated *in vivo* in flies expressing a Cl⁻ insensitive DmWNK (L421F). DmWNK regulates K⁺-flux in the fly's Malpighian tubule and the DmWNK-L421F is more active than its WT counterpart (Sun et al., 2018). Moreover, Chen and collaborators generated mice with a Cl⁻ insensitive WNK4 (L319F/L321F). These mice display an altered renal phenotype, reminiscent of FHHT, as shall be explained in a later section, showing that WNK4 is indeed a physiological Cl⁻ sensitive protein (Chen et al., 2019).

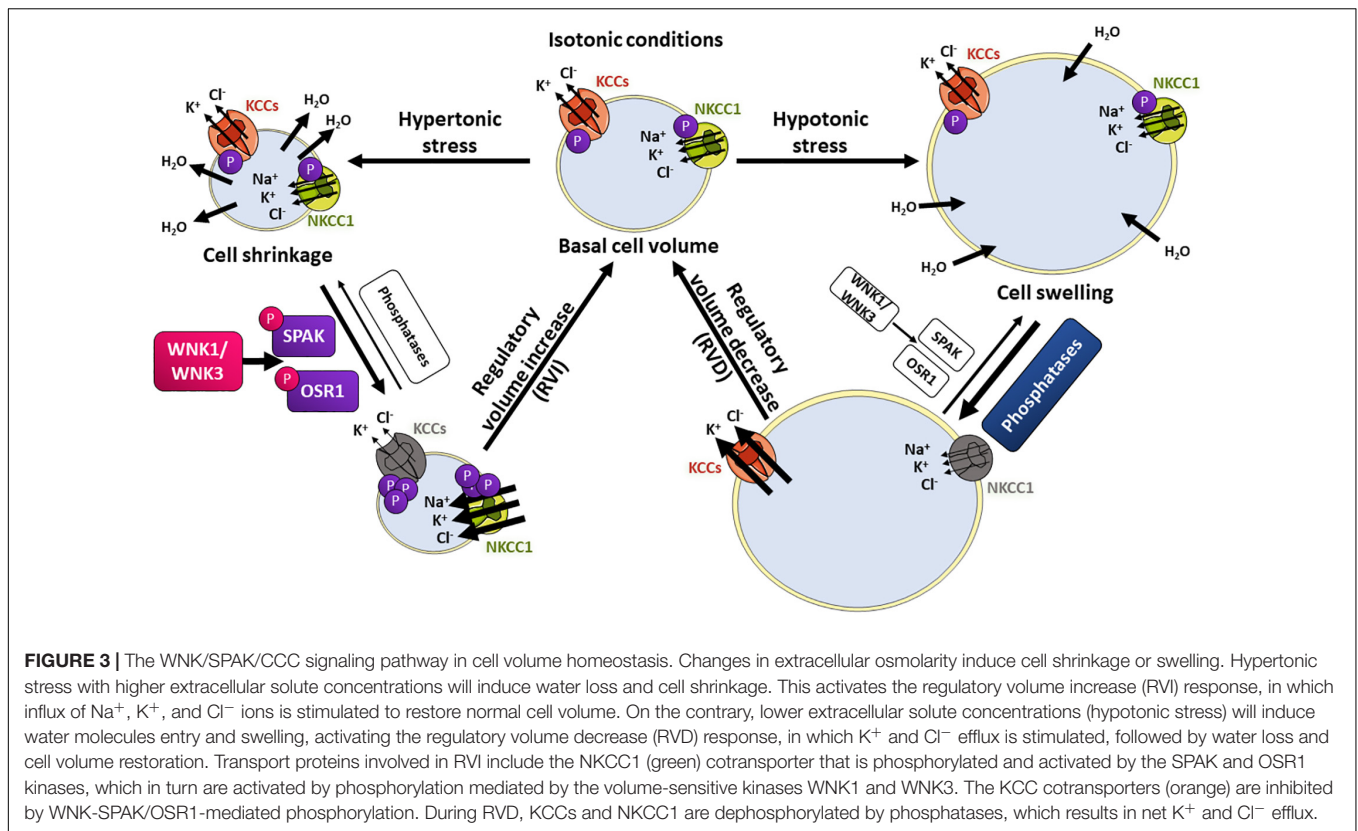
These recent findings related to WNKs regulation by [Cl⁻]_i are helping to elucidate how the WNK-SPAK/OSR1-CCC signaling pathway is involved in diverse physiological processes such as regulation of cell volume (Pacheco-Alvarez et al., 2020), potassium sensing and signaling in the renal distal convoluted tubule (Terker et al., 2015b), and differential neuronal response

to GABA (Alessi et al., 2014). These processes will be discussed in the following sections.

ROLE OF THE WNK-SPAK/OSR1-CCC PATHWAY IN CELL VOLUME REGULATION

Excluding bacterial and plant cells, all other cells are challenged constantly by changes in their volume due to differences in osmotic pressures between the intracellular and the extracellular milieu. Cell volume changes are proportional to the osmotic challenge they face. Water diffuses from the least concentrated solution to the more concentrated one, to equilibrate the osmotic pressure, causing cells to swell or shrink as osmotic balance is restored. However, basal cell volume must be promptly restored to minimize disruption of cellular functions and organization (Hoffmann et al., 2009).

When cells are exposed to hypotonic conditions, the resulting cell swelling triggers the regulatory volume decrease (RVD) response (Figure 3). The early phase of RVD involves activation of ion transporters that mediate K⁺ and Cl⁻ efflux. Water molecules will follow these ions until cell volume is restored. On the contrary, when cells are exposed to hypertonic conditions, cell



shrinkage triggers the regulatory volume increase (RVI) response, which involves intracellular solute accumulation causing the osmotic influx of water and the recovery to normal cell volume. Na^+ , K^+ , and Cl^- ions influx occurs in the early phase of this response (de los Heros et al., 2018; Delpire and Gagnon, 2018). Transport systems on the membrane are activated within seconds of volume deviation. Transport proteins involved in RVD include the K^+ - Cl^- cotransporters (KCCs), the volume-regulated Cl^- channel VRAC, as well as K^+ channels. For RVI, the main molecular players involved are the Na^+ - H^+ exchanger and the Na^+ - K^+ - 2Cl^- cotransporter (NKCC1) (Koivusalo et al., 2009). In this section we will focus on the mechanisms for CCCs' activation and deactivation during cell volume regulation.

As mentioned above, a key signaling event for modulation of CCCs in response to cell volume changes is the phosphorylation or dephosphorylation of specific residues in their N- and C-terminal tails. For instance, during cell swelling, dephosphorylation of conserved C-terminal threonine residues in KCCs induces their activation, while dephosphorylation of conserved N-terminal residues in NKCC1 inhibits its activity (Lytle and Forbush, 1992; Darman and Forbush, 2002; Rinehart et al., 2009). This results in increased K^+ - Cl^- efflux and decreased Na^+ influx, promoting water to follow ion movement. In contrast, during cell shrinkage, increasing phosphorylation of the above-mentioned sites, results in NKCC1 activation and KCCs inhibition, and thus, increased Na^+ , K^+ , and Cl^- influx, with the consequent influx of water that follows. This reciprocal regulation has led to propose the existence of a volume-sensing

enzyme cascade that regulates both NKCCs and KCCs in opposite ways. The identity of the sensors and transducers have been studied and examined, and the WNK-SPAK/OSR1 signaling cascade has emerged as the cascade involved in such regulation, with protein phosphatases playing also an essential regulatory role (de Los Heros et al., 2006; Zagórska et al., 2007; Pacheco-Alvarez et al., 2020).

***In vitro* Evidence of WNK1's Role in Cell Volume Regulation**

Different groups have shown that WNK1 activity is stimulated by hypertonic stress. For instance, Xu et al. (2000) and Zagórska et al. (2007) showed that WNK1 immunoprecipitated from HEK293 cells grown in hypertonic media displayed higher levels of autophosphorylation and higher ability to phosphorylate OSR1, respectively. Hypertonic stress promoted WNK1 autophosphorylation at S382, the T-loop's residue, an event that promotes kinase activation (Xu et al., 2002; Zagórska et al., 2007). Hypertonic stress has also been shown to promote activation of SPAK and OSR1 in cellular models (Chen et al., 2004; Anselmo et al., 2006; Zagórska et al., 2007). Such activation correlates with kinases' phosphorylation at activating sites targeted by WNK kinases (T-loop and S-motif sites). Additionally, siRNA-mediated WNK1 depletion in HeLa cells has been shown to partially prevent sorbitol-induced phosphorylation and activation of SPAK and OSR1 (Zagórska et al., 2007), suggesting that WNK1 activation in these cells is at least partially responsible for SPAK/OSR1 activation.

Regarding the mechanisms implicated in the modulation of WNK1 activity by hyperosmotic stress, it is interesting to note that Zagórska et al. (2007) observed that the truncated 1-667 WNK1 protein retained the ability of becoming activated by this stimulus, suggesting that the domain or domains involved in kinase activation are located within this region. In a more recent work, Naguro et al. (2012) showed that the MAP3K apoptosis signal-regulated kinase 3 (ASK3) is an osmotic stress-sensitive protein that can bind WNK1 and regulate its T-loop's phosphorylation. More specifically, they showed that ASK3 becomes phosphorylated and activated when stimulated by hypotonic stress and inhibited by hypertonic stress. They also showed that, when activated by hypotonicity, ASK3 inhibits WNK1 autophosphorylation, because in ASK3 depleted cells, but not in control cells, an increase in WNK1-mediated OSR1 phosphorylation was observed when the cells were subjected to hypotonic stimulation. Given that hypotonic stress promotes $[Cl^-]_i$ reduction, for example, via activation of the VRAC Cl^- channel, an appealing hypothesis is that ASK3 may be important for preventing Cl^- depletion-induced WNK1 activation under this condition.

In vitro Evidence of WNK3's Role in Cell Volume Regulation

As it was discussed previously, among the WNK family, WNK1 and WNK4 are sensitive to $[Cl^-]_i$, while WNK3 constitutes the non- Cl^- -sensitive member of the family and it might function as a cell volume-sensitive kinase. Indeed, WNK3 has shown unique biochemical and functional regulatory properties over the CCCs that have led to propose this protein as possible candidate for the volume sensor kinase. Initial characterization of WNK3 in 2005 performed in *Xenopus laevis* oocytes showed that WNK3 is a potent activator of NKCC1, NKCC2, and NCC, and an inhibitor of KCCs. In contrast, a catalytically inactive version of WNK3 (WNK3-KD) had opposite effects, most likely due to dominant negative effects on the endogenous WNK-SPAK/OSR1 cascade (Kahle et al., 2005; Rinehart et al., 2005; de Los Heros et al., 2006). No other WNK kinase has been shown to possess the ability to regulate all N(K)CCs and KCCs in such manner. It was also shown that WNK3 regulation of KCCs function, depend on phosphatase activity. By using phosphatase inhibitors, protein phosphatase 1 and 2B were proposed to be involved in the signaling pathway.

Experiments performed in HEK293 cells showed that WNK3 has a direct effect on the RVD and RVI volume compensatory mechanisms in mammalian cells. Cruz-Rangel et al. (2012) observed that cells that overexpress WNK3, achieved through stable transfection, showed less efficient RVD, which correlated with lower KCC activity and decreased Cl^- efflux. In contrast, cells overexpressing WNK3-KD showed more efficient RVD, as well and higher KCC activity and Cl^- efflux. Later on, in 2016, Zhang and coworkers used a combination of screening methods (kinome wide siRNA-screens, kinase inhibitor screen, and a kinase trapping- Orbitrap mass spectrometry screen) that allowed them to identify the major endogenous WNK kinase responsible for stimulating basal KCC3 C-terminal

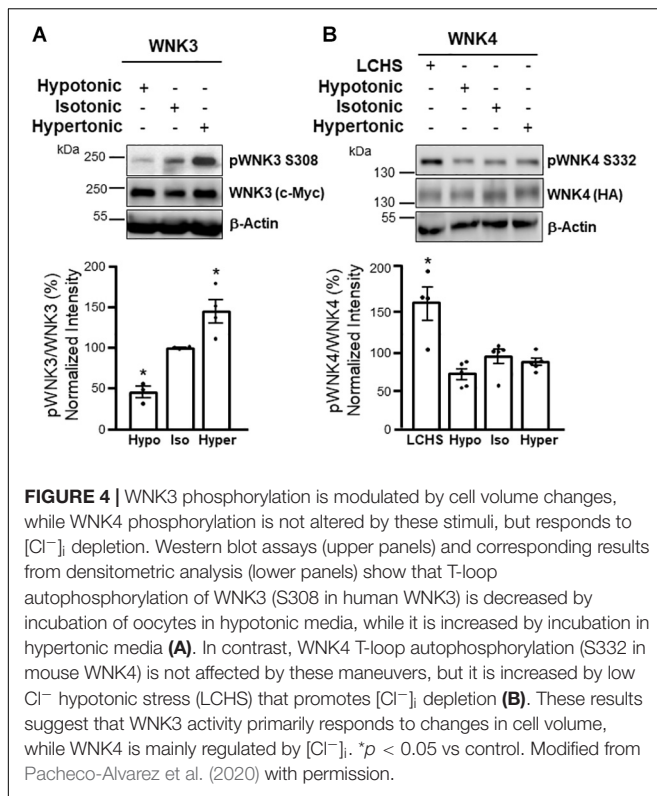
phosphorylation (T991 and T1048) in HEK293 cells (Zhang et al., 2016). WNK3 was identified in all three screening methods, suggesting that WNK3 basal activity is high in these cells. Subsequent targeted knockout experiments in the same model showed that not only WNK3 knockout, but also WNK1 knockout decreased KCC3 and NKCC1 phosphorylation in this model. They showed that HEK293 cells expressing KCC3 and transiently transfected with wild type WNK3 swelled under hypotonic stimulation, while expression of WNK3-KD prevented hypotonic swelling. This effect of WNK3-KD overexpression was reversed in the presence of the KCCs inhibitor furosemide, revealing that increased KCC activity was responsible for the more efficient RVD response in these cells. Finally, treatment of cells expressing wild type WNK3 with the SPAK/OSR1 inhibitor STOCK1S-50699, also prevented cells from swelling under hypotonic stress, demonstrating that inhibition of the WNK3-SPAK/OSR1 pathway promoted RVD. These experiments established the WNK3-SPAK/OSR1 complex as an integral component of the Cl^- /volume sensitive kinase system regulating the CCCs.

More recently, using the *X. laevis* oocytes heterologous expression system we have shown that WNK3 activity towards NCC is not affected neither by changes in $[Cl^-]_i$, nor by eliminating the putative Cl^- binding sites on the kinase (Pacheco-Alvarez et al., 2020). Instead, the activating phosphorylation of WNK3's T-loop, is modulated by changes in extracellular osmolarity (increased by hypertonicity and decreased by hypotonicity), whereas phosphorylation of WNK4 in the homologous residue is not affected by such stimuli (Figure 4). In contrast, WNK4 T-loop phosphorylation is stimulated by $[Cl^-]_i$ depletion. This supports the hypothesis that, at least toward the CCCs, while WNK4 and WNK1 are the Cl^- sensitive kinases, WNK3 is instead involved in volume-sensing. Key questions that remain open are whether this kinase can act as the actual cellular osmosensor or whether it is regulated instead by another protein with such activity. Also, whether WNK3 activity modulation by cell volume could also affect other players in the RVI or RVD response remains to be determined.

The Activity of the WNK3-SPAK/OSR1-CCC Pathway Is Altered in Cerebral Edema in Rodent Models

In vivo model experiments analyzed the role of the WNK3-SPAK/OSR1-CCC complex in cerebral edema, a condition where volume homeostasis of brain cells is disrupted. It is worth mentioning that increased glial cell volume is the major contributor to cerebral edema, given that in the mammalian brain glia outnumber neurons and also because glia, unlike neurons, express aquaporins that render them more vulnerable to osmotic stress (Kahle et al., 2015). NKCC1 and KCC3 are highly expressed in astrocytes where they participate in cell volume regulation (Pearson et al., 2001; Su et al., 2002).

Middle cerebral artery occlusion (MCAO) was performed to produce brain ischemia, a maneuver that induces cerebral edema, in wild type (WT), WNK3^{-/-}, and SPAK^{-/-} mice



(Begum et al., 2015; Zhang et al., 2016; Zhao et al., 2017). In comparison to WT mice, WNK3^{-/-} and SPAK^{-/-} mice showed reduced cerebral edema and infarct volume after MCAO, as well as less demyelination and faster neurobehavioral recovery. Phosphorylation levels of KCC3 and NKCC1 in brain homogenates of WNK3^{-/-} mice after brain ischemia were decreased compared to those in wild type mice (Begum et al., 2015; Zhang et al., 2016). It was suggested that these effects on CCCs phosphorylation could account for the decreased cerebral edema and other improved outcomes. Supporting the key role of SPAK in the regulation of NKCC1, KCC2, and KCC3 activity in brain tissue, it was shown that SPAK-CCT domain knock-in mice (SPAK^{L502A/L502A}), in which SPAK is unable to bind CCCs, have lower levels of phosphorylated NKCC1, KCC2, and KCC3 in brain homogenates. Co-immunoprecipitation experiments of KCC3 with SPAK performed with brain lysates of these mice confirmed that the KCC3-SPAK interaction is disrupted. Therefore, these results place the WNK3-SPAK complex as a “volume sensor-transducer” in mammalian brain that regulates CCC activity to achieve volume homeostasis.

REGULATION OF RENAL Na-Cl COTRANSPORTER (NCC) IN RESPONSE TO CHANGES IN EXTRACELLULAR K⁺ CONCENTRATION

The fine tuning of urinary Na⁺ and K⁺ excretion takes place within the mammalian distal nephron of which the distal

convoluted tubule (DCT) is the very first segment. The DCT actively participates in Na⁺, Ca²⁺, and Mg²⁺ reabsorption, and thus, its activity has an impact on blood pressure, Ca²⁺ and Mg²⁺ homeostasis. NCC constitutes the apical entry pathway for Na⁺ and Cl⁻ to DCT cells and its activity is the rate-limiting step for NaCl reabsorption in this segment. In addition, even though no net K⁺ reabsorption or secretion occurs in the DCT, NCC activity has an important impact on renal K⁺ handling, and thus, renal K⁺ excretion (Subramanya and Ellison, 2014; Bazúa-Valenti et al., 2016). This is evidenced by the phenotype displayed by patients with Gitelman’s syndrome, a genetic disease caused by inactivating mutations in the *SLC12A3* gene that encodes NCC (Simon et al., 1996b). Patients present with hypotension, hypocalciuria, and hypomagnesemia, but also, one of the most notable features is renal K⁺ loss and hypokalemia. NCC activity affects renal K⁺ handling by indirectly affecting the activity of the secretory K⁺ apparatus of the aldosterone sensitive distal nephron (ASDN) comprised by the connecting tubule and the cortical collecting duct. In these segments aldosterone drives K⁺ secretion by stimulating the concerted action of apical epithelial Na⁺ channels (ENaC) and Renal Outer Medullary K⁺ channels (ROMK). Electrogenic Na⁺ reabsorption via ENaC generates a lumen-negative transepithelial potential that drives K⁺ secretion via ROMK. Big K⁺ (BK) channels are also important contributors to K⁺ secretion under certain conditions (Meneton et al., 2004; Murillo-de-Ozores et al., 2019). The mechanisms explaining NCC’s impact on K⁺ secretion by the ASDN are currently controversial. It was initially thought that, by affecting distal Na⁺ delivery, NCC activity could impact on ENaC’s activity, and thus K⁺ secretion. However, some recent works have failed to confirm this mechanism, and instead, recent data point out to a more complex interaction that involves remodeling of distal tubule segments (Hunter et al., 2014; Grimm et al., 2017).

Whichever the mechanism, the importance that NCC plays on modulation of renal K⁺ excretion is evidenced by the fact that physiological mechanisms exist to modulate NCC activity in response to changes in dietary K⁺ intake. NCC activity, assessed by measuring activating phosphorylation (Pacheco-Alvarez et al., 2006), increases in mouse models subjected to low K⁺ diets and decreases in mouse models subjected to high K⁺ diets (Vallon et al., 2009; Sorensen et al., 2013; Castaneda-Bueno et al., 2014; Terker et al., 2015a). When this mechanism is broken, alterations in K⁺ homeostasis occur, like it is observed in Gitelman’s syndrome, caused by loss of function of NCC, or in Familial Hyperkalemic Hypertension (FHHt), which appears to be mainly caused by overactivation of NCC (Wilson et al., 2001; Lalioti et al., 2006). As the disease name indicates, FHHt patients present hypertension with hyperkalemia, as well as hyperchloremic metabolic acidosis. FHHt-causative mutations do not occur in the *SLC12A3* gene, but in genes encoding proteins that participate in the regulation of NCC activity. These genes include, as previously discussed, two that encode the WNK kinases WNK1 and WNK4 (Wilson et al., 2001), and two more (*CUL3* and *KLHL3*) that encode components of a protein complex with ubiquitin ligase activity that regulate WNK1 and WNK4 ubiquitylation and degradation (Boyden et al., 2012; Louis-Dit-Picard et al., 2012;

Ohta et al., 2013; Shibata et al., 2013; Wakabayashi et al., 2013).

The regulation of $[Cl^-]_i$ in DCT cells is a key part of the signaling mechanism that mediates regulation of NCC in response to the subtle changes in extracellular K^+ concentration ($[K^+]_e$) resulting, for example, from variations in dietary K^+ content. As explained below in detail, expression of a specific subset of monovalent ion channels in the basolateral membrane of these cells allows translating changes of extracellular K^+ levels into changes in membrane potential that in turn drive Cl^- fluxes that alter $[Cl^-]_i$ (Terker et al., 2015b). Such fluctuations in $[Cl^-]_i$ are sensed by the Cl^- sensitive WNK4, the master regulator of the signaling cascade involved in the regulation of NCC (Figure 5). In this section we describe the molecular players involved in this relatively novel signaling mechanism, as well as an overview of the *in vitro* and *in vivo* evidence that has been key for the description of this pathway.

Direct Effects of Plasma K^+ on DCT's $[Cl^-]_i$ and NCC Activity

A decrease in NCC phosphorylation (pNCC) levels can be observed within 15 minutes after an acute K^+ oral load. This effect parallels the rise in plasma K^+ levels and precedes the rise in plasma aldosterone and activation of ENaC. Interestingly, the rapid natriuresis and kaliuresis induced by the K^+ load seem to be dependent on the inhibition of NCC, because they are not observed in NCC^{-/-} mice (Sorensen et al., 2013). Decreased pNCC levels are also observed in mice in which hyperkalemia is induced pharmacologically by treatment with amiloride (Terker et al., 2015b) or in genetic mouse models with hyperkalemia, like in mice with specific deletion of ENaC subunits in the nephron (Perrier et al., 2016; Boscardin et al., 2017, 2018). Conversely, in rodent models with hypokalemia, e.g., in hyperaldosteronism models, NCC activation is observed (Kim et al., 1998; Terker et al., 2016). Finally, it has been shown by Terker et al. (2015a) that, across physiological levels of $[K^+]_e$, a linear correlation is observed between pNCC levels and $[K^+]_e$, and that subtle changes occur in $[K^+]_e$ in response to modest changes in dietary K^+ content, that are responsible for variations in pNCC observed.

Terker et al. (2015b) based on experiments performed in HEK293 cells, proposed that changes in $[K^+]_e$ modulate pNCC by inducing changes in the $[Cl^-]_i$, that in turn affect the activity of the WNK-SPAK/OSR1 pathway. The physiological relevance of this model was supported by *ex vivo* experiments performed by Penton et al. (2016) in which isolated mice kidneys were perfused or mouse kidney slices were incubated with solutions containing variable $[K^+]_e$. They confirmed that the $[K^+]_e$ has a direct effect on pNCC levels in the DCT. Moreover, such effects were not observed when changes in $[Cl^-]_i$ were prevented. Finally, they showed that whereas the activation of NCC on low $[K^+]_e$ is completely Cl^- -dependent, Cl^- -independent mechanisms also exist for the high $[K^+]_e$ -induced dephosphorylation of NCC.

Kir4.1/5.1 Heterotetramers

Recent works support the idea that K^+ channels formed by Kir4.1/5.1 heterotetramers are key for the direct sensing of

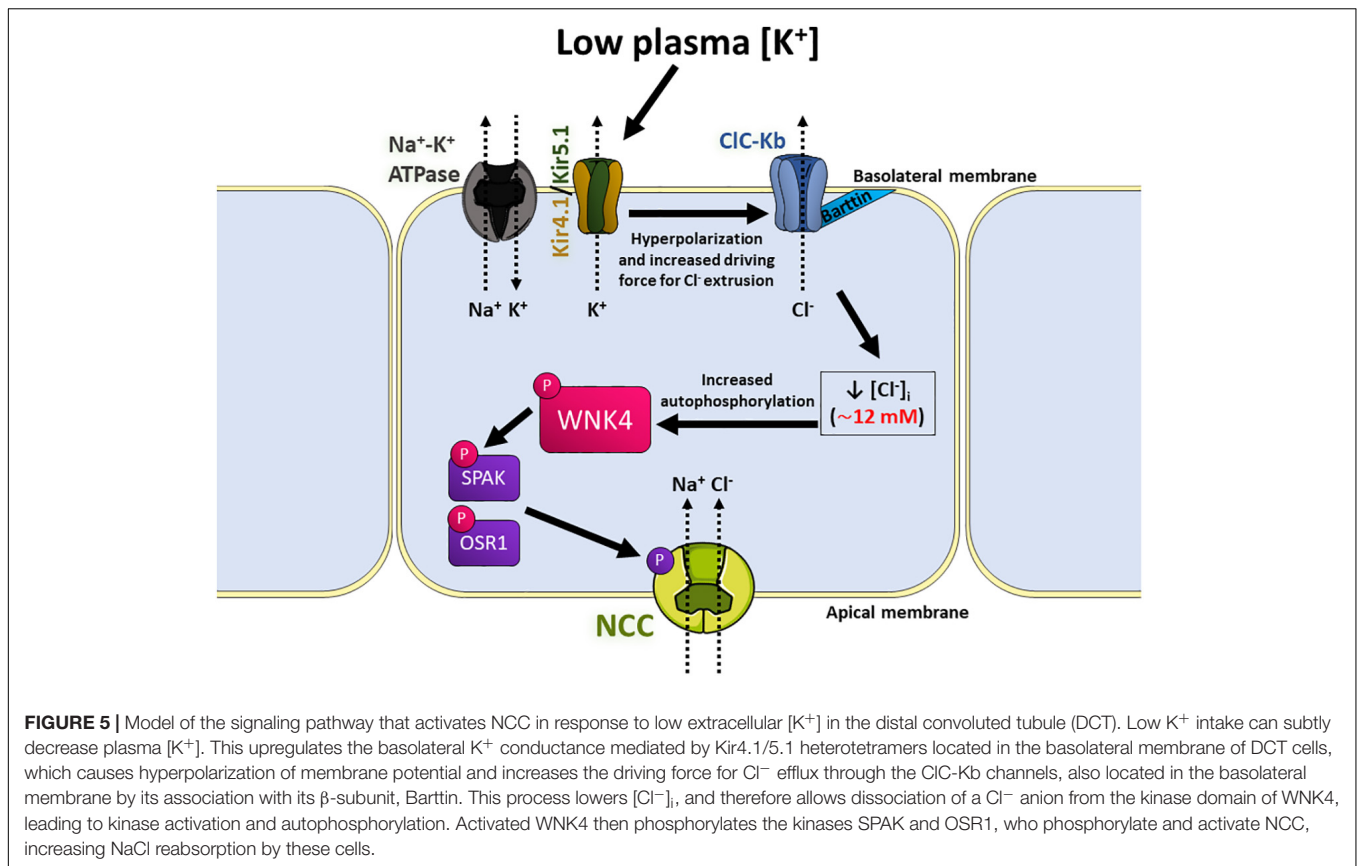
extracellular $[K^+]_e$ by DCT cells. Inwardly rectifying K^+ (Kir) channels are formed by homo- or hetero-tetramers, where each subunit is composed of two transmembrane regions with amino- and carboxyl-terminal regions located in the cytoplasm. These channels are expressed in a wide variety of cell types and are responsible for different functions (extensively reviewed by Hibino et al. (2010), one of which is the maintenance of resting membrane potential (Su and Wang, 2016).

In mouse microdissected DCT tubules, basolateral inwardly rectifying K^+ channels identified as Kir4.1/5.1 heterotetramers were characterized by patch-clamp experiments (Lourdel et al., 2002; Zhang et al., 2014), and the expression of these channels was confirmed by RT-PCR (Lourdel et al., 2002). Immunostaining assays have also shown basolateral localization of Kir4.1 (Bockenhauer et al., 2009; Zhang et al., 2014; Cuevas et al., 2017) and Kir5.1 (Tucker et al., 2000; Zhang C. et al., 2015) in the DCT, and proteomic data from microdissected tubules from rats shows high levels of Kir4.1 and Kir5.1 in the DCT (Limbutara et al., 2020). Coincidentally, *in vivo* interaction between Kir4.1 and Kir5.1 was first found in kidney samples (Tanemoto et al., 2000).

The activity of these channels is key for DCT function. In humans, loss of function mutations in the gene *KCNJ10* (encoding Kir4.1) are the cause of EAST/SESAME (epilepsy, ataxia, sensorineural deafness, and renal tubulopathy/seizures, sensorineural deafness, ataxia, mental retardation, and electrolyte imbalance) syndrome (Bockenhauer et al., 2009; Scholl et al., 2009), a complex disease characterized, among other manifestations, by hypokalemic metabolic alkalosis, hypomagnesemia, and hypocalciuria, a phenotype reminiscent of Gitelman syndrome. Accordingly, Kir4.1 global knockout mice have reduced levels of NCC (Zhang et al., 2014). As these mice display early lethality, mice with reduced Kir4.1 expression in the kidney (Malik et al., 2018) and kidney-specific-knockout mice (Cuevas et al., 2017) have also been generated and they also display decreased levels of expression and activity of NCC. DCT atrophy is also observed (Saritas et al., 2018).

Evidence supporting the role of the Kir4.1/5.1 heterotetramer in the establishment of membrane potential of DCT cells and its modulation by changes in $[K^+]_e$ include the following. Genetic disruption of *Kcnj10* in mice abolishes the basolateral K^+ conductance of DCT cells and promotes depolarization (Zhang et al., 2014; Cuevas et al., 2017). NCC regulation by changes in dietary K^+ content is completely blunted in kidney-specific-Kir4.1^{-/-} mice (Cuevas et al., 2017; Wang et al., 2018). Additionally, the activity of Kir4.1/Kir5.1 channels in the DCT has been shown to be modulated by $[K^+]_e$, as hyperpolarization and higher basolateral K^+ conductance is observed in the DCTs of mice on low K^+ diet. In contrast, high K^+ intake decreases basolateral K^+ currents and depolarizes DCT cells. These phenomena are not observed in cells from kidney-specific Kir4.1^{-/-} mice (Wang et al., 2018). All these findings together have led to the proposal of naming Kir4.1 as the 'potassium sensor' of the kidney.

Kir4.1 absence is not compensated by Kir5.1, as this latter subunit alone does not seem to form functional channels on the cell membrane (Pessia et al., 1996; Tanemoto et al., 2005). However, Kir5.1 does play an important role in establishing



the sensitivity to $[K^+]_e$ of DCT cells. The phenotype of Kir5.1^{-/-} mice differs from that of Kir4.1^{-/-} mice. Mice lacking Kir5.1 have higher NCC activity, measured as thiazide-sensitive natriuresis (Paulais et al., 2011), and total and phosphorylated NCC levels (Wu et al., 2019). The DCT cells of these mice display higher basolateral K^+ conductance and hyperpolarization compared to DCT cells of WT mice. Regulation of DCT basolateral K^+ conductance and levels of pNCC and NCC in response to changes in dietary K^+ content was impaired in Kir5.1^{-/-} mice (Wu et al., 2019).

Kir4.1/5.1 heterotetramers have different properties to Kir4.1 homotetramers (Pessia et al., 1996), such as increased intracellular pH sensitivity, as demonstrated by *in vitro* (Tanemoto et al., 2000; Tucker et al., 2000) and *ex vivo* experiments (Paulais et al., 2011). It has been suggested that decreased sensibility of Kir4.1 homotetramers to inhibition by H^+ ions may explain the higher DCT basolateral K^+ conductance of DCT cells on Kir5.1^{-/-} mice (Paulais et al., 2011).

CIC-Kb and Its β -Subunit, Barttin

The CIC family comprises nine genes that encode four plasmalemmal Cl^- channels (CIC-1, -2, -Ka and -Kb) and five intracellular Cl^-H^+ antiporters (CIC-3 to -7) (reviewed extensively by Jentsch and Pusch, 2018). CIC proteins assemble into homodimers, where each subunit mediates ion movement across the membrane.

CIC-Ka and CIC-Kb channels display different characteristics to the rest of the family, as they lack the 'gating glutamate' present in other family members and therefore, their voltage dependence is nearly ohmic (Waldegger and Jentsch, 2000). This allows them to mediate transmembrane movement of Cl^- over a wide range of membrane voltages, permitting the constant transepithelial transport of Cl^- (Jentsch and Pusch, 2018). Additionally, both CIC-Ka and CIC-kB require the presence of the β -subunit Barttin (Estévez et al., 2001), which acts like a chaperone that promotes localization of these channels in the plasma membrane (Waldegger et al., 2002).

In the kidney, CIC-Ka and -Kb channels play a prominent role. Both, human CIC-Ka (named CIC-K1 in mouse and rat) and CIC-Kb (CIC-K2 in mouse and rat) were initially identified and cloned from kidney (Kieferle et al., 1994), although their expression (as well as Barttin's) is also observed in epithelial cells of the inner ear (Estévez et al., 2001). While the main site of expression of CIC-Ka in the kidney is the thin ascending limb of Henle's loop, where it plays a role in urine concentration (Matsumura et al., 1999), CIC-Kb is primarily expressed in the basolateral membrane of the thick ascending limb of Henle's loop (TAL), DCT, and α -intercalated cells of the ASDN, as shown by RT-PCR (Vitzthum et al., 2002), immunostaining (Hennings et al., 2017), and proteomics (Limbutara et al., 2020).

Loss of function mutations in *CLCNKB* (which encodes CIC-Kb) and *BSND* (encoding Barttin) are the cause of Bartter syndrome type III (Simon et al., 1997) and type IV (Birkenhager

et al., 2001), respectively (see SLC12 section). These types of Bartter often share characteristics with Gitelman's syndrome, such as normo- or hypocalciuria and blunted response to thiazides (Konrad et al., 2000; Seyberth and Schlingmann, 2011; Cruz and Castro, 2013). This suggests that ClC-Kb and Barttin activities are not only relevant for NKCC2-mediated salt reabsorption in the TAL, but also for NCC-mediated salt reabsorption in the DCT.

Patch-clamp assays performed in microdissected tubules from ClC-K2^{-/-} mice have shown that ClC-K2 constitutes the main basolateral Cl⁻ conductance of TAL and DCT cells. Accordingly, ClC-K2^{-/-} mice have a Bartter type III-like phenotype with severe renal salt and potassium wasting. Furosemide-sensitive, as well as thiazide-sensitive NaCl transport are completely abolished (Grill et al., 2016; Hennings et al., 2017). Decreased levels of total and phosphorylated NCC are also observed (Hennings et al., 2017). While global Barttin^{-/-} mice die a few days after birth because of severe dehydration (Rickheit et al., 2008), hypomorphic mice for Barttin (with low expression levels of a mutated Barttin) are able to thrive and recapitulate a phenotype similar to Bartter syndrome type IV (Nomura et al., 2011). Interestingly, in baseline conditions these mice have similar levels of NCC expression and phosphorylation to WT mice, despite being hypokalemic and hypovolemic, which suggests impaired physiological response of the DCT (Nomura et al., 2018).

As explained in the previous section, changes in [K⁺]_e regulate the membrane potential of the DCT, thanks to the basolateral expression of Kir4.1/5.1 channels. This affects the driving force for Cl⁻ movement through ClC-Kb channels, as suggested by the reduced basolateral Cl⁻ conductance observed in Kir4.1^{-/-} mice (Zhang et al., 2014). Therefore, low [K⁺]_e promotes hyperpolarization, which increases Cl⁻ efflux and decreases [Cl⁻]_i, whereas, increased [K⁺]_e promotes depolarization, lowers Cl⁻ efflux, and increases [Cl⁻]_i (Terker et al., 2015b; Murthy and O'Shaughnessy, 2019). As explained previously in detail, [Cl⁻]_i is an important regulator of the WNK4-SPAK/OSR1 signaling pathway, which ultimately regulates NCC activity. The importance of [Cl⁻]_i as a second messenger that responds to changes in [K⁺]_e and translates them into modulation of NCC activity has been demonstrated *in vivo*, for example, by showing that hypomorphic Barttin mice do not upregulate NCC in the face of decreased K⁺ intake (Nomura et al., 2018).

WNK4

In mice and humans, mutations in *WNK4* that cause kinase overexpression are the cause of Familial Hyperkalemic Hypertension (FHHt), a disease that is mainly the consequence of the upregulation of NCC activity (Wilson et al., 2001; Lalioti et al., 2006; Yang et al., 2007; Shibata et al., 2013). *WNK4* expression has been reported in different tissues (Kahle et al., 2004; Murillo-de-Ozores et al., 2018) and in different renal cell types (Ohno et al., 2011), although in some reports definitive proof of antibody's signal specificity by comparison with *WNK4*^{-/-} samples was lacking. The strictly renal origin of the FHHt phenotype suggests that absence of *WNK4* activity in

extrarenal tissues can be compensated probably by the activity of other WNK kinases.

Within the DCT *WNK4* appears to be the major active WNK kinase. Recent evidence suggests that under basal, physiologic conditions *WNK4* and *KS-WNK1* (the truncated, kinase inactive version of *WNK1*) are probably the only WNK kinases expressed in DCT cells. Thus, *WNK4* is the only WNK kinase that can phosphorylate *SPAK* and *OSR1* in these cells. For instance, in *WNK4*^{-/-} mice NCC phosphorylation levels are completely ablated and a Gitelman-like syndrome is developed (Castaneda-Bueno et al., 2012). Accordingly, immunofluorescent staining using an antibody that detects phosphorylation at the S-motif serine of all WNK kinases shows that no signal is observed in kidney sections from *WNK4*^{-/-} mice (Thomson et al., 2020). This suggests that the catalytically active WNK in DCT is *WNK4* and that no other catalytically active WNK kinase becomes activated to compensate for its absence. Additionally, in mice carrying the FHHt mutation R528H in *KLHL3* that prevents WNK degradation, knocking down *WNK4* completely impairs NCC phosphorylation, even when *WNK1* expression levels observed in Western blot (probably *KS-WNK1* in DCT and perhaps *L-WNK1* in other nephron segments) remain upregulated (Susa et al., 2017).

WNK4 is also essential for low K⁺-mediated activation of NCC. No upregulation of NCC phosphorylation is observed in *WNK4*^{-/-} mice (Castaneda-Bueno et al., 2014; Yang et al., 2018) and, consequently, mice develop severe hypokalemia when maintained on a low K⁺ diet (Castaneda-Bueno et al., 2014).

DCT's [Cl⁻]_i has been estimated to be relatively low, ranging between 10 and 20 mM (Beck et al., 1988; Boettger et al., 2002; Weinstein, 2005; Terker et al., 2015b). Works by Bazua-Valenti et al. (2015) and Terker et al. (2015a) have shown that *WNK4* is more sensitive to inhibition by Cl⁻ than its related kinases *WNK1* and *WNK3*. In *in vitro* kinase assays performed by Terker et al. (2015a) it was shown that *WNK4* activity was inhibited even by the lowest [Cl⁻] tested which was 10 mM, whereas inhibition of *WNK1* and *WNK3* only began to be observed when [Cl⁻] reached 112 and 150 mM, respectively. These observations indicate that indeed *WNK4*'s Cl⁻ sensitivity lies within the range observed for [Cl⁻]_i in the DCT, and thus, makes it the appropriate WNK to be expressed in this cell type to allow modulation of WNK activity in response to changes in [Cl⁻]_i.

As mentioned before, mutations in the Cl⁻ binding domain of WNK kinases (L369F/L371F and L322F/L324F mutations in human *WNK1* and human *WNK4*, respectively) make them insensitive to Cl⁻ and constitutively active (Piala et al., 2014; Bazua-Valenti et al., 2015; Terker et al., 2015a). Introduction of these mutations in a genetic mouse model has provided the definitive proof that under basal conditions *WNK4* is indeed inhibited by Cl⁻ within DCT cells, because these mice display increased NCC phosphorylation and an FHHt-like phenotype (Chen et al., 2019). Interestingly, administering a low K⁺ diet or an acute K⁺ load by oral gavage did not promote the expected increase or decrease, respectively, in NCC phosphorylation levels, supporting the idea

that modulation of WNK4 kinase activity by intracellular Cl^- is behind the signaling mechanism implicated in such regulation.

SPAK and OSR1

In cultured HEK293 cells, incubation with low $[\text{K}^+]_i$ media promotes an increase in pSPAK/OSR1 levels. This increase is secondary to the intracellular Cl^- depletion that is induced by low $[\text{K}^+]_e$ (Terker et al., 2015b). In mice, dietary K^+ restriction induces an increase in renal SPAK/OSR1 phosphorylation levels. In DCT, apical localization of SPAK, OSR1, and pSPAK/OSR1 increases, as well as localization in cytoplasmic puncta (WNK bodies) whose formation is induced in conditions that promote pathway activation (Thomson et al., 2020). The increase in renal pSPAK/OSR1 is also observed when kidney slices are incubated on a low $[\text{K}^+]_i$ medium, suggesting that a direct effect of extracellular $[\text{K}^+]_i$ on DCT cells is implicated (Penton et al., 2016).

SPAK^{-/-} mice and SPAK knockin mice carrying a mutation that prevents phosphorylation of the T-loop's Thr243 that is essential for kinase's activation, both display lower levels of expression and phosphorylation of NCC and a Gitelman-like syndrome (Rafiqi et al., 2010; Yang et al., 2010; Lin et al., 2011; McCormick et al., 2011; Grimm et al., 2012). In contrast, kidney specific OSR1^{-/-} mice display normal to higher levels of pNCC (Lin et al., 2011; Ferdaus et al., 2016) and a Bartter-like phenotype with reduced pNKCC2 levels. These observations led to the idea that SPAK mainly participates in NCC regulation, while OSR1 may be more important for NKCC2 regulation. However, even though OSR1 cannot fully compensate to maintain NCC activity in the absence of active SPAK, several observations support the notion that OSR1 is also a physiological modulator of NCC.

First, Terker et al. (2014) showed that OSR1, but not SPAK is essential for β -adrenergic stimulation of NCC. Second, Chiga et al. (2011) showed that the FHHt phenotype of WNK4^{D561A/+} mice was not fully corrected by inactivation of SPAK (in WNK4^{D561A/+} SPAK^{T243A/T243A} mice). However, inactivation of one copy SPAK and one copy of OSR1 (WNK4^{D561A/+} SPAK^{T243A/+} OSR1^{T185A/+} mice) did normalize blood pressure, plasma $[\text{K}^+]_i$, and pNCC levels (Chiga et al., 2011). Third, Ferdaus et al. (2016) showed that, whereas in SPAK^{-/-} mice and kidney specific OSR1^{-/-} mice an increase in pNCC was observed when placed on K^+ deficient diet, double knockout mice were unable to upregulate NCC phosphorylation under this condition. Accordingly, plasma $[\text{K}^+]_i$ levels were significantly lower in the double mutants than in the single mutants. The severe hypokalemia developed in the double knockouts under dietary K^+ restriction was reminiscent to the one observed in WNK4^{-/-} mice on this same condition (Castaneda-Bueno et al., 2014). These results highlight the importance of the WNK4-SPAK/OSR1 signaling pathway for NCC activation and maintenance of K^+ homeostasis under K^+ deprivation. Finally, supporting this view, Grimm et al. (2017) recently showed that constitutive activation of SPAK exclusively in the DCT is sufficient to develop hyperkalemia, secondary to the activation of NCC.

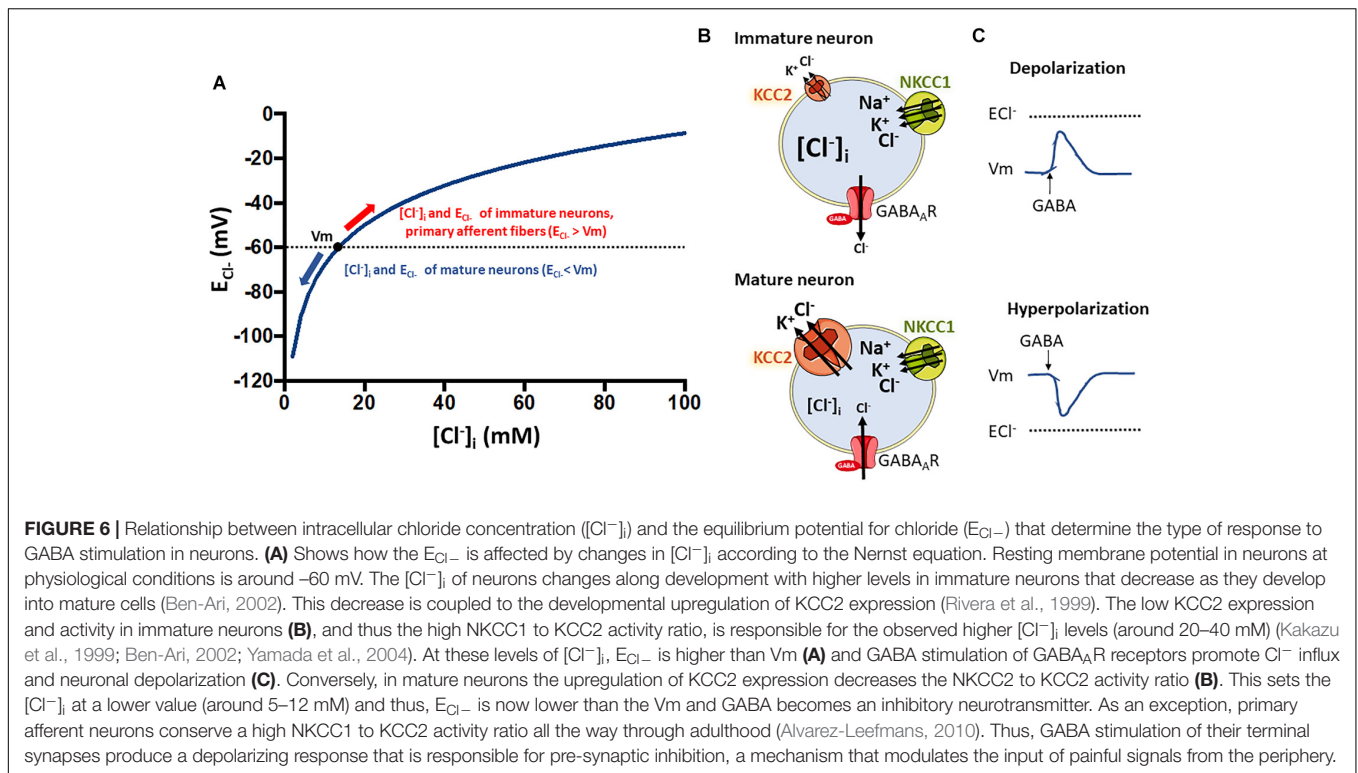
CATION-CHLORIDE COTRANSPORTERS IN THE REGULATION OF THE NEURONAL RESPONSE TO GABA

The $[\text{Cl}^-]_i$ and its regulation by a diverse family of Cl^- transporters is a crucial factor affecting GABAergic transmission during brain development and in the mature nervous system. In most neurons, $[\text{Cl}^-]_i$ concentration is largely dependent on the activity of two cotransporters of the CCC family: KCC2 and NKCC1, although KCC3 is also an important cotransporter in the CNS. The activity of these transporters can decrease or increase neuronal $[\text{Cl}^-]_i$, respectively, and therefore they can alter the polarity (inhibitory or excitatory) and the magnitude of GABAergic transmission. The abnormal function of these transporters can lead to neurologic disorders, including developmental disorders, epilepsy, schizophrenia, and autism. Knowledge of the expression levels and functional regulation of these Cl^- transporters in the central nervous system is crucial to understand the basis for Cl^- homeostasis under normal and pathological conditions. For reviews see Ben-Ari et al. (2007); Blaesse et al. (2009), Kaila et al. (2014); Titz et al. (2015), Kahle and Delpire (2016), and Ben-Ari (2017).

The ability of neurons in the CNS to inhibit each other is just as important as the ability to excite each other. While several excitatory neurotransmitters exist (glutamate, acetylcholine, ATP etc.), neuronal inhibition is mainly mediated by γ -aminobutyric acid (GABA) and to lesser extent by glycine. GABA binds to Cl^- -permeable GABA_A receptors (GABA_AR) and their resultant activation leads to the opening of the receptor's ion channel, resulting in Cl^- movement. The direction of the ion flux depends on the electrochemical driving force acting on the Cl^- ions, which is the difference between the cell's membrane potential (V_m) and the Cl^- equilibrium potential (E_{Cl^-}). The latter depends on the $[\text{Cl}^-]_i$ gradient across the cell membrane. With a $[\text{Cl}^-]_i$ of 8 mM, the E_{Cl^-} is about -70 mV (Figure 6). This value is often more negative than the neuron resting V_m (Kakazu et al., 1999; Rivera et al., 1999; Yamada et al., 2004; Glykys et al., 2014).

The regulation of neuronal $[\text{Cl}^-]_i$ by CCCs is essential for the normal activity of many neural circuits. In the mature brain, neuronal $[\text{Cl}^-]_i$ is low, and GABA binding to their postsynaptic receptors leads to Cl^- influx and post-synaptic hyperpolarization, which moves V_m away from the firing threshold, causing inhibition of excitability. Conversely, in the immature brain, $[\text{Cl}^-]_i$ is significantly higher, so E_{Cl^-} is more positive than V_m , and GABA produces Cl^- efflux, depolarizing responses, and increased excitability by moving V_m closer to the firing threshold (Ben-Ari, 2002).

The transition of GABA_A responses, from excitatory in immature neurons and neurons precursors to inhibitory in mature neurons, occurs because $[\text{Cl}^-]_i$ decreases and E_{Cl^-} shifts in the negative direction due to the high expression of NKCC1 (mediating Cl^- influx) and low expression of KCC2 (mediating Cl^- efflux) in immature neurons and the strong developmental upregulation of KCC2 in mature ones (Rivera et al., 1999; Ben-Ari et al., 2007). Onset of developmental upregulation of KCC2 seems to be species-specific, for example, occurring postnatally in rats (Rivera et al., 1999), and during the second half of



gestation in humans (Vanhatalo et al., 2005; Sedmak et al., 2016) (for review see Kaila et al., 2014). In the mature mammalian nervous system, KCC2 is highly expressed in most central neurons, but absent or expressed at low levels in peripheral neurons and in other nervous cell-types (Payne et al., 1996; Li et al., 2002).

NKCC1 and KCC2 Modulate Circadian Rhythms Determined by GABA

Another example of reversal of GABAergic responses, but that occur in a shorter timescale, has been reported in neurons from the suprachiasmatic nuclei (SCN). The reversal potential of GABAergic postsynaptic currents of these cells (the potential at which GABA responses changes from hyperpolarizing to depolarizing), displays diurnal variations of about 30 mV, suggesting daytime versus nighttime differences of $[Cl^-]_i$ levels (Irwin and Allen, 2009). Recent works have shown that NKCC1 expression in the SCN of the Syrian hamster is regulated by environmental light and displays circadian changes, suggesting that this may determine GABA polarity in a circadian manner (McNeill et al., 2020).

Similarly, in serotonergic neurons of the dorsal raphe nucleus (DRN), which participate in the sleep-wake cycle, GABAergic inhibition displays circadian variations. At daytime, hyperpolarizing responses to the $GABA_A$ R agonist muscimol are larger, and their equilibrium potential more negative compared to those measured at nighttime. Coincidentally, the expression of KCC2 (mediating Cl^- efflux) is higher during daytime than that during nighttime, with no changes in expression pattern

of NKCC1 (mediating Cl^- influx). Expression levels of the neuronal NO synthase (nNOS), present in most serotonergic DRN neurons, are higher at daytime than at night-time, and in brain slices treated with the NO donor sodium nitroprusside (SNP) the expression of KCC2, WNK1, WNK2, WNK3, SPAK, and OSR1 in the DRN increased, whereas phosphorylated SPAK decreased. Together, these results suggest that modulation of GABAergic inhibition of wake-inducing DRN neurons during the sleep-wake cycle is regulated by circadian variations in nNOS-derived NO concentration that in turn affect the WNK-SPAK/OSR1-KCC2 signaling (Kim et al., 2018).

Roles of KCC2 in the CNS: Lessons Learned From Genetic Mouse Models and Human Mutations Associated With Disease

$KCC2^{-/-}$ mice, lacking both KCC2a and KCC2b isoforms, exhibit elevated $[Cl^-]_i$ and GABA-induced neuronal excitation throughout the nervous system (Hubner et al., 2001) (Table 3). They die shortly after birth due to severe motor abnormalities that cause respiratory failure. Brainstem preparations of E18.5 $KCC2^{-/-}$ failed to show respiratory-related motor output of the pre-Bötzinger complex, a cluster of interneurons in the medulla that participate in the generation of respiratory rhythm. Treatment of medullary slices from newborn (P0–P7) WT mice with the KCC2 inhibitor (Dihydroindenyl)oxy alkanic acid (DIOA) has also been shown to decrease the frequency of the respiration-related rhythmic activity (Okabe et al., 2015). $KCC2b^{-/-}$ mice (the most abundant isoform in the nervous

TABLE 3 | Genetically engineered mouse models with mutations in KCC2.

Mouse model	Mutation	Effect on protein expression or function	Phenotype	References
KCC2 ^{-/-}	Elimination of exon 5	Complete absence of KCC2 expression	Neonatal death due to inability to breath, severe motor deficits, abnormal motoneuron activity due to excitatory response to GABA.	Hubner et al., 2001
KCC2b ^{-/-}	Elimination of exon 1	Absence of KCC2b, but not KCC2a expression	Die 12–17 days after birth. Abnormal posture (stiff limbs), frequent generalized seizures leading to brain injury, neuronal hyperexcitability (measured in hippocampal CA1 pyramidal neurons).	Woo et al., 2002
KCC2b ^{+/-}	Elimination of exon 1, heterozygous	Decreased expression of KCC2b isoform	Increased susceptibility to the proconvulsant pentylenetetrazole, sporadic seizures in aging mice.	Woo et al., 2002
KCC2 ^{E/E}	Phosphomimetic T906E/T1007E mutations, homozygous	Decreased KCC2 activity	Neonatal death due to inability to breath. In cesarean section-delivered mice at E18.5: spontaneous and touch-evoked generalized seizures. Abnormal neuronal distribution. Lower frequency of locomotor rhythm measured in lumbar 2 ventral roots.	Watanabe et al., 2019
KCC2 ^{A/A}	Phosphoablative T906A/T1007A mutations, homozygous	Increased KCC2 activity	Survive through adulthood with no overt phenotypes. Normal gross brain morphology and neuronal excitability. More negative E _{GABA} measured in hippocampal neurons. Delay of kainate-induced seizure onset and decrease in mortality rate from status epilepticus.	Moore et al., 2018
KCC2 ^{S940A/S940A}	Phosphoablative S940A mutation, homozygous	No effect on basal KCC2 activity in hippocampal neurons, but decreased KCC2 activity in glutamate stimulated neurons	Reach adulthood with no overt phenotypes. Increased sensitivity to kainate: accelerated onset of status epilepticus and increased seizure severity.	Silayeva et al., 2015

system) exhibit frequent generalized seizures that cause their death between postnatal days 12 and 17 (Woo et al., 2002). In these mice, KCC2a expression is intact (this isoform is produced from an alternative promoter and has an alternative exon 1 that was not targeted by the knockout strategy) and is estimated to represent between 5–10% of the normal total KCC2 expression in the mature brain cortex (Uvarov et al., 2007). Thus, the residual KCC2 activity is thought to explain the slight phenotypic differences between the two knockout models (Gagnon and Delpire, 2013). KCC2b^{+/-} mice show reduced KCC2 expression and can reach adulthood but are prone to suffer epileptic seizures (Woo et al., 2002).

Phosphorylation of KCC2 by the WNK-SPAK/OSR1 downregulates its activity, reducing the rate of Cl⁻ extrusion. Thus, if KCC2 phosphorylation is stimulated, GABAergic inhibition is expected to be weaker or null and the polarity of GABAergic responses could even reverse from inhibitory to excitatory. For instance, KCC2 phosphorylation in Thr906/Thr1007 by WNK1 decreased Cl⁻ extrusion and promoted GABAergic depolarization in cultured mature neurons (Inoue et al., 2012). Moreover, dephosphorylation of KCC2 in brain mouse has been shown to parallel the reversal of GABAergic responses (Friedel et al., 2015; Watanabe et al., 2019).

In the mouse model KCC2^{E/E} that expresses a KCC2 cotransporter harboring the phosphomimetic T906E/T1007E mutations in both alleles, touch-evoked epilepsy, disrupted locomotor rhythmicity, absence of spontaneous respiratory discharges in cervical spinal cord neurons, and early death due to respiratory arrest were reported (Watanabe et al., 2019). It has been shown that the disruption in the developmental switch in

polarity of GABAergic transmission can affect normal neuronal proliferation, migration, and dendritic spine maturation (Li et al., 2007; Ben-Ari et al., 2012). Accordingly, KCC2^{E/E} mice presented anomalous neuronal distribution, but dendritic spine morphology was normal.

In contrast, in KCC2^{T906A/T1007A} mice, in which mutations mimic a permanent dephosphorylated (hyperactive) state of KCC2, a reduction in kainate-induced epileptic seizures was observed, possibly due to stronger inhibitory GABAergic synapses throughout the CNS (Moore et al., 2018). Altogether, these results suggest that adequate KCC2-dependent Cl⁻ extrusion is essential for the correct function of a variety of neuronal circuits, and that its impairment or dysfunction causes inappropriate neuronal locomotor rhythmogenesis and touch-evoked epileptic seizures.

In humans, mutations that indirectly impair KCC2-Ser940 phosphorylation (R952H and R1049C) have been associated with idiopathic epilepsy (Kahle et al., 2014) and familial febrile seizures (Puskarjov et al., 2014). This latter condition associates with abnormal dendritic spine formation. While KCC2 phosphorylation in Thr residues (Rinehart et al., 2009; de los Heros et al., 2014) and Tyr residues (Watanabe et al., 2009; Lee et al., 2010) decrease its membrane availability and rate of ion transport, KCC2 phosphorylation in Ser940, mediated by protein kinase C (PKC), is associated with KCC2 stability in the plasma membrane and increased Cl⁻ transport (Lee et al., 2007). Thus, KCC2 phosphorylation in Ser940 leads to reduced [Cl⁻]_i and stronger GABAergic inhibition (Lee et al., 2007, 2011). In cultured cortical rat neurons, glutamate-mediated NMDA receptor activation triggers Ca²⁺ influx and PP1 activation that in turn mediates KCC2-Ser940 dephosphorylation (Lee et al.,

2011). This leads to diminished Cl^- extrusion and weaker GABAergic inhibition. However, if Ser940 dephosphorylation is blocked by treatment of cultured neurons with okadaic acid, the downregulation of KCC2 is prevented and the strength of GABAergic inhibition is unaffected. When Ser940 phosphorylation is prevented in vivo in the KCC2^{S940A/S940A} mouse, no effect is observed on basal Cl^- extrusion in hippocampal cultured neurons, but decreased KCC2 activity is observed in glutamate stimulated neurons. Onset of kainate-induced status epilepticus is accelerated and seizure severity is increased in these mice (Silayeva et al., 2015).

In mature neurons in culture, GABA_AR activation correlates with increased expression of KCC2 in the plasma membrane and KCC2 dephosphorylation at Thr906/Thr1007 (Heubl et al., 2017). Activation of GABA_AR allows Cl^- influx that significantly increases $[\text{Cl}^-]_i$. This in turn, as a homeostatic mechanism, turns off the WNK-SPAK/OSR1 pathway leading to increased membrane KCC2 expression, thus, its activity, favoring Cl^- extrusion. The opposite effect occurs when an antagonist blocks GABA transmission and produces activation of the WNK-SPAK cascade. $[\text{Cl}^-]_i$ depletion induces activating phosphorylation of WNK1 at Ser382, SPAK at Ser373, and inactivating phosphorylation of KCC2 at Thr906/Thr1007. This also increases NKCC1 phosphorylation at sites Thr203, Thr207, and Thr212. All these events promote net Cl^- influx. Thus, modulation of the WNK-SPAK/OSR1 pathway by $[\text{Cl}^-]_i$ is an important mechanism for restoration of $[\text{Cl}^-]_i$ levels after GABA_AR activation or blockade.

Association of CCCs Activities in the Development of Schizophrenia and Autism

The dysregulation of NKCC1 and KCC2 activity with the consequent altered $[\text{Cl}^-]_i$ homeostasis has been related to psychiatric disorders like autism and schizophrenia in which GABA induced inhibition is altered. Rare genetic variants in *SLC12A5* (encoding KCC2) that decrease the KCC2-mediated Cl^- extrusion have been linked to autism (R952H and R1049C) and schizophrenia (R952H) (Merner et al., 2015) and a gain of function missense variant in *SLC12A2* (encoding NKCC1; Y199C) has been reported in a large cohort of schizophrenic patients (Merner et al., 2016). In addition, Hyde et al. (2011) showed that the NKCC1/KCC2 expression ratio in the hippocampal formation of human brains from schizophrenic patients is higher than that observed in non-schizophrenic subjects. Furthermore, post-mortem analyzed brains from schizophrenic patients show higher transcript levels of *OXSRI* (coding OSR1 kinase) and *WNK3* (Arion et al., 2011). A role of NKCC1 in the pathophysiology of these brain diseases is also evidenced by the beneficial effects observed with bumetanide (an NKCC1 inhibitor) administration (Lemonnier et al., 2016, 2017; Merner et al., 2016; Ben-Ari, 2017; Rahmzadeh et al., 2017; Kharod et al., 2019; Mollajani et al., 2019; Zhang et al., 2020). In three different clinical trials, bumetanide administered to autistic patients showed significant improvement of the autistic symptoms and signs (Lemonnier et al., 2017; Zhou

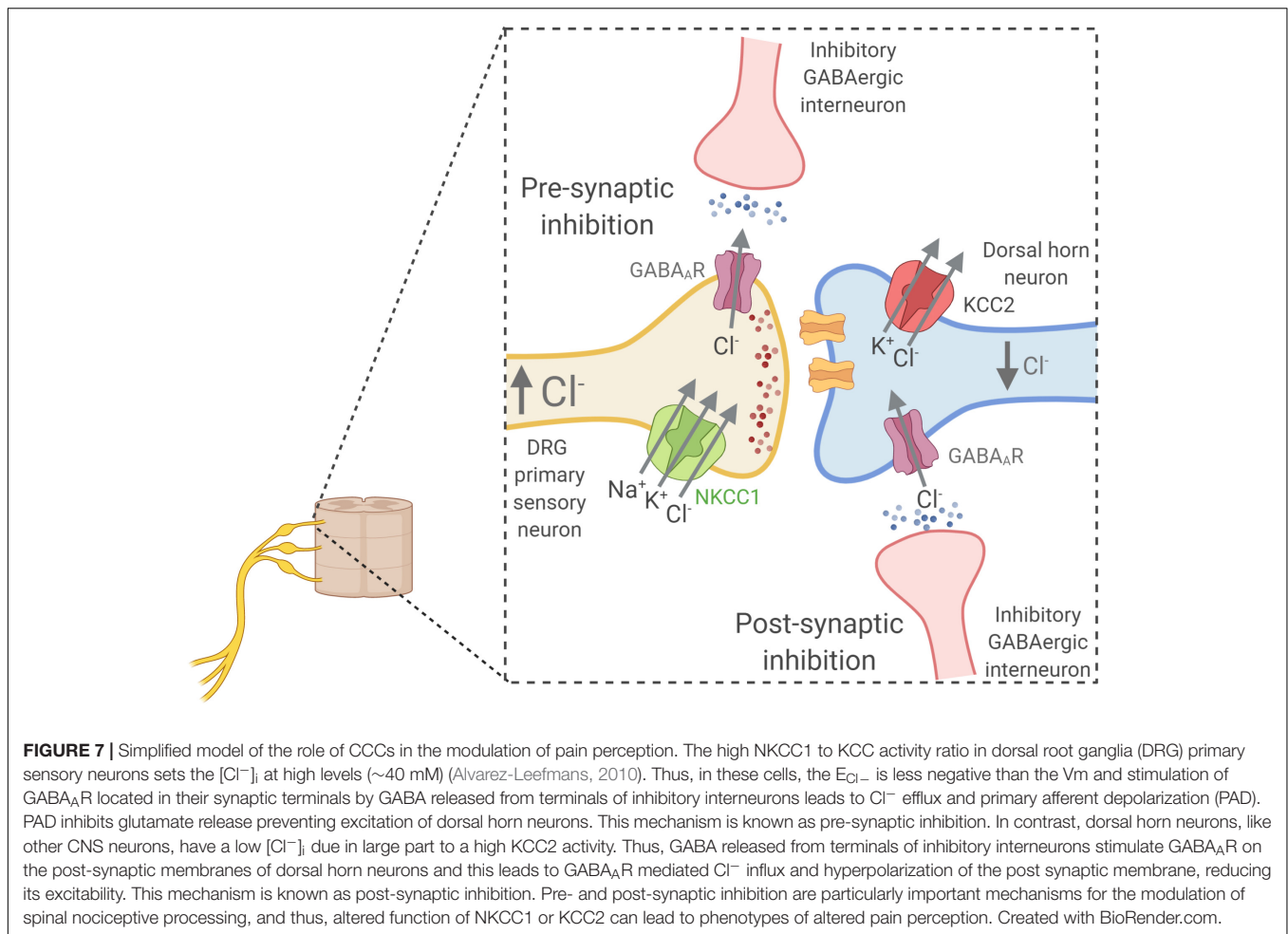
et al., 2020). These effects correlated with an increase in the GABA/Glutamate synapsis ratio recorded using magnetic resonance microscopy in the human insular cortex (Zhang et al., 2020). Encouraging effects of bumetanide have also been reported in schizophrenic patients (Lemonnier et al., 2016; Merner et al., 2016; Rahmzadeh et al., 2017).

KCC2 and NKCC1 Modulate Peripheral Sensory Transmission

CCCs are also expressed in neurons of the spinal cord and peripheral nervous system, where they play an important role in the processing of somatosensory information (Kahle et al., 2008; Alvarez-Leefmans, 2010). The observed effects of altered CCC function in different models suggest a particularly important role in the inhibition of spinal nociceptive processing (Sung et al., 2000; Coull et al., 2003; Laird et al., 2004; Tornberg et al., 2005; Gagnon and Delpire, 2013). The peripheral processes of primary sensory neurons (PSN), whose soma is located in the dorsal root ganglia (DRG), collect information from nociceptive receptors throughout the body. Their central processes conduct sensory signals into the dorsal horn of the spinal cord, the first relay in the central nervous system where nociceptive information is integrated and then transmitted to the brain through nociceptive specific projection neurons. Integration of these signals in the brain is necessary for conscious pain perception. GABAergic inhibition is an important mechanism for modulation of pain input from the periphery. Both, primary sensory neurons of the DRG and dorsal horn neurons are subject to GABAergic inhibition (Figure 7). GABA released from synaptic terminals of inhibitory interneurons of the dorsal horn and inhibitory descending fibers can modulate spinal nociceptive processing via two mechanisms: presynaptic inhibition of PSN and post-synaptic inhibition of spinal cord projection neurons (Rudomin and Schmidt, 1999; Alvarez-Leefmans, 2010; Guo and Hu, 2014).

The pre-synaptic inhibition of PSN involves GABA-induced depolarization of their excitatory synaptic terminals that causes a reduction in neurotransmitter release due to still controversial mechanisms (Guo and Hu, 2014). This phenomenon has been called primary afferent depolarization. The depolarizing effect of GABA is possible because PSN, unlike mature neurons from the CNS, maintain $[\text{Cl}^-]_i$ above electrochemical equilibrium due to a high NKCC1/KCC2 activity ratio (Sung et al., 2000; Alvarez-Leefmans et al., 2001; Price et al., 2006; Rocha-González et al., 2008; Mao et al., 2012). On the other hand, in post-synaptic inhibition, GABA_A receptor stimulation in spinal cord neurons induce hyperpolarization and thus reduce their excitability. Like in other mature CNS neurons, $[\text{Cl}^-]_i$ of these neurons is low due to greater KCC2 activity than NKCC1 activity (Price et al., 2005).

Dysregulation of CCCs function in PNS and spinal cord neurons that affect both inhibitory mechanisms has been associated to the pathogenesis of neuropathic pain. Regarding pre-synaptic inhibition, given that the high expression and activity of NKCC1 in DRG neurons is responsible for the high



$[Cl^-]_i$ that facilitates GABA-induced depolarization (Rocha-González et al., 2008; Alvarez-Leefmans, 2010), it has been proposed that the decreased sensitivity to pain observed in NKCC1^{-/-} mice might be explained by absence of pre-synaptic inhibition (Sung et al., 2000; Laird et al., 2004; Gagnon and Delpire, 2013).

On the other hand, altered KCC2 activity in dorsal horn pain neurons has been associated to neuropathic pain related to altered post-synaptic GABAergic inhibition. Mice with reduced expression of KCC2 showed reduced sensitivity to tactile and noxious thermal stimuli (Tornberg et al., 2005). Coull et al. (2003) showed that KCC2 is highly expressed in lamina I dorsal horn pain neurons and that pharmacological blockade or knockdown of spinal KCC2 in rats reduced the nociceptive threshold. Additionally, in the model of neuropathic pain induced by peripheral nerve injury Coull et al. (2003) observed a reduction in KCC2 expression in lamina I neurons that altered the E_{Cl^-} (making it less negative) and shifted the response to GABA stimulation from inhibitory to excitatory. Nomura et al. (2006) also showed a decrease in KCC2 expression in lamina I and lamina II neurons in a model of tissue injury-induced inflammatory pain. Thus, loss of post-synaptic inhibition due to KCC2 dysregulation seems to be a common mechanism

underlying neuropathic and inflammatory pain. Supporting this, it has been shown that the CLP257 compound that restores Cl^- transport and rescues KCC2 membrane expression in the dorsal horn following nerve injury, normalized stimulus-evoked responses in spinal nociceptive pathways and alleviated hypersensitivity (Gagnon et al., 2013).

Altered regulation of KCC2 activity has also been implicated in Hereditary Sensory and Autonomic Neuropathy type 2 (HSAN2, OMIM 201300). Patients with HSAN2 suffer from severe sensory loss of heat, touch or pain perception with a partial loss of peripheral sensory nerves (Rahmani et al., 2018). This is an autosomal recessive Mendelian disease caused by mutations in the HSN2 exon of WNK1 (Shekarabi et al., 2008; Pacheco-Cuellar et al., 2011). Interestingly, the case of a female patient has been reported who is a compound heterozygote for a 1 bp deletion in the HSN2 exon and a 2 bp deletion in exon 6 of the WNK1 gene (Shekarabi et al., 2008). The WNK1 gene encodes different WNK1 isoforms due to tissue-specific alternative splicing (Vidal-Petiot et al., 2012). Transcripts containing the HSN2 exon (located between exons 8 and 9) have been shown to be abundant in the dorsal horn, DRG, and peripheral nerves (Vidal-Petiot et al., 2012; Shekarabi et al., 2013). In a mouse model in which HSN2-containing WNK1 transcripts are absent due to the

introduction of loxP recombination sites flanking this exon, the HSN2 phenotype is not fully recapitulated, but the mice show reduced pain hypersensitivity after peripheral nerve injury (PNI) (Kahle et al., 2016). PNI increased WNK1-HSN2 expression and KCC2 phosphorylation (at Thr906 and Thr1007) in spinal cord homogenates of wild-type mice, but this increase was blunted in WNK1 Δ HSN2/ Δ HSN2 mice. Accordingly, the reversal potential for GABA-induced currents (E_{GABA}) measured in lamina II neurons of spinal cord slices was less negative in slices from WT mice with PNI than in those from sham operated mice. E_{GABA} was restored to more negative values by incubation of slices with the WNK-SPAK pathway inhibitor STOCK1S-50699. Moreover, E_{GABA} of lamina II neurons from WNK1 Δ HSN2/ Δ HSN2 mice was not altered after PNI. Thus, the PNI-induced increase in KCC2 phosphorylation is dependent on WNK1-HSN2 activity and the resulting decrease in KCC2 activity promotes an increase in $[Cl^-]_i$ of spinal cord neurons that shifts the E_{GABA} to more positive values.

Association of SPAK in Body Weight Control

Finally, there is a growing interest in understanding the importance of GABAergic transmission in regulating body weight balance (Tong et al., 2008; Kim et al., 2015; Sohrabipour et al., 2018). GABAergic transmission in hypothalamic areas and in the brainstem participates in a neuroendocrine network that modulates caloric intake, energy expenditure, and thermogenesis according to the level of food intake (Pigeyre et al., 2016). Neurons in the arcuate nucleus (ARC) express leptin receptors (LepR), whose activation triggers GABAergic inhibition by ARC neurons of PVN neurons (Kong et al., 2012). This in turn relieves the tonic inhibition that PVN neurons exert on brown adipose tissue (BAT), thus increasing energy expenditure through BAT-dependent thermogenesis. The effects of leptin on energy expenditure and thermogenesis are mediated by RIP neurons of the ARC (Tong et al., 2008; Vong et al., 2011; Kim et al., 2015). In mice in which GABA production is specifically impaired in RIP neurons, decreased oxygen consumption and BAT activity was observed, and they gained more body weight and fat mass than their wild type littermates when placed on a high fat diet (Kong et al., 2012). Given that in most neurons a key determinant of $[Cl^-]_i$, and thus of GABAergic response, is the NKCC1/KCC2 activity ratio, it is likely that this mechanism plays also an important role in GABA-sensitive neurons of the PVN. Interestingly, we have recently observed that mice expressing an inactive form of SPAK that is unable to phosphorylate NKCC1 and KCC2 (SPAK^{T243A/T243A} mice), are resistant to developing obesity when placed on a high-fat diet despite similar levels of food intake (Torre-Villalvazo et al., 2018). These mice show higher energy expenditure, reflected by an increase in thermogenesis in the brown adipose tissue, a higher muscle mitochondrial activity, and a lower hepatic steatosis than their wild-type littermates. Thus, it is possible that this phenotype could be related to altered $[Cl^-]_i$ and response to GABA in PVN neurons.

ADDITIONAL CELLULAR Cl^- SENSING MECHANISMS

Even though WNK kinases direct regulation by the anion Cl^- is clear now, it is likely that alternate mechanisms by which cells are able to respond to changes in $[Cl^-]_i$ exist, given that WNK kinases are not found in Bacteria and Archaea domains (Cao-Pham et al., 2018). While mammalian cells (Eagle, 1956) and some species of bacteria require Cl^- in order to grow (MacLeod and Onofrey, 1957; Roeßler and Müller, 1998), some other species of bacteria require Cl^- in order to adapt to different conditions in the environment, such as acidity or hyperosmolarity (Jordan and Davies, 2001; Roeßler et al., 2003). Cl^- also plays a role in signal transduction in bacteria, as it can modulate gene expression (Roeßler and Müller, 2002; Sewald et al., 2007) and enzymatic activity (Gut et al., 2006).

Accordingly, several studies have reported different genes whose expression is regulated in response to changes in $[Cl^-]_i$ in eukaryotes, such as *SCNNIA* (Niisato et al., 2004), *SCNNIB*, *SCNNIC* (Niisato et al., 2007), *COX2* (Cheng et al., 2000), *GLRX5* and *RPS27* (Valdivieso et al., 2016). GABA_AR receptor subunits levels are also regulated by $[Cl^-]_i$ (Succol et al., 2012). The detailed mechanisms responsible for these different phenomena are still unknown, even though the kinase p38 might be involved in the regulation of *SCNNIB*, *SCNNIG* (Niisato et al., 2007) and *COX2* (Cheng et al., 2000). Interestingly, the transcription factor RUNX1 has been shown to directly bind Cl^- ions (Bäckström et al., 2002), but further work will be necessary to elucidate its role in the context of intracellular Cl^- handling, or if there are other transcription factors that respond directly or indirectly to changes in $[Cl^-]_i$.

Finally, it is not clear if other kinases might function as direct Cl^- sensors. While the phosphorylation of different MAP kinases, such as JNK, p38, and MEK6 is increased in response to decreased $[Cl^-]_i$ (Ohsawa et al., 2010; Wu et al., 2016), it is still unknown if these proteins are able to directly bind Cl^- anions, or whether its activation depends on upstream activators that sense $[Cl^-]_i$. In the case of the kinase SGK1, *in vitro* kinase activity assays suggest that SGK1 can be directly activated by increasing $[Cl^-]_i$, as incubating recombinant SGK1 with increasing concentrations of NaCl or KCl (but not Na-gluconate or K-gluconate) promotes its phosphorylation (Zhang et al., 2018). Further analysis will be helpful to determine if SGK1 is indeed able to directly bind Cl^- anions. Additionally, the opposite regulation of WNK kinases and SGK1 by Cl^- is puzzling, and it will be an interesting avenue for future investigations, especially regarding epithelial physiology, where both kinases play important roles in fluid secretion and intracellular signaling.

CLOSING REMARKS

In the present manuscript we reviewed the role of the Cl^- anion as a second messenger participating in the modulation of several physiological processes, specifically by regulating the activity of WNK kinases and their downstream signaling

pathway, comprising the kinases SPAK and OSR1, as well as the cation-coupled Cl^- cotransporters (CCCs). Dynamic activation and inactivation of these kinases modulate the phosphorylation, and therefore activity of the CCCs. While initial description of the physiological roles of some of these proteins was facilitated by their association to genetic diseases, further investigations have shed additional light about their role in physiological and pathophysiological processes. For example, regulation of CCCs is relevant in maintaining normal cell volume in response to changes in extracellular osmolarity. In particular, the WNK3-SPAK complex seems to play an important role in cell volume regulation within the brain. Moreover, a complex $[\text{Cl}^-]_i$ -sensitive signaling pathway involving basolateral ion channels and the kinases WNK4, SPAK, and OSR1 is responsible for NCC regulation by physiological plasma $[\text{K}^+]$, an essential process in the homeostatic modulation of renal K^+ excretion. Finally, the WNK-SPAK/OSR1-CCC pathway has also been described to modulate GABAergic neuronal responses, where baseline $[\text{Cl}^-]_i$ dictates the direction of Cl^- currents elicited by binding of GABA to its receptor.

REFERENCES

- Alessi, D. R., Zhang, J., Khanna, A., Hochdorfer, T., Shang, Y., and Kahle, K. T. (2014). The WNK-SPAK/OSR1 pathway: master regulator of cation-chloride cotransporters. *Sci. Signal.* 7:re3. doi: 10.1126/scisignal.2005365
- Alvarez-Leefmans, F. J. (2010). "Chloride transporters in presynaptic inhibition, pain and neurogenic inflammation," in *Physiology and Pathology of Chloride Transporters and Channels in the Nervous System: From Molecules to Diseases*, eds F. J. Alvarez-Leefmans and E. Delpire (Amsterdam: Elsevier Inc), 439–470. doi: 10.1016/B978-0-12-374373-2.00022-4
- Alvarez-Leefmans, F. J., León-Olea, M., Mendoza-Sotelo, J., Alvarez, F. J., Antón, B., and Garduo, R. (2001). Immunolocalization of the Na⁺-K⁺-2Cl⁻ cotransporter in peripheral nervous tissue of vertebrates. *Neuroscience* 104, 569–582. doi: 10.1016/S0306-4522(01)00091-4
- Anselmo, A. N., Earnest, S., Chen, W., Juang, Y.-C., Kim, S. C., Zhao, Y., et al. (2006). WNK1 and OSR1 regulate the Na⁺, K⁺, 2Cl⁻ cotransporter in HeLa cells. *Proc. Natl. Acad. Sci. U.S.A.* 103, 10883–10888. doi: 10.1073/pnas.0604607103
- Arion, D., and Lewis, D. A. (2011). Altered expression of regulators of the cortical chloride transporters NKCC1 and KCC2 in schizophrenia. *Arch. Gen. Psychiatry* 68, 21–31. doi: 10.1001/archgenpsychiatry.2010.114
- Arroyo, J. P., Kahle, K. T., and Gamba, G. (2013). The SLC12 family of electroneutral cation-coupled chloride cotransporters. *Mol. Aspects Med.* 34, 288–298. doi: 10.1016/j.mam.2012.05.002
- Bäckström, S., Wolf-Watz, M., Grundström, C., Härd, T., Grundström, T., and Sauer, U. H. (2002). The RUNX1 Runt domain at 1.25 Å resolution: a structural switch and specifically bound chloride ions modulate DNA binding. *J. Mol. Biol.* 322, 259–272. doi: 10.1016/S0022-2836(02)00702-7
- Bazúa-Valenti, S., Castañeda-Bueno, M., and Gamba, G. (2016). Physiological role of SLC12 family members in the kidney. *Am. J. Physiol. Ren. Physiol.* 311, F131–F144. doi: 10.1152/ajprenal.00071.2016
- Bazua-Valenti, S., Chavez-Canales, M., Rojas-Vega, L., Gonzalez-Rodriguez, X., Vazquez, N., Rodriguez-Gama, A., et al. (2015). The effect of WNK4 on the Na⁺-Cl⁻ cotransporter is modulated by intracellular chloride. *J. Am. Soc. Nephrol.* 26, 1781–1786. doi: 10.1681/ASN.2014050470
- Beck, F.-X., Dörge, A., Rick, R., Schramm, M., and Thurau, K. (1988). The distribution of potassium, sodium and chloride across the apical membrane of renal tubular cells: effect of acute metabolic alkalosis. *Pflügers Arch. Eur. J. Physiol.* 411, 259–267. doi: 10.1007/BF00585112
- Begum, G., Yuan, H., Kahle, K. T., Li, L., Wang, S., Shi, Y., et al. (2015). Inhibition of WNK3 kinase signaling reduces brain damage and accelerates neurological

AUTHOR CONTRIBUTIONS

AM-d-O, MC-C, PH, GG, and MC-B wrote the manuscript, made the figures, edited the manuscript, revised and approved the final version. All the authors contributed to the article and approved the submitted version.

FUNDING

AM-d-O is a graduate student from the "Programa de Doctorado en Ciencias Biomédicas, Universidad Nacional Autónoma de México (UNAM)" and received a fellowship 606808 from CONACYT. The work in the researcher's lab is possible due to grant support no. DK51496 from NIH to GG, A1-S-8290, 283555, from Conacyt Mexico to GG and PH, respectively, IN201519, IN222320, IA203620, from PAPIIT UNAM to GG, PH, and MC-C, respectively, and RA202718 from Loreal L'Oréal-UNESCO-AMC-CONALMEX "For Women in Science, 2019" to MC-C.

- recovery after stroke. *Stroke* 46, 1956–1965. doi: 10.1161/STROKEAHA.115.008939
- Ben-Ari, Y. (2002). Excitatory actions of gaba during development: the nature of the nurture. *Nat. Rev. Neurosci.* 3, 728–739. doi: 10.1038/nrn920
- Ben-Ari, Y. (2017). NKCC1 chloride importer antagonists attenuate many neurological and psychiatric disorders. *Trends Neurosci.* 40, 536–554. doi: 10.1016/j.tins.2017.07.001
- Ben-Ari, Y., Gaiarsa, J.-L., Tyzio, R., and Khazipov, R. (2007). GABA: a pioneer transmitter that excites immature neurons and generates primitive oscillations. *Physiol. Rev.* 87, 1215–1284. doi: 10.1152/physrev.00017.2006
- Ben-Ari, Y., Khalilov, I., Kahle, K. T., and Cherubini, E. (2012). The GABA excitatory/inhibitory shift in brain maturation and neurological disorders. *Neuroscientist* 18, 467–486. doi: 10.1177/1073858412438697
- Birkenhager, R., Otto, E., Schurmann, M. J., Vollmer, M., Ruf, E. M., Maier-Lutz, I., et al. (2001). Mutation of BSND causes Bartter syndrome with sensorineural deafness and kidney failure. *Nat. Genet.* 29, 310–314. doi: 10.1038/ng752
- Blaesse, P., Airaksinen, M. S., Rivera, C., and Kaila, K. (2009). Cation-chloride cotransporters and neuronal function. *Neuron* 61, 820–838. doi: 10.1016/j.neuron.2009.03.003
- Bockenhauer, D., Feather, S., Stanescu, H. C., Bandulik, S., Zdebek, A. A., Reichold, M., et al. (2009). Epilepsy, ataxia, sensorineural deafness, tubulopathy, and KCNJ10 mutations. *N. Engl. J. Med.* 360, 1960–1970. doi: 10.1056/NEJMoa0810276
- Boettger, T., Hubner, C., Maier, H., Rust, M., Beck, F., and Jentsch, T. (2002). Deafness and renal tubular acidosis in mice lacking the K-Cl co-transporter Kcc4. *Nat. Lett.* 416, 13445–13452. doi: 10.1038/416874a
- Boettger, T., Rust, M. B., Maier, H., Seidenbecher, T., Schweizer, M., Keating, D. J., et al. (2003). Loss of K-Cl co-transporter KCC3 causes deafness, neurodegeneration and reduced seizure threshold. *EMBO J.* 22, 5422–5434. doi: 10.1093/emboj/cdg519
- Boscardin, E., Perrier, R., Sergi, C., Maillard, M., Loffing, J., Loffing-Cueni, D., et al. (2017). Severe hyperkalemia is rescued by low-potassium diet in renal βENaC -deficient mice. *Pflügers Arch. Eur. J. Physiol.* 469, 1387–1399. doi: 10.1007/s00424-017-1990-2
- Boscardin, E., Perrier, R., Sergi, C., Maillard, M. P., Loffing, J., Loffing-Cueni, D., et al. (2018). Plasma potassium determines NCC abundance in adult kidney-specific γENaC Knockout. *J. Am. Soc. Nephrol.* 29, 977–990. doi: 10.1681/ASN.2017030345
- Boulpaep, E. L., and Boron, W. F. (2016). *Medical Physiology*, 3rd Edn. Amsterdam: Elsevier.

- Boyden, L. M., Choi, M., Choate, K. A., Nelson-Williams, C. J., Farhi, A., Toka, H. R., et al. (2012). Mutations in kelch-like 3 and cullin 3 cause hypertension and electrolyte abnormalities. *Nature* 482, 98–102. doi: 10.1038/nature10814
- Breitwieser, G. E., Altamirano, A. A., and Russell, J. M. (1990). Osmotic stimulation of Na(+)-K(+)-Cl- cotransport in squid giant axon is [Cl-]i dependent. *Am. J. Physiol. Physiol.* 258, C749–C753. doi: 10.1152/ajpcell.1990.258.4.C749
- Cao-Pham, A. H., Urano, D., Ross-Elliott, T. J., and Jones, A. M. (2018). Nudge-nudge, WNK-WNK (kinases), say no more? *New Phytol.* 220, 35–48. doi: 10.1111/nph.15276
- Castañeda-Bueno, M., Arroyo, J. P., Zhang, J., Puthumana, J., Yarborough, O., Shibata, S., et al. (2017). Phosphorylation by PKC and PKA regulate the kinase activity and downstream signaling of WNK4. *Proc. Natl. Acad. Sci. U.S.A.* 114, E879–E886. doi: 10.1073/pnas.1620315114
- Castañeda-Bueno, M., Cervantes-Perez, L. G., Rojas-Vega, L., Arroyo-Garza, I., Vazquez, N., Moreno, E., et al. (2014). Modulation of NCC activity by low and high K+ intake: insights into the signaling pathways involved. *Am. J. Physiol. Ren. Physiol.* 306, F1507–F1519. doi: 10.1152/ajprenal.00255.2013
- Castañeda-Bueno, M., Cervantes-Perez, L. G., Vazquez, N., Uribe, N., Kantesaria, S., Morla, L., et al. (2012). Activation of the renal Na+:Cl- cotransporter by angiotensin II is a WNK4-dependent process. *Proc. Natl. Acad. Sci. U.S.A.* 109, 7929–7934. doi: 10.1073/pnas.1200947109
- Chang, H., Tashiro, K., Hirai, M., Ikeda, K., Kurokawa, K., and Fujita, T. (1996). Identification of a cDNA encoding a thiazide-sensitive sodium-chloride cotransporter from the human and its mRNA expression in various tissues. *Biochem. Biophys. Res. Commun.* 223, 324–328. doi: 10.1006/bbrc.1996.0893
- Chen, J.-C., Lo, Y.-F., Lin, Y.-W., Lin, S.-H., Huang, C.-L., and Cheng, C.-J. (2019). WNK4 kinase is a physiological intracellular chloride sensor. *Proc. Natl. Acad. Sci. U.S.A.* 116, 4502–4507. doi: 10.1073/pnas.1817220116
- Chen, W., Yazicioglu, M., and Cobb, M. H. (2004). Characterization of OSR1, a member of the mammalian Ste20p/Germinal center kinase subfamily. *J. Biol. Chem.* 279, 11129–11136. doi: 10.1074/jbc.M313562200
- Cheng, H., Wang, J., Zhang, M., McKanna, J., and Harris, R. (2000). Role of p38 in the regulation of renal cortical cyclooxygenase-2 expression by extracellular chloride. *J. Clin. Invest.* 106, 681–688. doi: 10.1172/JCI10318
- Chiga, M., Rafiqi, F. H., Alessi, D. R., Sohara, E., Ohta, A., Rai, T., et al. (2011). Phenotypes of pseudohypoaldosteronism type II caused by the WNK4 D561A missense mutation are dependent on the WNK-OSR1/SPAK kinase cascade. *J. Cell Sci.* 124, 1391–1395. doi: 10.1242/jcs.084111
- Coull, J. A. M., Boudreau, D., Bachand, K., Prescott, S. A., Nault, F., Sik, A., et al. (2003). Trans-synaptic shift in anion gradient in spinal lamina I neurons as a mechanism of neuropathic pain. *Nature* 424, 938–942. doi: 10.1038/nature01868
- Cruz, A. J., and Castro, A. (2013). Gitelman or bartter type 3 syndrome? A case of distal convoluted tubulopathy caused by CLCNKB gene mutation. *Case Rep.* 2013:bcr2012007929 doi: 10.1136/bcr-2012-007929
- Cruz-Rangel, S., Gamba, G., Ramos-Mandujano, G., and Pasantes-Morales, H. (2012). Influence of WNK3 on intracellular chloride concentration and volume regulation in HEK293 cells. *Pflugers Arch. Eur. J. Physiol.* 464, 317–330. doi: 10.1007/s00424-012-1137-4
- Csanády, L., Vergani, P., and Gadsby, D. C. (2019). Structure, gating, and regulation of the CFTR anion channel. *Physiol. Rev.* 99, 707–738. doi: 10.1152/physrev.00007.2018
- Cuevas, C. A., Su, X.-T., Wang, M.-X., Terker, A. S., Lin, D.-H., McCormick, J. A., et al. (2017). Potassium sensing by renal distal tubules requires Kir4.1. *J. Am. Soc. Nephrol.* 28, 1814–1825. doi: 10.1681/ASN.2016090935
- Darman, R. B., and Forbush, B. (2002). A regulatory locus of phosphorylation in the N terminus of the Na-K-Cl cotransporter. NKCC1. *J. Biol. Chem.* 277, 37542–37550. doi: 10.1074/jbc.M206293200
- de los Heros, P., Alessi, D. R., Gourlay, R., Campbell, D. G., Deak, M., Macartney, T. J., et al. (2014). The WNK-regulated SPAK/OSR1 kinases directly phosphorylate and inhibit the K+-Cl- co-transporters. *Biochem. J.* 458, 559–573. doi: 10.1042/BJ20131478
- de Los Heros, P., Kahle, K. T., Rinehart, J., Bobadilla, N. A., Vázquez, N., San Cristobal, P., et al. (2006). WNK3 bypasses the tonicity requirement for K-Cl cotransporter activation via a phosphatase-dependent pathway. *Proc. Natl. Acad. Sci. U.S.A.* 103, 1976–1981. doi: 10.1073/pnas.0510947103
- de los Heros, P., Pacheco-Alvarez, D., and Gamba, G. (2018). Role of WNK kinases in the modulation of cell volume. *Curr. Top. Membr.* 81, 207–235. doi: 10.1016/bs.ctm.2018.08.002
- Delalay, C., Lu, J., Houot, A.-M., Disse-Nicodeme, S., Gasc, J.-M., Corvol, P., et al. (2003). Multiple promoters in the WNK1 gene: one controls expression of a kidney-specific kinase-defective isoform. *Mol. Cell. Biol.* 23, 9208–9221. doi: 10.1128/MCB.23.24.9208-9221.2003
- Delpire, E., and Gagnon, K. B. (2018). Water homeostasis and cell volume maintenance and regulation. *Curr. Top. Membr.* 81, 3–52. doi: 10.1016/bs.ctm.2018.08.001
- Delpire, E., Lu, J., England, R., Dull, C., and Thorne, T. (1999). Deafness and imbalance associated with inactivation of the secretory Na-K-2Cl cotransporter. *Nat. Genet.* 22, 192–195. doi: 10.1038/9713
- Delpire, E., and Mount, D. B. (2002). Human and murine phenotypes associated with defects in cation-chloride cotransport. *Annu. Rev. Physiol.* 64, 803–843. doi: 10.1146/annurev.physiol.64.081501.155847
- Delpire, E., Rauchman, M. I., Beier, D. R., Hebert, S. C., and Gullans, S. R. (1994). Molecular cloning and chromosome localization of a putative basolateral Na+-K+-2Cl- cotransporter from mouse inner medullary collecting duct (mIMCD-3) cells. *J. Biol. Chem.* 269, 25677–25683.
- Delpire, E., Wolfe, L., Flores, B., Koumangoye, R., Schornak, C. C., Omer, S., et al. (2016). A patient with multisystem dysfunction carries a truncation mutation in human SLC12A2, the gene encoding the Na-K-2Cl cotransporter, NKCC1. *Mol. Case Stud.* 2:a001289. doi: 10.1101/mcs.a001289
- Dixon, M. J., Gazzard, J., Chaudhry, S. S., Sampson, N., Schulte, B. A., and Steel, K. P. (1999). Mutation of the Na-K-Cl co-transporter gene Slc12a2 results in deafness in mice. *Hum. Mol. Genet.* 8, 1579–1584. doi: 10.1093/hmg/8.8.1579
- Dowd, B. F. X., and Forbush, B. (2003). Pask (proline-alanine-rich STE20-related kinase), a regulatory kinase of the Na-K-Cl cotransporter (NKCC1). *J. Biol. Chem.* 278, 27347–27353. doi: 10.1074/jbc.M301899200
- Dvorak, M. M., De Jossineau, C., Carter, D. H., Pisitkun, T., Knepper, M. A., Gamba, G., et al. (2007). Thiazide diuretics directly induce osteoblast differentiation and mineralized nodule formation by interacting with a sodium chloride co-transporter in bone. *J. Am. Soc. Nephrol.* 18, 2509–2516. doi: 10.1681/ASN.2007030348
- Eagle, H. (1956). The salt requirements of mammalian cells in tissue culture. *Arch. Biochem. Biophys.* 61, 356–366. doi: 10.1016/0003-9861(56)90358-7
- El-Gebali, S., Mistry, J., Bateman, A., Eddy, S. R., Luciani, A., Potter, S. C., et al. (2019). The Pfam protein families database in 2019. *Nucleic Acids Res.* 47, D427–D432. doi: 10.1093/nar/gky995
- Estévez, R., Boettger, T., Stein, V., Birkenhäger, R., Otto, E., Hildebrandt, F., et al. (2001). Barttin is a Cl- channel β -subunit crucial for renal Cl- reabsorption and inner ear K+ secretion. *Nature* 414, 558–561. doi: 10.1038/35107099
- Evans, R. L., Park, K., James Turner, R., Watson, G. E., Nguyen, V. H., Dennett, M. R., et al. (2000). Severe impairment of salivation in Na+/K+/2Cl- cotransporter (NKCC1)-deficient mice. *J. Biol. Chem.* 275, 26720–26726. doi: 10.1074/jbc.M003753200
- Ferdaus, M. Z., Barber, K. W., López-Cayuqueo, K. I., Terker, A. S., Argai, E. R., Gassaway, B. M., et al. (2016). SPAK and OSR1 play essential roles in potassium homeostasis through actions on the distal convoluted tubule. *J. Physiol.* 594, 4945–4966. doi: 10.1113/JP272311
- Flagella, M., Clarke, L. L., Miller, M. L., Erway, L. C., Giannella, R. A., Andringa, A., et al. (1999). Mice lacking the basolateral Na-K-2Cl cotransporter have impaired epithelial chloride secretion and are profoundly deaf. *J. Biol. Chem.* 274, 26946–26955. doi: 10.1074/jbc.274.38.26946
- Foskett, J. K. (1990). [Ca2+]i modulation of Cl- content controls cell volume in single salivary acinar cells during fluid secretion. *Am. J. Physiol. Cell Physiol.* 259, C998–C1004. doi: 10.1152/ajpcell.1990.259.6.c998
- Friedel, P., Kahle, K. T., Zhang, J., Hertz, N., Pisella, L. I., Buhler, E., et al. (2015). WNK1-regulated inhibitory phosphorylation of the KCC2 cotransporter maintains the depolarizing action of GABA in immature neurons. *Sci. Signal.* 8:ra65. doi: 10.1126/scisignal.aaa0354
- Funabashi, K., Fujii, M., Yamamura, H., Ohya, S., and Imaizumi, Y. (2010). Contribution of chloride channel conductance to the regulation of resting membrane potential in chondrocytes. *J. Pharmacol. Sci.* 113, 94–99. doi: 10.1254/jphs.10026SC

- Gagnon, K. B., and Delpire, E. (2012). Molecular physiology of SPAK and OSR1: two ste20-related protein kinases regulating ion transport. *Physiol. Rev.* 92, 1577–1617. doi: 10.1152/physrev.00009.2012
- Gagnon, K. B., and Delpire, E. (2013). Physiology of SLC12 transporters: lessons from inherited human genetic mutations and genetically engineered mouse knockouts. *Am. J. Physiol. Physiol.* 304, C693–C714. doi: 10.1152/ajpcell.00350.2012
- Gagnon, K. B. E., England, R., and Delpire, E. (2006). Volume sensitivity of cation-Cl⁻ cotransporters is modulated by the interaction of two kinases: Ste20-related proline-alanine-rich kinase and WNK4. *Am. J. Physiol. Physiol.* 290, C134–C142. doi: 10.1152/ajpcell.00037.2005
- Gagnon, M., Bergeron, M. J., Lavertu, G., Castonguay, A., Tripathy, S., Bonin, R. P., et al. (2013). Chloride extrusion enhancers as novel therapeutics for neurological diseases. *Nat. Med.* 19, 1524–1528. doi: 10.1038/nm.3356
- Gamba, G. (2005). Molecular physiology and pathophysiology of electroneutral cation-chloride cotransporters. *Physiol. Rev.* 85, 423–493. doi: 10.1152/physrev.00011.2004
- Gamba, G., Miyanosita, A., Lombardi, M., Lytton, J., Lee, W. S., Hediger, M. A., et al. (1994). Molecular cloning, primary structure, and characterization of two members of the mammalian electroneutral sodium-(potassium)-chloride cotransporter family expressed in kidney. *J. Biol. Chem.* 269, 17713–17722.
- Gandolfi, B., Gruffydd-jones, T. J., Malik, R., Cortes, A., Jones, B. R., Helps, C. R., et al. (2012). First WNK4-hypokalemia animal model identified by genome-wide association in burmese cats. *PLoS One* 7:e0053173. doi: 10.1371/journal.pone.0053173
- Gillen, C. M., and Forbush, B. (1999). Functional interaction of the K-Cl cotransporter (KCC1) with the Na-K-Cl cotransporter in HEK-293 cells. *Am. J. Physiol. Physiol.* 276, C328–C336. doi: 10.1152/ajpcell.1999.276.2.C328
- Glykys, J., Dzhalal, V., Egawa, K., Balena, T., Saponjian, Y., Kuchibhotla, K. V., et al. (2014). Local impermeant anions establish the neuronal chloride concentration. *Science* 343, 670–675. doi: 10.1126/science.1245423
- Grill, A., Schießl, I. M., Gess, B., Fremter, K., Hammer, A., and Castrop, H. (2016). Salt-losing nephropathy in mice with a null mutation of the *Clcnk2* gene. *Acta Physiol.* 218, 198–211. doi: 10.1111/apha.12755
- Grimm, P. R., Coleman, R., Delpire, E., and Welling, P. A. (2017). Constitutively active SPAK causes hyperkalemia by activating NCC and remodeling distal tubules. *J. Am. Soc. Nephrol.* 28, 2597–2606. doi: 10.1681/ASN.2016090948
- Grimm, P. R., Taneja, T. K., Liu, J., Coleman, R., Chen, Y. Y., Delpire, E., et al. (2012). SPAK isoforms and OSR1 regulate sodium-chloride co-transporters in a nephron-specific manner. *J. Biol. Chem.* 287, 37673–37690. doi: 10.1074/jbc.M112.402800
- Gruber, M., Söding, J., and Lupas, A. N. (2006). Comparative analysis of coiled-coil prediction methods. *J. Struct. Biol.* 155, 140–145. doi: 10.1016/j.jsb.2006.03.009
- Guo, D., and Hu, J. (2014). Spinal presynaptic inhibition in pain control. *Neuroscience* 283, 95–106. doi: 10.1016/j.neuroscience.2014.09.032
- Gut, H., Pennacchietti, E., John, R. A., Bossa, F., Capitani, G., De Biase, D., et al. (2006). *Escherichia coli* acid resistance: pH-sensing, activation by chloride and autoinhibition in GadB. *EMBO J.* 25, 2643–2651. doi: 10.1038/sj.emboj.7601107
- Hennings, J. C., Andrini, O., Picard, N., Paulais, M., Huebner, A. K., Cayuqueo, I. K. L., et al. (2017). The ClC-K2 chloride channel is critical for salt handling in the distal nephron. *J. Am. Soc. Nephrol.* 28, 209–217. doi: 10.1681/ASN.2016010085
- Heubl, M., Zhang, J., Pressey, J. C., Al Awabdh, S., Renner, M., Gomez-Castro, F., et al. (2017). GABAA receptor dependent synaptic inhibition rapidly tunes KCC2 activity via the Cl⁻-sensitive WNK1 kinase. *Nat. Commun.* 8:1776. doi: 10.1038/s41467-017-01749-0
- Hibino, H., Inanobe, A., Furutani, K., Murakami, S., Findlay, I., and Kurachi, Y. (2010). Inwardly rectifying potassium channels: their structure, function, and physiological roles. *Physiol. Rev.* 90, 291–366. doi: 10.1152/physrev.00021.2009
- Hoffmann, E. K., Lambert, I. H., and Pedersen, S. F. (2009). Physiology of cell volume regulation in vertebrates. *Physiol. Rev.* 89, 193–277. doi: 10.1152/physrev.00037.2007
- Holden, S., Cox, J., and Raymond, F. L. (2004). Cloning, genomic organization, alternative splicing and expression analysis of the human gene WNK3 (PRKWNK3). *Gene* 335, 109–119. doi: 10.1016/j.gene.2004.03.009
- Howard, H. C., Mount, D. B., Rochefort, D., Byun, N., Dupré, N., Lu, J., et al. (2002). The K-Cl cotransporter KCC3 is mutant in a severe peripheral neuropathy associated with agenesis of the corpus callosum. *Nat. Genet.* 32, 384–392. doi: 10.1038/ng1002
- Hubner, C. A., Stein, V., Hermans-Borgmeyer, I., Meyer, T., Ballanyi, K., and Jentsch, T. J. (2001). Disruption of KCC2 reveals an essential role of K-Cl cotransport already in early synaptic inhibition. *Neuron* 30, 515–524. doi: 10.1016/s0896-6273(01)00297-5
- Hunter, R. W., Craigie, E., Homer, N. Z. M., Mullins, J. J., and Bailey, M. A. (2014). Acute inhibition of NCC does not activate distal electrogenic Na⁺ reabsorption or kaliuresis. *Am. J. Physiol. Ren. Physiol.* 306, F457–F467. doi: 10.1152/ajprenal.00339.2013
- Hutter, O. F. (2017). A personal historic perspective on the role of chloride in skeletal and cardiac muscle. *Physiol. Rep.* 5, 1–7. doi: 10.14814/phy2.13165
- Hyde, T. M., Lipska, B. K., Ali, T., Mathew, S. V., Law, A. J., Metitiri, O. E., et al. (2011). Expression of GABA signaling molecules KCC2, NKCC1, and GAD1 in cortical development and schizophrenia. *J. Neurosci.* 31, 11088–11095. doi: 10.1523/JNEUROSCI.1234-11.2011
- Inoue, K., Furukawa, T., Kumada, T., Yamada, J., Wang, T., Inoue, R., et al. (2012). Taurine inhibits K⁺-Cl⁻ cotransporter KCC2 to regulate embryonic Cl⁻ homeostasis via with-no-lysine (Wnk) protein kinase signaling pathway. *J. Biol. Chem.* 287, 20839–20850. doi: 10.1074/jbc.M111.319418
- Irwin, R. P., and Allen, C. N. (2009). GABAergic signaling induces divergent neuronal Ca²⁺ responses in the suprachiasmatic nucleus network. *Eur. J. Neurosci.* 30, 1462–1475. doi: 10.1111/j.1460-9568.2009.06944.x
- Jentsch, T. J., and Pusch, M. (2018). ClC chloride channels and transporters: structure, function, physiology, and disease. *Physiol. Rev.* 98, 1493–1590. doi: 10.1152/physrev.00047.2017
- Jordan, K. N., and Davies, K. W. (2001). Sodium chloride enhances recovery and growth of acid-stressed *E. Coli* O157:H7. *Lett. Appl. Microbiol.* 32, 312–315. doi: 10.1046/j.1472-765X.2001.00911.x
- Kahle, K. T., and Delpire, E. (2016). Kinase-KCC2 coupling: Cl⁻ rheostasis, disease susceptibility, therapeutic target. *J. Neurophysiol.* 115, 8–18. doi: 10.1152/jn.00865.2015
- Kahle, K. T., Gimenez, I., Hassan, H., Wilson, F. H., Wong, R. D., Forbush, B., et al. (2004). WNK4 regulates apical and basolateral Cl⁻ flux in extrarenal epithelia. *Proc. Natl. Acad. Sci. U.S.A.* 101, 2064–2069. doi: 10.1073/pnas.0308434100
- Kahle, K. T., Khanna, A. R., Alper, S. L., Adragna, N. C., Lauf, P. K., Sun, D., et al. (2015). K-Cl cotransporters, cell volume homeostasis, and neurological disease. *Trends Mol. Med.* 21, 513–523. doi: 10.1016/j.molmed.2015.05.008
- Kahle, K. T., Merner, N. D., Friedel, P., Silayeva, L., Liang, B., Khanna, A., et al. (2014). Genetically encoded impairment of neuronal KCC2 cotransporter function in human idiopathic generalized epilepsy. *EMBO Rep.* 15, 766–774. doi: 10.15252/embr.201438840
- Kahle, K. T., Rinehart, J., de los Heros, P., Louvi, A., Meade, P., Vazquez, N., et al. (2005). WNK3 modulates transport of Cl⁻ in and out of cells: implications for control of cell volume and neuronal excitability. *Proc. Natl. Acad. Sci. U.S.A.* 102, 16783–16788. doi: 10.1073/pnas.0508307102
- Kahle, K. T., Schmouth, J. F., Lavastre, V., Latremoliere, A., Zhang, J., Andrews, N., et al. (2016). Inhibition of the kinase WNK1/HSN2 ameliorates neuropathic pain by restoring GABA inhibition. *Sci. Signal.* 9, 1–9. doi: 10.1126/scisignal.aad0163
- Kahle, K. T., Staley, K. J., Nahed, B. V., Gamba, G., Hebert, S. C., Lifton, R. P., et al. (2008). Roles of the cation-chloride cotransporters in neurological disease. *Nat. Clin. Pract. Neurol.* 4, 490–503. doi: 10.1038/ncpneuro0883
- Kaila, K., Price, T. J., Payne, J. A., Puskarjov, M., and Voipio, J. (2014). Cation-chloride cotransporters in neuronal development, plasticity and disease. *Nat. Rev. Neurosci.* 15, 637–654. doi: 10.1038/nrn3819
- Kakazu, Y., Akaike, N., Komiyama, S., and Nabekura, J. (1999). Regulation of intracellular chloride by cotransporters in developing lateral superior olive neurons. *J. Neurosci.* 19, 2843–2851. doi: 10.1523/jneurosci.19-08-02843.1999
- Kharod, S. C., Kang, S. K., and Kadam, S. D. (2019). Off-label use of bumetanide for brain disorders: an overview. *Front Neurosci* 13:310. doi: 10.3389/fnins.2019.00310
- Kieferle, S., Fong, P., Bens, M., Vandewalle, A., and Jentsch, T. J. (1994). Two highly homologous members of the ClC chloride channel family in both rat and human kidney. *Proc. Natl. Acad. Sci. U.S.A.* 91, 6943–6947. doi: 10.1073/pnas.91.15.6943

- Kim, E. R., Wu, Z., Sun, H., Xu, Y., Mangieri, L. R., Xu, Y., et al. (2015). Hypothalamic Non-AgRP, Non-POMC GABAergic neurons are required for postweaning feeding and NPY hyperphagia. *J. Neurosci.* 35, 10440–10450. doi: 10.1523/JNEUROSCI.1110-15.2015
- Kim, G. H., Masilamani, S., Turner, R., Mitchell, C., Wade, J. B., and Knepper, M. A. (1998). The thiazide-sensitive Na-Cl cotransporter is an aldosterone-induced protein. *Proc. Natl. Acad. Sci. U.S.A.* 95, 14552–14557. doi: 10.1073/pnas.95.24.14552
- Kim, M. J., Yang, H. J., Kim, Y., Kang, I., Kim, S. S., and Cho, Y. W. (2018). Role of nitric oxide and WNK-SPAK/OSR1-KCC2 signaling in daily changes in GABAergic inhibition in the rat dorsal raphe neurons. *Neuropharmacology* 135, 355–367. doi: 10.1016/j.neuropharm.2018.03.035
- Koivusalo, M., Kapus, A., and Grinstein, S. (2009). Sensors, transducers, and effectors that regulate cell size and shape. *J. Biol. Chem.* 284, 6595–6599. doi: 10.1074/jbc.R800049200
- Kong, D., Tong, Q., Ye, C., Koda, S., Fuller, P. M., Krashes, M. J., et al. (2012). GABAergic RIP-Cre neurons in the arcuate nucleus selectively regulate energy expenditure. *Cell* 151, 645–657. doi: 10.1016/j.cell.2012.09.020
- Konrad, M., Vollmer, M., Lemmink, H. H., van den Heuvel, L. P., Jeck, N., Vargas-Poussou, R., et al. (2000). Mutations in the chloride channel gene CLCNKB as a cause of classic Bartter syndrome. *J. Am. Soc. Nephrol.* 11, 1449–1459.
- Koumangoye, R., Omer, S., and Delpire, E. (2018). Mistargeting of a truncated Na-K-2Cl cotransporter in epithelial cells. *Am. J. Physiol. Cell Physiol.* 315, C258–C276. doi: 10.1152/ajpcell.00130.2018
- Koumangoye, R., Omer, S., Kabeer, M. H., and Delpire, E. (2020). Novel human NKCC1 mutations cause defects in goblet cell mucus secretion and chronic inflammation. *Cell. Mol. Gastroenterol. Hepatol.* 9, 239–255. doi: 10.1016/j.jcmgh.2019.10.006
- Kumar, M., Gouw, M., Michael, S., Sámano-Sánchez, H., Panca, R., Glavina, J., et al. (2020). ELM-the eukaryotic linear motif resource in 2020. *Nucleic Acids Res.* 48, D296–D306. doi: 10.1093/nar/gkz1030
- Kursan, S., McMillen, T. S., Beesetty, P., Dias-Junior, E., Almutairi, M. M., Sajib, A. A., et al. (2017). The neuronal K+Cl- co-transporter 2 (Slc12a5) modulates insulin secretion. *Sci. Rep.* 7:1732. doi: 10.1038/s41598-017-01814-0
- Lai, Z. F., Chen, Y. Z., and Nishi, K. (2003). Modulation of intracellular Cl- homeostasis by lectin-stimulation in Jurkat T lymphocytes. *Eur. J. Pharmacol.* 482, 1–8. doi: 10.1016/S0014-2999(03)02076-4
- Laird, J. M. A., Garcia-Nicas, E., Delpire, E. J., and Cervero, F. (2004). Presynaptic inhibition and spinal pain processing in mice: a possible role of the NKCC1 cation-chloride co-transporter in hyperalgesia. *Neurosci. Lett.* 361, 200–203. doi: 10.1016/j.neulet.2003.12.015
- Lalioti, M. D., Zhang, J., Volkman, H. M., Kahle, K. T., Hoffmann, K. E., Toka, H. R., et al. (2006). Wnk4 controls blood pressure and potassium homeostasis via regulation of mass and activity of the distal convoluted tubule. *Nat. Genet.* 38, 1124–1132. doi: 10.1038/ng1877
- Lea, I. A., Borghoff, S. J., and Travlos, G. S. (2018). “Electrolytes, blood gases, and acid-base balance,” in *The Clinical Chemistry of Laboratory Animals*, eds D. M. Kurtz and G. S. Travlos (Boca Raton: CRC Press Taylor & Francis group), 873–927.
- Lee, H. H., Deeb, T. Z., Walker, J. A., Davies, P. A., and Moss, S. J. (2011). NMDA receptor activity downregulates KCC2 resulting in depolarizing GABA receptor-mediated currents. *Nat. Neurosci.* 14, 736–743. doi: 10.1038/nn.2806
- Lee, H. H., Jurd, R., and Moss, S. J. (2010). Tyrosine phosphorylation regulates the membrane trafficking of the potassium chloride cotransporter KCC2. *Mol. Cell Neurosci.* 45, 173–179. doi: 10.1016/j.mcn.2010.06.008
- Lee, H. H. C., Walker, J. A., Williams, J. R., Goodier, R. J., Payne, J. A., and Moss, S. J. (2007). Direct protein kinase C-dependent phosphorylation regulates the cell surface stability and activity of the potassium chloride cotransporter KCC2. *J. Biol. Chem.* 282, 29777–29784. doi: 10.1074/jbc.M705053200
- Lemonnier, E., Lazartigues, A., and Ben-Ari, Y. (2016). Treating schizophrenia with the diuretic bumetanide: a case report. *Clin. Neuropharmacol.* 39, 115–117. doi: 10.1097/wnf.0000000000000136
- Lemonnier, E., Villeneuve, N., Sonie, S., Serret, S., Rosier, A., Roue, M., et al. (2017). Effects of bumetanide on neurobehavioral function in children and adolescents with autism spectrum disorders. *Transl. Psychiatry* 7:e1124. doi: 10.1038/tp.2017.101
- Li, H., Khirug, S., Cai, C., Ludwig, A., Blaesse, P., Kolikova, J., et al. (2007). KCC2 Interacts with the dendritic cytoskeleton to promote spine development. *Neuron* 56, 1019–1033. doi: 10.1016/j.neuron.2007.10.039
- Li, H., Tornberg, J., Kaila, K., Airaksinen, M. S., and Rivera, C. (2002). Patterns of cation-chloride cotransporter expression during embryonic rodent CNS development. *Eur. J. Neurosci.* 16, 2358–2370. doi: 10.1046/j.1460-9568.2002.02419.x
- Limbutara, K., Chou, C.-L., and Knepper, M. A. (2020). Quantitative proteomics of all 14 renal tubule segments in rat. *J. Am. Soc. Nephrol.* 31, 1255–1266. doi: 10.1681/ASN.2020010071
- Lin, S.-H., Yu, I.-S., Jiang, S.-T., Lin, S.-W., Chu, P., Chen, A., et al. (2011). Impaired phosphorylation of Na+K+2Cl- cotransporter by oxidative stress-responsive kinase-1 deficiency manifests hypotension and Bartter-like syndrome. *Proc. Natl. Acad. Sci. U.S.A.* 108, 17538–17543. doi: 10.1073/pnas.1107452108
- Loffing, J., Vallon, V., Loffing-Cueni, D., Aregger, F., Richter, K., Pietri, L., et al. (2004). Altered renal distal tubule structure and renal Na+ and Ca2+ handling in a mouse model for gitelman's syndrome. *J. Am. Soc. Nephrol.* 15, 2276–2288. doi: 10.1097/01.ASN.0000138234.18569.63
- Louis-Dit-Picard, H., Barc, J., Trujillano, D., Miserey-Lenkei, S., Bouatia-Naji, N., Pylypenko, O., et al. (2012). KLHL3 mutations cause familial hyperkalemic hypertension by impairing ion transport in the distal nephron. *Nat. Genet.* 44, 456–460. doi: 10.1038/ng.2218
- Lourdell, S., Paulais, M., Cluzeaud, F., Bens, M., Tanemoto, M., Kurachi, Y., et al. (2002). An inward rectifier K(+) channel at the basolateral membrane of the mouse distal convoluted tubule: similarities with Kir4-Kir5.1 heteromeric channels. *J. Physiol.* 538, 391–404. doi: 10.1013/jphysiol.2001.012961
- Lüscher, B. P., Vachel, L., Ohana, E., and Muallem, S. (2020). Cl- as a bona fide signaling ion. *Am. J. Physiol. Physiol.* 318, C125–C136. doi: 10.1152/ajpcell.00354.2019
- Lytle, C., and Forbush, B. (1992). The Na-K-Cl cotransport protein of shark rectal gland. II. Regulation by direct phosphorylation. *J. Biol. Chem.* 267, 25438–25443.
- Lytle, C., and Forbush, B. (1996). Regulatory phosphorylation of the secretory Na-K-Cl cotransporter: modulation by cytoplasmic Cl-. *Am. J. Physiol. Physiol.* 270, C437–C448. doi: 10.1152/ajpcell.1996.270.2.C437
- MacLeod, R. A., and Onofrey, E. (1957). Nutrition and metabolism of marine bacteria: VI. Quantitative requirement for halides, magnesium, calcium, and iron. *Can. J. Microbiol.* 3, 753–759. doi: 10.1139/m57-085
- Macnamara, E. F., Koehler, A. E., D'Souza, P., Estwick, T., Lee, P., Vezina, G., et al. (2019). Kilquist syndrome: a novel syndromic hearing loss disorder caused by homozygous deletion of SLC12A2. *Hum. Mutat.* 40, 532–538. doi: 10.1002/humu.23722
- Malik, S., Lambert, E., Zhang, J., Wang, T., Clark, H. L., Cypress, M., et al. (2018). Potassium conservation is impaired in mice with reduced renal expression of Kir4.1. *Am. J. Physiol. Ren. Physiol.* 315, F1271–F1282. doi: 10.1152/ajprenal.00022.2018
- Mao, S., Garzon-Muvdi, T., Di Fulvio, M., Chen, Y., Delpire, E., Alvarez, F. J., et al. (2012). Molecular and functional expression of cation-chloride cotransporters in dorsal root ganglion neurons during postnatal maturation. *J. Neurophysiol.* 108, 834–852. doi: 10.1152/jn.00970.2011
- Matsumura, Y., Uchida, S., Kondo, Y., Miyazaki, H., Ko, S. B., Hayama, A., et al. (1999). Overt nephrogenic diabetes insipidus in mice lacking the CLC-K1 chloride channel. *Nat. Genet.* 21, 95–98. doi: 10.1038/5036
- McCormick, J. A., and Ellison, D. H. (2011). The WNKs: atypical protein kinases with pleiotropic actions. *Physiol. Rev.* 91, 177–219. doi: 10.1152/physrev.00017.2010
- McCormick, J. A., Mutig, K., Nelson, J. H., Saritas, T., Hoorn, E. J., Yang, C. L., et al. (2011). A SPAK isoform switch modulates renal salt transport and blood pressure. *Cell Metab.* 14, 352–364. doi: 10.1016/j.cmet.2011.07.009
- McNeill, J. K., Walton, J. C., Ryu, V., and Albers, H. E. (2020). The excitatory effects of GABA within the suprachiasmatic nucleus: regulation of Na-K-2Cl Cotransporters (NKCCs) by environmental lighting conditions. *J. Biol. Rhythms* 35, 275–286. doi: 10.1177/0748730420924271
- Meneton, P., Loffing, J., and Warnock, D. G. (2004). Sodium and potassium handling by the aldosterone-sensitive distal nephron: the pivotal role of the distal and connecting tubule. *Am. J. Physiol. Renal Physiol.* 287, F593–F601. doi: 10.1152/ajprenal.00454.2003

- Merner, N. D., Chandler, M. R., Bourassa, C., Liang, B., Khanna, A. R., Dion, P., et al. (2015). Regulatory domain or CpG site variation in SLC12A5, encoding the chloride transporter KCC2, in human autism and schizophrenia. *Front. Cell. Neurosci.* 9:386. doi: 10.3389/fncel.2015.00386
- Merner, N. D., Mercado, A., Khanna, A. R., Hodgkinson, A., Bruat, V., Awadalla, P., et al. (2016). Gain-of-function missense variant in SLC12A2, encoding the bumetanide-sensitive NKCC1 cotransporter, identified in human schizophrenia. *J. Psychiatr. Res.* 77, 22–26. doi: 10.1016/j.jpsychires.2016.02.016
- Mollajani, R., Joghataei, M. T., and Tehrani-Doost, M. (2019). Bumetanide therapeutic effect in children and adolescents with autism spectrum disorder: a review study. *Basic Clin. Neurosci.* 10, 433–441. doi: 10.32598/bcn.9.10.380
- Moon, T. M., Correa, F., Kinch, L. N., Piala, A. T., Gardner, K. H., and Goldsmith, E. J. (2013). Solution structure of the WNK1 autoinhibitory domain, a WNK-specific PF2 domain. *J. Mol. Biol.* 425, 1245–1252. doi: 10.1016/j.jmb.2013.01.031
- Moore, Y. E., Deeb, T. Z., Chadchankar, H., Brandon, N. J., and Moss, S. J. (2018). Potentiating KCC2 activity is sufficient to limit the onset and severity of seizures. *Proc. Natl. Acad. Sci. U.S.A.* 115, 10166–10171. doi: 10.1073/pnas.1810134115
- Moriguchi, T., Urushiyama, S., Hisamoto, N., Iemura, S. I., Uchida, S., Natsume, T., et al. (2005). WNK1 regulates phosphorylation of cation-chloride-coupled cotransporters via the STE20-related kinases. SPAK and OSR1. *J. Biol. Chem.* 280, 42685–42693. doi: 10.1074/jbc.M510042200
- Morris, R. G., Hoorn, E. J., and Knepper, M. A. (2006). Hypokalemia in a mouse model of Gitelman's syndrome. *Am. J. Physiol. Renal Physiol.* 290, F1416–F1420. doi: 10.1152/ajprenal.00421.2005
- Mount, D. B., Mercado, A., Song, L., Jason, X., George, A. L., Delpire, E., et al. (1999). Cloning and characterization of KCC3 and KCC4, new members of the cation-chloride cotransporter gene family. *J. Biol. Chem.* 274, 16355–16362. doi: 10.1074/jbc.274.23.16355
- Murillo-de-Ozores, A. R., Gamba, G., and Castañeda-Bueno, M. (2019). Molecular mechanisms for the regulation of blood pressure by potassium. *Curr. Top. Membr.* 83, 285–313. doi: 10.1016/bs.ctm.2019.01.004
- Murillo-de-Ozores, A. R., Rodríguez-Gama, A., Bazúa-Valenti, S., Leyva-Ríos, K., Vázquez, N., Pacheco-Álvarez, D., et al. (2018). C-terminally truncated, kidney-specific variants of the WNK4 kinase lack several sites that regulate its activity. *J. Biol. Chem.* 293, 12209–12221. doi: 10.1074/jbc.RA118.003037
- Murthy, M., and O'Shaughnessy, K. M. (2019). Modified HEK cells simulate DCT cells in their sensitivity and response to changes in extracellular K. *Physiol. Rep.* 7, 1–10. doi: 10.14814/phy2.14280
- Na, T., Wu, G., and Peng, J.-B. (2012). Disease-causing mutations in the acidic motif of WNK4 impair the sensitivity of WNK4 kinase to calcium ions. *Biochem. Biophys. Res. Commun.* 419, 293–298. doi: 10.1016/j.bbrc.2012.02.013
- Naguro, I., Umeda, T., Kobayashi, Y., Maruyama, J., Hattori, K., Shimizu, Y., et al. (2012). ASK3 responds to osmotic stress and regulates blood pressure by suppressing WNK1-SPAK/OSR1 signaling in the kidney. *Nat. Commun.* 3:1285. doi: 10.1038/ncomms2283
- Niisato, N., Eaton, D. C., and Marunaka, Y. (2004). Involvement of cytosolic Cl⁻ in osmoregulation of α -ENaC gene expression. *Am. J. Physiol. Ren. Physiol.* 287, F932–F939. doi: 10.1152/ajprenal.00131.2004
- Niisato, N., Taruno, A., and Marunaka, Y. (2007). Involvement of p38 MAPK in hypotonic stress-induced stimulation of β - and γ -ENaC expression in renal epithelium. *Biochem. Biophys. Res. Commun.* 358, 819–824. doi: 10.1016/j.bbrc.2007.04.192
- Nomura, H., Sakai, A., Nagano, M., Umino, M., and Suzuki, H. (2006). Expression changes of cation chloride cotransporters in the rat spinal cord following intraplantar formalin. *Neurosci. Res.* 56, 435–440. doi: 10.1016/j.neures.2006.08.012
- Nomura, N., Shoda, W., Wang, Y., Mandai, S., Furusho, T., Takahashi, D., et al. (2018). Role of Cl⁻-K⁺ and barttin in low-potassium induced sodium-chloride cotransporter activation and hypertension in mouse kidney. *Biosci. Rep.* 38:BSR20171243. doi: 10.1042/BSR20171243
- Nomura, N., Tajima, M., Sugawara, N., Morimoto, T., Kondo, Y., Ohno, M., et al. (2011). Generation and analyses of R8L barttin knockin mouse. *Am. J. Physiol. Renal Physiol.* 301, F297–F307. doi: 10.1152/ajprenal.00604.2010
- O'Doherty, J., and Stark, R. J. (1983). A transcellular route for Na-coupled Cl⁻ transport in secreting pancreatic acinar cells. *Am. J. Physiol. Gastrointest. Liver Physiol.* 8, 499–503. doi: 10.1152/ajpgi.1983.245.4.g499
- Ohno, M., Uchida, K., Ohashi, T., Nitta, K., Ohta, A., Chiga, M., et al. (2011). Immunolocalization of WNK4 in mouse kidney. *Histochem. Cell Biol.* 136, 25–35. doi: 10.1007/s00418-011-0827-x
- Ohsawa, R., Miyazaki, H., Niisato, N., Shiozaki, A., Iwasaki, Y., Otsuji, E., et al. (2010). Intracellular chloride regulates cell proliferation through the activation of stress-activated protein kinases in MKN28 human gastric cancer cells. *J. Cell. Physiol.* 223, 764–770. doi: 10.1002/jcp.22088
- Ohta, A., Schumacher, F., Mehellou, Y., Johnson, C., Knebel, A., Macartney, T. J., et al. (2013). The CUL3-KLHL3 E3 ligase complex mutated in Gordon's hypertension syndrome interacts with and ubiquitylates WNK isoforms: disease-causing mutations in KLHL3 and WNK4 disrupt interaction. *Biochem. J.* 451, 111–122. doi: 10.1042/bj20121903
- Oi, K., Sohara, E., Rai, T., Misawa, M., Chiga, M., Alessi, D. R., et al. (2012). A minor role of WNK3 in regulating phosphorylation of renal NKCC2 and NCC co-transporters in vivo. *Biol. Open* 1, 120–127. doi: 10.1242/bio.2011048
- Okabe, A., Shimizu-Okabe, C., Arata, A., Konishi, S., Fukuda, A., and Takayama, C. (2015). KCC2-mediated regulation of respiration-related rhythmic activity during postnatal development in mouse medulla oblongata. *Brain Res.* 1601, 31–39. doi: 10.1016/j.brainres.2015.01.007
- Osei-Owusu, J., Yang, J., Vitery, M., del, C., and Qiu, Z. (2018). "Molecular biology and physiology of volume-regulated anion channel (VRAC)," in *Current Topics in Membranes*, eds I. Levitan, E. Delpire, and H. Rasgado-Flores (Cambridge, MA: Academic Press Inc.), 177–203. doi: 10.1016/bs.ctm.2018.07.005
- Pace, A. J., Lee, E., Athirakul, K., Coffman, T. M., O'Brien, D. A., and Koller, B. H. (2000). Failure of spermatogenesis in mouse lines deficient in the Na⁺-K⁺-2Cl⁻ cotransporter. *J. Clin. Invest.* 105, 441–450. doi: 10.1172/JCI8553
- Pacheco-Álvarez, D., Carrillo-Perez, D. L., Mercado, A., Leyva-Ríos, K., Moreno, E., Hernandez-Mercado, E., et al. (2020). WNK3 and WNK4 exhibit opposite sensitivity with respect to cell volume and intracellular chloride concentration. *Am. J. Physiol. Physiol.* 19, C371–C380. doi: 10.1152/ajpcell.00488.2019
- Pacheco-Álvarez, D., San Cristóbal, P., Meade, P., Moreno, E., Vázquez, N., Muñoz, E., et al. (2006). The Na⁺-Cl⁻ cotransporter is activated and phosphorylated at the amino-terminal domain upon intracellular chloride depletion. *J. Biol. Chem.* 281, 28755–28763. doi: 10.1074/jbc.M603773200
- Pacheco-Cuellar, G., González-Huerta, L. M., Valdés-Miranda, J. M., Peláez-González, H., Zenteno-Bacheron, S., Cazarín-Barrientos, J., et al. (2011). Hereditary sensory and autonomic neuropathy II due to novel mutation in the HSN2 gene in Mexican families. *J. Neurol.* 258, 1890–1892. doi: 10.1007/s00415-011-6025-x
- Paulais, M., Bloch-Faure, M., Picard, N., Jacques, T., Ramakrishnan, S. K., Keck, M., et al. (2011). Renal phenotype in mice lacking the Kir5.1 (*Kcnj16*) K⁺ channel subunit contrasts with that observed in SeSAME/EAST syndrome. *Proc. Natl. Acad. Sci. U.S.A.* 108, 10361–10366. doi: 10.1073/pnas.1101400108
- Payne, J. A., Stevenson, J., and Donaldson, L. (1996). Molecular characterization of putative K⁺-Cl⁻ cotransporter in rat brain. *J. Biol. Chem.* 271, 16245–16252. doi: 10.1074/jbc.271.27.16245
- Pearson, M., Lu, J., Mount, D., and Delpire, E. (2001). Localization of the K⁺-Cl⁻ cotransporter, KCC3, in the central and peripheral nervous systems: expression in the choroid plexus, large neurons and white matter tracts. *Neuroscience* 103, 481–491. doi: 10.1016/S0306-4522(00)00567-4
- Pedemonte, N., and Galletta, L. J. V. (2014). Structure and function of tmem16 proteins (anoctamins). *Physiol. Rev.* 94, 419–459. doi: 10.1113/JP272504
- Penttonen, D., Czogalla, J., Wengi, A., Himmerkus, N., Löffing-Cueni, D., Carrel, M., et al. (2016). Extracellular K⁺ rapidly controls NaCl cotransporter phosphorylation in the native distal convoluted tubule by Cl⁻-dependent and independent mechanisms. *J. Physiol.* 594, 6319–6331. doi: 10.1113/JP272504
- Perrier, R., Boscardin, E., Malsure, S., Sergi, C., Maillard, M. P., Löffing, J., et al. (2016). Severe salt-losing syndrome and hyperkalemia induced by adult nephron-specific knockout of the epithelial sodium channel α -subunit. *J. Am. Soc. Nephrol.* 27, 2309–2318. doi: 10.1681/ASN.2015020154

- Pessia, M., Tucker, S. J., Lee, K., Bond, C. T., and Adelman, J. P. (1996). Subunit positional effects revealed by novel heteromeric inwardly rectifying K⁺ channels. *EMBO J.* 15, 2980–2987. doi: 10.1002/j.1460-2075.1996.tb00661.x
- Piala, A. T., Moon, T. M., Akella, R., He, H., Cobb, M. H., and Goldsmith, E. J. (2014). Chloride sensing by WNK1 involves inhibition of autophosphorylation. *Sci. Signal.* 7:ra41. doi: 10.1126/scisignal.2005050
- Piechotta, K., Lu, J., and Delpire, E. (2002). Cation chloride cotransporters interact with the stress-related kinases Ste20-related proline-alanine-rich kinase (SPAK) and oxidative stress response 1 (OSR1). *J. Biol. Chem.* 277, 50812–50819. doi: 10.1074/jbc.M208108200
- Pigeyre, M., Yazdi, F. T., Kaur, Y., and Meyre, D. (2016). Recent progress in genetics, epigenetics and metagenomics unveils the pathophysiology of human obesity. *Clin. Sci.* 130, 943–986. doi: 10.1042/CS20160136
- Ponce-Coria, J., San-Cristobal, P., Kahle, K. T., Vazquez, N., Pacheco-Alvarez, D., de los Heros, P., et al. (2008). Regulation of NKCC2 by a chloride-sensing mechanism involving the WNK3 and SPAK kinases. *Proc. Natl. Acad. Sci. U.S.A.* 105, 8458–8463. doi: 10.1073/pnas.0802966105
- Price, T. J., Certero, F., and de Koninck, Y. (2005). Role of cation-chloride-cotransporters (CCC) in pain and hyperalgesia. *Curr. Top. Med. Chem.* 5, 547–555. doi: 10.2174/1568026054367629
- Price, T. J., Hargreaves, K. M., and Certero, F. (2006). Protein expression and mRNA cellular distribution of the NKCC1 cotransporter in the dorsal root and trigeminal ganglia of the rat. *Brain Res.* 1112, 146–158. doi: 10.1016/j.brainres.2006.07.012
- Puskarjov, M., Seja, P., Heron, S. E., Williams, T. C., Ahmad, F., Iona, X., et al. (2014). A variant of KCC2 from patients with febrile seizures impairs neuronal Cl⁻ extrusion and dendritic spine formation. *EMBO Rep.* 15, 723–729. doi: 10.1002/embr.201438749
- Rafiqi, F. H., Zuber, A. M., Glouer, M., Richardson, C., Fleming, S., Jouanouić, S., et al. (2010). Role of the WNK-activated SPAK kinase in regulating blood pressure. *EMBO Mol. Med.* 2, 63–75. doi: 10.1002/emmm.200900058
- Rahmani, B., Fekrmandi, F., Ahadi, K., Ahadi, T., Alavi, A., Ahmadiani, A., et al. (2018). A novel nonsense mutation in WNK1/HSN2 associated with sensory neuropathy and limb destruction in four siblings of a large Iranian pedigree. *BMC Neurol.* 18:195. doi: 10.1186/s12883-018-1201-6
- Rahmanzadeh, R., Eftekhari, S., Shahbazi, A., Khodaei Ardakani, M. R., Rahmanzade, R., Mehrabi, S., et al. (2017). Effect of bumetanide, a selective NKCC1 inhibitor, on hallucinations of schizophrenic patients; a double-blind randomized clinical trial. *Schizophr. Res.* 184, 145–146. doi: 10.1016/j.schres.2016.12.002
- Reuter, D., Zierold, K., Schröder, W. H., and Frings, S. (1998). A depolarizing chloride current contributes to chemolectrical transduction in olfactory sensory neurons *in situ*. *J. Neurosci.* 18, 6623–6630. doi: 10.1523/JNEUROSCI.18-17-06623.1998
- Richardson, C., and Alessi, D. R. (2008). The regulation of salt transport and blood pressure by the WNK-SPAK/OSR1 signalling pathway. *J. Cell Sci.* 121, 3293–3304. doi: 10.1242/jcs.029223
- Rickheit, G., Maier, H., Strenzke, N., Andresescu, C. E., De Zeeuw, C. I., Muenscher, A., et al. (2008). Endocochlear potential depends on Cl⁻ channels: mechanism underlying deafness in Bartter syndrome IV. *EMBO J.* 27, 2907–2917. doi: 10.1038/emboj.2008.203
- Rinehart, J., Kahle, K. T., de Los Heros, P., Vazquez, N., Meade, P., Wilson, F. H., et al. (2005). WNK3 kinase is a positive regulator of NKCC2 and NCC, renal cation-Cl⁻ cotransporters required for normal blood pressure homeostasis. *Proc. Natl. Acad. Sci. U.S.A.* 102, 16777–16782. doi: 10.1073/pnas.0508303102
- Rinehart, J., Maksimova, Y. D., Tanis, J. E., Stone, K. L., Hodson, C. A., Zhang, J., et al. (2009). Sites of regulated phosphorylation that control K-Cl cotransporter activity. *Cell* 138, 525–536. doi: 10.1016/j.cell.2009.05.031
- Rivera, C., Voipio, J., Payne, J. A., Ruusuvuori, E., Lahtinen, H., Lamsa, K., et al. (1999). The K⁺/Cl⁻ co-transporter KCC2 renders GABA hyperpolarizing during neuronal maturation. *Nature* 397, 251–255. doi: 10.1038/16697
- Rocha-González, H. I., Mao, S., and Alvarez-Leefmans, F. J. (2008). Na⁺,K⁺,2Cl⁻ cotransport and intracellular chloride regulation in rat primary sensory neurons: thermodynamic and kinetic aspects. *J. Neurophysiol.* 100, 169–184. doi: 10.1152/jn.01007.2007
- Roessler, M., and Müller, V. (2002). Chloride, a new environmental signal molecule involved in gene regulation in a moderately halophilic bacterium, halobacillus halophilus. *J. Bacteriol.* 184, 6207–6215. doi: 10.1128/JB.184.22.6207-6215.2002
- Roessler, M., and Müller, V. (1998). Quantitative and physiological analyses of chloride dependence of growth of halobacillus halophilus. *Appl. Environ. Microbiol.* 64, 3813–3817. doi: 10.1128/AEM.64.10.3813-3817.1998
- Roessler, M., Sewald, X., and Müller, V. (2003). Chloride dependence of growth in bacteria. *FEMS Microbiol. Lett.* 225, 161–165. doi: 10.1016/S0378-1097(03)00509-3
- Rozansky, D. J., Cornwall, T., Subramanya, A. R., Rogers, S., Yang, Y. F., David, L. L., et al. (2009). Aldosterone mediates activation of the thiazide-sensitive Na-Cl cotransporter through an SGK1 and WNK4 signaling pathway. *J. Clin. Invest.* 119, 2601–2612. doi: 10.1172/JCI38323
- Rudomin, P., and Schmidt, R. F. (1999). Presynaptic inhibition in the vertebrate spinal cord revisited. *Exp. Brain Res.* 129, 1–37. doi: 10.1007/s002210050933
- Rust, M. B., Alper, S. L., Rudhard, Y., Shmukler, B. E., Vicente, R., Brugnara, C., et al. (2007). Disruption of erythroid K-Cl cotransporters alters erythrocyte volume and partially rescues erythrocyte dehydration in SAD mice. *J. Clin. Invest.* 117, 1708–1717. doi: 10.1172/JCI30630
- Saritas, T., Puellas, V. G., Su, X. T., McCormick, J. A., Welling, P. A., and Ellison, D. H. (2018). Optical clearing in the kidney reveals potassium-mediated tubule remodeling. *Cell Rep.* 25, 2668.e3–2675.e3. doi: 10.1016/j.celrep.2018.11.021
- Sasaki, S., Hasegawa, K., Higashi, T., Suzuki, Y., Sugano, S., Yasuda, Y., et al. (2016). A missense mutation in solute carrier family 12, member 1 (SLC12A1) causes hydrallantois in Japanese Black cattle. *BMC Genomics* 17:724. doi: 10.1186/s12864-016-3035-1
- Scholl, U. I., Choi, M., Liu, T., Ramaekers, V. T., Hausler, M. G., Grimmer, J., et al. (2009). Seizures, sensorineural deafness, ataxia, mental retardation, and electrolyte imbalance (SeSAME syndrome) caused by mutations in KCNJ10. *Proc. Natl. Acad. Sci. U.S.A.* 106, 5842–5847. doi: 10.1073/pnas.0901749106
- Schultheis, P. J., Lorenz, J. N., Meneton, P., Nieman, M. L., Riddle, T. M., Flagella, M., et al. (1998). Phenotype resembling gitelman's syndrome in mice lacking the apical Na⁺-Cl⁻ cotransporter of the distal convoluted tubule. *J. Biol. Chem.* 273, 29150–29155. doi: 10.1074/jbc.273.44.29150
- Sedmak, G., Jovanov-Milošević, N., Puskarjov, M., Ulamec, M., Krušlin, B., Kaila, K., et al. (2016). Developmental expression patterns of KCC2 and functionally associated molecules in the human brain. *Cereb. Cortex* 26, 4574–4589. doi: 10.1093/cercor/bhv218
- Seifter, J. L., and Chang, H.-Y. (2016). Disorders of acid-base balance: new perspectives. *Kidney Dis.* 2, 170–186. doi: 10.1159/000453028
- Sewald, X., Saum, S. H., Palm, P., Pfeiffer, F., Oesterheld, D., and Müller, V. (2007). Autoinducer-2-producing protein LuxS, a novel salt- and chloride-induced protein in the moderately halophilic bacterium halobacillus halophilus. *Appl. Environ. Microbiol.* 73, 371–379. doi: 10.1128/AEM.01625-06
- Seyberth, H. W., and Schlingmann, K. P. (2011). Bartter- and gitelman-like syndromes: salt-losing tubulopathies with loop or DCT defects. *Pediatr. Nephrol.* 26, 1789–1802. doi: 10.1007/s00467-011-1871-4
- Shekarabi, M., Girard, N., Rivière, J.-B., Dion, P., Houle, M., Toulouse, A., et al. (2008). Mutations in the nervous system-specific HSN2 exon of WNK1 cause hereditary sensory neuropathy type II. *J. Clin. Invest.* 118, 2496–2505. doi: 10.1172/JCI34088
- Shekarabi, M., Lafrenière, R., Gaudet, R., Laganière, J., Marcinkiewicz, M., Dion, P., et al. (2013). Comparative analysis of the expression profile of Wnk1 and Wnk1/Hsn2 splice variants in developing and adult mouse tissues. *PLoS One* 8:e0057807. doi: 10.1371/journal.pone.0057807
- Shibata, S., Zhang, J., Puthumana, J., Stone, K. L., and Lifton, R. P. (2013). Kelch-like 3 and Cullin 3 regulate electrolyte homeostasis via ubiquitination and degradation of WNK4. *Proc. Natl. Acad. Sci. U.S.A.* 110, 7838–7843. doi: 10.1073/pnas.1304592110
- Sievers, F., Wilm, A., Dineen, D., Gibson, T. J., Karplus, K., Li, W., et al. (2011). Fast, scalable generation of high-quality protein multiple sequence alignments using Clustal Omega. *Mol. Syst. Biol.* 7:539. doi: 10.1038/msb.2011.75
- Silayeva, L., Deeb, T. Z., Hines, R. M., Kelley, M. R., Munoz, M. B., Lee, H. H. C., et al. (2015). KCC2 activity is critical in limiting the onset and severity of status epilepticus. *Proc. Natl. Acad. Sci. U.S.A.* 112, 3523–3528. doi: 10.1073/pnas.1415126112

- Simon, D. B., Bindra, R. S., Mansfield, T. A., Nelson-Williams, C., Mendonca, E., Stone, R., et al. (1997). Mutations in the chloride channel gene, *CLCNKB*, cause Bartter's syndrome type III. *Nat. Genet.* 17, 171–178. doi: 10.1038/ng1097-171
- Simon, D. B., Karet, F. E., Hamdan, J. M., Di Pietro, A., Sanjad, S. A., and Lifton, R. P. (1996a). Bartter's syndrome, hypokalaemic alkalosis with hypercalciuria, is caused by mutations in the Na–K–2Cl cotransporter NKCC2. *Nat. Genet.* 13, 183–188. doi: 10.1038/ng0696-183
- Simon, D. B., Nelson-Williams, C., Bia, M. J., Ellison, D., Karet, F. E., Molina, A. M., et al. (1996b). Gitelman's variant of Bartter's syndrome, inherited hypokalaemic alkalosis, is caused by mutations in the thiazide-sensitive Na–Cl cotransporter. *Nat. Genet.* 12, 24–30. doi: 10.1038/ng0196-24
- Sohrabipour, S., Sharifi, M. R., Talebi, A., Sharifi, M., and Soltani, N. (2018). GABA dramatically improves glucose tolerance in streptozotocin-induced diabetic rats fed with high-fat diet. *Eur. J. Pharmacol.* 826, 75–84. doi: 10.1016/j.ejphar.2018.01.047
- Sorensen, M. V., Grossmann, S., Roesinger, M., Gresko, N., Todkar, A. P., Barmettler, G., et al. (2013). Rapid dephosphorylation of the renal sodium chloride cotransporter in response to oral potassium intake in mice. *Kidney Int.* 83, 811–824. doi: 10.1038/ki.2013.14
- Stöberg, T., McTague, A., Ruiz, A. J., Hirata, H., Zhen, J., Long, P., et al. (2015). Mutations in *SLC12A5* in epilepsy of infancy with migrating focal seizures. *Nat. Commun.* 6:8038. doi: 10.1038/ncomms9038
- Su, G., Kintner, D. B., Flagella, M., Shull, G. E., and Sun, D. (2002). Astrocytes from Na(+)-K(+)-Cl(-) cotransporter-null mice exhibit absence of swelling and decrease in EAA release. *Am. J. Physiol. Cell Physiol.* 282, C1147–C1160. doi: 10.1152/ajpcell.00538.2001
- Su, X.-T., and Wang, W.-H. (2016). The expression, regulation, and function of Kir4.1 (*Kcnj10*) in the mammalian kidney. *Am. J. Physiol. Ren. Physiol.* 311, F12–F15. doi: 10.1152/ajprenal.00112.2016
- Subramanya, A. R., and Ellison, D. H. (2014). Distal convoluted tubule. *Clin. J. Am. Soc. Nephrol.* 9, 2147–2163. doi: 10.1002/cphy.c140002
- Succol, F., Fiumelli, H., Benfenati, F., Cancedda, L., and Barberis, A. (2012). Intracellular chloride concentration influences the GABA A receptor subunit composition. *Nat. Commun.* 3:738. doi: 10.1038/ncomms1744
- Sun, Q., Wu, Y., Jonusaite, S., Pleinis, J. M., Humphreys, J. M., He, H., et al. (2018). Intracellular chloride and scaffold protein Mo25 cooperatively regulate transepithelial ion transport through WNK signaling in the malpighian tubule. *J. Am. Soc. Nephrol.* 29, 1449–1461. doi: 10.1681/ASN.2017101091
- Sung, K. W., Kirby, M., McDonald, M. P., Lovinger, D. M., and Delpire, E. (2000). Abnormal GABA_A receptor-mediated currents in dorsal root ganglion neurons isolated from Na–K–2Cl cotransporter null mice. *J. Neurosci.* 20, 7531–7538.
- Susa, K., Sahara, E., Takahashi, D., Okado, T., Rai, T., and Uchida, S. (2017). WNK4 is indispensable for the pathogenesis of pseudohypoadosteronism type II caused by mutant *KLHL3*. *Biochem. Biophys. Res. Commun.* 491, 727–732. doi: 10.1016/j.bbrc.2017.07.121
- Takahashi, N., Chernavvsky, D. R., Gomez, R. A., Igarashi, P., Gitelman, H. J., and Smithies, O. (2000). Uncompensated polyuria in a mouse model of Bartter's syndrome. *Proc. Natl. Acad. Sci. U.S.A.* 97, 5434–5439. doi: 10.1073/pnas.090091297
- Tamari, M., Daigo, Y., and Nakamura, Y. (1999). Isolation and characterization of a novel serine threonine kinase gene on chromosome 3p22-21.3. *J. Hum. Genet.* 44, 116–120. doi: 10.1007/s100380050121
- Tanemoto, M., Abe, T., and Ito, S. (2005). PDZ-Binding and Di-Hydrophobic motifs regulate distribution of Kir4.1 channels in renal cells. *J. Am. Soc. Nephrol.* 16, 2608–2614. doi: 10.1681/ASN.2005030266
- Tanemoto, M., Kittaka, N., Inanobe, A., and Kurachi, Y. (2000). In vivo formation of a proton-sensitive K⁺ channel by heteromeric subunit assembly of Kir5.1 with Kir4.1. *J. Physiol.* 525, 587–592. doi: 10.1111/j.1469-7793.2000.00587.x
- Terker, A. S., Yang, C. L., McCormick, J. A., Meermeier, N. P., Rogers, S. L., Grossmann, S., et al. (2014). Sympathetic stimulation of thiazide-sensitive sodium chloride cotransport in the generation of salt-sensitive hypertension. *Hypertension* 64, 178–184. doi: 10.1161/HYPERTENSIONAHA.114.03335
- Terker, A. S., Yarbrough, B., Ferdaus, M. Z., Lazelle, R. A., Erspamer, K. J., Meermeier, N. P., et al. (2016). Direct and indirect mineralocorticoid effects determine distal salt transport. *J. Am. Soc. Nephrol.* 27, 2436–2445. doi: 10.1681/ASN.2015070815
- Terker, A. S., Zhang, C., Erspamer, K. J., Gamba, G., Yang, C.-L., and Ellison, D. H. (2015a). Unique chloride-sensing properties of WNK4 permit the distal nephron to modulate potassium homeostasis. *Kidney Int.* 89, 1–8. doi: 10.1038/ki.2015.289
- Terker, A. S., Zhang, C., McCormick, J. A., Lazelle, R. A., Zhang, C., Meermeier, N. P., et al. (2015b). Potassium modulates electrolyte balance and blood pressure through effects on distal cell voltage and chloride. *Cell Metab.* 21, 39–50. doi: 10.1016/j.cmet.2014.12.006
- Thastrup, J. O., Rafiqi, F. H., Vitari, A. C., Pozo-Guisado, E., Deak, M., Mehellou, Y., et al. (2012). SPAK/OSR1 regulate NKCC1 and WNK activity: analysis of WNK isoform interactions and activation by T-loop trans-autophosphorylation. *Biochem. J.* 441, 325–337. doi: 10.1042/BJ20111879
- Thomson, M. N., Cuevas, C. A., Bewarder, T. M., Dittmayer, C., Miller, L. N., Si, J., et al. (2020). WNK bodies cluster WNK4 and SPAK/OSR1 to promote NCC activation in hypokalemia. *Am. J. Physiol. Physiol.* 318, F216–F228. doi: 10.1152/ajprenal.00232.2019
- Titz, S., Sammler, E. M., and Hormuzdi, S. G. (2015). Could tuning of the inhibitory tone involve graded changes in neuronal chloride transport? *Neuropharmacology* 95, 321–331. doi: 10.1016/j.neuropharm.2015.03.026
- Tong, Q., Ye, C. P., Jones, J. E., Elmquist, J. K., and Lowell, B. B. (2008). Synaptic release of GABA by AgRP neurons is required for normal regulation of energy balance. *Nat. Neurosci.* 11, 998–1000. doi: 10.1038/nm.2167
- Tornberg, J., Voikar, V., Savilahti, H., Rauvala, H., and Airaksinen, M. S. (2005). Behavioural phenotypes of hypomorphic *KCC2*-deficient mice. *Eur. J. Neurosci.* 21, 1327–1337. doi: 10.1111/j.1460-9568.2005.03959.x
- Torre-Villalvazo, I., Cervantes-Pérez, L. G., Noriega, L. G., Jiménez, J. V., Uribe, N., Chávez-Canales, M., et al. (2018). Inactivation of SPAK kinase reduces body weight gain in mice fed a high-fat diet by improving energy expenditure and insulin sensitivity. *Am. J. Physiol. Endocrinol. Metab.* 314, E53–E65. doi: 10.1152/ajpendo.00108.2017
- Tucker, S. J., Imbrici, P., Salvatore, L., D'Adamo, M. C., and Pessia, M. (2000). pH Dependence of the inwardly rectifying potassium channel. Kir5.1, and localization in renal tubular epithelia. *J. Biol. Chem.* 275, 16404–16407. doi: 10.1074/jbc.C000127200
- Ushiro, H., Tsutsumi, T., Suzuki, K., Kayahara, T., and Nakano, K. (1998). Molecular cloning and characterization of a novel Ste20-Related protein kinase enriched in neurons and transporting epithelia. *Arch. Biochem. Biophys.* 355, 233–240. doi: 10.1006/abbi.1998.0736
- Uvarov, P., Ludwig, A., Markkanen, M., Pruunsild, P., Kaila, K., Delpire, E., et al. (2007). A novel N-terminal isoform of the neuron-specific K–Cl cotransporter *KCC2*. *J. Biol. Chem.* 282, 30570–30576. doi: 10.1074/jbc.M705095200
- Valdivieso, Á.G., Clauzure, M., Massip-Copiz, M., and Santa-Coloma, T. A. (2016). The chloride anion acts as a second messenger in mammalian cells - modifying the expression of specific genes. *Cell. Physiol. Biochem* 38, 49–64. doi: 10.1159/000438608
- Valdivieso, Á.G., and Santa-Coloma, T. A. (2019). The chloride anion as a signalling effector. *Biol. Rev.* 94, 1839–1856. doi: 10.1111/brv.12536
- Vallon, V., Schroth, J., Lang, F., Kuhl, D., and Uchida, S. (2009). Expression and phosphorylation of the Na⁺-Cl⁻ cotransporter NCC in vivo is regulated by dietary salt, potassium, and SGK1. *Am. J. Physiol. Physiol.* 297, F704–F712. doi: 10.1152/ajprenal.00030.2009
- Van Poucke, M., Stee, K., Sonck, L., Stock, E., Bosseler, L., Van Dorpe, J., et al. (2019). Truncating *SLC12A6* variants cause different clinical phenotypes in humans and dogs. *Eur. J. Hum. Genet.* 27, 1561–1568. doi: 10.1038/s41431-019-0432-3
- Vanhatalo, S., Matias Palva, J., Andersson, S., Rivera, C., Voipio, J., and Kaila, K. (2005). Slow endogenous activity transients and developmental expression of K⁺-Cl⁻ cotransporter 2 in the immature human cortex. *Eur. J. Neurosci.* 22, 2799–2804. doi: 10.1111/j.1460-9568.2005.04459.x
- Verissimo, F., and Jordan, P. (2001). WNK kinases, a novel protein kinase subfamily in multi-cellular organisms. *Oncogene* 20, 5562–5569. doi: 10.1038/sj.onc.1204726
- Vidal-Petiot, E., Cheval, L., Faugeron, J., Malard, T., Doucet, A., Jeunemaitre, X., et al. (2012). A new methodology for quantification of alternatively spliced exons reveals a highly tissue-specific expression pattern of WNK1 isoforms. *PLoS One* 7:e0037751. doi: 10.1371/journal.pone.0037751

- Villa, F., Goebel, J., Rafiqi, F. H., Deak, M., Thastrup, J., Alessi, D. R., et al. (2007). Structural insights into the recognition of substrates and activators by the OSR1 kinase. *EMBO Rep.* 8, 839–845. doi: 10.1038/sj.embor.7401048
- Vitari, A. C., Deak, M., Morrice, N. A., and Alessi, D. R. (2005). The WNK1 and WNK4 protein kinases that are mutated in Gordon's hypertension syndrome phosphorylate and activate SPAK and OSR1 protein kinases. *Biochem. J.* 391, 17–24. doi: 10.1042/BJ20051180
- Vitzthum, H., Castrop, H., Meier-Meitingner, M., Riegger, G. A. J., Kurtz, A., Krämer, B. K., et al. (2002). Nephron specific regulation of chloride channel CLC-K2 mRNA in the rat. *Kidney Int.* 61, 547–554. doi: 10.1046/j.1523-1755.2002.00165.x
- Vong, L., Ye, C., Yang, Z., Choi, B., Chua, S. Jr., and Lowell, B. B. (2011). Leptin action on GABAergic neurons prevents obesity and reduces inhibitory tone to POMC neurons. *Neuron* 71, 142–154. doi: 10.1016/j.neuron.2011.05.028
- Wakabayashi, M., Mori, T., Isobe, K., Soharu, E., Susa, K., Araki, Y., et al. (2013). Impaired KLHL3-mediated ubiquitination of WNK4 causes human hypertension. *Cell Rep.* 3, 858–868. doi: 10.1016/j.celrep.2013.02.024
- Waldegger, S., Jeck, N., Barth, P., Peters, M., Vitzthum, H., Wolf, K., et al. (2002). Barttin increases surface expression and changes current properties of CLC-K channels. *Pflugers Arch. Eur. J. Physiol.* 444, 411–418. doi: 10.1007/s00424-002-0819-8
- Waldegger, S., and Jentsch, T. J. (2000). Functional and structural analysis of Cl⁻-K⁺ chloride channels involved in renal disease. *J. Biol. Chem.* 275, 24527–24533. doi: 10.1074/jbc.M001987200
- Wang, M. X., Cuevas, C. A., Su, X. T., Wu, P., Gao, Z. X., Lin, D. H., et al. (2018). Potassium intake modulates the thiazide-sensitive sodium-chloride cotransporter (NCC) activity via the Kir4.1 potassium channel. *Kidney Int.* 93, 893–902. doi: 10.1016/j.kint.2017.10.023
- Watanabe, M., Wake, H., Moorhouse, A. J., and Nabekura, J. (2009). Clustering of neuronal K⁺-Cl⁻ cotransporters in lipid rafts by tyrosine phosphorylation. *J. Biol. Chem.* 284, 27980–27988. doi: 10.1074/jbc.M109.043620
- Watanabe, M., Zhang, J., Shahid Mansuri, M., Duan, J., Karimy, J. K., Delpire, E., et al. (2019). Developmentally regulated KCC2 phosphorylation is essential for dynamic GABA-mediated inhibition and survival. *Sci. Signal.* 12:eaa9315. doi: 10.1126/scisignal.aaw9315
- Weinstein, A. M. (2005). A mathematical model of rat distal convoluted tubule. I. Cotransporter function in early DCT. *Am. J. Physiol. Physiol.* 289, F699–F720. doi: 10.1152/ajprenal.00043.2005
- Wilson, C. S., and Mongin, A. A. (2019). The signaling role for chloride in the bidirectional communication between neurons and astrocytes. *Neurosci. Lett.* 689, 33–44. doi: 10.1016/j.neulet.2018.01.012
- Wilson, F. H., Disse-Nicodém, S., Choate, K. A., Ishikawa, K., Nelson-Williams, C., Desitter, I., et al. (2001). Human hypertension caused by mutations in WNK Kinases. *Science* 293, 1107–1112. doi: 10.1126/science.1062844
- Wilson, F. H., Kahle, K. T., Sabath, E., Lalioti, M. D., Rapson, A. K., Hoover, R. S., et al. (2003). Molecular pathogenesis of inherited hypertension with hyperkalemia: the Na-Cl cotransporter is inhibited by wild-type but not mutant WNK4. *Proc. Natl. Acad. Sci. U.S.A.* 100, 680–684. doi: 10.1073/pnas.242735399
- Woo, N. S., Lu, J., England, R., McClellan, R., Dufour, S., Mount, D. B., et al. (2002). Hyperexcitability and epilepsy associated with disruption of the mouse neuronal-specific K-Cl cotransporter gene. *Hippocampus* 12, 258–268. doi: 10.1002/hipo.10014
- Wu, P., Gao, Z. X., Zhang, D. D., Su, X. T., Wang, W. H., and Lin, D. H. (2019). Deletion of Kir5.1 impairs renal ability to excrete potassium during increased dietary potassium intake. *J. Am. Soc. Nephrol.* 30, 1425–1438. doi: 10.1681/ASN.2019010025
- Wu, Q., Delpire, E., Hebert, S. C., and Strange, K. (1998). Functional demonstration of Na⁺-K⁺-2Cl⁻ cotransporter activity in isolated, polarized choroid plexus cells. *Am. J. Physiol. Physiol.* 275, C1565–C1572. doi: 10.1152/ajpcell.1998.275.6.C1565
- Wu, Q. Q., Liu, X. Y., Xiong, L. X., Shang, J. Y., Mai, X. Y., Pang, R. P., et al. (2016). Reduction of intracellular chloride concentration promotes foam cell formation. *Circ. J.* 80, 1024–1033. doi: 10.1253/circj.CJ-15-1209
- Xie, J., Wu, T., Xu, K., Huang, I. K., Cleaver, O., and Huang, C. L. (2009). Endothelial-specific expression of WNK1 kinase is essential for angiogenesis and heart development in mice. *Am. J. Pathol.* 175, 1315–1327. doi: 10.2353/ajpath.2009.090094
- Xie, J., Yoon, J., Yang, S., Lin, S., and Huang, C. (2013). WNK1 protein kinase regulates embryonic cardiovascular development through the OSR1 signaling cascade. *J. Biol. Chem.* 288, 8566–8574. doi: 10.1074/jbc.M113.451575
- Xie, Y., and Schafer, J. A. (2004). Inhibition of ENaC by intracellular Cl⁻ in an MDCK clone with high ENaC expression. *Am. J. Physiol. Ren. Physiol.* 287, F722–F731.
- Xu, B., English, J. M., Wilsbacher, J. L., Stippec, S., Goldsmith, E. J., and Cobb, M. H. (2000). WNK1, a novel mammalian serine/threonine protein kinase lacking the catalytic lysine in subdomain II. *J. Biol. Chem.* 275, 16795–16801. doi: 10.1074/jbc.275.22.16795
- Xu, B. E., Min, X., Stippec, S., Lee, B. H., Goldsmith, E. J., and Cobb, M. H. (2002). Regulation of WNK1 by an autoinhibitory domain and autophosphorylation. *J. Biol. Chem.* 277, 48456–48462. doi: 10.1074/jbc.M207917200
- Xue, H., Liu, S., Ji, T., Ren, W., Zhang, X. H., Zheng, L. F., et al. (2009). Expression of NKCC2 in the rat gastrointestinal tract. *Neurogastroenterol. Motil.* 21, 1068–e89. doi: 10.1111/j.1365-2982.2009.01334.x
- Yamada, J., Okabe, A., Toyoda, H., Kilb, W., Luhmann, H. J., and Fukuda, A. (2004). Cl⁻ uptake promoting depolarizing GABA actions in immature rat neocortical neurons is mediated by NKCC1. *J. Physiol.* 557, 829–841. doi: 10.1113/jphysiol.2004.062471
- Yang, C. L., Angell, J., Mitchell, R., and Ellison, D. H. (2003). WNK kinases regulate thiazide-sensitive Na-Cl cotransport. *J. Clin. Invest.* 111, 1039–1045. doi: 10.1172/JCI200317443
- Yang, S., Lo, Y., Wu, C., Lin, S., Yeh, C., Chu, P., et al. (2010). SPAK-knockout mice manifest gitelman syndrome and impaired vasoconstriction. *J. Am. Soc. Nephrol.* 21, 1868–1877. doi: 10.1681/ASN.2009121295
- Yang, S. S., Morimoto, T., Rai, T., Chiga, M., Soharu, E., Ohno, M., et al. (2007). Molecular pathogenesis of pseudohypoaldosteronism Type II: generation and analysis of a Wnk4D561A/+ knockin mouse model. *Cell Metab.* 5, 331–344. doi: 10.1016/j.cmet.2007.03.009
- Yang, Y. S., Xie, J., Yang, S. S., Lin, S. H., and Huang, C. L. (2018). Differential roles of WNK4 in regulation of NCC in vivo. *Am. J. Physiol. Ren. Physiol.* 314, F999–F1007. doi: 10.1152/ajprenal.00177.2017
- Zagórska, A., Pozo-Guisado, E., Boudeau, J., Vitari, A. C., Rafiqi, F. H., Thastrup, J., et al. (2007). Regulation of activity and localization of the WNK1 protein kinase by hyperosmotic stress. *J. Cell Biol.* 176, 89–100. doi: 10.1083/jcb.200605093
- Zambrowicz, B. P., Abuin, A., Ramirez-Solis, R., Richter, L. J., Piggott, J., BeltrandelRio, H., et al. (2003). Wnk1 kinase deficiency lowers blood pressure in mice: a gene-trap screen to identify potential targets for therapeutic intervention. *Proc. Natl. Acad. Sci. U.S.A.* 100, 14109–14114. doi: 10.1073/pnas.2336103100
- Zhang, C., Wang, L., Su, X.-T., Lin, D.-H., and Wang, W.-H. (2015). KCNJ10 (Kir4.1) is expressed in the basolateral membrane of the cortical thick ascending limb. *Am. J. Physiol. - Ren. Physiol.* 308, F1288–F1296. doi: 10.1152/ajprenal.00687.2014
- Zhang, J., Siew, K., Macartney, T., O'Shaughnessy, K. M., and Alessi, D. R. (2015). Critical role of the SPAK protein kinase CCT domain in controlling blood pressure. *Hum. Mol. Genet.* 24, 4545–4558. doi: 10.1093/hmg/ddv185
- Zhang, C., Wang, L., Zhang, J., Su, X. T., Lin, D. H., Scholl, U. I., et al. (2014). KCNJ10 determines the expression of the apical Na-Cl cotransporter (NCC) in the early distal convoluted tubule (DCT1). *Proc. Natl. Acad. Sci. U.S.A.* 111, 11864–11869. doi: 10.1073/pnas.1411705111
- Zhang, C., Wang, Z., Xie, J., Yan, F., Wang, W., Feng, X., et al. (2011). Identification of a novel WNK4 mutation in chinese patients with pseudohypoaldosteronism Type II. *Nephron Physiol.* 118, 53–61. doi: 10.1159/000321879
- Zhang, J., Gao, G., Begum, G., Wang, J., Khanna, A. R., Shmukler, B. E., et al. (2016). Functional kinomics establishes a critical node of volume-sensitive cation-Cl⁻ cotransporter regulation in the mammalian brain. *Sci. Rep.* 6, 1–19. doi: 10.1038/srep35986
- Zhang, L., Huang, C. C., Dai, Y., Luo, Q., Ji, Y., Wang, K., et al. (2020). Symptom improvement in children with autism spectrum disorder following bumetanide administration is associated with decreased GABA/glutamate ratios. *Transl. Psychiatry* 10:63. doi: 10.1038/s41398-020-0692-2
- Zhang, Y. L., Chen, P. X., Guan, W. J., Guo, H. M., Qiu, Z. E., Xu, J. W., et al. (2018). Increased intracellular Cl⁻ concentration promotes ongoing inflammation in

- airway epithelium article. *Mucosal Immunol.* 11, 1149–1157. doi: 10.1038/s41385-018-0013-8
- Zhao, H., Nepomuceno, R., Gao, X., Foley, L. M., Wang, S., Begum, G., et al. (2017). Deletion of the WNK3-SPAK kinase complex in mice improves radiographic and clinical outcomes in malignant cerebral edema after ischemic stroke. *J. Cereb. Blood Flow Metab.* 37, 550–563. doi: 10.1177/0271678X16631561
- Zhou, M. S., Nasir, M., Farhat, L. C., Kook, M., Artukoglu, B. B., and Bloch, M. H. (2020). Meta-analysis: pharmacologic treatment of restricted and repetitive behaviors in autism spectrum disorders. *J. Am. Acad. Child Adolesc. Psychiatry* 20:30265. doi: 10.1016/j.jaac.2020.03.007

Conflict of Interest: The authors declare that the research was conducted in the absence of any commercial or financial relationships that could be construed as a potential conflict of interest.

Copyright © 2020 Murillo-de-Ozores, Chávez-Canales, de los Heros, Gamba and Castañeda-Bueno. This is an open-access article distributed under the terms of the Creative Commons Attribution License (CC BY). The use, distribution or reproduction in other forums is permitted, provided the original author(s) and the copyright owner(s) are credited and that the original publication in this journal is cited, in accordance with accepted academic practice. No use, distribution or reproduction is permitted which does not comply with these terms.

REVIEW

WNK4 kinase: from structure to physiology

Adrián Rafael Murillo-de-Ozores,^{1,2} Alejandro Rodríguez-Gama,³ Héctor Carbajal-Contreras,^{1,5}
Gerardo Gamba,^{1,4,5} and María Castañeda-Bueno^{1,5}

¹Department of Nephrology and Mineral Metabolism, Instituto Nacional de Ciencias Médicas y Nutrición Salvador Zubirán, Tlalpan, Mexico City, Mexico; ²Facultad de Medicina, Universidad Nacional Autónoma de México, Coyoacan, Mexico City, Mexico; ³Stowers Institute for Medical Research, Kansas City, Missouri; ⁴Molecular Physiology Unit, Instituto de Investigaciones Biomédicas, Universidad Nacional Autónoma de México, Tlalpan, Mexico City, Mexico; and ⁵Combined Studies Program in Medicine MD/PhD (PECEM), Facultad de Medicina, Universidad Nacional Autónoma de México, Coyoacan, Mexico City, Mexico, Mexico

Abstract

With no lysine kinase-4 (WNK4) belongs to a serine-threonine kinase family characterized by the atypical positioning of its catalytic lysine. Despite the fact that WNK4 has been found in many tissues, the majority of its study has revolved around its function in the kidney, specifically as a positive regulator of the thiazide-sensitive NaCl cotransporter (NCC) in the distal convoluted tubule of the nephron. This is explained by the description of gain-of-function mutations in the gene encoding WNK4 that causes familial hyperkalemic hypertension. This disease is mainly driven by increased downstream activation of the Ste20/SPS1-related proline-alanine-rich kinase/oxidative stress responsive kinase-1-NCC pathway, which increases salt reabsorption in the distal convoluted tubule and indirectly impairs renal K⁺ secretion. Here, we review the large volume of information that has accumulated about different aspects of WNK4 function. We first review the knowledge on WNK4 structure and enumerate the functional domains and motifs that have been characterized. Then, we discuss WNK4 physiological functions based on the information obtained from in vitro studies and from a diverse set of genetically modified mouse models with altered WNK4 function. We then review in vitro and in vivo evidence on the different levels of regulation of WNK4. Finally, we go through the evidence that has suggested how different physiological conditions act through WNK4 to modulate NCC activity.

blood pressure; distal convoluted tubule; distal nephron; epithelial transport; familial hyperkalemic hypertension; potassium

INTRODUCTION

The With No Lysine Family of Kinases

The with no lysine (WNK) family of kinases is a conserved group of serine/threonine kinases found in eukaryotic organisms (1). They were first reported in 2000 with the cloning of *WNK1* from a rat cDNA library (2). Subsequent analysis of genomic sequences in the search for *WNK1* paralogs identified additional family members including *WNK2*, *WNK3*, and *WNK4* (3, 4). These proteins owe their name to the atypical positioning of its catalytic lysine (2). Whereas in most serine/threonine kinases this residue is located in subdomain II of the kinase domain, in the case of WNKs it is located in subdomain I. It has been speculated that this phenomenon is related to the Cl⁻-sensing ability of WNKs (5), as shall be explained below.

WNK kinases have been described to play a role in a variety of physiological and pathophysiological processes, such as cell volume regulation, modulation of transepithelial ion transport, and neurotransmission (6). Although several proteins have been shown to be modulated, directly or indirectly,

by WNK kinases (7, 8), their best-characterized role involves their participation in a signaling pathway comprised of their direct substrates STE20/SPS1-related proline-alanine-rich protein kinase (SPAK) and oxidative stress-responsive kinase-1 (OSR1) (9), which, in turn, act as serine/threonine kinases that phosphorylate and modulate cation-coupled Cl⁻ cotransporters (CCCs) of the SLC12 family (10).

In the past couple of decades, a large amount of information about the structure, regulation, and physiological functions of WNK kinases has accumulated (6, 7, 10, 11). Here, we review the current knowledge about one particular member of this family, WNK4, that plays a key role in kidney physiology.

WNK4

WNK4 is a highly conserved protein, as its orthologs in cartilaginous fishes show close to 50% identity with human WNK4 (hWNK4). In humans, the *WNK4* gene is located in chromosome 17, whereas its mouse ortholog is located in chromosome 11. It is composed of 19 exons, and it was first described due to human disease-causing mutations



found in 2001 by Richard Lifton's group (4). Missense mutations in *WNK4*, as well as intronic deletions in *WNK1*, were found in patients with familial hyperkalemic hypertension (FHHT), also called pseudohypoaldosteronism type II (PHAI) or Gordon syndrome. Additionally, it has been described that loss-of-function mutations in *WNK4* in Burmese cats are associated with feline hypokalemic periodic paralysis (12), which further suggests that *WNK4* plays an important role in K^+ homeostasis.

The fact that *WNK4* mutations were the cause of FHHT prompted several groups around the world to study its relationship to the thiazide-sensitive renal Na^+/Cl^- cotransporter (NCC), believed to be overactive and the cause of the electrolyte imbalance observed in FHHT (13). Several papers have shown that the presence of *WNK4* in the distal convoluted tubule (DCT) is indispensable for the activity of NCC (14, 15). *WNK4*-mediated phosphorylation of the kinases SPAK and OSR1 increases their activity and allows them to phosphorylate and activate NCC (9). It was later found that mutations in the genes Kelch-like family member 3 (*KLHL3*) and cullin 3 (*CUL3*) (16, 17) also cause FHHT, which led to the finding that *WNK4* protein abundance is negatively modulated by ubiquitin-mediated proteasome degradation promoted by the *KLHL3-CUL3* E3 ubiquitin ligase complex (18–20).

Although the most studied role of *WNK4* is the modulation of NCC in the distal nephron, several details are still not clear on the mechanisms that dictate the activity of the *KLHL3/CUL3-WNK4-SPAK/OSR1-NCC* pathway in response to different physiological states. Moreover, the roles of *WNK4* outside the kidney are still obscure, and further investigation is required in this respect.

STRUCTURAL FEATURES OF WNK4

General Description

WNK4 is the smallest member of the mammalian WNK kinase family, with a molecular mass of ~134 kDa. Roughly 35% of the primary sequence of *WNK4* is predicted to have a secondary structure, whereas the remaining 65% is predicted to be disordered (Fig. 1A). Around one-half of those disordered regions contain low-complexity sequences. The low presence of globular domains extends to the other family members, being more notable in the largest member, *WNK1*, that doubles the size of *WNK4*. To what extent such disordered regions influence WNK kinase function remains unclear. Increasing evidence has demonstrated the key role of low-complexity sequences in driving proteins from a dispersed phase to a condensed, assembled state (21). Notably, numerous reports have shown that *WNK-SPAK/OSR1* can form large cytoplasmic protein aggregates upon changes in potassium balance (22, 23).

Analysis of degree of conservation among different members of the WNK family shows sequence homology in three regions of the protein (Fig. 1A). These regions are also predicted to be globular domains by Globplot2 (<http://globplot.embl.de/>) and lie outside the predicted low-complexity regions shown in Fig. 1A. The first conserved region comprises the kinase domain, the first Pask-Fray 2-like (PF2-like) domain (initially described as the autoinhibitory domain

(24, 25), and the acidic domain (4). The second conserved region corresponds to the second PF2-like domain, termed 'PF2-like' by Gagnon et al. (24, 25). The third conserved region includes the COOH-terminal coiled-coil domain (CT-CCD; Fig. 1B) (26).

Below, we describe the regions mentioned above as well as additional domains and motifs that are important for *WNK4* function. We also integrate mechanistic insights derived from studies of other WNK kinases that may be applicable to *WNK4* at the structural and functional levels.

Unique Features of the WNK Kinase Domain

The most conserved region among the WNK kinases is the kinase domain, with ~90% sequence identity between *WNK1*, *WNK2*, and *WNK3*. The kinase domain of *WNK4* appears to be the most divergent one, with an average 82% conservation score with respect to other WNKs. The *WNK1* kinase domain crystal structure was first reported in 2004 and provided details for the mechanism of action of the WNK kinase family (27). Due to the high degree of homology, the same structural features may apply to the kinase domain of *WNK4*.

With a 25% identity to the kinase domains of other serine/threonine kinases, the kinase domain of *WNK1* presents a similar overall fold with a dual-lobe architecture and 12 conserved subdomains (27). The COOH-terminal lobe has a standard general architecture. However, in the NH_2 -terminal lobe, the β -sheet found in other kinases has an additional β -strand in *WNK1* and is rolled up, forming a nearly complete β -barrel.

Regarding the active site, WNK kinases present several particular features. As stated above, one of them is the absence of the catalytic lysine in subdomain II. The crystal structure of *WNK1* confirmed that Lys^{233} (Lys^{186} in hWNK4) that emanates from β -strand 2 (subdomain I) is positioned in the active site, replacing the ATP-binding function of the catalytic lysine found in β -strand 3 (subdomain II) in other kinases. Another distinctive feature is the presence of a DLG motif in subdomain VII instead of the DFG motif found in most protein kinases. The aspartic acid residue of this motif is involved in the binding of Mg^{2+} that interacts with ATP's β - and γ -phosphates and is important for catalysis. Interestingly, the leucine residue of the unique DLG motif of WNK kinases has been shown to be involved in the coordination of Cl^- , whose binding stabilizes *WNK1* in an inactive conformation (5). Substitution of this leucine residue with phenylalanine promotes higher levels of kinase autophosphorylation and prevents kinase inhibition at increasing NaCl concentrations. WNK kinases were long thought to be regulated, directly or indirectly, by intracellular Cl^- concentration, due to their ability to modulate the activation state of CCCs. The Cl^- -sensing protein turned out to be the WNK kinase domain itself. In addition to Leu^{369} of the DLG motif, other residues involved in Cl^- coordination are Phe^{283} , Leu^{299} , and Leu^{371} , which establish hydrophobic interactions with the Cl^- ion (Fig. 2). The backbone amides of Gly^{370} and Leu^{371} also establish hydrogen bonds with the Cl^- ion. Although at the structural level this site has only been described for *WNK1*, the observation that mutation of Leu^{322} of hWNK4 (equivalent to Leu^{369} of *WNK1*) also decreases its sensitivity to inhibition by Cl^- suggests that

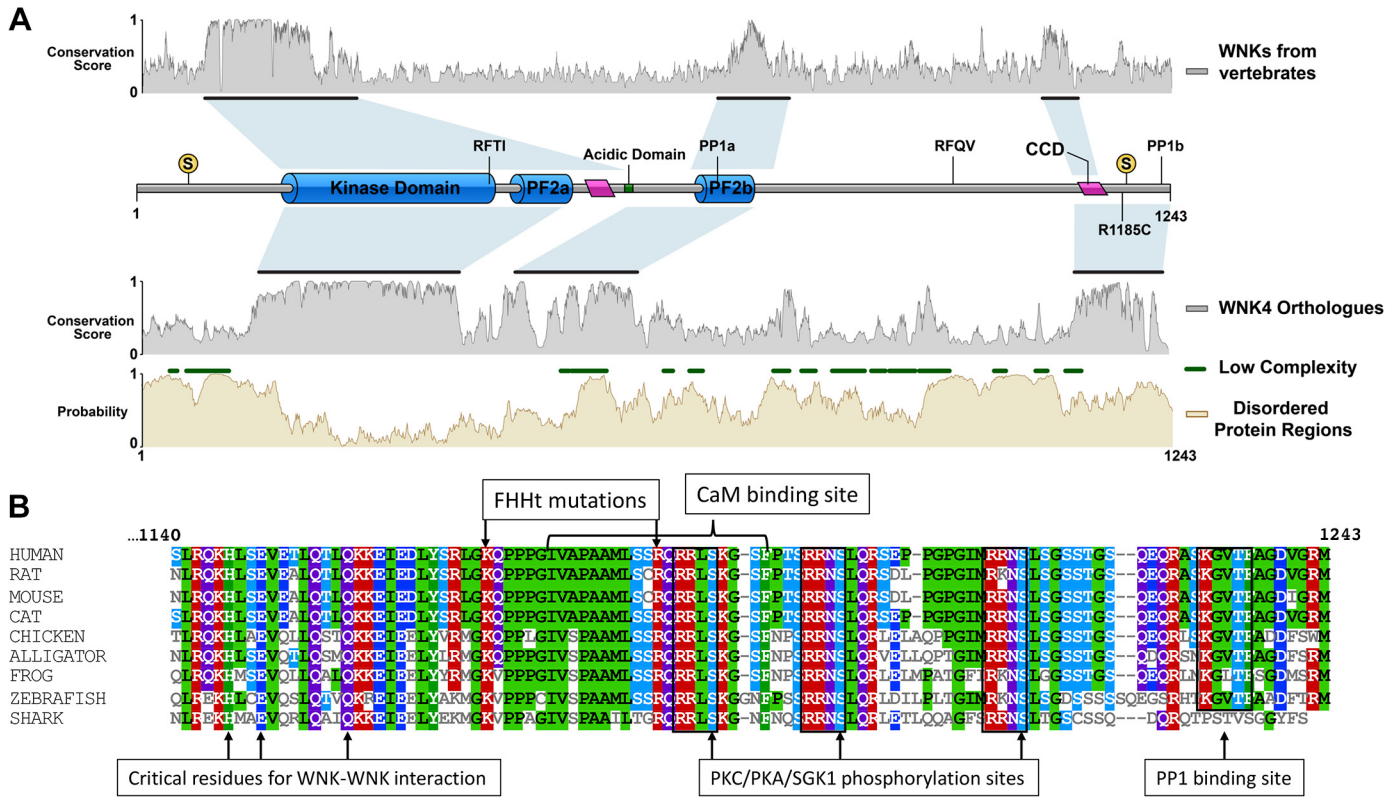


Figure 1. Conserved regions in with no lysine kinase 4 (WNK4). **A:** sequence conservation analysis was performed including the sequences of WNK1-4 kinases from the human, mouse, rat, zebrafish, pig, and clawed frog. Multiple sequence analysis was performed in Clustal Omega, and the conservation score was then calculated by <https://compbio.cs.princeton.edu/conservation/score.html>. The *top* graph shows the conservation score where three major conserved regions were identified. The first conserved region encompasses the kinase domain, the PF2a domain, and the acidic motif. The second and third conserved regions encompass the PF2b domain and the COOH-terminal coiled-coil domain (CT-CCD), respectively. The *middle* graph shows the conservation score observed along the WNK4 sequence in an analysis performed with the sequences of 27 WNK4 orthologs (including mammals, fishes, birds, reptiles, and amphibians). The analysis shows that, in addition to the domains and motifs that are conserved among different WNK kinases, a high degree of conservation was observed in the COOH-terminal segment, from the CT-CCD until the end of the protein. The *bottom* graph shows the results of the analysis of disordered protein regions. Many of these disordered regions overlap with low-complexity regions denoted by a green line. Low-complexity regions were predicted in <http://smart.embl.de/>. Disordered protein region probability was calculated in <https://iupred2a.elte.hu/>. **B:** amino acid sequence alignment of the COOH-terminal region of WNK4 of the human (KEGG entry 65266), rat (KEGG entry 287715), mouse (KEGG entry 69847), cat (KEGG entry 101100264), chicken (KEGG entry 777580), American alligator (KEGG entry 102565768), African clawed frog (KEGG entry 108701024), zebrafish (KEGG entry 100330953), and whale shark (KEGG entry 109912281). Numbers at the *top* represent the residue numbers of human WNK4. Different sites are indicated by arrows, such as critical residues for WNK-WNK binding located within the CT-CCD (153), familial hyperkalemic hypertension (FHHt) mutations (172, 188), calmodulin (CaM)-binding site (101), PKC/PKA/serum/glucocorticoid regulated kinase-1 (SGK1) phosphorylation sites (16, 124, 129), and a protein phosphatase-1 (PP1)-binding site (100). Alignment was generated in Clustal Omega (EMBL-EBI). KEGG, Kyoto Encyclopedia of Genes and Genomes.

this anion also binds to WNK4 in a structurally similar binding pocket (28).

Finally, two residues, Ser³⁷⁸ and Ser³⁸², have been shown to be *trans*-autophosphorylated in the activation loop of WNK1 (also known as the T-loop). These correspond to Ser³³¹ and Ser³³⁵ in hWNK4 (29, 30). As with other kinases, phosphorylation of the activation loop promotes kinase activation because it induces the correct positioning of the catalytic loop and other structures within the active site (31). Phosphorylation at Ser³⁸² of WNK1 has been shown to increase with maneuvers that promote kinase activation like exposure to hyperosmotic stress (29, 30). Thus, evaluation of phosphorylation levels of this site has been used as a surrogate to evaluate kinase activity.

PF2-Like Domains

All WNK kinases share the presence of a PF2-like domain immediately after their kinase domain. In SPAK and OSR1,

the best-known substrates of WNK kinases, two regulatory domains are found within their COOH-terminal region, which were named PF1 and PF2 (32). PASK was the name originally assigned to SPAK by the group that initially cloned it from the rat (33). Fray is the name of the *Drosophila* homolog (34). The PF2 domain in SPAK and OSR1 (also called CCT) can bind motifs with the consensus sequence Arg-Phe-Xxx-Val/Ile (RFxV/I) (35). These RFxV/I motifs are present in WNKs themselves and in CCCs, and they are essential to establish interactions with SPAK and OSR1 (36–39).

The first description of the PF2-like domain in WNK1 identified it as an autoinhibitory region. It was shown that the isolated domain had the ability to suppress the activity of WNK1's kinase domain (29). Later, Gagnon and Delpire noticed that this domain was homologous to the PF2 domain of SPAK and OSR1 and thus coined the term PF2-like (Fig. 3A) (24, 40). The solution of its structure revealed that

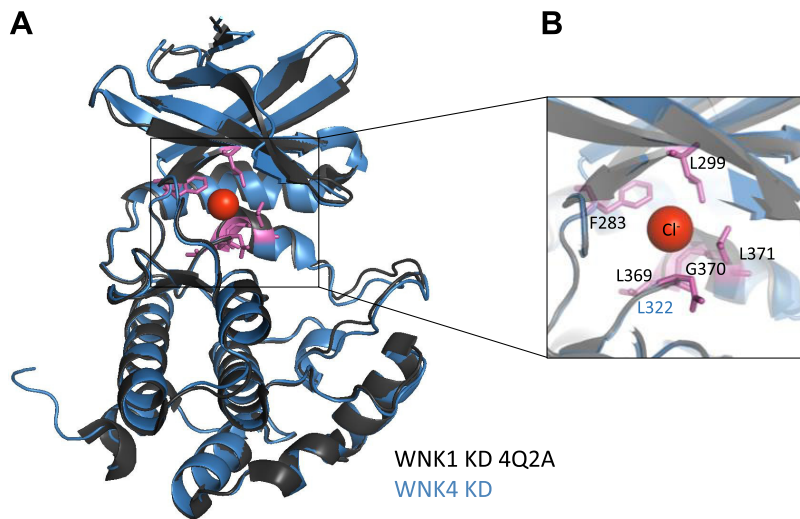


Figure 2. The with no lysine kinase (WNK) 4 kinase domain shares predicted structural features with WNK1. *A*: structural alignment of the WNK1 kinase domain (PDB 4Q2A) with the predicted structure of the kinase domain of WNK4 obtained from the sequence homology-based server <http://raptorx.uchicago.edu/>. *B*, inset: residues whose backbone amides and lateral chains are involved in the coordination of the Cl^- anion. Black labels indicate these amino acid residues in WNK1. Leu³²² in blue denotes the experimentally validated residue involved in Cl^- sensing in WNK4.

indeed it has a similar fold to that of the PF2 domain of SPAK and OSR1 (25, 35). It was also shown that this domain is able to bind RFxV/I-containing peptides with micromolar affinity (25), through similar interactions to those established between RFxV/I motifs and OSR1 (35). Gagnon and Delpire also identified another region in WNK kinases with homology to PF2 domains and referred to it as PF2-like' (24). This region corresponds to the second conserved region among WNK kinases shown in Fig. 1A. For simplicity, we here refer to the PF2-like domains of WNK kinases as PF2a and PF2b.

Modeling of the PF2a and PF2b domains of WNK4 suggests that they can fold in a similar way to other PF2 domains whose structure has been described (Fig. 3B) (24). Through sequence alignment analysis of the WNK4 PF2 domains with those of WNK1 and OSR1, it is possible to note the conservation of several key residues (Fig. 3A). For OSR1's PF2 domain, residues Asp⁴⁵⁹, Phe⁴⁵², and Ile⁴⁵⁰ drive the recognition of RFxV/I motifs within the groove formed by the β 2- α 1 interface (35). The same residues are observed to mediate interactions with the RFxV/I peptide in the WNK1-PF2a structure (corresponding to Asp⁵³¹, Phe⁵²⁴, and Ile⁵²² in WNK1) (25). Such residues are conserved in both PF2 domains of WNK4 as well (Fig. 3A), thus suggesting an inherent ability to recognize RFxV/I motifs.

The autoinhibitory role has been the only function attributed to the PF2a domain of WNK kinases, yet this function was proposed before it was identified as a PF2-like domain. More recently, we have shown that mutation of key residues within the PF2b domain of WNK4 impair its ability to phosphorylate SPAK (41), suggesting that it plays a positive role for kinase function. This effect is not due to impaired interaction with SPAK, as coimmunoprecipitation is still observed (Fig. 3C). Mutation of key residues within the PF2a domain of WNK4 also affect its ability to phosphorylate SPAK without impairing binding (Fig. 3C). Formation of homo- and heteromers among WNK monomers is key to their activity. For instance, it has been shown that mutation of two residues within the CT-CCD of WNKs prevents interaction between WNK monomers (26) and also prevents, for example, the ability of WNK1 to promote NCC activation in *Xenopus laevis*

oocytes (42). Thus, we tested the hypothesis that PF2 domains in WNKs could also be important for mediating WNK-WNK interactions as WNK proteins contain one or more RFxV/I motifs. However, mutation of key residues within PF2a, PF2b, or both domains did not affect interaction between WNK4 monomers (Fig. 3, D and E).

RFxV/I Motifs

As mentioned above, the PF2 domains of SPAK and OSR1 have been shown to mediate interactions with RFxV/I motifs present in CCCs and WNK kinases (36–39). Regarding RFxV/I motifs in WNK kinases, five RFxV/I motifs are distributed along the sequence of WNK1, three can be found in WNK3, and only two are found in WNK2 and WNK4. In all cases, one of these motifs is located in the kinase domain, whereas the additional motifs are located within the COOH-terminal domain. In WNK3, mutation of each one of the three RFxV/I motifs has shown that absence of the motif located within the kinase domain impairs WNK3's ability to activate NCC and $\text{Na}^+ - \text{K}^+ - \text{Cl}^-$ cotransporters (NKCCs) and inhibit $\text{K}^+ - \text{Cl}^-$ cotransporter 3 (KCC3) without impairing kinase activity. In contrast, mutation of the COOH-terminal RFxV/I motifs does not affect these functions (36). The kinase domain RFxV/I motif of WNK3 is conserved in WNK1 and WNK2 and localizes between α -helices 2 and 3. However, in WNK4, a glutamic acid replaces the valine in the last position of the RFxV/I motif. Instead, the kinase domain RFxV/I motif in WNK4 localizes before the α -helix 7 toward the end of the kinase domain. This motif is not conserved in other WNK members, as the phenylalanine is replaced by a tyrosine residue. In WNK4, this RFTI motif is conserved in mammals but changes to RYTI in reptiles, amphibians, birds, and fishes (Fig. 4A). We attempted to address the contributions of both RFxV/I motifs for WNK4's ability to bind and phosphorylate SPAK. Transfection of WNK4 mutants for each of the RFxV/I motifs showed that, whereas the second motif is required for SPAK binding, the first is necessary for SPAK activation (Fig. 4B). Notably, the phenylalanine in the RFTI motif in WNK4 can be replaced by a tyrosine without affecting

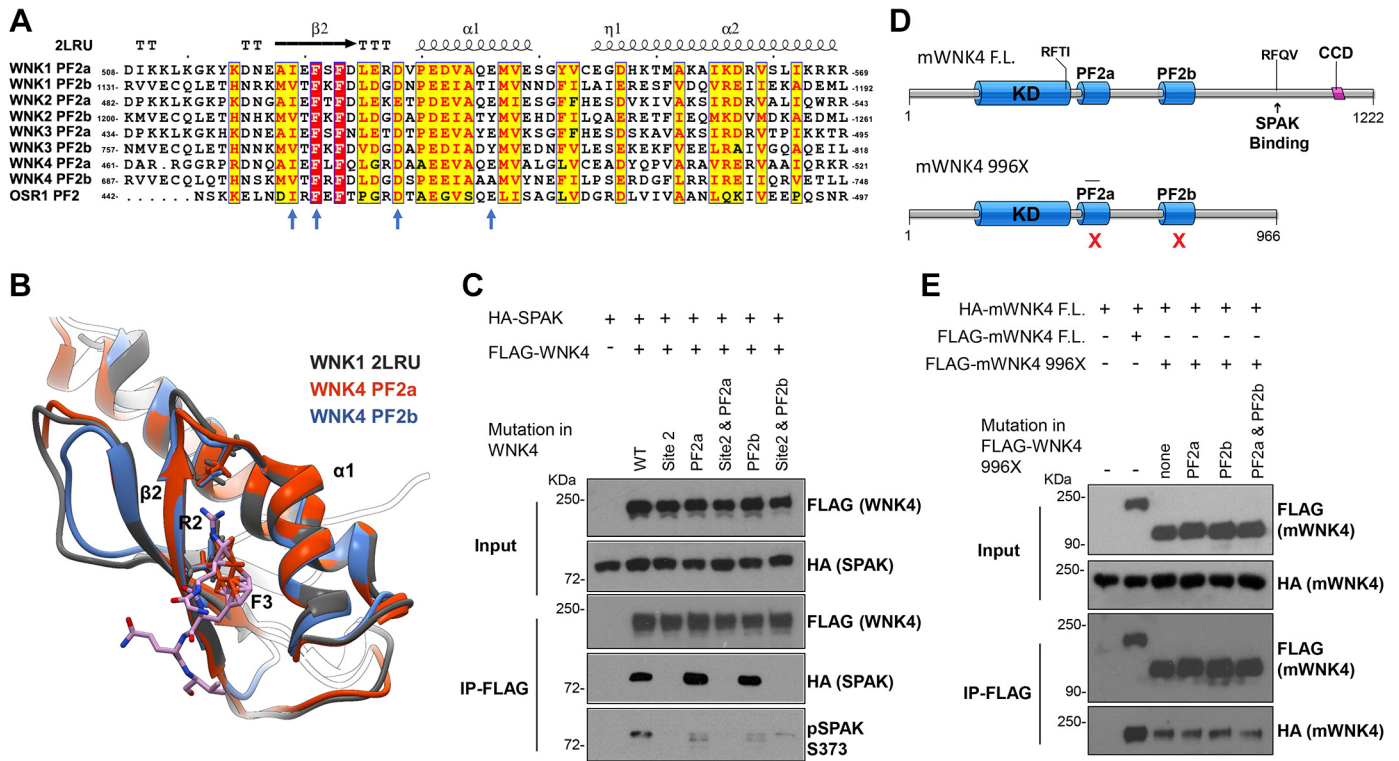


Figure 3. Sequence, structural, and functional analysis of the predicted PF2 domains in with no lysine kinase (WNK4). **A:** sequence homology analysis guided by structural information of the PF2a domain of WNK1 (2LRU) reveals high degree of conservation with PF2 domains of all WNK members and oxidative stress responsive kinase-1 (OSR1). Arrows indicate the conservation of the residues involved in the recognition of the RFXV/I motifs. All sequences correspond to human proteins. **B:** structural alignment of the PF2a domain of WNK1 with the predicted structure of WNK4 PF2a and PF2b domains. Structural prediction was obtained by <http://raptorx.uchicago.edu/>. The predicted structures for both WNK4 PF2 domains show the groove where the RFXV/I motifs bind. R2 and F3 indicate the positions of the Arg and Phe residues of the GRFQVT peptide (93). **C:** representative Western blot of coimmunoprecipitation of human WNK4 and STE20/SPS1-related proline-alanine-rich protein kinase (SPAK) coexpressed in human embryonic kidney (HEK)-293 cells. While the second RFXV/I motif found in mWNK4 (site 2, residues 1016-1019) drives the association of WNK4-SPAK, mutation of key residues within the PF2a (F476A,F478A) or PF2b (F703A,F705A) domains impacts the ability of WNK4 to optimally phosphorylate SPAK at Ser³⁷³. Similar results were observed in two independent experiments. **D:** the attributed function of WNK4's PF2 domains remain to be discovered. To assess whether these domains are important for WNK multimerization, we used a FLAG-tagged full-length mouse WNK4 clone (FLAG-mWNK4 F.L.) and a FLAG-tagged truncated mWNK4 clone at residue 996 (FLAG-mWNK4 996X) that lacks the coiled-coil domain (CCD) as well as RFXV/I site 2. In this last clone, mutations of PF2 domains' key residues were introduced individually or together (same mutations as those tested in C). **E:** by means of coimmunoprecipitation, we tested the interaction between FLAG-tagged WNK4 proteins and a HA-tagged mWNK4 full-length protein. We found that HA-mWNK4 F.L. interacted strongly with FLAG-mWNK4 F.L. (lane 2), but its ability to interact with mWNK4-996X decreased considerably (lane 3), probably due to lack of the COOH-terminal (CT)-CCD (153). However, mutation of the PF2 domains in FLAG-mWNK4-996X individually or together did not further decrease the interaction (lanes 4–6). This suggests that PF2 domains are not essential for multimerization of WNK4, and their function remains to be uncovered. Similar results were observed in two independent experiments.

WNK4's ability to phosphorylate SPAK (Fig. 4, C and D), consistent with the conservation seen in other vertebrates. This also suggests that this is not a bona fide SPAK-binding site, as the PF2 domain is unable to bind RYXV motifs (38).

The observation that the second RFXV/I motif of WNK4 is a bona fide SPAK-binding site might help us to understand the pathophysiology of nonsense mutations in WNK4 found in Burmese cats, as mutant WNK4 in these animals lacks this SPAK-binding motif and therefore behaves as loss of function (12).

Acidic Motif

Most of the FHHt-causative missense mutations in WNK4 characterized so far lie within a 10-amino acid region highly enriched in negatively charged amino acids that is known as the acidic motif (4). One major breakthrough in understanding how WNK4 mutations caused FHHt came with the

identification of mutations in *KLHL3* and *CUL3*, which are components of an E3 ubiquitin ligase complex (16). Normally, WNK4 is targeted for degradation through ubiquitination in at least 15 sites. However, mutations found in the acidic motif of WNK4, which constitutes the binding site for KLHL3, prevent the association with the KLHL3-CUL3 E3 complex leading to protein accumulation (19, 20). The crystal structure of the KLHL3 Kelch domain together with the acidic domain of WNK4 provided definitive evidence on the role of the acidic motif (43).

Coiled-Coil Domains

WNK4 contains two coiled-coil domains (CCD). The first CCD lies immediately after the PF2a domain, whereas the second is located toward the COOH terminus (CT-CCD). These are regions that present sequence conservation in all WNK kinases (Fig. 1). The first CCD has not been described to

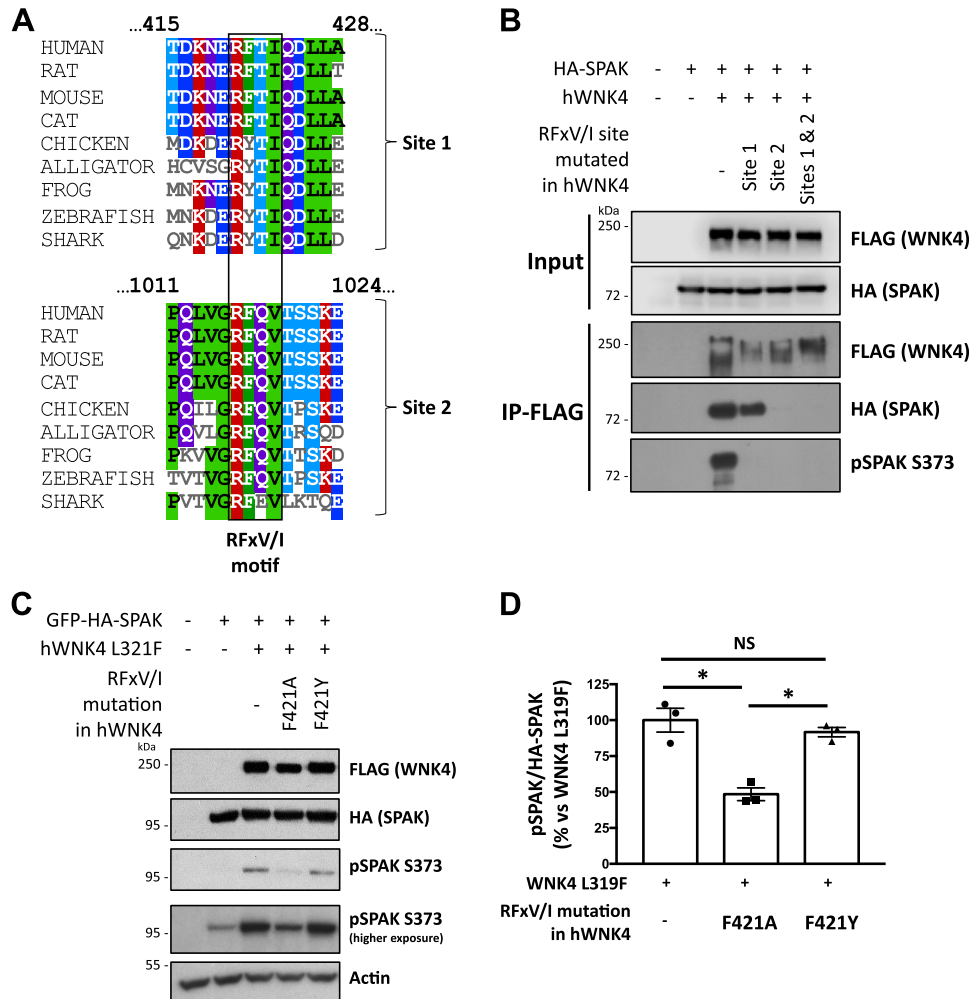


Figure 4. Sequence conservation and functional analysis of RFXV/I motifs in with no lysine kinase 4 (WNK4). **A:** multiple sequence alignment of WNK4 regions encompassing RFXV/I sites 1 and 2. Site 2 shows high degree of conservation, whereas site 1 is conserved in mammals but diverges in the second position (F changes to Y) in other classes. **B:** coimmunoprecipitation assay of STE20/SPS1-related proline-alanine-rich protein kinase (SPAK) and WNK4 proteins with mutated RFXV/I sites. SPAK and human (h)WNK4 clones were coexpressed in human embryonic kidney (HEK)-293 cells. Wild-type and mutant WNK4 proteins were immunoprecipitated, and their interaction with SPAK was assessed by Western blot. Appreciable interaction of SPAK with wild-type WNK4 and the WNK4 site 1 mutant (F421A) was observed. Nevertheless, only wild-type WNK4 was able to mediate SPAK phosphorylation at Ser³⁷³. Conversely, the WNK4 RFXV/I site 2 mutant (RF-1016,1017-AA) and the double mutant were unable to interact with SPAK. Similar results were observed in three independent experiments. **C:** the first RFXV/I motif in WNK4 is not a SPAK-binding site. Mutations affecting RFXV/I site 1 were introduced in a WNK4 clone that also carries the L321F mutation that affects the Cl⁻-binding site and thus impairs inhibition of kinase activity by Cl⁻. Expression of hWNK4-L321F in HEK-293 cells promoted SPAK Ser³⁷³ phosphorylation, whereas this effect was decreased with the F421A but not with F421Y mutation. As Tyr in this position would also affect binding to a PF2 domain (117), this suggests that RFXV/I site 1 is not a SPAK-binding site. Instead, it seems that the aromatic rings of Tyr and Phe establish key interactions that allow maintaining a functional structure. **D:** densitometric analysis of experiments corresponding to Fig. 1C (n = 3). *P < 0.05.

exert any regulatory function yet. Thastrup and colleagues showed that the CT-CCD mediates the formation of homo- and heteromers between WNK kinases (26). Through an alanine-scanning mutagenesis analysis, it was possible to identify that residues His¹¹⁴⁵, Glu¹¹⁴⁸, and Gln¹¹⁵⁶ in hWNK4 are essential for the interaction with WNK1. These three residues have a high degree of conservation in all WNK kinases from different species, including WNK1 from *Caenorhabditis elegans*. It was also shown that WNKs can form high-molecular-mass complexes as detected by size exclusion chromatography, and this is in part dependent on the CT-CCD. The multimerization dependent on the CT-CCD is essential for the functional role of WNK4 over SPAK/OSR1-CCC pathway (42).

Conserved COOH-Terminal Region

From the end of the CT-CCD domain until the end of the protein there is a region with a length of ~70 amino acids in WNK4 that is highly conserved in WNK4 orthologs across species of diverse vertebrate classes, including mammals, reptiles, birds, amphibians, and fishes (Fig. 1B). Within this region, several functional motifs are found. For instance, three phosphorylation sites that lie within RRxS motifs are present, whose modification has been shown to affect WNK4 function (see *Regulatory Mechanisms* below) (44–46). A calmodulin (CaM)-binding site has also been described in which the first RRxS motif is included. Interestingly, two dominant FHHt-causative mutations have been found

within this region: K1169E and R1185C. Arg¹¹⁸⁵ also lies within the proposed CaM-binding site and just five residues upstream of the first COOH-terminal RRxS phosphorylation site (Ser¹¹⁹⁰ in hWNK4 and Ser¹¹⁶⁹ in mWNK4).

Phosphorylation of RRxS sites has been shown to promote WNK4-mediated SPAK phosphorylation (44), to promote WNK4-mediated NKCC2 activation (45), and to prevent the WNK4-mediated NCC inhibition that is observed on basal conditions in *X. laevis* oocytes (46). Deletion of the CaM-binding site has also been shown to promote WNK4-mediated NKCC2 activation (45). Thus, it has been proposed that this region of the protein may play a negative regulatory role on WNK4 kinase activity that may be relieved by phosphorylation of RRxS sites, FHHt mutations, or CaM binding in the presence of Ca²⁺.

Finally, a protein phosphatase-1 (PPI)-binding site has been identified within the last 12 residues of WNK4. Absence of this site promotes hyperphosphorylation and constitutive activation of WNK4 in HEK-293 cells (41). For more details regarding these observations, see *Regulatory Mechanisms* below.

Kidney-Specific Short Forms of WNK4

Our group first reported the presence of short versions of WNK4 specifically in lysates of kidney tissue (41). These short forms are not observed in other tissues, and they lack the COOH-terminal region of WNK4, which contains several regulatory motifs including the SPAK-binding motif (RFxV/I). Thus, according to in vitro experiments with truncated WNK4 mutants, these short forms are predicted to be unable to phosphorylate and activate SPAK.

The presence of short isoforms has been previously described for SPAK (47). These appear to be, at least in part, the product of a proteolytic event (48). In a similar manner, WNK4 short isoforms appear to originate from a proteolytic event mediated by a Zn²⁺-dependent metalloprotease (41). The cleavage site was shown to lie within the amino acids 740–781. The abundance of these WNK4 short forms is not modulated by changes in Na⁺ or K⁺ intake, maneuvers that are known to modulate NCC activity. Thus, further characterization is necessary to decipher their functional contribution to the regulation of renal electrolyte transport.

WNK4 IN PHYSIOLOGY AND PATHOPHYSIOLOGY

Expression Pattern

Initial analysis of the pattern of expression of *WNK4* in humans indicated that this gene is highly expressed in the kidney, as determined by Northern blot (4), although it was also found in the colon and skin by RT-PCR (3). However, later RT-PCR assays in mouse tissues showed *WNK4* expression in the kidney, testis, colon, heart, liver, brain, lung, and spleen (49). Knockout mouse-validated protein expression has been observed in the kidney, testis, lung, and brain (41).

In the kidney, immunostaining assays showed that WNK4 is present in podocytes, the cortical thick ascending limb of Henle's loop (cTAL), the DCT, and cortical and medullary collecting ducts (50). Regarding subcellular localization, it was originally described that WNK4 localized to tight

junctions of renal epithelial cells based on colocalization with zonula occludens 1 (ZO-1) protein (4). However, more recent immunostaining experiments performed with knock-out-validated WNK4 antibodies have not confirmed this observation (23, 44, 50, 51). In the work by Ohno et al., strong staining was observed in the cytoplasmic subapical region of DCT, connecting tubule, and cortical thick ascending limb cells as well as principal cells of the cortical collecting duct. No colocalization was observed with ZO-1 in the DCT (50). In works by other authors, however, staining of kidney sections from mice maintained on standard conditions gives a very mild signal (most times indistinguishable from background signal) (23, 44, 51). However, in tissues from mice exposed to a low-K⁺ diet or volume depleted, conditions in which DCT Na⁺ reabsorption is stimulated, a strong punctuate cytoplasmic signal is observed in DCT cells (23, 44, 51). These structures have been termed “WNK bodies” as explained below in more detail.

Familial Hyperkalemic Hypertension

The DCT of the nephron participates in the regulation of electrolyte homeostasis, as it is involved in the renal handling of Na⁺, Cl⁻, Mg²⁺, and Ca²⁺. Specifically, the DCT mediates transcellular reabsorption of 5–10% of the filtered Na⁺ and Cl⁻ that cross the apical membrane via NCC (52). Interestingly, NCC also regulates K⁺ homeostasis, given that its activity indirectly modulates K⁺ secretion by principal cells in the aldosterone-sensitive distal nephron (ASDN) (53). This effect could be mediated by nephron remodeling (54). The importance of NCC in electrolyte and blood pressure homeostasis as well as acid-base balance became clear by the description of monogenic diseases affecting NCC activity, directly or indirectly, such as Gitelman syndrome and FHHt, respectively.

FHHt was initially described in 1970 (55). As the name indicates, it is a disease characterized by hypertension and hyperkalemia as well as hyperchloremic metabolic acidosis and normo- or hypercalciuria. Since the FHHt phenotype is opposite to the one observed in Gitelman syndrome [caused by loss-of-function mutations in the gene encoding NCC and characterized by hypokalemia, hypovolemia, metabolic alkalosis, and hypocalciuria (56)], and since it is corrected by a low dose of thiazide diuretics (specific inhibitors of NCC) (13, 57), it is thought that the main cause for the whole FHHt phenotype is NCC overactivation. This has been further supported by observations made in a transgenic mouse model where increased NCC activity is enough to promote the whole spectrum of FHHt abnormalities (54).

Despite NCC's involvement in FHHt, no mutations in the gene encoding this protein have been described as a cause for FHHt. Instead, mutations in genes that regulate NCC function have been found in patients with FHHt (Table 1), such as *WNK1*, *WNK4* (4, 59), *KLHL3*, and *CUL3* (16, 17).

FHHt due to mutations in WNK4 is an autosomal dominant trait with high penetrance. Most FHHt mutations within WNK4 are missense mutations that affect the acidic motif, such as E562K, D564A, Q565E (4), D564H (60), P561L (61), and E560G (62). As mentioned above, WNK4 mutations in the acidic motif disrupt its interaction with KLHL3 and prevent WNK4 degradation (18–20). A similar mechanism has been proposed to explain WNK4 activation by mutations

Table 1. Genetic mutations found in patients with FHHt

Gene	Mutation	Mendelian Inheritance	Proposed Mechanism	Corresponding Mouse Model
WNK1	Deletions in intron 1 (4)	Autosomal dominant	Ectopic L-WNK1 expression specifically in the DCT (58)	<i>Wnk1^{FHHt/+}</i> (intron 1 deletion) (58)
	Acidic domain missense mutations: E631K, A634T, D635E, D635N, Q636E, Q636R (59)	Autosomal dominant	Decreased KS-WNK1 degradation in the DCT (59)	<i>Wnk1^{delE631/+}</i> (59)
WNK4	Acidic domain missense mutations: E562K, D564A, Q565E (4), D564H (60), P561L (61), and E560G (62)	Autosomal dominant	Decreased WNK4 degradation in the DCT (20)	<i>Wnk4^{+/+Q562E/Q562E}</i> (63); <i>Wnk4^{D561A/+}</i> (64)
	COOH-terminal missense mutations: R1185C (4) and K1169E (65)	Autosomal dominant	Disruption of the inhibitory domain, promoting increased WNK4 activity (45)	Not reported yet
KLHL3	Several missense mutations (16,17)	Autosomal dominant	Decreased WNK4/KS-WNK1 degradation in the DCT (66,67)	<i>Klhl3^{R528H/+}</i> (66); <i>Klhl3^{M131V/+}</i> (68)
	Several missense mutations (16,17) as well as nonsense mutations and splicing-altering mutations (16)	Autosomal recessive	Decreased WNK4/KS-WNK1 degradation in the DCT (69)	<i>Klhl3^{-/-}</i> (69)
CUL3	Mutations in sites implicated in splicing of exon 9: intron 8 splice acceptor, intron 9 splice donor, putative intron 8 splice branch site, and a putative splice enhancer in exon 9 (12)	Autosomal dominant	Decreased WNK4/KS-WNK1 degradation in the DCT (70); impaired vascular relaxation through activation of the RhoA-ROCK pathway (71)	<i>Cul3^{Δ403-459/+}</i> (72); <i>Cul3^{Het/Δ9}</i> (70); <i>pgk-Cul3Δ⁹</i> (71)

WNK, with no lysine kinase; KLHL3, Kelch-like family member 3; CUL3, cullin 3; L-WNK1, full-length with WNK1; KS-WNK1 kidney-specific WNK1; DCT, distal convoluted tubule; ROCK, Rho kinase; FHHt, familial hyperkalemic hypertension.

in *KLHL3* and *CUL3*, where WNK4 protein levels are increased in the DCT, driving downstream activation of SPAK/OSR1 and ultimately NCC (66, 70, 72).

Additionally, FHHt-causative mutations within the COOH-terminal region of WNK4 have also been described: K1169E (65) and R1185C (4). Although it is not clear how these particular mutations affect the WNK4-SPAK/OSR1-NCC pathway, a possibility is that these mutations may eliminate the inhibitory properties of the COOH terminus of WNK4 (41, 45, 73) toward its kinase activity and/or downstream signaling (see *Structural Features* above).

Murine Models With Altered WNK4 Function

To recapitulate the phenotype of patients with FHHt, Lalioti et al. generated a mouse strain harboring two transgenic copies of the FHHt mutant *WNK4* Q562E, in addition to endogenous copies of *WNK4* (Table 2) (63). These mice displayed high blood pressure levels, hyperkalemia, metabolic acidosis, and hypercalciuria. DCT hyperplasia was also reported. As expected, the phenotype of *WNK4^{+/+Q562E/Q562E}* mice was completely reversed by genetic or pharmacological disruption of NCC, suggesting that FHHt is mainly driven by increased activity of this transporter in the DCT.

In a second FHHt mouse model, the D561A mutation was introduced in WNK4 (64). Heterozygous *WNK4^{+/D561A}* mice displayed higher blood pressure, hyperkalemia, hyperchloremia, and metabolic acidosis compared with *WNK4^{+/+}* mice as well as increased total and phosphorylated levels of NCC

and higher SPAK and OSR1 phosphorylation. Subsequent analysis also showed increased WNK4 protein levels in the kidneys of these mice (20). Accordingly, transgenic mice with additional copies of the *WNK4* gene (either 2 or 30 extra copies) showed higher WNK4 protein levels, as expected, as well as increased downstream phosphorylation of SPAK/OSR1 and NCC, which caused hypertension, hyperkalemia, and metabolic acidosis (20). These observations showed that FHHt-causing mutations in *WNK4* promote increased protein levels of WNK4 that are responsible for the FHHt phenotype.

As initial attempts to generate *WNK4* knockout mice were not successful, hypomorphic *WNK4* mice were generated by disrupting exon 7, which was expected to produce a COOH-terminally truncated WNK4 protein. However, splicing between exons 6 and 9 was observed, which had no frameshift, producing a WNK4 protein lacking the middle portion of WNK4, specifically, part of the PF2-like domain, the first CCD, and the acidic domain (74). Kinase assays showed that this mutant WNK4 immunoprecipitated from human embryonic kidney (HEK)-293 cells and mouse kidneys had a diminished kinase activity toward itself and SPAK. Hypomorphic *WNK4* mice displayed mild hypotension as well as mildly decreased levels of phosphorylated (p)OSR1 and NCC. This was the first in vivo evidence that hinted at the positive modulation of NCC by WNK4. Right after FHHt mutations were described in WNK4, initial observations made in certain in vitro and in vivo models suggested that WNK4 had an inhibitory role on NCC activity that was

Table 2. Genetically modified mouse models with altered WNK4 expression/function

Mouse Model	Mutation	Effect on Protein Function and/or Levels	Phenotype	Original Report
Transgenic WNK4 ^{+/+/Q562E/Q562E}	Two additional copies of the WNK4 gene harboring FHHT mutation Q562E (equivalent to Q565E in human WNK4)	Higher WNK4 levels (19)	FHHT-like: increased blood pressure, hyperkalemia, metabolic acidosis, and hypercalciuria as well as DCT hyperplasia	(63)
WNK4 ^{D561A/+}	D561A (equivalent to D564A in human WNK4)	Higher WNK4 levels, due to decreased degradation (20)	FHHT-like: increased blood pressure, hyperkalemia, hyperchloremic metabolic acidosis, higher NCC levels, and phosphorylation	(64)
WNK4 hypomorphic	Exon 7 deletion	Abnormal splicing between exons 6 and 9, with a protein lacking 14 kDa in the middle portion. WNK4 ^{ΔEx7-8} has decreased kinase activity	Gitelman-like: lower blood pressure and decreased OSR1 and NCC phosphorylation	(74)
WNK4 ^{-/-}	Deletion of exon 1	Absent WNK4 expression	Gitelman-like: hypokalemia, hypochloremic metabolic alkalosis, hypomagnesemia, increased plasma renin activity; virtually absent NCC phosphorylation and lower NCC levels (both at mRNA and protein levels)	(14)
Transgenic (WNK4 ^{WT})	Additional copies of WNK4 (2 copies or 30 extra copies)	Higher WNK4 protein levels	FHHT-like: high blood pressure, hyperkalemia with hyperchloremic metabolic acidosis, higher SPAK, OSR1 and NCC expression. and phosphorylation	(20)
WNK4 ^{-/-}	Deletion of exon 2	Absent WNK4 expression	Gitelman-like: lower blood pressure while on a low-NaCl diet and decreased SPAK and NCC expression and phosphorylation	(15)
WNK4 ^{-/-}	Deletion of exons 1 and 2	Absent WNK4 expression	Gitelman-like: lower NCC expression and phosphorylation	(75)
WNK4 ^{L319F,L321F/L319F,L321F}	L319F and L321F	Cl ⁻ -insensitive WNK4 and therefore, constitutively active kinase	FHHT-like: increased blood pressure, higher plasma K ⁺ concentration, and hyperchloremic metabolic acidosis, with higher NCC expression and phosphorylation	(76)

WNK, with no lysine kinase; FHHT, familial hyperkalemic hypertension; DCT, distal convoluted tubule; NCC, NaCl cotransporter; OSR1, oxidative stress-responsive 1; SPAK, STE20/SPS1-related proline-alanine-rich protein kinase.

reversed by FHHT mutations (63, 77, 78). However, these observations contrasted with the data later obtained by Vitari et al., showing that WNK4 can phosphorylate and activate SPAK and OSR1 in in vitro kinase assays (9), which, in turn, can phosphorylate and activate NCC (79).

Definitive confirmation of WNK4 as an activator of NCC came with the first report of a WNK4 knockout (-/-) mouse model generated by disruption of exon 1. These mice displayed a phenotype similar to that of Gitelman syndrome (14). Compared with their wild-type (WT) siblings, WNK4^{-/-} mice showed hypokalemia, hypochloremia, metabolic alkalosis, hypomagnesemia, and increased plasma renin activity. Hypokalemia was greatly accentuated by a low-K⁺ diet. WNK4^{-/-} mice had lower levels of NCC (both at transcript and protein levels) and virtually undetectable pNCC accompanied by a blunted response to thiazide diuretics. Increased response to amiloride suggested epithelial Na⁺ channel (ENaC) activation as a mechanism to compensate for NCC deficiency. Later, a second WNK4^{-/-} mouse model, with disruption of exon 2, was reported (15). These mice displayed a similar phenotype, showing a reduction of NCC expression and activity, with lower blood pressure levels while under a

low-Na⁺ diet. Interestingly, these mice did not show hypokalemia in basal conditions, possibly due to an effect of the genetic background, sample collection, and/or differences of the diet. Notably, DCT morphological changes were observed in these mice, specifically tubule dilation and lower cell height. A third WNK4^{-/-} mouse model with exon 1 and 2 deletion showed similar findings with respect to total and pNCC levels as well as blunted thiazide response (75). These mice also did not show hypokalemia while under a control diet; however, plasma K⁺ concentration was lower while under a low-K⁺ diet compared with WT mice, further confirming that WNK4 plays an important role in the modulation of K⁺ homeostasis.

Even though WNK4 is expressed in a variety of organs, it is puzzling that WNK4^{-/-} mice have a relatively mild phenotype, with alterations of renal origin only. This might suggest that other WNK kinases might have the ability to compensate for the absence of WNK4 in other cells. Of note, although the expected Mendelian frequencies were observed among the progeny of reproductive crosses between WNK4^{+/-} mice, it was reported that WNK4^{-/-} mice, when crossed with each other, had a lower number of offspring

(14). It is currently unknown whether this observation is related to a neurological or reproductive defect or both.

In 2019, a mouse model generated with CRISPR/Cas9 was reported where specific missense mutations were introduced in exon 3 of *WNK4*, causing the substitutions L319F and L321F in the *WNK4* protein [Chen et al. (76)]. In vitro, these changes render *WNK4* constitutively active, as it no longer has the ability to bind Cl^- (see *Regulatory Mechanisms* below). As expected, these mice showed a FHHt-like phenotype, with increased blood pressure and higher plasma K^+ and Cl^- concentrations as well as metabolic acidosis, and higher levels of pSPAK/OSR1 and total and pNCC.

All of these studies in murine models have been instrumental in establishing *WNK4* as a major positive regulator of SPAK/OSR1-NCC in the DCT in vivo, where this pathway is regulated by different mechanisms that will be detailed in later sections.

Interaction With Downstream Kinases SPAK and OSR1

As mentioned above, *WNK4* promotes NCC activation by phosphorylating and activating the intermediate kinases SPAK and OSR1, which, in turn, phosphorylate NCC. The initial description of the participation of SPAK and OSR1 in this pathway came when Piechotta et al. (38) identified the interaction of both kinases with the NH_2 terminus of multiple CCCs, mediated by the RFXV/I motifs present in the latter. Later on, Dowd and Forbush showed in HEK-293 cells that overexpression of wild-type SPAK significantly increased NKCC1 activity, which correlated with increased cotransporter phosphorylation, and that kinase-inactive SPAK exerted dominant-negative effects on NKCC1 function, inhibiting activity and phosphorylation (80).

A couple of years later, a link was made between *WNK* and SPAK/OSR1 activity, when Vitari et al. (9) discovered that SPAK and OSR1 were among the proteins interacting with *WNK1* and *WNK4* and, through kinase assays, showed that the kinase domains of *WNK1* and *WNK4* were able to phosphorylate and increase the activity of SPAK and OSR1. Similar observations were made simultaneously by Moriguchi et al. (81). Two phosphorylation residues targeted by *WNK* kinases were found: Thr²³³ and Ser³⁷³ in hSPAK and Thr¹⁸⁵ and Ser³²⁵ in hOSR1. The first of these residues lies in the kinases' T-loop and is critical for its activation. Meanwhile, the mutation of the second residue did not affect kinase activity (9), but its phosphorylation has been used as a readout of *WNK* activity toward SPAK/OSR1 (44, 64, 82, 83). A recent report has suggested that phosphorylation of this site might be involved in decreased SPAK degradation mediated by CUL4 (84).

In Vivo Models With Genetically Modified SPAK and OSR1 Reveal the Physiological Importance of These Kinases for the Modulation of NCC by *WNK4*

Several mouse models with gain- and loss-of-function mutations in SPAK or OSR1 have reinforced the concept that these kinases lie upstream to CCC phosphorylation. In addition, as explained below, these models have also been useful to demonstrate, for example, that SPAK and OSR1 serve as substrates of *WNK4* in the DCT and that most of the function

of *WNK4* within this nephron segment depends on SPAK/OSR1 phosphorylation.

In 2010, Rafiqi et al. (85) reported that C57BL/6 mice carrying an inactive version of SPAK (SPAK^{T243A/T243A} mice) have diminished phosphorylation of NCC, NKCC1, and NKCC2 in the kidney. The decrease in NCC activity appears to predominate, as the mice display a Gitelman syndrome-like phenotype with hypocalcemia instead of the characteristic hypercalciuria observed in patients with Bartter syndrome who have dysfunctional NKCC2. Other Gitelman syndrome-like features observed were hypotension and hypokalemia (the latter was observed only under a low- Na^+ diet) (85). A few years later, several groups reported the generation of SPAK^{-/-} mouse models, all of which also presented a Gitelman syndrome-like phenotype (47, 86, 87).

Attempts to generate a global OSR1 loss-of-function knockin or knockout mouse model have not been successful, as complete lack of function of this kinase is lethal during embryonic life (85, 87). However, heterozygous deletion of the kinase and kidney-specific knockout models have been studied. OSR1^{+/-} mice are hypotensive but have no differences in plasma or urinary electrolytes (87). Meanwhile, kidney-specific OSR1 knockout mice (KS-OSR1^{-/-}) are normotensive on a normal Na^+ diet but display hypokalemia and lower urinary osmolality, reduced sensitivity to loop diuretics, along with hypercalciuria and diminishment of pNKCC2, with an increase in total NCC and pNCC (88). Thus, it was proposed that OSR1 activity is more relevant for NKCC2 regulation in the thick ascending limb of Henle's loop, whereas in the DCT its absence can be compensated for by SPAK activity. In contrast, SPAK plays a more relevant role for NCC regulation in the DCT, where OSR1 cannot fully compensate for the absence of SPAK activity.

Nevertheless, further evidence has shown that OSR1 does play a role in NCC regulation and in the pathophysiology of FHHt caused by overexpression of *WNK4*. For instance, Chiga et al. (89) used *WNK4*^{D561A/+} mice and crossbred them with SPAK^{T243A/+} and OSR1^{T185A/+} mice to analyze the effect of reducing or impairing SPAK and OSR1 activity on the FHHt phenotype. They observed that *WNK4*^{D561A/+} SPAK^{T243A/T243A} mice had an intermediate phenotype between wild-type and *WNK4*^{D561A/+} mice (with systolic blood pressure, plasma K^+ concentration levels, and pNCC levels lower than in *WNK4*^{D561A/+} mice but higher than in wild-type mice). However, in *WNK4*^{D561A/+} SPAK^{T243A/T243A} OSR1^{T185A/+} mice, systolic blood pressure, plasma K^+ concentration levels, and pNCC levels were lower than in wild-type mice, showing that overactivation of both SPAK and OSR1 by *WNK4* is responsible for the FHHt phenotype.

A similar strategy was performed with SPAK^{-/-} and KS-OSR1^{-/-} mice on a *WNK4*^{D561A/+} background, where similar results were obtained (90). In this work, Chu et al. observed that *WNK4*^{D561A/+} SPAK^{-/-} mice had similar levels of NCC and pNCC to wild-type mice. Their systolic blood pressure and plasma electrolytes along with their thiazide-sensitive Na^+ and Cl^- urinary excretion were normal. However, *WNK4*^{D561A/+} SPAK^{-/-} mice had higher levels of pNCC and NCC than SPAK^{-/-} mice, suggesting that most likely OSR1 was responsible for the observed phosphorylation. Indeed, pNCC and NCC were further reduced in triple mutants (*WNK4*^{D561A/+} SPAK^{-/-} KS-OSR1^{-/-}).

Additional evidence pointing to a relevant role for OSR1 in DCT physiology comes from observations made in mice in which NCC activity is stimulated by administration of a low- K^+ diet. As discussed below in *Role of Wnk4 in the Regulation of NCC by Physiological Stimuli*, low K^+ intake is one of the more potent stimuli for NCC activation, and WNK4 plays a key role in the signaling pathway that mediates this effect (75, 91). Interestingly, low K^+ -induced activation of NCC can be clearly observed in SPAK^{T243A/T243A}, SPAK^{-/-}, and KS-OSR1^{-/-} mice (91, 92), whereas activation is dramatically reduced in double-knockout mice (SPAK^{-/-}KS-OSR1^{-/-}) (92).

Finally, Grimm et al. used an elegant strategy to generate an in vivo model of gain of function of SPAK in the early DCT (54). These mice express constitutively active SPAK exclusively in parvalbumin-expressing cells, which in the kidney are restricted to DCT cells. All other cell types are effectively SPAK null. The mice were named CA-SPAK and were shown to develop the classic FHHt phenotype with hyperkalemia, hypertension, and acidosis as well as a lower fractional urinary excretion of K^+ , all of which resolved with thiazides. These findings correlated with a significant increase in NCC and pNCC and an increase in the area and length of the DCT1 at the expense of a reduction of these measurements in the CNT. Thus, this model demonstrated that SPAK hyperactivity in the DCT is sufficient to produce FHHt and that NCC hyperactivity is sufficient to drive morphological changes in the ASDN.

In summary, as can be noted, mouse models of SPAK gain or loss of function have many similarities in their renal phenotype with WNK4 gain- or loss-of-function mouse models, respectively, as is expected for proteins that are in the same signaling pathway. Taken together, all these findings strongly suggest that the main mechanism through which WNK4 mediates both the phosphorylation of NCC and pathogenesis of FHHt is through the phosphorylation and activation of SPAK and OSR1.

SPAK/OSR1-Independent Regulation of Phosphorylation of CCCs

The presence of PF2-like domains in WNK4 led to the in vitro finding of WNK4 being able to bind and directly phosphorylate NKCC1 and NKCC2 in the residues known to be targeted by SPAK/OSR1 when overexpressed in conjunction with Cab39/MO25 in *X. laevis* oocytes (93). Whether direct phosphorylation of CCCs by WNK4 is physiologically relevant in any in vivo condition remains unknown.

WNK4 Functions Not Involving NCC

In addition to the best-described role of WNK4 in the regulation of the SPAK/OSR1-NCC pathway, some works, mainly performed in in vitro systems, have shown that WNK4 can regulate other membrane transport proteins, many of which also participate in renal electrolyte handling (Fig. 5). Below, we make a brief mention of some of these findings.

The SLC12 Family of Cotransporters

CCCs of the SLC12 family participate in a wide range of physiological processes (6, 94), which include the regulation of epithelial transport, regulation of intracellular Cl^- concentration of excitable cells, regulation of cellular volume, etc.

The seven well-characterized members of the SLC12 family (NCC, NKCC1, NKCC2, KCC1, KCC2, KCC3, and KCC4) are all subject to regulation by SPAK/OSR1-mediated phosphorylation (79, 80, 95, 96), and WNK4 is expressed in multiple tissues where different CCCs are expressed (3, 41, 97). Thus, it is possible that WNK4 could participate in the physiological regulation of CCCs other than NCC.

In vitro experiments have shown a possible role of WNK4 in the regulation of most members of the SLC12 family. For instance, it can increase the activity of NKCC1 and NKCC2 in *X. laevis* oocytes (45, 93, 98) and decrease the activity of KCCs (99). WNK4-induced phosphorylation of NKCC2 can also be observed in the HEK-293 cell system (100). However, only a couple of studies have analyzed the possible role of WNK4 in the regulation of these cotransporters in vivo.

For instance, a work by Terker et al. has recently suggested a role for WNK4 in NKCC2 regulation (100) (Fig. 5A). Given that WNK4^{-/-} mice present normocalciuria, Terker and co-workers hypothesized that this could be due to the additive dysfunction of NKCC2 and NCC, since the dysfunction of the former leads to hypercalciuria and dysfunction of the latter leads to hypocalciuria. They observed that WNK4^{-/-} mice have markedly decreased pNKCC2 levels in Western blot assays. However, recent findings have shown that, in mice bred on the C57BL/6 background (such as WNK4^{-/-} mice), the most frequently used antibodies targeting pNKCC2 (Thr⁹⁶/Thr¹⁰¹) mostly recognize NCC unspecifically in immunoblots (101). This is due to a genetic deletion of 15 bp encoding the highly conserved residues 96–100 of mouse (m) NKCC2 that prevents binding of the phosphoantibodies to NKCC2. Given this previously unknown fact, pNKCC2 levels in WNK4^{-/-} mice should be reassessed. However, a slight decrease in pNKCC2 was also observed by immunofluorescence in NKCC2-positive tubules by using antibodies directed against pThr⁹⁶/Thr¹⁰¹ and another phosphoacceptor site that is not affected by the deletion (pSer⁹¹).

Melo et al. also used WNK4^{-/-} mice on a low- Na^+ diet to show that WNK4 was not required for the upregulation of KCC4 in this condition (102). Whether the absence of WNK4 leads to different levels of baseline total or pKCC4 was not examined.

Epithelial Na^+ Channels

The description of FHHt-causative mutations in WNK4 and the renal origin of FHHt gave place to research focused not only on WNK4's regulation of NCC but also of other transport proteins in the nephron whose dysregulation could potentially contribute to the observed phenotype. One of these proteins was ENaC. ENaC is a heterotrimeric amiloride-sensitive channel formed by three subunits (α , β , and γ) expressed in many tissues. Within the kidney, it is expressed in principal cells of the ASDN, where its activity drives Na^+ reabsorption and K^+ secretion (103, 104). Heterologous overexpression in *X. laevis* oocytes showed that coexpression of WNK4 with ENaC subunits led to a reduction of amiloride-sensitive currents (Fig. 5C). This was preserved when catalytically inactive versions of WNK4 were coexpressed (105). Other in vitro studies in distal tubular cells showed that WNK4 facilitates the internalization of ENaC independently of Nedd4-2 (106).

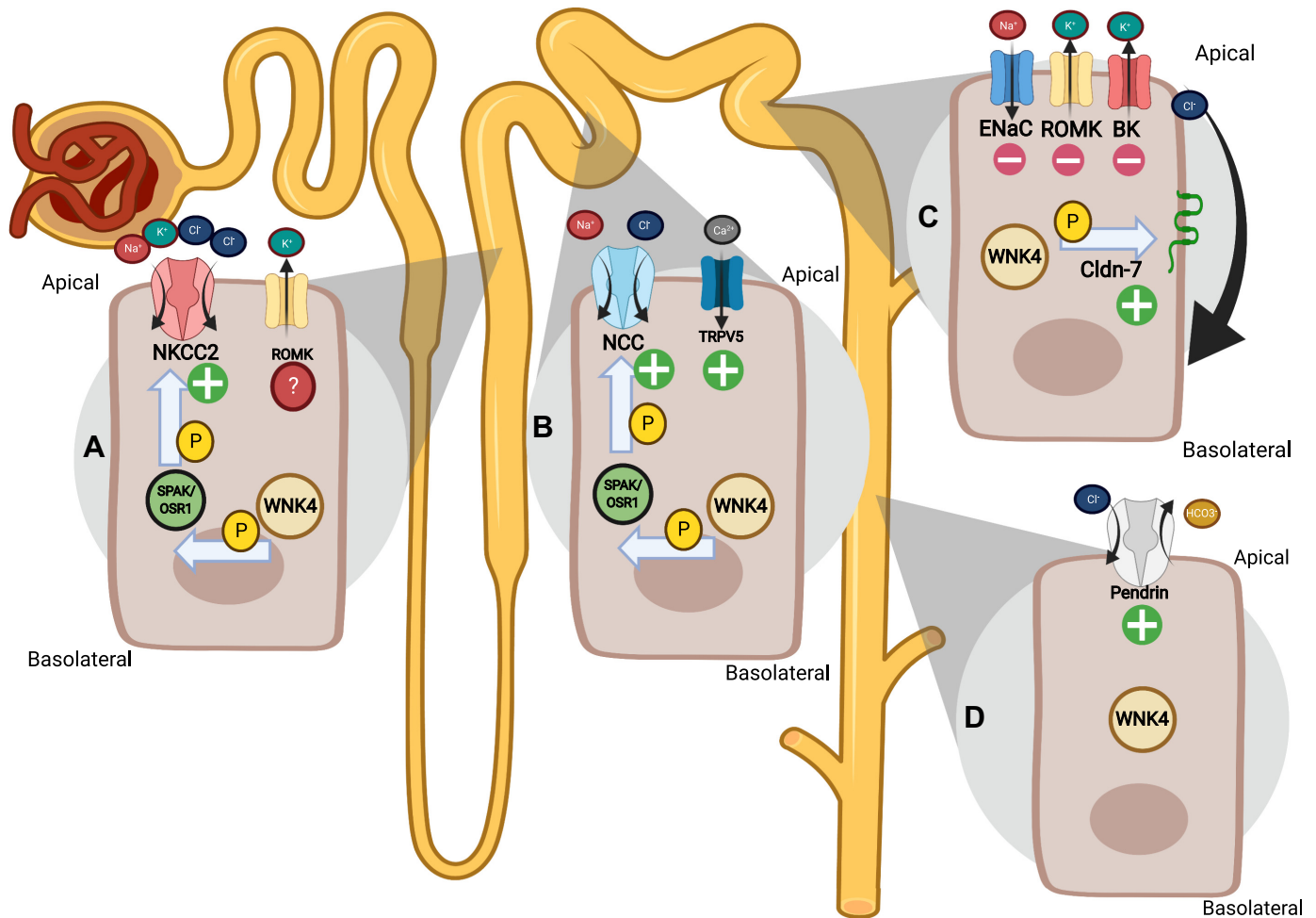


Figure 5. Proposed roles of with no lysine kinase 4 (WNK4) in the nephron. Works by different groups have suggested the participation of WNK4 in the regulation of multiple kidney transport proteins. *A:* in the thick ascending limb of the loop of Henle, WNK4 has been reported to positively regulate the activity of $\text{Na}^+ - \text{K}^+ - 2\text{Cl}^-$ cotransporter (NKCC2) through the phosphorylation of STE20/SPS1-related proline-alanine-rich protein kinase (SPAK)/oxidative stress-responsive 1 (OSR1). Although a role for WNK4 in the regulation of renal outer medullary K^+ channels (ROMK) has been postulated, it is unknown whether WNK4 specifically modulates this channel in the thick ascending limb. *B:* in the distal convoluted tubule (DCT), WNK4 is a positive regulator of NaCl cotransporter (NCC) through the phosphorylation of SPAK/OSR1. It also seems to play a role in Ca^{2+} handling through the positive regulation of transient receptor potential vanilloid 5 (TRPV5) channels. *C:* in the principal cells of the aldosterone-sensitive distal nephron (ASDN), WNK4 has been implicated as a negative regulator of electrogenic Na^+ reabsorption and K^+ secretion through epithelial Na^+ channels (ENaC) and ROMK/large-conductance K^+ (BK) channels, respectively. *D:* the $\text{Cl}^-/\text{HCO}_3^-$ antiporter pendrin has been postulated to be upregulated by WNK4, at least in the context of familial hyperkalemic hypertension (FHHt). No mechanisms are known for this phenomenon (figure created with Biorender.com).

WNK4^{-/-} and WNK4 hypomorphic mice show an increase in ENaC function (14, 74), consistent with these inhibitory properties. However, it is unclear whether this is a direct consequence of the absence of WNK4 or an adaptation that occurs to compensate for NCC dysfunction. In the FHHt WNK4^{+/+}/Q562E/Q562E mouse model, in which WNK4 is overexpressed, an inverse phenomenon is observed: ENaC subunit levels and amiloride-sensitive currents are diminished in the kidneys of these animals (107). Interestingly, CA-SPAK mice also have a decreased abundance of ENaC subunits in total kidney lysates, which can be reversed with thiazides (54). This model strongly suggests that NCC overactivation is sufficient to produce a compensatory decrease in ENaC expression levels.

Renal Outer Medullary K^+ Channels

Kir1.1, also known as the renal outer medullary K^+ channel (ROMK), mediates both K^+ recycling in the thick

ascending limb of the loop of Henle and K^+ secretion in the ASDN when coupled with the activity of ENaC (108).

Kahle et al. showed that WNK4 is an inhibitor of ROMK in *X. laevis* oocytes (109) (Fig. 5C). FHHt versions of WNK4 were more efficient inhibitors of ROMK in this system. This effect was also independent of the kinase activity of WNK4, was prevented by the phosphorylation of Ser¹¹⁶⁹ of WNK4 (105), and was shown to be mediated by intersectin, a scaffolding protein that participates in vesicle endocytosis (110). The phosphorylation of tyrosine residues in WNK4 (Tyr¹⁰⁹² and Tyr¹¹⁴³) by c-Src have been postulated to enhance ROMK inhibition by WNK4 (111, 112). WNK4^{+/+}/Q562E/Q562E animals have been recently found to possess lower activities of ROMK in patch-clamp, single-channel current experiments of their tubular cells (107), giving in vivo proof of the regulation of this channel by WNK4 in whole organisms. How much of a contribution is made to the FHHt phenotype by

the direct dysregulation of ENaC and ROMK is not understood, since overactivity of WNK4 in the DCT is both necessary (63) and sufficient (54) to induce the phenotype in its totality.

Large-Conductance K⁺ or Maxi-K Channels

Large-conductance K⁺ (BK) channels are Ca²⁺-activated K⁺ channels involved in the regulation of neuronal excitability. They have also been described as flow-activated K⁺ channels that mediate K⁺ secretion in the ASDN (108).

WNK4 can inhibit BK channels in HEK-293 cells expressing α - and β -BK channel subunits (Fig. 5C). Unlike what has been observed for ENaC and ROMK, this inhibition is dependent on its kinase activity (113). Inhibition is achieved through a reduction in total and cell surface BK subunits through lysosomal degradation, as was shown by the rescue of the proteins with treatment with bafilomycin A1 or leupeptin. Wang et al. (114) found that the first CCD and first PF2-like domain of WNK4 (residues 1–584 of mWNK4) are necessary for its inhibition of BK channels. It is difficult to reconcile this knowledge with the recent finding of SPAK increasing BK channel activity (115), which is at odds with a WNK4 kinase-dependent inhibition of BK.

Claudins

Claudins are some of the main components of tight junctions, can facilitate paracellular epithelial transport of specific ions, and affect transepithelial resistance (116).

In mammalian cells expressing WNK4, claudin-1, -2, -3, and -4 have been coimmunoprecipitated with WNK4, and mutant WNK4 (D564A in hWNK4) showed an enhanced interaction with these tight-junction components. The presence of WNK4 also increased the phosphorylation of these claudins in different cell lines, with WNK4-D564A showing higher activity than wild-type WNK4 (117). Transepithelial Cl⁻ permeability was increased in cells expressing wild-type WNK4 and even more so in cells expressing FHHt mutants (49, 117). In these cell systems, WNK4 FHHt mutants may have been expressed at higher levels than wild-type WNK4. However, this was not assessed by the authors.

Tatum et al. later found that WNK4 colocalizes with claudin-7 in kidney tubules and coimmunoprecipitated both proteins from native tissues (Fig. 5C). Ser²⁰⁶ in claudin-7 was characterized as a putative WNK4 phosphoacceptor site. Its phosphorylation was determined to increase in the presence of wild-type WNK4 and to a greater extent with WNK4-Q562E, correlating with a decrease in transepithelial resistance (118). Conversely, immortalized collecting duct cells from mice lacking claudin-7 were shown to have increased transepithelial resistance. Interestingly, greater levels of WNK4 at the mRNA and protein levels were observed in these cells. This was speculated to occur as part of a compensatory mechanism to promote claudin-7 function (119).

Transient Receptor Potential Vanilloid Channels

The transient receptor potential (TRP) vanilloid (TRPV) subfamily of channels, which belongs to the TRP superfamily, is composed of a group of Ca²⁺-permeable channels that, in the kidney, can mediate Ca²⁺ reabsorption and have been postulated to play a role in osmolality and flow sensing

(119a). In other cells, they play other important roles, such as heat and pain perception (119b).

Of all the TRPV channels, TRPV4 and TRPV5 have been shown to be modulated by WNK4. Regarding TRPV4, downregulation of the channel occurs when it is coexpressed with WNK4 in HEK-293 cells through a decrease in the surface expression of the channel, which cannot be activated by hypotonicity in the presence of this kinase (120).

Regarding TRPV5 (Fig. 5B), conflicting conclusions have been reached by different groups. In *X. laevis* oocytes, TRPV5 Ca²⁺ currents are stimulated in the presence of WNK4. A dose-dependent inhibition of WNK4 stimulation of TRPV5 occurs with increasing doses of NCC, which could possibly be mediated by an increase in intracellular Cl⁻ (121). FHHt mutants of WNK4 show similar activation of this channel. WNK4 might facilitate the forward trafficking of TRPV5 to the plasma membrane (121). On the other hand, negative regulation of TRPV5 by WNK4 has also been reported, with HEK-293 cells expressing WNK4 having an enhanced endocytosis of the channel (122). In vivo, lack of WNK4 causes a substantial reduction in TRPV5 measured by immunofluorescence. Furosemide-sensitive calciuria is enhanced in WNK4^{-/-} mice, which might be the consequence of a decrease in Ca²⁺ reabsorption proteins of the distal nephron, including TRPV5 (123). It must be noted that this finding goes in the opposite direction of the hypocalciuria normally observed with NCC downregulation or inhibition.

Cystic Fibrosis Transmembrane Conductance Regulator Channels

Cystic fibrosis transmembrane conductance regulator (CFTR) is a Cl⁻/HCO₃⁻-permeable channel that is expressed in many epithelial and glandular cells, where, in concert with the activity of NKCC1, it mediates Cl⁻ and water secretion (124). The regulation of CFTR by WNK4 is unclear. An initial report showed that, in *X. laevis* oocytes, WNK4 downregulated the presence of CFTR in the plasma membrane independently of its kinase activity in a dose-dependent manner (125). A more recent report in mammalian cells showed an enhancement of surface expression of CFTR by WNK4, also independently of kinase activity (126).

Pendrin

Pendrin is an anion antiporter involved in ear and thyroid physiology (127). In the kidney, it mediates Cl⁻/HCO₃⁻ exchange in β -intercalated cells and thus participates in HCO₃⁻ secretion in the collecting duct. It has also been shown to mediate electroneutral NaCl reabsorption when its activity is coupled to Na⁺/Cl⁻/HCO₃⁻ transport mediated by the Na⁺-driven Cl⁻/HCO₃⁻ exchanger (128) and has been implicated in Na⁺ retention by aldosterone (129).

WNK4^{+/+/Q562E/Q562E} animals have been shown to have increased pendrin activity in their β -intercalated cells and increased β -intercalated cell mass (Fig. 5D) (130). The authors of that work argued that this protein could potentially contribute to metabolic acidosis and Na⁺ retention in FHHt, as deletion of pendrin in WNK4^{+/+/Q562E/Q562E} mice led to normalization of plasma HCO₃⁻ and K⁺ and an increase in renin mRNA levels. It is unknown whether the

pathophysiological dysregulation of pendrin observed in *WNK4*^{+/+}/*Q562E/Q562E* mice occurs in all models of FHHt and whether it is mediated directly by WNK4. The only published in vitro assay of pendrin function in the presence of WNK4 was made in *X. laevis* oocytes, where no effect was seen with coexpression of both proteins (97).

REGULATORY MECHANISMS OF WNK4 FUNCTION

WNK4 function is regulated at different levels. At the transcriptional level, no information is yet available about the regulation of *WNK4* mRNA levels. Posttranslationally, however, a pathway for regulation of WNK4 protein levels has been well described. This pathway involves regulation of the WNK4 degradation rate by the CUL3-KLHL3 E3 ubiquitin ligase complex. In addition, kinase activity of WNK4 is also tightly regulated, and more than one mechanism appears to be involved (Fig. 6).

Regulation of the WNK4 Degradation Rate by the CUL3-KLHL3 E3 Complex in the Kidney

Cullin-RING ligases (CRLs) are ubiquitin E3 enzymes that regulate the ubiquitylation of a wide variety of substrates. It has been estimated that ~300 different CRL complexes may exist in humans (131), each of them with different substrate specificities that are determined by the cullin subtype and substrate adaptor molecule that make up the complex.

As mentioned above, mutations in the genes encoding for two proteins that are part of a CRL complex are responsible for the most severe forms of FHHt (16, 17). These are CUL3, the protein that forms the heterodimeric scaffold of the CRL complex, and KLHL3, the protein that acts as the substrate adaptor and that also binds to the NH₂-terminal domain of CUL3. Following the description of these mutations, it was rapidly identified that WNK kinases are substrates for the CUL3-KLHL3 E3 ligase complex. It was shown that, in vitro, KLHL3 can bind WNK1, WNK2, WNK3, and WNK4 (18–20), that the CUL3-KLHL3 E3 complex can promote ubiquitylation of WNK1 and WNK4 (18–20), and that this decreases WNK4 protein levels in cultured cells, suggesting that ubiquitylation promotes proteasomal degradation (19, 20). The observed binding, ubiquitylation, and degradation were impaired when tested with KLHL3 or WNK4 FHHt mutants. The acidic motif of WNK kinases, in which FHHt mutations in WNK4 are clustered, was shown to function as the binding site for KLHL3 (18).

In mutant mice carrying WNK4-FHHt mutations, increased renal levels of WNK4 were observed (19, 20), and in mutant mice carrying the KLHL3-R528H and KLHL3-M131V FHHt mutations, increased WNK4 and WNK1 renal expression levels were observed (66, 68). Given that KLHL3 expression in the kidney is largely restricted to the DCT (17, 132, 133), this upregulation is likely to exclusively occur within this nephron segment. Interestingly, it was shown that impaired activity of the CUL3-KLHL3 E3 complex (in *KLHL3*^{-/-} mice) increased WNK1 and WNK4 expression in the kidney but did not affect their expression levels in extrarenal tissues (134). Thus, in other tissues, WNK1 and WNK4 levels may not be subject to CRL-mediated regulation or,

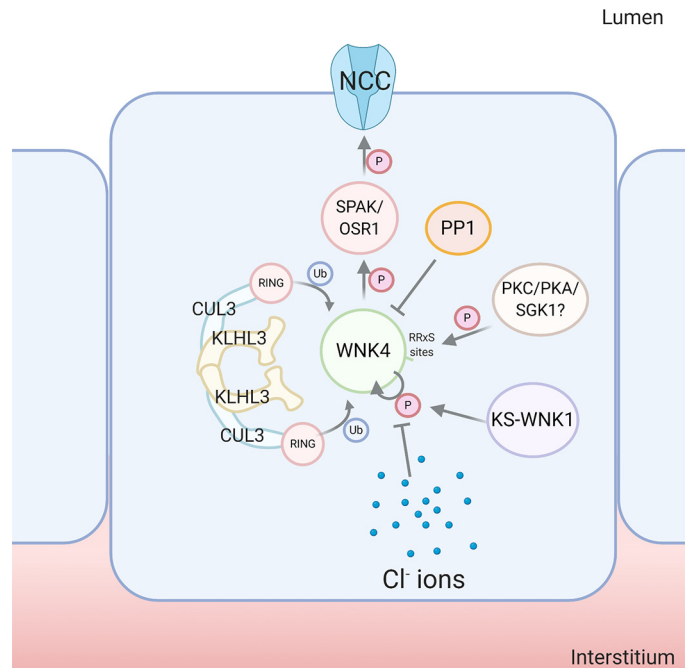


Figure 6. Regulatory mechanisms of with no lysine kinase (WNK4) function. In the distal convoluted tubule (DCT), WNK4 protein levels are regulated by the activity of the cullin 3 (CUL3)-Kelch-like family member 3 (KLHL3) E3 complex, which targets WNK4 for degradation by promoting its ubiquitylation at several sites (94, 136). KLHL3 binds to the acidic motif of WNK kinases through its propeller domain. Another level of regulation involves the modulation of WNK4 kinase activity. Several mechanisms have been described that participate in this regulation, which are the following. 1) Binding of Cl⁻ to a pocket within the active site of the kinase stabilizes an inactive conformation and prevents kinase autophosphorylation (4, 115). Intracellular Cl⁻ concentration levels are thus determinant on WNK4 activity. 2) WNK4 contains five phosphorylation sites within a RRXS motif, two located in the NH₂-terminal domain and three located in a COOH-terminal region. All five sites can be phosphorylated in vitro by PKC and PKA (16), and at least the three COOH-terminal sites can be phosphorylated by serum/gluocorticoid regulated kinase-1 (SGK1) (101, 124, 129). Phosphorylation levels of two of these sites (Ser⁶⁴ and Ser¹¹⁹⁶) correlate with levels of kinase activity [measured by its ability to autophosphorylate and to phosphorylate STE20/SPS1-related proline-alanine-rich protein kinase (SPAK)]. Phosphoablative mutations at Ser⁶⁴ and Ser¹¹⁹⁶ prevent WNK4-mediated phosphorylation of SPAK in response to certain stimuli, like ANG II (16). 3) A protein phosphatase 1 (PP1)-binding site has been described close to the COOH-terminal end of the protein. Absence of this motif promotes WNK4 hyperphosphorylation and constitutive activation in cultured cells (100). 4) Kidney-specific (KS)-WNK1 interacts with WNK4 through the COOH-terminal coiled-coil domain (CT-CCD). Coexpression of KS-WNK1 in *Xenopus laevis* oocytes promotes WNK4 autophosphorylation and activation by a mechanism that is currently unknown (3). *WNK1* mutations that produce amino acid substitutions within the acidic domain produce a mild familial hyperkalemic hypertension (FHHt) phenotype in humans and mice that has been speculated to be due to increased KS-WNK1-mediated activation of WNK4 (83) (figure created with Biorender.com).

alternatively, they could be subject to regulation by a different CRL complex. A third possibility, given that KLHL3 expression is not kidney specific, is that KLHL3 absence may be compensated for by another KLHL protein. For instance, KLHL2 has been shown to be able to bind and promote ubiquitylation of WNK kinases (135). *KLHL2*^{-/-} mice were shown to display higher WNK4 expression levels in the renal medulla but not in the renal cortex. Expression levels of WNK kinases in extrarenal tissues were not reported.

Finally, it is interesting to note that the upregulation of SPAK and NCC activity (measured as phosphorylation) observed in KLHL3-R528H mice was completely prevented when these mice were crossed with WNK4^{-/-} mice, despite persistent WNK1 overexpression (67). Thus, the increased WNK1 levels were unable to compensate for WNK4 absence, and WNK4 seems to be key in the pathogenesis of FHHt caused by mutations in KLHL3. It remains to be determined whether the overexpressed WNK1 reported by Susa et al. corresponds to full-length WNK1 (L-WNK1) or the KS-WNK1 isoform. Interestingly, it has been recently shown that KS-WNK1 is much more sensitive to CUL3-KLHL3 E3-induced degradation than L-WNK1 (59).

All FHHt-causative mutations in *CUL3* characterized so far cluster in sites implicated in splicing of exon 9 and cause the skipping of this exon. Thus, a protein with a 57-amino acid deletion is produced (CUL-Δ403–459) (16). It has been shown that expression of CUL3-Δ403–459 protein prevents ubiquitylation of WNK kinases even in the presence of wild-type CUL3 (72). CUL3^{+ /Δ403–459} mice display higher levels of WNK4 protein, which drives downstream phosphorylation and activations of SPAK and NCC, causing FHHt. As CUL3-Δ403–459 promotes its autoubiquitylation and degradation and, thus, CUL3^{+ /Δ403–459} mice have lower levels of CUL3 expression, it was initially proposed that haploinsufficiency was the cause for FHHt. However, it was later shown that Cul3^{+/-} (CUL3^{Het}) mice did not have a FHHt-like phenotype. In contrast, Cul3^{Het} mice that also carried a copy of a transgene that allowed inducible expression of CUL3-Δ403–459 (which were identified as CUL3^{HET/Δ9} mice) did develop the FHHt phenotype. CUL3 protein levels were similarly decreased in both CUL3^{Het} and CUL3^{HET/Δ9} mice. However, only CUL3^{HET/Δ9} mice had higher WNK4, NCC, and pNCC protein levels (70). These results suggested that CUL3-Δ403–459 protein has a dominant-negative effect on CUL3-KLHL3 E3-mediated degradation of WNK kinases, resulting in higher WNK4 levels and increased downstream activation of NCC.

FHHt-causative CUL3 mutations are responsible for the most severe form of FHHt (16). There is evidence that such severe phenotype may be due, at least in part, to additive effects of altered CUL3 function of renal electrolyte handling and vascular function (71). However, given that CUL3 expression seems to be ubiquitous, the absence of other manifestations of extrarenal origin are intriguing.

WNK4 Kinase Activity Is Sensitive to Intracellular Cl⁻ Levels

Modulation of the activity of CCCs by intracellular Cl⁻ levels is a well-known phenomenon supported by a large body of experimental evidence (136–139). Initial observations were made as far back as 1983, when John Russell described that intracellular Cl⁻ inhibited bumetanide-sensitive Na⁺-K⁺-Cl⁻ transport in the squid giant axon (140).

Later on, modulation of CCC activity by intracellular Cl⁻ concentration was shown to be related to their phosphorylation state (137, 141), and SPAK and OSR1 were shown to be the kinases responsible for such phosphorylation (38, 80). Thus, when WNK kinases were described as the upstream regulators of SPAK and OSR1 (9, 81), it was immediately

tested and confirmed that WNK activity is upregulated by intracellular Cl⁻ depletion (81).

Direct modulation of WNK activity by Cl⁻ was not confirmed, however, until Piali and collaborators (5) described the crystallographic structure of the WNK1 kinase domain and the existence of a Cl⁻-binding site within the catalytic site of the protein. This site is structurally similar to the Cl⁻-binding sites found in Cl⁻ channels of the ClC family, with interactions to backbone amides and lateral chains of hydrophobic residues. It was shown that Cl⁻ binding stabilizes an inactive conformation of the kinase, preventing kinase autophosphorylation and activation. Mutation of one of the residues that makes up the Cl⁻-binding site (Leu³⁶⁹) decreased the inhibition of autophosphorylation observed at increasing concentrations of Cl⁻.

Bazua-Valenti et al. showed that the ability of WNK4 to activate NCC is also modulated by intracellular Cl⁻ concentration (28). This observation helped to resolve the long-lasting controversy of whether WNK4 acts as a positive or negative modulator of NCC. According to observations of Bazua-Valenti et al., in the *X. laevis* oocyte system, in which initial characterization of WNK4-regulatory activity of CCCs was performed, the intracellular Cl⁻ concentration is high, which renders WNK4 inactive. Thus, under basal conditions, WNK4 expression exerts an inhibitory effect on NCC activity, probably due to a dominant-negative effect over the endogenous WNK kinase or kinases (42). However, decreasing intracellular Cl⁻ concentrations by different maneuvers promoted WNK4 activation, measured as kinase autophosphorylation and through its ability to activate NCC (28). In addition, introduction of mutation L322F in hWNK4 (the residue equivalent to Leu³⁶⁹ in WNK1) rendered the kinase constitutively active.

Bazua-Valenti et al.'s work and a later work by Terker et al. suggested that WNK kinases, despite having very similar kinase domains, present different sensitivities to inhibition by Cl⁻. Interestingly, WNK4 has the more divergent kinase domain (with ~80% identity with other WNKs, whereas the kinase domains of other WNKs have ~90% identity among them) (6) and appears to be the family member that is more sensitive to inhibition by Cl⁻ (28, 83). It has been suggested that such high affinity of WNK4 for Cl⁻ is important for its physiological role in the regulation of NCC, given that intracellular Cl⁻ concentration in the DCT has been estimated to be rather low (142–144). Thus, the low intracellular Cl⁻ concentration of DCT cells allows WNK4 to remain active under basal conditions and allows rapid modulation of its activity in response to changes in intracellular Cl⁻ concentration. Definitive proof that modulation of WNK4 activity by intracellular Cl⁻ concentration is physiologically relevant, at least in the DCT, came with the description of a mouse model carrying the L319F/L321F-WNK4 mutation (L322F/L324F in hWNK4) (76). As mentioned above in *WNK4 in Physiology and Pathophysiology*, these mice present higher levels of NCC activity accompanied by the expected FHHt phenotype.

WNK4 Activity Is Modulated by Phosphorylation of Residues Located in Its Regulatory NH₂- and COOH-Terminal Domains

The initial description of a phosphorylation site located within the regulatory COOH-terminal domain of WNK4,

whose modification affects WNK4 function, was made by Ring et al. (105). This site, Ser¹¹⁶⁹ (in mouse WNK4), was identified through a search for serum/glucocorticoid-regulated kinase-1 (SGK1) consensus phosphorylation motifs, as it was hypothesized that WNK4 may act as a transducer of aldosterone signaling in the distal nephron. In *in vitro* kinase assays, it was shown that SGK1 can indeed phosphorylate this WNK4 residue. Additionally, it was shown that introduction of the phosphomimetic mutation S1169D impaired the ability of WNK4 to inhibit ENaC and ROMK in *X. laevis* oocytes.

Later on, the works by Rozansky et al. and Na et al. described two additional phosphorylation sites within the COOH terminus of WNK4 that can be phosphorylated *in vitro* by SGK1: Ser¹¹⁸⁰ and Ser¹¹⁹⁶ in mouse WNK4 (Ser¹²⁰¹ and Ser¹²¹⁷ in hWNK4) (45, 46). As mentioned above (in *Structural Features*), these sites are clustered within a highly conserved region of WNK4 and are present from zebrafish to humans (44). Rozansky et al. showed that, in *X. laevis* oocytes, coexpression of SGK1 with WNK4 and NCC prevented WNK4 inhibitory activity on NCC and that the phosphomimetic mutant WNK4-S1169D/S1196D lost its ability to inhibit NCC (46). In addition, Na et al. showed, in the same expression system, that the phosphomimetic mutants S1169D/S1196D and S1169D/S1180D/S1196D had an enhanced positive effect on NKCC2 activity (45).

Several years later, we performed a comprehensive study of WNK4 phosphorylation sites by mass spectrometry analysis of WNK4 peptides generated from the immunoprecipitated protein from HEK-293 extracts (44). Eighteen phosphorylation sites were reproducibly identified, including the T-loop Ser³³² autophosphorylation site (Ser³³⁵ in hWNK4). We were particularly interested in five sites present within an RRxS motif, all of them located in segments of the protein that are highly conserved. These included, in addition to the Ser¹¹⁶⁹, Ser¹¹⁸⁰, and Ser¹¹⁹⁶ sites previously described as SGK1 targets, the Ser⁴⁷ and Ser⁶⁴ sites, located in the NH₂-terminal domain of the protein. Given that PKC and PKA show a preference for phosphorylation of sites within the RRxS sequence (145, 146), we explored the possibility that these sites might be targeted by these kinases. Indeed, we observed that pharmacological activation of PKC or PKA in HEK-293 cells promoted phosphorylation of all RRxS sites. The ability of PKC and PKA to phosphorylate these sites was also demonstrated in *in vitro* kinase assays. Importantly, phosphorylation of these sites was shown to promote WNK4 activation, measured by its ability to autophosphorylate and to phosphorylate SPAK. In particular, impaired phosphorylation of Ser⁶⁴ and Ser¹¹⁹⁶ had the greatest effect on WNK4 activity and kinase activity was completely abrogated in the S64A/S1196A double mutant. With the use of phosphospecific antibodies, we showed that these sites are phosphorylated *in vivo* in mouse kidney samples and that their phosphorylation levels increase in volume-depleted mice and in WNK4-FHHt mice. By immunofluorescent staining, the volume depletion-induced increase in phosphorylation at Ser⁶⁴ was observed to occur in the DCT.

Further studies will be necessary to determine whether these sites are mainly targeted *in vivo* by PKC, PKA, and/or SGK1. WNK4 phosphorylation by SGK1 was initially thought to occur in response to aldosterone stimulation (46, 105), since SGK1 expression is regulated by aldosterone (147).

However, the sensitivity of DCT cells to aldosterone stimulation has recently been questioned (see *Role of WNK4 in the Regulation of NCC by Physiological Stimuli*) (148, 149). Thus, aldosterone-mediated regulation of WNK4 phosphorylation may only occur in the ASDN, which excludes the DCT. Within the DCT, phosphorylation of these sites may occur through aldosterone-independent regulated activity of SGK1 or through activity of PKC and/or PKA.

Possible Regulation of WNK4 Activity by Calmodulin Binding

Within the conserved region in which the COOH-terminal RRxS sites are located, Na et al. have additionally described the presence of a binding site for CaM (45). Their *in vitro* experiments demonstrated that CaM binds to the 1175–1194 segment of hWNK4 (1154–1173 of mWNK4), which presents a consensus CaM-binding site sequence, and that binding requires the presence of Ca²⁺. Deletion of the CaM-binding site in WNK4 prevented binding and also increased the ability of WNK4 to activate NKCC2 in *X. laevis* oocytes. On the basis of those observations, Na and coworkers proposed that this segment of the protein exerts a negative effect on WNK4 activity that may be relieved by binding to Ca²⁺/CaM or by RRxS phosphorylation, although demonstration that WNK4 activity increases in the presence of Ca²⁺/CaM is still missing. Indeed, Yang et al. have previously described a “negative regulatory signal region” within the last 47 amino acids of WNK4 (73).

Regulation of WNK4 Activity by PP1

Protein phosphatases target many components of the WNK-SPAK/OSR1-CCC pathway. In WNK4, there are two predicted PP1 sites with the consensus sequence KxVxF. Lin and colleagues described that PP1 binds to mouse WNK4 in amino acid regions 695–699 and 1211–1215, which both contain PP1-binding sites (150). In 2018, our group showed that the interaction between WNK4 and PP1 still occurred even in the absence of the two PP1-binding sites previously identified by Lin et al. (41). This suggested that other regions in WNK4 may contribute to the binding of PP1, or perhaps indirect binding through other endogenous WNKs was observed. However, mutation or deletion of the second PP1 motif near the COOH terminus of WNK4 resulted in a gain of function with increased WNK4 phosphorylation levels at the T-loop site Ser³³² (in mWNK4) and RRxS sites as well as increased WNK4-mediated phosphorylation of SPAK at Ser³⁷³. Accordingly, coimmunoprecipitation between PP1 and a shorter WNK4 COOH-terminal construct showed specific binding to the second PP1 motif, confirming it as a bona fide PP1-binding site that negatively modulates WNK4 phosphorylation and activity. PP1 α - and γ -isoforms, but not the β -isoform, were shown to promote dephosphorylation of WNK4 RRxS sites.

Interestingly, mutation of the first PP1 motif in WNK4 ablated the gain of function caused by the mutation of the second PP1 motif. Since this first PP1 motif lies within the predicted PF2b domain of WNK4 (see *Structural Features*), this raises the question of whether this mutation disrupts the function of the PF2 instead of preventing PP1 binding. Notably, this site is conserved in other WNKs, and it has

been shown that it does not mediate PP1 binding in the case of WNK1 (151). In addition to PP1 sites, WNK4 also contains predicted PP2A and PP2B motifs, but none of them have been functionally described (<http://elm.eu.org/>).

Regulation of WNK4 Activity by Interaction With KS-WNK1

KS-WNK1 is a short isoform of WNK1 that is produced by transcriptional initiation at an upstream region regulated by an alternative promoter located within intron 4 of the *WNK1* gene. Transcription from this promoter introduces into the transcript an alternative exon known as exon 4a. Thus, KS-WNK1 differs from L-WNK1 in that it lacks the segment encoded by exons 1–4 (that comprise most of the kinase domain) and contains a unique 30-residue segment in its NH₂ terminus encoded by exon 4a (152, 153). As the name indicates, this isoform is expressed only in the kidney, and its transcript levels are much higher in the DCT than in other nephron segments, although low levels have also been observed in the CNT (154).

Despite lacking a kinase domain, work from our group showed that KS-WNK1 can promote NCC activation when expressed in *X. laevis* oocytes (155). Such activation seems to be dependent on the interaction with an endogenous WNK kinase, as it is prevented by WNK463 (a specific inhibitor of WNK kinase activity). Coexpression of KS-WNK1 with WNK4 in the oocyte system promotes WNK4 autophosphorylation at Ser³³². The effect is not observed when a KS-WNK1 clone with mutations in the CT-CCD that prevent binding to WNK4 is expressed (26). Thus, interaction of WNK4 with KS-WNK1 within the DCT may be key to modulate WNK4 activity. Interestingly, it has recently been shown that missense mutations in the acidic domain of WNK1 produce a mild form of FHHt (59), and it was suggested that this phenotype is probably due to upregulation of KS-WNK1 protein expression, which then leads to increased activation of WNK4-SPAK/OSR1-NCC. This proposal is based on the following observations: 1) KS-WNK1 is more sensitive to CUL3-KLHL3 E3-induced degradation than L-WNK1 (59), and 2) KS-WNK1 is much more abundant in the DCT than L-WNK1. At the transcript level, the abundance of KS-WNK1 is 80 times higher than that of L-WNK1 (154). At the protein level, certain lines of evidence suggest that, in the DCT, L-WNK1 levels may be negligible. This is best highlighted by the effects of knockout of WNK4 in two different FHHt mouse models. In the KLHL3-R528H model, knockout of WNK4 completely abrogates NCC activity (measured by phosphorylation) (67). Western blots show that KLHL3-R528H mice have higher renal WNK1 levels. Although it was unclear to which isoform they correspond, it may be deduced that WNK1 upregulation in the DCT probably corresponds to KS-WNK1, as it does not compensate for the absence of WNK4. In contrast, in the WNK1-FHHt model (with an intronic deletion in *WNK1* that promotes ectopic expression of L-WNK1 in the DCT), knockout of WNK4 does not prevent the pathway upregulation (42). Thus, in this model, the pathological ectopic expression of L-WNK1 appears to override the WNK4-mediated regulation of NCC. It is noteworthy that L-WNK1 is less sensitive to inhibition by Cl⁻ than WNK4 and thus may be constitutively active in intracellular Cl⁻ concentration levels of the DCT.

ROLE OF WNK4 IN THE REGULATION OF NCC BY PHYSIOLOGICAL STIMULI

NCC is regulated by multiple physiological stimuli (156). Given that, as explained above, WNK4 appears to be the major WNK kinase responsible for SPAK/OSR1 phosphorylation and activation in the DCT, this kinase plays a central role in many of the signaling pathways that transduce the extracellular signals that modulate NCC activity.

Extracellular K⁺ Concentration

Dietary K⁺ intake levels have been correlated with the level of NCC activity (assessed by its phosphorylation status). In rodent models, higher levels of NCC and pNCC are observed in animals on low-K⁺ diet (vs. control diet), and lower levels of NCC and pNCC are observed on high-K⁺ diet. Such modulation is triggered by subtle changes in extracellular K⁺ concentration that occur in response to the changes in dietary K⁺ content (51, 83, 157–159). Changes in extracellular K⁺ concentration affect the driving force for K⁺ movement through Kir4.1/Kir5.1 K⁺ channels expressed in the basolateral membrane of DCT cells (Fig. 7) (160, 161). Movement of K⁺ provokes changes in the membrane potential of DCT cells that, in turn, drive Cl⁻ fluxes through basolateral ClC-Kb channels (162, 163), ultimately affecting intracellular Cl⁻ concentration. These fluctuations in intracellular Cl⁻ concentration affect WNK4 activity and, thus, activity of the SPAK/OSR1-NCC pathway. Hence, a low-K⁺ diet promotes K⁺ efflux from DCT cells, membrane hyperpolarization, reduction of intracellular Cl⁻ concentration, and WNK4 activation; the opposite effects are produced by a high-K⁺ diet.

It has been proposed that among WNK kinases WNK4 is especially suited to participate in this mechanism, since, as mentioned above (see *Regulatory Mechanisms*), its sensitivity to inhibition by Cl⁻ is higher than that of other WNK kinases (28, 83). As DCT intracellular Cl⁻ concentration has been estimated to be rather low (142–144), it has been suggested that the other less sensitive WNK kinases would be constitutively active under these intracellular Cl⁻ concentration levels. The relevance that WNK4 plays in this regulatory mechanism was evidenced by the absence of upregulation of NCC phosphorylation in WNK4^{-/-} mice when placed on a low-K⁺ diet (75, 91). Consequently, mice developed severe hypokalemia. In addition, in mice expressing Cl⁻-insensitive WNK4 (harboring the L319F/L321F mutations), administration of a low-K⁺ diet did not promote NCC upregulation, and administration of an acute oral K⁺ load did not stimulate the NCC downregulation that was observed in wild-type controls, supporting the idea that the regulation of WNK4 activity by Cl⁻ is a key element in the signaling pathway for the regulation of NCC by extracellular K⁺ (76).

Besides the direct Cl⁻-sensing ability of WNK4, recent evidence from our group has shown that WNK4 phosphorylation at RRxS sites can be stimulated by a decrease in extracellular K⁺ concentration (164). This may be important to potentiate the activation of NCC. Interestingly, our data show that phosphorylation of these sites upon exposure to a decrease in extracellular K⁺ concentration is also secondary to the reduction in intracellular Cl⁻ concentration but is

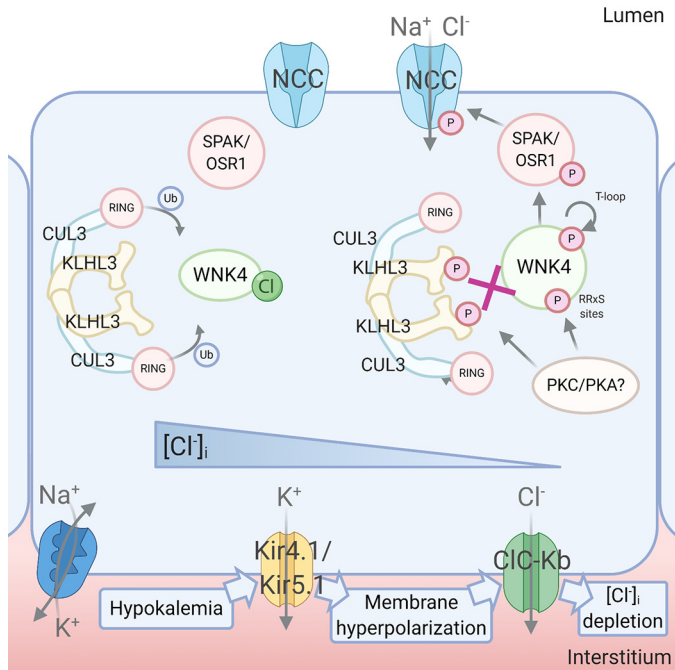


Figure 7. Role of with no lysine kinase 4 (WNK4) in the regulation of NaCl cotransporter (NCC) by extracellular K^+ . In the face of hypokalemia, the extracellular K^+ concentration ($[K^+]_e$) gradient favors K^+ exit from the distal convoluted tubule (DCT) cell through basolateral K^+ channels formed by Kir4.1 and Kir5.1 subunits. This leads to membrane hyperpolarization, which, in turn, promotes exit of Cl^- . The resulting decrease in intracellular Cl^- concentration ($[Cl^-]_i$) promotes WNK4 activation due to release of Cl^- from the Cl^- -binding site, leading to increased STE20/SPS1-related proline-alanine-rich protein kinase (SPAK)/oxidative stress-responsive 1 (OSR1) and NCC phosphorylation and activation (152). An opposite mechanism may operate in hyperkalemia, although additional mechanisms are thought to participate in this setting. The decrease in $[Cl^-]_i$ induced by hypokalemia appears also to be responsible for the increase in WNK4 phosphorylation levels at RRxS sites that is observed in response to decreases in $[K^+]_e$ (99). The detailed mechanism is currently under investigation, but it may involve activation of PKC and/or PKA, given that these kinases can phosphorylate RRxS sites in vitro. In addition, phosphorylation of Kelch-like family member 3 (KLHL3) in the RRxS site located within the substrate-binding propeller domain is also induced by decreases in $[K^+]_e$ (58). Given the similarity of this last mechanism to the regulation of WNK4 by phosphorylation at RRxS sites, it is possible that KLHL3-RRxS phosphorylation may also be secondary to $[Cl^-]_i$ depletion in the setting of hypokalemia (figure created with Biorender.com).

independent of WNK kinase activity. The molecular players that link intracellular Cl^- concentration depletion to WNK4 phosphorylation at RRxS sites are currently under investigation.

Finally, Ishizawa et al. have shown that CUL3-KLHL3 E3-induced degradation of WNK4 decreases in mice exposed to a low- K^+ diet by a mechanism that involves KLHL3 phosphorylation at an RRxS site located within the substrate binding propeller domain (see *Angiotensin II* below) (165). Interestingly, such phosphorylation would prevent not only WNK4 degradation but also KS-WNK1 degradation (59). In 2018, Boyd-Shiwarski and colleagues coined the term “WNK bodies” to refer to WNK signaling complexes that are formed in the DCT under certain conditions (22). They also showed that KS-WNK1 expression is essential for the formation of WNK bodies, as these were absent in KS-WNK1^{-/-} mice. One of the conditions that have consistently been shown to

induce the formation of WNK bodies is K^+ deprivation (22, 51, 166). Thus, it is possible that KS-WNK1 induction under these conditions could promote the formation of these complexes. Interestingly, WNK bodies composed of WNK1 and SPAK/OSR1 are still formed in mice lacking WNK4; however, the phosphorylation of SPAK/OSR1 within the WNK bodies entirely depends on WNK4 (23). This evidence suggests that the localization of WNK4 to WNK bodies has functional relevance.

Aldosterone

Until relatively recently, NCC was thought to be a target of aldosterone. This idea was based on the observation that aldosterone infusion in rats increases NCC expression (167). The current view, however, is that aldosterone affects NCC activity indirectly, by affecting the levels of extracellular K^+ concentration. That is, aldosterone promotes renal K^+ secretion eventually leading to hypokalemia, and hypokalemia promotes NCC activation. This view is supported by the following observations. First, kidney-specific mineralocorticoid receptor (MR)-deficient mice have lower levels of NCC expression and activity that are reversed when hyperkalemia is corrected by a low- K^+ diet (149). Second, in mice in which random deletion of MR occurs in only ~20% of renal tubule cells (148), low- Na^+ diet-induced upregulation of NCC and pNCC was observed in all cells irrespective of the absence or presence of MR. Third, 11 β -hydroxysteroid dehydrogenase (11 β -HSD) expression has been shown to be absent in the DCT of mice (168, 169), although this may vary between species (170, 171). This enzyme catalyzes the inactivation of glucocorticoids, thus preventing their binding to MRs. Cells that do not express 11 β -HSD are aldosterone insensitive, because in these cells MR is mainly occupied by glucocorticoids that circulate in plasma at much higher levels than aldosterone. In contrast, in cells that express 11 β -HSD, intracellular levels of glucocorticoids are much lower, and MR activity is mainly regulated by aldosterone.

All these pieces of evidence together have put into question the role that SGK1 plays on the regulation of the WNK4-SPAK/OSR1-NCC pathway. SGK1 expression is regulated by aldosterone in the ASDN, where phosphorylation of WNK4 by this enzyme could be important for the modulation of ENaC and ROMK. However, in the aldosterone-insensitive DCT, SGK1-mediated phosphorylation of WNK4 would have to be regulated by stimuli other than aldosterone. Alternatively, SGK1 target sites may be phosphorylated by another kinase. As mentioned above, we have observed that phosphorylation of RRxS sites (including Ser¹¹⁹⁶) increases when extracellular K^+ concentration decreases (164). Thus, aldosterone-induced hypokalemia may promote NCC activation not only by decreasing Cl^- binding to the active site of WNK4 but also by promoting RRxS phosphorylation. Nevertheless, the kinase responsible for these phosphorylation events remains to be uncovered. It is unlikely, however, that SGK1 is involved, as the aldosterone-independent stimulation of SGK1 activity is triggered by hyperkalemia (172).

Angiotensin II

NCC expression and phosphorylation levels are modulated by dietary NaCl intake. Low-NaCl diets promote NCC

activation and high-NaCl diets promote NCC inhibition (173–176). Aldosterone was initially thought to be behind such modulation, as low NaCl intake is a well-known stimulus for the activation of the renin-angiotensin-aldosterone system. However, as explained above, current evidence suggests that aldosterone does not regulate NCC directly.

Van der Lubbe et al. showed that NCC and pNCC levels are regulated by ANG II independently of aldosterone by observing a stimulatory effect of ANG II infusion on NCC and pNCC levels in adrenalectomized rats (177). Later on, we showed that WNK4 is a key element in the signaling pathway that transduces ANG II stimulation into NCC activation. In *WNK4*^{-/-} mice, ANG II infusion did not promote the increase in SPAK/OSR1 or NCC phosphorylation that was observed in their wild-type littermates.

Subsequent works described two different mechanisms by which WNK4 activity is regulated by ANG II (Fig. 8). First, Shibata et al. showed that stimulation of the ANG II type 1 (AT₁) receptor in HEK-293 cells (a G_{αq}-coupled seven-transmembrane receptor) upregulates WNK4 levels by promoting PKC-mediated phosphorylation of KLHL3 within a site located in the substrate-binding propeller domain (178). Phosphorylation of this site prevents KLHL3 binding to WNK4 and thus prevents WNK4 degradation. In vivo, increases in WNK4 levels were reported in mice infused with ANG II. Second, stimulation of cells with ANG II can also promote PKC-mediated phosphorylation of WNK4 at RRXS sites. As discussed above, phosphorylation of these sites, especially Ser⁶⁴ and Ser¹¹⁹⁶, promotes an increase in WNK4 activity. In HEK-293 cells stimulated with ANG II, pSPAK levels increased only in the presence of WNK4. However, this effect was not observed in the presence of mutant WNK4 with phosphoablative mutations in Ser⁶⁴ and Ser¹¹⁹⁶. Phosphorylation levels of these sites were shown to increase in volume-depleted mice (44).

More recently, NCC expression and phosphorylation were analyzed in AT₁ receptor knockout models (179, 180). No differences were observed between wild-type and AT₁^{-/-} mice. It remains to be determined whether this absence of effect is due to compensatory mechanisms that maintain NCC expression and activity in the absence of AT₁ receptor signaling or whether the reported ANG II effects on the DCT are independent of AT₁ receptor activity.

Calcium-Sensing Receptor

Stimulation of the calcium-sensing receptor (CaSR) in HEK-293 cells transfected with WNK4 and SPAK has been recently shown to promote SPAK-activating phosphorylation (82). This activation is WNK4 dependent and occurs through similar mechanisms to the those described above for ANG II-mediated regulation of WNK4 (Fig. 8). CaSR can be coupled to G_{αq} proteins; thus, its stimulation can lead to activation of PKC. PKC then phosphorylates KLHL3 and WNK4, leading to increased levels of WNK4 expression and activity. It has been postulated that this mechanism is important for promoting NCC activation in circumstances in which increased extracellular Ca²⁺ levels promote CaSR-mediated NKCC2 inhibition that leads to a decrease in Ca²⁺ but also NaCl reabsorption in the thick ascending limb of Henle's loop. In this scenario, NCC activation would help to recover the NaCl to prevent urinary salt losses.

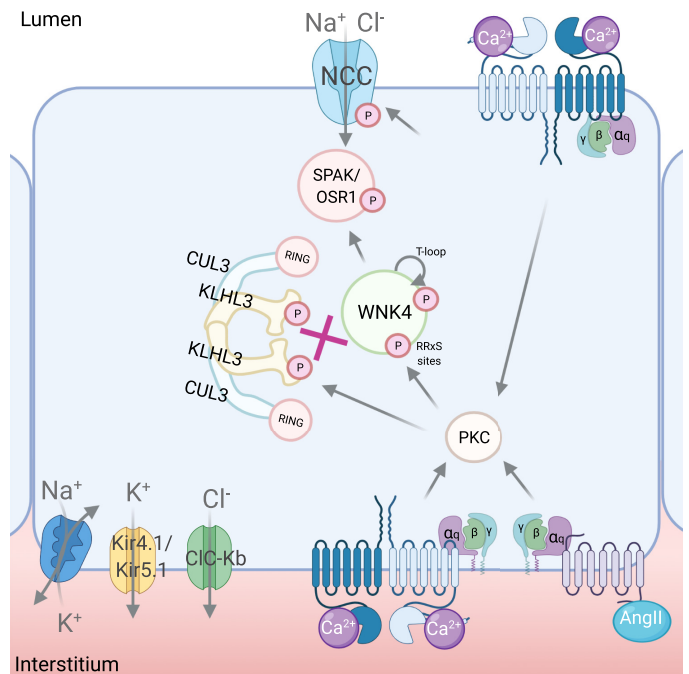


Figure 8. Role of with no lysine kinase 4 (WNK4) in the regulation of NaCl cotransporter (NCC) by ANG II and by extracellular Ca²⁺. Stimulation of ANG II type 1 receptors (AT₁) or calcium-sensing receptor (CaSR) in human embryonic kidney (HEK)-293 cells promotes PKC activation that, in turn, phosphorylates RRXS sites in WNK4 and Kelch-like family member 3 (KLHL3) (5, 16, 135). KLHL3 phosphorylation prevents WNK4 degradation (135), and WNK4 phosphorylation promotes kinase activation (16). In mice, high circulating ANG II levels correlate with increased KLHL3 and WNK4 phosphorylation levels at RRXS sites as well as increased levels of WNK4 protein expression (16, 135). Higher levels of WNK4 expression and phosphorylation at an RRXS site are also observed in mice administered the calcimimetic R-568, which acts as a positive allosteric modulator of CaSR (5). On the basis of this evidence, our group has proposed that activation of ANG II receptors and CaSR receptors in distal convoluted tubule cells promotes NCC activation via the depicted pathway (figure created with Biorender.com).

Distal Luminal NaCl Delivery

Several groups have reported that increased distal NaCl delivery to the DCT, induced by either loop diuretic administration or NaCl loading, promotes NCC activation and DCT hypertrophy (75, 173, 181, 182). In some of these models, loop diuretic administration produced a decrease in plasma K⁺ concentration; thus, it remains to be reassessed whether the observed effects on DCT were not due to changes in extracellular K⁺ concentration. In a more recent work, Yang et al. investigated such phenomena by inducing increased distal NaCl delivery in mice by subcutaneous injection of 0.5 mL of normal saline (with 0.1% KCl) for 3 days (75). With this maneuver, no changes in extracellular K⁺ concentration or renin levels occur. The amount of NaCl administered was low compared with that used in high-NaCl diet experiments in which NCC inhibition was observed. Interestingly, they found that their NaCl loading protocol promoted NCC activation (increased pNCC and thiazide sensitivity) in wild-type mice but also in *WNK4*^{-/-} mice. They proposed that activation of NCC by increased luminal NaCl delivery is independent of WNK4.

Other Hormonal Regulators of NCC Activity

Other hormones that have been shown to promote NCC activation include norepinephrine, insulin, fibroblast growth protein-23 (FGF23), prolactin, estrogens, and progesterone (180, 183–187). Insulin was also shown to promote SPAK and OSR1 phosphorylation (187) as well as estradiol and progesterone (186). Interestingly, Terker et al. reported that the effect of norepinephrine on NCC activation is dependent on OSR1 but not on SPAK activity (180). Regarding WNK4, Takahashi et al. showed that the insulin-induced activation of NCC is not observed in WNK4^{-/-} mice (15), suggesting that insulin promotes NCC activation via WNK4. In addition, work by Andrukhova et al. suggested that WNK4 is also involved in NCC activation induced by FGF23, given that they observed increased phosphorylation levels of WNK4 in renal cortex proteins extracted from mice treated with recombinant FGF23 (183).

CONCLUDING REMARKS

The study of the kinase WNK4 and its central role in renal physiology began with the identification of gain-of-function mutations causing inherited salt-sensitive hypertension in humans. Even though FHHt is a rare disease, that finding opened a field of research that had led to understanding several physiological and pathophysiological processes. It has now been established that the signaling pathway comprised of WNK4-SPAK/OSR1-NCC plays a pivotal role in the regulation of electrolyte homeostasis, such as Na⁺, Cl⁻, and K⁺ homeostasis, which have an impact on physiological parameters like blood pressure and extracellular K⁺ concentration levels. Additionally, these physiological parameters regulate the activity of WNK4 through different mechanisms, such as direct Cl⁻ binding, phosphorylation of different sites, and/or proteasomal degradation, forming negative feedback loops responsible for homeostatic balance. All this has been achieved in a record amount of time by the work of several groups of renal physiologists, increasingly collaborating at the international level. A lot of interesting discoveries are ahead of us in this exciting field.

ACKNOWLEDGMENTS

We are grateful to members of the Molecular Physiology Unit for suggestions and stimulating discussions.

GRANTS

Work in the researchers' laboratories is possible due to the support of National Institute of Diabetes and Digestive and Kidney Diseases Grant DK51496 (to G.G.) and Consejo Nacional de Ciencia y Tecnología Mexico Grants A1-S-8290 and 101720 (to G.G. and M.C.B., respectively).

DISCLOSURES

No conflicts of interest, financial or otherwise, are declared by the authors.

AUTHOR CONTRIBUTIONS

A.R.M., A.R. and M.C. conceived and designed research; A.R.M. and A.R. performed experiments; A.R.M., A.R., G.G. and M.C.

analyzed data; A.R.M., A.R., G.G. and M.C. interpreted results of experiments; A.R.M., A.R., H.C. and M.C. prepared figures; A.R.M., A.R., H.C., G.G. and M.C. drafted manuscript; A.R.M., A.R., H.C., G.G. and M.C. edited and revised manuscript; A.R.M., A.R., H.C., G.G. and M.C. approved final version of manuscript.

REFERENCES

1. Cao-Pham AH, Urano D, Ross-Elliott TJ, Jones AM. Nudge-nudge, WNK-WNK (kinases), say no more? *New Phytol* 220: 35–48, 2018. doi:10.1111/nph.15276.
2. Xu B, English JM, Wilsbacher JL, Stippec S, Goldsmith EJ, Cobb MH. WNK1, a novel mammalian serine/threonine protein kinase lacking the catalytic lysine in subdomain II. *J Biol Chem* 275: 16795–16801, 2000. doi:10.1074/jbc.275.22.16795.
3. Verissimo F, Jordan P. WNK kinases, a novel protein kinase subfamily in multi-cellular organisms. *Oncogene* 20: 5562–5569, 2001. doi:10.1038/sj.onc.1204726.
4. Wilson FH, Disse-Nicodème S, Choate KA, Ishikawa K, Nelson-Williams C, Desitter I, Gunel M, Milford DV, Lipkin GW, Achard JM, Feely MP, Dussol B, Berland Y, Unwin RJ, Mayan H, Simon DB, Farfel Z, Jeunemaitre X, Lifton RP. Human hypertension caused by mutations in WNK kinases. *Science* 293: 1107–1112, 2001. doi:10.1126/science.1062844.
5. Piali AT, Moon TM, Akella R, He H, Cobb MH, Goldsmith EJ. Chloride sensing by WNK1 involves inhibition of autophosphorylation. *Sci Signal* 7: ra41, 2014. doi:10.1126/scisignal.2005050.
6. Murillo-de-Ozores AR, Chávez-Canales M, de los Heros P, Gamba G, Castañeda-Bueno M. Physiological processes modulated by the chloride-sensitive WNK-SPAK/OSR1 kinase signaling pathway and the cation-coupled chloride cotransporters. *Front Physiol* 11: 1–28, 2020. doi:10.3389/fphys.2020.585907.
7. McCormick JA, Ellison DH. The WNKs: atypical protein kinases with pleiotropic actions. *Physiol Rev* 91: 177–219, 2011. doi:10.1152/physrev.00017.2010.
8. Rodan AR, Jenny A. WNK kinases in development and disease. *Curr Top Dev Biol* 123: 1–47, 2017. doi:10.1016/bs.ctdb.2016.08.004.
9. Vitari AC, Deak M, Morrice NA, Alessi DR. The WNK1 and WNK4 protein kinases that are mutated in Gordon's hypertension syndrome phosphorylate and activate SPAK and OSR1 protein kinases. *Biochem J* 391: 17–24, 2005. doi:10.1042/BJ20051180.
10. Alessi DR, Zhang J, Khanna A, Hochdorfer T, Shang Y, Kahle KT. The WNK-SPAK/OSR1 pathway: master regulator of cation-chloride cotransporters. *Sci Signal* 7: re3–re3, 2014. doi:10.1126/scisignal.2005365.
11. Hadchouel J, Ellison DH, Gamba G. Regulation of renal electrolyte transport by WNK and SPAK-OSR1 kinases. *Annu Rev Physiol* 78: 367–389, 2016. doi:10.1146/annurev-physiol-021115-105431.
12. Gandolfi B, Gruffydd-Jones TJ, Malik R, Cortes A, Jones BR, Helps CR, Prinzenberg EM, Erhardt G, Lyons LA. First WNK4-hypokalemia animal model identified by genome-wide association in Burmese cats. *PLoS One* 7: e53173, 2012. doi:10.1371/journal.pone.0053173.
13. Mayan H, Vered I, Mouallem M, Tzadok-Witkon M, Pautzner R, Farfel Z. Pseudohypoaldosteronism Type II: marked sensitivity to thiazides, hypercalciuria, normomagnesemia, and low bone mineral density. *J Clin Endocrinol Metab* 87: 3248–3254, 2002. doi:10.1210/jcem.87.7.8449.
14. Castaneda-Bueno M, Cervantes-Perez LG, Vázquez N, Uribe N, Kantesaria S, Morla L, Bobadilla NA, Doucet A, Alessi DR, Gamba G. Activation of the renal Na⁺:Cl⁻ cotransporter by angiotensin II is a WNK4-dependent process. *Proc Natl Acad Sci U S A* 109: 7929–7934, 2012. doi:10.1073/pnas.1200947109.
15. Takahashi D, Mori T, Nomura N, Khan MZH, Araki Y, Zeniya M, Sohara E, Rai T, Sasaki S, Uchida S. WNK4 is the major WNK positively regulating NCC in the mouse kidney. *Biosci Rep* 34: 195–206, 2014. doi:10.1042/BSR20140047.
16. Boyden LM, Choi M, Choate KA, Nelson-Williams CJ, Farhi A, Toka HR, et al. Mutations in kelch-like 3 and cullin 3 cause hypertension and electrolyte abnormalities. *Nature* 482: 98–102, 2012. doi:10.1038/nature10814.
17. Louis-Dit-Picard H, Barc J, Trujillano D, Miserey-Lenkei S, Bouatia-Naji N, Pylpenko O, International Consortium for Blood Pressure (ICBP), et al. KLHL3 mutations cause familial hyperkalemic

- hypertension by impairing ion transport in the distal nephron. *Nat Genet* 44: 456–460, 2012. [Erratum in *Nat Genet* 44: 609, 2012]. doi:10.1038/ng.2218.
18. Ohta A, Schumacher FR, Mehellou Y, Johnson C, Knebel A, Macartney TJ, Wood NT, Alessi DR, Kurz T. The CUL3-KLHL3 E3 ligase complex mutated in Gordon's hypertension syndrome interacts with and ubiquitylates WNK isoforms: disease-causing mutations in KLHL3 and WNK4 disrupt interaction. *Biochem J* 451: 111–122, 2013. doi:10.1042/BJ20121903.
 19. Shibata S, Zhang J, Puthumana J, Stone KL, Lifton RP. Kelch-like 3 and Cullin 3 regulate electrolyte homeostasis via ubiquitination and degradation of WNK4. *Proc Natl Acad Sci U S A* 110: 7838–7843, 2013. doi:10.1073/pnas.1304592110.
 20. Wakabayashi M, Mori T, Isobe K, Sahara E, Susa K, Araki Y, Chiga M, Kikuchi E, Nomura N, Mori Y, Matsuo H, Murata T, Nomura S, Asano T, Kawaguchi H, Nonoyama S, Rai T, Sasaki S, Uchida S. Impaired KLHL3-mediated ubiquitination of WNK4 causes human hypertension. *Cell Rep* 3: 858–868, 2013. doi:10.1016/j.celrep.2013.02.024.
 21. Khan T, Kandola TS, Wu J, Venkatesan S, Ketter E, Lange JJ, Rodríguez Gama A, Box A, Unruh JR, Cook M, Halfmann R. Quantifying nucleation in vivo reveals the physical basis of prion-like phase behavior. *Mol Cell* 71: 155–168, 2018. doi:10.1016/j.molcel.2018.06.016.
 22. Boyd-Shiwerski CR, Shiwerski DJ, Roy A, Namboodiri HN, Nkashama LJ, Xie J, McClain KL, Marciszyn A, Kleyman TR, Tan RJ, Stolz DB, Puthenveedu MA, Huang CL, Subramanya AR. Potassium-regulated distal tubule WNK bodies are kidney-specific WNK1 dependent. *Mol Biol Cell* 29: 499–509, 2018. doi:10.1091/mbc.E17-08-0529.
 23. Thomson MN, Cuevas CA, Bewarder TM, Dittmayer C, Miller LN, Si J, Cornelius RJ, Su X-T, Yang C-L, McCormick JA, Hadchouel J, Ellison DH, Bachmann S, Mutig K. WNK bodies cluster WNK4 and SPAK/OSR1 to promote NCC activation in hypokalemia. *Am J Physiol Renal Physiol* 318: F216–F228, 2020. doi:10.1152/ajprenal.00232.2019.
 24. Gagnon KB, Delpire E. Molecular physiology of SPAK and OSR1: two Ste20-related protein kinases regulating ion transport. *Physiol Rev* 92: 1577–1617, 2012. doi:10.1152/physrev.00009.2012.
 25. Moon TM, Correa F, Kinch LN, Piali AT, Gardner KH, Goldsmith EJ. Solution structure of the WNK1 autoinhibitory domain, a WNK-specific PF2 domain. *J Mol Biol* 425: 1245–1252, 2013. doi:10.1016/j.jmb.2013.01.031.
 26. Thastrup JO, Rafiqi FH, Vitari AC, Pozo-Guisado E, Deak M, Mehellou Y, Alessi DR. SPAK/OSR1 regulate NKCC1 and WNK activity: analysis of WNK isoform interactions and activation by T-loop trans-autophosphorylation. *Biochem J* 441: 325–337, 2012. doi:10.1042/BJ20111879.
 27. Min X, Lee BH, Cobb MH, Goldsmith EJ. Crystal structure of the kinase domain of WNK1, a kinase that causes a hereditary form of hypertension. *Structure* 12: 1303–1311, 2004. doi:10.1016/j.str.2004.04.014.
 28. Bazua-Valenti S, Chávez-Canales M, Rojas-Vega L, González-Rodríguez X, Vázquez N, Rodríguez-Gama A, Argai ER, Melo Z, Plata C, Ellison DH, García-Valdés J, Hadchouel J, Gamba G. The effect of WNK4 on the Na⁺-Cl⁻ cotransporter is modulated by intracellular chloride. *J Am Soc Nephrol* 26: 1781–1786, 2015. doi:10.1681/ASN.2014050470.
 29. Xu BE, Min X, Stippec S, Lee BH, Goldsmith EJ, Cobb MH. Regulation of WNK1 by an autoinhibitory domain and autophosphorylation. *J Biol Chem* 277: 48456–48462, 2002. doi:10.1074/jbc.M207917200.
 30. Zagórska A, Pozo-Guisado E, Boudeau J, Vitari AC, Rafiqi FH, Thastrup J, Deak M, Campbell DG, Morrice NA, Prescott AR, Alessi DR. Regulation of activity and localization of the WNK1 protein kinase by hyperosmotic stress. *J Cell Biol* 176: 89–100, 2007. doi:10.1083/jcb.200605093.
 31. Huse M, Kuriyan J. The conformational plasticity of protein kinases. *Cell* 109: 275–282, 2002. doi:10.1016/S0092-8674(02)00741-9. doi:10.1016/S0092-8674(02)00741-9.
 32. Chen W, Yazicioglu M, Cobb MH. Characterization of OSR1, a member of the mammalian Ste20p/germinal center kinase subfamily. *J Biol Chem* 279: 11129–11136, 2004. doi:10.1074/jbc.M313562200.
 33. Ushiro H, Tsutsumi T, Suzuki K, Kayahara T, Nakano K. Molecular cloning and characterization of a novel Ste20-related protein kinase enriched in neurons and transporting epithelia. *Arch Biochem Biophys* 355: 233–240, 1998. doi:10.1006/abbi.1998.0736.
 34. Leiserson WM, Harkins EW, Keshishian H. Fray, a *Drosophila* serine/threonine kinase homologous to mammalian PASK, is required for axonal ensheathment. *Neuron* 28: 793–806, 2000. doi:10.1016/S0896-6273(00)00154-9.
 35. Villa F, Goebel J, Rafiqi FH, Deak M, Thastrup J, Alessi DR, van Aalten DM. Structural insights into the recognition of substrates and activators by the OSR1 kinase. *EMBO Rep* 8: 839–845, 2007. doi:10.1038/sj.embor.7401048.
 36. Pacheco-Alvarez D, Vázquez N, Castañeda-Bueno M, De-Los-Heros P, Cortes-González C, Moreno E, Meade P, Bobadilla NA, Gamba G. WNK3-SPAK interaction is required for the modulation of NCC and other members of the SLC12 family. *Cell Physiol Biochem* 29: 291–302, 2012. doi:10.1159/000337610.
 37. Piechotta K, Garbarini N, England R, Delpire E. Characterization of the interaction of the stress kinase SPAK with the Na⁺-K⁺-2Cl⁻ cotransporter in the nervous system: Evidence for a scaffolding role of the kinase. *J Biol Chem* 278: 52848–52856, 2003. doi:10.1074/jbc.M309436200.
 38. Piechotta K, Lu J, Delpire E. Cation chloride cotransporters interact with the stress-related kinases Ste20-related proline-alanine-rich kinase (SPAK) and oxidative stress response 1 (OSR1). *J Biol Chem* 277: 50812–50819, 2002. doi:10.1074/jbc.M208108200.
 39. Vitari AC, Thastrup J, Rafiqi FH, Deak M, Morrice NA, Karlsson HKR, Alessi DR. Functional interactions of the SPAK/OSR1 kinases with their upstream activator WNK1 and downstream substrate NKCC1. *Biochem J* 397: 223–231, 2006. doi:10.1042/BJ20060220.
 40. Delpire E, Gagnon KB. SPAK and OSR1: STE20 kinases involved in the regulation of ion homeostasis and volume control in mammalian cells. *Biochem J* 409: 321–331, 2008. doi:10.1042/BJ20071324.
 41. Murillo-de-Ozores AR, Rodríguez-Gama A, Bazúa-Valenti S, Leyva-Ríos K, Vázquez N, Pacheco-Alvarez D, De La Rosa-Velázquez IA, Wengi A, Stone KL, Zhang J, Loffing J, Lifton RP, Yang CL, Ellison DH, Gamba G, Castañeda-Bueno M. C-terminally truncated, kidney-specific variants of the WNK4 kinase lack several sites that regulate its activity. *J Biol Chem* 293: 12209–12221, 2018. doi:10.1074/jbc.RA118.003037.
 42. Chávez-Canales M, Zhang C, Soukaseum C, Moreno E, Pacheco-Alvarez D, Vidal-Petiot E, Castañeda-Bueno M, Vázquez N, Rojas-Vega L, Meermeier NP, Rogers S, Jeunemaitre X, Yang CL, Ellison DH, Gamba G, Hadchouel J. WNK-SPAK-NCC cascade revisited: WNK1 stimulates the activity of the Na-Cl cotransporter via SPAK, an effect antagonized by WNK4. *Hypertension* 64: 1047–1053, 2014. doi:10.1161/HYPERTENSIONAHA.114.04036.
 43. Schumacher F-R, Sorrell FJ, Alessi DR, Bullock AN, Kurz T. Structural and biochemical characterization of the KLHL3-WNK kinase interaction important in blood pressure regulation. *Biochem J* 460: 237–246, 2014. doi:10.1042/BJ20140153.
 44. Castañeda-Bueno M, Arroyo JP, Zhang J, Puthumana J, Yarborough O 3rd, Shibata S, Rojas-Vega L, Gamba G, Rinehart J, Lifton RP. Phosphorylation by PKC and PKA regulate the kinase activity and downstream signaling of WNK4. *Proc Natl Acad Sci U S A* 114: E879–E886, 2017. doi:10.1073/pnas.1620315114.
 45. Na T, Wu G, Zhang W, Dong W-J, Peng J-B. Disease-causing R1185C mutation of WNK4 disrupts a regulatory mechanism involving calmodulin binding and SGK1 phosphorylation sites. *Am J Physiol Renal Physiol* 304: F8–F18, 2013. doi:10.1152/ajprenal.00284.2012.
 46. Rozansky DJ, Cornwall T, Subramanya AR, Rogers S, Yang YF, David LL, Zhu X, Yang CL, Ellison DH. Aldosterone mediates activation of the thiazide-sensitive Na-Cl cotransporter through an SGK1 and WNK4 signaling pathway. *J Clin Invest* 119: 2601–2612, 2009. doi:10.1172/JCI38323.
 47. McCormick JA, Mutig K, Nelson JH, Saritas T, Hoorn EJ, Yang CL, Rogers S, Curry J, Delpire E, Bachmann S, Ellison DH. A SPAK isoform switch modulates renal salt transport and blood pressure. *Cell Metab* 14: 352–364, 2011. doi:10.1016/j.cmet.2011.07.009.
 48. Markadieu N, Rios K, Spiller BW, McDonald WH, Welling PA, Delpire E. Short forms of Ste20-related proline/alanine-rich kinase (SPAK) in the kidney are created by aspartyl aminopeptidase (Dnpep)-mediated proteolytic cleavage. *J Biol Chem* 289: 29273–29284, 2014. doi:10.1074/jbc.M114.604009.

49. Kahle KT, Macgregor GG, Wilson FH, Van Hoek AN, Brown D, Ardito T, Kashgarian M, Giebisch G, Hebert SC, Boulpaep EL, Lifton RP. Paracellular Cl⁻ permeability is regulated by WNK4 kinase: insight into normal physiology and hypertension. *Proc Natl Acad Sci U S A* 101: 14877–14882, 2004. doi:10.1073/pnas.0406172101.
50. Ohno M, Uchida K, Ohashi T, Nitta K, Ohta A, Chiga M, Sasaki S, Uchida S. Immunolocalization of WNK4 in mouse kidney. *Histochem Cell Biol* 136: 25–35, 2011. doi:10.1007/s00418-011-0827-x.
51. Terker AS, Zhang C, McCormick JA, Lazelle RA, Zhang C, Meermeier NP, Siler DA, Park HJ, Fu Y, Cohen DM, Weinstein AM, Wang WH, Yang CL, Ellison DH. Potassium modulates electrolyte balance and blood pressure through effects on distal cell voltage and chloride. *Cell Metab* 21: 39–50, 2015. doi:10.1016/j.cmet.2014.12.006.
52. Boulpaep EL, Boron WF. *Medical Physiology*. 3rd edition. New York: Elsevier, 2016.
53. Murillo-de-Ozores AR, Gamba G, Castañeda-Bueno M. Molecular mechanisms for the regulation of blood pressure by potassium. In: *Current Topics in Membranes*. New York: Elsevier Inc., 2019. p. 285–313.
54. Grimm PR, Coleman R, Delpire E, Welling PA. Constitutively active SPAK causes hyperkalemia by activating NCC and remodeling distal tubules. *J Am Soc Nephrol* 28: 2597–2606, 2017. doi:10.1681/ASN.2016090948.
55. Gordon RD, Geddes RA, Pawsey CG, O'Halloran MW. Hypertension and severe hyperkalemia associated with suppression of renin and aldosterone and completely reversed by dietary sodium restriction. *Australas Ann Med* 19: 287–294, 1970. doi:10.1111/imj.1970.19.4.287.
56. Simon DB, Nelson-Williams C, Bia MJ, Ellison D, Karet FE, Molina A M, Vaara I, Iwata F, Cushner HM, Koolen M, Gainza FJ, Gitelman HJ, Lifton RP. Gitelman's variant of Bartter's syndrome, inherited hypokalaemic alkalosis, is caused by mutations in the thiazide-sensitive Na-Cl cotransporter. *Nat Genet* 12: 24–30, 1996. doi:10.1038/ng0196-24.
57. Pasman JW, Gabreëls FJM, Semmekrot B, Renier WO, Monnens LAH. Hyperkalemic periodic paralysis in Gordon's syndrome: a possible defect in atrial natriuretic peptide function. *Ann Neurol* 26: 392–395, 1989. doi:10.1002/ana.410260314.
58. Vidal-Petiot E, Elvira-Matelot E, Mutig K, Soukaseum C, Baudrie V, Wu S, Cheval L, Huc E, Cambillau M, Bachmann S, Doucet A, Jeunemaitre X, Hadchouel J. WNK1-related familial hyperkalemic hypertension results from an increased expression of L-WNK1 specifically in the distal nephron. *Proc Natl Acad Sci U S A* 110: 14366–14371, 2013. doi:10.1073/pnas.1304230110.
59. Louis-Dit-Picard H, Kouranti I, Rafael C, Loisel-Ferreira I, Chavez-Canales M, Abdel-Khalek W, Argai ER, Baron S, Vacle S, Migeon T, Coleman R, Do Cruzeiro M, Hureauux M, Thuraijasingam N, DeCramer S, Girerd X, O'Shaughnessy K, Mulatero P, Roussey G, Tack I, Unwin R, Vargas-Poussou R, Staub O, Grimm R, Welling PA, Gamba G, Clauser E, Hadchouel J, Jeunemaitre X. Mutation affecting the conserved acidic WNK1 motif causes inherited hyperkalemic hyperchloremic acidosis. *J Clin Invest* 26: 94171, 2020. doi:10.1172/jci94171.
60. Golbang AP, Murthy M, Hamad A, Liu CH, Cope G, Van't Hoff W, Cuthbert A, O'Shaughnessy KM. A new kindred with pseudohypoaldosteronism type II and a novel mutation (564D>H) in the acidic motif of the WNK4 gene. *Hypertension* 46: 295–300, 2005. doi:10.1161/01.HYP.0000174326.96918.d6.
61. Gong H, Tang Z, Yang Y, Sun L, Zhang W, Wang W, Cui B, Ning G. A patient with pseudohypoaldosteronism type II caused by a novel mutation in WNK4 gene. *Endocrine* 33: 230–234, 2008. doi:10.1007/s12020-008-9084-8.
62. Brooks AM, Owens M, Sayer JA, Salzmann M, Ellard S, Vaidya B. Pseudohypoaldosteronism type 2 presenting with hypertension and hyperkalemia due to a novel mutation in the WNK4 gene. *Qjm* 105: 791–794, 2012. doi:10.1093/qjmed/hcr119.
63. Lalioti MD, Zhang J, Volkman HM, Kahle KT, Hoffmann KE, Toka HR, Nelson-Williams C, Ellison DH, Flavell R, Booth CJ, Lu Y, Geller DS, Lifton RP. Wnk4 controls blood pressure and potassium homeostasis via regulation of mass and activity of the distal convoluted tubule. *Nat Genet* 38: 1124–1132, 2006. doi:10.1038/ng1877.
64. Yang SS, Morimoto T, Rai T, Chiga M, Sahara E, Ohno M, Uchida K, Lin SH, Moriguchi T, Shibuya H, Kondo Y, Sasaki S, Uchida S. Molecular pathogenesis of pseudohypoaldosteronism type ii: generation and analysis of a Wnk4D561A/+ knockin mouse model. *Cell Metab* 5: 331–344, 2007. doi:10.1016/j.cmet.2007.03.009.
65. Zhang C, Wang Z, Xie J, Yan F, Wang W, Feng X, Zhang W, Chen N. Identification of a Novel WNK4 Mutation in Chinese Patients with Pseudohypoaldosteronism Type II. *Nephron Physiol* 118: 53–61, 2011. doi:10.1159/000321879.
66. Susa K, Sahara E, Rai T, Zeniya M, Mori Y, Mori T, Chiga M, Nomura N, Nishida H, Takahashi D, Isobe K, Inoue Y, Takeishi K, Takeda N, Sasaki S, Uchida S. Impaired degradation of WNK1 and WNK4 kinases causes PHAII in mutant KLHL3 knock-in mice. *Hum Mol Genet* 23: 5052–5060, 2014. doi:10.1093/hmg/ddu217.
67. Susa K, Sahara E, Takahashi D, Okado T, Rai T, Uchida S. WNK4 is indispensable for the pathogenesis of pseudohypoaldosteronism type II caused by mutant KLHL3. *Biochem Biophys Res Commun* 491: 727–732, 2017. doi:10.1016/j.bbrc.2017.07.121.
68. Lin CM, Cheng CJ, Yang SS, Tseng MH, Yen MT, Sung CC, Lin SH. Generation and analysis of a mouse model of pseudohypoaldosteronism type II caused by KLHL3 mutation in BTB domain. *FASEB J* 33: 1051–1061, 2019. doi:10.1096/fj.201801023R.
69. Sasaki E, Susa K, Mori T, Isobe K, Araki Y, Inoue Y, Yoshizaki Y, Ando F, Mori Y, Mandai S, Zeniya M, Takahashi D, Nomura N, Rai T, Uchida S, Sahara E. KLHL3 knockout mice reveal the physiological role of KLHL3 and the pathophysiology of pseudohypoaldosteronism type ii caused by mutant KLHL3. *Mol Cell Biol* 37: e00508–e00516, 2017. doi:10.1128/MCB.00508-16.
70. Ferdous MZ, Miller LN, Agbor LN, Saritas T, Singer JD, Sigmund CD, McCormick JA. Mutant Cullin 3 causes familial hyperkalemic hypertension via dominant effects. *JCI Insight* 2: e96700, 2017. doi:10.1172/jci.insight.96700.
71. Abdel Khalek W, Rafael C, Loisel-Ferreira I, Kouranti I, Clauser E, Hadchouel J, Jeunemaitre X. Severe arterial hypertension from Cullin 3 mutations is caused by both renal and vascular effects. *J Am Soc Nephrol* 30: 811–823, 2019. doi:10.1681/ASN.2017121307.
72. Schumacher F-R, Siew K, Zhang J, Johnson C, Wood N, Cleary SE, Al Maskari RS, Ferryman JT, Hardege I, Yasmin Figg NL, Enchev R, Knebel A, O'Shaughnessy KM, Kurz T. Characterisation of the Cullin-3 mutation that causes a severe form of familial hypertension and hyperkalemia. *EMBO Mol Med* 7: 1285–1306, 2015. doi:10.15252/emmm.201505444.
73. Yang CL, Zhu X, Ellison DH. The thiazide-sensitive Na-Cl cotransporter is regulated by a WNK kinase signaling complex. *J Clin Invest* 117: 3403–3411, 2007. doi:10.1172/JCI32033.
74. Ohta A, Rai T, Yui N, Chiga M, Yang SS, Lin SH, Sahara E, Sasaki S, Uchida S. Targeted disruption of the Wnk4 gene decreases phosphorylation of Na-Cl cotransporter, increases Na excretion and lowers blood pressure. *Hum Mol Genet* 18: 3978–3986, 2009. doi:10.1093/hmg/ddp344.
75. Yang Y, Xie J, Yang S, Lin S, Huang C. Differential roles of WNK4 in regulation of NCC in vivo. *Am J Physiol Renal Physiol* 314: F999–F1007, 2018. doi:10.1152/ajprenal.00177.2017.
76. Chen JC, Lo YF, Lin YW, Lin SH, Huang CL, Cheng CJ. WNK4 kinase is a physiological intracellular chloride sensor. *Proc Natl Acad Sci U S A* 116: 4502–4507, 2019. doi:10.1073/pnas.1817220116.
77. Wilson FH, Kahle KT, Sabath E, Lalioti MD, Rapson AK, Hoover RS, Hebert SC, Gamba G, Lifton RP. Molecular pathogenesis of inherited hypertension with hyperkalemia: the Na-Cl cotransporter is inhibited by wild-type but not mutant WNK4. *Proc Natl Acad Sci U S A* 100: 680–684, 2003. doi:10.1073/pnas.242735399.
78. Yang CL, Angell J, Mitchell R, Ellison DH. WNK kinases regulate thiazide-sensitive Na-Cl cotransport. *J Clin Invest* 111: 1039–1045, 2003. doi:10.1172/JCI17443.
79. Richardson C, Rafiqi FH, Karlsson HK, Moleleki N, Vandewalle A, Campbell DG, Morrice NA, Alessi DR. Activation of the thiazide-sensitive Na⁺-Cl⁻ cotransporter by the WNK-regulated kinases SPAK and OSR1. *J Cell Sci* 121: 675–684, 2008. doi:10.1242/jcs.025312.
80. Dowd BFX, Forbush B. Pask (proline-alanine-rich STE20-related kinase), a regulatory kinase of the Na-K-Cl cotransporter (NKCC1). *J Biol Chem* 278: 27347–27353, 2003. doi:10.1074/jbc.M301899200.
81. Moriguchi T, Urushiyama S, Hisamoto N, Iemura SI, Uchida S, Natsume T, Matsumoto K, Shibuya H. WNK1 regulates phosphorylation of cation-chloride-coupled cotransporters via the STE20-related kinases, SPAK and OSR1. *J Biol Chem* 280: 42685–42693, 2005. doi:10.1074/jbc.M510042200.






82. **Bazúa-Valenti S, Rojas-Vega L, Castañeda-Bueno M, Barrera-Chimal J, Bautista R, Cervantes-Pérez LG, Vázquez N, Plata C, Murillo-de-Ozores AR, González-Mariscal L, Ellison DH, Riccardi D, Bobadilla NA, Gamba G.** The calcium-sensing receptor increases activity of the renal NCC through the WNK4-SPAK pathway. *J Am Soc Nephrol* 29: 1838–1848, 2018. doi:10.1681/ASN.2017111155.
83. **Terker AS, Zhang C, Erspamer KJ, Gamba G, Yang C-L, Ellison DH.** Unique chloride-sensing properties of WNK4 permit the distal nephron to modulate potassium homeostasis. *Kidney Int* 89: 1–8, 2015. doi:10.1038/ki.2015.289.
84. **Dhiani BA, Mehellou Y.** The Cul4-DDB1-WDR3/WDR6 complex binds SPAK and OSR1 kinases in a phosphorylation-dependent manner. *ChemBioChem* 21: 638–643, 2020. doi:10.1002/cbic.201900454.
85. **Rafiqi FH, Zuber AM, Glover M, Richardson C, Fleming S, Jovanović S, Jovanović A, O'Shaughnessy KM, Alessi DR.** Role of the WNK-activated SPAK kinase in regulating blood pressure. *EMBO Mol Med* 2: 63–75, 2010. doi:10.1002/emmm.200900058.
86. **Grimm PR, Taneja TK, Liu J, Coleman R, Chen YY, Delpire E, Wade JB, Welling PA.** SPAK isoforms and OSR1 regulate sodium-chloride co-transporters in a nephron-specific manner. *J Biol Chem* 287: 37673–37690, 2012. doi:10.1074/jbc.M112.402800.
87. **Yang S, Lo Y, Wu C, Lin S, Yeh C, Chu P, Sytwu H-K, Uchida S, Sasaki S, Lin S-H.** SPAK-knockout mice manifest Gitelman syndrome and impaired vasoconstriction. *J Am Soc Nephrol* 21: 1868–1877, 2010. doi:10.1681/ASN.2009121295.
88. **Lin SH, Yu IS, Jiang ST, Lin SW, Chu P, Chen A, Sytwu HK, Sohara E, Uchida S, Sasaki S, Yang SS.** Impaired phosphorylation of Na⁺-K⁺-2Cl⁻ cotransporter by oxidative stress-responsive kinase-1 deficiency manifests hypotension and Bartter-like syndrome. *Proc Natl Acad Sci U S A* 108: 17538–17543, 2011. doi:10.1073/pnas.1107452108.
89. **Chiga M, Rafiqi FH, Alessi DR, Sohara E, Ohta A, Rai T, Sasaki S, Uchida S.** Phenotypes of pseudohypoaldosteronism type II caused by the WNK4 D561A missense mutation are dependent on the WNK-OSR1/SPAK kinase cascade. *J Cell Sci* 124: 1391–1395, 2011. doi:10.1242/jcs.084111.
90. **Chu PY, Cheng CJ, Wu YC, Fang YW, Chau T, Uchida S, Sasaki S, Yang SS, Lin SH.** SPAK deficiency corrects pseudohypoaldosteronism II caused by WNK4 mutation. *PLoS One* 8: e72969, 2013. doi:10.1371/journal.pone.0072969.
91. **Castaneda-Bueno M, Cervantes-Perez LG, Rojas-Vega L, Arroyo-Garza I, Vazquez N, Moreno E, Gamba G.** Modulation of NCC activity by low and high K⁺ intake: insights into the signaling pathways involved. *Am J Physiol Renal Physiol* 306: F1507–F1519, 2014. doi:10.1152/ajprenal.00255.2013.
92. **Ferdaus MZ, Barber KW, López-Cayuqueo KI, Terker AS, Argaiz ER, Gassaway BM, Chambrey R, Gamba G, Rinehart J, McCormick JA.** SPAK and OSR1 play essential roles in potassium homeostasis through actions on the distal convoluted tubule. *J Physiol* 594: 4945–4966, 2016. doi:10.1113/JP272311.
93. **Ponce-Coria J, Markadieu N, Austin TM, Flammang L, Rios K, Welling PA, Delpire E.** A novel Ste20-related Proline/Alanine-rich Kinase (SPAK)-independent pathway involving Calcium-binding Protein 39 (Cab39) and Serine Threonine Kinase with No Lysine Member 4 (WNK4) in the activation of Na-K-Cl cotransporters. *J Biol Chem* 289: 17680–17688, 2014. doi:10.1074/jbc.M113.540518.
94. **Gamba G.** Molecular physiology and pathophysiology of electroneutral cation-chloride cotransporters. *Physiol Rev* 85: 423–493, 2005. doi:10.1152/physrev.00011.2004.
95. **de los Heros P, Alessi DR, Gourlay R, Campbell DG, Deak M, Macartney TJ, Kahle KT, Zhang J.** The WNK-regulated SPAK/OSR1 kinases directly phosphorylate and inhibit the K⁺-Cl⁻ co-transporters. *Biochem J* 458: 559–573, 2014. doi:10.1042/BJ20131478.
96. **Richardson C, Sakamoto K, de los Heros P, Deak M, Campbell DG, Prescott AR, Alessi DR.** Regulation of the NKCC2 ion cotransporter by SPAK-OSR1-dependent and -independent pathways. *J Cell Sci* 124: 789–800, 2011. doi:10.1242/jcs.077230.
97. **Kahle KT, Gimenez I, Hassan H, Wilson FH, Wong RD, Forbush B, Aronson PS, Lifton RP.** WNK4 regulates apical and basolateral Cl⁻ flux in extrarenal epithelia. *PNAS* 101: 2064–2069, 2004. doi:10.1073/pnas.0308434100.
98. **Gagnon KB, England R, Delpire E.** Characterization of SPAK and OSR1, regulatory kinases of the Na-K-2Cl cotransporter. *Mol Cell Biol* 26: 689–698, 2006. doi:10.1128/MCB.26.2.689-698.2006.
99. **Garzon-Muvdi T, Pacheco-Alvarez D, Gagnon KBE, Vazquez N, Ponce-Coria J, Moreno E, Delpire E, Gamba G.** WNK4 kinase is a negative regulator of K⁺-Cl⁻ cotransporters. *Am J Physiol Renal Physiol* 292: F1197–F1207, 2007. doi:10.1152/ajprenal.00335.2006.
100. **Terker AS, Castañeda-Bueno M, Ferdaus MZ, Cornelius RJ, Erspamer KJ, Su X-T, Miller LN, McCormick JA, Wang W-H, Gamba G, Yang C-L, Ellison DH.** With no lysine kinase 4 modulates sodium potassium 2 chloride cotransporter activity in vivo. *Am J Physiol Renal Physiol* 315: F781–F790, 2018. doi:10.1152/ajprenal.00485.2017.
101. **Moser S, Loffing J.** Different NKCC2 amino acid sequences between 129/Sv and C57BL/6 mice affect analysis of NKCC2 phosphorylation with phosphoform-specific antibodies (Abstract). *J Am Soc Nephrol* 30: 599, 2019.
102. **Melo Z, Cruz-Rangel S, Bautista R, Vázquez N, Castañeda-Bueno M, Mount DB, Pasantes-Morales H, Mercado A, Gamba G.** Molecular evidence for a role for K⁺-Cl⁻ cotransporters in the kidney. *Am J Physiol Renal Physiol* 305: F1402–F1411, 2013. doi:10.1152/ajprenal.00390.2013.
103. **Kleyman TR, Kashlan OB, Hughey RP.** Epithelial Na⁺ channel regulation by extracellular and intracellular factors. *Annu Rev Physiol* 80: 263–281, 2018. doi:10.1146/annurev-physiol-021317-121143.
104. **Rossier BC, Pradervand S, Schild L, Hummler E.** Epithelial sodium channel and the control of sodium balance: interaction between genetic and environmental factors. *Annu Rev Physiol* 64: 877–897, 2002. doi:10.1146/annurev.physiol.64.082101.143243.
105. **Ring AM, Leng Q, Rinehart J, Wilson FH, Kahle KT, Hebert SC, Lifton RP.** An SGK1 site in WNK4 regulates Na⁺ channel and K⁺ channel activity and has implications for aldosterone signaling and K⁺ homeostasis. *Proc Natl Acad Sci U S A* 104: 4025–4029, 2007. doi:10.1073/pnas.0611728104.
106. **Yu L, Cai H, Yue Q, Ali AA, Wang D, Al-Khalili O, Bao HF, Eaton DC.** WNK4 inhibition of ENaC is independent of Nedd4-2-mediated ENaC ubiquitination. *Am J Physiol Renal Physiol* 305: F31–F41, 2013. doi:10.1152/ajprenal.00652.2012.
107. **Zhang C, Wang L, Su X-T, Zhang J, Lin D-H, Wang W-H.** ENaC and ROMK activity are inhibited in the DCT2/CNT of TgWnk4 PHAI1 mice. *Am J Physiol Renal Physiol* 312: F682–F688, 2017. doi:10.1152/ajprenal.00420.2016.
108. **Welling PA.** Roles and regulation of renal K channels. *Annu Rev Physiol* 78: 415–435, 2016. doi:10.1146/annurev-physiol-021115-105423.
109. **Kahle KT, Wilson FH, Leng Q, Lalioti MD, O'Connell AD, Dong K, Rapson AK, MacGregor GG, Giebisch G, Hebert SC, Lifton RP.** WNK4 regulates the balance between renal NaCl reabsorption and K⁺ secretion. *Nat Genet* 35: 372–376, 2003. doi:10.1038/ng1271.
110. **He G, Wang HR, Huang SK, Huang CL.** Intersectin links WNK kinases to endocytosis of ROMK1. *J Clin Invest* 117: 1078–1087, 2007. doi:10.1172/JCI30087.
111. **Laghmani K, Beck BB, Yang S-S, Seayafan E, Wenzel A, Reusch B, et al.** Polyhydramnios, transient antenatal Bartter's syndrome, and MAGED2 mutations. *N Engl J Med* 374: 1853–1863, 2016. doi:10.1056/NEJMoa1507629.
112. **Lin DH, Yue P, Yarborough O 3rd, Scholl UI, Giebisch G, Lifton RP, Rinehart J, Wang WH.** Src-family protein tyrosine kinase phosphorylates WNK4 and modulates its inhibitory effect on KCNJ1 (ROMK). *Proc Natl Acad Sci U S A* 112: 4495–4500, 2015. doi:10.1073/pnas.1503437112.
113. **Zhuang J, Zhang X, Wang D, Li J, Zhou B, Shi Z, Gu D, Denson DD, Eaton DC, Cai H.** WNK4 kinase inhibits Maxi K channel activity by a kinase-dependent mechanism. *Am J Physiol Renal Physiol* 301: F410–F419, 2011. doi:10.1152/ajprenal.00518.2010.
114. **Wang Z, Subramanya AR, Satlin LM, Pastor-Soler NM, Carattino MD, Kleyman TR.** Regulation of large-conductance Ca²⁺-activated K⁺ channels by WNK4 kinase. *Am J Physiol Cell Physiol* 305: C846–C853, 2013. doi:10.1152/ajpcell.00133.2013.
115. **Bi Y, Li C, Zhang Y, Wang Y, Chen S, Yue Q, Hoover RS, Wang XH, Delpire E, Eaton DC, Zhuang J, Cai H.** Stimulatory role of SPAK signaling in the regulation of large conductance Ca²⁺-activated potassium (BK) channel protein expression in kidney. *Front Physiol* 11: 1–10, 2020. doi:10.3389/fphys.2020.00638.
116. **Hou J, Rajagopal M, Yu AS.** Claudins and the kidney. *Annu Rev Physiol* 75: 479–501, 2013. doi:10.1146/annurev-physiol-030212-183705.

117. Yamauchi K, Rai T, Kobayashi K, Sahara E, Suzuki T, Itoh T, Suda S, Hayama A, Sasaki S, Uchida S. Disease-causing mutant WNK4 increases paracellular chloride permeability and phosphorylates claudins. *Proc Natl Acad Sci USA* 101: 4690–4694, 2004. doi:10.1073/pnas.0306924101.
118. Tatum R, Zhang Y, Lu Q, Kim K, Jeanson BG, Chen YH. WNK4 phosphorylates ser206 of claudin-7 and promotes paracellular Cl⁻ permeability. *FEBS Lett* 581: 3887–3891, 2007. doi:10.1016/j.febslet.2007.07.014.
119. Fan J, Tatum R, Hoggard J, Chen YH. Claudin-7 modulates Cl⁻ and Na⁺ homeostasis and WNK4 expression in renal collecting duct cells. *IJMS* 20: 3798, 2019. doi:10.3390/ijms20153798.
- 119a. Tomilin V, Mamenko M, Zaika O, Pochynyuk O. Role of renal TRP channels in physiology and pathology. *Semin Immunopathol* 38: 371–383, 2016. doi:10.1007/s00281-015-0527-z.
- 119b. Nilius B, Owsianik G, Voets T, Peters JA. Transient receptor potential cation channels in disease. *Physiol Rev* 87: 165–217, 2007. doi:10.1152/physrev.00021.2006.
120. Fu Y, Subramanya A, Rozansky D, Cohen DM. WNK kinases influence TRPV4 channel function and localization. *Am J Physiol Renal Physiol* 290: F1305–F1314, 2006. doi:10.1152/ajprenal.00391.2005.
121. Jiang Y, Ferguson WB, Peng JB. WNK4 enhances TRPV5-mediated calcium transport: potential role in hypercalciuria of familial hyperkalemic hypertension caused by gene mutation of WNK4. *Am J Physiol Renal Physiol* 292: F545–F554, 2007. doi:10.1152/ajprenal.00187.2006.
122. Cha SK, Huang CL. WNK4 kinase stimulates caveola-mediated endocytosis of TRPV5 amplifying the dynamic range of regulation of the channel by protein kinase C. *J Biol Chem* 285: 6604–6611, 2010. doi:10.1074/jbc.M109.056044.
123. Ferdous MZ, Gratreak BDK, Miller L, Si J, McCormick JA, Yang C, Ellison DH, Terker AS. WNK4 limits distal calcium losses following acute furosemide treatment. *Physiol Rep* 7: e14195, 2019. doi:10.14814/phy2.14195.
124. Frizzell RA, Hanrahan JW. Physiology of epithelial chloride and fluid secretion. *Cold Spring Harb Perspect Med* 2: a009563, 2012. doi:10.1101/cshperspect.a009563.
125. Yang CL, Liu X, Paliege A, Zhu X, Bachmann S, Dawson DC, Ellison DH. WNK1 and WNK4 modulate CFTR activity. *Biochem Biophys Res Commun* 353: 535–540, 2007. doi:10.1016/j.bbrc.2006.11.151.
126. Mendes AI, Matos P, Moniz S, Luz S, Amaral MD, Farinha CM, Jordan P. Antagonistic regulation of cystic fibrosis transmembrane conductance regulator cell surface expression by protein kinases WNK4 and spleen tyrosine kinase. *Mol Cell Biol* 31: 4076–4086, 2011. doi:10.1128/MCB.05152-11.
127. Everett LA, Glaser B, Beck JC, Idol JR, Buchs A, Heyman M, Adawi F, Hazani E, Nassir E, Baxevasis AD, Sheffield VC, Green ED. Pendred syndrome is caused by mutations in a putative sulphate transporter gene (PDS). *Nat Genet* 17: 411–422, 1997. doi:10.1038/ng1297-411.
128. Levief F, Hübner CA, Houillier P, Morla L, El Moghrabi S, Brideau G, Hassan H, Hatim H, Parker MD, Kurth I, Kougioumtzes A, Sinning A, Pech V, Riemondy KA, Miller RL, Hummler E, Shull GE, Aronson PS, Doucet A, Wall SM, Chambrey R, Eladari D. The Na⁺-dependent chloride-bicarbonate exchanger SLC4A8 mediates an electroneutral Na⁺ reabsorption process in the renal cortical collecting ducts of mice. *J Clin Invest* 120: 1627–1635, 2010. [Erratum in *J Clin Invest* 121: 1668, 2011]. doi:10.1172/JCI40145.
129. Wall SM, Verlander JW, Romero CA. The renal physiology of pendrin-positive intercalated cells. *Physiol Rev* 100: 1119–1147, 2020. doi:10.1152/physrev.00011.2019.
130. López-Cayuqueo KI, Chavez-Canales M, Pillot A, Houillier P, Jayat M, Baraka-Vidot J, Trepiccione F, Baudrie V, Büsst C, Soukaseum C, Kumai Y, Jeunemaitre X, Hadchouel J, Eladari D, Chambrey R. A mouse model of pseudohypoaldosteronism type II reveals a novel mechanism of renal tubular acidosis. *Kidney Int* 94: 514–523, 2018. doi:10.1016/j.kint.2018.05.001.
131. Keuss MJ, Thomas Y, McArthur R, Wood NT, Knebel A, Kurz T. Characterization of the mammalian family of DCN-type NEDD8 E3 ligases. *J Cell Sci* 129: 1441–1454, 2016. doi:10.1242/jcs.181784.
132. Limbutara K, Chou CL, Knepper MA. Quantitative proteomics of all 14 renal tubule segments in rat. *J Am Soc Nephrol* 31: 1255–1266, 2020. doi:10.1681/ASN.2020010071.
133. Park J, Shrestha R, Qiu C, Kondo A, Huang S, Werth M, Li M, Barasch J, Suszták K. Single-cell transcriptomics of the mouse kidney reveals potential cellular targets of kidney disease. *Science* 360: 758–763, 2018. doi:10.1126/science.aar2131.
134. Kasagi Y, Takahashi D, Aida T, Nishida H, Nomura N, Zeniya M, Mori T, Sasaki E, Ando F, Rai T, Uchida S, Sahara E. Impaired degradation of medullary WNK4 in the kidneys of KLHL2 knockout mice. *Biochem Biophys Res Commun* 487: 368–374, 2017. doi:10.1016/j.bbrc.2017.04.068.
135. Takahashi D, Mori T, Wakabayashi M, Mori Y, Susa K, Zeniya M, Sahara E, Rai T, Sasaki S, Uchida S. KLHL2 interacts with and ubiquitinates WNK kinases. *Biochem Biophys Res Commun* 437: 457–462, 2013. doi:10.1016/j.bbrc.2013.06.104.
136. Breitwieser GE, Altamirano AA, Russell JM. Osmotic stimulation of Na⁺-K⁺-Cl⁻ cotransport in squid giant axon is [Cl⁻]_i dependent. *Am J Physiol* 258: C749–C753, 1990. doi:10.1152/ajpcell.1990.258.4.C749.
137. Lytle C, Forbush B. Regulatory phosphorylation of the secretory Na-K-Cl cotransporter: modulation by cytoplasmic Cl⁻. *Am J Physiol* 270: C437–C448, 1996. doi:10.1152/ajpcell.1996.270.2.C437.
138. Pacheco-Alvarez D, San Cristóbal P, Meade P, Moreno E, Vazquez N, Muñoz E, Díaz A, Juárez ME, Giménez I, Gamba G. The Na⁺:Cl⁻ cotransporter is activated and phosphorylated at the amino-terminal domain upon intracellular chloride depletion. *J Biol Chem* 281: 28755–28763, 2006. doi:10.1074/jbc.M603773200.
139. Ponce-Coria J, San-Cristobal P, Kahle KT, Vazquez N, Pacheco-Alvarez D, de Los Heros P, Juárez P, Muñoz E, Michel G, Bobadilla NA, Giménez I, Lifton RP, Hebert SC, Gamba G. Regulation of NKCC2 by a chloride-sensing mechanism involving the WNK3 and SPAK kinases. *Proc Natl Acad Sci U S A* 105: 8458–8463, 2008. doi:10.1073/pnas.0802966105.
140. Russell JM. Cation-coupled chloride influx in squid axon: Role of potassium and stoichiometry of the transport process. *J Gen Physiol* 81: 909–925, 1983. doi:10.1085/jgp.81.6.909.
141. Lytle C, Forbush B 3rd. The Na-K-Cl cotransport protein of shark rectal gland. II. Regulation by direct phosphorylation. *J Biol Chem* 267: 25438–25443, 1992. doi:10.1016/S0021-9258(19)74060-5.
142. Beck FX, Dörge A, Rick R, Schramm M, Thurau K. The distribution of potassium, sodium and chloride across the apical membrane of renal tubular cells: effect of acute metabolic alkalosis. *Pflugers Arch* 411: 259–267, 1988. doi:10.1007/BF00585112.
143. Boettger T, Hubner C, Maier H, Rust M, Beck F, Jentsch T. Deafness and renal tubular acidosis in mice lacking the K-Cl cotransporter Kcc4. *Nat Lett* 416: 874–13452, 2002. doi:10.1038/416874a.
144. Su X, Klett NJ, Sharma A, Allen CN, Wang W, Yang C, Ellison DH. Distal convoluted tubule Cl⁻ concentration is modulated via K⁺ channels and transporters. *Am J Physiol Renal Physiol* 319: F534–F540, 2020. doi:10.1152/ajprenal.00284.2020.
145. Nishikawa K, Toker A, Johannes FJ, Songyang Z, Cantley LC. Determination of the specific substrate sequence motifs of protein kinase C isozymes. *J Biol Chem* 272: 952–960, 1997. doi:10.1074/jbc.272.2.952.
146. Pearson RB, Kemp BE. Protein kinase phosphorylation site sequences and consensus specificity motifs: tabulations. *Methods Enzymol* 200: 62–81, 1991. doi:10.1016/0076-6879(91)00127-1. doi:10.1016/0076-6879(91)00127-i.
147. Verrey F, Loffing J, Zecevic M, Heitzmann D, Staub O. SGK1: aldosterone-induced relay of Na⁺ transport regulation in distal kidney nephron cells. *Cell Physiol Biochem* 13: 21–28, 2003. doi:10.1159/000070246.
148. Czogalla J, Vohra T, Penton D, Kirschmann M, Craigie E, Loffing J. The mineralocorticoid receptor (MR) regulates ENaC but not NCC in mice with random MR deletion. *Pflugers Arch Eur Arch* 468: 849–858, 2016. doi:10.1007/s00424-016-1798-5.
149. Terker AS, Yarbrough B, Ferdous MZ, Lazelle RA, Erspamer KJ, Meermeier NP, Park HJ, McCormick JA, Yang CL, Ellison DH. Direct and indirect mineralocorticoid effects determine distal salt transport. *J Am Soc Nephrol* 27: 2436–2445, 2016. doi:10.1681/ASN.2015070815.
150. Lin D-H, Yue P, Rinehart J, Sun P, Wang Z, Lifton R, Wang W-H. Protein phosphatase 1 modulates the inhibitory effect of With-no-Lysine kinase 4 on ROMK channels. *Am J Physiol Renal Physiol* 303: F110–F119, 2012. doi:10.1152/ajprenal.00676.2011.

151. **Hendrickx A, Beullens M, Ceulemans H, Den Abt T, Van Eynde A, Nicolaescu E, Lesage B, Bollen M.** Docking motif-guided mapping of the interactome of protein phosphatase-1. *Chem Biol* 16: 365–371, 2009. doi:10.1016/j.chembiol.2009.02.012.
152. **Delalay C, Lu J, Houot AM, Disse-Nicodeme S, Gasc JM, Corvol P, Jeunemaitre X.** multiple promoters in the WNK1 gene: one controls expression of a kidney-specific kinase-defective isoform. *Mol Cell Biol* 23: 9208–9221, 2003. doi:10.1128/MCB.23.24.9208-9221.2003. doi:10.1128/mcb.23.24.9208-9221.2003.
153. **O'Reilly M, Marshall E, Speirs HJ, Brown RW.** *Wnk1*, a gene within a novel blood pressure control pathway, tissue-specifically generates radically different isoforms with and without a kinase domain. *J Am Soc Nephrol* 14: 2447–2456, 2003. doi:10.1097/O1.ASN.0000089830.97681.3B.
154. **Vidal-Petiot E, Cheval L, Faugetoux J, Malard T, Doucet A, Jeunemaitre X, Hadchouel J.** A new methodology for quantification of alternatively spliced exons reveals a highly tissue-specific expression pattern of WNK1 isoforms. *PLoS One* 7: e37751–9, 2012. doi:10.1371/journal.pone.0037751.
155. **Argaiz ER, Chavez-Canales M, Ostrosky-Frid M, Rodríguez-Gama A, Vázquez N, Gonzalez-Rodríguez X, Garcia-Valdes J, Hadchouel J, Ellison D, Gamba G.** Kidney-specific WNK1 isoform (KS-WNK1) is a potent activator of WNK4 and NCC. *Am J Physiol Renal Physiol* 315: F734–F745, 2018. doi:10.1152/ajprenal.00145.2018.
156. **Rojas-Vega L, Gamba G.** Mini-review: regulation of the renal NaCl cotransporter by hormones. *Am J Physiol Renal Physiol* 310: F10–F14, 2016. doi:10.1152/ajprenal.00354.2015.
157. **Penton D, Czogalla J, Wengi A, Himmerkus N, Loffing-Cueni D, Carrel M, Rajaram RD, Staub O, Bleich M, Schweda F, Loffing J.** Extracellular K^+ rapidly controls NaCl cotransporter phosphorylation in the native distal convoluted tubule by Cl^- -dependent and independent mechanisms. *J Physiol* 594: 6319–6331, 2016. doi:10.1113/JP272504.
158. **Rengarajan S, Lee DH, Oh YT, Delpire E, Youn JH, McDonough AA.** Increasing plasma $[K^+]$ by intravenous potassium infusion reduces NCC phosphorylation and drives kaliuresis and natriuresis. *Am J Physiol - Ren Physiol* 306: F1059–F1068, 2014. [Erratum in *Am J Physiol Renal Physiol* 310: F688, 2016]. doi:10.1152/ajprenal.00015.2014.
159. **Sorensen MV, Grossmann S, Roesinger M, Gresko N, Todkar AP, Barmettler G, Ziegler U, Odermatt A, Loffing-Cueni D, Loffing J.** Rapid dephosphorylation of the renal sodium chloride cotransporter in response to oral potassium intake in mice. *Kidney Int* 83: 811–824, 2013. doi:10.1038/ki.2013.14.
160. **Cuevas CA, Su XT, Wang MX, Terker AS, Lin DH, McCormick JA, Yang CL, Ellison DH, Wang WH.** Potassium Sensing by Renal Distal Tubules Requires Kir4.1. *J Am Soc Nephrol* 28: 1814–1825, 2017. doi:10.1681/ASN.2016090935.
161. **Wang MX, Cuevas CA, Su XT, Wu P, Gao ZX, Lin DH, McCormick JA, Yang CL, Wang WH, Ellison DH.** Potassium intake modulates the thiazide-sensitive sodium-chloride cotransporter (NCC) activity via the Kir4.1 potassium channel. *Kidney Int* 93: 893–902, 2018. doi:10.1016/j.kint.2017.10.023.
162. **Nomura N, Shoda W, Wang Y, Mandai S, Furusho T, Takahashi D, Zeniya M, Sohara E, Rai T, Uchida S.** Role of ClC-K and barttin in low-potassium induced sodium-chloride cotransporter activation and hypertension in mouse kidney. *Biosci Rep* 38: BSR20171243, 2018. doi:10.1042/BSR20171243.
163. **Zhang C, Wang L, Zhang J, Su XT, Lin DH, Scholl UI, Giebisch G, Lifton RP, Wang WH.** KCNJ10 determines the expression of the apical Na-Cl cotransporter (NCC) in the early distal convoluted tubule (DCT1). *Proc Natl Acad Sci U S A* 111: 11864–11869, 2014. doi:10.1073/pnas.1411705111.
164. **Murillo-de-Ozores AR, Grajeda-Medina LI, Gamba G, Castañeda-Bueno M.** Intracellular chloride depletion promotes WNK4-RRXS phosphorylation by a PKC/PKA dependent mechanism [Abstract]. *J Am Soc Nephrol* 29: 1005, 2018.
165. **Ishizawa K, Xu N, Loffing J, Lifton RP, Fujita T, Uchida S, Shibata S.** Potassium depletion stimulates Na-Cl cotransporter via phosphorylation and inactivation of the ubiquitin ligase Kelch-like 3. *Biochem Biophys Res Commun* 480: 745–751, 2016. doi:10.1016/j.bbrc.2016.10.127.
166. **Thomson MN, Schneider W, Mutig K, Ellison DH, Kettritz R, Bachmann S.** Patients with hypokalemia develop WNK bodies in the distal convoluted tubule of the kidney. *Am J Physiol Renal Physiol* 316: F292–F300, 2019. doi:10.1152/ajprenal.00464.2018.
167. **Kim GH, Masilamani S, Turner R, Mitchell C, Wade JB, Knepper MA.** The thiazide-sensitive Na-Cl cotransporter is an aldosterone-induced protein. *Proc Natl Acad Sci U S A* 95: 14552–14557, 1998. doi:10.1073/pnas.95.24.14552.
168. **Hunter RW, Ivy JR, Flatman PW, Kenyon CJ, Craigie E, Mullins LJ, Bailey MA, Mullins JJ.** Hypertrophy in the distal convoluted tubule of an 11 β -hydroxysteroid dehydrogenase type 2 knockout model. *J Am Soc Nephrol* 26: 1537–1548, 2015. doi:10.1681/ASN.2013060634.
169. **Náray-Fejes-Tóth A, Fejes-Tóth G.** Novel mouse strain with Cre recombinase in 11 β -hydroxysteroid dehydrogenase-2-expressing cells. *Am J Physiol Ren Physiol* 292: 486–494, 2007. doi:10.1152/ajprenal.00188.2006.
170. **Bostanjoglo M, Reeves WB, Reilly RF, Velázquez H, Robertson N, Laitwak G, Morsing P, Dørup J, Bachmann S, Ellison DH.** 11 β -hydroxysteroid dehydrogenase, mineralocorticoid receptor, and thiazide-sensitive Na-Cl cotransporter expression by distal tubules. [Online]. *J Am Soc Nephrol* 9: 1347–1358, 1998. <http://www.ncbi.nlm.nih.gov/pubmed/9697656>.
171. **Velázquez H, Náray-Fejes-Tóth A, Silva T, Andújar E, Reilly RF, Desir GV, Ellison DH.** Rabbit distal convoluted tubule coexpresses NaCl cotransporter and 11 β -hydroxysteroid dehydrogenase II mRNA. *Kidney Int* 54: 464–472, 1998. doi:10.1046/j.1523-1755.1998.00036.x.
172. **Sorensen MV, Saha B, Jensen IS, Wu P, Ayasse N, Gleason CE, Svendsen SL, Wang WH, Pearce D.** Potassium acts through mTOR to regulate its own secretion. *JCI Insight* 5: e126910, 2019. doi:10.1172/jci.insight.126910.
173. **Ellison DH, Velázquez H, Wright FS.** Adaptation of the distal convoluted tubule of the rat. Structural and functional effects of dietary salt intake and chronic diuretic infusion. *J Clin Invest* 83: 113–126, 1989. doi:10.1172/JCI113847.
174. **Frindt G, Palmer LG.** Surface expression of sodium channels and transporters in rat kidney: effects of dietary sodium. *Am J Physiol Renal Physiol* 297: F1249–F1255, 2009. doi:10.1152/ajprenal.00401.2009.
175. **Sandberg MB, Maunsbach AB, McDonough AA.** Redistribution of distal tubule Na⁺-Cl⁻ cotransporter (NCC) in response to a high-salt diet. *Am J Physiol Renal Physiol* 291: F503–F508, 2006. doi:10.1152/ajprenal.00482.2005.
176. **Vallon V, Schroth J, Lang F, Kuhl D, Uchida S.** Expression and phosphorylation of the Na⁺-Cl⁻ cotransporter NCC in vivo is regulated by dietary salt, potassium, and SGK1. *Am J Physiol Renal Physiol* 297: F704–F712, 2009. doi:10.1152/ajprenal.00030.2009.
177. **van der Lubbe N, Lim CH, Fenton RA, Meima ME, Danser AHJ, Zietse R, Hoorn EJ.** Angiotensin II induces phosphorylation of the thiazide-sensitive sodium chloride cotransporter independent of aldosterone. *Kidney Int* 79: 66–76, 2011. doi:10.1038/ki.2010.290.
178. **Shibata S, Arroyo JP, Castañeda-Bueno M, Puthumana J, Zhang J, Uchida S, Stone KL, Lam TT, Lifton RP.** Angiotensin II signaling via protein kinase C phosphorylates Kelch-like 3, preventing WNK4 degradation. *Proc Natl Acad Sci U S A* 111: 15556–15561, 2014. doi:10.1073/pnas.1418342111.
179. **Li J, Hatano R, Xu S, Wan L, Yang L, Weinstein AM, Palmer L, Wang T.** Gender difference in kidney electrolyte transport. I. Role of AT1a receptor in thiazide-sensitive Na⁺-Cl⁻ cotransporter activity and expression in male and female mice. *Am J Physiol Physiol* 313: F505–F513, 2017. doi:10.1152/ajprenal.00087.2017.
180. **Terker AS, Yang CL, McCormick JA, Meermeier NP, Rogers SL, Grossmann S, Trompf K, Delpire E, Loffing J, Ellison DH.** Sympathetic stimulation of thiazide-sensitive sodium chloride cotransport in the generation of salt-sensitive hypertension. *Hypertension* 64: 178–184, 2014. doi:10.1161/HYPERTENSIONAHA.114.03335.
181. **Kaissling B, Stanton BA.** Adaptation of distal tubule and collecting duct to increased sodium delivery. I. Ultrastructure. *Am J Physiol Physiol* 255: F1256–F1268, 1988. doi:10.1152/ajprenal.1988.255.6.F1256.
182. **Stanton BA, Kaissling B.** Adaptation of distal tubule and collecting duct to increased Na delivery. II. Na⁺ and K⁺ transport. *Am J Physiol Physiol* 255: F1269–F1275, 1988. doi:10.1152/ajprenal.1988.255.6.F1269.
183. **Andrukhova O, Slavic S, Smorodchenko A, Zeitz U, Shalhoub V, Lanske B, Pohl EE, Erben RG.** FGF23 regulates renal sodium

- handling and blood pressure. *EMBO Mol Med* 6: 744–759, 2014. doi:10.1002/emmm.201303716.
184. **Chávez-Canales M, Arroyo JP, Ko B, Vázquez N, Bautista R, Castañeda-Bueno M, Bobadilla NA, Hoover RS, Gamba G.** Insulin increases the functional activity of the renal NaCl cotransporter. *J Hypertens* 31: 303–311, 2013. doi:10.1097/HJH.0b013e32835bbb83.
185. **Komers R, Rogers S, Oyama TT, Xu B, Yang C-L, McCormick J, Ellison DH.** Enhanced phosphorylation of Na⁺-Cl⁻ co-transporter in experimental metabolic syndrome: role of insulin. *Clin Sci (Lond)* 123: 635–647, 2012. doi:10.1042/CS20120003.
186. **Rojas-Vega L, Reyes-Castro LA, Ramírez V, Bautista-Pérez R, Rafael C, Castañeda-Bueno M, Meade P, de los Heros P, Arroyo-Garza I, Bernard V, Binart N, Bobadilla NA, Hadchouel J, Zambrano E, Gamba G.** Ovarian hormones and prolactin increase renal NaCl cotransporter phosphorylation. *Am J Physiol Renal Physiol* 308: F799–F808, 2015. doi:10.1152/ajprenal.00447.2014.
187. **Sohara E, Rai T, Yang SS, Ohta A, Naito S, Chiga M, Nomura N, Lin SH, Vandewalle A, Ohta E, Sasaki S, Uchida S.** Acute insulin stimulation induces phosphorylation of the Na-Cl cotransporter in cultured distal mpkDCT cells and mouse kidney. *PLoS One* 6: e24277, 2011. doi:10.1371/journal.pone.0024277.
188. **Mori Y, Wakabayashi M, Mori T, Araki Y, Sohara E, Rai T, Sasaki S, Uchida S.** Decrease of WNK4 ubiquitination by disease-causing mutations of KLHL3 through different molecular mechanisms. *Biochem Biophys Res Commun* 439: 30–34, 2013. doi:10.1016/j.bbrc.2013.08.035.

The Calcium-Sensing Receptor Increases Activity of the Renal NCC through the WNK4-SPAK Pathway

Silvana Bazúa-Valenti ^{1,2}, Lorena Rojas-Vega,² María Castañeda-Bueno,² Jonatan Barrera-Chimal,¹ Rocío Bautista,³ Luz G. Cervantes-Pérez,⁴ Norma Vázquez,¹ Consuelo Plata,² Adrián R. Murillo-de-Ozores,^{1,2} Lorenza González-Mariscal,⁵ David H. Ellison ^{6,7}, Daniela Riccardi ⁸, Norma A. Bobadilla ^{1,2} and Gerardo Gamba ^{1,2,9}

¹Molecular Physiology Unit, Instituto de Investigaciones Biomédicas, Universidad Nacional Autónoma de México, Mexico City, Mexico; ²Department of Nephrology and Mineral Metabolism, Instituto Nacional de Ciencias Médicas y Nutrición Salvador Zubirán, Mexico City, Mexico; ³Departments of Molecular Biology and ⁴Pharmacology, Instituto Nacional de Cardiología Ignacio Chávez, Mexico City, Mexico; ⁵Department of Physiology, Biophysics and Neuroscience, Center for Research and Advanced Studies (Cinvestav), Mexico City, Mexico; ⁶Department of Medicine, Oregon Health and Science University, Portland, Oregon; ⁷Renal Section, Veterans Administration Portland Health Care System, Portland, Oregon; ⁸School of Biosciences, Cardiff University, Cardiff, United Kingdom; and ⁹Tecnológico de Monterrey, Escuela de Medicina y Ciencias de la Salud, Monterrey, Nuevo León, Mexico

ABSTRACT

Background Hypercalciuria can result from activation of the basolateral calcium-sensing receptor (CaSR), which in the thick ascending limb of Henle's loop controls Ca^{2+} excretion and NaCl reabsorption in response to extracellular Ca^{2+} . However, the function of CaSR in the regulation of NaCl reabsorption in the distal convoluted tubule (DCT) is unknown. We hypothesized that CaSR in this location is involved in activating the thiazide-sensitive NaCl cotransporter (NCC) to prevent NaCl loss.

Methods We used a combination of *in vitro* and *in vivo* models to examine the effects of CaSR on NCC activity. Because the KLHL3-WNK4-SPAK pathway is involved in regulating NaCl reabsorption in the DCT, we assessed the involvement of this pathway as well.

Results Thiazide-sensitive $^{22}\text{Na}^+$ uptake assays in *Xenopus laevis* oocytes revealed that NCC activity increased in a WNK4-dependent manner upon activation of CaSR with Gd^{3+} . In HEK293 cells, treatment with the calcimimetic R-568 stimulated SPAK phosphorylation only in the presence of WNK4. The WNK4 inhibitor WNK463 also prevented this effect. Furthermore, CaSR activation in HEK293 cells led to phosphorylation of KLHL3 and WNK4 and increased WNK4 abundance and activity. Finally, acute oral administration of R-568 in mice led to the phosphorylation of NCC.

Conclusions Activation of CaSR can increase NCC activity via the WNK4-SPAK pathway. It is possible that activation of CaSR by Ca^{2+} in the apical membrane of the DCT increases NaCl reabsorption by NCC, with the consequent, well known decrease of Ca^{2+} reabsorption, further promoting hypercalciuria.

J Am Soc Nephrol 29: ●●-●●, 2018. doi: <https://doi.org/10.1681/ASN.2017111155>

The calcium-sensing receptor (CaSR) is a member of class C of the G protein-coupled receptors (GPCR) and its role is to constantly monitor Ca^{2+} in the extracellular environment.¹ In the kidney, CaSR is essential for sensing Ca^{2+} in both the urinary filtrate and interstitial fluid to adequately modulate calcium excretion. To achieve this, CaSR is expressed all along the nephron.²⁻⁵

Received November 3, 2017. Accepted April 10, 2018.

Published online ahead of print. Publication date available at www.jasn.org.

Correspondence: Dr. Gerardo Gamba, Molecular Physiology Unit, Vasco de Quiroga No. 15, Tlalpan 14080, Mexico City, Mexico. Email: gamba@biomedicas.unam.mx

Copyright © 2018 by the American Society of Nephrology

Ca²⁺ and salt (NaCl) handling in the kidney are particularly integrated in two segments of the nephron: the thick ascending limb of Henle's loop (TALH) and the distal convoluted tubule (DCT). In the TALH Ca²⁺ is reabsorbed by a paracellular route, a process which is largely dependent on NaCl reabsorption.^{6,7} Apical NaCl influx *via* the Na⁺-K⁺-2Cl⁻ cotransporter (NKCC2) is accompanied by potassium recycling to the lumen, through the apical renal outer medullary K⁺ channel (ROMK, KCNJ1), and by the basolateral extrusion of NaCl by the Na⁺/K⁺-ATPase and the chloride channel Kb (CLCNKB).⁸ The apical recycling of K⁺ generates a transepithelial voltage difference providing a driving force that drags paracellular reabsorption of cations, among them, Ca²⁺.⁹ Consequently, a positive correlation exists between NaCl and Ca²⁺ reabsorption in this nephron segment. For instance, patients with Bartter syndrome exhibit a salt-losing nephropathy and hypercalciuria.¹⁰ Likewise, clinicians have taken advantage of this positive correlation phenomenon by using loop diuretics to treat hypercalcemia.¹¹

In the TALH, CaSR is expressed in the basolateral membrane^{2,5} where it senses increased interstitial Ca²⁺ and promotes its urinary excretion by halting NKCC2 and ROMK activity.^{4,12–15} In this manner, the increase in Ca²⁺ excretion is due to decreased NaCl reabsorption in the TALH that must be reabsorbed beyond the macula densa. Indeed, gain-of-function mutations of CaSR have been reported to produce a Bartter-like syndrome.^{16,17}

The DCT reabsorbs approximately 5%–10% of the filtered NaCl and Ca²⁺.^{6,7,18} Its effect on BP and Ca²⁺ excretion is prominent because NaCl reabsorption beyond the macula densa is not regulated by tubuloglomerular feedback and no specific Ca²⁺ reabsorption pathways are present beyond this point.⁷ In the DCT, reabsorption of NaCl occurs through the thiazide-sensitive Na⁺-Cl⁻ cotransporter (NCC), whereas that of Ca²⁺ occurs through the apical transient receptor potential cation channel subfamily V (TRPV5).¹⁸ In this part of the nephron, NaCl and Ca²⁺ transport occurs in opposite directions; increased NaCl reabsorption is associated with decreased Ca²⁺ reabsorption.¹⁹ For instance, patients with Gitelman syndrome present a salt-losing nephropathy accompanied by hypocalciuria.²⁰ Clinicians have taken advantage of this inverse reabsorption by using thiazide diuretics to promote Ca²⁺ reabsorption in patients with urolithiasis.²¹ The exact mechanism for this inverse relationship is still unclear. CaSR is expressed both in the basolateral and apical membranes of DCT cells.^{4,5,22} However, the role CaSR might play in regulating NaCl reabsorption in this nephron segment is not known.

The activity of NCC is modulated by a kinase pathway consisting of the with-no-lysine-kinases (WNKs) acting upon the Ste20-related proline alanine-rich kinase (SPAK).²³ Active WNK kinases phosphorylate SPAK,²⁴ which subsequently phosphorylates and activates NCC.²⁵ Two proteins, Cullin 3 (CUL3) and Kelch-like 3 (KLHL3), are part of an E3-RING ubiquitin ligase complex that in turn regulates WNK kinases. KLHL3 specifically binds to WNKs marking them for

Significance Statement

Extracellular calcium modulates calciuria by acting on the basolateral membrane calcium-sensing receptor (CaSR) of the thick ascending limb of Henle's loop (TALH), reducing calcium reabsorption at the expense of apical NaCl absorption. CaSR is also expressed in the apical membrane of the distal convoluted tubule. Here, we show using *in vitro* and *in vivo* models that stimulation of the CaSR induces activation of the NaCl cotransporter (NCC), by a pathway that involves a PKC-induced activation of the KLHL3-WNK4-SPAK pathway that ultimately phosphorylates NCC, increasing its activity. This study proposes a mechanism through which NaCl reabsorption is upregulated beyond the TALH to recover NaCl, while calcium is excreted.

degradation.^{26,27} Disease-causing mutations in WNK4, KLHL3, or CUL3 result in impaired degradation of WNK kinases leading to increased NCC activity that results in a syndrome called pseudohypoaldosteronism type II.^{28,29}

Hormones that regulate NaCl reabsorption in the DCT do so by affecting the KLHL3-WNK-SPAK-NCC pathway. Angiotensin II (AngII) regulates NCC activity in a WNK4-dependent manner.^{30,31} This regulation occurs *via* protein kinase C (PKC), which directly phosphorylates WNK4 in two main sites, S64 and S1196, increasing WNK4 activity.³² PKC also promotes phosphorylation of KLHL3 in a serine residue (S433) that lays in the WNK4-binding domain preventing degradation of WNK4.³³ The effects of AngII in the DCT are mediated by the AT1 receptor, a pleiotropic GPCR whose intracellular signaling mechanisms are similar to that of CaSR.³⁴ Both receptors are preferentially coupled to Gαq and thus activate PLC transduction pathway, increasing intracellular Ca²⁺ and activating PKC.^{14,35} In this work, using a combination of *in vitro* and *in vivo* approaches, we sought to test the hypothesis that activation of CaSR modulates NCC activity through the KLHL3-WNK4-SPAK pathway.

METHODS

In Vitro Experiments

To test the effects of CaSR on NCC activity *in vitro* we assessed NCC activity in *Xenopus laevis* oocytes by measuring tracer ²²Na⁺ uptake when CaSR was stimulated with gadolinium chloride (GdCl₃), as described in the complete methods (Supplemental Material). In mammalian cells, the effect of CaSR activation was assessed in HEK-293 cells transiently transfected with CaSR wild type (WT), CaSR mutants, mWNK4-HA, and hSPAK-GFP-HA, with/without KLHL3 and mWNK4-5A-HA mutant. Cells were stimulated with the calcimimetic NPS R-568 (R-568) (Tocris Biosciences) and SPAK phosphorylation, and WNK4 abundance and phosphorylation were assessed by western blot analysis (complete methods, Supplemental Material).

In Vivo Experiments

To test the effect of activating CaSR on the WNK4-SPAK-NCC pathway *in vivo* we used C57BL/6 male mice, 12–16 weeks old,

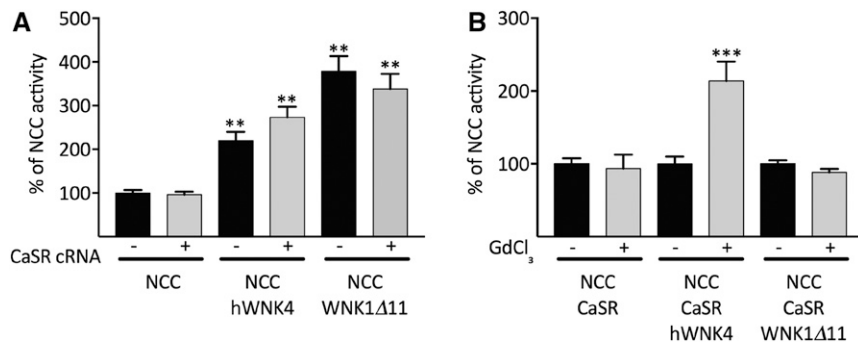


Figure 1. CaSR activates NCC in a WNK4-dependent manner in *X. laevis* oocytes. (A) The presence of non-activated CaSR has no effect on WNK4- or WNK1-induced activation of NCC. Functional expression assay shows the thiazide-sensitive Na⁺ uptake in groups of oocytes injected with NCC, NCC+hWNK4, and NCC+WNK1Δ11 cRNA (black bars), or together with CaSR cRNA (gray bars), as stated. Uptake in oocytes injected with NCC cRNA alone was arbitrarily set to 100% and the corresponding groups were normalized accordingly. ***P*<0.01 versus NCC. (B) Activation of CaSR with GdCl₃ increased the activity of NCC only in the presence of WNK4. Uptake was performed in control conditions (black bars) or after stimulation with GdCl₃ 80 μM for 15 minutes. Each group in control conditions (black bars) was arbitrarily set to 100% and the corresponding group with GdCl₃ was normalized accordingly (gray bars). ****P*<0.001 versus its own control. Supplemental Figure 1 shows the same experiments but with data expressed as picomoles per oocyte per hour. cRNA, complementary RNA.

exposed to vehicle or R-568 (3.0 μg/g of weight) by oral gavage,^{36,37} or a single furosemide (Sigma) ip dose of 15 mg/kg⁵⁸. Three hours later, kidneys were extracted and proteins were prepared for western blot (complete methods, Supplemental Information). We also used *ex vivo* kidney preparations such as the Langendorff system, as previously described.^{38,39} Kidneys were perfused with vehicle or the calcimimetic, R-568, at a rate of 0.60 μg/ml per minute for 30 minutes.

Statistical Analyses

Unpaired *t* test (two tailed) was used for comparison between two groups. One-way ANOVA with Dunnett's multiple comparison test was performed for comparison between multiple groups. *P*<0.05 was considered significant. Values are reported as mean ± SEM.

RESULTS

CaSR Activates NCC in a WNK4-Dependent Manner in *X. laevis* Oocytes

Xenopus oocytes were coinjected with WT CaSR and NCC cRNA, with or without WNK4 or WNK1 cRNA, and subjected to thiazide-sensitive tracer ²²Na⁺ transport assays as previously reported.⁴⁰ Coexpressing NCC with WNK4 or WNK1 promoted marked increases in basal NCC activity of two- and four-fold (*P*<0.01), respectively (Figure 1A), as previously described.^{41,42} However, this increase was not affected by the presence of CaSR (Figure 1A). Thus, unstimulated CaSR by

itself had no effect on NCC activity. We then tested the effect of CaSR stimulation in the absence or presence of WNK1 or WNK4 kinases. As Figure 1B shows, after exposing oocytes to the type 1 CaSR agonist, Gd³⁺, NCC uptake increased two-fold (*P*<0.001) only in oocytes coexpressing both CaSR and WNK4 (Figure 1B). We observed no effect of Gd³⁺ in oocytes injected with NCC+CaSR or NCC+WNK1Δ11+CaSR. These results suggest that, similar to the effects of AngII,^{30,31} WNK4 is required for the activation of CaSR to have an effect on NCC.

CaSR Phosphorylates SPAK in a WNK4-Dependent Manner in HEK-293 Cells

To test whether the CaSR-NCC effect could also be observed in a human cell model, we analyzed the effects of activating CaSR on SPAK phosphorylation (pSPAK), as a surrogate of SPAK-NCC activation by WNKs in HEK-293 cells.²⁴ Cells were transiently transfected with SPAK-GFP-HA, WNK4-HA, and CaSR and then treated with the calcimimetic

R-568.^{43–45} Results show that R-568 induced a time- and dose-dependent pSPAK increase in cells fasted in a serum-free medium (Supplemental Figure 2, A and B). We next evaluated the role of WNK4 on SPAK phosphorylation by CaSR. HEK-293 cells were transfected with SPAK-GFP-HA, CaSR, and/or WNK4-HA. In cells transfected with CaSR alone, pSPAK did not increase after treatment with the calcimimetic. Only in the presence of CaSR and WNK4 together did the calcimimetic promote a significant increase in pSPAK (*P*<0.05) (Figure 2, A and B). To further test that WNK4 is required for translating CaSR activation to SPAK phosphorylation, we assessed the effect of the highly specific WNK inhibitor, WNK463,⁴⁶ on CaSR-induced SPAK phosphorylation. As shown in Figure 2, C and D, the positive effect of R-568 on pSPAK was completely prevented by the presence of WNK463 inhibitor, confirming that in mammalian cells the effect of CaSR is WNK4-dependent. It is known that CaSR activation leads to activation by phosphorylation of the mitogen-activated protein kinase ERK1,2.⁴⁷ Therefore, we analyzed ERK1,2 phosphorylation to verify CaSR activation in these experiments. As shown in Figure 2A, a clear functional activation of CaSR was achieved with R-568 in CaSR-transfected cells, as demonstrated by increased ERK1,2 phosphorylation, but SPAK phosphorylation by CaSR only increases in the presence of WNK4.

An Activating Mutation of CaSR Increases WNK4 Abundance

Mutations in the *CASR* gene result in Mendelian disorders characterized by altered Ca²⁺ homeostasis.⁴⁸ Activating mutations of the receptor cause autosomal dominant

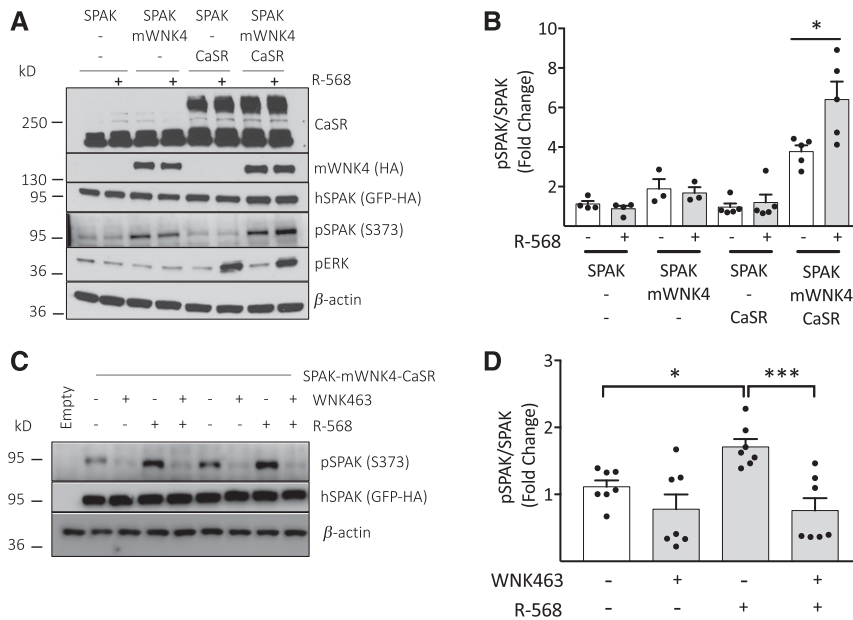


Figure 2. CaSR phosphorylates SPAK in a WNK4-dependent manner in HEK-293 cells. (A) Representative immunoblot of cells transfected with hSPAK-GFP-HA, mWnk4-HA, and hCaSR in different combinations, as stated. The day before the experiment, cells were serum-starved in the normal growth medium and left overnight. The next day, cells were stimulated with R-568 (200 nM) for 30 minutes. (B) Densitometric analysis of (A). SPAK transfection alone in control conditions was arbitrarily set to 1 and the corresponding groups were normalized accordingly. Bars represent mean \pm SEM of at least three independent experiments. * P <0.05 versus control. (C) Representative immunoblot showing two experiments of cells transfected with empty vector (Empty), hSPAK-GFP-HA, mWnk4-HA, and hCaSR and treated as in (A). The WNK inhibitor Wnk463 was added to the medium for 2 hours on the day of the experiment to a final concentration of 4 μ M. (D) Densitometric analysis of (C). SPAK in control conditions was arbitrarily set to 1 and the corresponding groups were normalized accordingly. Bars represent mean \pm SEM of at least three independent experiments. * P <0.05 versus control (no stimulation with R-568 and no Wnk463). *** P <0.01 versus R-568.

hypocalcemia, whereas inactivating mutations cause dominant familial hypocalciuric hypercalcemia or recessive neonatal severe hyperparathyroidism.^{15,49,50} We used two reported mutations, one activating, CaSR-E228K, and one inactivating, CaSR-R185Q, to assess their effects on the WNK4-SPAK-NCC pathway.^{51–53} We transfected HEK-293 cells with the WT CaSR or the mutants with WNK4 and observed that CaSR-E228K increased WNK4 abundance (Figure 3, A and C). We reasoned that if CaSR was acting by the same signal transduction pathway as the AT1 receptor, the presence of KLHL3 would enhance this effect on WNK4. As expected, cotransfection of KLHL3 induced a significant decrease of WNK4 abundance (Figure 3, A and B) that was prevented by CaSR-E228K, but not by CaSR-R185Q, establishing a significant KLHL3-dependent increase in WNK4 total protein levels only in the presence of the active mutant CaSR-E228K (Figure 3D). These results are consistent with the proposal that active CaSR may elicit the same signal transduction pathway as that of AT1

receptor, resulting in decreased degradation of WNK4, likely due to inhibition of KLHL3.³³

CaSR Promotes KLHL3 and WNK4 Phosphorylation by PKC

Two previous studies have demonstrated that AngII effects on WNK4 are due to a G α q-PKC signaling transduction pathway.^{32,33} To further determine whether CaSR activation elicited similar effects, we assessed if PKC-mediated phosphorylation of KLHL3 and WNK4 occurred after CaSR activation. KLHL3-Flag was immunoprecipitated from lysates of HEK-293 cells cotransfected with CaSR WT or CaSR mutants and subjected to immunoblotting with an mAb that recognizes PKC phosphorylation site, pRRXS.^{32,33,54} In the presence of the active mutant CaSR-E228K, KLHL3 pRRXS phosphorylation remarkably increased (P <0.01), whereas this was not observed with the inactive mutant CaSR-R185Q (Figure 4A). If PKC was responsible for these effects, we would expect that inhibition of PKC would prevent CaSR-induced pRRXS increase in KLHL3. As shown in Figure 4B, bisindolylmaleimide I, used at a concentration considered to be an inhibitor of PKC,⁵⁵ significantly reduced KLHL3 pRRXS phosphorylation.

We next evaluated if CaSR-induced activation of PKC also promoted WNK4 phosphorylation. To this end we analyzed whether activating CaSR in HEK-293 cells with R-568 promoted phosphorylation of a key WNK4 PKC phosphorylation site, serine residue S1196.³² After transfection of WNK4-HA, SPAK-GFP-HA, and CaSR, incubation with the calcimimetic resulted in a clear increase in S1196 phosphorylation P <0.05 (Figure 4C). Because the experiment was done with an acute CaSR activation of 30 minutes, no changes were seen in total WNK4 abundance; however, activation by phosphorylation of this site has been previously established³², partially explaining why we can see an effect before WNK4 abundance increases. Furthermore, we used a WNK4 mutant that has all five serines of the PKC consensus sites (RRXS sites) mutated to alanines (WNK4-5A), which prevents PKC-induced phosphorylation.³² The 5A mutation did not alter WNK4 abundance but remarkably reduced the CaSR effect on SPAK phosphorylation (Figure 4D), suggesting that phosphorylation of these sites, and the consequent activation of WNK4 by PKC, is necessary for the complete effect of CaSR on the WNK4-SPAK pathway.

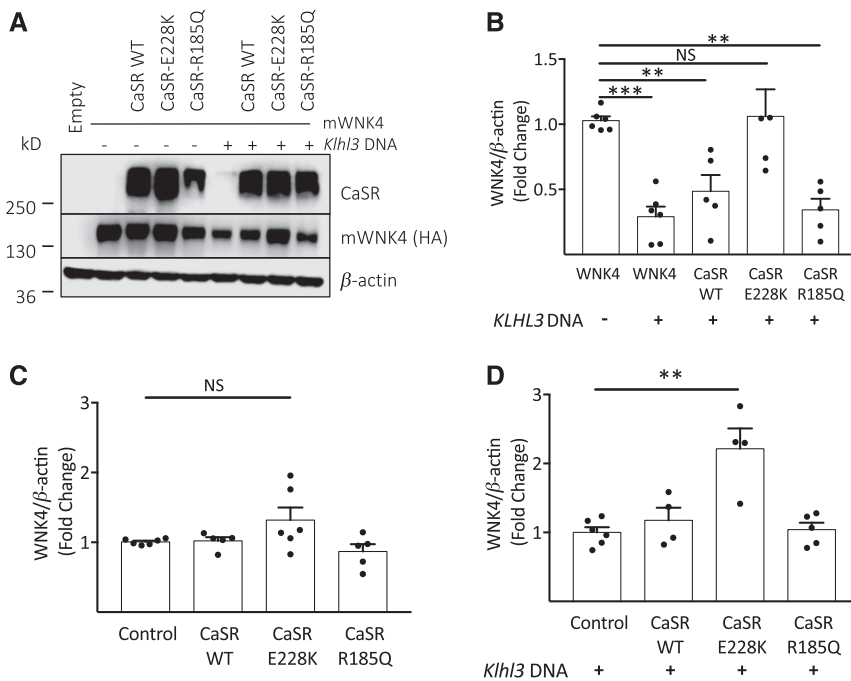


Figure 3. An activating mutation of CaSR increases WNK4 abundance. (A) Representative immunoblot of HEK-293 cells transfected with mWNK4-HA, hCaSR WT, and CaSR mutants with or without *KLHL3* DNA (40 ng). For this set of experiments, cells were maintained in normal growth medium after transfection. (B) Densitometric analysis of (A), where the expression of WNK4 alone (WNK4) was set to 1 and the rest of the groups were normalized accordingly. Bars represent mean \pm SEM of at least three independent experiments. *** $P < 0.001$ and ** $P < 0.05$ versus WNK4. (C and D) Densitometric analysis where WNK4 (Control) (C) without *KLHL3* cotransfection or (D) with *KLHL3* were set to 1 and the rest of the groups were normalized accordingly. Bars depict mean \pm SEM of at least three independent experiments. ** $P < 0.001$ versus WNK4+*KLHL3* (Control of [D]).

CaSR Promotes NCC Phosphorylation *In Vivo*

To define whether the CaSR effect on NCC occurred *in vivo*, we administered C57BL/6 male WT mice with an acute oral treatment of R-568 (3 μ g/g body wt)^{36,37} and, 3 hours later, mice were euthanized to investigate the effects on NCC phosphorylation by immunoblotting. Calcimimetics directly target the TALH CaSR function,¹² thereby decreasing NKCC2 activity (hence, phosphorylation) and promoting increased luminal Ca^{2+} and NaCl delivery to the distal nephron.¹² To test if this effect occurred in our *in vivo* model we assessed NKCC2 phosphorylation after the administration of the calcimimetic. Figure 5, A and B, shows that mice treated with the calcimimetic exhibited a significant decrease of NKCC2 phosphorylation $P < 0.05$.

Activation of NCC is associated with increased phosphorylation of three residues, T55, T60, and S73, in human NCC^{25,56}; therefore, phosphorylation of any of these residues has been extensively used as surrogate of NCC activation.⁵⁶ As expected, treatment with the calcimimetic induced a 1.5-fold increase in NCC phosphorylation ($P < 0.05$) (Figure 5, C and D), without promoting changes in total NCC (NCC/ β -actin 1.00 versus 0.96531, $P = NS$). Moreover, in concordance with

our *in vitro* data, activation of CaSR resulted in a significant increase in total WNK4 protein (1.7-fold increase, $P < 0.05$) (Figure 5, C and D). To evaluate if the increased WNK4 protein was activated by PKC, we analyzed the phosphorylation of residue S64, as previously reported.³² We found that most of the WNK4 protein in the calcimimetic-administered group was phosphorylated in S64 (Figure 5C). However, the pS64/WNK4 ratio between vehicle and R-568 groups remained similar (pS64/WNK4 1.00 versus 1.3050, $P = NS$). The absence of significance between the vehicle- and R-568-administered groups could be due to the concurrent increase in WNK4 protein. Additionally, immunofluorescence microscopy of kidneys extracted from WT mice showed increased membrane abundance after an acute dose of the calcimimetic (Figure 5E). Interestingly, the increase in NCC phosphorylation was not present in knock-in mice in which SPAK cannot be activated by WNKs (mutation T243A)⁵⁷ (pNCC/NCC 1.00 versus 0.99, $P = NS$) (Figure 5, F and G).

CaSR is expressed at both the apical and basolateral membranes of DCT cells. To investigate if increasing Ca^{2+} delivery to the DCT, and therefore, only activation of the apical CaSR is sufficient to elicit NCC phosphorylation, we administered C57BL/6 male WT mice with an acute treatment of furosemide (15 mg/kg over 3 hours), as previously described.⁵⁸ This specific dosage and

short time of treatment has been described to increase Ca^{2+} and NaCl delivery to the DCT, without promoting dehydration.⁵⁸ No changes in plasma potassium after 3 hours were observed (vehicle 4.3 ± 0.73 versus furosemide 4.3 ± 0.25 , $P = NS$). As expected, furosemide administration increased NCC phosphorylation four-fold ($P < 0.05$) while not increasing total NCC (NCC/ β -actin 1.00 versus 0.9456, $P = NS$) (Figure 6, A and B). In addition, furosemide administration was associated with increased WNK4 total protein and increased phosphorylation of WNK4 at S64 (Figure 6, C and D). Taken together, these results suggest that the acute inhibition of NKCC2 is associated with increased WNK4-NCC phosphorylation that was probably triggered by increased luminal Ca^{2+} .

CaSR Promotes NCC Phosphorylation *Ex Vivo*

The administration of the calcimimetic in the previous experiments could have promoted NCC activation either by a direct effect on the kidney, through the mechanism proposed in our hypothesis, or by a secondary effect due to activation/modification of any of the multiple hormonal systems that can activate NCC.⁵⁹ Acute calcimimetic administration is

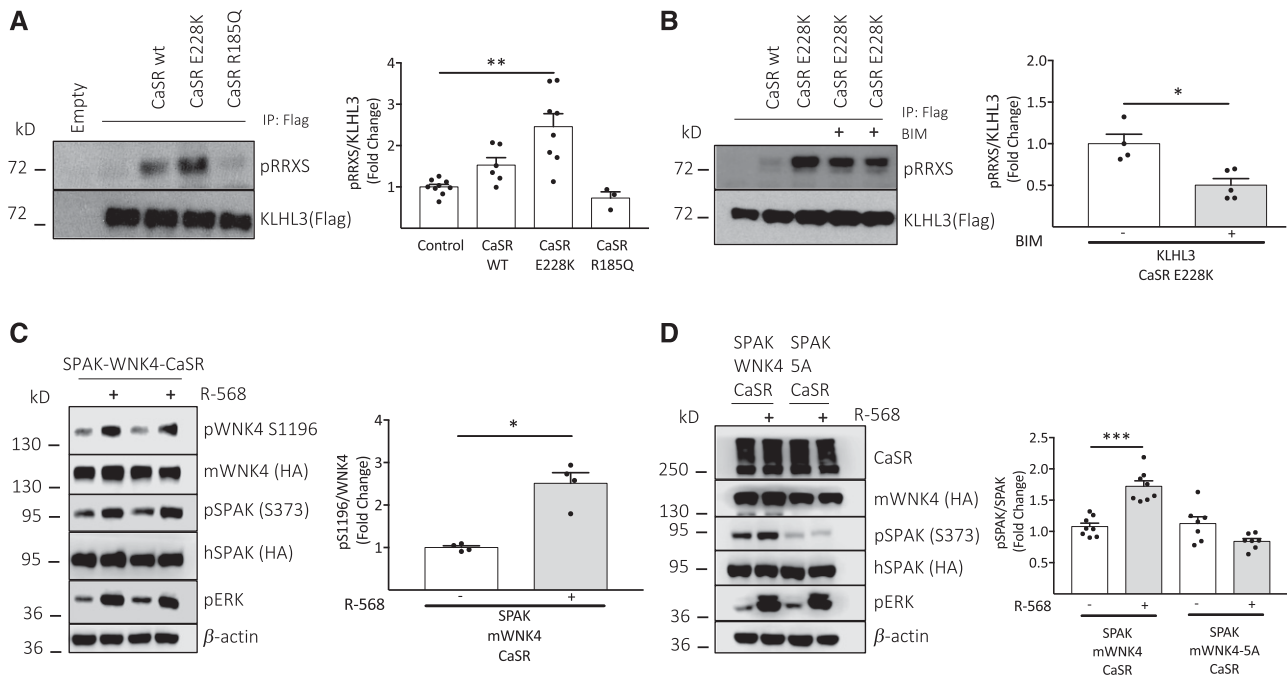


Figure 4. CaSR promotes KLHL3 and WNK4 phosphorylation by PKC. (A) Representative immunoblot of immunopurified KLHL3-Flag from HEK-293 cells transfected with KLHL3, WT hCaSR, and CaSR mutants. Cells were maintained in normal growth medium after transfection. Graph depicts densitometric analysis of at least three independent experiments. KLHL3 immunopurified from transfection alone (Control) was set as 1 and the rest of the groups were normalized accordingly. Bars represent mean ± SEM. ***P* < 0.01 versus Control. (B) Representative image of immunopurified KLHL3-Flag from HEK-293 cells transfected with KLHL3, CaSR-E228K, and treated with a PKC inhibitor (bisindolylmaleimide I [BIM]). BIM (4 μM) was added to the normal growth medium and left overnight. The next day, cells were lysed and immunoblotted. Graph shows densitometric analysis of at least three independent experiments. Bars represent mean ± SEM. **P* < 0.05 versus KLHL3 CaSR-E228K without BIM. (C) Representative immunoblot of cells transfected with SPAK-GFP-HA, mWNK4-HA, and WT hCaSR, serum-starved and stimulated with R-568 (200 nM) for 30 minutes. Lysates were blotted with the indicated antibodies. The graph depicts densitometric analysis. **P* < 0.05 versus Control (no stimulation with R-568). (D) Cells were transfected with SPAK-GFP-HA, mWNK4-HA, and WT hCaSR or the mutant mWNK4-5A, which has all PKC-phosphorylation sites mutated to alanines, and then stimulated as in (C). The graph represents densitometric analysis of at least three independent experiments for the mWNK45A mutant. Bars are mean ± SEM. ****P* < 0.001 versus its own control (data for SPAK-mWNK4-CaSR are shared with Figure 2D). IP, immunoprecipitation.

associated with decreased activity of the renin-AngII system,^{60,61} making this possibility unlikely. Nevertheless, we studied NCC phosphorylation using an *ex vivo* system where intervention of the central nervous system and other extra renal hormonal systems are not expected to be present. Kidneys of WT male Wistar rats were perfused with physiologic saline with vehicle or with R-568 (0.60 μg/ml per minute). The concentration of R-568 used in these experiments did not change the perfusion pressure, arguing against the presence of an intrarenal AngII effect. As shown in Figure 7, A and B, NCC and SPAK phosphorylation levels were significantly higher in kidneys perfused with the calcimimetic.

DISCUSSION

In this study, we show that CaSR activation is associated with increased NCC activity *in vitro* and *in vivo*. This increase

involves PKC activation of the WNK4-SPAK pathway, supporting the hypothesis that CaSR modulates NCC activity. As previously shown for AngII, modulation of NCC *via* WNK4-SPAK occurs by two different pathways—phosphorylation and concurrent activation of WNK4, and prevention of WNK4 degradation by KLHL3 phosphorylation. CaSR-induced activation of NCC has an implication in the physiologic response to increased extracellular Ca²⁺, which requires the kidney to promote its excretion at the apparent expense of reducing NaCl reabsorption in the TALH, thus increasing the delivery of NaCl and Ca²⁺ to the distal nephron.¹⁴ Integration of NaCl and Ca²⁺ homeostasis by CaSR in the DCT could prevent unwanted NaCl loss, while further permitting Ca²⁺ excretion. In this regard, CaSR expression in the apical membrane of the DCT has been clearly established by many groups and recent studies colocalize CaSR with NCC in human and mouse kidneys.^{5,22} Taking together the observations in this study, we propose the existence of a mechanism in the DCT, where apical CaSR responds to increased intratubular Ca²⁺ concentration evoking a

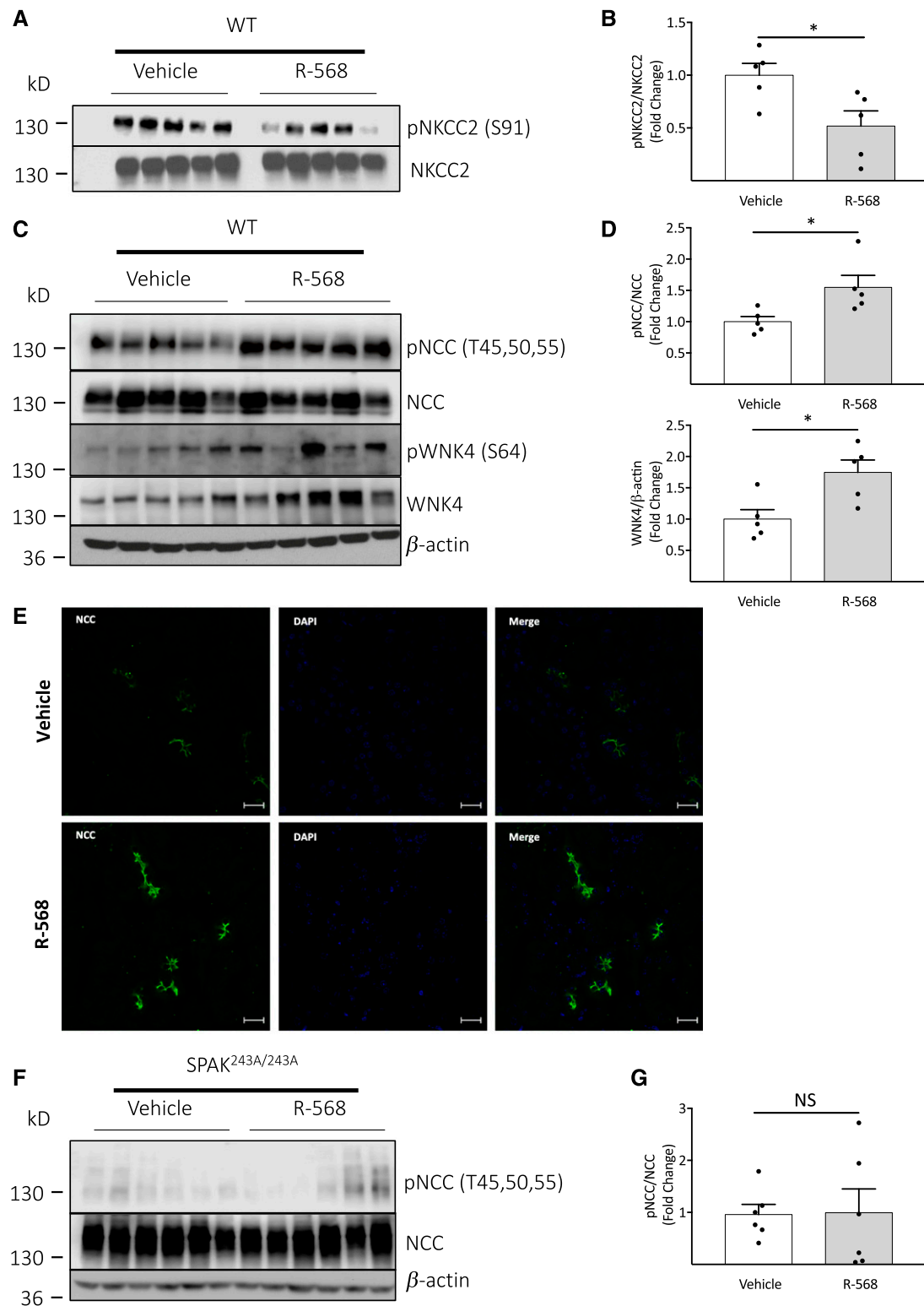


Figure 5. CaSR promotes NCC phosphorylation *in vivo*. Animals were administered with vehicle or with R-568, 3 μ g/g body wt through oral gavage. Three hours later, kidneys were harvested and processed for immunoblot. Each column of the representative immunoblot represents the kidneys from one animal. (A and C) Representative immunoblot of the effect of oral R-568 administration on NCC and NKCC2 phosphorylation, WNK4 abundance, and phosphorylation in S64 in WT mice (upper image). pS64/WNK4 1.00 versus 1.3050, P =NS. (E) Immunofluorescent staining of kidney sections from WT mice treated with Vehicle or R-568. Scale bars, 20 μ m. (F) Representative immunoblot of the effect of R-568 on NCC phosphorylation in SPAK knock-in mice (SPAK^{243A/243A}). (B, D, and G) Densitometric analysis of representative immunoblots. Bars represent mean \pm SEM. * P <0.05 versus Vehicle.

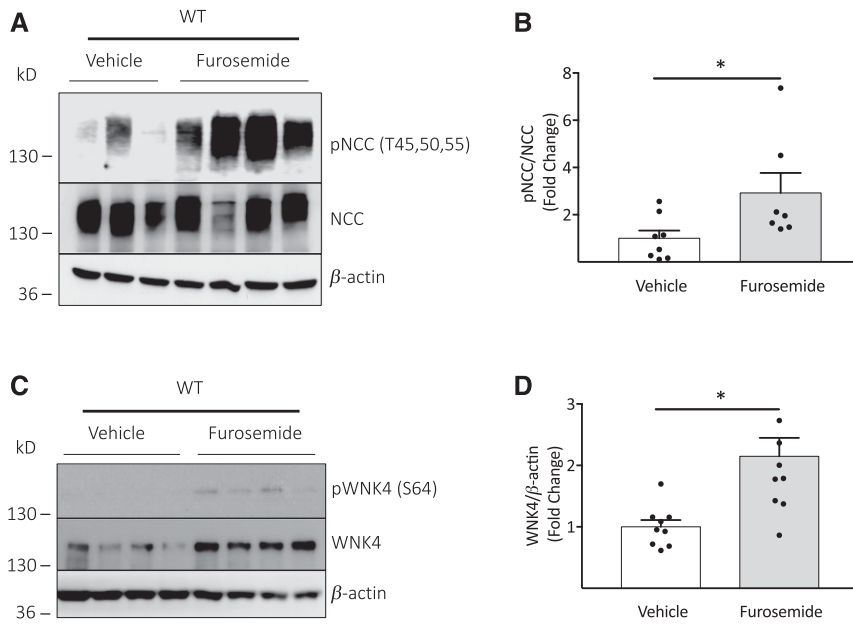


Figure 6. An acute furosemide treatment promotes NCC phosphorylation *in vivo*. Animals were administered with vehicle or with furosemide, 15 mg/kg body wt through ip injection. Three hours later, kidneys were harvested and processed for immunoblot. Each column of the representative immunoblot represents the kidney from one animal. (A and C) Representative immunoblots of the effect of the acute administration of furosemide on NCC phosphorylation, WNK4 abundance, and phosphorylation in S64 in WT mice. pS64/WNK4 1.00 versus 1.53, $P=NS$. (B and D) Densitometric analysis of $n=8$ controls and $n=7$ furosemide-administered mice. Bars represent mean \pm SEM. * $P<0.05$ versus Vehicle (B was analyzed with Mann-Whitney U test).

CaSR- $G\alpha_q$ -PKC-WNK4-SPAK signaling transduction pathway that promotes NCC activation to recover the NaCl that was not reabsorbed in the TALH, due to NKCC2 and ROMK inhibition (Figure 8). Because it is known that increased NaCl reabsorption in the DCT is associated with decreased Ca^{2+} absorption,¹⁴ this mechanism not only claims the NaCl, but also further promotes

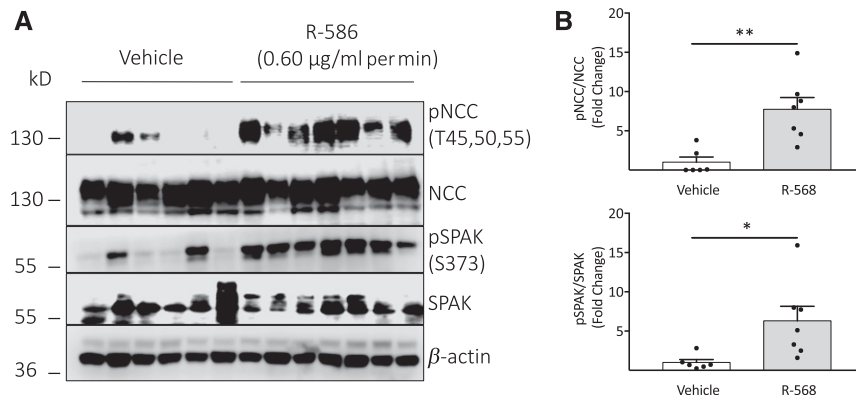


Figure 7. CaSR promotes NCC phosphorylation *ex vivo*. (A) Representative immunoblot of protein extracts from *ex vivo* perfused rat kidneys. The kidneys were perfused with physiologic saline with vehicle or with R-568 at a rate of 0.60 $\mu\text{g/ml}$ per minute. Each column of the immunoblot represents one kidney. (B) Bars represent mean \pm SEM of the densitometric analysis of (A). $n=6$ vehicles and $n=7$ R-568. ** $P<0.01$ versus vehicle. * $P<0.05$ versus vehicle.

hypercalciuria. The controversy of whether the thiazide effect on Ca^{2+} excretion occurs directly in the DCT or elsewhere^{62,63} does not contradict our findings.

We are aware of the possibility that the basolateral CaSR in DCT may also elicit a response to activate NCC, and our results do not rule out this possibility. In this scenario, increased extracellular Ca^{2+} could simultaneously reduce NKCC2 activity in the TALH but increase NCC activity in the DCT, by activating the basolateral receptor in both segments. However, because of the presence of CaSR and NCC in the apical membrane, is it likely that luminal Ca^{2+} is also involved in this response. NCC activation elicited by a single acute dose of furosemide, known to promote increased Ca^{2+} delivery to DCT, supports the fact that activation of apical CaSR is enough to provoke the proposed response. It is also worth mentioning that patients with autosomal dominant hypocalcemia (due to CaSR activating mutations) may exhibit a Bartter-like syndrome (also known as Bartter syndrome type V) that has been described as mild in most patients.^{16,17} Perhaps CaSR activation in the DCT helps to reduce natriuresis, as compared with other types of Bartter syndrome.

A similar mechanism prompted by CaSR in the nephron has been described before. It has been clinically recognized for many years that hypercalcemia induces polyuria.^{64,65} Increasing urinary Ca^{2+} to the distal nephron could also promote precipitation of Ca^{2+} and phosphate salts. Sands *et al.*⁶⁶ elegantly demonstrated that apical CaSR in the collecting duct responds to increased luminal Ca^{2+} to blunt vasopressin-induced insertion of AQP-2 water channels into the apical membrane. The latter would prevent water reabsorption in the collecting duct, allowing the urine to be diluted and thus preventing Ca^{2+} precipitation and formation of renal stones. The authors also demonstrated that the signaling pathway and molecular mechanisms initiated by CaSR was by $G\alpha_q$ and PKC proteins.⁶⁶ More recently, other groups have further established the association of active apical CaSR with decreased AQP2 abundance.^{67–69}

The observation that CaSR activation modulates NCC activity *via* WNK4-SPAK pathway may have further implications beyond the physiologic mechanism of how NaCl is recovered in DCT when TALH NaCl reabsorption is decreased by Ca^{2+} .

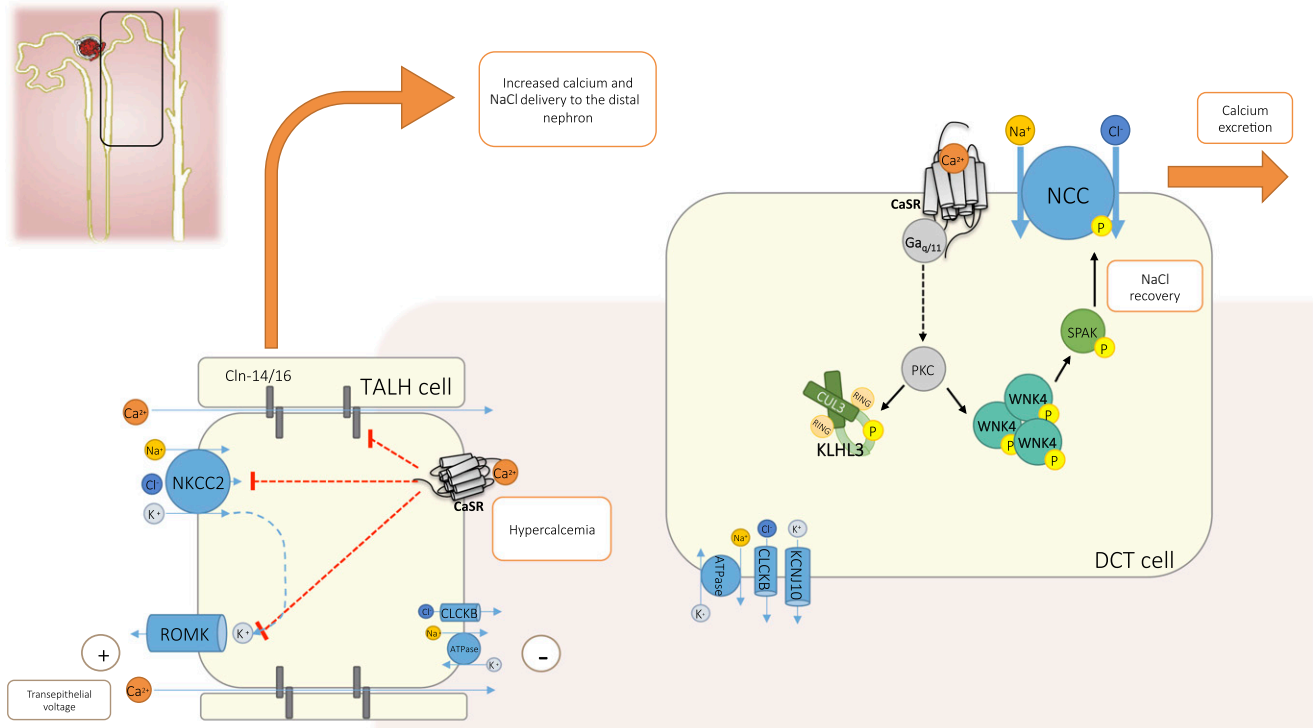


Figure 8. Proposed model for CaSR activation of NCC through a PKC-WNK4-SPAK pathway. Increased extracellular Ca^{2+} leads to CaSR-mediated inhibition of NKCC2 and ROMK, halting the transepithelial voltage difference that drags paracellular reabsorption of Ca^{2+} ions. Reduction in Ca^{2+} reabsorption in the TALH causes increased NaCl and Ca^{2+} delivery to the distal nephron. In the DCT, integration of calcium and NaCl homeostasis by the CaSR must respond to prevent unwanted NaCl loss. We propose the existence of a mechanism in the DCT where apically expressed CaSR responds to increased intratubular Ca^{2+} concentration, evoking a CaSR- $\text{G}\alpha_{q/11}$ -PKC-WNK4 signaling transduction pathway that promotes NCC activation. Cln-14/16, Claudin 14 and 16 heterodimers.

First, it is known that arterial hypertension is highly prevalent in primary hyperparathyroidism, ranging from 40% to 65%, which is much higher than the expected 25%–30% of hypertension in the general adult population.⁷⁰ Given our observations, a possible mechanism could be that increased Ca^{2+} in the tubular fluid, as occurs in hypercalcemia, stimulates the activity of NCC promoting NaCl reabsorption and, hence, the development of hypertension. Second, it has been recently demonstrated that glucose and other sugars act as type II calcimimetics, enhancing CaSR affinity for Ca^{2+} .⁷¹ This could be relevant in the apical membrane of the DCT because all of the filtered glucose is reabsorbed in the proximal tubule and therefore these cells are not continuously exposed to glucose. In patients with diabetes, the excess filtered glucose often escapes reabsorption in the proximal tubule, allowing a significant amount of glucose in the tubular fluid that reaches the DCT. It is possible that the presence of glucose acting as a calcimimetic increases apical CaSR sensibility, enhancing NCC activity of thus NaCl reabsorption, which could help to explain the higher prevalence of hypertension in patients with diabetes.⁷² These possibilities are speculative but can certainly be explored in future studies.

ACKNOWLEDGMENTS

We thank Dario Alessi for the kind gift of WNK463 inhibitor. We thank Dr. Norma O. Uribe-Uribe and Dr. Jazmín de Anda-González for the help with the kidney slicing for immunofluorescence analysis.

This work was supported by the Consejo Nacional de Ciencia y Tecnología (CONACyT) Grant No. 23 from the “Fronteras de la ciencia” program and 188712 to G.G., No. 257726 to M.C.-B. and No. 290056 to L.R.-V., and the National Institute of Diabetes and Digestive and Kidney Diseases RO1 grant No. DK051496-15 to D.H.E. and G.G. S.B.-V. was supported by a scholarship from CONACyT-Mexico and is a graduate student in the Doctorado en Ciencias Bioquímicas program of the Universidad Nacional Autónoma de México.

S.B.-V., L.R.-V., M.C.-B., D.H.E., D.R., N.A.B., and G.G. designed the study, planned experiments, interpreted data, and edited the manuscript. S.B.-V., L.R.-V., J.B.-C., R.B., L.G.C.-P., N.V., A.R.M.-d.-O., C.P., and L.G.-M. performed experiments and reviewed the manuscript. S.B.-V. and G.G. wrote the paper.

DISCLOSURES

None.

REFERENCES

- Brown EM, Gamba G, Riccardi D, Lombardi M, Butters R, Kifor O, et al: Cloning and characterization of an extracellular Ca²⁺-sensing receptor from bovine parathyroid. *Nature* 366: 575–580, 1993
- Riccardi D, Hall AE, Chattopadhyay N, Xu JZ, Brown EM, Hebert SC: Localization of the extracellular Ca²⁺/polyvalent cation-sensing protein in rat kidney. *Am J Physiol* 274: F611–F622, 1998
- Riccardi D, Lee WS, Lee K, Segre GV, Brown EM, Hebert SC: Localization of the extracellular Ca²⁺-sensing receptor and PTH/PTHrP receptor in rat kidney. *Am J Physiol* 271: F951–F956, 1996
- Riccardi D, Valenti G: Localization and function of the renal calcium-sensing receptor. *Nat Rev Nephrol* 12: 414–425, 2016
- Graca JAZ, Schepelmann M, Brennan SC, Reens J, Chang W, Yan P, et al: Comparative expression of the extracellular calcium-sensing receptor in the mouse, rat, and human kidney. *Am J Physiol Renal Physiol* 310: F518–F533, 2016
- Palmer LG, Schnermann J: Integrated control of Na transport along the nephron. *Clin J Am Soc Nephrol* 10: 676–687, 2015
- Blaine J, Chonchol M, Levi M: Renal control of calcium, phosphate, and magnesium homeostasis. *Clin J Am Soc Nephrol* 10: 1257–1272, 2015
- Gamba G, Wang W, Schild L: Sodium chloride transport in the loop of Henle, distal convoluted tubule and collecting duct. In: *Seldin and Giebisch's The Kidney: Physiology and Pathophysiology*, edited by Alpern RJ, Caplan MJ, Moe OW, 5th Ed., London, Elsevier, 2013, pp 1143–1180
- Mandon B, Siga E, Roinel N, de Rouffignac C: Ca²⁺, Mg²⁺ and K⁺ transport in the cortical and medullary thick ascending limb of the rat nephron: influence of transepithelial voltage. *Pflugers Arch* 424: 558–560, 1993
- Simon DB, Karet FE, Hamdan JM, DiPietro A, Sanjad SA, Lifton RP: Bartter's syndrome, hypokalaemic alkalosis with hypercalciuria, is caused by mutations in the Na-K-2Cl cotransporter NKCC2. *Nat Genet* 13: 183–188, 1996
- Suki WN, Yium JJ, Von Minden M, Saller-Hebert C, Eknayan G, Martinez-Maldonado M: Acute treatment of hypercalcemia with furosemide. *N Engl J Med* 283: 836–840, 1970
- Loupy A, Ramakrishnan SK, Wootla B, Chambrey R, de la Faille R, Bourgeois S, et al: PTH-independent regulation of blood calcium concentration by the calcium-sensing receptor. *J Clin Invest* 122: 3355–3367, 2012
- Toka HR, Al-Romaih K, Koshy JM, DiBartolo S 3rd, Kos CH, Quinn SJ, et al: Deficiency of the calcium-sensing receptor in the kidney causes parathyroid hormone-independent hypocalciuria. *J Am Soc Nephrol* 23: 1879–1890, 2012
- Gamba G, Friedman PA: Thick ascending limb: the Na(+):K(+):2Cl(-) co-transporter, NKCC2, and the calcium-sensing receptor, CaSR. *Pflugers Arch* 458: 61–76, 2009
- Toka HR, Pollak MR, Houillier P: Calcium sensing in the renal tubule. *Physiology (Bethesda)* 30: 317–326, 2015
- Vargas-Poussou R, Huang C, Hulin P, Houillier P, Jeunemaître X, Paillard M, et al: Functional characterization of a calcium-sensing receptor mutation in severe autosomal dominant hypocalcemia with a Bartter-like syndrome. *J Am Soc Nephrol* 13: 2259–2266, 2002
- Watanabe S, Fukumoto S, Chang H, Takeuchi Y, Hasegawa Y, Okazaki R, et al: Association between activating mutations of calcium-sensing receptor and Bartter's syndrome. *Lancet* 360: 692–694, 2002
- Subramanya AR, Ellison DH: Distal convoluted tubule. *Clin J Am Soc Nephrol* 9: 2147–2163, 2014
- Friedman PA: Codependence of renal calcium and sodium transport. *Annu Rev Physiol* 60: 179–197, 1998
- Sabath E, Meade P, Berkman J, de los Heros P, Moreno E, Bobadilla NA, et al: Pathophysiology of functional mutations of the thiazide-sensitive Na-Cl cotransporter in Gitelman disease. *Am J Physiol Renal Physiol* 287: F195–F203, 2004
- Reilly RF, Peixoto AJ, Desir GV: The evidence-based use of thiazide diuretics in hypertension and nephrolithiasis. *Clin J Am Soc Nephrol* 5: 1893–1903, 2010
- Topala CN, Schoeber JPH, Searchfield LE, Riccardi D, Hoenderop JGJ, Bindels RJM: Activation of the Ca²⁺-sensing receptor stimulates the activity of the epithelial Ca²⁺ channel TRPV5. *Cell Calcium* 45: 331–339, 2009
- Hadchouel J, Ellison DH, Gamba G: Regulation of renal electrolyte transport by WNK and SPAK-OSR1 kinases. *Annu Rev Physiol* 78: 367–389, 2016
- Richardson C, Rafiqi FH, Karlsson HKR, Moleleki N, Vandewalle A, Campbell DG, et al: Activation of the thiazide-sensitive Na⁺-Cl⁻ cotransporter by the WNK-regulated kinases SPAK and OSR1. *J Cell Sci* 121: 675–684, 2008
- Pacheco-Alvarez D, Cristóbal PS, Meade P, Moreno E, Vazquez N, Muñoz E, et al: The Na⁺:Cl⁻ cotransporter is activated and phosphorylated at the amino-terminal domain upon intracellular chloride depletion. *J Biol Chem* 281: 28755–28763, 2006
- Shibata S, Zhang J, Puthumana J, Stone KL, Lifton RP: Kelch-like 3 and Cullin 3 regulate electrolyte homeostasis via ubiquitination and degradation of WNK4. *Proc Natl Acad Sci U S A* 110: 7838–7843, 2013
- Ohta A, Rai T, Yui N, Chiga M, Yang S-S, Lin S-H, et al: Targeted disruption of the Wnk4 gene decreases phosphorylation of Na-Cl cotransporter, increases Na excretion and lowers blood pressure. *Hum Mol Genet* 18: 3978–3986, 2009
- Wilson FH, Disse-Nicodème S, Choate KA, Ishikawa K, Nelson-Williams C, Desitter I, et al: Human hypertension caused by mutations in WNK kinases. *Science* 293: 1107–1112, 2001
- Boyden LM, Choi M, Choate KA, Nelson-Williams CJ, Farhi A, Toka HR, et al: Mutations in kelch-like 3 and cullin 3 cause hypertension and electrolyte abnormalities. *Nature* 482: 98–102, 2012
- San-Cristobal P, Pacheco-Alvarez D, Richardson C, Ring AM, Vazquez N, Rafiqi FH, et al: Angiotensin II signaling increases activity of the renal Na-Cl cotransporter through a WNK4-SPAK-dependent pathway. *Proc Natl Acad Sci U S A* 106: 4384–4389, 2009
- Castañeda-Bueno M, Cervantes-Pérez LG, Vázquez N, Uribe N, Kantesaria S, Morla L, et al: Activation of the renal Na⁺:Cl⁻ cotransporter by angiotensin II is a WNK4-dependent process. *Proc Natl Acad Sci U S A* 109: 7929–7934, 2012
- Castañeda-Bueno M, Arroyo JP, Zhang J, Puthumana J, Yarborough O 3rd, Shibata S, et al: Phosphorylation by PKC and PKA regulate the kinase activity and downstream signaling of WNK4. *Proc Natl Acad Sci U S A* 114: E879–E886, 2017
- Shibata S, Arroyo JP, Castañeda-Bueno M, Puthumana J, Zhang J, Uchida S, et al: Angiotensin II signaling via protein kinase C phosphorylates Kelch-like 3, preventing WNK4 degradation. *Proc Natl Acad Sci U S A* 111: 15556–15561, 2014
- AbdAlla S, Lother H, Quittner U: AT1-receptor heterodimers show enhanced G-protein activation and altered receptor sequestration. *Nature* 407: 94–98, 2000
- Ward DT: Calcium receptor-mediated intracellular signalling. *Cell Calcium* 35: 217–228, 2004
- Fox J, Lowe SH, Petty BA, Nemeth EF: NPS R-568: a type II calcimimetic compound that acts on parathyroid cell calcium receptor of rats to reduce plasma levels of parathyroid hormone and calcium. *J Pharmacol Exp Ther* 290: 473–479, 1999
- Fenton RA, Murray F, Dominguez Rieg JA, Tang T, Levi M, Rieg T: Renal phosphate wasting in the absence of adenylyl cyclase 6. *J Am Soc Nephrol* 25: 2822–2834, 2014
- Chávez-Canales M, Arroyo JP, Ko B, Vázquez N, Bautista R, Castañeda-Bueno M, et al: Insulin increases the functional activity of the renal NaCl cotransporter. *J Hypertens* 31: 303–311, 2013
- Rojas-Vega L, Reyes-Castro LA, Ramírez V, Bautista-Pérez R, Rafael C, Castañeda-Bueno M, et al: Ovarian hormones and prolactin increase renal NaCl cotransporter phosphorylation. *Am J Physiol Renal Physiol* 308: F799–F808, 2015

40. Monroy A, Plata C, Hebert SC, Gamba G: Characterization of the thiazide-sensitive Na(+)-Cl(-) cotransporter: a new model for ions and diuretics interaction. *Am J Physiol Renal Physiol* 279: F161–F169, 2000
41. Bazúa-Valenti S, Chávez-Canales M, Rojas-Vega L, González-Rodríguez X, Vázquez N, Rodríguez-Gama A, et al: The effect of WNK4 on the Na+-Cl- cotransporter is modulated by intracellular chloride. *J Am Soc Nephrol* 26: 1781–1786, 2015
42. Chávez-Canales M, Zhang C, Soukaseum C, Moreno E, Pacheco-Alvarez D, Vidal-Petiot E, et al: WNK-SPAK-NCC cascade revisited: WNK1 stimulates the activity of the Na-Cl cotransporter via SPAK, an effect antagonized by WNK4. *Hypertension* 64: 1047–1053, 2014
43. Ward DT, Riccardi D: New concepts in calcium-sensing receptor pharmacology and signalling. *Br J Pharmacol* 165: 35–48, 2012
44. Nemeth EF, Steffey ME, Hammerland LG, Hung BC, Van Wagenen BC, DelMar EG, et al: Calcimimetics with potent and selective activity on the parathyroid calcium receptor. *Proc Natl Acad Sci U S A* 95: 4040–4045, 1998
45. Nemeth EF, Heaton WH, Miller M, Fox J, Balandrin MF, Van Wagenen BC, et al: Pharmacodynamics of the type II calcimimetic compound cinacalcet HCl. *J Pharmacol Exp Ther* 308: 627–635, 2004
46. Yamada K, Park H-M, Rigel DF, DiPetrillo K, Whalen EJ, Anisowicz A, et al: Small-molecule WNK inhibition regulates cardiovascular and renal function. *Nat Chem Biol* 12: 896–898, 2016
47. Holstein DM, Berg KA, Leeb-Lundberg LMF, Olson MS, Saunders C: Calcium-sensing receptor-mediated ERK1/2 activation requires Galphai2 coupling and dynamin-independent receptor internalization. *J Biol Chem* 279: 10060–10069, 2004
48. Toka HR, Pollak MR: The role of the calcium-sensing receptor in disorders of abnormal calcium handling and cardiovascular disease. *Curr Opin Nephrol Hypertens* 23: 494–501, 2014
49. Brown EM, Pollak M, Hebert SC: The extracellular calcium-sensing receptor: its role in health and disease. *Annu Rev Med* 49: 15–29, 1998
50. Bai M, Quinn S, Trivedi S, Kifor O, Pearce SH, Pollak MR, et al: Expression and characterization of inactivating and activating mutations in the human Ca²⁺-sensing receptor. *J Biol Chem* 271: 19537–19545, 1996
51. Zhang C, Miller CL, Gorkhali R, Zou J, Huang K, Brown EM, et al: Molecular basis of the extracellular ligands mediated signaling by the calcium sensing receptor. *Front Physiol* 7: 441, 2016
52. Mayr B, Glaudo M, Schöfl C: Activating calcium-sensing receptor mutations: Prospects for future treatment with calcilytics. *Trends Endocrinol Metab* 27: 643–652, 2016
53. Mayr B, Schnabel D, Dörr H-G, Schöfl C: GENETICS IN ENDOCRINOLOGY: Gain and loss of function mutations of the calcium-sensing receptor and associated proteins: current treatment concepts. *Eur J Endocrinol* 174: R189–R208, 2016
54. Pearson RB, Kemp BE: Protein kinase phosphorylation site sequences and consensus specificity motifs: tabulations. *Methods Enzymol* 200: 62–81, 1991
55. Davies SP, Reddy H, Caivano M, Cohen P: Specificity and mechanism of action of some commonly used protein kinase inhibitors. *Biochem J* 351: 95–105, 2000
56. Gamba G: Regulation of the renal Na+-Cl- cotransporter by phosphorylation and ubiquitylation. *Am J Physiol Renal Physiol* 303: F1573–F1583, 2012
57. Rafiqi FH, Zuber AM, Glover M, Richardson C, Fleming S, Jovanović S, et al: Role of the WNK-activated SPAK kinase in regulating blood pressure. *EMBO Mol Med* 2: 63–75, 2010
58. Lee C-T, Chen H-C, Lai L-W, Yong K-C, Lien Y-HH: Effects of furosemide on renal calcium handling. *Am J Physiol Renal Physiol* 293: F1231–F1237, 2007
59. Rojas-Vega L, Gamba G: Mini-review: regulation of the renal NaCl cotransporter by hormones. *Am J Physiol Renal Physiol* 310: F10–F14, 2016
60. Atchison DK, Ortiz-Capisano MC, Beierwaltes WH: Acute activation of the calcium-sensing receptor inhibits plasma renin activity in vivo. *Am J Physiol Regul Integr Comp Physiol* 299: R1020–R1026, 2010
61. Atchison DK, Beierwaltes WH: The influence of extracellular and intracellular calcium on the secretion of renin. *Pflugers Arch* 465: 59–69, 2013
62. Gesek FA, Friedman PA, van der Kemp AWCM, Loffing J, Hoenderop JGJ, Bindels RJM: Mechanism of calcium transport stimulated by chlorothiazide in mouse distal convoluted tubule cells. *J Clin Invest* 90: 429–438, 1992
63. Choi KH, Shin CH, Yang SW, Cheong HI: Autosomal dominant hypocalcemia with Bartter syndrome due to a novel activating mutation of calcium sensing receptor, Y829C. *Korean J Pediatr* 58: 148–153, 2015
64. Levi M, Peterson L, Berl T: Mechanism of concentrating defect in hypercalcemia. Role of polydipsia and prostaglandins. *Kidney Int* 23: 489–497, 1983
65. Gill JR Jr, Bartter FC: On the impairment of renal concentrating ability in prolonged hypercalcemia and hypercalciuria in man. *J Clin Invest* 40: 716–722, 1961
66. Sands JM, Naruse M, Baum M, Jo I, Hebert SC, Brown EM, et al: Apical extracellular calcium/polyvalent cation-sensing receptor regulates vasopressin-elicited water permeability in rat kidney inner medullary collecting duct. *J Clin Invest* 99: 1399–1405, 1997
67. Bustamante M, Hasler U, Leroy V, de Seigneux S, Dimitrov M, Mordasini D, et al: Calcium-sensing receptor attenuates AVP-induced aquaporin-2 expression via a calmodulin-dependent mechanism. *J Am Soc Nephrol* 19: 109–116, 2008
68. Renkema KY, Velic A, Dijkman HB, Verkaar S, van der Kemp AW, Nowik M, et al: The calcium-sensing receptor promotes urinary acidification to prevent nephrolithiasis. *J Am Soc Nephrol* 20: 1705–1713, 2009
69. Earm JH, Christensen BM, Frøkiaer J, Marples D, Han JS, Knepper MA, et al: Decreased aquaporin-2 expression and apical plasma membrane delivery in kidney collecting ducts of polyuric hypercalcemic rats. *J Am Soc Nephrol* 9: 2181–2193, 1998
70. Pepe J, Cipriani C, Sonato C, Raimo O, Biamonte F, Minisola S: Cardiovascular manifestations of primary hyperparathyroidism: a narrative review. *Eur J Endocrinol* 177: R297–R308, 2017
71. Medina J, Nakagawa Y, Nagasawa M, Fernandez A, Sakaguchi K, Kitaguchi T, et al: Positive allosteric modulation of the calcium-sensing receptor by physiological concentrations of glucose. *J Biol Chem* 291: 23126–23135, 2016
72. Colosia AD, Palencia R, Khan S: Prevalence of hypertension and obesity in patients with type 2 diabetes mellitus in observational studies: a systematic literature review. *Diabetes Metab Syndr Obes* 6: 327–338, 2013

This article contains supplemental material online at <http://jasn.asnjournals.org/lookup/suppl/doi:10.1681/ASN.2017111155/-/DCSupplemental>.



OPEN

Vegfa promoter gene hypermethylation at HIF1 α binding site is an early contributor to CKD progression after renal ischemia

Andrea Sánchez-Navarro^{1,2}, Rosalba Pérez-Villalva^{1,2}, Adrián Rafael Murillo-de-Ozores^{1,2}, Miguel Ángel Martínez-Rojas^{1,2}, Jesús Rafael Rodríguez-Aguilera³, Norma González², María Castañeda-Bueno², Gerardo Gamba^{1,2}, Félix Recillas-Targa³ & Norma A. Bobadilla^{1,2}✉

Chronic hypoxia is a major contributor to Chronic Kidney Disease (CKD) after Acute Kidney Injury (AKI). However, the temporal relation between the acute insult and maladaptive renal response to hypoxia remains unclear. In this study, we analyzed the time-course of renal hemodynamics, oxidative stress, inflammation, and fibrosis, as well as epigenetic modifications, with focus on HIF1 α /VEGF signaling, in the AKI to CKD transition. Sham-operated, right nephrectomy (UNx), and UNx plus renal ischemia (IR + UNx) groups of rats were included and studied at 1, 2, 3, or 4 months. The IR + UNx group developed CKD characterized by progressive proteinuria, renal dysfunction, tubular proliferation, and fibrosis. At first month post-ischemia, there was a twofold significant increase in oxidative stress and reduction in global DNA methylation that was maintained throughout the study. *Hif1 α* and *Vegfa* expression were depressed in the first and second-months post-ischemia, and then *Hif1 α* but not *Vegfa* expression was recovered. Interestingly, hypermethylation of the *Vegfa* promoter gene at the HIF1 α binding site was found, since early stages of the CKD progression. Our findings suggest that renal hypoperfusion, inefficient hypoxic response, increased oxidative stress, DNA hypomethylation, and, *Vegfa* promoter gene hypermethylation at HIF1 α binding site, are early determinants of AKI-to-CKD transition.

Clinical, epidemiological, and experimental studies have shown that AKI is an independent risk factor for the development of CKD and end-stage renal disease (ESRD)^{1,2}. In this transition, the initial insult severity and duration is proportional to the risk of CKD, besides, age is another preponderant factor³⁻⁶.

AKI is characterized by an abrupt reduction in renal blood flow with consequent hypoxia, endothelial and proximal epithelial injury, and renal dysfunction. After an AKI episode, a cascade of events occurs, such as brush border loss, cell polarity alterations, increased oxidative stress, and mitochondrial dysfunction of proximal tubular epithelial cells^{7,8}, as a result, some of these cells undergo necrosis or apoptosis⁹. These processes are also accompanied by macrophage infiltration and inflammation^{7,10,11}. Although the tubular epithelium has the capacity for regeneration¹², the injured epithelium is no longer the same. A subpopulation of dedifferentiated and proliferating tubular cells that recover from the acute renal insult suffer cell cycle arrest and cannot be re-differentiated, leading to tubular atrophy; all these events contribute greatly to the tubulointerstitial fibrosis that is observed in the long term^{12,13}.

Consequently, a maladaptive repair occurs^{11,14,15}, where there is persistent macrophage infiltration¹⁶⁻¹⁸, dissociation of pericytes from the tubular capillaries¹⁹, and arrest of some tubular cells in the G2/M phase²⁰, leading to a progressive fibrotic kidney²⁰⁻²². Some mechanisms involved have been elucidated, such as trans-differentiation of pericytes into myofibroblasts^{19,23}, uncontrolled proliferation of epithelial cells²², the emergence of an abnormal proximal-tubule phenotype²⁴, excessive production of TGF β by both the tubular epithelium²² and

¹Molecular Physiology Unit, Instituto de Investigaciones Biomédicas, Universidad Nacional Autónoma de México, Av. Universidad 3000, UNAM, CU, 04510 Coyoacán, Mexico City, Mexico. ²Department of Nephrology, Instituto Nacional de Ciencias Médicas y Nutrición Salvador Zubirán, Vasco de Quiroga No. 15, Tlalpan 14080, Mexico City, Mexico. ³Department of Molecular Genetics, Instituto de Fisiología Celular, Universidad Nacional Autónoma de México, Mexico City, Mexico. ✉email: nab@iibiomedicas.unam.mx

local myofibroblasts^{25,26}, accumulation of extracellular matrix proteins^{27,28}, vascular rarefaction^{29–31}, chronic hypoxia^{30,32}, and chronic stress of the endoplasmic reticulum³³.

In addition, it has been recently shown that epigenetic modifications may be involved in several renal pathologies. However, the specific molecular mechanisms by which epigenetic modifications alter renal physiology are little known. The most studied epigenetic regulations in AKI are the chromatin compaction, DNA methylation and histone acetylation/deacetylation. In AKI, obstructive renal injury, and diabetic nephropathy, epigenetic modifications induced an increase in proinflammatory and profibrotic cytokines such as monocyte chemoattractant protein-1 (MCP-1), complement protein 3 (C3), transforming growth factor β (TGF- β), which in turn perpetuate inflammation and promote epithelial-to-mesenchymal transition (EMT) that contributes to renal fibrosis^{34–38}. Although some mechanisms have been elucidated, many others remain unknown, and less is known about temporal changes during CKD progression, such as renal hemodynamics, structural injury, HIF signaling, and epigenetic modifications.

We have previously shown that an AKI episode induced by moderate or severe bilateral renal ischemia/reperfusion (IR) in male rats is sufficient to induce CKD progression after nine months^{22,27}. Interestingly, this transition was not observed in female rats, despite a similar magnitude of AKI in both male and female rats. The unique difference in the early phase post-ischemia was that females did not exhibit oxidative stress, suggesting a pivotal role of reactive oxygen species generation in this transition²¹.

Thus, it is relevant to establish a temporal understanding of the pathophysiological mechanisms throughout the AKI-to-CKD transition. In this study, we used the model of unilateral renal IR plus contralateral nephrectomy, which allowed us to induce CKD after four months. We found abnormal renal hemodynamics, reduced HIF-1 α signaling, increased oxidative stress, and global DNA hypomethylation in the early phase of the AKI to CKD transition. We also showed that the *HIF-1 α /Vegfa* signaling reduction was associated with the DNA hypermethylation of the *Vegfa* gene promoter, beginning at an early stage post-ischemia and suggesting that reduced VEGF expression is an early contributor that triggers renal hypoxia and the consequent fibrosis.

Results

Renal injury induced by unilateral ischemia after 24 h of reperfusion. First, we corroborated that the initial insult induced by IR in the uninephrectomized rats was similar among the groups studied at 1, 2, 3, or 4 months postischemia. All IR + UNx rats were randomly assigned to the different periods of follow-up. After 24 h of inducing renal ischemia, all the IR + UNx rats exhibited significant proteinuria that was of the same magnitude among the groups assigned to 1, 2, 3 and, 4 months of follow-up (Fig. 1A), together with a similar reduction in renal function (Fig. 1B); these alterations were not observed in the S (n = 16) or UNx (n = 16) groups after 24 h of the surgery as is shown by the individual data presented in Fig. 1A, B. Consequently, the S or UNx rats were also randomly assigned to the different periods of follow-up. The urinary hydrogen peroxide levels were also evaluated and reflected significant oxidative stress in all IR + UNx groups (Fig. 1C). The urinary HSP72 levels, known to be a sensitive AKI biomarker, were also analyzed^{39–42}. As expected, all rats that underwent IR + UNx exhibited a significant and similar increase in urinary HSP72 levels corrected by urinary creatinine (UHSP72/UCreat), (Fig. 1D). These findings show that all the IR + UNx rats exhibited a similar AKI degree. This was important to ensure that the changes observed in the long term were due to the initial insult itself rather than differences in the severity of the ischemic injury.

Temporal progression of renal dysfunction and structural injury after an AKI episode. To evaluate the precise moment at which the functional, structural, and molecular alterations occur along with AKI to CKD transition, the groups were euthanized at 1, 2, 3, or 4 months after the initial ischemic insult. No differences in body weight were found among the studied groups (Fig. 2A). As expected, the UNx and IR + UNx groups showed a significant increase in kidney weight/body weight (KW/BW) starting in the first-month compared to that of the S group (Fig. 2B). All experimental groups remained normotensive at the time of evaluation (Fig. 2C). The IR + UNx group exhibited a progressive increase in proteinuria starting in the second month of follow-up that was not evident in the S and UNx groups (Fig. 2D). Due to the renal mass reduction, the UNx group exhibited renal hyperperfusion, but when it was corrected to the kidney weight, renal blood flow (RBF) was similar to the S group (Fig. 2E). This finding, in the UNx group, was related to the maintenance of normal renal function (Fig. 2F). Interestingly, this compensatory response was not seen in the IR + UNx group. RBF/KW was significantly lower than that of the S and UNx groups, starting in the first-month, and renal hypoperfusion was maintaining along the study course (Fig. 2E). At the end of the study, the IR + UNx group had significant renal dysfunction (Fig. 2F). The renal urinary biomarker HSP72 and KIM1 normalized by urinary creatinine, were significantly elevated starting in the first-month and third-month respectively, and increased even more by the end of the study (Fig. 2G, H). In Table 1 appears urinary flow, fractional excretion of sodium (FENa) and osmolarity. No differences were found among the groups along the study, except that the osmolarity was lower in the IR + UNx group at fourth-month compared to S group.

The long-term consequences of an AKI episode were also evidenced by the presence of tubulointerstitial fibrosis starting in the second-month post-ischemia, which progressively increased, whereas this injury was not detected in the UNx group (Fig. 3A). Although increased *Tgfb1* mRNA levels were not observed in the early stages of the AKI to CKD transition, a significant upregulation in *Tgfb1* mRNA and protein levels was evident in the fourth-month post-ischemia compared to that of the S and UNx groups (Fig. 3B, C). Accordingly with this, *Col1a1* (collagen 1) mRNA levels were significantly increased in the fourth-month (Fig. 3D). We only measured TGF β protein levels at the fourth-month, because the *Tgfb1* mRNA levels and its target gene *Col1a1* were only significantly increased in this point of the follow-up. Besides, the IR + UNx group exhibited higher levels of Ki67 positive tubular cells (Fig. 3E, F), similar to our previous findings²².

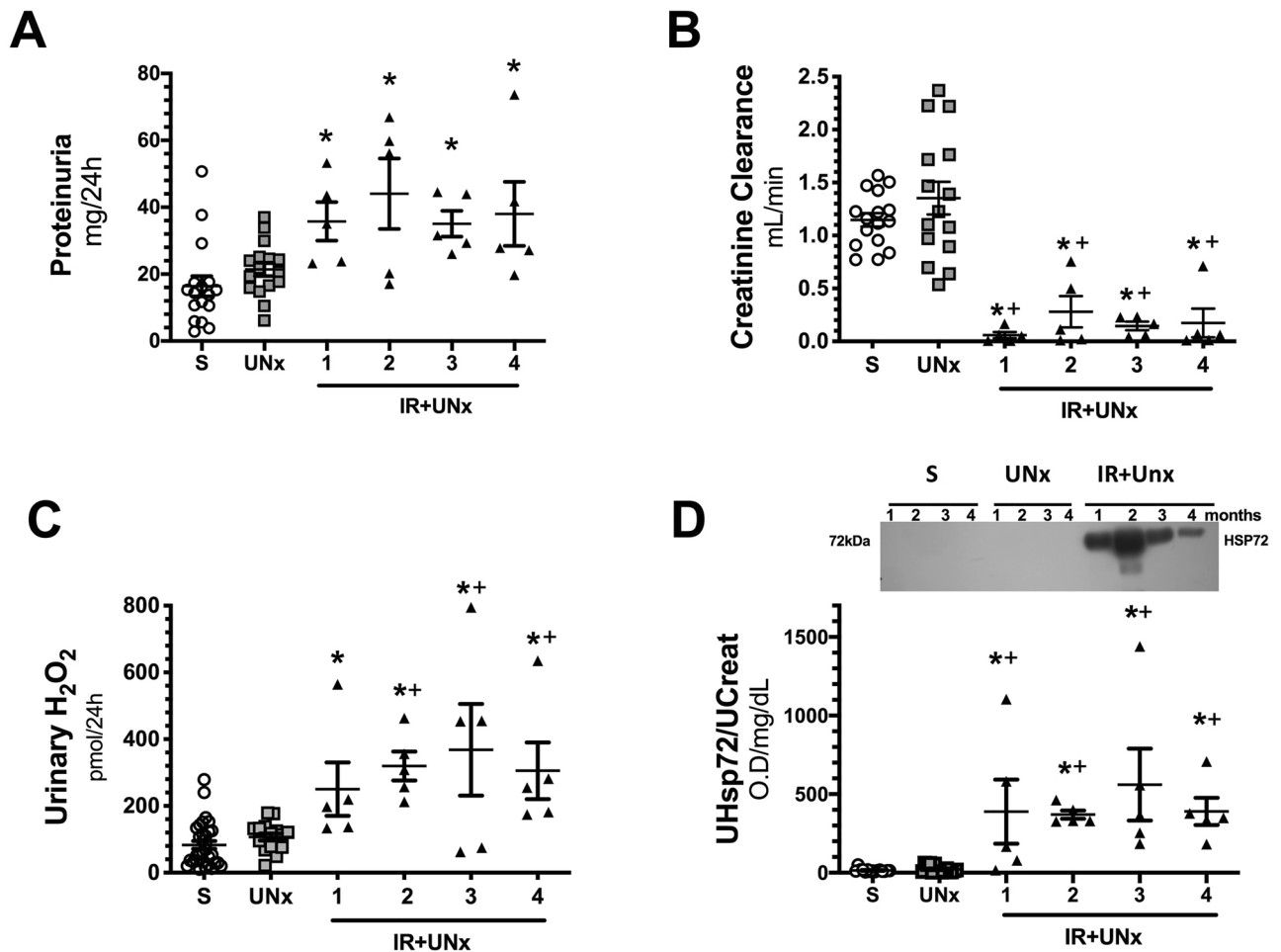


Figure 1. Renal injury induced by unilateral ischemia after 24 h of reperfusion. (A) Proteinuria, (B) Creatinine clearance, (C) Urinary hydrogen peroxide, and (D) Urinary HSP72 corrected by urinary creatinine, including a representative cropped blot image. Data are represented as the mean \pm SE (for S, $n = 16$, for UNx, $n = 16$ and $n = 20$ for IR + UNx groups). White bars represent the S, gray bars represent UNx, and black bars represent IR + UNx groups. The one-way analysis of variance (ANOVA) was used to determine statistical differences, using the Bonferroni correction for multiple comparisons. * $p < 0.05$ versus S group and + $p < 0.05$ versus UNx group. Full-length blots are presented in Supplementary Fig. 3.

These results show that an AKI episode induced functional and structural alterations that mostly appear beginning at an early stage, highlighting the fact that there was no compensatory renal hyperperfusion expected by the renal mass lost in the IR + UNx group.

Temporal course of oxidative stress and vasoactive factors in the CKD progression induced by an AKI episode.

Oxidative stress and renal inflammation have a pivotal role in CKD progression; thus, the temporality of these two pathways was also analyzed. An increase in oxidative stress (Fig. 4A) and a reduction in mRNA levels of the transcription factor *Nfe2l2*, which stimulates the antioxidant response, was observed beginning in the initial stage of the AKI to CKD transition (Fig. 4B), even though *Nox4* mRNA levels were reduced in the late stage of the disease (Fig. 4C). An imbalance in vasoactive factors was also observed at the end of the study. *NOS3* mRNA levels were significantly decreased (Fig. 4D), whereas the endothelin vasoconstrictor effect was increased (Fig. 4E, F).

Inflammatory pathways in the time course of CKD induced by AKI.

The mRNA levels of interleukin 6 (*Il6*), monocyte chemoattract protein (*Mcp1*), and interleukin 10 (*Il10*) were measured throughout the study. *Il6* was upregulated in the IR + UNx group in the fourth-month after renal ischemia, as demonstrated by the significant elevation in interleukin 6 mRNA and protein levels (Fig. 5A, B). Because, we only observed a significant increase in *Il6* mRNA levels in the IR + UNx group at fourth-month post-ischemia, the IL6 protein levels were only evaluated in the Sham and IR + UNx groups in this specific time of the study. *Mcp1* mRNA levels increased in the first-month, and this elevation was observed again in the fourth month (Fig. 5C). The mRNA levels of the anti-inflammatory cytokine *Il10* showed a reduction starting in the first-month that became

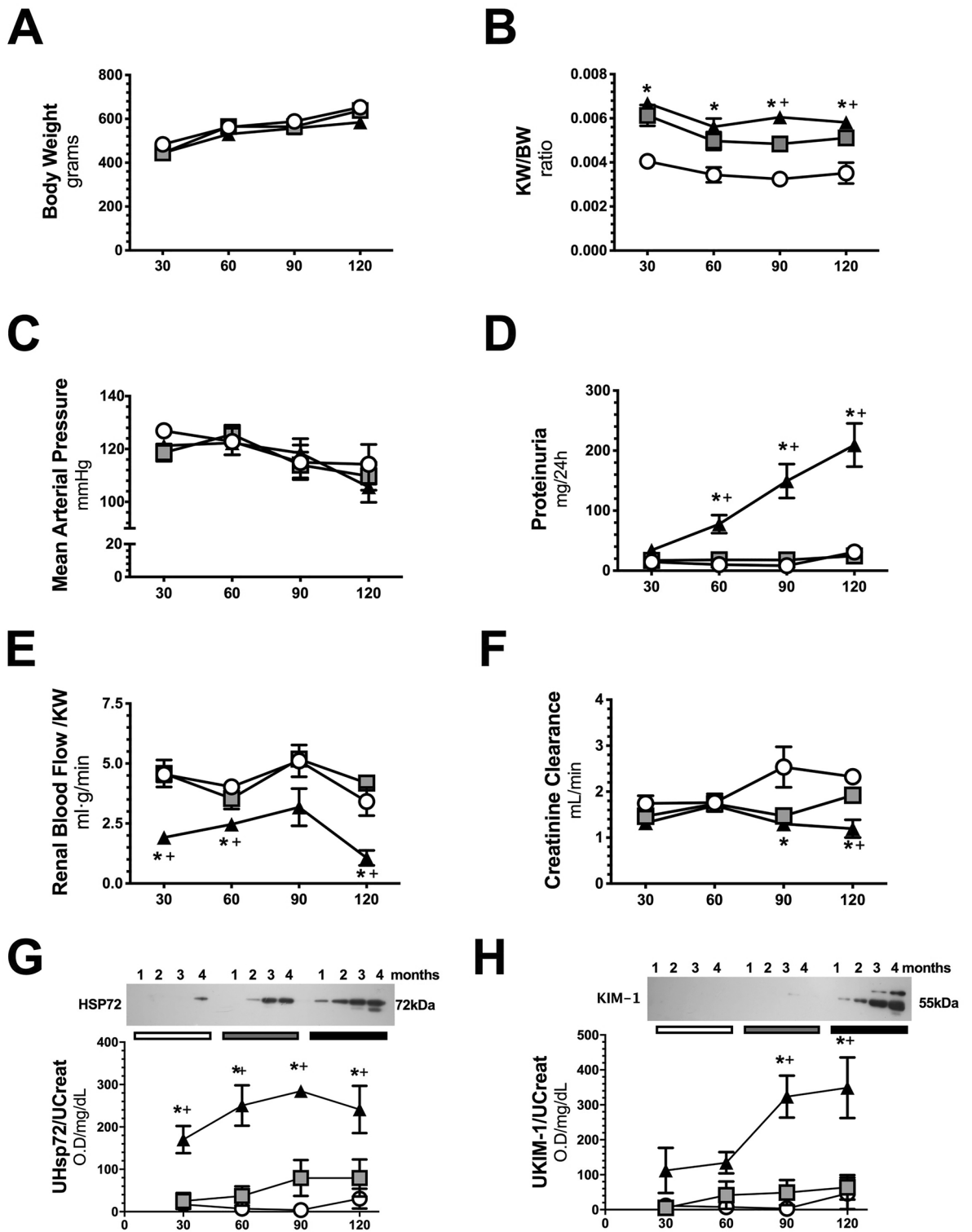


Figure 2. Follow-up of renal function in the AKI to CKD transition. (A) Body weight, (B) Ratio kidney weight/body weight, (C) Mean arterial Pressure, (D) Proteinuria, (E) Renal blood flow / kidney weight, (F) Creatinine clearance, (G) Urinary HSP72 corrected by urinary creatinine, and (H) Urinary KIM-1 corrected by urinary creatinine, including representative cropped blots, along the follow-up. Data are represented as the mean \pm SE. $n = 4, 4,$ and 5 for the S, UNx, and IR + UNx groups in each studied period: 30, 60, 90, and 120 days post-ischemia. White circles represent the S, gray squares represent UNx and black triangles represent IR + UNx groups. The one-way analysis of variance (ANOVA) was used to determine statistical differences, using the Bonferroni correction for multiple comparisons. * $p < 0.05$ versus S group and + $p < 0.05$ versus UNx group in their respective period. Full-length blots are presented in Supplementary Figs. 4 and 5.

	Urinary flow (mL/min)	FENa (%)	Osmolarity (mOsm/L)
Sham			
30 days	0.031 ± 0.004	0.17 ± 0.03	350 ± 77
60 days	0.026 ± 0.007	0.10 ± 0.00	481 ± 107
90 days	0.023 ± 0.003	0.11 ± 0.02	729 ± 123
120 days	0.014 ± 0.003	0.08 ± 0.03	1226 ± 178
UNx			
30 days	0.029 ± 0.005	0.19 ± 0.04	494 ± 172
60 days	0.025 ± 0.005	0.15 ± 0.05	703 ± 119
90 days	0.014 ± 0.007	0.16 ± 0.04	936 ± 72
120 days	0.024 ± 0.004	0.09 ± 0.02	746 ± 129
IR + UNx			
30 days	0.026 ± 0.005	0.21 ± 0.07	448 ± 59
60 days	0.037 ± 0.003	0.26 ± 0.14	440 ± 39
90 days	0.030 ± 0.002	0.24 ± 0.07	501 ± 30
120 days	0.024 ± 0.004	0.20 ± 0.08	678 ± 145*

Table 1. Urine Chemistries along the study for all the included groups. * $p < 0.05$ versus respective Sham.

significant in the second month and returned to normal levels by the third month compared to that of the S and UNx groups (Fig. 5D).

These findings suggest that oxidative stress, rather than renal inflammation, is an initial trigger of the subsequent damage.

Hypoxic response in the timing of CKD progression. As we showed, the UNx group exhibited renal hyperperfusion starting in the first-month post ischemia (Fig. 2E). In contrast, because renal compensatory hyperperfusion was absent in the IR + UNx group, the HIF1 α signaling pathway was studied. The gene expression *Hif1a* and one of its target genes, *Vegfa*, were assessed during AKI to CKD transition. In the UNx group, *Hif1a* mRNA levels were significantly reduced in the first and second-month post-ischemia, whereas HIF1 α protein levels remained unaltered during follow-up. This response was explained and expected in part by the compensatory renal hyperperfusion seen in these rats. In contrast, there was an inefficient response to hypoxia in the IR + UNx group that exhibited renal hypoperfusion because there was a significant decrease in *Hif1a* mRNA levels in the first and second-month after ischemia (Fig. 6A). In support of this inefficient response, *Vegfa* mRNA and protein levels were significantly reduced starting in the first-month and remained so on during follow-up (Fig. 6B–D), despite *Hif1a* mRNA and protein levels being reestablished by the third-month, suggesting that an independent mechanism maintains *Vegfa* gene expression downregulation and could be related with the vascular rarefaction characteristic of the AKI to CKD transition^{29–31}.

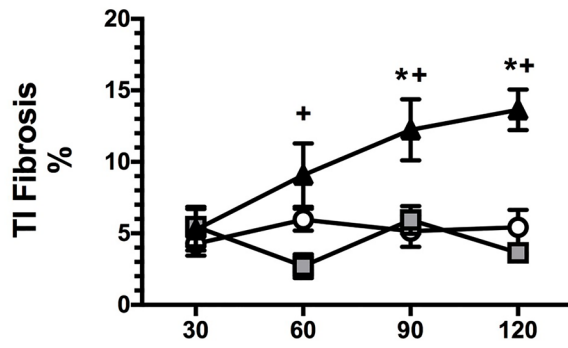
Time course global DNA methylation during CKD progression induced by AKI. Numerous studies have demonstrated that renal injury is associated with epigenetic changes, including histone modifications, DNA methylation, and the expression of various non-coding RNAs⁴³. We found that rats experiencing the AKI to CKD transition exhibited mainly hypomethylation of global DNA, which started in the first-month post-ischemia and was maintained throughout follow-up (Fig. 7A). These changes were only seen in the renal cortex, whereas no differences were observed in the renal medulla (Fig. 7B). In general, the renal medulla exhibited lower levels of DNA methylation compared to that of the renal cortex.

Based on the changes observed in the global methylation of DNA and the possible independent mechanisms regulating the decreased expression of VEGF in the AKI to CKD transition, we decided to evaluate the specific methylation of the *Vegfa* gene promoter.

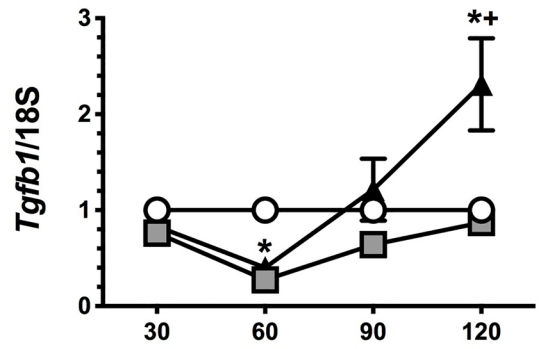
***Vegfa* gene promoter DNA methylation during AKI to CKD transition.** With the interest to know if DNA methylation was associated with the modulation of *Vegfa* and *Hif1a* expression in AKI to CKD transition, we assessed the methylation state on 5'-upstream promoter region by bisulfite sequencing. According to the decreased *Vegfa* gene expression, we localized a DNA hypermethylated region in the noncoding upstream region of this gene, since the first-month post-ischemia (Fig. 8A), which was maintained until the fourth-month of follow-up (Fig. 8B). Therefore, we discovered that in the binding site for HIF1 α , located at the region 2 of the *Vegfa* gene promoter, contains a specific CpG that was highly methylated in the IR + UNx group since the first-month and (75%) compared to that of the S (12%) and UNx groups (30%) (Fig. 8A). Moreover, the hypermethylated region was maintained at the end of the study in the IR + UNx group (91%) compared to that of the S (18%) and UNx (40%) groups (Fig. 8B).

Consistent with our transcriptional findings, we did not find any methylation in the noncoding upstream promoter region of *Hif1a* among the groups (Suppl. Fig. 2).

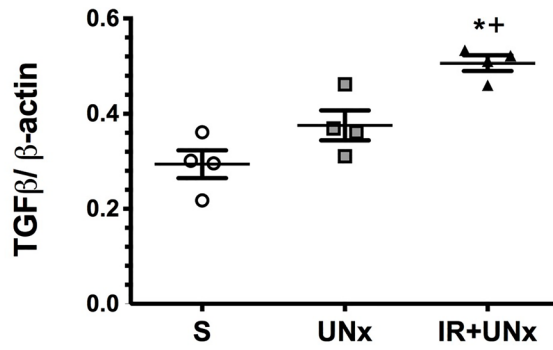
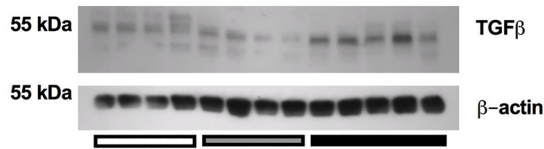
A



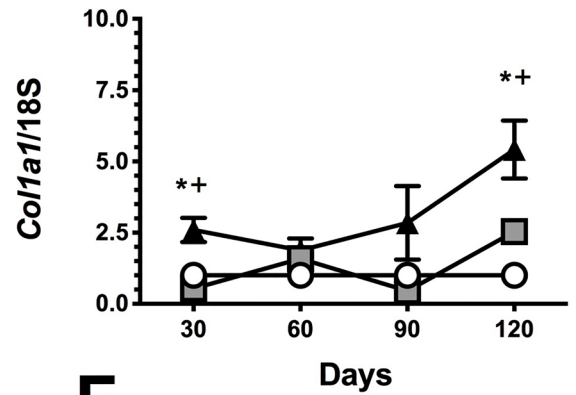
B



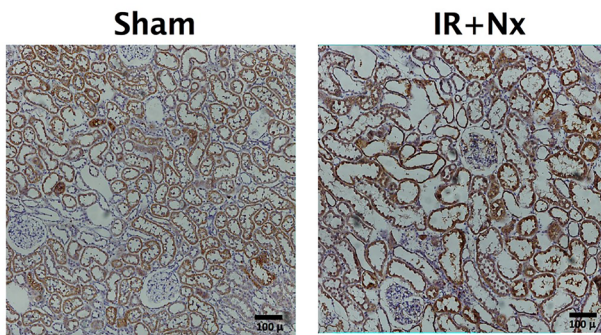
C



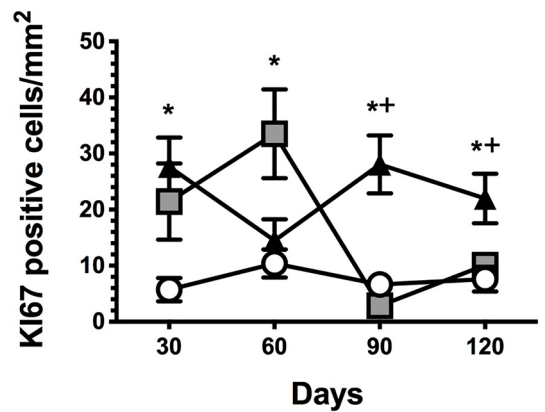
D



E



F



◀ **Figure 3.** Temporally induction of tubulointerstitial fibrosis by TGF β activation. (A) Tubulointerstitial fibrosis, (B) mRNA levels of *Tgfb1*, (C) Protein levels of TGF β , at fourth-month post-ischemia, including a representative cropped blots. (D) mRNA levels of *Collagen1a1*, (E) Representative microphotographs of Ki67 immunostaining for the S and IR + UNx groups. (F) Quantification of Ki67 positive epithelial cells (cells/mm²). Data are represented as the mean \pm SE. n = 4, 4, and 5 for S, UNx, and IR + UNx groups, in each studied period: 30, 60, 90, and 120 days post-ischemia. White circles/bar represent the S, gray squares/bar represent the UNx and black triangles/bar represent the IR + UNx groups. The one-way analysis of variance (ANOVA) was used to determine statistical differences, using the Bonferroni correction for multiple comparisons. * $p < 0.05$ versus S group and + $p < 0.05$ versus UNx group in their respective period. Full-length blots are presented in Supplementary Fig. 6.

Discussion

Acute kidney injury is a public health problem and despite the advances in modern medicine, its incidence has not diminished in recent decades⁴⁴. Also, the alarming increase in patients with CKD worldwide⁴⁵, coupled with the recent recognition that AKI is an independent risk factor for CKD development^{1,2} requires joint work between biomedical and clinical researchers to avoid this complication. Therefore, it is imperative to study the temporality of the mechanisms that affect and lead to the AKI to CKD transition, which will allow for the identification of the key points and mediators in the development of this disease and propose specific therapeutic targets according to the stages of CKD. Many efforts have been made, and some pathways, such as trans-differentiation of pericytes into myofibroblasts^{19,23}, uncontrolled proliferation of epithelial cells²², excessive production of TGF β by both tubular epithelium²² and local myofibroblasts^{25,26}, accumulation of extracellular matrix proteins^{27,28}, chronic hypoxia^{30,32}, vascular rarefaction^{29,31,46}, and chronic stress of the endoplasmic reticulum³³, have been identified, but many others remain to be elucidated.

In this study, we evaluated ischemic renal damage after 24 h of reperfusion plus right nephrectomy compared to that of the S and UNx groups. AKI induced by IR was characterized by elevated proteinuria, renal dysfunction, and oxidative stress. All IR + UNx rats exhibited the same magnitude of AKI. In the long term, the nephrectomy plus I/R model was able to accelerate the development of CKD. After four months, the IR + UNx group presented a progressive increase in proteinuria and a significant decrease in renal function. Among the alterations that occurred in the early phase of the transition, we found a significant increase in oxidative stress that was maintained throughout the study follow-up and a significant decrease in global DNA methylation, suggesting that both are early key players in the AKI to CKD transition.

As expected, the UNx group exhibited renal hyperperfusion and hyperfiltration to compensate the renal mass reduction for maintaining renal function within standard values, as the S group had. Interestingly, the IR + UNx group displayed sustained hypoperfusion that was observed beginning at an early phase and impacted the expected renal function compensation. Our results suggest that this poor renal hemodynamic response after an AKI episode could be one of the responsible mechanisms involved in the AKI to CKD transition, contributing to chronic renal hypoxia.

Previous studies have demonstrated that chronic hypoxia is a trigger mechanism in the AKI to CKD transition that coordinates the interaction between inflammation, oxidative stress, and progressive fibrosis^{13,16–18,20–22,47}. HIF1 α serves as a master regulator of adaptive responses against hypoxia, although, the levels of HIF1 α can also be regulated by oxygen independent pathways⁴⁸. This transcription factor induces an angiogenic pathway throughout the induction of *Vegfa* gene expression^{49,50}. In this regard, we found an inefficient response against renal hypoxia in the IR + UNx group. *Hif1a* mRNA levels were decreased in the first and second-month post-ischemia, similar to those observed in the UNx group. Although, this response could be explained in the UNx group due to the compensatory elevation in RBE, which when normalized by kidney weight was similar to the S group. Since, HIF1 α is regulated by proteasomal degradation pathways in response to oxygen levels⁵¹, it is very likely that in the UNx group, there is a greater metabolic work to maintain renal function and therefore, the state of renal oxygenation could not have changed. But this HIF1 α response was unexpected in the IR + UNx group that exhibited renal hypoperfusion, a condition in which proteasomal degradation is not expected to occur. This inefficient response of HIF1 α was also demonstrated by the reduction in its target gene *Vegfa*. Thus, *Vegfa* mRNA levels were reduced starting in the first-month, and interestingly, they remained reduced throughout the study, despite the restoration of HIF1 α levels. The decreased *Vegfa* expression was also corroborated at the protein level throughout the study. Recent studies have reported that the late response of HIF1 α could be related to the activation of inflammatory processes and the generation of renal fibrosis⁵². It is well known that the reduction in *Vegfa* gene expression is partly responsible for vascular rarefaction^{46,53–55} that accompanies the AKI to CKD transition, which also perpetuates chronic hypoxia. Although *Hif1a* mRNA levels were restored at the end of the study and protein levels remained unaltered, *Vegfa* levels continued diminishing; this opened the possibility of an alternative regulation of *Vegfa* gene expression through the involvement of epigenetic mechanisms.

It has been shown that the hypoxia response element (HRE) in the *Vegfa* promoter gene contains several cytosines in a CpG context that are potentially methylated. This methylation could reduce the HIF1 α interaction with the *Vegfa* gene promoter^{56,57}. In vitro studies have demonstrated that DNA hypermethylation in the *Vegfa* promoter region induces silencing of this gene⁵⁸. To understand the reduction in *Vegfa* expression despite sustained renal hypoperfusion and recovery of *Hif1a* mRNA levels, we analyzed the methylation of the noncoding upstream region of *Vegfa* during the AKI to CKD transition. Interestingly, we found DNA hypermethylation in the promoter region of *Vegfa*. More importantly, we demonstrated that the HRE, as well as the core region for HIF1 α interaction was hypermethylated since the first-month post-ischemia and it was maintained at the fourth-month of the follow-up. This site matches with the region 2, previously described to be important in *Vegf*

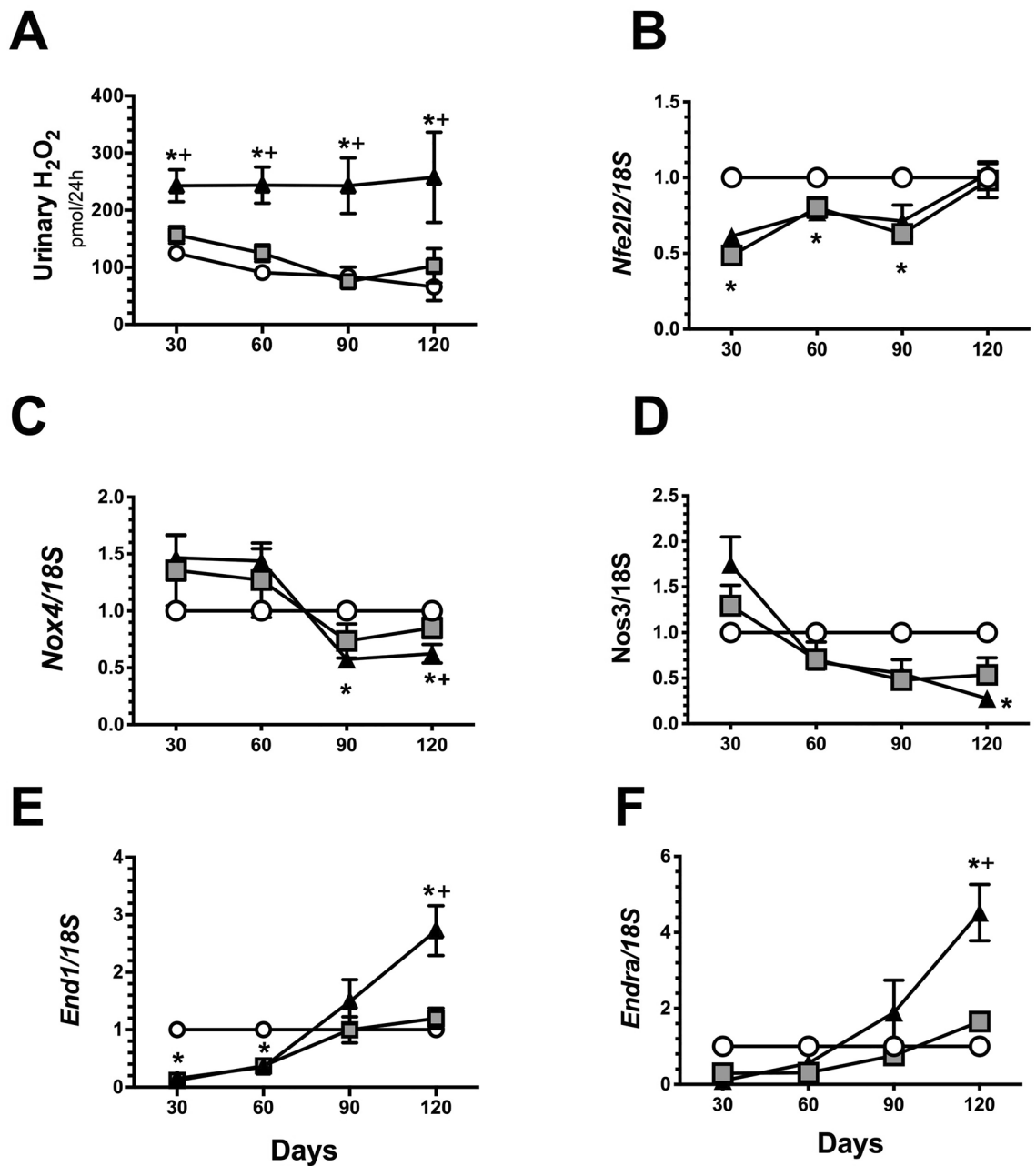


Figure 4. Oxidative stress and vasoactive mediators over the course of AKI to CKD transition. (A) Urinary hydrogen peroxide, (B) mRNA levels of *Nfe2l2* (C) mRNA levels of *Nos3*, (D) mRNA levels of NOX4, (E) mRNA levels of *Edn1* and (F) mRNA levels of endothelin receptor A (*Endra*). Data are represented as the mean \pm SE. $n = 4$, $n = 4$, and $n = 5$ for the S, UNx, and IR + UNx groups, in each studied period: 30, 60, 90, and 120 days post-ischemia. The one-way analysis of variance (ANOVA) was used to determine statistical differences, using the Bonferroni correction for multiple comparisons. * $p < 0.05$ versus S group and + $p < 0.05$ versus UNx group in their respective period.

gene transcription regulation⁵⁹. Using the transcription factor binding site predictor tool PROMO (version 8.3 of TRANSFAC, <http://algggen.lsi.upc.es>), TFsitscan (<http://www.ifti.org/cgi-bin/ifti/Tfsitescan.pl>) and JASPAR database (<http://dbcat.cgm.ntu.edu.tw>), we found that this hypermethylated region contains a putative binding sequence responsible for the interaction of Hif1 α , C/EBP α and the p300. This complex is essential for *Vegfa* transcription regulation and contributes to the pro-angiogenic pathway^{60,61}. Our findings suggest that the reduction in *Vegfa* gene expression in the IR + UNx group resulted from epigenetic regulation, which could be partially responsible for inducing vascular rarefaction and chronic renal hypoxia, which are mechanisms implicated in the AKI to CKD transition^{19,29–31,46}. In agreement with our results, it has been demonstrated that treatment with VEGF-121 was effective in suppressing the AKI to CKD transition induced by IR in rats. Although VEGF-121 did not affect AKI, the loss of peritubular capillaries in the cortex and outer stripe of the outer medulla was

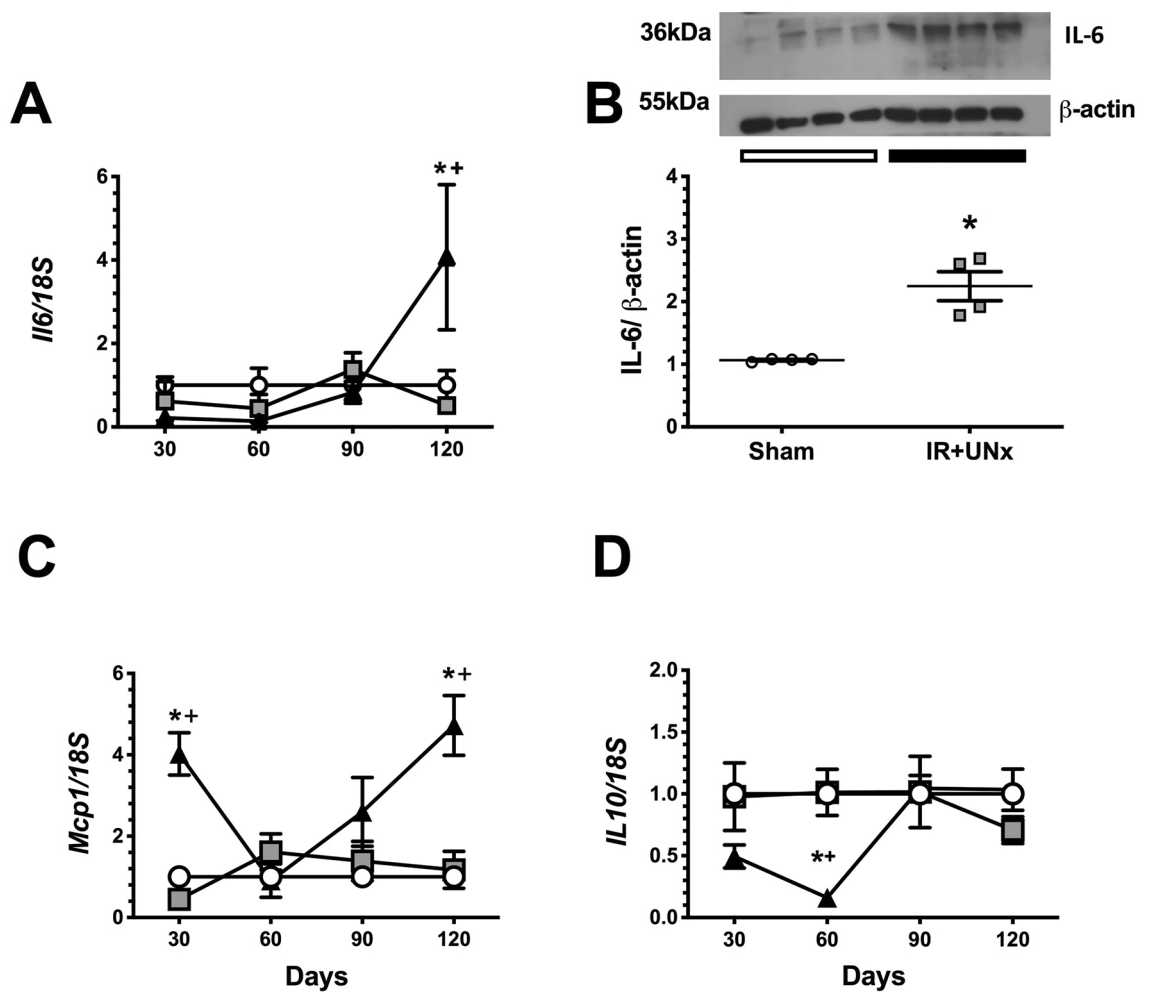


Figure 5. Inflammatory mediators participation during AKI to CKD transition. (A) mRNA levels of *Il6*, (B) Protein levels of IL-6 at fourth-month post-ischemia, including a representative cropped blots, (C) mRNA levels of *Mcp1* and (D) mRNA levels of *Il10*. Data are represented as the mean \pm SE. $n = 4, 4,$ and 5 for the S, UNx, and IR + UNx groups in each studied period: 30, 60, 90, and 120 days post-ischemia. White circles/bar represent the S, gray squares represent the UNx and black triangles/bar represent the IR + UNx groups. The one-way analysis of variance (ANOVA) was used to determine statistical differences, using the Bonferroni correction for multiple comparisons. * $p < 0.05$ versus S group and + $p < 0.05$ versus UNx group in their respective period. Full-length blots are presented in Supplementary Fig. 7.

significantly attenuated⁵⁵. Further experimental and clinical studies are required to evaluate VEGF therapeutic power in preventing the AKI to CKD transition. In this hypermethylated region, we also found a putative binding site for Nrf2, which is a master regulator of the antioxidant response⁶². Because hypermethylation of the *Vegfa* promoter region occurred from the first-month post-ischemia, it suggests that this epigenetic mechanism plays an important role in the onset of the disease, promoting chronic hypoxia and concomitant development of renal fibrosis. In a recent study, it was observed that indeed, epigenetic modifications occur early after folic acid-induced kidney damage. In particular, it was observed that de novo methylation of histone H3K4 is necessary for the differentiated cells to re-enter mitosis and regenerate the proximal tubular epithelium⁶³. These findings together, highlighted the crucial role of the early epigenetic modifications in the long consequences after an ischemic insult. Furthermore, our results open an exciting research field to explore the mechanisms by which hypermethylation of the *Vegfa* promoter gene is occurring, in which cell subpopulations occur, as well as the molecular mediators of this phenomenon, such as histone modifications and the enzymes involved in this pathophysiological condition. In this context, previous reports have demonstrated that the up-regulation of DNA methyltransferase 1 (Dnmt1), DNA methylation, and transcriptional silencing are linked to fibroblast activation and kidney fibrosis³⁷.

In addition to the mentioned changes, the IR + UNx group exhibited activation of renal inflammation. Pro-inflammatory molecules, as indicated by *Mcp1* and *Il6* mRNA levels, increased, while the anti-inflammatory molecule, *Il10*, decreased beginning at the early phase of the transition of this disease. These changes could result from the global DNA hypomethylation observed in the IR + UNx, as previous studies have shown in AKI, diabetic nephropathy, and CKD models^{34,37,38}.

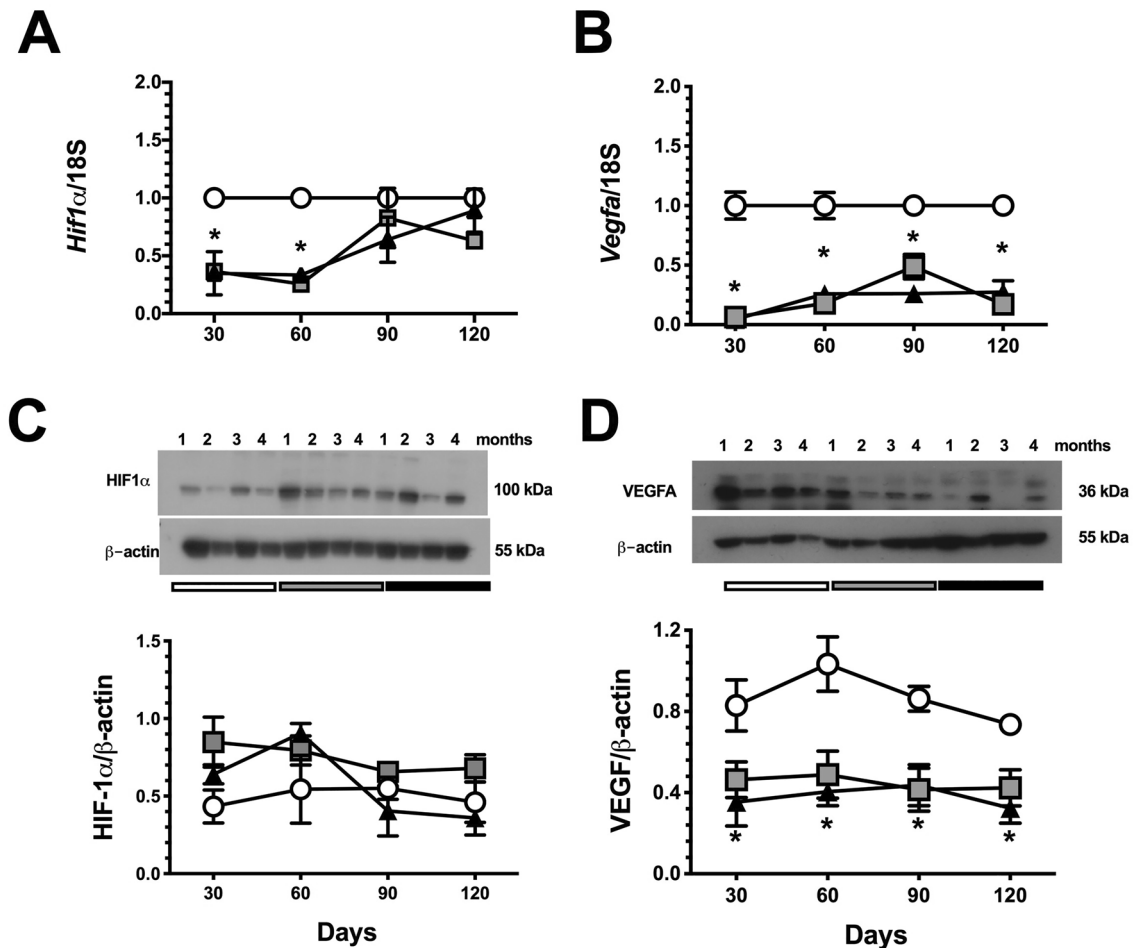


Figure 6. Temporal course of HIF-1 α signaling during AKI to CKD transition. (A) mRNA levels of *Hif1a*, (B) mRNA levels of *Vegfa*, (C) Protein levels of HIF-1 α , including a representative cropped blot, and (D) Protein levels of VEGF, including a representative cropped blot. Data are represented as the mean \pm SE. $n = 4$, for S, UNx, and IR + UNx groups, in each studied period: 30, 60, 90, and 120 days post-ischemia. White circles represent the S, gray squares represent the UNx and black triangles represent the IR + UNx groups. The one-way analysis of variance (ANOVA) was used to determine statistical differences, using the Bonferroni correction for multiple comparisons. * $p < 0.05$ versus S group and + $p < 0.05$ versus UNx group in their respective period. Full-length blots are presented in Supplementary Figs. 8 and 9.

In summary, our study shows that early renal hypoperfusion, inefficient hypoxia response, increased oxidative stress, and increased inflammation play an important role in the AKI to CKD transition. Specifically, the inefficient hypoxia response results from the inadequate hypermethylation of the *Vegfa* promoter gene at the site of HIF1 α binding that occurs in the early stage post-ischemia.

Methods

All the experimental procedures in the animals were conducted following the Guide for the Care and Use of Laboratory Animals and were approved by the animal research ethics committee of the *Instituto Nacional de Ciencias Médicas y Nutrición Salvador Zubirán* with the approval number NMM-1852. The study was carried out in compliance with the ARRIVE guidelines.

Experimental model: right nephrectomy and contralateral ischemia. Fifty-nine male Wistar rats weighing between 300 and 320 g were included. Seven rats did not meet our inclusion and exclusion criteria, two were excluded due to bleeding during the nephrectomy surgical procedure and five due to postoperative death in the first 72 h as a consequence of renal ischemia–reperfusion injury. Therefore, a total of 52 rats were included and randomly divided into three groups: the sham surgery group (S, $n = 16$), the right nephrectomy group (UNx, $n = 16$), and the group with right nephrectomy and simultaneous left renal ischemia of 45 min in the left kidney (IR + UNx, $n = 20$). Based on our previous experience with the IR experimental model, we calculated the sample size for comparison of two means, using the creatinine elevation after 24 h post-ischemia. Although, we did not use a method to generate the randomization sequence, each block of 3 rats was randomly assigned to each of the studied groups: S, UNx or IR + UNx and so on. The study was not blinded because no pharmacological intervention was carried out.

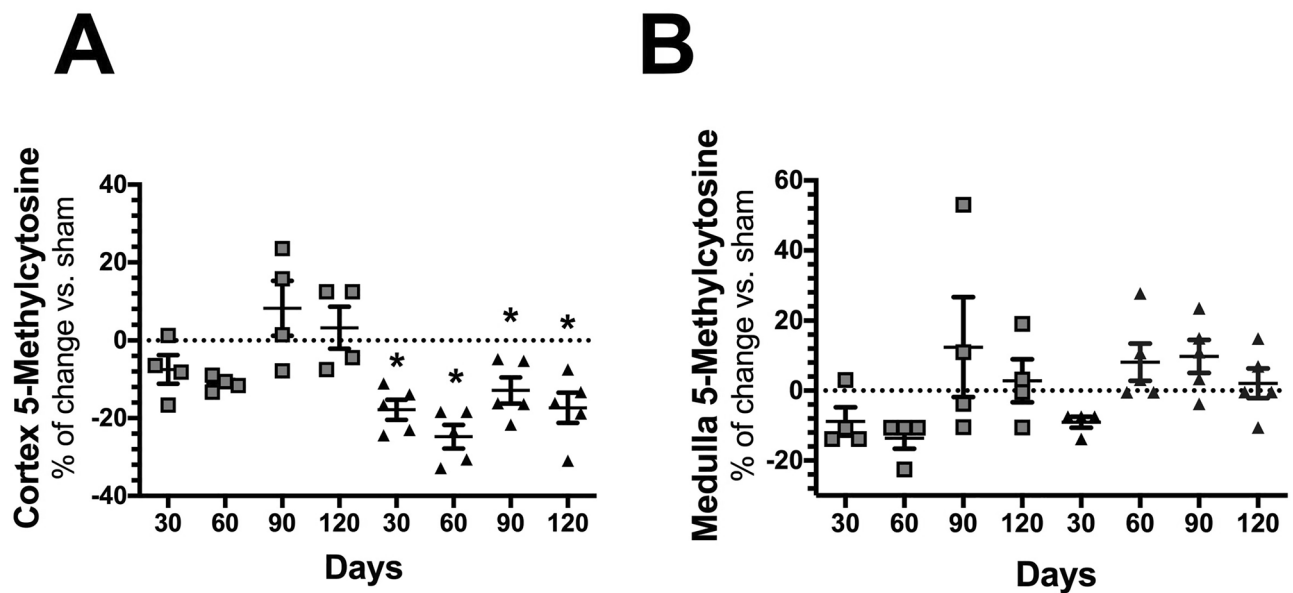


Figure 7. Global DNA methylation over the course of AKI to CKD transition. (A) Percentage change of global DNA methylation in renal cortex from the UNx (gray squares) and IR + UNx (black triangles) groups. (B) Percentage change of global DNA methylation in renal medulla from the UNx (gray squares) and IR + UNx (black triangles) groups, for each studied period: 30, 60, 90, and 120 days. The one-way analysis of variance (ANOVA) was used to determine statistical differences, using the Bonferroni correction for multiple comparisons. * $p < 0.05$ versus S group.

The animals were anesthetized with sodium pentobarbital (30 mg/kg) and kept in a thermoregulated bed to perform the surgery at 37 °C. Under anesthesia, an abdominal incision was made to expose the two kidneys, first, the nephrectomy of the right kidney was performed, dissecting the peri-renal fat, as well as, separating the adrenal gland from the kidney with delicacy to avoid damaging it. For the IR + UNx group, in addition to the nephrectomy, a clip was placed in the left kidney for 45 min, to induce the ischemic process and the reperfusion was achieved when the clip was removed, using the recovery of the coloration of the kidney, as an indicator. The animals were bred and kept in our animal facility; on a 12/12 h light/dark cycles and permitted ad libitum access to food and water. Each studied group was followed for 1, 2, 3, and 4 months, respectively. At the end of each experimental period, the following parameters were assessed: mean arterial pressure (MAP), renal blood flow (RBF), creatinine clearance, glomerular diameter, tubule-interstitial fibrosis, Ki67 positive cells, urinary H₂O₂ excretion urinary biomarkers of renal injury, RNA and protein levels of antioxidant enzymes and anti-inflammatory cytokines, DNA methylation and promoter VEGF methylation.

Renal functional studies. The animals were placed in metabolic cages every month, to collect urine for at least 18 h to determine urinary protein excretion and creatinine clearance. A blood sample from the retro-orbital plexus was also collected monthly. Urine collections were carried out at the same schedule in all animals, starting between 4 and 6 pm and ended 18 h later, to avoid diurnal variations. For the determination of serum and urine creatinine, the colorimetric method of picric acid was used and quantified at 510 nm in a spectrophotometer. To calculate the creatinine clearance, the formula of $C = (U \cdot V) / S$ was used, where U is the urinary creatinine multiplied by the urinary volume (V), and S corresponds to the serum creatinine. Urinary protein excretion was determined by the turbidimetric method of trichloroacetic acid (TCA) and quantified at 420 nm in a spectrophotometer.

By the end of each experimental period, the animals were anesthetized with sodium pentobarbital (30 mg/kg) and were placed in a thermoregulated pad. The trachea was cannulated with a PE-240 polyethylene tube and the femoral arteries were catheterized with a polyethylene tube PE-90. The mean arterial pressure was recorded by one of the catheters placed in the femoral artery, using a pressure transducer (Model p23 db, Gould, Puerto Rico). Subsequently, an abdominal incision was made to expose the left kidney, the renal artery was dissected and an ultrasound probe was placed to register the renal blood flow (1RB, Transonic, Ithaca, NY).

The right kidney from the S group was ligated and removed and the left kidney upper and lower pole for the UNx and the IR + UNx groups were excised to separate renal medulla and cortex, both sections were immediately frozen at -70 °C for further molecular analysis. The left kidney was then perfused through the femoral artery catheter with 20 mL of saline and then fixed with 20 mL of 4% formaldehyde, and removed immediately after. The animals were euthanized with an intraperitoneal delivery of an overdose of pentobarbital (100 mg/kg) after 1, 2, 3, and 4 months of renal reperfusion.

Light microscopy and immunohistochemistry analysis. After tissue fixation, the kidneys were dehydrated and embedded in paraffin. Renal slices of 4 μm were obtained and stained with Periodic Acid Schiff

Vegfa Regulatory region

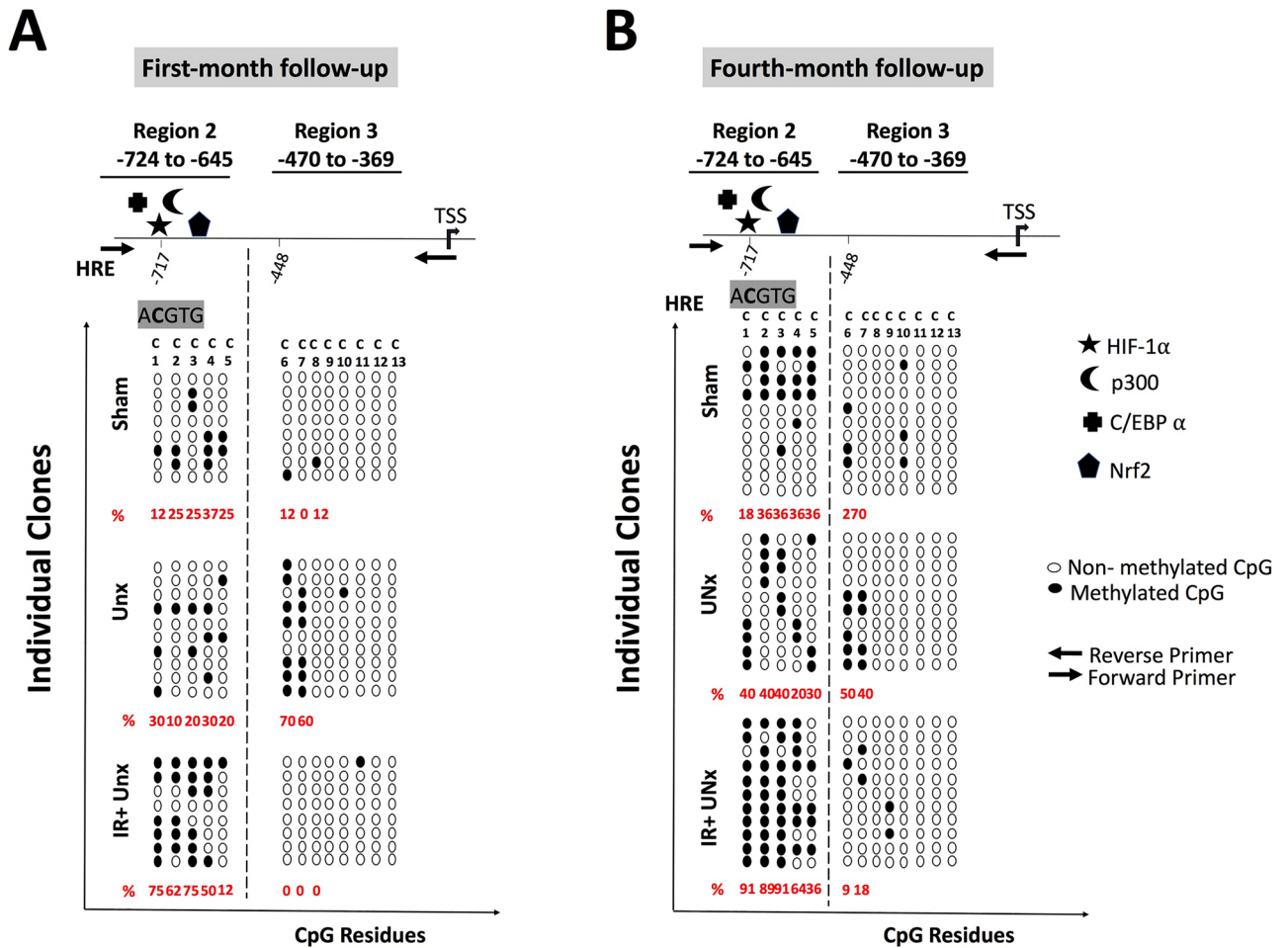


Figure 8. Bisulfite sequencing of two non-coding upstream regions of *Vegfa* promoter for (A) the first-month and (B) the fourth month of follow-up for the Sham, UNx and IR + UNx groups, respectively. Arrows represented the forward and reverse primers for each amplicon. HIF-1 α , p300, C/EBP α , and Nrf2 binding sites as is stated. White circles represented non-methylated CpG, and black circles represented methylated CpG, each circle represented an individual clone. Each C represented a cytosine in CpG context. TSS-Transcription start site; HRE-Hypoxia response element (ACGTG).

(PAS) or Sirius red. In the slices stained with PAS, ten microphotographs (Magnification 400x) were obtained from different renal cortex fields of each kidney and glomerular diameter was quantified in at least 40 glomeruli per rat using a Nixon camera incorporated to the microscope. In the slices stained with Sirius red, five to eight subcortical periglomerular fields per section were randomly selected in kidneys from the groups studied (Magnification 100x). Tubulo-interstitial fibrosis consisted of extracellular matrix expansion with collagen deposition together with distortion and collapse of the tubules; fibrosis was evidenced by red coloration in Sirius red-stained slides. The affected area was delimited and the percentage of tubulointerstitial fibrosis was calculated by dividing the fibrotic by the total area, excluding the glomerular area. Researchers were blind to the experimental group.

To evaluate tubular cell proliferation, conventional immunoperoxidase assays for Ki67 (anti-Ki67 antibody, Abcam Cat. No. ab66155) were performed. For signal detection, HRP/DAB Detection System (Bio SB, Santa Barbara CA, USA Cat. No. BSB 0001) was used, slides were counterstain with hematoxylin. The number of Ki-67-positive epithelial cells on each slide was counted in at least 10-subcortical fields (100 \times magnification).

Hydrogen peroxide urinary excretion. In the urine collected during the follow-up time, the determination of urine hydrogen peroxides as an oxidative stress marker was carried out, using a commercial kit (Amplex Red Hydrogen Peroxide/Peroxidase Assay, Roche, Cat. No. A22188) following the manufacturer's instructions. The determination is based on the presence of peroxidase which, when reacted with hydrogen peroxide, produces a red-fluorescent compound, which was quantified in a spectrophotometer at 560 nm and extrapolated with a standard curve.

RNA extraction and quantitative PCR. The total RNA was isolated from the kidneys using the TRIzol method (Invitrogen, Carlsbad, CA, Cat. No. 15596026) and checked for integrity using 1% agarose gel electrophoresis. To avoid DNA contamination, total RNA samples were treated with DNase (DNase I; Invitrogen, Carlsbad, CA, Cat. No. 18068015). Reverse transcription (RT) was carried out with 1 μ g of total RNA and 200 U of Moloney murine leukemia virus reverse transcriptase (Invitrogen). The mRNA levels of *Hif1a*, *Vegfa*, pre-pro-endothelin (*Edn1*), endothelin receptor A (*Ednra*), endothelial NOS 3 (*NOS3*), transforming growth factor (*Tgfb1*), monocyte chemoattractant protein 1 (*Mcp1*), nuclear factor erythroid 2 like 2 (*Nfe2l2*), NADPH oxidase 4 (*Nox4*), collagen-1 (*Col1a1*) interleukin 6 (*Il6*), and interleukin 10 (*Il10*) were quantified by real-time PCR on an ABI Prism 7300 Sequence Detection System (TaqMan, ABI, Foster City, CA, Cat. No. 4331182). Primers and probes were ordered as a kit as follows: *Hif1a*, (Rn0057756_m1), *Vegfa* (Rn01511602_m1), *Edn1* (Rn00561129_m1), *Ednra* (Rn00561137_m1), *NOS3* (Rn004352204_m1), *Tgfb1* (Rn00572010_m1), *Mcp1* (Rn00580555_m1), *Nfe2l2* (Rn00582415_m1), *Nox4* (Rn00585380_m1), *Col1a1* (Rn1463848_m1), *Il6* (Rn01410330_m1), and *Il10* (Rn99999012_m1). As an endogenous control, eukaryotic 18S rRNA (predesigned assay reagent Applied by ABI, external run, Rn03928990_g1, Cat. No. 4319413E was used. The relative quantification of each gene expression was performed with the comparative threshold cycle (Ct) method.

Western blot and antibodies. The renal cortex proteins were homogenized with a lysis buffer containing: 50 mM HEPES pH 7.4, 250 mM NaCl, 5 mM EDTA, 0.1% NP-40 and complete protease inhibitor (Roche, Cat. No. 11,697,498,001). The proteins concentration was assessed by Lowry protein assay (Bio-Rad, Cat. No. 5000113 and 5,000,114). Renal cortex protein levels were detected by Western blot, tissue proteins (20–40 μ g) were electrophoresed in a denaturing 8.5% acrylamide gel with SDS. The samples were prepared with loading buffer in a 1:1 ratio with a final volume of 20 μ L. The membranes were incubated with the primary antibody TGF β (Thermo Fisher, Cat. No. MA5-15,065, 1:1000), HIF-1 α (Abcam, Cat. No. ab2185, 1:5000) VEGFA (Invitrogen, MA1-16,629, 1:5000), IL-6 (Abcam, Cat. No. ab9324, 1:1000), and HRP β -Actin antibody [AC-15] (Abcam, Cat. No. ab49900, 1:1,000,000) overnight at 4 $^{\circ}$ C. Three 10-min washes were performed with TBS-1 \times Tween and then incubated with the secondary antibody coupled to HRP, anti-rabbit or anti-mouse IgG (Santa Cruz, Cat. No. sc-2031 or sc-2004, respectively 1: 5000). Tissue proteins assessed by Western blot were normalized by β -Actin detection.

Detection of urinary biomarkers by western blot. Urinary HSP72 levels were detected by Western blot, each urine was diluted 1:10 in 0.9% saline solution, and 10 μ L of each dilution was loaded and resolved by 8.5% SDS-PAGE, as previously described^{39–42,64}. The membranes were incubated with mouse anti-HSP72 antibody (ENZO Life Sciences, Cat. No. ADI-SPA-819F, 1:5000 dilution) or KIM-1 (Boster, Cat. No. PA1632, 1:5000) overnight at 4 $^{\circ}$ C. Thereafter; membranes were incubated with a secondary antibody, HRP-conjugated goat anti-mouse IgG, or anti-rabbit IgG, respectively (1:5000, Cat. No. sc-2031 or sc-2004, respectively, Santa Cruz). The proteins were detected using a commercial chemiluminescence kit (Millipore, Cat. No. WBKLS0500) and were normalized by urinary creatinine (UCreat).

Genomic DNA extraction and quantification of global DNA methylation. For genomic DNA extraction, 50 mg of tissue was homogenized in 200 μ L of 1X PBS (10 mM PO₄, 137 mM NaCl, and 2.7 mM KCl), 60 μ L of digestion buffer (Tris-HCl 1 M, EDTA 0.5 M, SDS 10%, NaCl 5 M, pH = 8), then 26 μ L of Proteinase K (Sigma, Cat. No. P2308-100 mg, 10 mg/mL) was added and kept on ice for 5 min. Subsequently, the mixture was left overnight at 56 $^{\circ}$ C, then the samples were treated with 3 μ L of RNase A (Qiagen, Cat. No. 19101, 10 mg/mL) and incubated for 3 h at 37 $^{\circ}$ C. By the end, 250 μ L of phenol-chloroform-isoamyl alcohol (Sigma, Cat. No. 77617-100ML) was added, centrifuged for 20 min, 16.1 g at 4 $^{\circ}$ C. Only the upper phase was taken and 83 μ L of ammonium acetate (7.5 M) and 250 μ L of absolute ethanol were added. The samples were incubated at –20 $^{\circ}$ C overnight, centrifuged and the supernatant was discarded. Two washes were made with 250 μ L of 70% ethanol. The pellet was re-suspended in 200 μ L of DNase/RNase-Free Distilled Water. To analyze the global DNA methylation, the commercial methylation kit of 5mC DNA (Zymo Research Cat. No. D5326) was used, 100 ng of DNA from each sample was used and it was taken to a volume of 100 μ L with 5mC of coating buffer. The mix was incubated at 98 $^{\circ}$ C for 5 min and then left on ice for 10 min. Then it was added to the plate and incubated at 37 $^{\circ}$ C for 1 h and the excess was discarded and washed with 200 μ L of 5mC Elisa Buffer. Thereafter, 200 μ L of 5mC Elisa buffer was added to each well and incubated at 37 $^{\circ}$ C for 30 min. A mixture of 5-methyl cytosine primary antibody (1:2,000) and HRP-coupled secondary anti-rabbit antibody (1:1000) was added. Finally, 100 μ L of HRP developer was added to each well, incubated 1 h, and measured in a spectrometer at 405–450 nm. The results were extrapolated with a standard curve and the correction was made for the percentage of cytosines and guanine dinucleotides (CpGs), which have been previously reported for the rat genome⁶⁵.

Sequence analysis and bisulfite primer design. Three binding Hif1 α sequences in the promoter *Vegf* gene in the rat have been previously identified and were named as region 1 (–976 to –857), region 2 (–724 to –645), and region 3 (–470 to –369), respectively (Suppl. Fig. 1)⁵⁹. DataBase of CpG islands and Analytical Tool (DBCAT) (<http://dbcat.cgm.ntu.edu.tw>) software-assisted us to identify the CpG islands in the promoter and the first part of the coding regions of *Vegf* gene. This analysis showed that only regions 2 and 3 were enriched of CpG islands, suggesting that these regions are susceptible to methylation. Consequently, optimal primers were designed in the Methyl Primer Express software for bisulfite sequencing of *Hif-1 α* and *Vegf* gene promoters. For *Hif-1 α* the primers were: 5'-GTAGAGAGTAGAGATTGAGTT-3' (forward) and 5'-CAAAACCTAACC AAACACTAC-3' (reverse) that amplified the region from –1390 to –688 (702 bp): As was commented before there are three HIF1 α binding sequences in the promoter of *Vegfa*, but only two are susceptible to methylation:

the region 2, from –724 to –645, and the region 3, from –470 to –369, we amplified together with the following primers: 5'-GGTTTGTAGATTTATAGTG-3' (forward) and 5'-CCATAACCTAAAATTATCTATC-3' (reverse) yielding a product of 763 bp.

Sodium bisulfite DNA conversion and sequencing. Genomic DNA (3 µg) was processed with sodium bisulfite⁶⁶, DNA fragments of interest were PCR-amplified. The amplified DNA fragments were cloned into the pGEM-T Easy system (Promega, Cat. No. A1360), and Sanger sequenced using its respective reverse primer. At least 8 clones were evaluated for each region.

Statistical analysis. The results are presented as the mean ± SE. The significance of the differences between groups was assessed by 1-way ANOVA using the Bonferroni correction for multiple comparisons. All comparisons passed the normality test. Statistical significance was defined when the *p*-value was <0.05. All the graphs and statistical analyses were performed using the statistical GraphPad Prisma 8 software for Mac (GraphPad Software, San Diego, CA, USA).

Received: 5 November 2020; Accepted: 6 April 2021

Published online: 22 April 2021

References

- Chawla, L. S., Eggers, P. W., Star, R. A. & Kimmel, P. L. Acute kidney injury and chronic kidney disease as interconnected syndromes. *N. Engl. J. Med.* **371**, 58–66 (2014).
- Hsu, C. Y. *et al.* Impact of AKI on urinary protein excretion: analysis of two prospective cohorts. *J. Am. Soc. Nephrol.* **30**, 1271–1281. <https://doi.org/10.1681/ASN.2018101036> (2019).
- Bucaloiu, I. D., Kirchner, H. L., Norfolk, E. R., Hartle, J. E. & Perkins, R. M. Increased risk of death and de novo chronic kidney disease following reversible acute kidney injury. *Kidney Int.* **81**, 477–485 (2012).
- Chawla, L. S., Amdur, R. L., Amodeo, S., Kimmel, P. L. & Palant, C. E. The severity of acute kidney injury predicts progression to chronic kidney disease. *Kidney Int.* **79**, 1361–1369 (2011).
- Hatakeyama, Y. *et al.* Transition from acute kidney injury to chronic kidney disease: a single-centre cohort study. *Clin. Exp. Nephrol.* **22**, 1281–1293. <https://doi.org/10.1007/s10157-018-1571-5> (2018).
- Ishani, A. *et al.* Acute kidney injury increases risk of ESRD among elderly. *J. Am. Soc. Nephrol.* **20**, 223–228 (2009).
- Funk, J. A. & Schnellmann, R. G. Persistent disruption of mitochondrial homeostasis after acute kidney injury. *Am. J. Physiol. Ren. Physiol.* **302**, F853–F864. <https://doi.org/10.1152/ajprenal.00035.2011> (2012).
- Zuk, A. & Bonventre, J. V. Acute kidney injury. *Annu. Rev. Med.* **67**, 293–307. <https://doi.org/10.1146/annurev-med-050214-013407> (2016).
- Linkermann, A. *et al.* Two independent pathways of regulated necrosis mediate ischemia-reperfusion injury. *Proc. Natl. Acad. Sci. U. S. A.* **110**, 12024–12029. <https://doi.org/10.1073/pnas.1305538110> (2013).
- Dong, Y. *et al.* Ischemic duration and frequency determines AKI-to-CKD progression monitored by dynamic changes of tubular biomarkers in IRI mice. *Front Physiol.* **10**, 153. <https://doi.org/10.3389/fphys.2019.00153> (2019).
- Fiorentino, M., Grandaliano, G., Gesualdo, L. & Castellano, G. Acute kidney injury to chronic kidney disease transition. *Contrib. Nephrol.* **193**, 45–54. <https://doi.org/10.1159/000484962> (2018).
- Bonventre, J. V. Dedifferentiation and proliferation of surviving epithelial cells in acute renal failure. *J. Am. Soc. Nephrol.* **14**(Suppl 1), S55–61. <https://doi.org/10.1097/01.asn.0000067652.51441.21> (2003).
- Bonventre, J. V. & Yang, L. Cellular pathophysiology of ischemic acute kidney injury. *J. Clin. Invest.* **121**, 4210–4221 (2011).
- Bonventre, J. V. Maladaptive proximal tubule repair: cell cycle arrest. *Nephron Clin. Pract.* **127**, 61–64. <https://doi.org/10.1159/000363673> (2014).
- Okamura, D. M. & Pennathur, S. The balance of powers: redox regulation of fibrogenic pathways in kidney injury. *Redox Biol.* **6**, 495–504. <https://doi.org/10.1016/j.redox.2015.09.039> (2015).
- Lech, M. *et al.* Macrophage phenotype controls long-term AKI outcomes—kidney regeneration versus atrophy. *J. Am. Soc. Nephrol.* **25**, 292–304 (2014).
- Lee, S. *et al.* Distinct macrophage phenotypes contribute to kidney injury and repair. *J. Am. Soc. Nephrol.* **22**, 317–326 (2011).
- Zhang, M. Z. *et al.* CSF-1 signaling mediates recovery from acute kidney injury. *J. Clin. Invest.* **122**, 4519–4532 (2012).
- Kramann, R., Wongboonsin, J., Chang-Panesso, M., Machado, F. G. & Humphreys, B. D. Gli1(+) pericyte loss induces capillary rarefaction and proximal tubular injury. *J. Am. Soc. Nephrol.* **28**, 776–784. <https://doi.org/10.1681/ASN.2016030297> (2017).
- Yang, L., Besschetnova, T. Y., Brooks, C. R., Shah, J. V. & Bonventre, J. V. Epithelial cell cycle arrest in G2/M mediates kidney fibrosis after injury. *Nat. Med.* **16**, 535–543, 531p (2010).
- Lima-Posada, I. *et al.* Gender differences in the acute kidney injury to chronic kidney disease transition. *Sci. Rep.* **7**, 12270. <https://doi.org/10.1038/s41598-017-09630-2> (2017).
- Rodriguez-Romo, R. *et al.* AT1 receptor antagonism before ischemia prevents the transition of acute kidney injury to chronic kidney disease. *Kidney Int.* **89**, 363–373. <https://doi.org/10.1038/ki.2015.320> (2016).
- Humphreys, B. D. *et al.* Fate tracing reveals the pericyte and not epithelial origin of myofibroblasts in kidney fibrosis. *Am. J. Pathol.* **176**, 85–97. <https://doi.org/10.2353/ajpath.2010.090517> (2010).
- Kirita, Y., Wu, H., Uchimura, K., Wilson, P. C. & Humphreys, B. D. Cell profiling of mouse acute kidney injury reveals conserved cellular responses to injury. *Proc. Natl. Acad. Sci. U. S. A.* **117**, 15874–15883. <https://doi.org/10.1073/pnas.2005477117> (2020).
- Iwano, M. *et al.* Evidence that fibroblasts derive from epithelium during tissue fibrosis. *J. Clin. Invest.* **110**, 341–350. <https://doi.org/10.1172/JCI15518> (2002).
- Moll, S. *et al.* Epithelial cells as active player in fibrosis: findings from an in vitro model. *PLoS ONE* **8**, e56575 (2013).
- Barrera-Chimal, J. *et al.* Spironolactone prevents chronic kidney disease caused by ischemic acute kidney injury. *Kidney Int.* **83**, 93–103 (2013).
- Horbelt, M. *et al.* Acute and chronic microvascular alterations in a mouse model of ischemic acute kidney injury. *Am. J. Physiol. Ren. Physiol.* **293**, F688–F695 (2007).
- Basile, D. P., Donohoe, D., Roethe, K. & Osborn, J. L. Renal ischemic injury results in permanent damage to peritubular capillaries and influences long-term function. *Am. J. Physiol. Ren. Physiol.* **281**, F887–F899 (2001).
- Basile, D. P., Donohoe, D. L., Roethe, K. & Mattson, D. L. Chronic renal hypoxia after acute ischemic injury: effects of L-arginine on hypoxia and secondary damage. *Am. J. Physiol. Ren. Physiol.* **284**, F338–F348 (2003).

31. Kramann, R., Tanaka, M. & Humphreys, B. D. Fluorescence microangiography for quantitative assessment of peritubular capillary changes after AKI in mice. *J. Am. Soc.* **25**, 1924–1931 (2014).
32. Li, L. *et al.* FoxO3 activation in hypoxic tubules prevents chronic kidney disease. *J. Clin. Invest.* **130**, 2374–2389. <https://doi.org/10.1172/JCI122256> (2019).
33. Shu, S. *et al.* Endoplasmic reticulum stress is activated in post-ischemic kidneys to promote chronic kidney disease. *EBioMedicine* **37**, 269–280. <https://doi.org/10.1016/j.ebiom.2018.10.006> (2018).
34. Huang, N., Tan, L., Xue, Z., Cang, J. & Wang, H. Reduction of DNA hydroxymethylation in the mouse kidney insulted by ischemia reperfusion. *Biochem. Biophys. Res. Commun.* **422**, 697–702 (2012).
35. Pang, M. *et al.* Inhibition of histone deacetylase activity attenuates renal fibroblast activation and interstitial fibrosis in obstructive nephropathy. *Am. J. Physiol. Ren. Physiol.* **297**, F996–F1005 (2009).
36. Naito, M., Zager, R. A. & Bomsztyk, K. BRG1 increases transcription of proinflammatory genes in renal ischemia. *J. Am. Soc. Nephrol.* **20**, 1787–1796 (2009).
37. Bechtel, W. *et al.* Methylation determines fibroblast activation and fibrogenesis in the kidney. *Nat. Med.* **16**, 544–550 (2010).
38. Rodriguez-Romo, R., Berman, N., Gomez, A. & Bobadilla, N. A. Epigenetic regulation in the acute kidney injury (AKI) to chronic kidney disease transition (CKD). *Nephrol. (Carlton)* **20**, 736–743 (2015).
39. Barrera-Chimal, J. *et al.* Hsp72 is an early and sensitive biomarker to detect acute kidney injury. *EMBO Mol. Med.* **3**, 5–20 (2011).
40. Morales-Buenrostro, L. E. *et al.* Hsp72 is a novel biomarker to predict acute kidney injury in critically ill patients. *PLoS ONE* **9**, e109407 (2014).
41. Ortega-Trejo, J. A. *et al.* Heat shock protein 72 (Hsp72) specific induction and temporal stability in urine samples as a reliable biomarker of acute kidney injury (AKI). *Biomarkers* **20**, 453–459. <https://doi.org/10.3109/1354750X.2015.1096305> (2015).
42. Perez-Villalva, R. *et al.* HSP72 is an early biomarker to detect cisplatin and acetaminophen nephrotoxicity. *Biomarkers* **22**, 548–556. <https://doi.org/10.1080/1354750X.2017.1315616> (2017).
43. Reddy, M. A. & Natarajan, R. Recent developments in epigenetics of acute and chronic kidney diseases. *Kidney Int.* **88**, 250–261. <https://doi.org/10.1038/ki.2015.148> (2015).
44. Ronco, C., Bellomo, R. & Kellum, J. A. Acute kidney injury. *Lancet* **394**, 1949–1964. [https://doi.org/10.1016/S0140-6736\(19\)32563-2](https://doi.org/10.1016/S0140-6736(19)32563-2) (2019).
45. Mehta, R. L. *et al.* International society of nephrology's 0by25 initiative for acute kidney injury (zero preventable deaths by 2025): a human rights case for nephrology. *Lancet* **385**, 2616–2643. [https://doi.org/10.1016/S0140-6736\(15\)60126-X](https://doi.org/10.1016/S0140-6736(15)60126-X) (2015).
46. Basile, D. P. Rarefaction of peritubular capillaries following ischemic acute renal failure: a potential factor predisposing to progressive nephropathy. *Curr. Opin. Nephrol. Hypertens.* **13**, 1–7 (2004).
47. Rius, J. *et al.* NF-kappaB links innate immunity to the hypoxic response through transcriptional regulation of HIF-1alpha. *Nature* **453**, 807–811. <https://doi.org/10.1038/nature06905> (2008).
48. Iommarini, L., Porcelli, A. M., Gasparre, G. & Kurelac, I. Non-canonical mechanisms regulating hypoxia-inducible factor 1 alpha in cancer. *Front Oncol.* **7**, 286. <https://doi.org/10.3389/fonc.2017.00286> (2017).
49. Liu, Y., Cox, S. R., Morita, T. & Kourembanas, S. Hypoxia regulates vascular endothelial growth factor gene expression in endothelial cells. Identification of a 5' enhancer. *Circ. Res.* **77**, 638–643. <https://doi.org/10.1161/01.res.77.3.638> (1995).
50. Pugh, C. W. & Ratcliffe, P. J. Regulation of angiogenesis by hypoxia: role of the HIF system. *Nat. Med.* **9**, 677–684. <https://doi.org/10.1038/nm0603-677> (2003).
51. Semenza, G. L. Hydroxylation of HIF-1: oxygen sensing at the molecular level. *Physiol. Bethesda* **19**, 176–182. <https://doi.org/10.1152/physiol.00001.2004> (2004).
52. Yu, X. *et al.* The balance of beneficial and deleterious effects of hypoxia-inducible factor activation by prolyl hydroxylase inhibitor in rat remnant kidney depends on the timing of administration. *Nephrol. Dial. Trans.* **27**, 3110–3119 (2012).
53. Basile, D. P. *et al.* Impaired endothelial proliferation and mesenchymal transition contribute to vascular rarefaction following acute kidney injury. *Am. J. Physiol. Ren. Physiol.* **300**, F721–F733 (2011).
54. Basile, D. P., Friedrich, K., Chelladurai, B., Leonard, E. C. & Parrish, A. R. Renal ischemia reperfusion inhibits VEGF expression and induces ADAMTS-1, a novel VEGF inhibitor. *Am. J. Physiol. Ren. Physiol.* **294**, F928–F936 (2008).
55. Leonard, E. C., Friedrich, J. L. & Basile, D. P. VEGF-121 preserves renal microvessel structure and ameliorates secondary renal disease following acute kidney injury. *Am. J. Physiol. Ren. Physiol.* **295**, F1648–F1657 (2008).
56. Pisani, F. *et al.* Potential role of the methylation of VEGF gene promoter in response to hypoxia in oxygen-induced retinopathy: beneficial effect of the absence of AQP4. *J. Cell Mol. Med.* **22**, 613–627. <https://doi.org/10.1111/jcmm.13348> (2018).
57. Sundrani, D. P. *et al.* Differential placental methylation and expression of VEGF, FLT-1 and KDR genes in human term and preterm preeclampsia. *Clin. Epigenet.* **5**, 6. <https://doi.org/10.1186/1868-7083-5-6> (2013).
58. Siddique, A. N. *et al.* Targeted methylation and gene silencing of VEGF-A in human cells by using a designed Dnmt3a-Dnmt3L single-chain fusion protein with increased DNA methylation activity. *J. Mol. Biol.* **425**, 479–491. <https://doi.org/10.1016/j.jmb.2012.11.038> (2013).
59. Shinagawa, M. *et al.* C/EBPbeta regulates Vegf gene expression in granulosa cells undergoing luteinization during ovulation in female rats. *Sci. Rep.* **9**, 714. <https://doi.org/10.1038/s41598-018-36566-y> (2019).
60. Lando, D., Peet, D. J., Whelan, D. A., Gorman, J. J. & Whitelaw, M. L. Asparagine hydroxylation of the HIF transactivation domain a hypoxic switch. *Science* **295**, 858–861. <https://doi.org/10.1126/science.1068592> (2002).
61. Mahon, P. C., Hirota, K. & Semenza, G. L. FIH-1: a novel protein that interacts with HIF-1alpha and VHL to mediate repression of HIF-1 transcriptional activity. *Genes Dev.* **15**, 2675–2686. <https://doi.org/10.1101/gad.924501> (2001).
62. Schmidlin, C. J., Dodson, M. B., Madhavan, L. & Zhang, D. D. Redox regulation by NRF2 in aging and disease. *Free Radic. Biol. Med.* **134**, 702–707. <https://doi.org/10.1016/j.freeradbiomed.2019.01.016> (2019).
63. Soofi, A., Kutschat, A. P., Azam, M., Laszczyk, A. M. & Dressler, G. R. Regeneration after acute kidney injury requires PTIP-mediated epigenetic modifications. *JCI Insight* <https://doi.org/10.1172/jci.insight.130204> (2020).
64. Institute of Laboratory Animal Resources (U.S.). Committee on care and use of laboratory animals. In *NIH Publication Volumes* (U.S. Dept. of Health and Human Services, Public Health Service, Bethesda, Md.).
65. Han, L., Su, B., Li, W. H. & Zhao, Z. CpG island density and its correlations with genomic features in mammalian genomes. *Genome Biol.* **9**, R79. <https://doi.org/10.1186/gb-2008-9-5-r79> (2008).
66. Valdes-Quezada, C., Arriaga-Canon, C., Fonseca-Guzman, Y., Guerrero, G. & Recillas-Targa, F. CTCF demarcates chicken embryonic alpha-globin gene autonomous silencing and contributes to adult stage-specific gene expression. *Epigenetics* **8**, 827–838. <https://doi.org/10.4161/epi.25472> (2013).

Acknowledgements

We are grateful to Mariela Contreras's staff for their aid with animal care. The results presented in this paper have not been published previously in whole or in part, except as an abstract presented at the American Society of Nephrology Kidney Week Meeting 2016 (Chicago, IL), and World Congress of Nephrology ISN 2017 (Mexico City, Mexico).

Author contributions

Conception and design A.S.N. and N.A.B. Performed the experiments and analytical techniques A.S.N., R.P.V., A.R.M.O., M.A.M.R., J.R.R.A., N.G. and M.C.B. Acquisition of data: A.S.N., and N.A.B. Analysis and interpretation of data; N.A.B., A.S.N. and F.R.T. Drafting the article and revising it critically for important intellectual content; N.A.B., A.S.N., F.R.T. and G.G.

Funding

This study was supported by Grants from the Mexican Council of Science and Technology (CONACyT) (A1-S-8715, 300151, 235855, and 235964 to NAB) and from the Universidad Nacional Autónoma de México (IN201619 to NAB). This study was performed in partial fulfillment of the requirements for the PhD degree, Andrea Sánchez-Navarro is a doctoral student from Programa de Doctorado en Ciencias Biomédicas, Universidad Nacional Autónoma de México (UNAM) and received a fellowship from CONACYT (607517).

Competing interests

The authors declare no competing interests.

Additional information

Supplementary Information The online version contains supplementary material available at <https://doi.org/10.1038/s41598-021-88000-5>.

Correspondence and requests for materials should be addressed to N.A.B.

Reprints and permissions information is available at www.nature.com/reprints.

Publisher's note Springer Nature remains neutral with regard to jurisdictional claims in published maps and institutional affiliations.



Open Access This article is licensed under a Creative Commons Attribution 4.0 International License, which permits use, sharing, adaptation, distribution and reproduction in any medium or format, as long as you give appropriate credit to the original author(s) and the source, provide a link to the Creative Commons licence, and indicate if changes were made. The images or other third party material in this article are included in the article's Creative Commons licence, unless indicated otherwise in a credit line to the material. If material is not included in the article's Creative Commons licence and your intended use is not permitted by statutory regulation or exceeds the permitted use, you will need to obtain permission directly from the copyright holder. To view a copy of this licence, visit <http://creativecommons.org/licenses/by/4.0/>.

© The Author(s) 2021

RESEARCH ARTICLE

Mechanisms of Renal Electrolyte Transport and Ion Channel Regulation in Honor of Dr. Gerhard Giebisch

Role of KLHL3 and dietary K⁺ in regulating KS-WNK1 expression

Mauricio Ostrosky-Frid,^{1,2} María Chávez-Canales,³ Jinwei Zhang,⁴ Olena Andrukhova,^{5†} Eduardo R. Argáiz,¹ Fernando Lerdo-de-Tejada,³ Adrian Murillo-de-Ozores,^{6,7} Andrea Sanchez-Navarro,^{1,7} Lorena Rojas-Vega,⁷ Norma A. Bobadilla,^{1,7} Norma Vazquez,¹ María Castañeda-Bueno,⁷ Dario R. Alessi,⁵ and Gerardo Gamba^{1,2,7}

¹Molecular Physiology Unit, Instituto de Investigaciones Biomédicas, Universidad Nacional Autónoma de México, Mexico City, Mexico; ²PECEM (MD/PhD), Facultad de Medicina, Universidad Nacional Autónoma de México, Mexico City, Mexico; ³Unidad de Investigación UNAM-INC, Instituto Nacional de Cardiología Ignacio Chávez and Instituto de Investigaciones Biomédicas, Universidad Nacional Autónoma de México, Mexico City, Mexico; ⁴Institute of Biomedical and Clinical Sciences, Medical School, College of Medicine and Health, University of Exeter, Hatherly Laboratories, Exeter, United Kingdom; ⁵MRC Protein Phosphorylation and Ubiquitylation Unit, College of Life Sciences, University of Dundee, Dundee, United Kingdom; ⁶Facultad de Medicina, Universidad Nacional Autónoma de México, Mexico City, Mexico; and ⁷Department of Nephrology and Mineral Metabolism, Instituto Nacional de Ciencias Médicas y Nutrición Salvador Zubirán, Mexico City, Mexico

Abstract

The physiological role of the shorter isoform of with no lysine kinase (WNK)1 that is exclusively expressed in the kidney (KS-WNK1), with particular abundance in the distal convoluted tubule, remains elusive. KS-WNK1, despite lacking the kinase domain, is nevertheless capable of stimulating the NaCl cotransporter, apparently through activation of WNK4. It has recently been shown that a less severe form of familial hyperkalemic hypertension featuring only hyperkalemia is caused by missense mutations in the WNK1 acidic domain that preferentially affect cullin 3 (CUL3)-Kelch-like protein 3 (KLHL3) E3-induced degradation of KS-WNK1 rather than that of full-length WNK1. Here, we show that full-length WNK1 is indeed less impacted by the CUL3-KLHL3 E3 ligase complex compared with KS-WNK1. We demonstrated that the unique 30-amino acid NH₂-terminal fragment of KS-WNK1 is essential for its activating effect on the NaCl cotransporter and recognition by KLHL3. We identified specific amino acid residues in this region critical for the functional effect of KS-WNK1 and KLHL3 sensitivity. To further explore this, we generated KLHL3-R528H knockin mice that mimic human mutations causing familial hyperkalemic hypertension. These mice revealed that the KLHL3 mutation specifically increased expression of KS-WNK1 in the kidney. We also observed that in wild-type mice, the expression of KS-WNK1 was only detectable after exposure to a low-K⁺ diet. These findings provide new insights into the regulation and function of KS-WNK1 by the CUL3-KLHL3 complex in the distal convoluted tubule and indicate that this pathway is regulated by dietary K⁺ levels.

NEW & NOTEWORTHY In this work, we demonstrated that the kidney-specific isoform of with no lysine kinase 1 (KS-WNK1) in the kidney is modulated by dietary K⁺ and activity of the ubiquitin ligase protein Kelch-like protein 3. We analyzed the role of different amino acid residues of KS-WNK1 in its activity against the NaCl cotransporter and sensitivity to Kelch-like protein 3.

distal convoluted tubule; hypertension; salt transport; STE20/SPS1-related proline-alanine-rich protein kinase; with no lysine kinase 4

INTRODUCTION

Familial hyperkalemic hypertension (FHHT) encompasses a spectrum of diseases that are mainly the consequence of over-activity of the renal thiazide-sensitive NaCl cotransporter (NCC) of the distal convoluted tubule (DCT) (1). NCC activity is modulated by with no lysine kinase (WNK)1 and WNK4, whose half-life is, in turn, regulated by the cullin-RING E3

ligase complex containing Kelch-like protein 3 (KLHL3) and cullin 3 (CUL3) proteins. The severity of FHHT depends on which one of these genes is affected and is defined by age of diagnosis, K⁺ levels, blood pressure levels, and percentage of affected individuals with hypertension before the age of 18 yr old. The more severe disease presentation is due to exon 9 deletion of CUL3, followed by dominant or recessive mutations in KLHL3 (2, 3). These mutations impair the ubiquitylation



† Deceased 3 October 2017.

Correspondence: G. Gamba (gamba@iibiomedicas.unam.mx).

Submitted 27 October 2020 / Revised 3 March 2021 / Accepted 3 March 2021



and degradation of WNK kinases in the DCT. Less severe is FHHt due to missense mutations in the acidic motif of WNK4, which constitutes the recognition site for KLHL3 (4, 5) and thus abrogate only WNK4 ubiquitylation (6). Finally, the mildest form of FHHt is due to intronic deletions in the *WNK1* gene that apparently result in ectopic expression of the full-length catalytic isoform of this kinase (known as L-WNK1) in the DCT (7). Louis-Dit-Picard et al. (8) have recently described, however, an even milder form of FHHt. In this work, humans and mice with heterozygous mutations in the acidic domain of WNK1 display an inherited phenotype with hyperkalemia, hyperchloremia, and metabolic acidosis, but without arterial hypertension, that is nevertheless accompanied by low renin expression levels, suggesting a mild volume expansion that is, however, not enough to produce hypertension.

The major product of the *WNK1* gene in the kidney is a shorter isoform known as kidney-specific WNK1 (KS-WNK1) (9–11). This isoform is transcribed from an alternative promoter located between exons 4 and 4a that lacks the kinase domain and contains a unique 30-amino acid residues sequence encoded by exon 4a. Despite lacking a kinase domain, recent evidence suggests that KS-WNK1 may function as an activator of NCC. First, in *Xenopus laevis* oocytes, we have shown that KS-WNK1 is able to induce phosphorylation and activation of NCC by interacting with other WNKs and reducing its sensitivity to Cl^- . For instance, in the presence of KS-WNK1, WNK4 is active at higher levels of intracellular Cl^- concentration, increasing the activity of the intermediate kinase, STE20/SPS1-related proline-alanine-rich protein kinase (SPAK), toward NCC (12). Second, it has been observed that under conditions in which NCC activity is expected to be increased, like in response to low dietary K^+ , conglomerations of WNKs, known as WNK bodies, are formed in DCT cells, and their formation requires the presence of KS-WNK1 (13, 14), also supporting that KS-WNK1 is associated with activation of NCC. Third, Louis-Dit-Picard et al. (8) suggested that the FHHt phenotype observed in patients with mutations in the acidic domain of WNK1 is likely due to increased protein expression of KS-WNK1 in DCT cells because it was observed that the sensitivity of KS-WNK1 to the CUL3-KLHL3 E3 ligase complex is several times higher than that of L-WNK1 and, thus, mutations of the acidic motif in WNK1 seem to preferentially protect KS-WNK1 from ubiquitylation by the CUL3-KLHL3 E3 ligase complex.

Given that both KS-WNK1 and L-WNK1 contain the acidic motif involved in KLHL3 binding, the different sensitivity to CUL3-KLHL3 E3 ligase complex-mediated degradation is surprising. Our goal in the present study was to analyze and characterize the effect of the CUL3-KLHL3 E3 ligase complex on KS-WNK1 and to define the protein domains responsible for the difference in sensitivity. In addition, we began to explore the physiological stimuli that regulate KS-WNK1 protein expression levels by modulating its targeting to degradation by the CUL3-KLHL3 E3 complex.

METHODS

Generation of *KLHL3*^{+/R528H} Mice

KLHL3^{+/R528H} knockin mice were generated through homologous recombination strategies by TaconicArtemis

(<https://www.taconic.com/>). For vector construction, mouse genomic fragments (obtained from the C57BL/6J RPCIB-731 BAC library) and selected features (such as desired point mutation, recombination sites, and selection markers, as provided in Supplemental Fig. S1; see <https://doi.org/10.6084/m9.figshare.13721791>) were assembled into the targeting vector.

The linearized vector was transfected into the TaconicArtemis C57BL/N Tac embryonic stem (ES) cell line. Homologous recombinant clones were isolated using positive (PuroR) and negative [thymidine kinase (TK)] selection. Specific ES clones were selected by Southern blot analysis of genomic DNA. Blastocysts were isolated from the uterus of pregnant BALB/c females at *day postcoitum* 3.5 and injected with 10–15 targeted C57BL/6NTac ES cells. After recovery, eight injected blastocysts were transferred to each uterine horn of 2.5 days postcoitum, pseudopregnant Naval Medical Research Institute (NMRI) females. Chimerism was measured in chimeras (G_0) by coat color contribution of ES cells to the BALB/c host (black/white). Highly chimeric mice were bred to C57BL/6-Tg(CAG-Flpe)2 Arte females for elimination of the puromycin resistance cassette. This produced mice that constitutively express mutated KLHL3 protein. The remaining FRT recombination site in these mice is located in a nonconserved region of the genome. Primers 6560_31 (5'-CACTGTGTTCTGCCTTTCAGG-3') and 6560_32 (5'-CAGACCAAGAC-CAGAGAGAAGG-3') were used to confirm the presence of the R528H mutation by PCR amplification and product sequencing.

For genotyping analysis, genomic DNA was extracted from tail biopsies and analyzed by PCR. *Primer 1* (5'-GATACCCACTGGCATTGG-3') and *primer 2* (5'-GGTAAGGGCAG-CATTACTGG-3') were used to detect wild-type and knockin alleles. The wild-type allele generates a 308-bp product, whereas the knockin allele generates a 383-bp product. The latter product is larger due to the presence of the FRT site and flanking region that remains in an intronic region following Flp-mediated excision of the puromycin selection cassette.

Generation of *KLHL3*^{R528H/R528H}/*KS-WNK1*^{-/-} Mice

KS-WNK1^{-/-} mice were a kind gift from Hadchouel (15) (INSERM Paris), and the generation and genotyping have been described in the supporting information of the cited article.

Mice were crossed with *KLHL3*^{+/R528H} to produce the desired genotypes: wild type, *KLHL3*^{R528H/R528H}, *KS-WNK1*^{-/-}, and *KLHL3*^{R528H/R528H}/*KS-WNK1*^{-/-}. Male mice were used for experimental purposes.

Low- K^+ Diet Experiments

Wild-type and *KLHL3*^{+/R528H} mice were placed on normal (1% K^+) or K^+ -deficient diets (0.0% K^+) for 4 days. The OpenStandard diet with no added K^+ (D16120202) was purchased from Research Diets and used as the K^+ -deficient diet. The normal- K^+ diet was prepared by adding KCl. By the end of the 4-day period, mice were euthanized under isoflurane anesthesia, and kidney samples were collected.

Western Blot Analysis of Mouse Kidney Proteins

Kidney lysates were prepared with lysis buffer containing 50 mM Tris-HCl (pH 7.5), 1 mM EGTA, 1 mM EDTA, 50 mM sodium fluoride, 5 mM sodium pyrophosphate, 1 mM

sodium orthovanadate, 1% (w/v) Nonidet P-40, 0.27 M sucrose, 0.1% (v/v) 2-mercaptoethanol, and protease inhibitors (1 tablet per 50 mL). Lysates (20 µg) in SDS sample buffer were subjected to electrophoresis on polyacrylamide gels and transferred to nitrocellulose membranes. Membranes were incubated for 30 min with Tris-buffered saline-Tween 20 (TBS-T) containing 5% (w/v) skim milk. Membranes were then immunoblotted in 5% (w/v) skim milk in TBS-T with the indicated primary antibodies overnight at 4°C. Sheep antibodies were used at a concentration of 1–2 µg/mL. The incubation with phospho-specific sheep antibodies was performed with the addition of 10 µg/mL of the dephospho-peptide antigen used to raise the antibody. Blots were then washed six times with TBS-T and incubated for 1 h at room temperature with secondary horseradish peroxidase (HRP)-conjugated antibodies diluted 5,000-fold in 5% (w/v) skim milk in TBS-T. After the washing steps were repeated, the signal was detected with an enhanced chemiluminescence reagent. Immunoblots were developed using a film automatic processor (SRX-101, Konica Minolta Medical), and films were scanned with 600-dpi resolution on a scanner (PowerLook 1000, UMAX).

For the detection of KS-WNK1, kidney tissue was homogenized in lysis buffer containing 250 mM sucrose, 10 mM triethanolamine, 1× protease inhibitors (Roche), 50 mM sodium fluoride, 10 mM sodium pyrophosphate, and 1 mM sodium orthovanadate.

Protein samples were subjected to polyacrylamide gel electrophoresis and then transferred to PVDF membranes for 2 h at 10 mV. Membranes were blocked for 2 h in 10% nonfat dry milk dissolved in TBS-T solution (2 mM Tris-HCl, 150 mM NaCl, and 0.2% Tween 20, pH 7.5).

Membranes were incubated overnight with the indicated antibodies diluted in 5% nonfat dry milk in TBS-T, followed by incubation for 1 h at room temperature with HRP-conjugated secondary antibodies diluted in 5% nonfat dry milk in TBS-T. After the incubation, membranes were washed six times for 10 min with TBS-T. For signal detection by chemiluminescence, Luminata Forte Western HRP substrate (Merck Millipore) was used, and LI-COR equipment was used to perform the reading.

The following antibodies were used. Rabbit anti-WNK4 (1:4,000) was a gift from David Ellison (Oregon Health & Science University) (16). For WNK1 detection, we used commercially available rabbit anti-WNK1 antibody from Bethyl Laboratories (1:1,000, A301-515A, pan-WNK1). The following antibodies were raised in the sheep and affinity purified on the appropriate antigen by the Division of Signal Transduction Therapy Unit of the University of Dundee: WNK4 total antibody (S064B, second bleed, raised against residues 1,221–1,243 of human WNK4), NCC phospho-Thr⁶⁰ antibody (S995B, residues 54–66 of human NCC phosphorylated at Thr⁶⁰, RTFGYNpTIDVVPT), NCC total antibody (S965B, residues 906–925 of human NCC, CHTKRFEDM-IAPFRLNDGFKD), SPAK NH₂-terminal antibody (S668D, raised against residues 2–76 of mouse SPAK), oxidative stress response-1 (OSR1) mouse antibody (S149C, residues 389–408 of mouse OSR1, SAHLPQAGQMPTQPAQVSL), SPAK/OSR1 (S motif) phospho-Ser³⁷³/Ser³²⁵ antibody [S670B, raised against residues 367–379 of human SPAK, RRVPGS(S)GHLHKT, which is highly similar to residues 319–331 of human OSR1, in which the sequence is RRVPGS(S)GRLHKT]. α-Epithelial Na⁺

channel (ENaC) antibody was kindly provided by Land (17); p44/42 MAPK (Erk1/2) antibody (3062) was purchased from Cell Signaling Technology. Secondary antibodies coupled to HRP used for immunoblot analysis were obtained from Pierce. All antibodies used and their corresponding validation studies are cited in Supplemental Table S1; see <https://doi.org/10.6084/m9.figshare.13721797>.

Immunofluorescent Staining of Mouse Kidney Sections

Harvested mouse kidneys were immersion fixed in fresh 4% (w/v) formaldehyde-PBS (pH 6.9) for 16 h at 37°C, washed three times in PBS, and stored at 4°C until paraffin embedded. Sections (5 µm) were deparaffinized in Histoclear (National Diagnostics) and rehydrated in graded methanol steps. An antigen retrieval step was performed with R-Universal buffer in the 2100 antigen retriever for a single heat-pressure cycle (Aptum Biologics). Sections were permeabilized with 0.05% (v/v) Triton X-100-PBS for 20 min and blocked for 1 h at 37°C with 2% (v/v) donkey serum in 0.05% (v/v) Triton X-100-PBS. Primary antibodies were incubated overnight for 16 h at 4°C at the following concentrations diluted in 1% (v/v) donkey serum in 0.05% (v/v) Triton X-100-PBS: 2 µg/mL for total SPAK and phospho-SPAK S373 and anti-α-ENaC (Novus Biologicals, 1:500). Phospho-specific antibodies included the addition of 10 µg/mL of the nonphosphopeptide used to raise the antibody per 2 µg/mL of antibody used. Negative controls omitted the primary antibody and were processed in parallel. Slides were then washed for 20 min in 0.05% (v/v) Triton X-100-PBS and incubated in secondary antibody for 1 h at 37°C. Preabsorbed donkey IgG-conjugated Alexa Fluor 488, 633, and 647 secondary antibodies (Life Technologies/Abcam) were used at 1:200 diluted in 1% (v/v) donkey serum in 0.05% (v/v) Triton X-100-PBS for immunofluorescent labeling. Slides were washed as above, counterstained using Sytox orange nucleic acid stain (S11368, Life Technologies), mounted using Prolong gold antifade (P36930, Life Technologies), and shielded from light.

Mutagenesis and Constructs

Rat NCC, human WNK4-Flag, human L-WNK1-Δ11-c-Myc, and human KS-WNK1-Δ11-c-Myc have been previously described (12, 18, 19). KS-WNK1-Δ4a, KS-WNK1-2CxS (KS-2CxS), KS-WNK1-6CxS (KS-6CxS), KS-WNK1-5Q (KS-5Q), KS-WNK1-V11A, KS-WNK1-F12A, KS-WNK1-V13A, KS-WNK1-I14A, and KS-WNK1-I15A were made from KS-WNK1-Δ11 using the QuikChange mutagenesis system (Stratagene). All modifications were confirmed by DNA sequencing. cRNA was made from linearized cDNA using the T7 RNA polymerase mMESSAGE kit (Ambion). The KLHL3-Flag clone was a gift from Richard P. Lifton (Rockefeller University). The open reading frame was subcloned into a pGEMHE vector.

Functional Expression of NCC

Oocytes were extracted in clusters from adult female *X. laevis* frogs anesthetized by submerging them in 0.17% Tricaine. Oocytes were incubated with collagenase type 2 (3 mg/mL) eluted in Ca²⁺-free ND-96 (96 mM NaCl, 2 mM KCl, 1.0 mM MgCl₂, and 5 mM HEPES, pH 7.4) for 1.5 h, washed three times with Ca²⁺-free ND-96, and incubated again with collagenase type 2 for 1.5 h. Oocytes were washed with ND-

96 solution (96.0 mM NaCl, 2.0 mM KCl, 1.8 mM CaCl₂, 1.0 mM MgCl₂, and 5.0 mM HEPES, pH 7.4) three times and incubated overnight at 16°C.

Oocytes were injected with 20 ng of each of the indicated cRNAs and then incubated at 16°C for 48 h in ND-96 before protein extraction for Western blot analysis or 72 h before transport experiments. MG132 (100 μM) was added to the media 16 h before protein extraction in the described cases.

Consent for the Performance of Animal Experiments

The use of *X. laevis* oocytes as well as wild-type and transgenic mice were approved by Institutional Animal Care and Use Committee of the Instituto Nacional de Ciencias Medicas y Nutricion Salvador Zubiran and in accordance with regulations set by the Universities of Cambridge and Dundee and the United Kingdom Home Office. Only male mice at 12–16 wk old were used.

Western Blot Analysis of *X. laevis* Oocyte Proteins

Twenty oocytes per experimental group were collected, and samples were extracted using 5 μL/oocyte of lysis buffer containing 50 mM Tris-HCl (pH 7.5), 1 mM EGTA, 1 mM EDTA, 50 mM sodium fluoride, 10 mM sodium pyrophosphate, 1 mM sodium orthovanadate, 1% (w/v) Nonidet P-40, 0.27 M sucrose, and protease inhibitors (Complete tablets, Roche).

Western blots were performed as described above. The antibody concentrations used were anti-Flag 1:5,000 (Sigma), anti-Myc 1:1,000 (Sigma), and anti-actin 1:2,500 (Santa Cruz Biotechnology). Densitometric analysis was performed using ImageStudioLite software.

Transport Assays

NCC activity was evaluated using the radioactive tracer ²²Na⁺ (Perkin Elmer Life Sciences). Oocytes were injected as previously described; 72 h later, 15 oocytes per group were incubated at room temperature for 30 min in Cl⁻-free ND-96 medium [containing (in mM) 96 sodium isethionate, 2 potassium gluconate, 1.8 calcium gluconate, 1 magnesium gluconate, and 5 HEPES, pH 7.4] containing 1 mM ouabain, 100 μM amiloride, and 100 μM bumetanide in the presence or absence of 100 μM trichlormethiazide. Oocytes were transferred to K⁺-free uptake medium [containing (in mM) 40 NaCl, 56 NMDG-Cl, 1.8 CaCl₂, 1 MgCl₂, and 5 HEPES, pH 7.4] with ouabain, amiloride, and bumetanide with or without trichlormethiazide and with 0.5 μCi of ²²Na⁺ for 60 min at 32°C. Oocytes were washed five times in an ice-cold radioactive-free medium and placed in individual tubes with 1%

SDS. After lysis scintillation counting, liquid (ecolume, MP Biomedicals) was added.

Statistical Analysis

In experiments with $n \geq 3$, statistical significance was calculated with one-way ANOVA with multiple comparisons using GraphPad Prism 8.4.3. Significance was defined as $P \leq 0.05$. Results are presented as means ± SEM.

RESULTS

Generation and Characterization of a New Strain of KLHL3 Knockin Mice

KLHL3 knockin mice carrying the FHHt mutation R528H that prevents binding to WNK kinases (20, 21) were generated by TaconicArtemis (<http://www.taconic.com/wmspage.cfm?parm1=1453>).

Phenotypic characterization under basal conditions showed that the mice displayed the expected FHHt-like phenotype with hyperkalemia, metabolic acidosis, and hyperchloremia (Table 1). The abundance and phosphorylation of relevant renal transporters and regulatory proteins were also studied. As previously reported for a *KLHL3*^{+ /R528H} strain generated by Susa and collaborators (22), higher WNK4 and NCC expression levels as well as higher NCC (Thr⁶⁰) and SPAK (Ser³⁷³) phosphorylation levels were observed in *KLHL3*^{+ /R528H} mice compared with wild-type mice. These differences were more dramatic in *KLHL3*^{R528H/R528H} mice (Fig. 1). In homozygotes, SPAK and OSR1 expression levels were also higher than in wild-type mice. Additionally, in contrast to what was reported by Susa et al., a clear decrease in the abundance of the full-length and cleaved forms of α-ENaC was observed in both *KLHL3*^{+ /R528H} and *KLHL3*^{R528H/R528H} mice made for this study. This finding was corroborated by immunofluorescent staining of kidney sections (Fig. 2). Finally, in sections stained with SPAK and phospho-SPAK (Ser³⁷³) antibodies, a punctate signal was observed in the cytoplasm of some cortical tubular cells of *KLHL3*^{+ /R528H} and *KLHL3*^{R528H/R528H} mice that contrasted with the apical signal observed in wild-type mice. In the medullary portion, an apical expression pattern was observed in some tubules of wild-type and mutant mice, and this signal intensity was higher in mutant mice.

KS-WNK1 Is Highly Sensitive to CUL3-KLHL3 E3 Ligase Complex-Mediated Degradation in Vivo

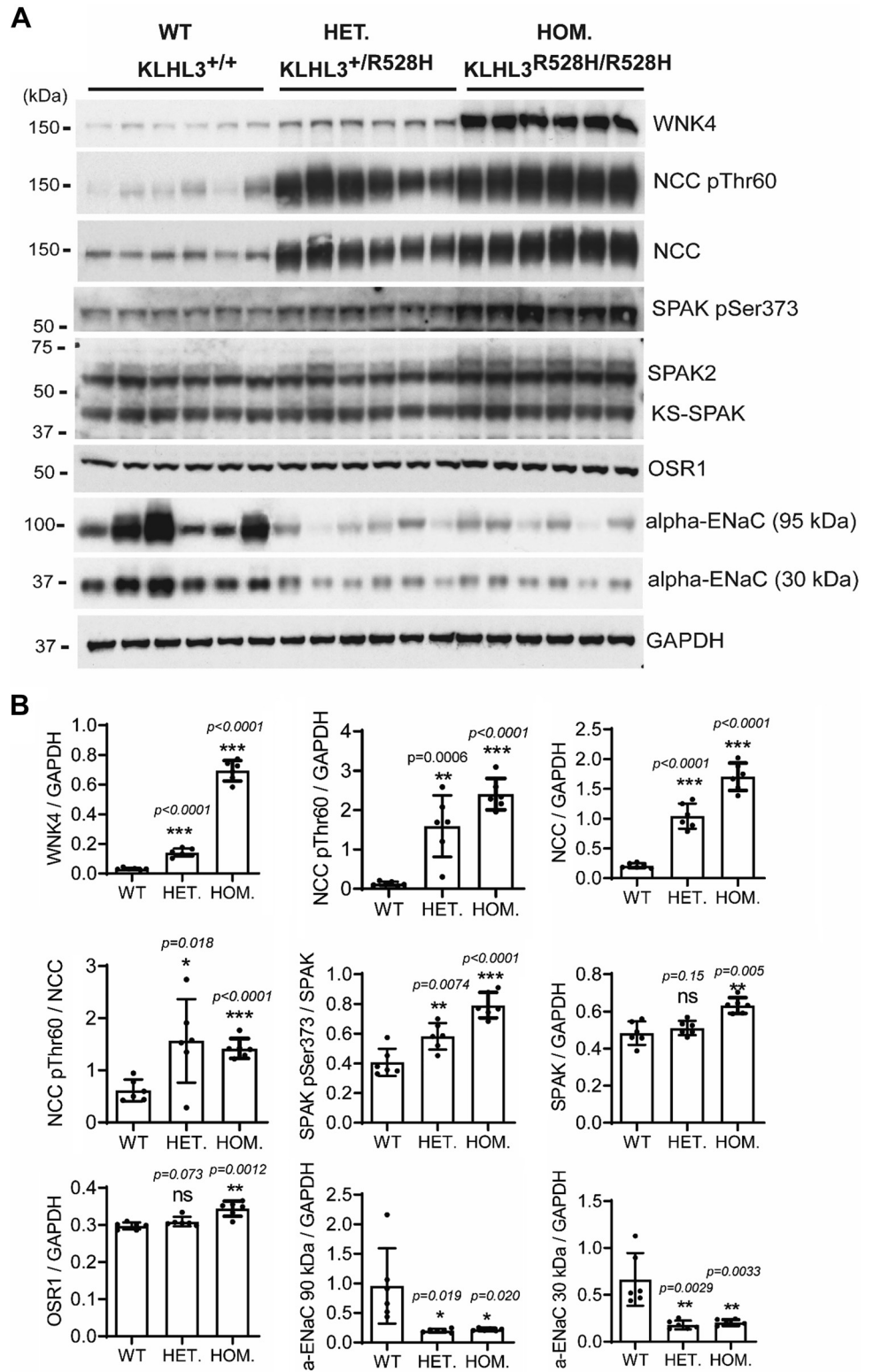
To analyze the effect of the KLHL3-R528H mutation on WNK1 expression, we used an antibody directed against a COOH-termi-

Table 1. Serum electrolytes of wild-type, *KLHL3*^{+ /R528H}, and *KLHL3*^{R528H/R528H} mice

	<i>KLHL3</i> ^{+ /+}	<i>KLHL3</i> ^{+ /R528H}	<i>KLHL3</i> ^{R528H/R528H}
Na ⁺ , mM	146.6 ± 1.06 (n = 17)	147.3 ± 0.45 (n = 28)	148.5 ± 0.77 (n = 16)
K ⁺ , mM	4.63 ± 0.09 (n = 18)	5.40 ± 0.1 (n = 28)*	5.56 ± 0.13 (n = 16)*
Cl ⁻ , mM	115.3 ± 1.46 (n = 17)	123.8 ± 1.94 (n = 24)*	123.3 ± 2.03 (n = 14)*
Ca ²⁺ , mM	2.21 ± 0.05 (n = 4)	2.28 ± 0.05 (n = 5)	2.36 ± 0.09 (n = 5)
pH	7.32 ± 0.03 (n = 6)	ND	7.18 ± 0.03 (n = 3)*

Data are means ± SE; n represents the number of mice included in the analyses. KLHL3, Kelch-like protein 3. * $P < 0.05$ versus wild-type mice.

Figure 1. Kelch-like protein 3 (*KLHL3*^{+ /R528H} and *KLHL3*^{R528H/R528H} mice display the expected changes in the expression and phosphorylation levels of components of the with no lysine kinase 4 (WNK4)-STE20/SPS1-related proline-alanine-rich protein kinase (SPAK)/oxidative stress response-1 (OSR1)-NaCl cotransporter (NCC) pathway. **A:** total kidney extracts from wild-type (WT), *KLHL3*^{+ /R528H} [heterozygous (HET)] and *KLHL3*^{R528H/R528H} [homozygous (HOM)] mice were subjected to Western blot analysis with the indicated antibodies. Each sample was derived from a separate littermate animal. **B:** band intensities were quantified using ImageJ, and the results are presented relative to the expression of GAPDH. Increased expression of NCC and WNK4 as well as increased phosphorylation of SPAK (Ser³⁷³) and NCC (Thr⁶⁰) were observed in *KLHL3*^{+ /R528H} mice. Such differences were more dramatic in *KLHL3*^{R528H/R528H} mice, in which an increase in the expression of SPAK and OSR1 was also observed. ENaC, epithelial Na⁺ channel; ns, not significant.



nal epitope of the protein that can recognize both L-WNK1 and KS-WNK1 (pan-WNK1 antibody). Given that several bands were observed in the blots performed with this antibody, in order to identify the band corresponding to KS-WNK1, we included in these experiments lysates from KS-WNK1 knockout mice [*KS-*

WNK1^{-/-}, a kind gift of Hadchouel (15), INSERM Paris] and *KLHL3*^{R528H/R528H}; *KS-WNK1*^{-/-} double mutants.

Interestingly, we observed no band at the expected size for KS-WNK1 in wild-type mice, but a robust band of this size was observed in *KLHL3*^{R528H/R528H} mice (Fig. 3). Its absence in

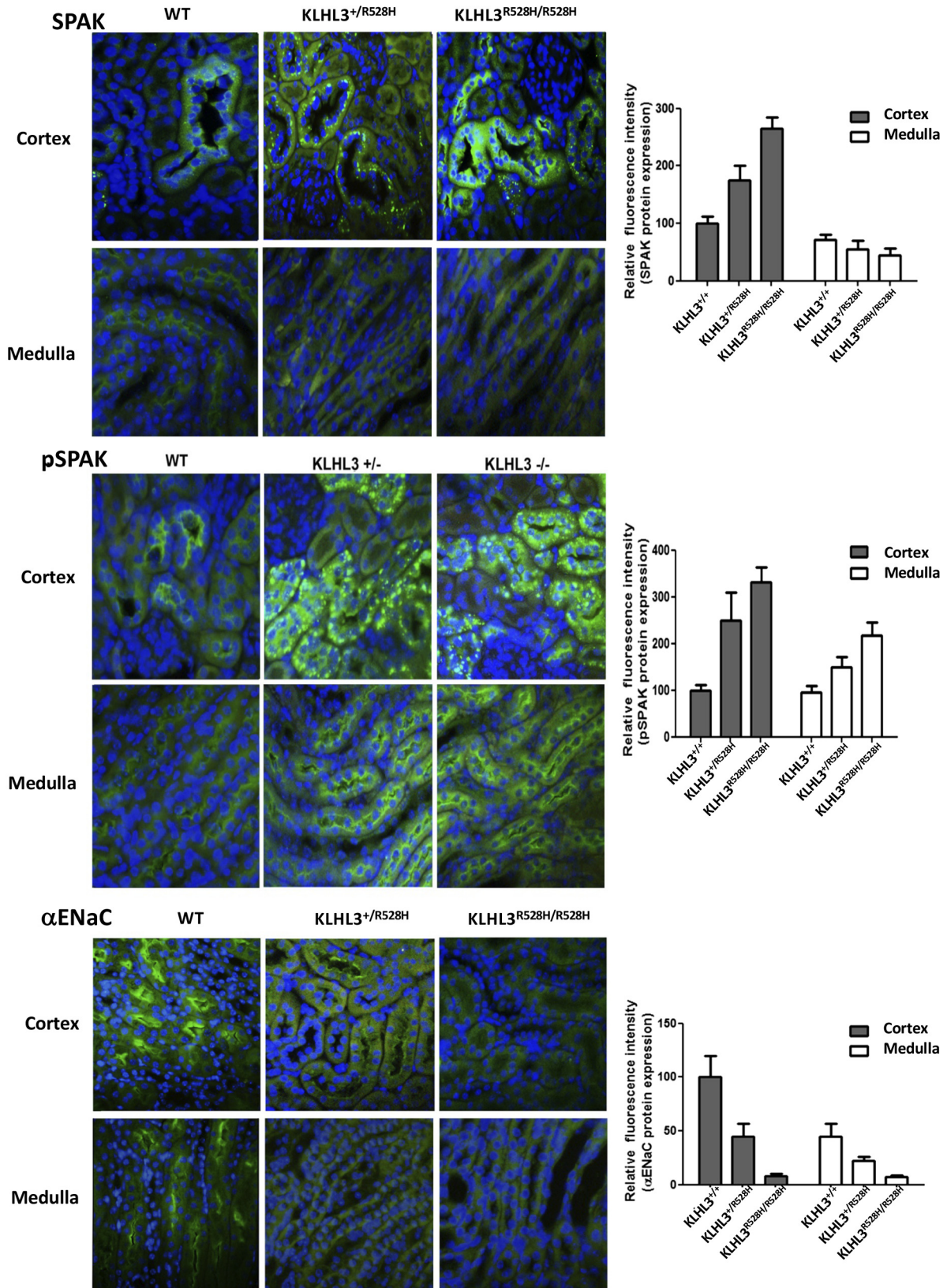


Figure 2. Immunofluorescent staining of kidney sections was performed. The primary antibodies used are indicated. Representative images from cortical and medullary regions are shown. Fluorescence intensity was quantified using ImageJ, and the results are presented in the corresponding bar graphs. ENaC, epithelial Na⁺ channel; KLHL3, Kelch-like protein 3; pSPAK, phospho-SPAK; SPAK, STE20/SPS1-related proline-alanine-rich protein kinase; WNK1, with no lysine kinase 1.

double-mutant mice confirmed that indeed this band corresponds to KS-WNK1. These observations suggest that the KS-WNK1 protein expression level is very low (undetectable by Western blot) in kidneys from wild-type mice under basal conditions, which is striking given the high KS-WNK1 mRNA levels that have been reported for renal tissue (11). This observation supports, as suggested by Luis-Dit-Picard et al. (8), that KS-WNK1 is highly sensitive to CUL3-KLHL3 E3-mediated degradation, given the large upregulation observed in *KLHL3*^{R528H/R528H} mice in which WNK-KLHL3 binding is impaired.

Finally, a band of higher molecular weight that may correspond to L-WNK1 was observed with the pan-WNK1 antibody, whose intensity was similar in all genotypes. We cannot rule out, however, that this may be a nonspecific band. WNK4 expression in the kidneys from wild-type and *KS-WNK1*^{-/-} mice was similar, whereas, as expected, it was increased in *KLHL3*^{R528H/R528H} mice and double-mutant mice.

Knockout of KS-WNK1 Does Not Prevent the FHHt Phenotype of *KLHL3*^{R528H/R528H} Mice

Given the striking KS-WNK1 protein upregulation that we observed in *KLHL3*^{R528H/R528H} mice, we decided to evaluate whether this upregulation is implicated in the pathogenesis of FHHt. Thus, we studied the phenotype of *KLHL3*^{R528H/R528H}; *KS-WNK1*^{-/-} mice and compared it with the phenotype of *KLHL3*^{R528H/R528H} mice. We observed that double-knockout mice have an FHHt phenotype with serum K⁺, Cl⁻, HCO₃⁻, and pH levels similar to those observed in *KLHL3*^{R528H/R528H}

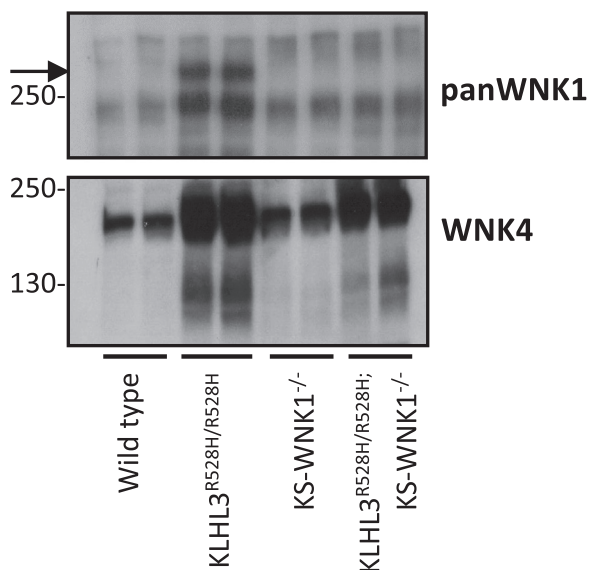


Figure 3. Kidney-specific with no lysine kinase (WNK)1 (KS-WNK1) protein levels are undetectable in kidney tissue of wild-type mice but are high in mice in which cullin 3-Kelch-like protein 3 (KLHL3) E3-mediated degradation is prevented. Total kidney lysates from *KLHL3*^{R528H/R528H} mice, *KS-WNK1*^{-/-} mice, and double mutants (*KLHL3*^{R528H/R528H}; *KS-WNK1*^{-/-} mice) were analyzed by Western blot to assess the expression of WNK1 isoforms (as measured by the pan-WNK1 antibody). The robust band observed in *KLHL3*^{R528H/R528H} mice (arrow) that was absent in wild-type mice corresponds to KS-WNK1, as corroborated by its absence in the double mutants. The WNK4 blot is presented at the bottom. The expected increase in WNK4 expression was observed in *KLHL3*^{R528H/R528H} samples and in *KLHL3*^{R528H/R528H}; *KS-WNK1*^{-/-} mice.

mice (Table 2). Thus, KS-WNK1 upregulation does not seem to play a central role in the pathogenesis of FHHt. In further experiments, administration of diets with altered content of K⁺ and Na⁺ may help to uncover phenotypic differences. However, this was out of the scope of this work.

KS-WNK1 and L-WNK1 Exhibit Different Sensitivity to CUL3-KLHL3 E3-Mediated Degradation

Our preliminary data, published in Luis-Dit-Picard et al. (8), showed that KS-WNK1 is heterologously expressed in *X. laevis* oocytes and in human embryonic kidney (HEK)-293 cells is readily degraded when coexpressed with KLHL3. In contrast, L-WNK1 is resistant to such degradation. To further explore this phenomenon, we began by analyzing the effect of KLHL3 coexpression on KS-WNK1 and L-WNK1-mediated activation of NCC. We microinjected *X. laevis* oocytes with NCC cRNA in the absence or presence of L-WNK1 or KS-WNK1 cRNA with or without KLHL3 cRNA. Three days later, thiazide-sensitive tracer Na⁺ uptake was assessed. As we have previously shown (12), both KS-WNK1 and L-WNK1 were able to increase the activity of NCC, despite the fact that KS-WNK1 has no kinase domain (Fig. 4A). Our previous work supported that the effect of KS-WNK1 on NCC is likely due to an interaction of KS-WNK1 with an endogenous WNK kinase, since the presence of KS-WNK1 increased the phosphorylation of SPAK and NCC, and the effect was prevented by the specific WNK inhibitor WNK463 (12). Consistent with our preliminary observations (8), the effect of KS-WNK1 on NCC was completely prevented by coinjection with KLHL3 cRNA, whereas the effect of L-WNK1 on NCC was not.

We then analyzed the effect of KLHL3 expression on L-WNK1, KS-WNK1, WNK3, and WNK4 abundances. This effect has been previously described. However, no study has compared the effect of KLHL3 on all these WNK isoforms in parallel (4, 5, 21). Figure 4B shows a representative image of such analysis. Oocytes were injected with each WNK cRNA alone or coinjected with KLHL3 cRNA. L-WNK1, KS-WNK1, and WNK3 expression was assessed with anti-c-myc antibodies and WNK4 and KLHL3 with anti-Flag antibodies. Consistent with the results shown in Fig. 4A, the presence of KLHL3 had little to no effect on the L-WNK1 expression level, whereas the expression of KS-WNK1 in the presence of KLHL3 was completely abrogated. In addition, we observed that WNK3 and WNK4 exhibited high sensitivity to CUL3-KLHL3 E3-mediated degradation. Thus, according to the densitometric analysis (Fig. 4C), it appears that at least in *X. laevis* oocytes the sensitivity of L-WNK1 to the effect of the CUL3-KLHL3 E3 complex was significantly lower than that observed for the other WNKs. A similar observation has also been reported in HEK-293 cells by Luis-Dit-Picard et al. (8).

The Unique KS-WNK1 Segment Encoded by Exon 4a Is Involved in the Sensitivity to the CUL3-KLHL3 E3 Ligase Complex

L-WNK1 and KS-WNK1 have different NH₂-terminal portions but are identical from the beginning of the segment encoded by exon 5 until the end of the protein. Thus, they

Table 2. Serum electrolytes of wild-type, *KLHL3*^{R528H/R528H}, *KS-WNK1*^{-/-}, and double-mutant mice

	<i>KLHL3</i> ^{+/+} ; <i>KS-WNK1</i> ^{+/+}	<i>KLHL3</i> ^{R528H/R528H} ; <i>KS-WNK1</i> ^{+/+}	<i>KLHL3</i> ^{+/+} ; <i>KS-WNK1</i> ^{-/-}	<i>KLHL3</i> ^{R528H/R528H} ; <i>KS-WNK1</i> ^{-/-}
Na ⁺ , mM	151 ± 0.56 (n = 6)	152 ± 0.56 (n = 6)	150 ± 0.61 (n = 6)	153 ± 0.58 (n = 6)
K ⁺ , mM	4.5 ± 0.16 (n = 6)	5.1 ± 0.10 (n = 6)*	4.7 ± 0.12 (n = 6)	5.0 ± 0.12 (n = 6)*
Cl ⁻ , mM	118 ± 0.61 (n = 6)	123 ± 0.22 (n = 6)*	118 ± 0.53 (n = 6)	122 ± 0.40 (n = 6)*
Ca ²⁺ , mM	4.2 ± 0.3 (n = 6)	4.5 ± 0.06 (n = 6)	4.2 ± 0.12 (n = 6)	4.3 ± 0.04 (n = 6)
pH	7.3 ± 0.03 (n = 6)	7.2 ± 0.01 (n = 6)	7.3 ± 0.02 (n = 6)	7.2 ± 0.01 (n = 6)
HCO ₃ ⁻ , mM	20 ± 0.76 (n = 6)	14 ± 0.42 (n = 6)*	17 ± 0.36 (n = 6)	15 ± 0.52 (n = 6)*

Data are means ± SE; *n* represents the number of mice included in the analyses. KLHL3, Kelch-like protein 3; WNK1, with no lysine kinase 1. **P* < 0.05 versus wild-type mice.

both contain the acidic motif (EPEEPEADQHQ) that mediates interactions with KLHL3 (Supplemental Fig. S2; see <https://doi.org/10.6084/m9.figshare.13721794>).

The first 30-amino acid residues of KS-WNK1 are unique to this isoform because they are encoded by exon 4a, which is not included in the L-WNK1 transcript. Exon 4a is highly conserved across evolution since its amino acid sequence is almost identical from coelacanths to humans (13), suggesting that it plays a key role in species that have evolved a renal tubule. This segment has been shown to be key for the formation of KS-WNK1-dependent WNK bodies (13). Thus, to evaluate its effect on KS-WNK1 activity and CUL3-KLHL3 E3-mediated degradation, we generated the *KS-WNK1-Δ4a* clone that lacks this fragment. We assessed its ability to activate NCC and its sensitivity to degradation promoted by CUL3-KLHL3 E3. As previously described (12), the absence of the 4a fragment prevents the positive effect of KS-WNK1 on NCC activity (Fig. 5A). Interestingly, this modification prevented KS-WNK1 functionality and also prevented its degradation, as demonstrated by the representative blot shown in Fig. 5B and the densitometric analysis shown in Fig. 5C. We observed a mild protective effect of the proteasome inhibitor MG132 against CUL3-KLHL3-RING-induced degradation of KS-WNK1, suggesting that other pathways may also be involved in degradation (Fig. 5B).

The Cysteines in Region 4a Are Important for KS-WNK1 Function but Not for Its CUL3-KLHL3 E3-Mediated Degradation

Boyd-Shiwarski et al. (13) have previously analyzed the degree of conservation of individual residues within the 4a segment and have identified a cluster of conserved cysteines and a cluster of conserved hydrophobic residues (Fig. 6A). Mutagenic analysis led them to conclude that these clusters, which they termed the “cysteine-rich hydrophobic motif,” are key for the formation of KS-WNK1-dependent WNK bodies. Thus, we decided to evaluate their role on KS-WNK1-dependent NCC activation and sensitivity to CUL3-KLHL3 E3-induced degradation.

We first decided to analyze the role of conserved cysteines. For this purpose, we generated a clone with the six conserved cysteines mutated to serine (*KS-6CxS* mutant) and a clone in which only the outer two cysteines were mutated to serine (*KS-2CxS* mutant; Fig. 6A). According to the data by Boyd-Shiwarski et al. (13), the *KS-6CxS* mutation prevents the formation of WNK bodies, but the *KS-2CxS* mutation only partially does so.

We injected oocytes with NCC and wild-type KS-WNK1 or mutants *KS-6CxS* or *KS-2CxS* and treated them with or without MG132 to evaluate their function and degradation. We observed that the ability of the *KS-6CxS* mutant to activate NCC was completely abrogated, whereas that of the *KS-2CxS* mutant was only partially impaired (Fig. 6B). Regarding CUL3-KLHL3 E3-mediated degradation, we observed that both mutants were degraded in the presence of KLHL3, suggesting that, although the whole exon 4a seems to be important in conferring sensitivity to CUL3-KLHL3 E3-mediated degradation, the cysteine residues are not involved (Fig. 6, C and D).

The Cluster of Hydrophobic Residues in the 4a Segment of KS-WNK1 Are Key for NCC Activation and Confers KS-WNK1 Sensitivity to CUL3-KLHL3 E3-Mediated Degradation

We next analyzed the role of the cluster of hydrophobic residues on KS-WNK1 ability to activate NCC and on its sensitivity to CUL3-KLHL3 E3-mediated degradation. This cluster includes the five hydrophobic amino acid residues between the positions 11 and 15 (valine, phenylalanine, valine, isoleucine, and isoleucine; Fig. 6A). We generated a clone in which these five residues were mutated to glutamine (*KS-5Q* mutant). We decided to mutate these residues to glutamine given that Boyd-Shiwarski et al. (13) used this strategy to substitute the hydrophobic residues for hydrophilic ones and showed that these mutations prevented WNK body formation. Thus, we evaluated if the same mutations can also affect kidney-specific function and KLHL3-induced degradation. We observed that the ability of this mutant to activate NCC was completely impaired (Fig. 7A). Interestingly, however, we observed that this mutant was insensitive to CUL3-KLHL3 E3-induced degradation (Fig. 7, B and C).

Valine 11 and Valine 13 of KS-WNK1 Are Relevant for Its CUL3-KLHL3 E3-Mediated Degradation

To evaluate the role of individual residues within the hydrophobic cluster on KS-WNK1 activity and degradation, we generated the five single residue mutants and studied them in the oocyte system as performed for the other mutants. For the individual mutants, we decided to mutate each of the hydrophobic amino acid residues to alanine to explore whether the sole absence of the hydrophobic lateral chain is sufficient to produce these effects. We observed that the V11A mutant was unable to activate NCC and that this function was significantly reduced for the V13A mutant. For

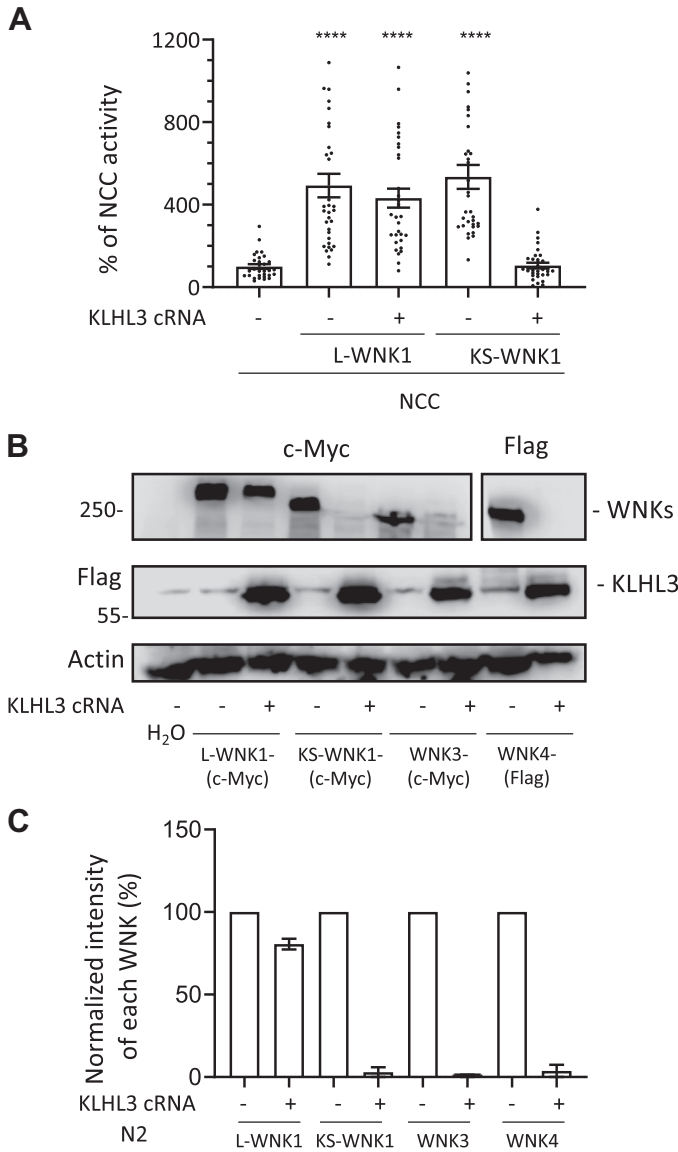


Figure 4. Kidney-specific with no lysine kinase (WNK)1 (KS-WNK1), WNK3, and WNK4, but not full-length WNK1 (L-WNK1), are degraded when coexpressed with Kelch-like protein 3 (KLHL3) in oocytes. **A:** thiazide-sensitive $^{22}\text{Na}^+$ uptake was assessed in *Xenopus laevis* oocytes injected with the indicated cRNAs. Uptake values observed in the control group (NCC only) were set to 100%, and the other groups were normalized accordingly. While both L-WNK1 and KS-WNK1 increased Na^+ uptake, KLHL3 coexpression prevented NaCl cotransporter (NCC) activation by KS-WNK1 but not by L-WNK1. Dots represent uptake values for individual oocytes. At least three independent experiments were performed with >10 oocytes per group (**** $P < 0.0001$ vs. NCC; three points outside graphic limits). **B:** representative Western blots showing the effect of KLHL3 coexpression on L-WNK1, KS-WNK1, WNK3, and WNK4 levels. Oocytes were injected with cRNAs encoding for c-Myc-tagged L-WNK1, KS-WNK1, or WNK3 or Flag-tagged WNK4 with or without Flag-tagged KLHL3. All kinases except L-WNK1 were degraded in the presence of KLHL3. **C:** densitometric analysis of the Western blots presented in **B**. Two independent experiments were performed with similar results. c-Myc-tagged L-WNK1, KS-WNK1, or WNK3 or Flag-tagged WNK4 were normalized to 100% and compared with those observed in groups expressing KLHL3.

the remaining three mutants, this function was only slightly reduced (Fig. 8A). CUL3-KLHL3 E3-mediated degradation was impaired for the V11A and V13A mutants (Fig. 8, B and C), suggesting that these residues may participate

in conferring the sensitivity to CUL3-KLHL3E3-mediated degradation.

KS-WNK1 Protein Expression Is Upregulated in Kidneys of Mice Maintained on Low- K^+ Diet

Ishizawa et al. (23) recently showed that phosphorylation of KLHL3 in a residue located within the substrate-binding domain is upregulated in mice that are maintained on a low- K^+ diet. This reduces CUL3-KLHL3 E3-targeted degradation

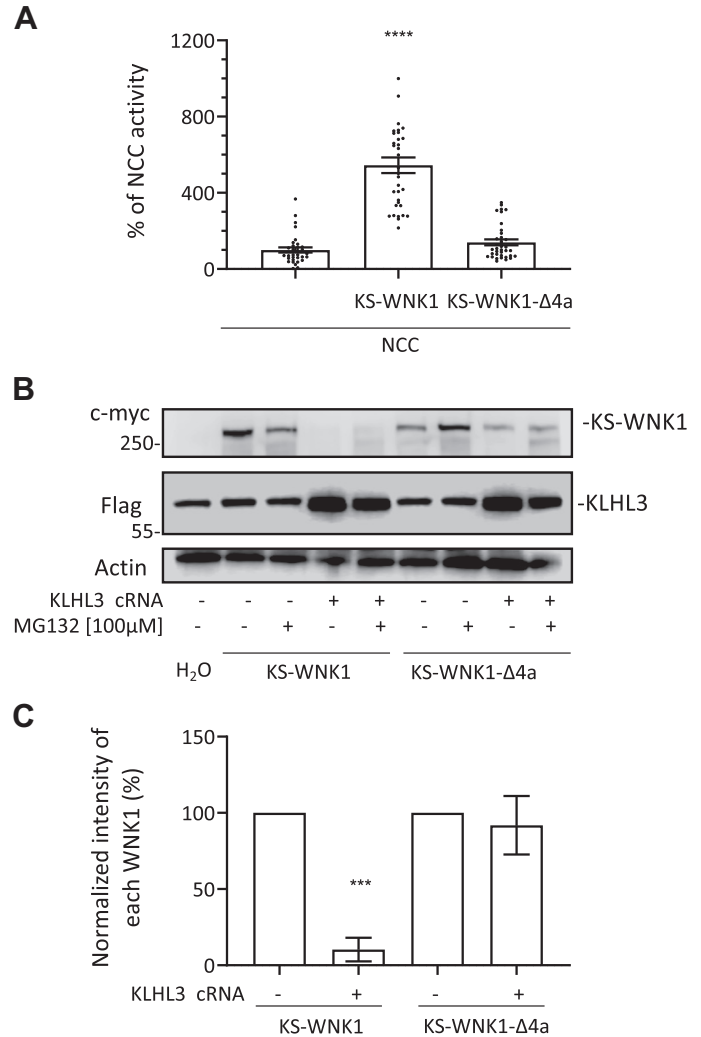


Figure 5. The segment encoded by exon 4a in kidney-specific with no lysine kinase 1 (KS-WNK1) is needed to activate NaCl cotransporter (NCC) and to be targeted for degradation by cullin-3 (CUL3)-Kelch-like protein 3 (KLHL3) E3. **A:** thiazide-sensitive Na^+ uptake of NCC cRNA-injected oocytes was set to 100%, and uptake values of additional groups were normalized accordingly. KS-WNK1 coexpression increased NCC activity, but the KS-WNK1-Δ4a mutant failed to activate ($n = 3$ transport assays, **** $P < 0.0001$ vs. NCC; one point outside graphic limits). **B:** representative Western blots showing KS-WNK1 and KS-WNK1-Δ4a expression in the absence or presence of KLHL3. CUL3-KLHL3 E3-induced degradation of KS-WNK1 is observed regardless of proteasome inhibition, whereas KS-WNK1-Δ4a is expressed but resistant to CUL3-KLHL3 E3-induced degradation. **C:** densitometric analysis of the Western blots presented in **B**. Results from four different experiments were included. Expression of KS-WNK1 or KS-WNK1-Δ4a in the absence of KLHL3 were arbitrarily set to 100% and compared with expression levels observed in the presence of KLHL3 ($n = 4$ Western blots, *** $P > 0.001$ vs. control without KLHL3).

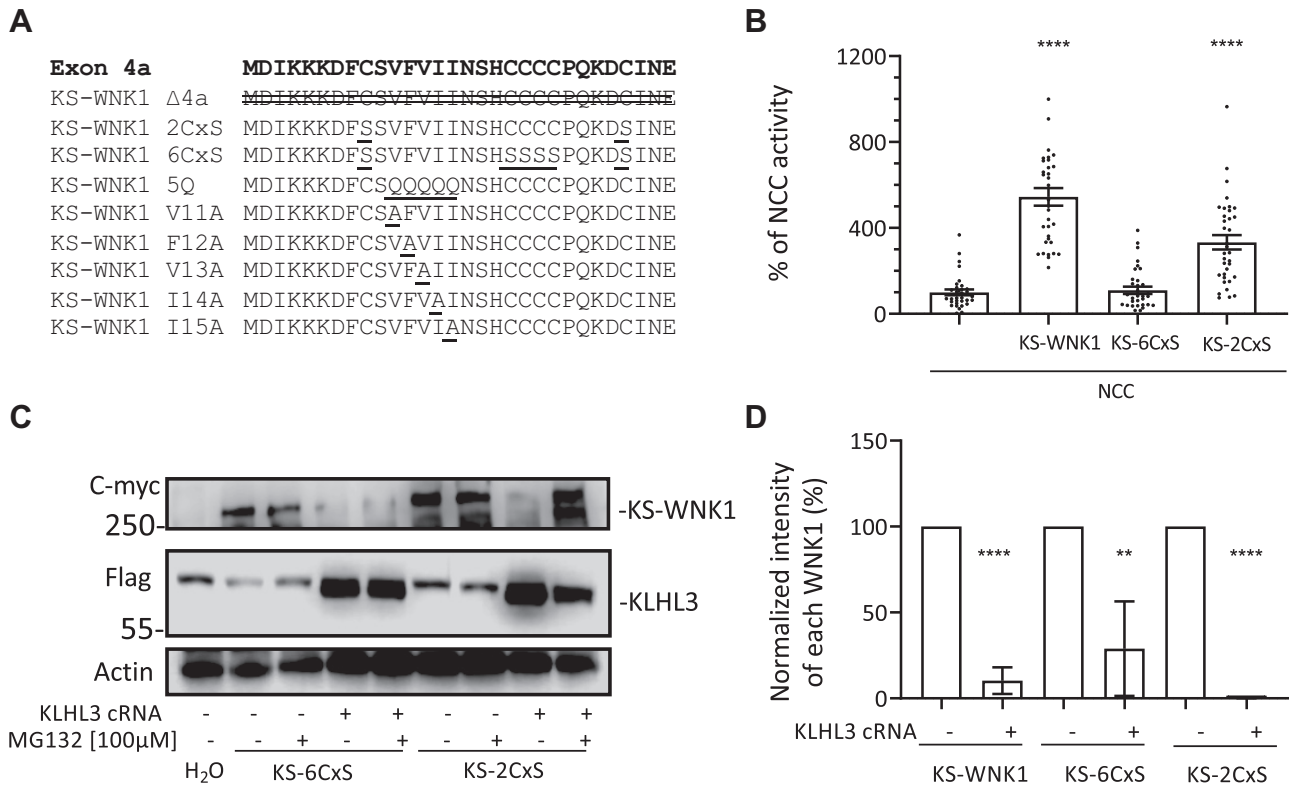


Figure 6. Mutation of the six conserved cysteines encoded in exon 4a impairs the ability of kidney-specific with no lysine kinase 1 (KS-WNK1) to activate NaCl cotransporter (NCC) but does not prevent cullin-3 (CUL3)-Kelch-like protein 3 (KLHL3) E3-induced degradation. **A:** amino acid sequence encoded by exon 4a. Different KS-WNK1 mutants were generated for this work with variations in the sequence of this region. The modifications introduced in each mutant are indicated. **B:** NCC was coexpressed in oocytes with KS-WNK1, KS-6CxS (in which all six cysteines were mutated to serine), or KS-2CxS (in which the two peripheral cysteines were mutated to serine). Thiazide-sensitive Na^+ uptake of NCC-expressing oocytes was set to 100% and compared with all other groups, which were normalized accordingly. KS-WNK1-6CxS did not activate NCC, whereas KS-WNK1-2CxS did activate NCC, albeit at a lower level than wild-type KS-WNK1 ($n = 3$ transport assays, **** $P < 0.0001$ vs. NCC; 3 points outside graphic limits). **C:** representative Western blots showing the expression of KS-WNK1-6CxS and KS-WNK1-2CxS. Both mutant proteins are targeted for degradation by CUL3-KLHL3 E3, whereas treatment with MG132 could prevent KS-WNK1-2CxS degradation. **D:** compiled results of densitometric analysis from at least two different Western blot experiments like that presented in (B). Expression levels of KS-WNK1, KS-WNK1-6CxS, and KS-WNK1-2CxS in the absence of KLHL3 were normalized to 100% and compared with groups expressing KLHL3 ($n = 2-4$ Western blots, ** $P < 0.01$ and **** $P < 0.0001$ vs. control without KLHL3).

of WNK4. Thus, to evaluate whether K^+ restriction is a possible physiological stimuli for induction of KS-WNK1 expression, wild-type, and *KLHL3*^{+/R528H} mice were placed on low- K^+ diet for 7 days and then euthanized for renal tissue collection. Kidney lysates were prepared and analyzed by Western blot analysis with pan-WNK1 and WNK4 antibodies (Fig. 9).

The band corresponding to KS-WNK1 was only barely observed in samples from *KLHL3*^{+/R528H} mice (Fig. 9), in contrast to what we previously observed with *KLHL3*^{R528H/R528H} mouse samples (Fig. 3). This suggests that the residual activity of the CUL3-KLHL3 E3 complex present in heterozygous mice is sufficient to almost entirely degrade KS-WNK1. A more robust band was observed in samples from wild-type and *KLHL3*^{+/R528H} mice maintained on the low- K^+ diet, showing that indeed KS-WNK1 expression is induced under conditions of dietary K^+ restriction. WNK4 upregulation was also observed, as previously reported (23).

DISCUSSION

In the present study, we show that KS-WNK1 is more sensitive to CUL3-KLHL3 E3-mediated degradation than L-

WNK1, and we began to explore the elements of their primary sequence that are responsible for this difference. Given that the known binding site for KLHL3 in WNK kinases is the acidic motif, the observation is puzzling as both proteins present the exact same binding site. Interestingly, we observed that removal of the unique sequence of KS-WNK1 encoded by exon 4a decreases its sensitivity to CUL3-KLHL3 E3-mediated degradation. This shows that targeting by KLHL3 of the COOH-terminal segment of WNK1 (comprising the sequence encoded from exon 5 until the end that includes the acidic motif) is not efficient unless this 30-amino acid residue segment is present. We also showed that this segment is critical for the ability of KS-WNK1 to activate NCC. Other works also support the key role of exon 4a for KS-WNK1 function. For instance, Argaz et al. (12) showed that the ability of KS-WNK1 to activate NCC by promoting WNK4 phosphorylation is impaired by the removal of this segment, although KS-WNK1 binding to WNK4 was not affected, and Boyd-Shiowski et al. (13) showed that exon 4a is necessary for the KS-WNK1-dependent formation of WNK bodies.

Interestingly, the analysis of the effects of mutation of certain conserved residues within exon 4a showed that some of

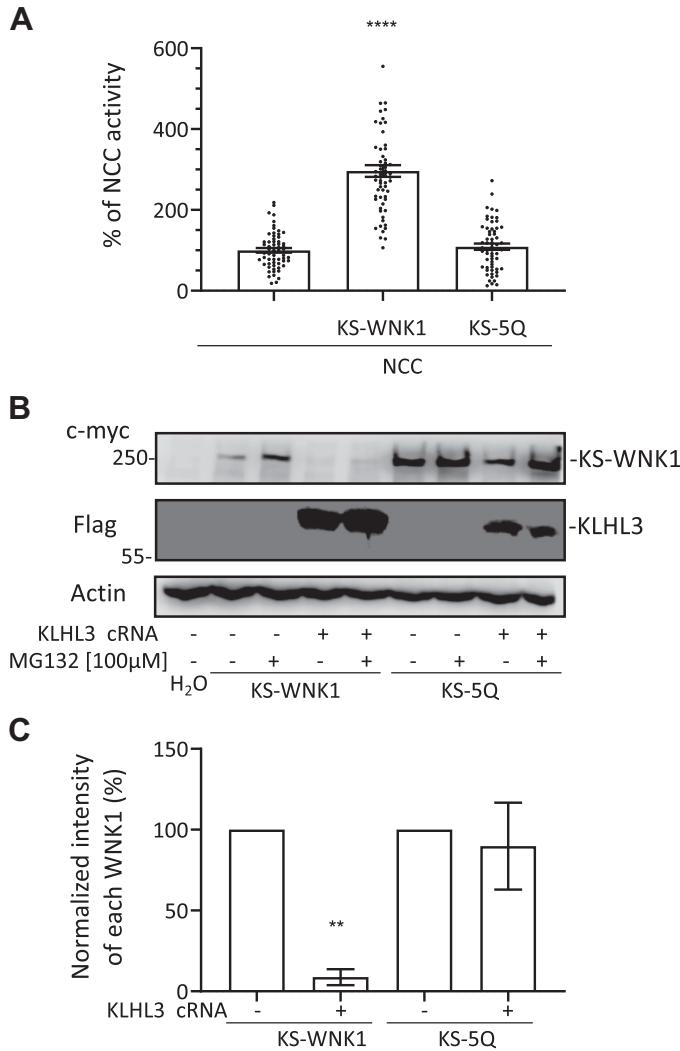


Figure 7. Mutation of the five conserved hydrophobic residues encoded in exon 4a impairs the ability of kidney-specific with no lysine kinase 1 (KS-WNK1) to activate NaCl cotransporter (NCC) and prevent cullin-3-Kelch-like protein 3 (KLHL3) E3-induced degradation. **A:** NCC was coexpressed in oocytes with KS-WNK1 or KS-5Q (in which all five hydrophobic residues were mutated to glutamine), and thiazide-sensitive Na⁺ uptake was assessed. Uptake levels observed for NCC-expressing oocytes were normalized to 100% and compared with those observed for groups expressing KS-WNK1 and KS-5Q. The strong activation of NCC induced by KS-WNK1 was not observed in the KS-5Q mutant (*n* = 5 transport assays, *****P* < 0.0001 vs. NCC; 2 points outside graphic limits). **B:** representative Western blots showing the expression of KS-WNK1 and KS-5Q. KS-WNK1 was degraded in the presence of KLHL3, whereas KS-5Q was not degraded. Treatment with MG132 increased KS-5Q expression, probably by impairing degradation even more. **C:** compiled results of densitometric analysis from three different experiments like that presented in **B**. Expression levels of KS-WNK1 and KS-5Q in the absence of KLHL3 were normalized to 100% and compared with those observed in groups expressing KLHL3 (*n* = 3 Western blots, ***P* < 0.01 vs. control without KLHL3).

these modifications alter KS-WNK1 ability to activate NCC, but not its targeting by KLHL3, whereas those that affect KLHL3 targeting also affect the ability to activate NCC. Thus, although the same segment is key to define the sensitivity to CUL3-KLHL3 E3 and the ability of KS-WNK1 to activate NCC, these properties can be dissociated, suggesting that they are not strictly dependent on one another.

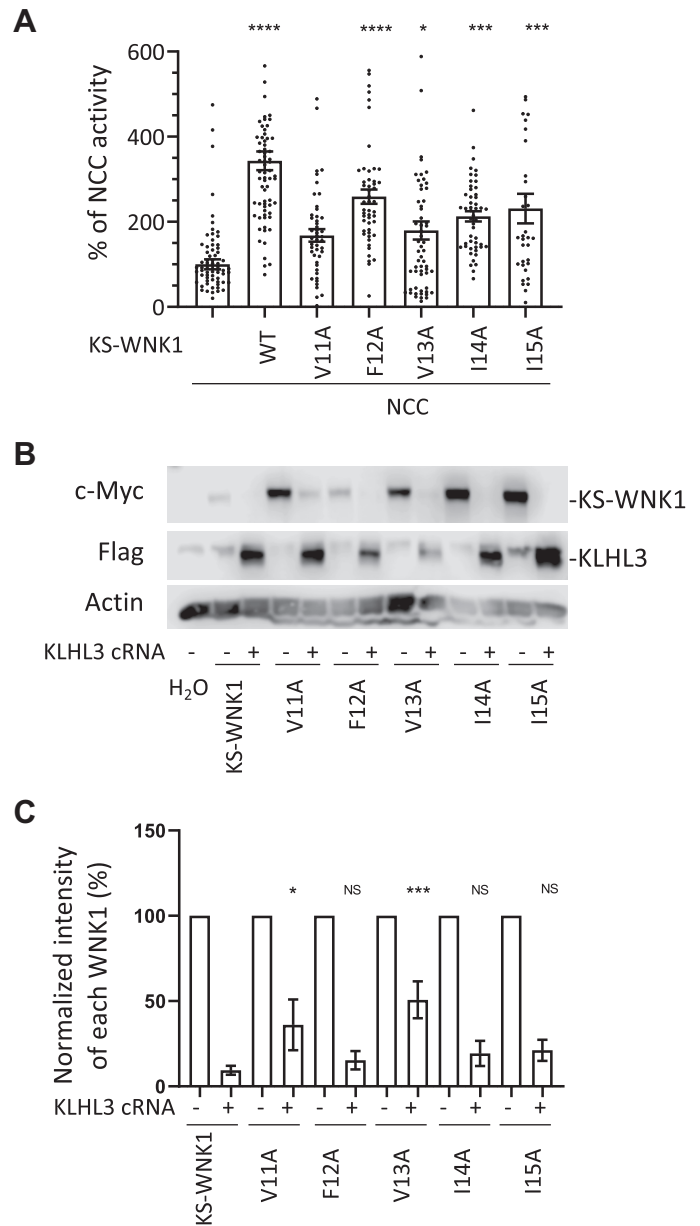


Figure 8. Mutation of valine 11 or valine 13 located in the hydrophobic motif of exon 4a impairs the ability of kidney-specific with no lysine kinase 1 (KS-WNK1) to activate NaCl cotransporter (NCC) and cullin-3-Kelch-like protein 3 (KLHL3) E3-induced degradation of KS-WNK1. **A:** NCC was coexpressed in oocytes with KS-WNK1 or with KS-WNK1 mutants containing one of the following single amino acid substitutions: V11A, F12A, V13A, I14A, or I15A. Uptake levels observed for NCC-expressing oocytes were normalized to 100% and compared with those observed for groups expressing KS-WNK1 mutants. All mutants except KS-WNK1-V11A were capable of activating NCC (*n* = 3–5 transport assays, **P* < 0.05, ****P* < 0.001, and *****P* < 0.0001 vs. NCC; 16 points outside graphic limits). **B:** representative Western blots showing the expression of KS-WNK1 and of each single-residue mutant in the absence or presence of KLHL3. Compared with wild-type (WT) KS-WNK1, there was significantly less degradation of the V11A and V13A mutants in the presence of KLHL3. Other mutants degraded similarly to the WT. **C:** compiled results of densitometric analysis from at least five different experiments like that presented in **B**. Expression levels of KS-WNK1 and single-residue mutants in the absence of KLHL3 were normalized to 100%. Degradation of single-residue mutants were compared with WT KS-WNK1 in the presence of KLHL3 (*n* = 5–8 Western blots, **P* < 0.05 and ****P* < 0.001 vs. control with KLHL3).

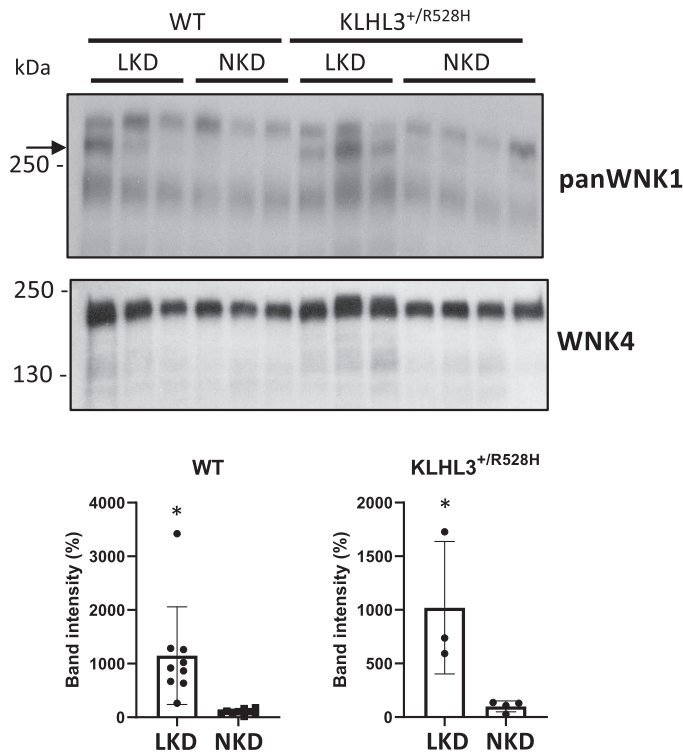


Figure 9. Renal kidney-specific with no lysine kinase 1 (KS-WNK1) expression is induced by a low- K^+ diet (LKD). Total kidney lysates from wild-type (WT) and Kelch-like protein 3 (KLHL3)^{+/R528H} mice maintained on a normal- K^+ diet (NKD) or LKD were analyzed by Western blot to assess the expression of KS-WNK1. Compared with WT mice, moderately higher expression was observed in KLHL3^{+/R528H} mice. In addition, a robust increase in KS-WNK1 expression was observed in WT mice but also in KLHL3^{+/R528H} mice, suggesting that KLHL3-targeted degradation was further affected under this condition. Results of quantitation of the band corresponding to KS-WNK1 are shown at the bottom. Band intensity values of mice on a NKD were normalized to 100%. A WNK4 blot is also shown. The expected increase in WNK4 expression was observed in KLHL3^{+/R528H} samples. Expression was further increased when mice were placed on a LKD, as previously reported (10). $n = 9$ for WT mice on the LKD and NKD, $n = 3$ for KLHL3^{+/R528H} mice on the NKD, and $n = 4$ for KLHL3^{+/R528H} mice on the LKD. * $P < 0.05$ versus the NKD. WNK1, with no lysine kinase 1.

Substitution of either one of two specific residues within the conserved hydrophobic motif in exon 4a was enough to prevent CUL3-KLHL3 E3-mediated degradation of KS-WNK1. The mechanisms underlying 4a segment's role on KS-WNK1 activity and sensitivity to targeting by KLHL3 remain as open questions for future studies. Possible mechanisms are, for example, that this segment may be involved in establishing key interactions or that perhaps it could be a determinant to achieve a specific conformational state of the protein.

Our data suggest that KS-WNK1 is also highly sensitive to CUL3-KLHL3 E3-mediated degradation in vivo. Vidal-Petiot et al. (11) reported that KS-WNK1 mRNA levels are high in the kidney (higher than L-WNK1 mRNA levels). Despite this, we were unable to detect KS-WNK1 protein in kidney lysates from wild-type mice by Western blot analysis. However, robust KS-WNK1 protein expression was detected in lysates from KLHL3^{R528H/R528H} mice in which KLHL3-WNK binding is impaired. Thus, the low protein expression observed in wild-type mice may result from a high degradation rate of KS-WNK1. The physiological significance of this observation

remains to be determined. Analogous biological phenomena have been described. For example, the ubiquitous transcription factor hypoxia-inducible factor-1 α (HIF-1 α) is normally undetectable at the protein level due to highly active proteasomal degradation that is dependent on the presence of O_2 (24). HIF-1 α is marked for degradation by a cullin-RING E3 ligase complex in which the von Hippel-Lindau (VHL) tumor suppressor protein acts as the substrate recognition element. VHL can only recognize HIF-1 α when it is hydroxylated at two proline residues, and hydroxylation is dependent on the activity of prolyl-hydroxylases that are activated in the presence of O_2 . Thus, in conditions of hypoxia, hydroxylation is prevented and HIF-1 α expression is rapidly induced, as well as expression of its target genes.

In the case of KS-WNK1, the physiological stimuli that can upregulate its expression remain to be elucidated. We show here, however, that one of these stimuli is dietary K^+ restriction. Ishizawa et al. (23) have shown that KLHL3 phosphorylation in the substrate recognition domain is induced by low- K^+ intake in mice. Thus, low- K^+ -induced phosphorylation of KLHL3 may underlie the observed upregulation of KS-WNK1 in mice on a low- K^+ diet. This observation is in line with the fact that the formation of WNK bodies, which is induced by low- K^+ intake, requires the presence of KS-WNK1, suggesting that indeed the DCT response to low- K^+ intake involves KS-WNK1 upregulation due to KLHL3 inhibition by phosphorylation. This agrees with the observation that WNK bodies are present in KLHL3^{R528H/R528H} mice (Fig. 2) but not in mice with FHHt caused by mutations in WNK4 (14).

The physiological role of KS-WNK1 is currently a very controversial issue. However, knowledge of the conditions in which KS-WNK1 protein is expressed in the DCT may help guide experiments to uncover this physiological role. In the present work, we show that despite the high KS-WNK1 protein upregulation observed in FHHt mice due to a mutation in KLHL3, KS-WNK1 is not essential to develop the FHHt phenotype. That is, WNK4 overexpression appears to be sufficient to produce the disease, consistent with prior results (25).

Different lines of evidence obtained from a diversity of transgenic mouse models suggest that the WNK1 isoform expressed in the DCT is KS-WNK1 and that L-WNK1 is not normally present (1). Absence of WNK4 expression completely impairs the phosphorylation and activity of NCC (26), demonstrating that WNK4 absence cannot be compensated by L-WNK1 activity. Additionally, in KLHL3^{R528H/R528H} mice, expression of both L-WNK1 and WNK4 is increased but the FHHt phenotype is completely abrogated by elimination of WNK4, although L-WNK1 remains upregulated, strongly suggesting that L-WNK1 is not present in the DCT (25). Thomson et al. (14) have shown that, within the large WNK bodies observed in WNK4 knockout mice, no active WNK1 is present, as indicated by the lack of signal obtained with the pT-loop WNK antibody, supporting that the WNK1 product in the WNK bodies is KS-WNK1, not L-WNK1. Finally, it has been demonstrated that intronic WNK1 deletions responsible for FHHt cause ectopic expression of L-WNK1 in the DCT (7), and this is the unique situation in which the absence of WNK4 does not result in NCC downregulation (18). Thus, given that L-WNK1 activity is less sensitive to inhibition by

Cl⁻ than WNK4 (27, 28) and less sensitive to CUL3-KLHL3 E3-induced degradation, as shown by this work, it is likely that ectopic expression of L-WNK1 promotes higher levels of NCC activity at any given value of intracellular Cl⁻ concentration and activity level of the CUL3-KLHL3 E3 complex. In this regard, it is noteworthy that *WNK1* intronic deletions cause FHH even in the absence of WNK4 (18), supporting that if L-WNK1 is expressed in the DCT, the presence of WNK4 would be irrelevant. In future work, it would be interesting to establish how low-K⁺ interferes with CUL3-KLHL3 E3-mediated degradation of KS-WNK1.

Finally, as mentioned in the INTRODUCTION, Louis-Dit-Picard et al. (8) have shown that humans and mice with heterozygous mutations in the acidic motif of WNK1 display a mild FHH phenotype that is easily corrected with thiazide treatment in both species. They also showed that the SPAK/OSR1-NCC pathway is upregulated in *WNK1*^{+ /del^{EG31}} mice. Thus, they proposed that NCC upregulation is the primary defect leading to the phenotypic alterations. Also, based on results from in vitro experiments, they proposed that the increased expression of KS-WNK1 in the DCT is largely responsible for NCC upregulation as KS-WNK1 abundance is preferentially affected by these mutations. The large WNK bodies observed in DCT cells of these mice also support this idea, as well as the in vitro and in vivo data presented in this work, showing that KS-WNK1 is very sensitive to CUL3-KLHL3 E3-induced degradation. However, as KS-WNK1 activates NCC via WNK4, the effect of an increase in KS-WNK1 may be buffered by the amount of WNK4, causing only a mild activation of NCC. This activation is probably enough to cause slight hyperkalemia and volume retention but not enough to produce a rise in blood pressure.

In conclusion, our work shows, both in vivo and in vitro, that KS-WNK1 is highly sensitive to CUL3-KLHL3 E3-induced degradation, whereas L-WNK1 is much less sensitive. The high sensitivity of KS-WNK1 seems to be due to the presence of the unique segment encoded in exon 4a. This segment is also key for KS-WNK1 function and its ability to activate NCC. We propose that this exquisite sensibility of KS-WNK1 to targeting by KLHL3 may be relevant to achieve rapid induction of KS-WNK1 protein expression under certain conditions, one of which appears to be extracellular K⁺ depletion. The mechanisms by which exon 4a affects the activity and sensitivity to degradation of KS-WNK1 and the role that KS-WNK1 upregulation plays under conditions of dietary K⁺ deprivation remain to be explored.

ACKNOWLEDGMENTS

We thank Dr. Juliette Hadchouel for the kind gift of KS-WNK1 knockout colony and Hilda Sánchez for assistance.

GRANTS

This work was supported by National Institute of Diabetes and Digestive and Kidney Diseases Grant DK51496 (to G.G.), Grants 87794, 101720, and A1-S-8290 from Conacyt Mexico (to M.C.-C., M.C.-B., and G.G., respectively), Grants IA203620 and RA202718 from PAPIIT UNAM and Loreal L'Oréal-UNESCO-AMC-CONALMEX "For Women in Science, 2019" (to M.C.-C.), and Grant IN201519 from PAPIIT UNAM (to G.G.). M.O.-F. was supported by a scholarship from Conacyt-Mexico and is a graduate student in the PECM

MD/PhD program of the Universidad Nacional Autónoma de México. G.G. is the guarantor of the study. D.R.A. is supported by Medical Research Council Grant MC_UU_12016/2.

DISCLOSURES

No conflicts of interest, financial or otherwise, are declared by the authors.

AUTHOR CONTRIBUTIONS

M.O.-F., M.C.-C., J.Z., E.R.A., L.R.-V., N.A.B., M.C.-B., D.R.A., and G.G. conceived and designed research; M.O.-F., N.V., M.C.-B., J.Z., O.A., E.R.A., F.L.d-T., A.M.d-O., A.S.-N., and L.R.-V. performed experiments; M.O.-F., M.C.-C., J.Z., O.A., E.R.A., F.L.d-T., A.M.d-O., A.S.-N., L.R.-V., N.A.B., N.V., M.C.-B., D.R.A., and G.G. analyzed data; M.O.-F., M.C.-C., M.C.-C., J.Z., E.R.A., D.R.A., G.G., A.M.d-O., and A.S.-N. interpreted results of experiments; M.O.-F., M.C.-B., J.Z., N.V., and G.G. prepared figures; M.O.-F., M.C.-C., M.C.-B., and G.G. drafted manuscript; M.O.-F., M.C.-C., M.C.-C., J.Z., E.R.A., A.M.d-O., A.S.-N., L.R.-V., N.A.B., D.R.A., and G.G. edited and revised manuscript; M.O.-F., M.C.-C., E.R.A., F.L.d-T., A.M.d-O., J.Z., A.S.-N., L.R.-V., N.A.B., N.V., M.C.-B., D.R.A., and G.G. approved final version of manuscript.

REFERENCES

- Ostrosky-Frid M, Castaneda-Bueno M, Gamba G. Regulation of the renal NaCl cotransporter by the WNK/SPAK pathway: lessons learned from genetically altered animals. *Am J Physiol Renal Physiol* 316: F146–F158, 2019. doi:10.1152/ajprenal.00288.2018.
- Boyden LM, Choi M, Choate KA, Nelson-Williams CJ, Farhi A, Toka HR, et al. Mutations in kelch-like 3 and cullin 3 cause hypertension and electrolyte abnormalities. *Nature* 482: 98–102, 2012. doi:10.1038/nature10814.
- Louis-Dit-Picard H, Barc J, Trujillano D, Miserey-Lenkei S, Bouatia-Naji N, Pylypenko O; International Consortium for Blood Pressure (ICBP), et al. KLHL3 mutations cause familial hyperkalemic hypertension by impairing ion transport in the distal nephron. *Nat Genet* 44: 456–460, 2012 [Erratum in *Nat Genet* 44: 609, 2012]. doi:10.1038/ng.2218.
- Shibata S, Zhang J, Puthumana J, Stone KL, Lifton RP. Kelch-like 3 and Cullin 3 regulate electrolyte homeostasis via ubiquitination and degradation of WNK4. *Proc Natl Acad Sci USA* 110: 7838–7843, 2013. doi:10.1073/pnas.1304592110.
- Wakabayashi M, Mori T, Isobe K, Sahara E, Susa K, Araki Y, Chiga M, Kikuchi E, Nomura N, Mori Y, Matsuo H, Murata T, Nomura S, Asano T, Kawaguchi H, Nonoyama S, Rai T, Sasaki S, Uchida S. Impaired KLHL3-mediated ubiquitination of WNK4 causes human hypertension. *Cell Rep* 3: 858–868, 2013. doi:10.1016/j.celrep.2013.02.024.
- Lifton RP, Gharavi AG, Geller DS. Molecular mechanisms of human hypertension. *Cell* 104: 545–556, 2001. doi:10.1016/s0092-8674(01)00241-0.
- Vidal-Petiot E, Elvira-Matelot E, Mutig K, Soukaseum C, Baudrie V, Wu S, Cheval L, Huc E, Cambillau M, Bachmann S, Doucet A, Jeunemaitre X, Hadchouel J. WNK1-related Familial Hyperkalemic Hypertension results from an increased expression of L-WNK1 specifically in the distal nephron. *Proc Natl Acad Sci USA* 110: 14366–14371, 2013. doi:10.1073/pnas.1304230110.
- Louis-Dit-Picard H, Kouranti I, Rafael C, Loisel-Ferreira I, Chavez-Canales M, Abdel KW, Argaza E, Baron S, Vacle S, Migeon T, Coleman R, Do Cruzeiro M, Hureauux M, Thuraijasingam N, Decramer S, Girerd X, O'Shaughnessy KM, Mulatero P, Roussey G, Tack I, Unwin RJ, Vargas-Poussou R, Staub O, Grimm PR, Welling PA, Gamba G, Clauser E, Hadchouel J, Jeunemaitre X. Mutations affecting the conserved acidic WNK1 motif cause inherited hyperkalemic hyperchloremic acidosis. *J Clin Invest* 130: 6379–6394 2020. doi:10.1172/JCI94171.
- Delaloy C, Lu J, Houot AM, Disse-Nicodeme S, Gasc JM, Corvol P, Jeunemaitre X. Multiple promoters in the WNK1 gene: one controls

- expression of a kidney-specific kinase-defective isoform. *Mol Cell Biol* 23: 9208–9221, 2003. doi:10.1128/mcb.23.24.9208-9221.2003.
10. O'Reilly M, Marshall E, Speirs HJ, Brown RW. WNK1, a gene within a novel blood pressure control pathway, tissue-specifically generates radically different isoforms with and without a kinase domain. *J Am Soc Nephrol* 14: 2447–2456, 2003. doi:10.1097/01.asn.0000089830.97681.3b.
 11. Vidal-Petiot E, Cheval L, Faugeron J, Malard T, Doucet A, Jeunemaitre X, Hadchouel J. A new methodology for quantification of alternatively spliced exons reveals a highly tissue-specific expression pattern of WNK1 isoforms. *PLoS One* 7: e37751, 2012. doi:10.1371/journal.pone.0037751.
 12. Argaiz ER, Chavez-Canales M, Ostrosky-Frid M, Rodriguez-Gama A, Vazquez N, Gonzalez-Rodriguez X, Garcia-Valdes J, Hadchouel J, Ellison DH, Gamba G. Kidney-specific WNK1 isoform (KS-WNK1) is a potent activator of WNK4 and NCC. *Am J Physiol Renal Physiol* 315: F734–F745, 2018. doi:10.1152/ajprenal.00145.2018.
 13. Boyd-Shiwarski CR, Shiwerski DJ, Roy A, Nkashama LJ, Namboodiri HN, Xie J, McClain KL, Marciszyn A, Kleyman TR, Tan RJ, Stolz DB, Puthenveedu MA, Huang CL, Subramanya AR. Potassium-regulated distal tubule WNK bodies are kidney-specific WNK1 dependent. *Mol Biol Cell* 29: 499–509, 2018. doi:10.1091/mbc.E17-08-0529.
 14. Thomson MN, Cuevas CA, Bewarder TM, Dittmayer C, Miller LN, Si J, Cornelius RJ, Su XT, Yang CL, McCormick JA, Hadchouel J, Ellison DH, Bachmann S, Mutig K. WNK bodies cluster WNK4 and SPAK/OSR1 to promote NCC activation in hypokalemia. *Am J Physiol Renal Physiol* 318: F216–F228, 2020. doi:10.1152/ajprenal.00232.2019.
 15. Hadchouel J, Soukaseum C, Busst C, Zhou XO, Baudrie V, Zurrer T, Cambillau M, Elghozi JL, Lifton RP, Loffing J, Jeunemaitre X. Decreased ENaC expression compensates the increased NCC activity following inactivation of the kidney-specific isoform of WNK1 and prevents hypertension. *Proc Natl Acad Sci USA* 107: 18109–18114, 2010. doi:10.1073/pnas.1006128107.
 16. McCormick JA, Yang CL, Zhang C, Davidge B, Blankenstein KI, Terker AS, Yarbrough B, Meermeier NP, Park HJ, McCully B, West M, Borschewski A, Himmerkus N, Bleich M, Bachmann S, Mutig K, Argaiz ER, Gamba G, Singer JD, Ellison DH. Hyperkalemic hypertension-associated cullin 3 promotes WNK signaling by degrading KLHL3. *J Clin Invest* 124: 4723–4736, 2014. doi:10.1172/JCI76126.
 17. Watt GB, Ismail NA, Caballero AG, Land SC, Wilson SM. Epithelial Na(+) channel activity in human airway epithelial cells: the role of serum and glucocorticoid-inducible kinase 1. *Br J Pharmacol* 166: 1272–1289, 2012.
 18. Chavez-Canales M, Zhang C, Soukaseum C, Moreno E, Pacheco-Alvarez D, Vidal-Petiot E, Castaneda-Bueno M, Vazquez N, Rojas-Vega L, Meermeier NP, Rogers S, Jeunemaitre X, Yang CL, Ellison DH, Gamba G, Hadchouel J. WNK-SPAK-NCC cascade revisited: WNK1 stimulates the activity of the Na-Cl cotransporter via SPAK, an effect antagonized by WNK4. *Hypertension* 64: 1047–1053, 2014. doi:10.1161/HYPERTENSIONAHA.114.04036.
 19. Gamba G, Miyanoshita A, Lombardi M, Lytton J, Lee WS, Hediger MA, Hebert SC. Molecular cloning, primary structure and characterization of two members of the mammalian electroneutral sodium-(potassium)-chloride cotransporter family expressed in kidney. *J Biol Chem* 269: 17713–17722, 1994. doi:10.1016/S0021-9258(17)32499-7.
 20. Mori Y, Wakabayashi M, Mori T, Araki Y, Sohara E, Rai T, Sasaki S, Uchida S. Decrease of WNK4 ubiquitination by disease-causing mutations of KLHL3 through different molecular mechanisms. *Biochem Biophys Res Commun* 439: 30–34, 2013. doi:10.1016/j.bbrc.2013.08.035.
 21. Ohta A, Schumacher FR, Mehellou Y, Johnson C, Knebel A, Macartney TJ, Wood NT, Alessi DR, Kurz T. The CUL3-KLHL3 E3 ligase complex mutated in Gordon's hypertension syndrome interacts with and ubiquitylates WNK isoforms; disease-causing mutations in KLHL3 and WNK4 disrupt interaction. *Biochem J* 451: 111–122, 2013. doi:10.1042/BJJ20121903.
 22. Susa K, Sohara E, Rai T, Zeniya M, Mori Y, Mori T, Chiga M, Nomura N, Nishida H, Takahashi D, Isobe K, Inoue Y, Takeishi K, Takeda N, Sasaki S, Uchida S. Impaired degradation of WNK1 and WNK4 kinases causes PHaII in mutant KLHL3 knock-in mice. *Hum Mol Genet* 23: 5052–5060, 2014. doi:10.1093/hmg/ddu217.
 23. Ishizawa K, Xu N, Loffing J, Lifton RP, Fujita T, Uchida S, Shibata S. Potassium depletion stimulates Na-Cl cotransporter via phosphorylation and inactivation of the ubiquitin ligase Kelch-like 3. *Biochem Biophys Res Commun* 480: 745–751, 2016. doi:10.1016/j.bbrc.2016.10.127.
 24. Semenza GL. Hydroxylation of HIF-1: oxygen sensing at the molecular level. *Physiology (Bethesda)* 19: 176–182, 2004.
 25. Susa K, Sohara E, Takahashi D, Okado T, Rai T, Uchida S. WNK4 is indispensable for the pathogenesis of pseudohypoaldosteronism type II caused by mutant KLHL3. *Biochem Biophys Res Commun* 491: 727–732, 2017. doi:10.1016/j.bbrc.2017.07.121.
 26. Castaneda-Bueno M, Cervantes-Perez LG, Vazquez N, Uribe N, Kantesaria S, Morla L, Bobadilla NA, Doucet A, Alessi DR, Gamba G. Activation of the renal Na⁺:Cl⁻ cotransporter by angiotensin II is a WNK4-dependent process. *Proc Natl Acad Sci USA* 109: 7929–7934, 2012. doi:10.1073/pnas.1200947109.
 27. Bazua-Valenti S, Chavez-Canales M, Rojas-Vega L, Gonzalez-Rodriguez X, Vazquez N, Rodriguez-Gama A, Argaiz ER, Melo Z, Plata C, Ellison DH, Garcia-Valdes J, Hadchouel J, Gamba G. The effect of WNK4 on the Na⁺-Cl⁻ cotransporter is modulated by intracellular chloride. *J Am Soc Nephrol* 26: 1781–1786, 2015. doi:10.1681/ASN.2014050470.
 28. Terker AS, Zhang C, Erspamer KJ, Gamba G, Yang CL, Ellison DH. Unique chloride-sensing properties of WNK4 permit the distal nephron to modulate potassium homeostasis. *Kidney Int* 89: 127–134, 2016. doi:10.1038/ki.2015.289.